Bib. Nat. Lab.
reg. Bib. Contr.
8 JUNI 1937
N.V. PHILIPS' GLOEILAMPENFABRIEKEN.

PHILIPS TECHNICAL REVIEW

VOLUME I
1936

PHILIPS RESEARCH LABORATORY — EINDHOVEN

CONTENTS

VOLUME I 1936

LIGHTSOURCES

page
Comparison between discharge phenomena in sodium and mercury vapour lamps 2, 70
Brightness greater than on the sun 62
High-frequency oscillations in sodium lamps 87
The development of the coiled-coil lamp . . 97
The photometry of metal vapour lamps . . . 120
The mercury vapour lamp HP 300 129
A new apparatus for testing the fastness-to-light of materials 277
The "Photoflux", a light-source for flashlight photography 289

LIGHT AND ILLUMINATION

Characteristics of the eye with special reference to road lighting 102
The definitions of brightness and apparent brightness and their importance in road lighting and photometry 142
The perception of brightness contrasts in road lighting 166
Irradiation of plants with Neon light 193
Visual acuity and speed of vision in road lighting 215
The problem of glare in highway lighting . . 225
Sodium lighting of tennis courts 252
The perception of colour 283
How can one judge the efficiency of road lighting 349

RADIO AND TELEVISION

An experimental television transmitter and receiver 16
Relaxation oscillations 39
Demonstration model illustrating superheterodyne reception 76
The VR 18 transmitting and receiving equipment 114
Some characteristics of receiving valves in short-wave reception 171
Electrical filters 240, 270, 298, 327 363
The communal aerial 246
Improvements in radio receivers 264
Television 321
Gas-filled triodes 367

SOUND, RECORDING AND REPRODUCTION

The loudspeaker and sound-amplifying installation on the T.S.S. "Normandie" 22
Optical model experiments for studying the acoustics of theatres 46
Absolute sound-pressure measurements . . . 82
The Philips-Miller system of sound recording 107
The sound recorder of the Philips-Miller system 135
The sound-recording cutter in the Philips-Miller system 211
The recording strip in the Philips-Miller system 231

TELEPHONY

Optical telephony 152
Electrical filters 240, 270, 298, 327, 363
Rectifiers for telephone exchanges 295
The use of loading coils in telephony 353

X-RAYS

page
A modern high-voltage equipment 6
Practical applications of X-rays for the examination of materials 29, 60, 95, 158, 188, 220, 253, 373
Dosage control in X-ray Laboratories and Works 62
Systematic X-ray examination for the detection of pulmonary tuberculosis 335

CATHODE RAYS

The production of sharp fluorescent spots in cathode ray tubes 33
Control of the beam intensity in cathode ray tubes 91
An oscillograph apparatus 147
The electron-microscope as an aid in research 312
Electron-optical X-ray observations on the transition of Alpha to Gamma iron 317

ELECTROTECHNICAL APPARATUS

A modern high-voltage equipment 6
Relay valves as timing devices in seam-welding practice 11
A high-frequency furnace with valve generator 53
A new metal rectifying valve with mercury cathode 65
An oscillograph apparatus 147
A controllable rectifier unit for 20 000 volts/18 amperes 161
Heavy-current condensers 178
Automatic starting resistances 205
An impulse-voltage generator for two million volts 236
Rectifiers for telephone exchanges 295
A surveillance system using infra-red rays . . 306
The Philips twin current welding unit . . . 338

MATERIALS AND THEIR RESEARCH

How does a welding electrode fuse? 26
Practical applications of X-rays for the examination of materials 29, 60, 95, 158, 188, 220, 253, 373
A speed-increment test as a short-time testing method for estimating the machinability of steels 183, 200
An impulse-voltage generator for two million volts 236
Properties and applications of artificial resin products 257
A new apparatus for testing the fastness-to-light of materials 277
The electron-microscope as an aid in research 312
Electron-optical X-ray observations on the transition of Alpha to Gamma iron 317
Telescope mirrors 358
The damping of mechanical vibrations 370

MISCELLANEOUS

Introduction 1
Abstracts of publications 32, 63, 96, 127, 160, 190, 223, 255, 288, 346, 376
High-frequency oscillations in sodium lamps 87
A very sensitive spring balance 126
Irradiation of plants with Neon light 193
A new apparatus for testing the fastness-to-light of materials 277
A surveillance system using infra-red rays . . 306
Telescope mirrors 358
The damping of mechanical vibrations 370

VOL. 1 No. 1 JANUARY 1936

Philips Technical Review

DEALING WITH TECHNICAL PROBLEMS
RELATING TO THE PRODUCTS, PROCESSES AND INVESTIGATIONS OF
N.V. PHILIPS' GLOEILAMPENFABRIEKEN

EDITED BY THE RESEARCH LABORATORY OF N.V. PHILIPS' GLOEILAMPENFABRIEKEN, EINDHOVEN, HOLLAND

INTRODUCTION

With the appearance of the first issue of this new periodical, the policy and aims should be outlined which will be pursued in these pages. The Philips Research Laboratories are continually receiving an everincreasing number of enquiries and requests from many quarters for more detailed data and particulars of the extensive range of Philips products, and especially for information as to their specific characteristics and practical applications. A large proportion of these enquiries comes from the engineering world and it is hoped by means of this periodical to establish permanent contact with these circles.

This journal will deal with the following items:

a) Technical descriptions of new Philips products, and reports on investigations relating thereto,

b) Information concerning the applications of these products, and

c) Technical articles of a more general nature on various questions relating to the above, which may be of interest to the reader.

An endeavour will be made to present the subject matter of the articles as simply as possible. Mathematical treatment will be resorted to neither more nor less than is necessary. Facts which can be concisely stated by mathematical formulae will in addition be explained in simple language, which will make it possible for those who do not wish to follow the mathematics to gather the gist of the article from the text alone. Additional clarity will further be strived for by the free use of diagrams and graphs. In this way every unnecessary show of learnedness will be avoided, but on the other hand care will be taken that this simplicity of expression does not lead to superficiality and indefiniteness when dealing with really complicated subjects.

Each contribution to this periodical will be, as far as possible, complete in itself. Owing to the wide range of products manufactured by Philips every article cannot be expected to command the same measure of interest from every reader. Nevertheless, it may be expected that many readers wil find matter of interest also in those contributions which do not concern their own immediate activities.

This periodical therefore will be not merely a journal embracing the activities of the Philips organisation nor a technical journal on popular lines, but a source of information of value and interest to the whole engineering profession. Our hope is that this publication will prove of practical interest and use to many, and in consequence merit a wide circle of readers.

G. HOLST.

COMPARISON BETWEEN DISCHARGE PHENOMENA IN SODIUM AND MERCURY VAPOUR LAMPS

I.

Summary. The visible radiations of sodium and mercury vapour lamps are generated by entirely different processes. Sodium is excited by the impact of electrically accelerated electrons against atoms in the normal state. In high-pressure mercury vapour lamps the radiation is produced by the temperature of the mercury vapour.

Introduction

The technical features of sodium and mercury vapour lamps as regards the state of the metal vapours have developed along very different lines, which in many respects have been tending in opposite directions. Thus it has been found that in general the efficiency of light production in sodium vapour was the higher, the lower the vapour pressure, the current density and the luminous intensity, while that of the mercury vapour lamp in the range investigated increased with these factors. *Table I* brings out the marked difference between these two types of gas-discharge lamps in their present stages of development. This table compares certain essential data of the metal vapours of a commercial sodium lamp with an experimental type of mercury vapour discharge tube of very high efficiency.

Table I. Characteristics of the metal vapour of a sodium tube lamp of 100 watts (Philora type SO 100) and of a super-high-pressure mercury lamp of 1400 watts (experimental type).

	Na	Hg
Pressure in atmos.	10^{-5}	200
Current density in amp/sq.cm.	0.4	280
Cross-section in sq.cm.	1.43	0.0075
Luminous intensity in candles/sq.cm.	10—20	180000
Vapour temperature in deg.C	280	8600
Light output in lumens/watt	68	78

The sodium lamp is surrounded by a double walled vacuum flask which diminishes heat conduction; the mercury vapour discharge, however, is cooled by running water.

The complete divergence in the behaviour of sodium vapour and mercury vapour cannot be readily reconciled with the assumption that the processes responsible for the emission of light from these two classes of lamps are analogous. Closer examination does in fact show that, in spite of a fundamental similarity in the mechanism of the two forms of discharge, there is yet an essential difference between the processes generating the visible radiation. Those prosesses which furnish the useful light in the mercury lamp represent, on the other hand, undesirable losses in the case of the sodium lamp, and vice versa. The explanation of this must be sought in the different structure of the sodium and mercury atoms, and makes it necessary for us to consider the fundamental principles of atomic physics regarding the emission of light from atoms.

Luminous Radiation due to Atomic Processes

In discussing this problem the principles will be followed enunciated in the atomic theory of Bohr. The sodium atom consists of a positively-charged nucleus about which 11 electrons revolve. A measure of the forces linking the electrons to the atom is the energy which must be expended to remove an electron from the rest of the atom. With both the sodium and mercury atoms it has been found much easier to remove the first electron from the atomic system than subsequent electrons, whose separation requires the expenditure of a much larger amount of energy. Ionisation may be produced, for instance, by bombarding the atom with electrons which have been sufficiently accelerated by an electric field that they are able to impart the requisite energy for ionisation to one of the atomic electrons. If an electron with charge e has passed through a voltage drop of V volts and stored the energy:

$$\varepsilon = e\,V \qquad (1)$$

acquired in this process, it will be termed an electron of V volts.

To be able to ionize sodium an electron must have acquired at least 5.12 volts, while in order to ionize mercury 10.38 volts are required. If electrons with a lower energy collide with the atoms, they will prove too weak to break up the atoms into positive ions and electrons.

The atoms, are, however, able to absorb certain amounts of energy which are smaller than the ionisation energy, but any energy values irrespective of magnitude cannot be absorbed; the energy absorbed must be in specific quanta.

The consequences will be discussed somewhat in detail for sodium atoms bombarded with electrons of steadily increasing velocities. As long as an electron has passed only through a voltage range which is smaller than 2.1 volts, collision is perfectly elastic since the sodium cannot absorb such small energy quanta. But as soon as the electron has passed through a voltage drop of 2.1 volts, it is able to impart the corresponding energy quantum of 2.1 e to the atom. By absorbing this amount of energy ε the atom passes into a socalled excited state, from which it is usually able to return very rapidly to its initial normal state (e.g. after the elapse of about 10^{-8} sec.). During this process it radiates light of a perfectly definite wave-length λ or frequency ν, as expressed by Planck's equation:

$$\varepsilon = h\nu = \frac{hc}{\lambda} \quad . \quad . \quad . \quad (2)$$

where c is the velocity of light and h the constant of Planck ($h = 6.55 \cdot 10^{-27}$ ergsec).

Equation (2) not only applies to the transition from the first excited state to the normal state, but in fact to every transition from one specific energy level to another during which the energy liberated is radiated as light. ε is here the difference in energy between the two states. In the particular case where sodium is excited by electrons of at least 2.1 volts, a yellow light is radiated. Analysing this radiation with the spectroscope, two lines are found, with wave-lengths of 5890 and 5896 Å respectively. These lines correspond to transitions from two states whose energies differ by such a small margin that in practice it is not possible to obtain the lower excited state alone. The wave-lengths agree with equations (2) and (1), from which we obtain the following relationship between the wave-length λ of the luminous radiation in Å and the potential difference passed through:

$$\lambda = \frac{hc}{eV/300}\,10^8 = \frac{6.55 \cdot 10^{-27}\, 3 \cdot 10^{10}}{4.77 \cdot 10^{-10} \cdot V}\, 300 \cdot 10^8$$

$$= \frac{12340}{V}\ \text{Ångström} \quad . \quad . \quad . \quad (3)$$

With mercury, electrons of 4.86 volts are similarly found capable of generating the ultra-violet mercury line with a wave-length of 2537 Å.

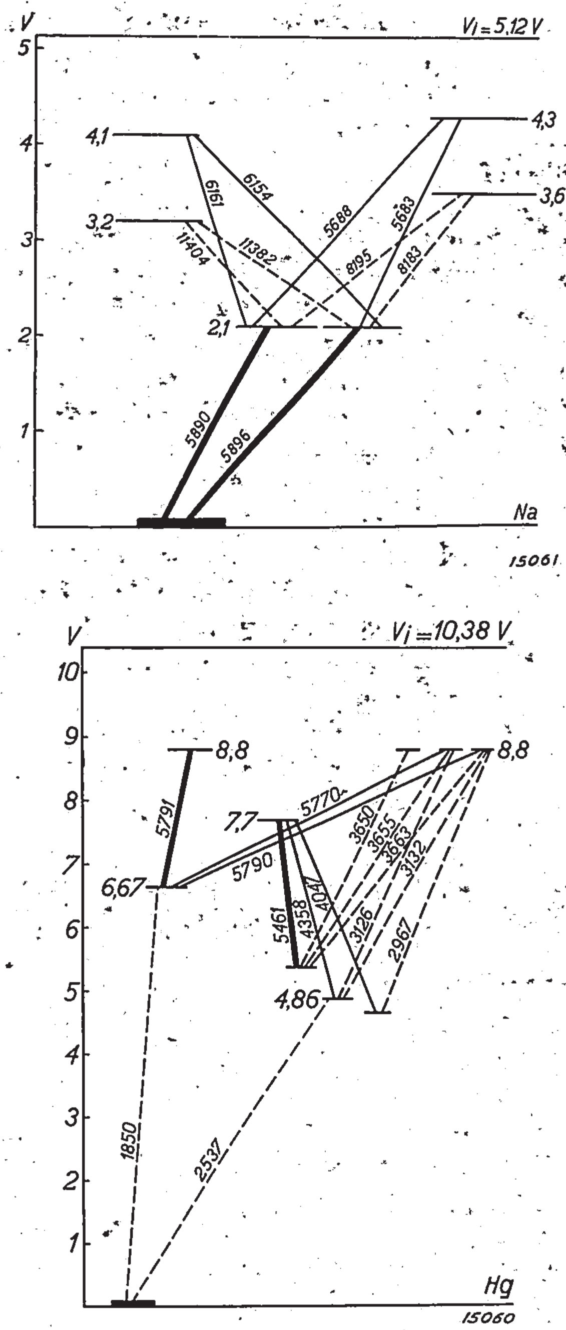

Fig. 1. Energy levels of Sodium and Mercury. The thickness of the lines denotes the visibility of the transition phenomena; invisible (ultraviolet and infrared) transitions are shown as broken lines. V_i is the ionisation voltage. With sodium, visible light is produced mainly by resonance lines (5890 and 5896 Å); higher transitions give infrared radiation. With mercury, visible radiation is produced by higher transitions (mainly 5461 and 5791 Å); the resonance lines (1850 and 2537 Å) are ultraviolet.

If in the case of sodium the velocity of the bombarding electrons is increased, various other lines of the sodium spectrum appear successively. Thus at 3.2 volts two infrared lines in the neighbourhood of 11400 Å are obtained, corresponding to a transition from the 3.2 volt level to the 2.1 volt level, and from 3.5 volts onward there appear the lines 8183 and 8195 Å. In this way the whole of the sodium spectrum is gradually produced, until at 5.12 volts the sodium is ionized. Similarly with mercury, at 6.67 volts there appears in the extreme ultraviolet a line with a wavelength of 1850 Å. From 7.7 volts onwards one gets the wellknown green, blue and violet lines of mercury with wavelengths of 5461, 4358 and 4047 Å, while in the neighbourhood of 9 volts the yellow mercury line 5791 Å appears, as well as a large number of lines which are on the threshold between the visible violet and the ultraviolet.

The energy levels of sodium and mercury may be represented as shown in *fig. 1.* Along the vertical axis the minimum voltage is plotted which the electron must pass through in order to be able to bring the atom into the corresponding state. The individual levels between which a transition accompanied by radiation may occur are joined by lines, whose thickness corresponds roughly to the intensity of the visible light obtained. These diagrams clearly show that not all possible transitions are obtained with noticeable intensity, thus e.g. there are no combinations between the energy levels in one and the same column. In fact, whether reciprocal combinations are possible or not with the emission of radiation has determined this distribution of the different energy levels over a number of columns. This question cannot be discussed in detail within the scope of this article.

The diagram shows that the common yellow sodium lines which make up the larger part of the visible light emitted by sodium lamps are radiated on the transition of the sodium atom from the lowest excited state to its normal state. The analogous process with mercury gives an invisible ultraviolet line and must therefore be regarded as undesirable. On the other hand, the visible mercury lines in the green and yellow are due to transitions between higher levels, which in the case of sodium mostly produce infrared lines. To this is due the fundamental difference in the behaviour of the sodium and mercury vapour lamps.

Energy can be imparted to an atom not merely by bombarding it with high-speed electrons, but also by causing the atom to absorb radiation or raising the gas to a high temperature. In these processes also it is found that the atom can absorb energy only in definite quanta. If the temperature is not too high, practically all the atoms are in the normal state and they then absorb only such light quanta, as are radiated on return to the normal state. The smallest light quantum which can be absorbed is that corresponding to a transition from the normal state to the nearest excited state. A spectral line radiated on return to the normal state is termed a resonance line.

The resonance lines play an important part, as they are strongly absorbed by the gas itself. If the pressure of the metal vapour is not extremely small, the intensity of the resonance radiation is considerably weakened by self-absorption. Self-absorption is not intrinsically a loss in luminosity, as the absorbed energy is usually emitted again in the form of a light quantum of the same wave length. But it may happen that an atom before radiating the absorbed light quantum is excited to a higher degree by collision with an electron (cumulative excitation) or transfers its energy to an electron and thus returns to the normal state without emitting radiation (collision of the second kind).

It is obvious that the weakening of the resonance radiation in gaseous discharges is determined not only by the intensity of self-absorption, but also by the relative occurrence of the secondary processes referred to. Self-absorption increases with the pressure, while the secondary processes increase with the current density.

Conclusions bearing on the Design of Sodium and Mercury Vapour Lamps

The above considerations show that to obtain a high output of visible radiation from sodium vapour and mercury vapour lamps entirely different methods must be adopted. To obtain a high yield of light rays with sodium, it is essential for the resonance radiation to predominate and transitions between higher energy levels to be suppressed as far as possible. On the other hand in the mercury vapour lamp the discharge must be such that the maximum radiation is obtained by transitions between high energy levels.

As already indicated in the previous section, resonance lines are easily and considerably weakened by self-absorption. This weakening is undesired in the sodium lamp, but highly desirable in the case of the mercury lamps. As this weakening due to self-absorption increases with the gas pressure and the current density, it appears that to obtain the best results, sodium lamps should have a low vapour pressure and be run on a low current density, and mercury lamps have a very high vapour pressure as well as a very high current density.

How far the adoption of these principles would result in an increase in the light output of sodium and mercury lamps will be discussed in a later paper. Certain results will, however, be briefly referred to here owing to their general interest, although they do not completely bear out the considerations above. It has been found that in the sodium lamp radiation is produced as a result of excitation by electronic collision. On the other hand, when passing a discharge through mercury vapour at a high pressure, the conditions of excitation and ionization are determined by the temperature of the vapour, in other words the vapour atoms behave as if they were contained in a closed vessel at a constant temperature. In spite of the input of energy by the current and the output of energy by radiation, a thermal equilibrium is roughly established. This is due to the fact that owing to the high concentration of the mercury atoms the energy stored in the gaseous column as heat is much greater than the energy input and output during a specific time interval sufficient for thermal equilibrium to be established.

In the case of sodium, nearly the whole of the energy of the electrons is converted to resonance radiation, when the current density is extremely low and the vapour pressure has a suitable value. In practice this limiting case is not approached, because inter alia part of the energy must be converted to heat in order to maintain the walls at such a temperature that the vapour pressure of sodium has a satisfactory value. The energy lost by thermal radiation increases with the area of the radiating surface. Therefore a specific luminous flux should not be radiated through an excessive area. The luminous density and hence also the current density must therefore not be too low.

The spectral distribution of energy in the radiation of high pressure mercury vapour presents a very complex problem. With rising vapour pressure, the relative concentration of mercury molecules Hg_2 also increases. These molecules give a spectrum, composed of wide bands instead of sharply defined lines. As a result the line spectrum will gradually become covered by a continuous background, the transition becoming the more marked as the vapour pressure rises. *Fig. 2* shows the spectra obtained with a super-high-pressure mercury vapour lamp at different vapour pressures.

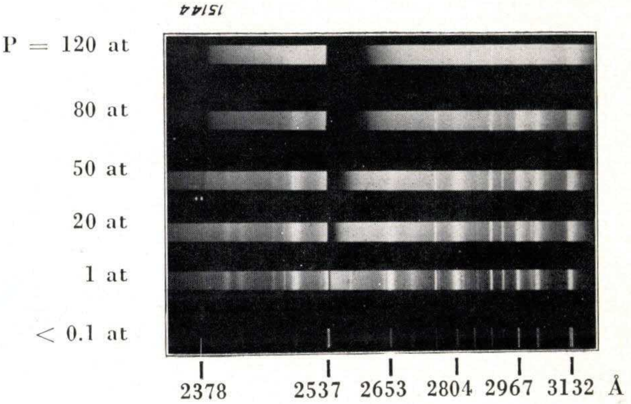

Fig. 2. Spectrum of a mercury vapour discharge, cooled with a stream of water, at different vapour pressures P. With rising vapour pressure, the spectrum lines will progressively be covered by emission and absorption bands. (Internal diameter of tube 2 mm, current intensity approx. 1.3 A).

The most striking difference in these spectra is the steady intensification of the continuous background beginning at the resonance line 2537 Å and spreading mainly in the direction of the longer wavelengths. With the increase in vapour pressure an absorption band progressively covers a greater part of the spectrum owing to self-absorption of the resonance radiation. The appearence of the bands may be regarded as the first stage of the transition of radiation into a state of thermal equilibrium, where the spectral distribution of intensity is no longer determined by the characteristics of the individual atoms but merely by Planck's law of black body radiation. Since a black body at the temperature of the radiating zone in the discharge emits comparatively more red radiation and less ultraviolet radiation than a mercury vapour lamp, it may be concluded already from thermodynamical considerations that with rising vapour pressure the center of gravity of the intensity distribution becomes shifted towards longer wavelengths. This effect is indeed clearly brought out in fig. 2. The wide absorption bands produced by a broadening of the resonance lines weaken the ultraviolet radiation of the mercury vapour to a degree which increases with the rise in vapour pressure, while the continuous background which increases in intensity with the pressure stretches far into the red and infrared region of the spectrum.

Compiled by G. HELLER.

A MODERN HIGH-VOLTAGE EQUIPMENT

Summary. The equipment described furnishes peak voltages up to 1000 kV, and a D.C. voltage of 700 kV, a current of 4 milliamps being derived. Compactness and simplicity of control are its features. The installation is composed of two symmetrical units. One unit comprises four stages, each consisting of a condenser and valve; each structural element is subject to a quarter only of the total voltage. Owing to their special design, the valves are able to cope with a 200 kV backfiring voltage. The oxide cathodes are heated by means of a high-frequency generator.

Introduction

The problem of generating D.C. voltages up to several hundreds of kilovolts has been stimulated in a high degree by the development of atomic physics, which has acquired considerable proportions during the last few years. For experiments on the disintegration of atoms a very large number of high-voltage equipments complying more or less with the special requirements have been designed and constructed. But most of these equipments take up a great deal of room and demand much of the experimenter's attention, which, therefore, has to be necessarily divided between the actual experiments in hand and the apparatus supplying the requisite high voltage. An installation which, while not relieving the experimenter from every such duty, yet does simplify supervision to a marked degree, has been developed in the X-ray laboratory of the Philips Works 1). This equipment, which supplies a direct current of 4 mA at 700 kV and peak voltages up to 1000 kV, takes up very little space and is remarkable for the simplicity of its construction and operation.

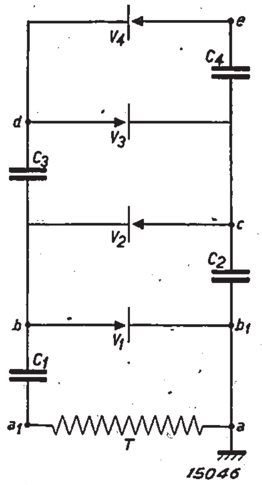

Fig. 1. Principle of the Greinacher circuit. If transformer T supplies an A.C. voltage of amplitude E, point c is at a constant voltage 2 E and point e at a constant voltage 4 E with respect to earth. The circuit can be expanded as required.

The theoretical lay-out of this installation is based upon a circuit, first described by Greinacher. Cockcroft (Cambridge), and Bouwers (Eindhoven), working independently almost simultaneously thought of applying this principle for generating very high voltages.

Principle of circuit

The fundamental diagram is shown in *fig. 1.* The secondary winding T of a high-tension transformer furnishes an A.C. voltage of amplitude E. Point a is earthed and is thus always at zero potential. (This fact is not essential, but it is stated to facilitate a clear understanding of the circuit). Point a_1 has a voltage with respect to earth, which is represented by the voltage-time sine curve a_1 in *fig. 2.* How will the voltage at point b vary with time?

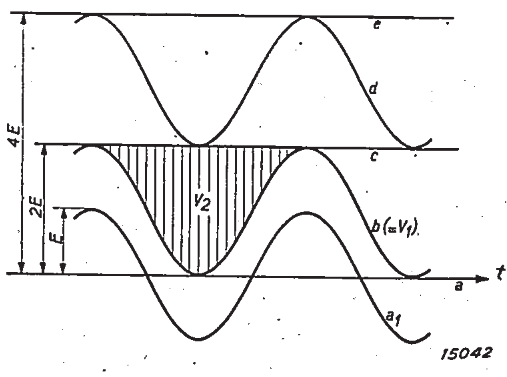

Fig. 2. Voltage-time curves for various points of the circuit in fig. 1. Across each valve the voltage fluctuates between zero and 2 E; for adjacent valves the phase-displacement is half a cycle.

In the absence of valve V_1, the upper plate of condenser C_1 would alternately assume a positive and negative charge, whose maximum value would

---

1) A short description of the equipment — which has since been much improved — has been published by A. Bouwers ("Modern X-ray Development", British Journal of Radiology 7, 21, 1934).

correspond to the peak value E of the transformer (it amounts to E times the capacity of C_1). As, however, valve V_1 permits the current to flow in circuit $a\ a_1\ b\ b_1\ a$ in one direction only (viz. to the left) [2]), the positive charge once accumulated on the upper condenser plate will be maintained, as the deficiency of electrons cannot be made up via V_1. Condenser C_1 is thus charged to the peak voltage E, and the potential at b consequently remains $+$ E in excess of that at a_1 (or —E, if the valve is reversed). The potential at b which with respect to earth is identical to the voltage across valve V_1 can obviously be represented by curve *b*: it oscillates between zero and 2E.

The same reasoning may be followed for ascertaining the fluctuation of the potential at point c of the adjacent circuit. The voltage across valve V_1 which oscillates between zero and 2E, here performs the function of the A.C. voltage supplied by the transformer; owing to the action of valve V_2, condenser C_2 is charged to the highest voltage occurring at V_1, viz. 2E. Point c, therefore, has a constant potential 2E with respect to b_1 (= earth) (cf. line c, fig. 2).

Between points c and b, i.e. across valve V_2, a voltage occurs which can readily be found as the difference of the potentials at these points, that is, the difference between the ordinates of curves c and b (cf. the shaded area V_2.) It is seen that the valve-voltage V_2 oscillates between zero and 2E (which was also the case with valve V_1), this voltage being displaced by half a cycle with respect to that of V_1. Starting with V_2 and proceeding by the same method, it is similarly found that at point d the voltage fluctuates between 2E and 4E; and also, that point e acquires a constant voltage 4E (cf. curves d and c in fig. 2).

If, for instance, the original A.C. voltage E is 100 kV, a D.C. voltage 4E = 400 kV is obtained at c; by means of a second unit devised on the same lines but having valves operating in the opposite direction, a voltage of —400 kV can be obtained. Between the terminals of the two systems a total voltage 8E = 800 kV will therefore obtain. From fig. 2 it will be evident that in the unit described, voltages still higher than 4E occur: between points e and a_1, the voltage fluctuates between 3E and 5E. By earthing point a_1 instead of a, a peak voltage as high as 5E per unit may be obtained, so that two units in combination are able to supply a peak voltage of 10E.

The main advantage of this circuit is that all condensers and valves are subjected to a fraction of the voltage only (viz. 2E, and even E only in C_1). This has enabled the dimensions of all components to be kept within reasonable limits. Moreover, each unit is composed of identical stages, so that still higher voltages can be attained by increasing the number of stages per unit.

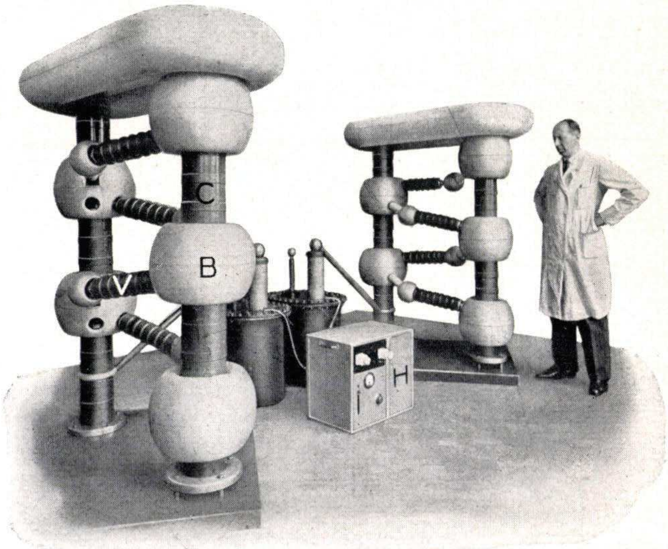

Fig. 3. Complete equipment consisting of two units. The metal globes B enclose the connecting points to eliminate corona phenomena. Between the globes the condensers C which form the vertical structural elements are visible; the valves V are fitted in the sloping interconnections. The transformer is at the rear, the transmitter H for high-frequency heating is in the front.

Description of equipment

Fig. 3 shows a photograph of the complete equipment, comprising two units of four stages each. At both sides of each unit the condensers C(paper condensers of about 0.01 μF) can be seen mounted vertically; the valves V are contained in the sloping connecting members. The connecting points b, c, d and e are surrounded by globe-shaped metal shields B to decrease corona phenomena. Theoretically, a maximum D.C. voltage of 800 kV is obtained between the terminals if the amplitude of the transformer voltage amounts to E = 100 kV. (When the system is loaded this voltage will be somewhat lower because the condensers cannot maintain their peak voltages. Also, a ripple amounting to a small percentage will occur in that case). By a slight modification of the circuit, it is possible, as already mentioned, to obtain a voltage fluctuating between 600 and 1000 kV.

It has already been pointed out that this type of installation is not by any means bulky, the equipment shown in fig. 3 occupying a floor area of only 1.5×3 m and being only 2 m high. It can, therefore, be accommodated in a comparatively small room.

---

[2]) In the symbol for the valves used in fig. 1, the arrow denotes the cathode; the arrow consequently indicates the direction of the flow of electrons.

The valves

Among the various components constituting the equipment, the valves designed by Mulder[3]) (Eindhoven) call for special mention. They contain mercury vapour at saturation pressure (approximately $2 \cdot 10^{-3}$ mm at 15° C) and are provided

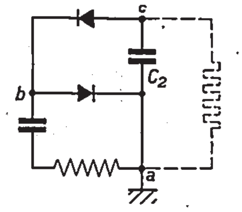

Fig. 4A. Two-stage unit. Starting at instant t_0 a current is taken from *c*.

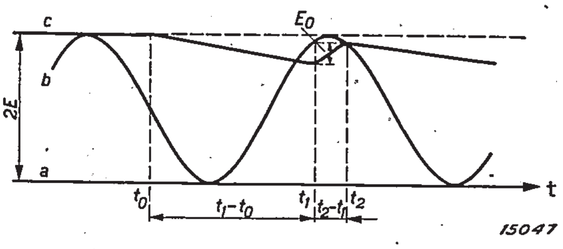

Fig. 4B. The variation of potential at points *b* and *c* is similar to that in fig. 2, but the potential of *c* slowly decreases from the instant t_0. At t_1, the potential difference across the valves (between points *b* and *c*) attains the value of the ignition voltage E_0; ignition is effected, the potential at *c* increases up to t_2. During the short interval t_2—t_1 the whole charge of condenser C_2 lost during the long interval t_1—t_0 has to be made up. The charging current must therefore assume high momentary values during this short interval.

with oxide cathodes. It is true that, compared with high-vacuum valves, gasfilled tubes have the disadvantage of a high ignition voltage (about 7 kV). Moreover, their operation sets a limit to the ambient temperature, such that in view of the mercury-pressure required, the permissible temperature range is restricted to between about 15° and 40° C. On the other hand, they offer the advantage of a very low voltage drop (50 volts); their main feature, however, is that they enable oxide cathodes to be used which require very little heating and thus facilitate the application of "high-frequency heating", described below (the power required for heating tungsten cathodes is about ten times greater).

Notwithstanding the fact that the high-tension equipment has to supply a current of a few milliamps only, the cathodes must be designed for an emission current of about 100 milliamps, for the instantaneous values of the charging currents in the valves are many times greater than the current to be ultimately supplied. This point will be considered in some detail, as it is of paramount importance to the efficient functioning of the installation.

When the equipment has to supply current, the functioning of the installation is explained on the same lines as outlined above, except that the potentials of the condensers are somewhat reduced as a discharge occurs. The state of affairs is shown in *fig. 4B*, for an installation of only two stages, up to *c* (*fig. 4A*), and assuming that at a certain instant t_0 the current is drawn from point *c*. The potential at *c*, which was initially 2E, now slowly drops as condenser C_2 is discharged. At a certain instant the potential at *b*, which, as previously stated, fluctuates between zero and 2E, will be in excess of the decreased potential at *c*; when the excess voltage reaches the value E_0 of the ignition voltage — at the instant t_1 — the valve is started up and the condenser C_2 becomes recharged. The potential at *b*, however, remains only a short time at the peak around 2E; it decreases again, whilst the potential at *c* increases. Shortly after, at the instant t_2, the potential difference at the valve becomes zero and the charging current is interrupted. From this point, the cycle is repeated. In order to prevent the condenser voltage from decreasing regularly at intervals, it is necessary to restore to the condenser in the short period t_2—t_1 that charge which has been lost during the long period t_1—t_0 by the discharge current. As the charge is represented by the integral of the current over the time, it is clear that owing to the short duration of the charging current its magnitude must be correspondingly greater; it should exceed the discharge current by the ratio between the time intervals t_1—t_0 and t_2—t_1[4]).

The oscillogram of the current of condenser C_2, shown in *fig. 5*, clearly shows how the condenser is discharged with a small current and how the charge is restored in a few peaks.

Moreover, the importance of using valves with a low ignition voltage will now be evident. If the ignition voltage is high, it may happen that, at the first "crossing" of the potential at *b* and *c* (point t_1 in fig. 4B), no ignition of the valve at all takes place, so that the condenser is still further discharged, until recharging occurs at the next "crossing", or even later! In this case the time interval for restoring the charge has become still more unfavourable.

---

[3]) cf. J. G. W. Mulder, Dissertation, Delft 1934.

[4]) If the potential at *c* is decreasing more quickly, point t_1 is shifted to the left and the ratio of the time intervals becomes more favourable, but the potential "ripple" at *c* is then very large.

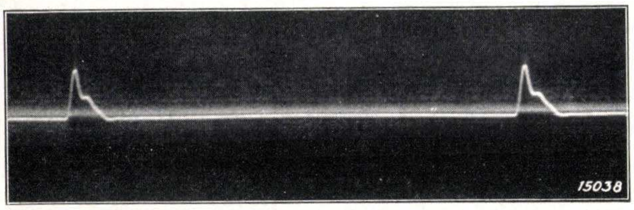

Fig. 5. Oscillogram of current in condenser C_2 (of fig. 4A), showing the small discharge current (below the zero-line) and the peaks of the charging current (above the zero-line, about 10 times as large).

The valves used are provided with oxide cathodes consuming about 8 watts, which is ample for obtaining the necessary emission current.

As the cathode is at a potential of several 100 kV, the heating power supply presents a problem in itself. Cockcroft made use of small storage batteries, which were placed directly on the condensers. This seems to be a simple solution, but the regular charging and supervision of the batteries necessary are serious drawbacks and prove very inconvenient. In the case of the equipment described here, the cathodes have for some time been heated by small generators, a method also employed by Cockcroft. The generators were mounted on the condensers and were driven in pairs by a motor on the floor through a common insulating pertinax shaft. This solution is fairly satisfactory, but has the drawback that operation is not noiseless.

The high-frequency heating

The heating problem was later solved in a more elegant way by the application of high-frequency heating, a method suggested by Kuntke (Eindhoven). The circuit at present used is shown diagrammatically in *fig. 6* (only one of the two units is shown).

The condensers C_1-C_4 act as insulators for the D.C. voltage produced, but allow a high-frequency alternating current to pass freely. Between the points *a* and b_1 (*a* is at zero potential) an alternating voltage is applied with a frequency of $7.5 \cdot 10^5$ c/s (corresponding to a wavelength of 400 metres) and derived from a small 150-watt transmitter H. This A.C. voltage now delivers current to the high-tension circuit without affecting the high tension and without being affected thereby. This implies, however, that the circuit must be suitably dimensioned to carry both kinds of current; the condensers for instance must be designed in such a way that, apart from the required capacity and disruptive strength, they involve only small high-frequency losses. Notwithstanding the special design, the high-frequency losses in the condensers are still comparatively high. Therefore it was desirable to restrict the high-frequency current intensity to 0.7 amp. To obtain the 3.5 amp current required for heating the cathodes, small air-core trnasformers of a 5 : 1 ratio have therefore to be included in the circuit (cf. fig. 6). The necessary power of 8 watts is arrived at by constructing the air-core transformers with a tight coupling and low leakage; the secondary voltage is derived from taps on the coil, as in an auto-transformer. All cathodes are thus heated in a series circuit.

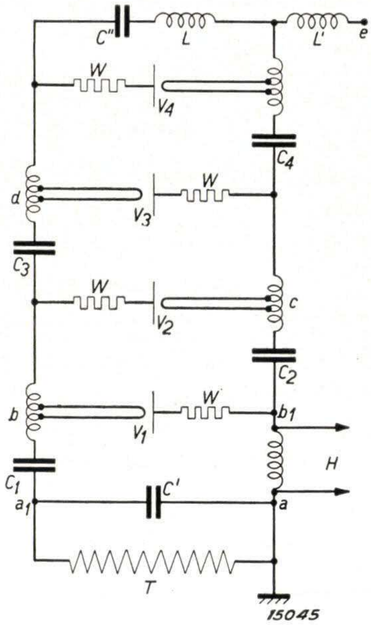

Fig. 6. Circuit diagram of a single unit, with supplementary high-frequency heating. Through the high-tension circuit there also flows a 750 kc current of 0.7 amp; by means of specially-designed air-core transformers (at *b*, *c*, *d* and above C_1), the requisite value of 3.5 amp for heating the cathodes is obtained. The functions of the supplementary components (capacities, inductances and resistances) are explained in the text.

Some details of the diagram shown in fig. 6 may be referred to. The resistances W of 20000 ohms, connected in series with the valves, were originally designed to limit the initial current at the moment of ignition; now they also serve to prevent the valves from providing a shunt for the high-frequency current. For the high-frequency current the capacity C′ shorts the transformer, while capacity C″ bridges the last valve. The self-inductance L is used to tune the circuit to resonance and, therefore, to reduce the impedance of the high-frequency circuit to the minimum possible. The choke coil L′ prevents the high-frequency circuit from passing over to the loading circuit.

The design of the valves is such that the discharge path between cathode and anode is subdivided by a number of short metal tubes. The valves are glass tubes about 50 cm long and 3 cm in diameter; the cathode-anode distance d is about 30 cm and is sub-divided by means of 60 tubes in such a way that the distance c between the small tubes amounts to about 0.5 cm (cf. *fig.* 7).

The function of the tubes, which may be regarded as intermediate electrodes, is to increase the backfiring voltage; this is briefly explained as follows: The break-down voltage depends on the vapour pressure and the distance between the electrodes. When the distance between the electrodes is decreased, with a fixed vapour pressure, a region is ultimately reached in which the break-down voltage increases with decreasing electrode-distance 5)). Roughly speaking, this condition prevails when the mean free path of the electrons in the vapour is of the same order of magnitude as the distance between the electrodes. Then, owing to the deficiency of the number of collisions, the electrons do not produce a sufficient quantity of ions to cause a discharge. Now the mean free path of the electrons in mercury vapour at a pressure of about $2 \cdot 10^{-3}$ mm is of the order of a few centimetres and is therefore comparable to the distance between the small tubes. The latter are interconnected by condensers; this affords a linear potential distribution along the discharge-path, which is necessary during the period during which the tube has to stand the full voltage (2E). The dielectrics of these condensers are constructed as rings of high-tension Philite and fitted round the valve-tube, and thus give the valves the striking appearance shown in fig. 3.

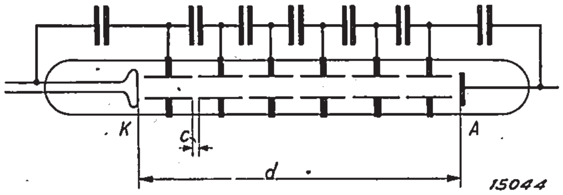

Fig. 7. Construction of valve: the distance d = 30 cm between cathode K and anode A is subdivided by 6 tubes each separated by a distance c = 0.5 cm to increase the backfiring voltage. The bridging condensers produce uniform distribution of the total voltage along the tube.

Compiled by S. GRADSTEIN.

---

5) Cf. e.g. J. J. Thomson and G. P. Thomson, Conduction of electricity through gases, Cambridge 1933, Vol. 2, p. 475 ff.

RELAY VALVES AS TIMING DEVICES IN SEAM-WELDING PRACTICE

By D. M. DUINKER.

Summary. The usual method of bonding two pieces of metal by spot-welding is to pass a very high-ampere alternating current through them. Practical experience in recent years has shown that to obtain a reliable bond it is essential to limit the time the current is passing to a few hundredths of a second, i.e. to a small number of periods at a 50-cycle frequency. In welding long seams the parts to be bonded are passed between roller-type electrodes at a constant speed, a series of welding-spots being produced by passing a current impuls of the above mentioned duration through the electrodes at uniform intervals. A timing device designed for this purpose must therefore allow the current to pass for a certain number of cycles x, then arrest the current for a further number of cycles y and repeat this sequence (x+y) continually. Mechanical timing devices are not suitable for this purpose owing to the extremely short period of time involved (of the order of 0,02 second) and the powerful current used (usually several 100 amps). The employment of a relay valve controlled by a relaxation oscillation offers considerable advantages as it operates with perfect synchronism and can be readily and instantaneously regulated within wide limits. The design and operation of a timing device of this type are described below.

In addition to arc welding, two pieces of metal can also be bonded electrically by resistance welding in which a powerful current is passed through the metal. In this process the greatest resistance to the flow of current is encountered at the gap between the two surfaces, the heat generated at this point causing the metals to fuse together to give the desired bond. Usually the current is supplied to the two pieces of metal by means of more or less tapered electrodes, the weld covering an area with a diameter of only a few millimetres. Hence the term "spot-welding". To produce long seams, a series of welding-spots are required, to obtain which the electrodes are made in the form of rollers that are brought in contact with the metal surfaces to be bonded. The metal is then passed between the rollers at a speed determined by the distance required between the welding-spots, which in turn depends on the required mechanical strength and impermeability to liquids of gases. The present paper deals essentially with this method of seam-welding.

The heat generated at a welding-spot is determined by the strength of the current passed and its duration of flow. Investigations during recent years have shown that it is important for the current to be sufficiently powerful to allow it to pass through the metal for only an extremely short period of time, in order that the heat generated is restricted to the spot where it is required. The heating of the surrounding material, which is avoided by this means, is not only of no practical value but may also have a most deleterious effect on the quality of the weld, since it may cause oxidation and other undesirable chemical and physical changes.

The method of interrupting the flow of the welding current periodically signifies an important advance in this method of welding, as compared with a non-periodic interruption. In the first place it has led to a marked speeding up of welding, and secondly it has enabled such metals as stainless steels and aluminium alloys to be welded satisfactorily. In some cases it may be necessary to restrict the passage of the current to a few hundredths of a second, in other words to a few cycles of the alternating current, and it is evident that to give a satisfactory uniform weld a circuit breaker capable of performing this duty must operate in perfect synchronism with the mains supply and permit of such accurate adjustment that the intervals between the opening and closing of the associated circuit can be maintained absolutely constant. With the short times of current flow involved here, a difference of half a periode (0,01 second) either way is already sufficient to produce a marked alteration in the amount of heat produced. Furthermore, as the primary current of the transformer is several 100 amps (the secondary current being 1000 to 10000 amps at 3 to 10 volts), it is apparent that a mechanical device is quite impracticable, especially as it would be exposed to the most severe wear.

A more satisfactory and more efficient method for the synchronous opening and closing of the circuit is obtained by means of relay valves. These are gas-filled hot-cathode rectifiers with control grid; the ignition voltage of such valves can be adjusted by means of the grid voltage, as shown by *fig. 1*, the characteristic for Philips relay valve DCG 5/30. It will be noticed that at positive grid voltages exceeding 12 volts the ignition voltage is low (<100 volts), whereas in the case for instance of —2 volts grid voltage the valve ignites only at 11000 volts anode voltage.

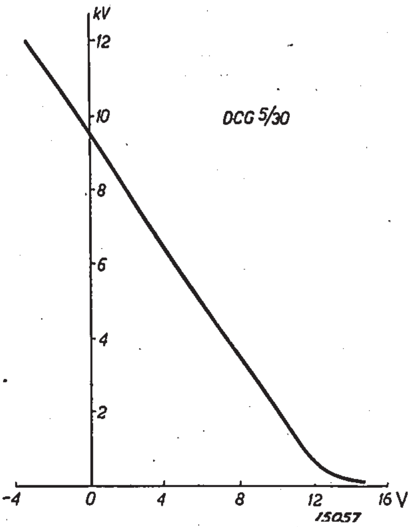

Fig. 1. Characteristic of Philips Relay Valve type DCG 5/30: Ignition voltage as a function of grid voltage.
Principal data: Max. peak inverse voltage 12000 volts
Max. anode current peak value, 25 amps
Max. anode current mean value, 6 amps

These relay valves render it possible, by means of certain circuits (see below) to close the current for any desirable number of cycles (x = 1, 2, 3, ...) and to open it for any other number of cycles (y = 1, 2, 3, ...), and this sequence x+y to be repeated periodically. The values of x and y can be varied independently of each other within wide limits. The principal advantages of a timing device of this type are:

1. Absence of all moving and revolving parts, no wear or noise;
2. Perfect synchronism with the mains supply;
3. Ready and instantaneous regulation of time intervals x and y;
4. The value of x can be reduced to a single cycle (0,02 second);
5. Uniformity in operation in any setting when once made.

Fig. 2 shows the various circuits making up the timing device, and which consist essentially of the three following:

A. The oscillating circuit;
B. The time-delay circuit;
C. The interrupter circuit;

these circuits are also shown separately and slightly simplified in figs. 3, 7 and 5.

The primary circuit of the welding transformer (T_1, *fig. 3*) includes the primary winding of a transformer (T_2), whose secondary winding is connected to the cathode and anode of a relay valve (M_1). Transformer T_3 serves for heating the cathode of valve M_1. When the potential difference between the grid and the cathode of M_1 reaches such a value that the valve passes current, transformer T_2 is shorted [1]), practically the whole of the mains voltage is applied across the terminals of T_1 and welding takes place. The grid of M_1 is now given a negative potential sufficiently large to prevent ignition of the valve: the secondary circuit of T_2 remains open, and only the weak magnetising current flows through the primary circuit; the welding current is then practically zero. A grid potential of $-V_g$ volts (e.g. derived from a battery) is sufficient to prevent ignition of the valve. What potential difference must be applied to the grid between the points 1 and 2 (fig. 3) so that the primary current can flow for a single cycle (x=1) and be cut off for y cycles (y being integral)? It follows from the above that this is obtained by imparting to the grid a positive potential impulse every (1+y) cycles, at the instant the anode becomes positive with respect to the cathode. We therefore require a potential of the

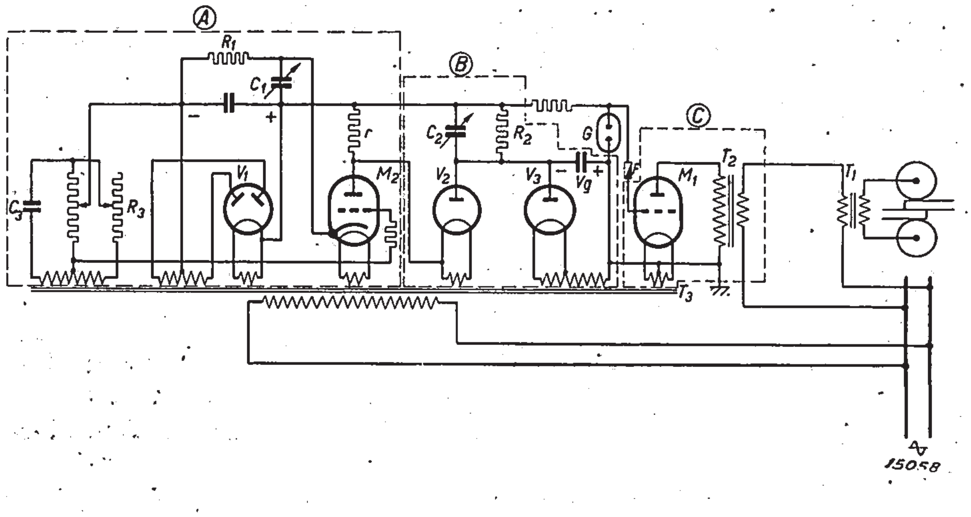

Fig. 2. Circuit diagram of timing device for seam welding.
T_1 = Welding transformer.
A = Oscillating circuit (see fig. 5).
B = Time-delay circuit (see fig. 7).
C = Interrupter circuit (see fig. 3).

---

[1]) This applies only for one direction of the secondary current, but for the primary current this has practically the same effect as a complete short-circuit (cf. e.g. P. Lenz, Archiv für Elektrotechnik **27**, 497, 1933).

form shown in *fig. 4*, i.e. an alternating voltage with a fundamental frequency $1/(1+y)$ times the mains frequency. Such demultiplication of the frequency may be conveniently obtained by means of relaxation oscillations 2), which brings us to the oscillating circuit shown in *fig. 5*.

A small relay valve (M_2) of low output is connected in parallel with the condenser C_1, which

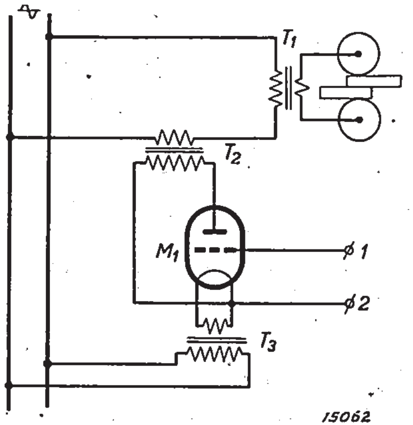

Fig. 3. Interrupter circuit (cf. "C" in fig. 2).
T_1 = Welding transformer.
T_2 = Series-transformer.
T_3 = Filament heating transformer.
M_1 = Main relay valve.
Grid (1) is negative with respect to cathode (2): the anode current of the valve is blocked and only no-load current flows through the primary circuit of T_2. Grid (1) is given a potential causing ignition of the valve: transformer T_2 is shorted and practically the whole of the mains voltage is applied across the welding transformer T_1.

is slowly charged from a source of direct current through a high resistance R_1 after the circuit is closed by the switch; the anode voltage, which is equal to the condenser voltage, therefore increases. As the potential of C_1 increases, there is a decrease of the voltage drop at R_1, which drop serves as negative grid voltage for valve M_2; after a certain time the valve ignites, the condenser is rapidly discharged through the valve and the small resistance r. This cycle then starts all over again. A free relaxation oscillation of this type has a frequency proportional to $1/R_1C_1$, although it can be very readily synchronised with a higher or lower harmonic of any other frequency introduced into the system. This is illustrated in *fig. 6*: anode and condenser voltage with respect to the cathode K show an exponential trend (A, C_1). The trend of the critical grid voltage (dotted line g) has been deduced from this by means of the characteristic, i.e the grid voltage required for ignition at the anode voltage in question. Actually the grid voltage G consists of the voltage-drop across R_1 (V_{R_1}) with the superimposed A.C. voltage V_S. Ignition takes place the moment the actual grid voltage exceeds the critical one, i.e. at the point of intersection of the curves G and g. As this point of intersection will always be situated near the peak of V_S, only such conditions will occur at which an integral number (1, 2, 3 ...) of cycles of the frequency of the synchronising voltage elapses between two successive ignitions. The frequency of the free relaxation oscillation will therefore adapt itself to that of the adjacent lower harmonic (1/1, 1/2, 1/3 ...) of the imposed mains-frequency. It is, for instance, sufficient to apply to the grid circuit a low-voltage 50-cycle alternating current (fig. 5) in order to limit the possible frequencies of the relaxation oscillations to 50, 25, $16^2/_3$, $12^1/_2$ and 10 cycles, etc. If to the capacity of C_1 values are given at which

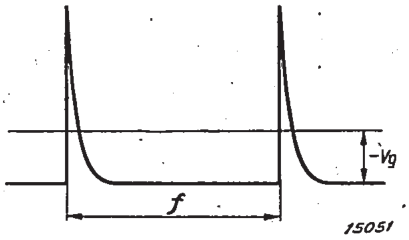

Fig. 4. Required voltage waveform between terminals 1 and 2 (fig. 3) in order to obtain welding-spots during a single cycle at intervals of y cycles.

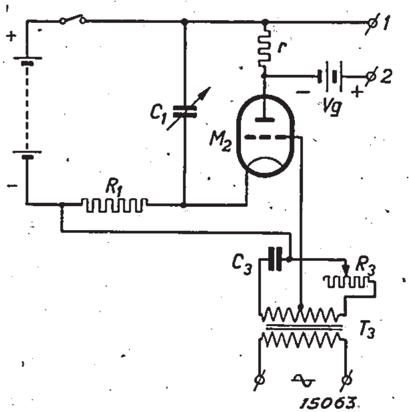

Fig. 5. Oscillating circuit (simplified) (Cf. "A" in fig. 2).
C_1 = Variable condenser.
R_1 = Charging resistance.
r = Discharging resistance.
M_2 = Relay valve.
T_3 = Transformer to furnish a potential of mains frequency at the grid of M_2.
Valve M_2 is ignited with a frequency which is a sub-harmonic of the mains frequency. The degree of frequency demultiplication is determined by the product C_1R_1. Circuit C_3R_3 permits the phase displacement to be varied between the relaxation oscillation obtained and the mains.

---

2) Cf. e.g. B. van der Pol, Phil. mag. **2**, 978, 1926, and B. van der Pol and J. van der Mark, Frequency Demultiplication, Nature **120**, 363, 1927.

the free relaxation frequency would be in the neighbourhood of these fractions of the mains frequency, a current impulse will flow through the resistance r (fig. 5) every 2, 3, 4 or more periods of the mains supply. The potential at r, combined with the battery voltage $-V_g$, then fluctuates as shown in fig. 4. The condenser C_3 and resistance R_3 (fig. 5) permit the phase displacement between the mains voltage and the grid potential of M_2 to be adjusted in such a way that M_2 is ignited exactly at the instant the anode of M_1 becomes positive. The phase displacement requires adjustment only once and remains constant.

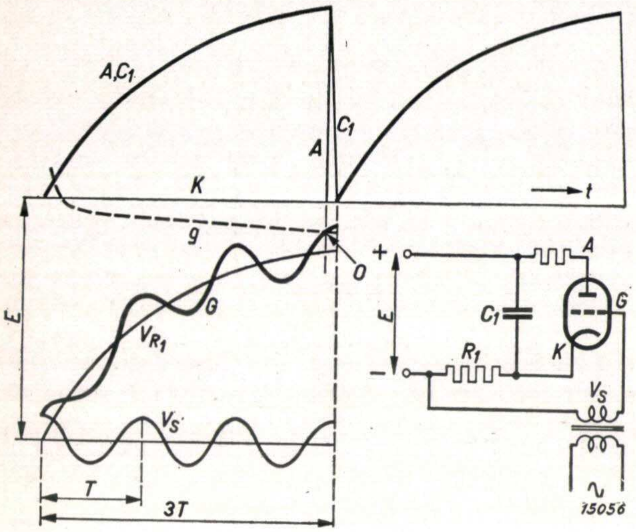

Fig. 6. Diagram of a free relaxation oscillation synchronised with a lower harmonic (in this case $^1/_3$) of an imposed A.C. voltage.

By connecting terminals 1 and 2 in fig. 5 with terminals 1 and 2 in fig. 3, an arrangement is obtained which allows current to be passed through the associated circuit for one single cycle at intervals of 2, 3, 4 or more cycles. For some purposes this duration of current flow may be too short, and one would like to be able to prolong it as required to 2, 3, 4 or more periods, retaining at the same time a suitable interval with no current-flowing. This can be readily achieved by inserting a time-delay circuit between the circuits C and A in figs. 3 and 5, which will prolong as required the time the positive impulse is applied to the grid of M_1. A circuit of this type is shown in *fig.* 7; it has a condenser C_2 in parallel with the resistance r (fig. 5) which is charged the instant the valve M_2 becomes ignited and is discharged slowly through the high resistance R_2 (a rapid discharge of C_2 through r is prevented by the valve V_2). By increasing the capacity of C_2 (or the resistance R_2) the interval during which the grid of M_1 remains positive with respect to the cathode can be increased as required, this interval corres-

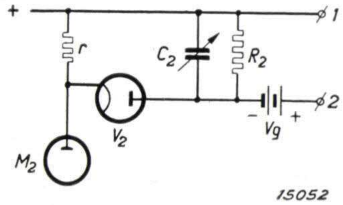

Fig. 7. Time-delay circuit (simplified) (cf. "B" in fig. 2). This circuit which is made up of a variable condenser C_2, a resistance R_2 and a valve V_2, serves for prolonging the interval during which welding current is flowing.

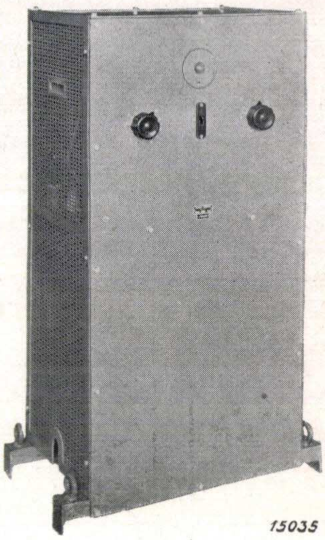
15035

Fig. 8. Front view of apparatus. On the left is the knob for controlling the "on + off" cycle (x+y) which is variable between 1 and 75 periods of the 50-cycle current, and on the right the knob for controlling the "on" interval (x); in the middle at the top is a pilot lamp, and below the switch for the auxiliary circuits.

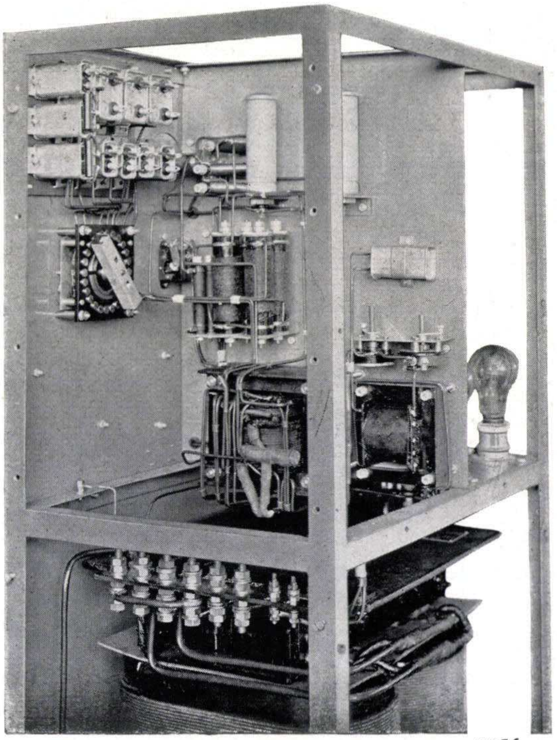
15036

Fig. 9. Interior view of apparatus. Below, the series-transformer (T_2), on the left at the top the condensers and a step switch. The valves are on the right hand side behind the partition.

ponding to the number of cycles x the welding-current flows. The apparatus thus has two control knobs by means of which the capacities of C_1 and C_2 can be varied: With C_2 x is adjusted and with C_1 the whole sequence x+y.

Returning to the complete diagram (fig. 2), which incorporates the individual circuits shown in figs. 3, 5 and 7, it is seen that the batteries in the latter have been replaced by rectifiers (valves V_1 and V_3) which are provided with condensers for smoothing the rectified voltage. The apparatus is protected against the high tension of the transformer T_2 on the one hand by earthing the cathode of M_1, and on the other hand by the fuse F and the the rare gas cartridge G (fig. 2). In the event of a short-circuit between the grid and anode of valve M_1, the cartridge G ignites and blows out the fuse F, thus disconnecting the valve from the rest of the circuit.

An apparatus of the type described here is shown in *figs. 8 and 9*. The controls referred to above are mounted on the front panel. Transformer T_2 is accommodated in the lower part of the housing, and the relay valves M_1 and the auxiliary circuits in the top part. A number of oscillograms of the primary current obtained with this apparatus are reproduced in *fig. 10*; it is seen that there is perfect periodicity in the opening and closing of the circuit in synchronism with the mains supply. These curves also show that a wide variety of settings can be obtained with this apparatus.

The above description brings out the many practical advantages of a relay-valve timing circuit as compared with mechanical devices.

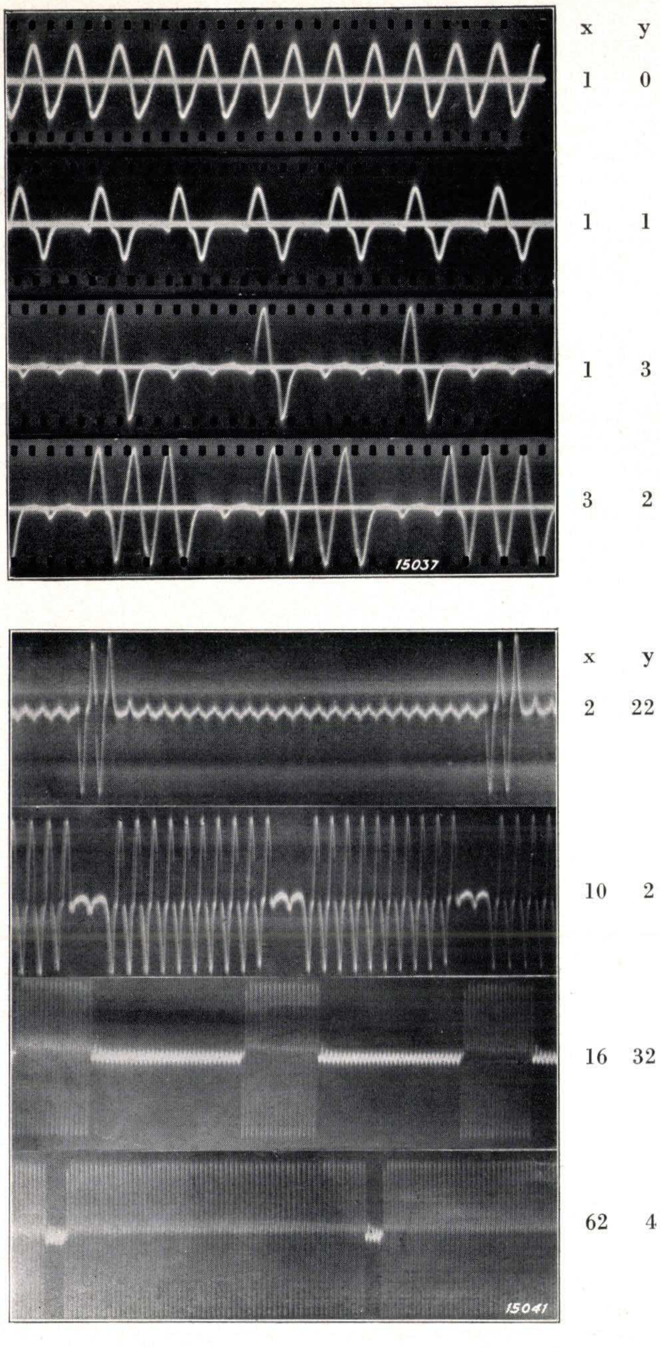

Fig. 10. Oscillograms of the primary current: Circuit closed for x cycles, and opened for y cycles.

AN EXPERIMENTAL TELEVISION TRANSMITTER AND RECEIVER

By J. VAN DER MARK.

Summary. On the occasion of the erection of a television transmitter at the Philips Laboratory, some of the main principles of modern television are discussed. The circuit and components of a modern television transmitter and receiver are described with special reference to the Philips experimental unit.

Principle of Television

The human eye is a very complex and sensitive organ, whose optical mechanism functions briefly as follows: The crystalline lens of the eye produces an image of the field of view on the retina which is made up of a very large number of minute lightsensitive cells. Each of these cells through its own nerve filament communicates to the brain the stimulus it receives from the amount of light falling on it, and from the sum-total of the stimuli received by it the brain builds up the image seen by the eye.

In the human eye Nature has provided us with the basic principles of television fully worked out; also in televising the area of the picture to be transmitted is resolved into a large number of small elements or cells (*fig. 1*). Each of these elements is given a number and the light value of each element is telegraphed to the receiver in sequential order. Exactly as at the transmitter, the picture surface at the receiver is also resolved into elements which are numbered in the same way, and each element is given the light value telegraphed for its particular number. In this way the picture reproduced at the receiver is the same as that transmitted by the sender.

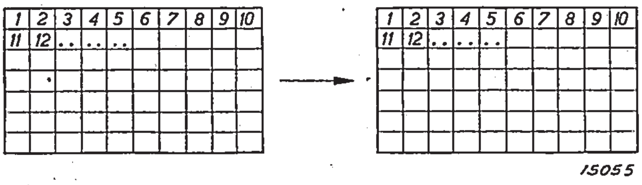

Fig. 1. Principle of television. The surface of the picture to be televised is resolved into a number of small elements which are numbered in succession. The brightness of each individual element is telegraphed. At the receiver where the picture surface is subdivided into similar elements each element is given the brightness transmitted for its respective number, so that the received picture exactly reproduces the original.

In the eye every element of the picture in the transmitter (cell of retina) has its own conductor (optic nerve filament) to the receiver (brain), and the light values of all elements are telegraphed simultaneously. In television this simultaneity naturally cannot be effected, as only one conductor (a single carrier wave) is available for all picture elements, so that the separate light values must be telegraphed in succession. In consequence television technique is rather complex, as may be exemplified by a simple calculation. To obtain a picture of satisfactory quality, the area of a picture measuring 4×4.8 in. must be resolved into about 40000 elements. In televising moving pictures, it is necessary, as in cinematography, to send a sufficient number of pictures per second, at least 25, in order to produce a connective image on spectator's eye. Thus, only 1/25th of a second is available for the transmission of each picture, in other words each second the light values of $25 \times 40000 = 1{,}000{,}000$ elements of the picture must be telegraphed 1).

Conversion of a Picture into a Modulated Radio Wave. Resolution of the Picture into Elements or Cells

Both at the transmitter and receiver the picture is resolved into a series of elements or cells by "scanning" it with a beam of electrons furnished by a cathode ray tube. The scanning spot at which the electronic beam strikes the surface of the picture describes a path on this surface of the type shown in *fig. 2*. This path is made up of a series of nearly horizontal lines packed close together, the beam passing over these lines in

---

1) This is aptly brought out by the following example: For some years facsimile and picture telegraphy has enabled pictures to be transmitted by telegraphy, the transmission of a single picture taking from 10 to 20 seconds or even longer. In the Melbourne Air Race in October, 1934, a film was made of the arrival of the winners at Melbourne and was transmitted to London. This short film, which was on exhibition at London cinemas on the same day already, took a $^3/_4$ minute to project, while the time of transmission from Australia was about 6 hours. In television the same transmission must be completed in a $^3/_4$ minute.

succession. When the beam reaches the end of one line, it jumps to the beginning of the next line, scans it in exactly the same way and so on over the whole picture, until it arrives at the end of the last line. Then it flies back to the beginning of the first line and goes through the same sequence of operations again. During scanning, the scanning beam measures the brightness of each element of the picture as described in the next section. The beam is guided along its scanning path by two voltages which deflect the beam to varying degrees simultaneously, each voltage fluctuating with a saw-tooth voltage-time diagram as shown in *fig. 3*. The slow voltage controls the scanning motion in the vertical direction with a frequency equal to the number of pictures per second, while the fast voltage controls the motion in the horizontal direction with a frequency equal to the product of the number of pictures per second and the number of lines in the picture.

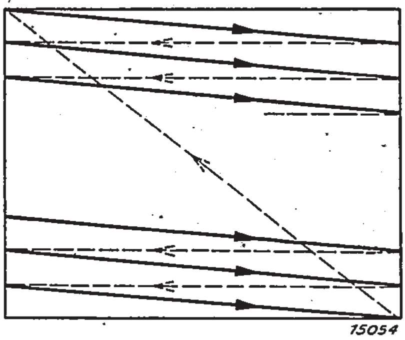

Fig. 2. The numbering in fig. 1 is replaced by "scanning" the picture in a definite sequence. The path of the scanning spot shown here determines the order in which the various elements are telegraphed.

In order to reassemble the picture at the receiver from the elements in the same manner, as it was resolved at the transmitter, the electron beam in the cathode ray tube of the receiver must at every moment occupy exactly the same position relative to the picture as the electron beam of the transmitter, i.e. the scanning sequence in the receiver and transmitter must be completely synchronised. This is realised by means of two distinct types of synchronising signals which are radiated from the transmitter at the end of every line and each picture respectively. We shall return to this point later.

The modulation of the light value when scanning a horizontal line may be regarded as equivalent to a resolution into a definite number of elements. If the picture is a square and has the same sharpness both horizontally and vertically, the number of these elements must be equal to the number of lines N in the whole picture. Usually rectangular pictures with sides in a ratio of 6:5 are televised[2]. The total number of elements in the picture is then 1.2 N^2. The number of picture elements to be transmitted per second, which determines the maximum modulating frequency of the radio wave required for televising the picture, is then 30 N^2 with a picture frequency of 25. In this way very high frequencies are soon reached. Since an alternating current of p cycles per second already corresponds to 2p alternations per second of light and dark, the required modulating frequency can be halved, so that with 180 lines the maximum modulating frequency is 500,000 cycles and with 450 lines 3,000,000 cycles.

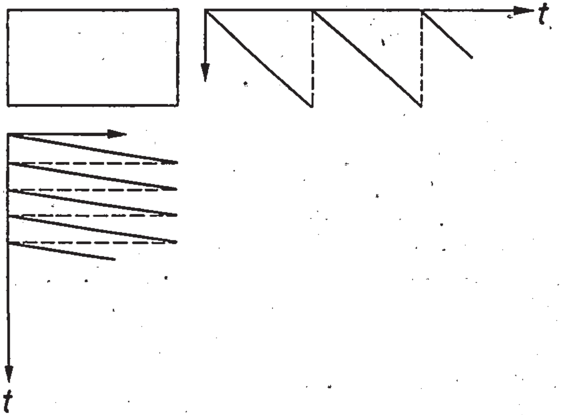

Fig. 3. Composition of the two motions of the scanning beam. A deflecting voltage with a saw-tooth time diagram controls motion along each line (left), while a similar voltage (right) N times slower (N being the number of lines in the picture) controls the beam motion in such a way that it does not incessantly scan the same line but passes along the N lines in succession and then flies back to its starting point again.

As already stated, television signals are transmitted in the same way as microphone signals in broadcasting by modulation of a carrier wave whose frequency must be considerably higher than the modulating frequency. For televising it is therefore necessary to use a carrier wave in the ultra short-wave range between 7 and 5 metres.

This very short wave, however, has a particular drawback. Contrary to broadcasting waves of several 100 m in length these waves do not propagate along the curved surface of the earth. They can therefore only be received within a radius which barely exceeds the distance at which the transmitting aerial is still in sight of the receiving aerial[3]. To make this area as large as possible, the aerial must be suspended from very high masts. In the case of the transmitter at Eindhoven, the primary aim has not been to obtain a range of reception as large as possible; the aerial has therefore only been made about 150 ft. high and is fixed to a small mast on the roof of one of the works buildings. The Eindhoven transmitter operates on a wave-length of about 7 m and has a maximum output of about 400 watts; it has been designed for a maximum modulating frequency of about 3,000,000 cycles and can therefore televise pictures of the finest screen yet attained.

---

[2] This is the usual size ratio of sound-film pictures.

[3] Recently these waves have been detected for short intervals also at greater distances, but reception has been so patchy that satisfactory transmission to points beyond the visible horizon is quite impracticable.

Conversion of Light Values into Voltages with the Iconoscope

How are the light values, registered by the electron beam on scanning the picture elements, converted into a modulating voltage? The apparatus here used for this purpose, is the iconoscope which was developed by Zworykin. It here fulfils the same function as the human eye in the seeing mechanism.

This apparatus (*fig. 4*) consists of a cathode ray tube, which, in addition to the usual hot cathode, the anode and the deflector system in part K, also has a photo-electric plate P prepared in a special manner mounted in place of the usual fluorescent screen. The picture to be televised is projected on to this plate by means of an ordinary photographic lens. The whole arrangement, comprising the iconoscope with the attached optical system for projecting the picture on the plate P, may be termed a "television camera". Plate P, which may be regarded as the retina in the eye of the transmitter, is made of very thin non-conducting material (cf. fig. 4), which has a uniformily-distributed mosaic of separate cells in the form of drops of metal on the illuminated side. These cells are insulated from each other and have photoelectric surfaces. The number of these cells is so great that several fall within the area covered by the scanning beam. On the back the insulated plate P is covered with a continuous conducting layer, which with the metal cells on the upper surface forms a corresponding number of minute condensers from which current can be taken at the outside.

As soon as the scanning spot strikes a cell, the latter acquires a negative charge from the beam up to a certain maximum value; this means that the associated condenser gets a definite potential. The beam now moves onward and only returns to this cell again after having scanned the whole picture. In the meantime, the photo-electric cell emits photoelectrons under the action of the incident light and thus looses a part of its charge, this diminution being proportional to the light value of the picture at the respective point. When the scanning spot again reaches the cell, the latter's depleted stock of electrons is immediately replenished until the same maximum charge is restored as it possessed at the outset. At the instant this occurs, a charging current proportional to the brightness of the picture at this particular point flows from the outside to the condenser. A potential is hence produced at the resistance R (fig. 4) in the external circuit of the iconoscope which at each instant is proportional to the light value of the various picture elements in the sequence they are scanned. This potential is now amplified and serves for modulating the radiated carrier wave.

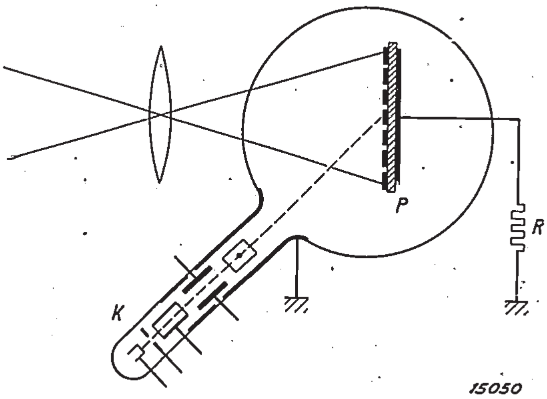

Fig. 4. The iconoscope. In a cathode ray tube which contains the usual components in part K (hot cathode, anode and deflection systems), the fluorescent screen is replaced by a photo-electric plate P (the "retina") prepared in a special way, on to which the picture to be televised is projected.

The great advantage of the iconoscope as compared with other systems, such as for instance Nipkow's disc, is its high sensitivity: while in other cases the brightness of each picture element must be measured in the extremely short period the scanning spot is in contact with the element, in the iconoscope the light at each such point can act as a stimulus during the far longer period between successive scanning moments and the effect produced is stored as an electric charge in the individual condensers. Only by means of this enormous gain in sensitivity is it at all possible to televise ordinary daylight scenes without spotlights, etc.

Films are transmitted by a somewhat different process, as here a sufficient interval must be provided to allow for the motion of the film. To enable the television camera designed for out-door scenes to be used without alteration also for films, the film is only illuminated during the period of the synchronising impulse at the end of each picture

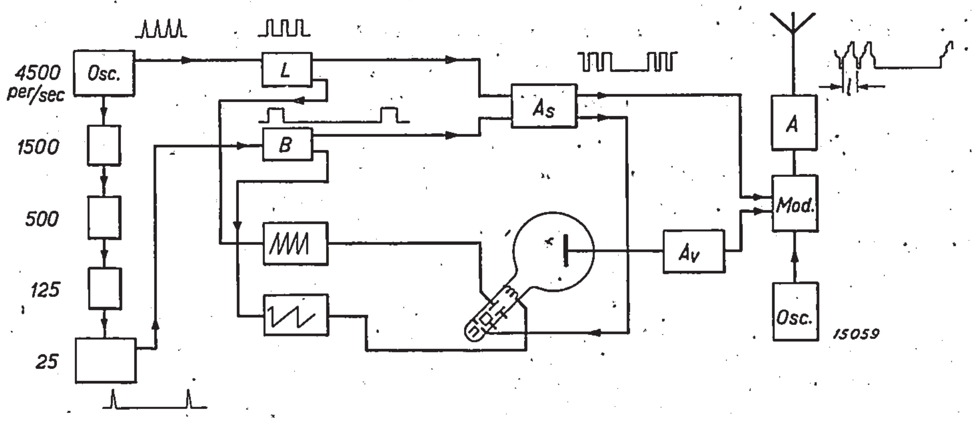

Fig. 5. Circuit diagram of television transmitter (simplified). In the top left hand corner is the oscillator which generates the line impulses of 25 × 180 = 4500 cycles (with 450 lines in the picture this value would be 25 × 450 = 11250 cycles). In the stages immediately below, this frequency is demultiplied until the picture frequency of 25 per second is reached. From these two types of impulses the line and picture synchronising signals (rectangular voltage wave-form) are generated in circuits L and B respectively. These have firstly to synchronise the two relaxation voltage units which control the movement of the iconoscope scanning beam, and secondly they are amplified in As and used for modulating the carrier wave generated by the oscillator in the bottom right hand corner. The voltage fluctuations furnished by the iconoscope are amplified in the video-frequency amplifier Av and also modulated on the carrier wave. A is the last amplifier for the modulated carrier wave.

scanning cycle. As the film also can be illuminated with a greater light intensity according to requirements, the short period of illumination is not a drawback. For the same reason, however, the iconoscope offers no pronounced advantage in this case.

The Transmitter. Synchronising Signals

We shall now briefly review the circuit and components of the television transmitter. In the first place the voltages for the synchronous control of the scanning beams must be generated.

An oscillator (in the left hand top corner of the diagram in *fig.* 5) generates relaxation oscillations of line-frequency, i.e. 25 N (thus with N = 180, a frequency of 4500 cycles). This frequency is demultiplied in successive stages until the picture frequency of about 25 cycles is obtained. Frequency demultiplication is very simple with relaxation oscillations 4).

The line and picture impulses 5) generated do not yet possess the voltage wave-form required for the synchronising signals, but these signals can be obtained quite simply from them, exactly as they have to be modulated on the radiated carrier wave: These signals are right-angled voltage impulses of specific duration. The duration of the signal for each line is about 5 per cent of the time required for scanning a line; the synchronising signal for each picture is equal to the scanning time of several lines. As a result a width of several lines is lost at the bottom of the picture; but even if hence say only 170 lines are contained in the visible picture instead of 180, we must still take N = 180 when calculating the line frequency.

Control of Scanning Beam

Each of the two synchronising signals controls one of the relaxation voltage units, which together provide the components for controlling the motion of the scanning beam as already shown in fig. 3. Each voltage unit consists essentially of a condenser which is charged by a constant current (thus giving a potential which increases linearly with the time), and a discharge tube which is ignited by the corresponding synchronising signal so that the condenser is discharged (the potential rapidly drops to zero). The potential generated is applied to the deflecting system of the cathode ray tube and causes the scanning beam to move to and fro in the manner required.

While with Nipkow's disc, the number of lines in the picture is invariable, as it is equal to the number of perforations in the disc, it is comparatively simple with the iconoscope to adapt a transmitter for televising different numbers of

---

4) The properties of relaxation oscillations, particularly for frequency demultiplication, have for some years been the subject of close investigation in this laboratory. Cf.e.g. B. van der Pol, Phil. Mag. **2**, 978, 1926, and B. van der Pol and J. van der Mark, Nature **120**, 363, 1927.

5) In televising films, the frequencies of the line and picture impulses generated must also be in a fixed ratio to the frequency of the local mains supply, as in film projection a mains-fed synchronous motor is usually employed. The picture synchronising signal (period of illumination) must always coincide with the moment the film is stationary. This supplementary synchronising with the mains will not be further discussed here.

lines per picture. To do this it is only necessary to alter the velocity of the component motions of the scanning beam by adjusting the relaxation voltage units and the synchronising signals. It is proposed to modify the transmitter, which is now under test, on these lines at some later date and to carry out experiments with the various systems of transmission.

In the iconoscope the photo-electric plate (the picture surface) is at an angle to the scanning beam, so that the picture can be projected vertically on it (see fig. 4). This requires certain additional corrections in the relaxation voltages generated in order to scan properly the picture with the electron beam.

Amplification of the Modulated Voltage

The small voltage fluctuations furnished by the iconoscope must be amplified before they can be modulated on the radiated carrier wave. The "video-frequency" amplifier provided for this purpose (A_V in fig. 5) has to perform a far more difficult task here than the "audio-frequency" amplifier commonly used for sound reproduction in broadcasting. For while in television the voltage wave-form at the receiver must be exactly similar to that at the transmitter, in broadcasting if we regard the modulating voltage as resolved into all its component frequencies (its Fourier spectrum) the various frequencies are permitted to reach the loudspeaker with a larger or a smaller phase displacement: in music we are unable to detect differences in phase. In television, however, a phase displacement of the component frequencies would completely destroy the original voltage wave-form and fluff the picture received. It follows therefore that the transit times of each frequency through the amplifier must be equal within certain limits. The frequencies in question here cover a spread from a few cycles to more than 3000000 cycles, as already calculated above. Again in this respect there is a radical difference to ordinary radio amplifiers, as in broadcasting the highest modulating frequencies do not exceed 5000 cycles.

By using various special circuits it has been possible to construct amplifiers which satisfy the above requirements for televising 25 pictures per second and 450 lines per picture. The voltages amplified in this way, together with the synchronising signals amplified separately by A_S in fig. 5, are now used for modulating the carrier wave. The radiated signal is of the form shown in the right hand top corner of fig. 5, where l corresponds to a line in the picture.

In addition to the components already mentioned the transmitter is also equipped with a number of auxiliary units, such as oscillographs to control the relaxation voltages, and for further control of the modulated voltages a receiver in which the radiated picture is reassembled. Sound is radiated by a separate apparatus on an adjoining wave length, which facilitates tuning of the receiver. Reference to these points must be dispensed with here.

The receiver

In the receiver (circuit shown in *fig. 6*) a picture has to be reassembled from the incoming signals. This is done in a cathode ray tube B of which a modified form has already been met with in the television camera. The tube in the receiver is, however, of the standard form as employed in cathode ray oscillographs, i.e. with a fluorescent screen F on which the electron beam inscribes the image in the usual way. This beam is again controlled by two relaxation voltage units in the same way as in the transmitter, so that the light spot on the screen describes a path as shown in fig. 2. At the same time the intensity of fluorescence is varied by modulating the intensity of the scanning beam by means of a control grid which functions in exactly the same way as the grid in a radio valve. The incoming picture signals are applied to the control grid, so that the brightness of the fluorescent spot fluctuates with the variations in light value registered on the original picture by the scanning beam of the transmitter. In this way the same picture as transmitted is reproduced on the fluorescent screen ⁶).

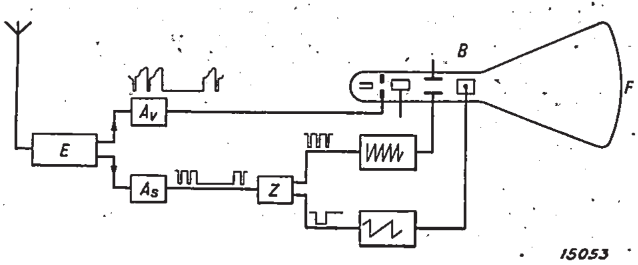

Fig. 6. Circuit diagram for television receiver. The television signals received and rectified at the receiver E are amplified in the video-frequency amplifier A_V and applied to the control grid of the cathode ray tube B, after the synchronising signals have been filtered out in A_S by means of their particular amplitude. In the two filter circuits Z the (short) line and the (long) picture synchronising signals are separated from each other and passed to the respective relaxation voltage units which control the motion of the scanning beam. The picture is produced on the fluorescent screen F.

The received signals are amplified by a video-

---

⁶) The cathode ray tube will shortly be the subject of further separate articles in this journal.

frequency amplifier (A_V) similar to that used in the transmitter. They also include the synchronising signals which here have to maintain the displacements of the scanning beams of the receiver and transmitter in perfect synchronism. These signals have been modulated on the carrier wave in a certain manner, so that they can be separated from the picture modulation by an amplifier (A_S) responding to specific amplitudes only. Exactly as in the transmitter, the saw-tooth motion of the receiver scanning beam (fig. 3) is obtained by means of oscillating circuits, which generate the requisite type of relaxation oscillations having a frequency which in unconstrained vibration is already close to the required frequency and which is corrected to obtain the right rhythm by the synchronising signals which come in at regular intervals. By using two filter circuits (Z), of which one responds to only short potential impulses and the other to only long impulses, the (short) line-synchronising signals can be separated from the (long) picture-synchronising signals and passed separately to the corresponding relaxation voltage units.

Receivers constructed on these principles were evolved some time ago in this laboratory and have operated with complete satisfaction. *Fig. 7* reproduces two photographs of televised pictures (180 lines) which show the quality of reproduction already here attained.

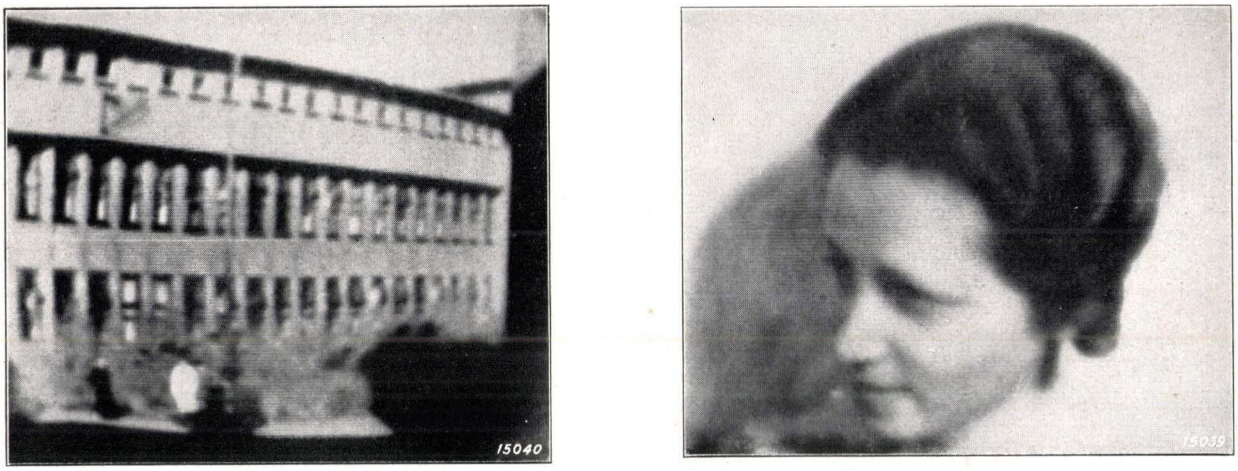

Fig. 7. Two television pictures (180 lines) produced with the new television plant at this laboratory.

a) An out-door scene (without artificial lighting).

b) A studio-portrait.

THE LOUDSPEAKER AND SOUND-AMPLIFYING INSTALLATION ON THE T.S.S. "NORMANDIE"

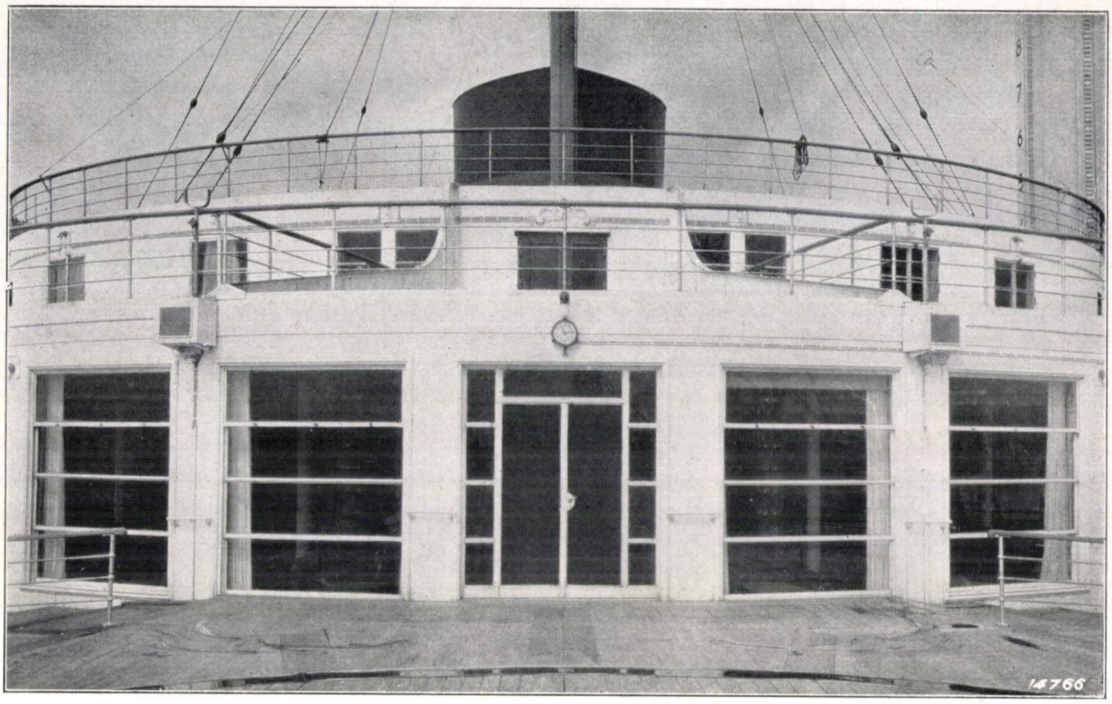

Fig. 1. Watertight loudspeakers on the fore-deck.

With the steady perfection in the efficiency of microphones, amplifiers and loudspeakers in recent years, sound-amplifying installations have come more and more into favour for the transmission of speech and music and their amplified reproduction without loss of naturalness.

Installations of this type have recently also been carried out in ships. For the TSS. "Normandie", Philips has evolved and constructed a very comprehensive loudspeaker and sound-amplifying installation, a description of which will give some idea of what has already been achieved in this direction.

Seventy-four loudspeakers are distributed throughout the vessel. These are of watertight construction where necessary (*fig. 1*), being protected against sea-water and rain by the addition of weatherboards which in no way affect the radiation of sound.

In the passenger saloons the loudspeakers are installed as inconspicuously as possible; in fact in the 1st Class saloon it is almost impossible to detect that the gilt rosette over the escutcheon at the entrance hides a loudspeaker horn (*fig. 2*). In the 1st Class smoking saloon, the loudspeakers are fixed behind a lamp over the upright wall fittings (*fig. 3*); in the winter garden the loudspeaker is recessed in the wall under the clock (*fig. 4*), while in the dining room the speakers are hidden from sight in the ceiling panels. At all points where "acoustic reaction" is likely to cause interference (i.e. the sound radiated from a loudspeaker can again be picked up by the transmitting microphone) when broadcasting speeches and addresses, etc., the particular loudspeakers likely to cause trouble can be switched off.

The loudspeaker installation on the TSS. "Normandie" is designed for the following purposes:

Transmission of musical programmes by the ship's orchestra.
Transmission of gramophone records, e.g. organ music for religious services in the chapel.
Transmission of speeches and news.
Transmission of radio programmes.
Transmission of religious services in the chapel to other parts of the ship.
Transmission of orders from the bridge to the passenger decks in the event of accident or danger.

For the transmission of music and speech, microphones are installed in the chapel, the 1st Class dining saloon, the large 1st Class saloon, the theatre, in the grill room and on the bridge. The bridge microphone has precedence over all other microphones, the captain being always in a position to address every one of the 2000 passengers from the bridge. Oral communications regarding landing arrangements, explanations of delays, notices of festivities, etc., can now be transmitted to all passengers from the bridge much quicker than by the method employed hitherto of posting up notices at various points in the vessel. Loudspeakers are also provided on the boat deck, so that orders and instructions can similarly be issued during boat drill.

Should the space available in the chapel be insufficient to accomodate the whole of the congregation, arrangements can be made for the Tourist Class passengers to remain in their saloon and receive the service through the medium of the loudspeakers installed there. These speakers are connected to the microphone in the chapel through one of the amplifiers.

The theatre which has 400 seats is not large enough to accommodate all the First Class passengers, but with the aid of the loudspeaker installation it is possible to transmit theatrical productions, musical recitals and other stage productions to all those passengers unprovided with seats.

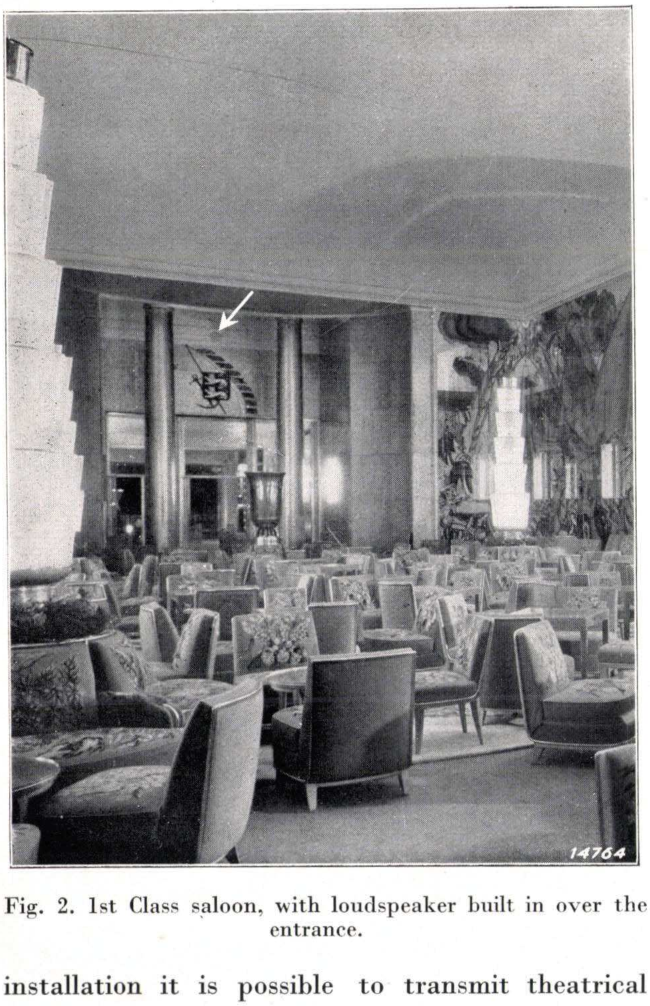

Fig. 2. 1st Class saloon, with loudspeaker built in over the entrance.

The ship's orchestra plays alternatively in the dining room and in the grill room, both of which are provided with microphones; the grill room can moreover be converted for dancing. For the reproduction and transmission of gramophone records, a playing desk with two turntables in a cardan suspension is provided so that the records remain perfectly horizontal also during the rolling of the vessel.

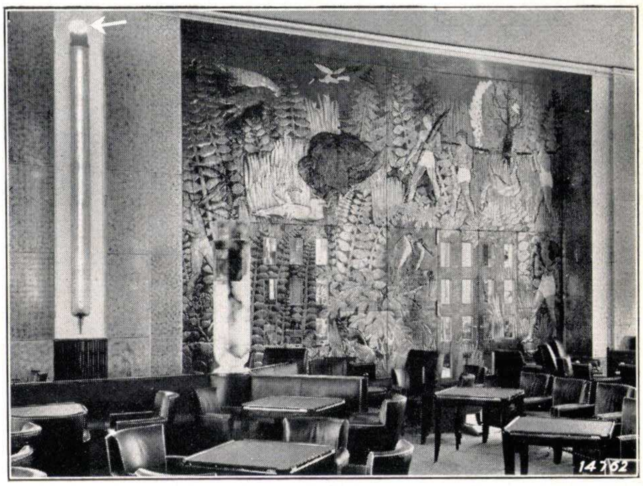

Fig. 3. 1st Class smoking saloon, with loudspeakers built in over the entrance.

To ensure maximum reliability and continuity in the functioning of the whole equipment, all essential components, such as the amplifiers and the 3-kw D.C.-A.C. converters, have been duplicated. In addition to the two principal amplifiers, each of 350 watts output (the output can be reduced to 175 watts by cutting out two of the four last-stage valves), two smaller amplifiers, each of 20 watts, are also provided.

The 74 loudspeakers of 6, 10 and 20 watts are rated for 680 watts at full load. As a rule the loudspeakers will not be run all at the same time or all at their maximum power (the volume of each loudspeaker can be adjusted independently); a reduced amplifier output, e.g. 350 watts + 175 watts or 350 watts, will then prove sufficient to feed all speakers in operation. One of the 20-watt amplifiers is sufficient for transmitting a service in the chapel to one of the Tourist Class or Third Class saloons. By means of a switchboard in the amplifier room (see *fig.* 5), the 40 loudspeaker circuits terminating at the board can be connected to the 4 amplifiers (fig. 5, b, d and e) in various ways as required.

A simplified circuit diagram of the installation on the TSS. "Normandie" is shown in *fig. 6.*

All amplifiers have a maximum output voltage of 100 volts at normal full load. The cone coils of the electrodynamic loudspeakers must be built for a much lower voltage, and these are therefore provided with transformers to enable them to be connected to the standard 100-volts supply.

Owing to the comparatively high voltage and hence the low current intensity in the circuits, the voltage losses remain within reasonable limits in spite of the great length of the many conductors required on this large vessel. A still higher voltage has not been chosen on account of the risk of accidents and because the capacity of the extensive cable system might then adversely affect the quality of reproduction.

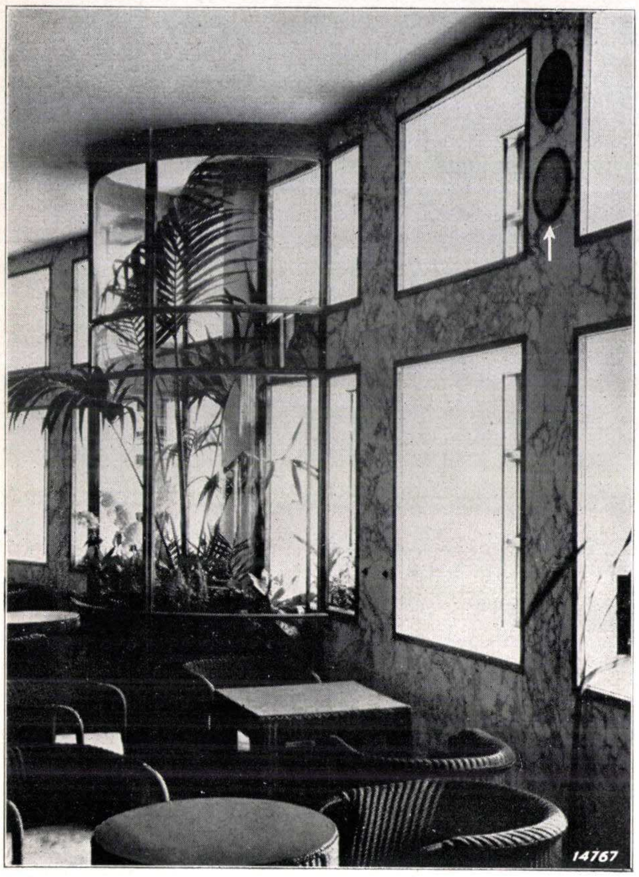

Fig. 4. Wintergarden with loudspeaker built in under the clock.

When connecting one or more loudspeakers to an amplifier, it is necessary to take as a basis the principle that the rated consumption of the loudspeakers is equal to the rated output of the amplifier; furthermore, the total impedance of all loudspeakers must be such that they can actually take the output of the amplifier. To arrive at this adaptation, a number of tappings on the secondary winding of the output transformer may be useful. As commercial types of loudspeakers have very different impedance values, it may be very difficult or even impossible in some circumstances to obtain the required total impedance by merely connecting the loudspeakers in series or parallel. Frequently a number of loudspeakers are connected in series in order to avoid excessive current intensities and voltage losses. In power current practice complicated circuits of this type have long been abandoned, and it is now the practice to provide a constant voltage supply to which only apparatus rated for this specific supply voltage are connected in parallel.

This method has also been adopted by Philips for sound-amplifying installations. The amplifiers at complete modulation (i.e. at the highest possible voltage of the signal to be amplified) and on full load furnish an output of 100 volts. As already pointed out above, the loudspeakers are provided with transformers with ratios of transformation such that on connection to a 100-volt input the power absorbed is equal to that rated power for which the loudspeakers are built.

Thus it is unnecessary to sum the reciprocal values of the loudspeaker impedances, which constitute the load, in order to obtain the total impedance determining the correct adaptation. The problem of correct adaptation is now easier to deal with. For if the total rated consumption of the loudspeakers, which individually may have very different consumption ratings, is made equal to the rated output of the amplifier, one is assured that the amplifier will really give this output.

If the rated output of the amplifier is slightly exceeded by the rated consumption of the loudspeakers, this will not cause any appreciable reduction in the output of the amplifier. Heavy overloading of the amplifier is however undesirable, since inter alia the voltage drop resulting therefrom is frequently accompanied by an increase

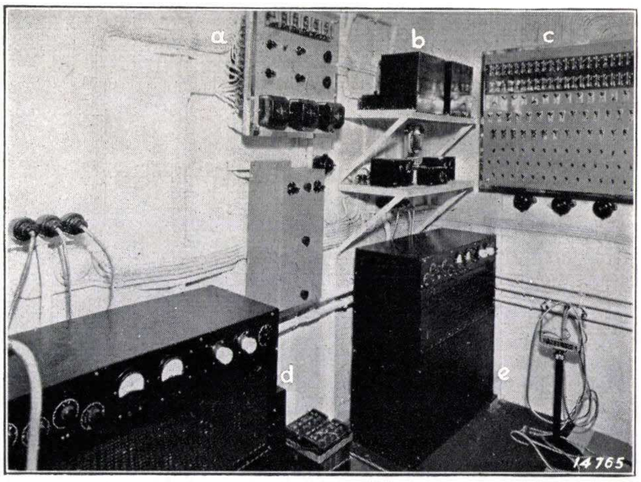

Fig. 5. Amplifier room.

a) Switchboard for the microphone circuits
b) Two 20-W amplifiers with impedance matching boxes below
c) Switchboard for the loudspeaker circuits
d) and e) Two 350 W amplifiers.

in the current intensity, which in the long run may e.g. damage the end-stage valves. On the other hand, there is no objection to a subnormal load, as long as the voltage does not rise too much that the loudspeakers become overloaded.

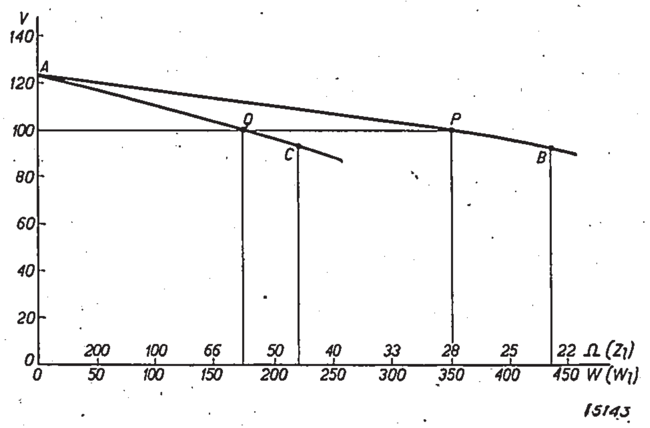

Fig. 7. Voltage curves of the amplifier as a function of the rated power consumption of the connected loudspeakers. The line A-B is for the 350-W amplifier at full output, and A-C for the same amplifier when set for supply of half the power.

In installations of this type where a fluctuating load has to be dealt with, the output voltage must not be too closely dependent on the load. This requirement is met by the Philips 350-watt amplifier as may be seen from *fig.* 7 where the voltage is plotted against the power consumption of the connected loudspeakers. On no-load the voltage does not exceed 123 volts, which can do no harm to the Philips loudspeakers. In practice it is very unlikely that one loudspeaker only will be connected to the 350-watt amplifier; besides, the overload of the loudspeaker implied in this case will be audible only at the loudest passages of the music.

The permissible maximum load on the amplifier is shown in fig. 7 by the points B and C respectively.

Compiled by N. A. HALBERTSMA.

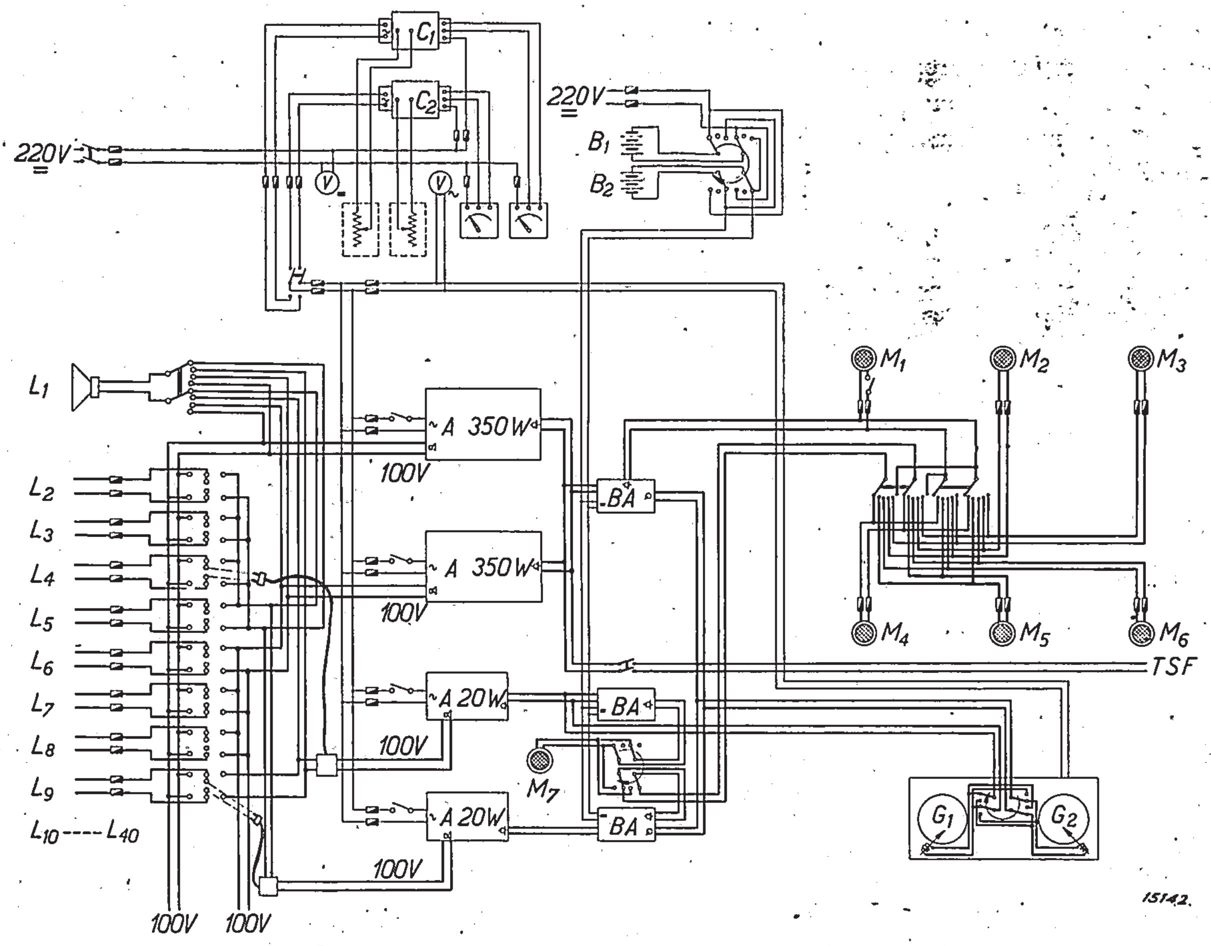

Fig. 6. Simplified circuit diagram of the sound-amplifying installation.

A	Amplifiers
BA	Impedance matching boxes
B	Microphone batteries
C	Convertors
G	Turntables
L	Loudspeaker or loudspeakergroup
M	Microphones
V	Voltmeters

HOW DOES A WELDING ELECTRODE FUSE?

By J. SACK.

If an arc-welder is asked what he thinks of two particular welding electrodes, he will usually answer that one welds better than the other. The ease or difficulty of welding is closely associated with the conditions of fusion at the end of the electrode. In this article it is not intended to give a complete explanation of the conditions of fusion of an electrode, since many aspects of the problem are still obscure and form the subject of current research. Reference here will be limited to a few of the more common methods of investigation now being employed for studying this problem.

The fusion of a welding electrode cannot be followed in detail with unprotected eyes merely screened against glare by coloured glasses; in fact the formation of drops of metal is only just distinguishable with electrodes which melt slowly and form large drops. The drops are seen to grow, and at the moment of coming into contact with the molten metal in the pool, they become detached from the electrode and merge into the pool. The currents of gas and vapour at the arc and their dazzling light are very troublesome when observations are made with the naked eye.

Observation is facilitated by projecting an enlarged image of the arc on to a projection screen, a method used by Creedy[1]) in his investigations on the influence of the electromagnetic forces on drop formation. It has been found that by a considerable reduction in the welding current, the rate of drop-formation can be decreased so much that the process can be followed on the screen. On the other hand, the fusion process at these low current intensities of, say, 5 amps, differs fundamentally from that obtained at normal currents, e.g. 150 amps. In the former case the drops detach themselves from the electrode in the same way as water drips from a tap, while in the latter case the drops disappear very suddenly with a more or less loud click. This observation was made in investigations with bare electrodes.

The registration of welding conditions on a photographic film, and in particular by means of a slow-motion cine-camera, has constituted a marked advance in these investigations. If an ordinary type of film is used, the interesting part of the process, i.e. the formation and separation of the metal drops is completely masked by the arc. The Chicago Steel and Wire Co[2]) has therefore made use of a special infrared sensitive film and a filter only permitting the passage of infrared (thermal) radiation. These rays are mainly emanating from the glowing metal and the incandescent gases and are able to penetrate through the cloud of vapour surrounding the arc. Pictures were taken at the rate of 60 exposures per second, which on projecting at the rate of 20 pictures per second gave a threefold slowing-down of the actual process. This method for the first time revealed photographically the transfer of material during welding and was applied to all types of bare and coated electrodes. In particular the influence of the chemical composition and the physical properties of the core and coating was studied.

A short time later Hilpert[3]) in Germany also made film records of the welding arc. His apparatus constructed by Thun took 800 pictures per second and thus gave a 40-fold expansion of the actual time of welding. Precautions to cut out the intense glare were, however, omitted, with the result that the light rays from the arc strongly predominated and the drop-transfer could hardly be followed. Nevertheless these records have been useful. They showed that even with a 40-fold retardation, the arc still moved to and fro very quickly. The number of pictures per second was therefore further increased to a maximum of 4000, and the arc and the ambient region no longer registered by means of the intrinsic light but as a silhouette obtained with a more powerful source of light. With these modifications the transfer of material with bare electrodes was studied. In addition to photographic registration, the welding current, the welding voltage and as a time standard an A.C. voltage of 50 cycles were also recorded by means of an oscillograph. In films made at the rate of about 1600 to 2400 pictures per second, corresponding to a slowing down of 80 to 120 times, two types of drop transfer were observed, viz.,

---

[1]) F. Creedy, R. O. Lerch, P. W. Seal, E. P. Sordon: Forces of electric origin in the iron arc. (Abstract A.I.E.E. Paper Nr. 32—41). Electrical Engineering **51**, 49, 1932.

[2]) Cf. K. Bung: Der Werkstoffübergang im elektrischen Schweisslichtbogen. Zeitschrift des V.D.I. **72**, 750, 1928.

[3]) A. Hilpert: Werkstoffübergang im Schweisslichtbogen. Zeitschrift des V.D.I. **73**, 798, 1929.

1. a thread-shaped transfer, which may be compared to a narrow stream of metal being poured from the molten end of the electrode on to the piece of work, and
2. a mushroom-shaped transfer where a very thick drop of irregular shape moves to and fro and seems to be reluctant to combine with the piece of work.

The French investigator L. Bull[4]), also took cinematograph pictures of silhouettes of the welding arc. Using heavily-coated electrodes and taking 60 to 80 pictures per second, he observed the rapid transfer of spherical drops without any short-circuit occurring, such as was usually observed with bare and thinly-coated electrodes. These pictures were taken with solar rays, a heliostat being employed to direct a powerful ray of sunlight on to the object being photographed.

From these methods of direct observation of the welding process, we shall turn to the indirect methods which have been devised for the same purpose. First of all the method mentioned above of registrating the welding current and voltage as a function of the time by means of the oscillograph should be considered. A short-circuit on drop-transfer is indicated in the oscillogram as a voltage drop to nearly zero and an increase of the current to the short-circuit value. We are primarily interested in the instant the short-circuit occurs and how long this condition lasts. This information is not only of value as regards the behaviour of the electrodes, but principally as an indication of the efficiency of the welding aggregate as a whole. To this end oscillograms have been employed to determine the intensity of the current-impulses and the speed of adaptation of the welding set to variations of arc length.

As already mentioned the oscillograms show that in general two periods have to be distinguished viz.,

1. the arc-period B, during which the arc burns, and
2. the short-circuit-period K.

If the total time of the drop-period is T, (i.e. $T = B + K$), it will be interesting to know the ratio $B:T$ or $K:T$, either as a fuction of the time or as an average over a certain lapse of time. A circuit where a meter indicates and registers the ratio

---

[4]) Cf. M. Lebrun: La soudure électrique à l'arc et ses applications (1931), p. 39-44.

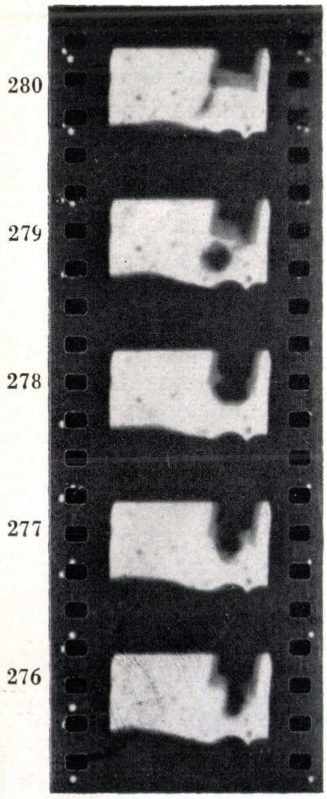

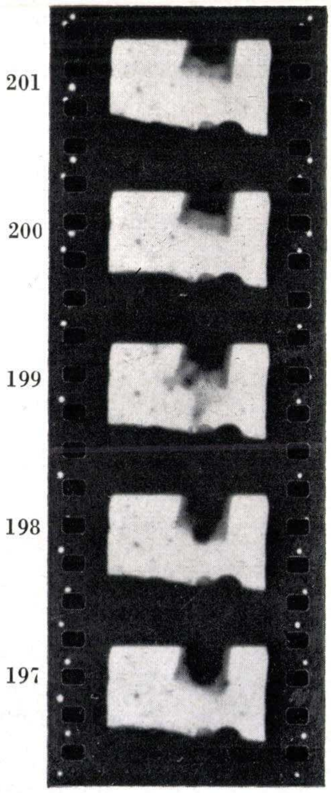

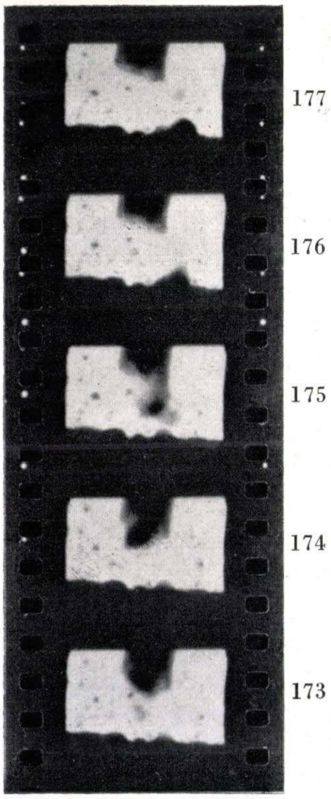

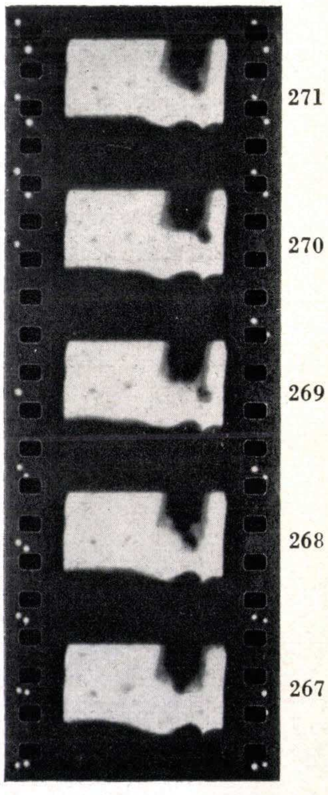

Film exposures recorded by the X-ray cine-camera (cf. p. 29)
The pictures must always be read from bottom to top.

Fig. 1. Drop-transfer. The drop is completely enclosed by coating material.

Fig. 2. The melting point of the metal core and the softening range of the coating must be adapted to each other so that on fusion a sleeve is formed (see fig. 10).

Fig. 3. After contracting (picture 173) an elongated drop (picture 174) is formed which moves to and fro (picture 175) and is eventually transferred to the piece of work (picture 176).

Fig. 4. A metal drop is thrown back to the welding electrode.

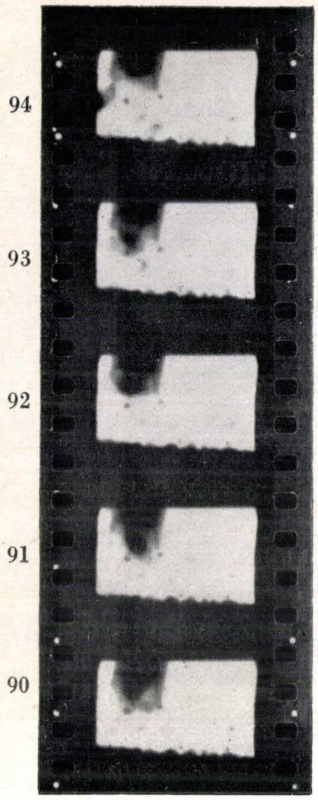

Fig. 5. Gas bubble in the coating (picture 90); 0,02 second later the gas bubble has burst (picture 91). In pictures 92 and 93, the material of the coating appears to "neck" the coating drop.

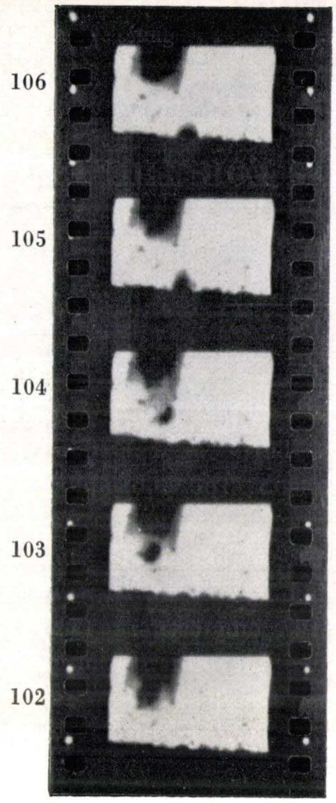

Fig. 6. A coated drop becomes detached from the welding electrode: during its descent the drop explodes (picture 104).

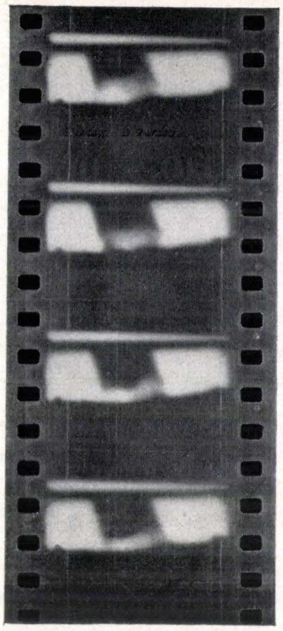

Fig. 7. $12^1/_2$ pictures per second. Over the whole surface of the sleeve the coating fuses into droplets. Core and coating are difficult to distinguish.

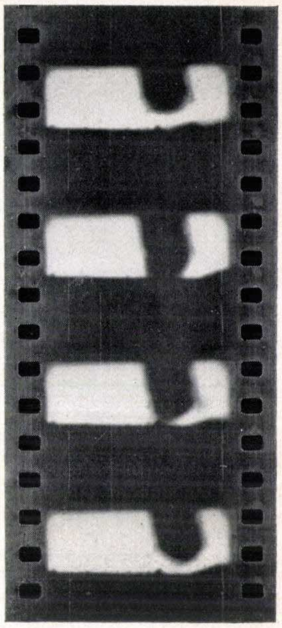

Fig. 8. $12^1/_2$ pictures per second. Thinly-coated electrode. The drop falls and causes a short-circuit. The bulk of the molten metal flows into the welding seam.

B:T was used by Flamm⁵), and afterwards by Bela Ronay⁶), who called his apparatus an "arcronograph". It was found that with heavily-coated electrodes the ratio B:T was nearly equal to unity, in other words that the drops during transfer produce no short-circuit (K:T = 0). This result confirms the film records obtained by Bull.

Finally, reference must also be made to those methods of investigation which cannot be called either direct or indirect methods. We shall group these under the general head of **model experiments**, as a model is made of that part of the welding process which it is desired to study in greater detail.

A typical example of this class is given by the experiments of Flamm⁷), who studied the formation and transfer of drops and the capillary forces accompanying these processes by using oil as a medium. From his observations he drew various conclusions regarding the transfer of material during welding.

The investigations of Doan and his collaborators⁸) also come under this head: they consisted in welding on a continuously-moving band so that successive drops were collected separately. The same applies to the experiments already described at the beginning of this article¹), where the period

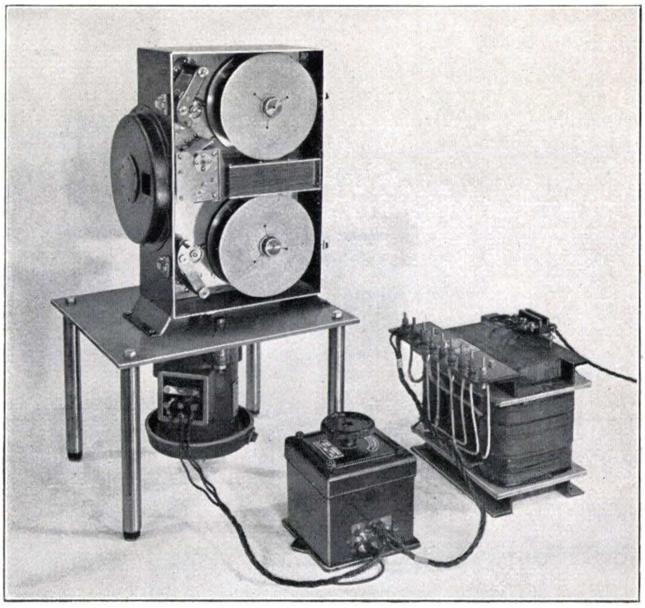

Fig. 9. X-ray cine-camera for taking 50 pictures per second, with cover removed.

---

⁵) P. Flamm: Messmethoden und Messungen bei der elektrischen Lichtbogenschweissung. Die Elektroschweissung **3,** 50, 1932.

⁶) Bela Ronay: Evolution of the Arcronograph. J. Amer. Soc. Nav. Eng. **46,** 285, 1934.

⁷) P. Flamm: Die elektrische Lichtbogenschweissung als Kapillarvorgang. Die Schmelzschweissung **9,** 105 and 162, 1930.

⁸) Gilbert E. Doan and J. Murray Weed: Metal disposition in electric arc welding. Electrical Engineering **51,** 852, 1932.

of drop-formation was extended by employing very small currents, and the experiments of Ronay[6]) in which the electrode was fused against a carbon base.

A method has recently been developed at the Philips Laboratory[9]) to make radiographic film pictures of the transfer of material. The welding process is recorded with X-rays on a special X-ray-sensitive film; if the X-ray tube is run on a suitable voltage it is found that the core and coating of the electrode can be readily distinguished on the radiograph, the method thus being of special value with coated electrodes. But also for bare electrodes the method presents advantages, as the gas and vapour clouds surrounding the arc can be completely penetrated by the X-rays and are hence not reproduced on the film. This enhances the clearness of reproduction.

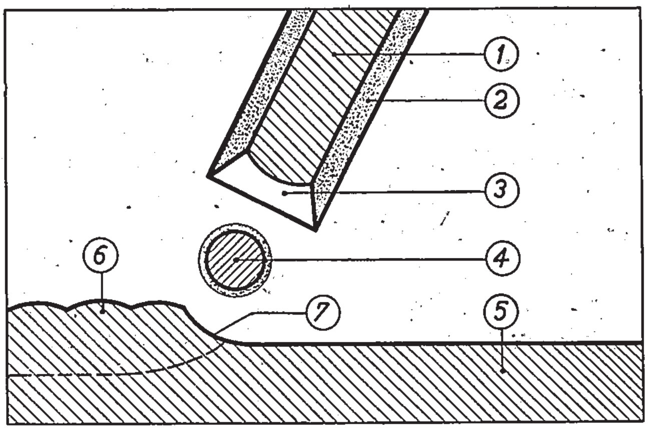

Fig. 10. Diagrammatic sketch of drop transfer from the welding electrode to the workpiece (cross-sectional view): 1 core, 2 coating of the welding electrode, 3 sleeve, 4 drop enclosed by coating material, 5 piece of work, 6 bead, 7 pool.

The first pictures were made with an ordinary amateur cine-camera which was reconstructed for X-ray exposures. With this unit $12^{1}/_{2}$ pictures per second could be taken on an X-ray-sensitive film. Subsequent pictures were made with an X-ray cine-camera (*fig. 9*) specially designed for this purpose and with which 50 pictures per second (slow-motion film) could be obtained. *Fig. 10* gives a schematical representation of the drop-transfer; the reproductions *fig. 1-8* shown above are parts of the film and show various stages during the drop-transfer.

---

[9]) J. Sack: The Iron and Steel Institute. Symposium on the welding of iron and steel, London 1935, Vol. 2, p. 553.

PRACTICAL APPLICATIONS OF X-RAYS FOR THE EXAMINATION OF MATERIALS[1])

I.

By W. G. BURGERS.

Introduction

The successful application of X-rays to the technical examination of materials does not by any means require a fundamental theoretical knowledge of the laws of crystallography and physics, such as is essential for an exhaustive scientific investigation. X-ray methods have therefore become very useful aids for testing materials and enable valuable results to be obtained also in cases where other means of examination do not succeed. In the modern laboratory, in researches concerned with the structure of matter, an apparatus for taking X-ray diffraction patterns is nowadays as indispensable as the microscope.

It is obvious that satisfactory results cannot be expected without suitable apparatus, which comprise a high-tension generator, an X-ray tube and an X-ray camera. During recent years, X-ray diffraction apparatus have been evolved which are no more difficult to manipulate than the ordinary microscope. The adjoining picture (*fig. 1*) shows the apparatus employed in the Philips laboratory for registering diffraction patterns. The base of this apparatus has a diameter of 10 in., the overall height being 2.5 ft. It is run directly off the alternating-current mains.

---

[1]) In this section we propose to discuss applications of the socalled interference method only, in which diffraction of the X-rays takes place at the atoms of the radiographed material. No consideration will be given to the absorption method by which structural flaws and other internal abnormalities of a material can be deduced from differences in the absorption of the rays.

The use of this apparatus is quite simple in the majority of its applications. The actual camera is merely a cylindrical box on the inside wall of which the photographic film is secured by springs (in fig. 1 a camera is seen on either side of the X-ray tube); a diagrammatic sketch of the arrangement is shown in *fig. 2*. In the middle of the camera top is the specimen holder which can be rotated about its axis and at the end of which the specimen P is secured. The material to be examined should be pulverised if possible and a little of the powder (a few tenths of a gram suffice, the small quantity required being in fact one of the main advantages of the X-ray method) placed in a thin-walled glass capillary with a diameter of about 1 mm. The X-rays pass through a small metal tube B (diaphragm) inserted in the cylinder wall of the camera and impinge on the prepared specimen, where they are dispersed and produce a series of characteristic interference lines on the film F.

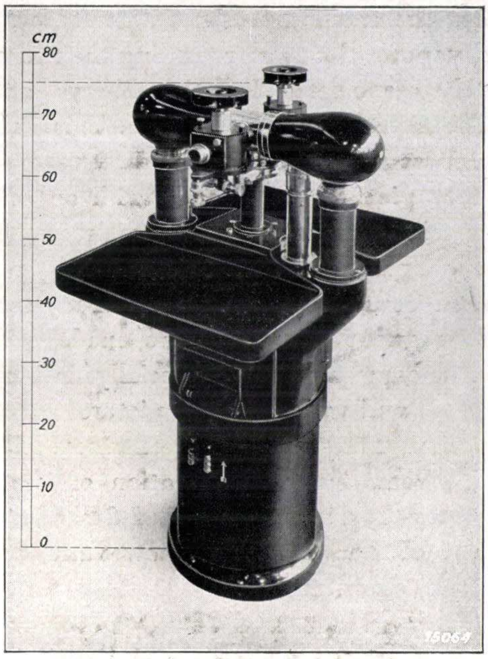

Fig. 1. Apparatus for taking X-ray diffraction patterns.

If the material cannot or must not be pulverised, a different arrangement is used. Thus if the test-pieces are of larger size, they can be secured to the base of the camera with wax so that the X-rays just graze them. Other models of camera with a flat film can also be employed.

With the aid of this handy and portable apparatus it is quite simple to extend the application of X-ray analysis from the laboratory to the work-shop. It is, however, not generally recognised that in practice many cases occur which are particularly suitable for the successful application of this method of analysis, as for instance where definite information is sought on specific points without extensive and complicated investigation. Information of this character can frequently be obtained with surprising simplicity and great accuracy from X-ray diagrams. The diffraction patterns do not require careful measurement nor have complicated theories to be applied; simple inspection is enough, provided a certain amount of experience has been acquired. It is evident that a series of diagrams for a number of commonly occurring materials is very useful for comparison purposes and as a guide in this work.

That up to the present the X-ray diffraction method is applied to practical problems in a limited number of cases only, is probably due to the fact that, on the one hand radiologists have not come in contact with these problems, and, on the other hand investigators employed in the practical testing of materials have not yet fully realised the potentialities of X-rays in their work. Only as a result of a more intense exchange of views and experience will X-ray diffraction methods and apparatus acquire the general application in industrial practice which their practical utility merits.

To contribute to the wider adoption of this method is the purpose of this section, in which we propose to publish periodically examples of applications and results achieved in this laboratory. We shall intentionally limit ourselves to the discussion of problems and cases in which mere inspection of the diffraction patterns is sufficient

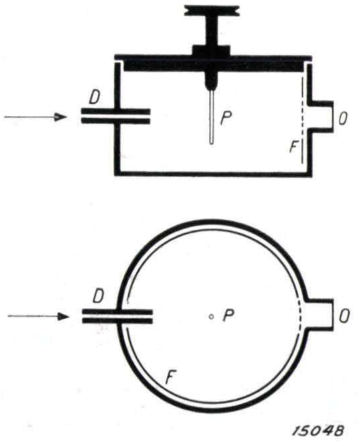

Fig. 2. Camera for obtaining X-ray diffraction patterns. The arrow denotes the entrant direction of the rays emitted by the X-ray tube. D is a diaphragm for producing a narrow pencil of rays, P is the specimen attached to the rotatable holder, F the strip of film clamped to the inner wall. The camera has an aperture at O for the emergence of those X-rays which are not diffracted, in order to prevent disturbing interferences. For the same purpose a hole is cut in the film at this point.

to give the desired result. Problems, whether of a practical nature or not, which necessitate a more fundamental examination will not be embraced in this section.

The examples [2]) to follow will demonstrate the manifold applications of X-ray analysis in practice.

1. Comparison of Porcelains

To determine whether a new porcelain mixture was identical with an existing one, diffraction patterns were obtained for different specimens. *Fig. 3a* reproduces the pattern obtained with the new mixture before firing and fig. 3b the same mixture after firing; fig. 3c shows the pattern obtained with an existing porcelain. The distances between the lines in fig. 3b differ from those in fig. 3a, thus indicating that a structural change has taken place during firing, while on the other hand the exact agreement between the lines in figs. 3b and 3c shows that the fired product is identical with that already known.

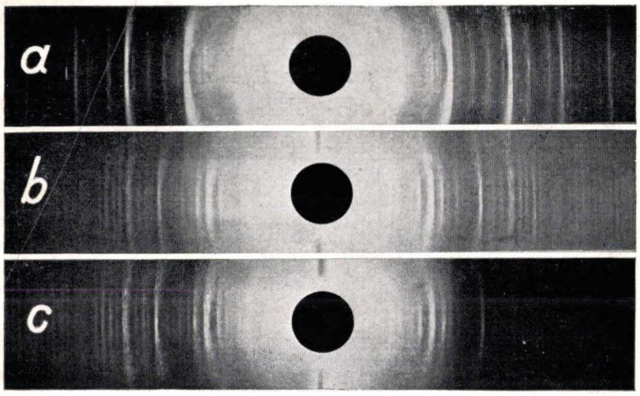

Fig. 3. Comparison of porcelain mixtures.
a) New mixture before firing
b) New mixture after firing
c) Existing porcelain mixture

2. Identification of Surface Film on Steel Balls

Steel balls which had been in rolling contact with brass bushes gradually acquired a dark surface film, which evidently was extremely thin and adhered tenaciously to the steel surface.

It was required to establish the nature of this film without in any way treating the balls either chemically or mechanically. The X-ray patterns for a new steel ball (a) and two balls (b and c) which had been in use for increasing times are reproduced in *fig. 4*; the photographs were obtained by means of radiations just grazing the spherical surface [3]).

While the pattern for an unused ball contains only lines due to α-iron (fig. 4a), another group of lines is seen to become gradually more and more apparent as the period of service increases (fig. 4b and c). Simple comparison with a diagram obtained for copper (fig. 4d) shows that the balls are covered with a thin film of copper.

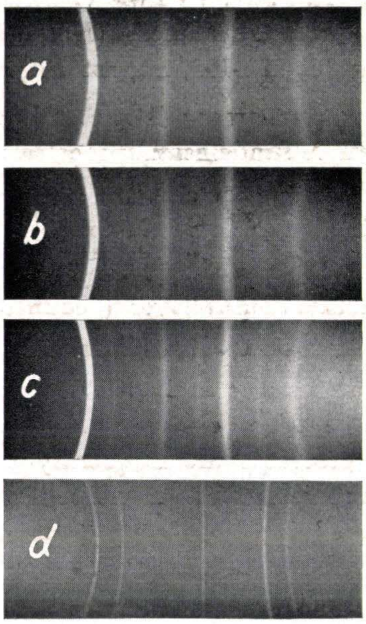

Fig. 4. Identification of a surface film on steel balls.
a) New steel ball before use
b) and c) Steel ball after increasing periods of service
d) Copper

It may also be concluded from the constant distance between the iron lines in all three diagrams, a to c, that the copper film on the balls has not penetrated into the steel with the formation of a solid solution, as otherwise the iron lines would reveal a displacement.

---

[2]) The majority of these investigations were carried out in collaboration with M. F. M. Jacobs.

[3]) The different appearance of fig. 4 and fig. 3 is due to the fact that a different method of registration was used. The essential characteristic is the relative position of the lines.

ABSTRACTS OF RECENT SCIENTIFIC PUBLICATIONS OF THE N.V. PHILIPS' GLOEILAMPENFABRIEKEN

This section will be devoted to a monthly review of the latest scientific papers published by the N.V. Philips' Gloeilampenfabrieken. Reprints of the majority of these papers can be obtained on application to the Administration of the Research Laboratory, Kastanjelaan, Eindhoven, Holland. Those papers of which only a limited number of reprints are available are marked with an asterisk (*).

No. 1030: E. J. W. Verwey, Ionenadsorpton und Austausch (Kolloid-Zeitschrift **72**, 187-192, August 1935).

Adsorption phenomena in electrolytes may be reduced to three fundamental processes:

a. The adsorption of ions which determine the potential of the double layer;

b. The interchange of oppositely-charged mobile ions in the double layer ("counterions");

c. True adsorption of an electrolyte.

It is shown on the basis of ion interchange in the crystal lattice observed by Kolthoff that these processes are frequently inter-related in a complex manner. The mechanism of "adsorption indicators" is also discussed in some detail. The author shows in conclusion that there is a systematic error in precipitation titrations where the equivalence point is taken as the end point. The practical utility of these titration methods is however not adversely affected by this.

No. 1031: M. J. O. Strutt, Anode bend detection (Proc. Institute of Radio Engineers **23**, 945-957, August 1935.)

The anode direct current is as a function of the grid potential expressed as a series which enables the characteristics of certain modern commercial valves to be accurately represented by no more than three terms. The principal advantage of this form of expression is that the rectification gradient and the distortion effects can be calculated exactly from the static valve characteristics. Certain general conclusions are also drawn regarding the rectification of various incoming waves. Results of measurement and calculation are in very good agreement.

No. 1032*: B. van der Pol, Oplossing van potentiaalvergelijking en golfvergelijking in n, n+1, n+2.... dimensies (Handelingen van het XXV Ned. Nat.- en Geneesk. Congres, 1935).

The fact that a small rotation of a potential or wave function gives rise to another potential or wave function can be employed to derive functions for an n+1 dimensional space from functions in n dimensions. Simple derivation and extension of the general solution according to Whittaker.

No. 1033*: C. G. A. von Lindern, Magnetrons (Handelingen van het XXV Ned. Nat.- en Geneesk. Congres, 1935).

With rotating field oscillations described by Nordlohne and Posthumus, the high-frequency radiation energy generated is considerably greater than with the two earlier known types of oscillations of the magnetrons valve. With a wave length of 100 cm both theory and experiment give an efficiency of 65 percent.

No. 1034*: H. Bruining, Secundaire electronenemissie (Handelingen van het XXV Ned. Nat.- en Geneesk. Congres, 1935).

The depths from which secondary electrons are emitted from metal surfaces are investigated and it is found that these electrons are not derived from the upper atomic layer but from those at a greater depth. Electrons which graze a smooth metal surface cause the emission of more secondary electrons from this surface than obtained on vertical incidence, as the secondary elec rons emitted have freer access to the surface.

No. 1035*: W. de Groot, Aard en meting van straling (Handelingen van het XXV Ned. Nat.- en Geneesk. Congres, 1935).

This paper, which was read at a joint meeting of physicists and medical men, deals mainly with the nature and properties of electromagnetic radiations throughout the whole known range of wavelengths. At the end of the paper reference is also made to the latest work on corpuscular radiations.

VOL. 1 No. 2 FEBRUARY 1936

Philips Technical Review

DEALING WITH TECHNICAL PROBLEMS
RELATING TO THE PRODUCTS, PROCESSES AND INVESTIGATIONS OF
N.V. PHILIPS' GLOEILAMPENFABRIEKEN

EDITED BY THE RESEARCH LABORATORY OF N.V. PHILIPS' GLOEILAMPENFABRIEKEN, EINDHOVEN, HOLLAND

THE PRODUCTION OF SHARP FLUORESCENT SPOTS IN CATHODE RAY TUBES

Summary. The problem of producing sharply-defined light spots on a fluorescent screen with the aid of a beam of electrons is studied in this article, use being made as far as practicable of the analogy between light-rays and the cathode rays.

Introduction

During recent years, the cathode ray (or Braun) tube which was originally only employed for physical experiments has been adapted to permit of its use for various technical purposes. The earliest use of the cathode ray tube was in the cathode-ray oscillograph in which the motion of a sharp spot of light on a fluorescent screen was studied. The television apparatus, which has already been described in the first number of this Review [1]), is one of the latest applications of the cathode ray tube. In this apparatus the image is produced on the fluorescent screen by causing a spot of light (or scanning beam), whose intensity is subject to rapid fluctuations, to travel at great speed over the whole picture-surface. A third important application of the cathode ray tube is the electron microscope, in which the cathode ray throws an enlarged image of the hot cathode surface on the fluorescent screen. *Fig. 1* reproduces a series of photographs of the crystal structure of a cathode surface, which were obtained by Dr. W. G. Burgers with the aid of an electron microscope.

In the various applications of the cathode ray tube, the specific requirements were such as to necessitate a closer investigation and improvements of various details. It appears desirable, therefore, in this introductory article to review the principles governing the construction and method of operation of the cathode ray tube.

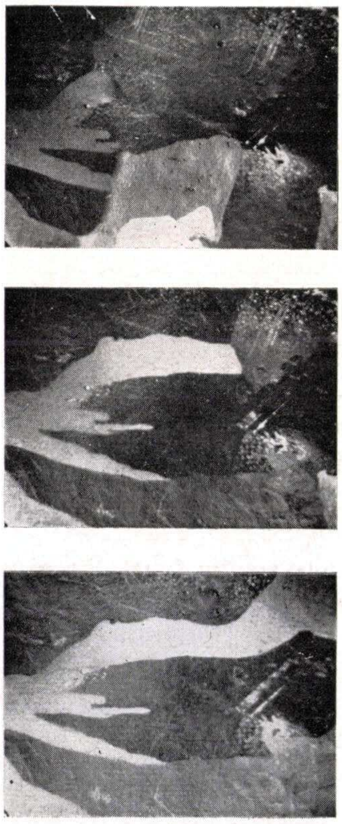

Fig. 1. Series of pictures of a cathode surface produced by cathode rays (magnification 15 times).

---

[1]) Philips techn. Rev. **1**, 16, 1936.

Fig. 2 shows the construction of a gasfilled cathode ray tube of very simple design. The hot cathode K is surrounded by the cylinder C, which is given a negative bias of such magnitude that owing to attraction by the gas ions the electrons emitted from the cathode are focussed as far as possible to a single point (*fig.* 3). If a potential difference is applied to the pair of plates P_1 and P_2, the beam of electrons is deflected. Owing to the small rout-time of the electrons from the cathode to the screen, the beam of electrons can respond to electrical oscillations much more quickly than mechanical oscillographs. Only at frequencies higher than 10^8 per sec (i.e. at a wavelength of less than 3m) in high vacuum tubes the cathode ray does no longer follow the impressed oscillations.

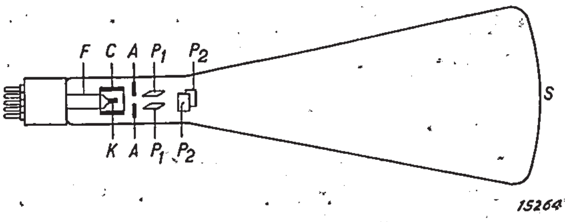

Fig. 2. Diagrammatic sketch of a gas-filled cathode ray tube. K = cathode. F = leading-in wires. C = Wehnelt cylinder. A = anode. P_1 and P_2 = deflecting plates. S = screen.

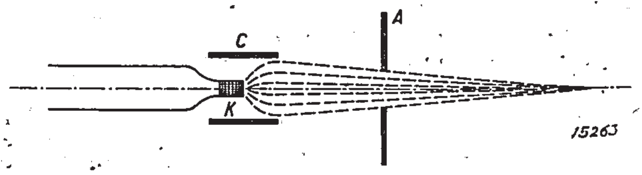

Fig. 3. Image of the cathode obtained with the aid of the Wehnelt cylinder C. Owing to the electric field of C and the attraction of the gas ions the electrons emitted by the cathode are concentrated on a point of the axis forming an image of the cathode.

Electron Lenses

Although the cylinder C (fig. 2) is quite effective for focussing the beam of electrons in gasfilled tubes, sharply defined cathode images can indeed only be obtained with the aid of more complex electrical arrangements. This is the only successful method in high-vacuum tubes. To visualise clearly the method of operation of such additional electric fields, we will discuss the electrical system by analogy with optical systems. We therefore also speak of electron lenses, etc..

The path of light-rays in geometrical optics is governed by Fermat's principle, according to which the path of these rays between two points is such that the time for passing from one point to the other is a minimum. In a medium with a refractive index n, the velocity of light is c/n, where c is the speed of light in vacuo. Fermats' principle may be expressed mathematically as follows:

$$\int dt = \int \frac{n}{c}\, ds = \frac{1}{c}\int n\, ds = minimum \quad (1)$$

In order to describe the path of a beam of electrons, we must start from the fundamental laws of point mechanics. These laws may be summarised in the principle of minimum action, according to which the space-integral of the product of the mass m and the velocity v (mv = impulse p) between any two points of the space traversed is smaller for the actual path taken than for any other conceivable path terminating at the same two points with the same velocities. It is presupposed here that the velocity of the body at every point in its path is as great as required by the energy theorem. We thus obtain the following condition for a minimum:

$$\int p\, ds = m \int v\, ds = minimum\ . \quad . \quad (2)$$

Comparing equations (1) and (2), it is seen that the velocity v of the electrons in electronic optics plays exactly the same part as the refractive index n in geometrical optics. If, with the aid of metal lattices, lenticular areas in cathode ray tubes (*fig.* 4) are raised by a constant amount of potential above the surrounding space, the electrons will travel within such areas at greater velocities than outside them. The velocity within the electron lens is determined by the potential difference the electrons passed through:

$$e\ V + \frac{1}{2}\ m\ v^2 = const.$$

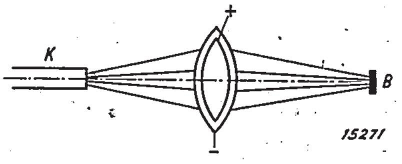

Fig. 4. Electronic lens of wire lattice. K = cathode. B = image. The wire lattices are electrical double layers. At the small distance between them the electrons are much accelerated or retarded; outside and inside the electron lens their velocity is a constant.

V being the potential and e, m [2]) and v respectively the charge, the mass and the velocity of the electron.

The lenticular area thus acts on the electrons in an analogous way to an ordinary optical lens.

---

[2]) $e = 4{,}77.10^{-10}$ e. s. u.
$m = 9.10^{-28}$ gr.

The practical production of lenses by means of wire lattices has, however, certain disadvantages as the electrons are scattered at the lattice wires.

Immersion Systems for Electrons

Of an efficient cathode ray tube it is not only required that the image of the cathode on the fluorescent screen shall be as small as possible, but also that the optical system and the screen shall be sufficiently far apart (fig. 2). This large intervening distance is necessary so that the fairly small angular deflections, which the pair of plates P_1 and P_2 impart to the beam of electrons, are rendered visible on the screen on a magnified scale. On the fluorescent screen we thus obtain an image O' of small area as well as a beam of small angle Ω'. On the other hand, to obtain a sufficient intensity it is necessary to make the area of the cathode O as well as the angle of emission Ω of the electron beam as large as possible.

According to a theorem in geometrical optics, the product of the area O, the angle Ω of the beam and the square of the refractive index n^2 is the same for both image and object, thus:

$$O'\,\Omega'\,n'^2 = O\,\Omega\,n^2 \tag{3}$$

A corresponding formula also applies in electronic optics, except that the refractive index n is replaced by the velocity v of the electrons. The requirements to be met by the cathode ray tube set forth in the previous section can obviously only be satisfied if the electrons striking the screen have a much greater velocity than those leaving the cathode. In optics, systems in which the object and image are embedded in media with different refractive indices are termed immersion systems. The same nomenclature may be applied in electronic optics to systems in which the velocities of the electrons at the cathode and at the screen are not the same.

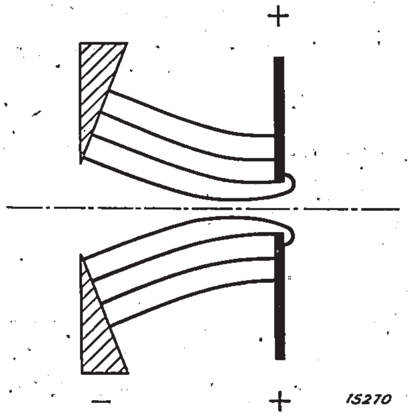

Fig. 5. Electrostatic field of an immersion system for electrons. It can be deduced from the shape of the lines of force that the electrons moving from left to right are accelerated; so they pass through the aperture of the anode at a high velocity.

For light rays the refractive indices vary only between 1 and 2; with cathode rays, however, any desired ratio between the velocities corresponding to the refractive indices, can be obtained by accelerating the electrons sufficiently. In this way both the angle of the beam and the image of the cathode can be made as small as desired. The beam of electrons is focussed by means of electric fields with a rotational symmetry instead of by wire lattices. An example of this is shown in *fig. 5*. The focussing action of such electric fields can be readily deduced from the configuration of the lines of force. *Fig. 6* shows the arrangement of the electronic lenses in the Philips 3951/3952 cathode ray tubes. The Wehnelt cylinder is provided with a metal plate which has a small aperture just in front of the hot cathode. Owing to the negative bias of the Wehnelt cylinder, the beam of electrons on admission into the first anode cylinder is already subject to preliminary focussing. The electric field between the two anode cylinders ensures accurate concentration of the electron beam.

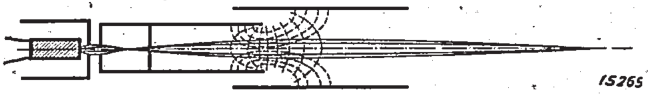

Fig. 6. Arrangement of an electronic lens in the Philips 3951/3952 cathode ray tube. Lines of force: — — — — —; equipotential surfaces: — . — . — . —; path of electrons: ——

Magnetic Electron Lenses

Besides electrical systems, magnetic systems such as a homogeneous magnetic field with the same direction as the electron beam, can also be employed for focussing the cathode ray. For the action of such a magnetic field there is no optical analogy. If a slightly divergent beam of electrons travels in the longitudinal direction of a magnetic field, the electrons are deflected by Lorentz forces which are perpendicular to the direction of motion of the electrons and to the magnetic field. Under the action of these Lorentz forces, the electrons describe elongated spiral paths whose axes are in the direction of the magnetic field. As these spiral paths (*fig.* 7) all have the same pitch, the electron beam is concentrated to a single focus.

We shall analyse this process in greater detail. Take an electron with a velocity v which makes a small angle α with the direction of the magnetic field, so that the radial component of the velocity is $v \sin \alpha$, while the axial component is almost equal to v. The projection of the path of the electron on a surface perpendicular to the axis of the magnetic field is then a circle of radius r. The centripetal force

$$\frac{m\,v^2\,\sin^2\alpha}{r}$$

required to produce this motion is provided by the magnetic field H, which is therefore equal to $H\,(e/c)\,v\,\sin\alpha$ (c is the velocity of light). This gives the radius of the circle as:

$$r = \frac{c\,m\,v}{eH}\sin\alpha \quad . \quad . \quad . \quad (4)$$

The radii of the circles are therefore proportional to the velocities of the electrons v and inversely proportional to the magnetic field strength H.

At a given field-strength, all circular paths will be described in the same time, viz:

$$\tau = \frac{2\pi r}{v\,\sin\alpha} = 2\pi\,\frac{m\,c}{eH} \quad . \quad . \quad . \quad (5)$$

During this time of motion the electrons will traverse the same distance s in an axial direction:

$$s = v\tau = 2\pi\,\frac{m\,c\,v}{eH} \quad . \quad . \quad . \quad (6)$$

The spiral paths thus all have the same pitch (fig. 7).

With magnetic focussing very good results are obtained. It is also used in the electron microscope with which the photographs of fig. 1 were made.

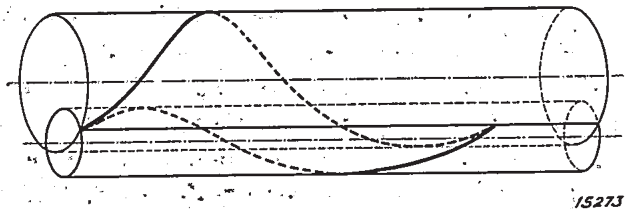

Fig. 7. Spiral paths described by electrons in a homogeneous magnetic field. The cylindrical surfaces enclosing these spiral paths are shown solid for the sake of elucidation. The axis of the system is the common generator of all cylinders.

Distortion of the image

As a rule light-rays of different colours are refracted to different degrees at the surfaces bounding two media, so that two rays of light of different colours coming from the same point are usually not focussed in exact coincidence, and so-called chromatic aberration is obtained. The corresponding distortion in electronic optics is obtained with non-homogeneous beams, a beam being defined as non-homogeneous when the constituent electrons have different velocities and are therefore deflected to different degrees in the electric field. The electrons being emitted by the cathode with various velocities, the electron beam is always non-homogeneous. The difference between the velocities of the electrons can, however, be kept within sufficiently narrow limits by accelerating the electrons already close to the cathode to such a degree that their velocity is large compared with different emission velocities.

If in geometrical optics the apertures through which the ray passes are not made too small, then the rays emitted from one point in the axis will be combined at different points according as they travel close to the axis or make a large angle with it. Distortion of the image due to this factor is termed spherical aberration. The corresponding analogy in electronic optics is the aberration of homogeneous beams of electrons with a finite angle of emission, but in practice such distortion is small as the apertures employed are not very large.

If a plane perpendicular to the axis appears as a curved surface in the image, we have what is called curvilinear distortion, which is of little trouble in electronic optics as we are dealing with beams of great depth of definition (cf. the section of space-charge phenomena, fig. 10) in which the surface of the image does not occupy a strictly defined position.

A beam of light-rays which does not travel parallel to the axis of the lens will as a rule not be concentrated at a focus, but along two focal lines perpendicular to each other and perpendicular to the axis of the lens at different distances from the lens. This form of distortion is termed the astigmatism of inclined beams. In optical systems not accurately centred, astigmatic distortion of beams parallel to the axis also occurs. In electronic optics this phenomenon may be very troublesome, for the beam of electrons here gives rise to two lines perpendicular to each other, which are thrown on the screen at different potentials. To obtain sharply-defined images astigmatic distortion must therefore be kept as small as possible. It has been found that the deviations from rotational symmetry and the error in centring the cathode and the Wehnelt cylinder must not exceed 0.01 mm. In other parts of the optical system the dimensions in question are greater, so that the geometrical and centring errors may also be somewhat greater (about 0.1 mm). Furthermore, non-homogeneities of the surface of the cathode may also cause deviations in the rotational symmetry of the beam of electrons, resulting in the production of so-called cathodic astigmatism. Fortunately this distortion usually disappears in course of time as the surface of the cathode becomes sufficiently homogeneous after a few hours' heating.

When using magnetic lenses, for which there is no analogy in geometrical optics, distortion of the image is also obtained, but for whose elucidation no optical analogy can be of any assistance. In the case of rays which only deviate slightly from the direction of the axis, we obtain in a homogeneous magnetic field H a specific rotation of eH/cmv per unit of length in the direction of the axis. If the electrons are also accelerated during their passage through the magnetic coil, their total rotation in the magnetic field is the integral of this specific rotation along the path of the electron. Non-homogeneous magnetic fields also enable well-defined images to be obtained, whereby the image is not only rotated but also magnified or reduced. If the rays make a larger angle with the axis, their rotation may differ from that of the rays travelling almost parallel to the axis, and for this reason straight lines perpendicular to the axis are frequently shown in the image as curved. In this case we speak of rotational distortion (*fig. 8*).

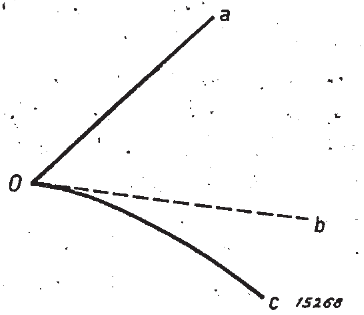

Fig. 8. Rotational distortion projected on a surface perpendicular to the axis. O is the axis, a is a line cutting the axis perpendicularly; b is its rotated image according to equation 6; c is the figure produced by rotational distortion.

Deflection Systems

The deflecting fields naturally possess no rotational symmetry but usually an enantiomorphic symmetry, and thus behave as cylindrical lenses in geometrical optics. Care must be taken that the astigmatism caused by them is as small as possible, for if for instance one of the deflecting plates is connected to the anode and an alternating voltage applied only to the other, the astigmatism at the same potential difference between the plates will be much greater than when the two plates are connected up symmetrically with respect to the anode.

If the electrons are deflected to a marked extent, they will approach the edges of the deflecting plates where the field is very non-homogeneous. Deflection will then no longer be proportional to the deflecting potential difference. To avoid this source of error, the ends of the deflecting plates are splayed outwards (*fig. 9*) so that the electrons on leaving the deflecting system can travel along equipotential surfaces for as great a distance as possible.

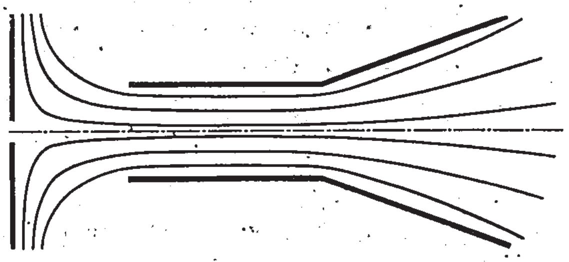

Fig. 9. A deflecting system in which the electrons on emission are almost parallel to the equipotential lines.

Space-Charge Phenomena

The mutual repulsion of the electrons has no corresponding analogy in geometrical optics and the distortion of the cathode ray resulting from this action must therefore be discussed independently. The fluorescent spot owing to the space-charge becomes greater than it should do according to geometrical optics. If in a 2000-volt oscillograph the maximum diameter of the spot is stipulated as 1 mm the greatest permissible current intensity is then 0.1 milliamp. In modern cathode ray tubes for television purposes this current value is reached although only at higher voltages. Perhaps the current strength of the cathode ray could be further increased by using systems with a greater aperture and in which the current density remained sufficiently low up to the neighbourhood of the screen.

With a cathode ray the position of the image obtained is not by any means fixed as precisely as with light-rays, for the beam of electrons in the neighbourhood of its maximum constriction has practically a constant cross-section over a fairly considerable distance (*fig. 10*). A cathode ray has therefore a much greater depth of definition, so that curvilinear distortion (see section on distortion of the image) is of no moment.

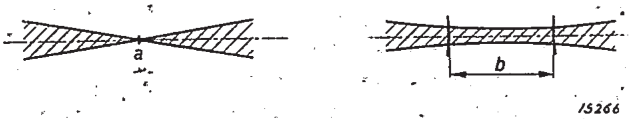

Fig. 10. Production of an image: (a) by light-rays, (b) by a beam of cathode rays. With light-rays the outlines of the beam are straight lines, with cathode rays they are curved by mutual repulsion of the electrons. Therefore these electron beams possess approximately their minimum diameter along a large distance.

The thickness of the graphed line in an oscillogram obtained with a cathode ray tube is also determined by the graphing speed. This phenomenon is termed the "charging spread" and is due to irregularities in the charging of the screen caused by the greater or lower velocity of the scanning cathode ray. Charging produces an electrostatic field in front of the screen which scatters the electron beam.

The electric charge of the cathode ray, in addition to the troublesome effects mentioned above, has fortunately also an advantageous action. The so-called gas concentration which can be obtained in gas-filled tubes, results from the ionisation of the gaseous atoms by the high-speed electrons. In this way the passage of the cathode ray produces a track of positive ions, which, as they are far less mobile than the electrons generated at the same time, remain in their original positions, while the electrons diffuse into the surrounding space. In the path traversed a space-charge field is thus produced which not only counteracts the mutual repulsion of the electrons but is also even capable of focussing the beam of electrons. In gas-filled tubes sufficiently small spots can be obtained without special electric fields.

For the gas concentration gas pressures of 10^{-2} to 10^{-3} mm are required. Neon, argon or mercury vapour are among the gases used for filling the tubes. Cathode ray tubes of this type give satisfactory spots already with a few hundred volts. A disadvantage of the gas filling is the danger of causing deterioration of the cathode by bombardment with positive ions. To prevent this action the anode is so constructed that it isolates the cathode space as far as possible from the deflection space where the majority of the ions are produced.

The focussing action of the space-charge field is closely determined by the radiation intensity. On varying the intensity the equilibrium between the electrons, ions and gaseous atoms in the neighbourhood of the ray is naturally also altered. For television purposes, in which the intensity of the ray varies considerably, it is not a simple matter to obtain satisfactory results with gas concentration. For this reason also, high-vacuum tubes are used for television which are run on several kilovolts, so that owing to the much greater velocity of the electrons their mutual repulsion is not given time to spread out the beam.

Compiled by G. P. ITTMANN.

RELAXATION OSCILLATIONS

Summary. The characteristics of relaxation oscillations are a fixed amplitude (and not an amplitude determined by the initial conditions, as in the case of harmonic vibrations) and a period determined by a relaxation time (i.e. the time-delay of the formation of an equilibrium). This class of oscillations is widely distributed and is met with in the most varied branches of science and technology. They fulfil a special function in the maintenance of harmonic vibrations, a motion with which the engineer is much more closely acquainted. A very useful property of relaxation oscillations from the practical standpoint is the ease with which they can be synchronised. Between the two limiting cases of perfect relaxation oscillations and perfect harmonic motion there are transitional forms which can be produced experimentally as well as derived from a differential equation.

Introduction

In the case of many natural phenomena, progress in our knowledge of them and their subsequent technical application do not date from the time of their discovery but from the time they were given a distinguishing name. The acquisition of a specific name is an indication that the phenomenon in question, although it may have been known already for centuries, has become a focus of interest and that the research worker commencing to study and investigate it in greater detail, now requires some means of readily identifying it.

Relaxation oscillations were given this name [1]) in 1926 when a number of investigators, among which are also those in the Philips Laboratory, began to show a deeper interest in this type of phenomenon. It was soon realized that very many periodic processes in the most divergent branches of science could be interpreted as relaxation oscillations. The newly-christened type of oscillation was also found to be a useful tool to the engineer, which he had unknowingly already been employing for a long time. In the first issue of this Review special applications of these oscillations have already been described in two different articles (J. van der Mark, An Experimental Television Transmitter and Receiver, p. 16; D. M. Duinker, Relay Valves as Timing Devices in Seam Welding, p. 11).

The mechanism and most important properties of those systems which are subject to relaxation oscillations will be discussed here.

A Special Relaxation Oscillation as Example

To demonstrate without preamble the particular class of processes which enter into consideration here, we shall start with the discussion of an example which has indeed been known for a long time, viz. the intermittent discharge of a glow discharge tube having a condenser connected in parallel.

The circuit of this system is shown in *fig. 1.* B is a discharge tube of any type, which has a specific ignition voltage V_1 and a specific extinction voltage V_2.

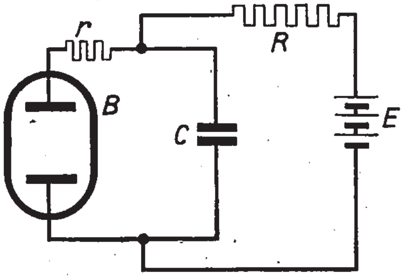

Fig. 1. A system which can perform relaxation oscillations: The condenser C is charged from battery E through the suitably-rated resistance R. The discharge tube B has initially an infinitely high resistance. However, as soon as the potential of the condenser exceeds the ignition voltage of B, the tube becomes ignited, i.e. its resistance drops abruptly to a low value r. The condenser discharges itself rapidly through this low resistance until its potential has dropped to the extinction voltage of B, whereupon the resistance of the tube again becomes infinite and the same cycle recommences.

---

[1]) By B. van der Pol in the Tijdschr. v. h. Nederl. Radio Genootsch. 3, 25, 1926, (cf. also Phil. Mag. 2, 978, 1926). About the same time, E. Friedländer, Arch. f. Elektrotechnik 17, 1, 1926, termed these oscillations "Kippschwingungen", which name has been adopted in Germany.

The tube commences to conduct current as soon as the potential across its terminals exceeds V_1. The condenser C, which is charged from a battery E through the high resistance R, is discharged through the low resistance r of the tube B as soon as it has reached the potential V_1. The potential of the condenser on discharge through the low resistance r drops rapidly to the extinction voltage V_2, at which the tube allows no further current to pass and the discharge again ceases. The condenser is then recharged and its potential again rises from V_2 to V_1 when the same cycle is repeated. The potential V of the condenser thus fluctuates as shown in *fig. 2*.

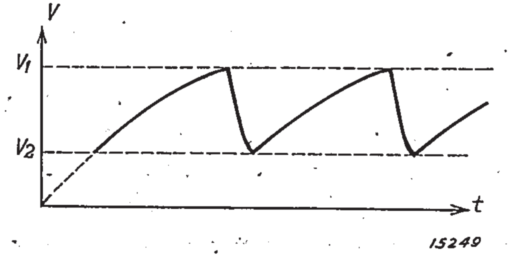

Fig. 2. Variation of the potential V of the condenser in the circuit in fig. 1. V_1 is the ignition voltage, V_2 the extinction voltage. The curve represents a relaxation oscillation.

It is seen that the oscillation obtained is very different from an ordinary sinusoidal one. In the curve in fig. 2, as in other forms of relaxation oscillations (see fig. 7c), characteristic features are the steep discontinuities which occur at the end of each period corresponding to the sudden discharge. The length of the period is therefore mainly determined by the time required for charging the condenser (from the potential V_2 to V_1); this interval of time is determined by the resistance R and the capacity C. An interval of time of this kind, which quite generally represents the delay with which an equilibrium is arrived at (in the present case the equilibrium between the potential of the condenser and the battery voltage) is termed a relaxation time. In the class of oscillations which are discussed here, the vibration period is always determined by a relaxation time, hence the term "relaxation oscillations" proposed by van der Pol.

Apart from this rather superficial difference between relaxation oscillations and the well-known harmonic (sinusoidal) motion, there are other reasons which justify relaxation oscillations being regarded and investigated as independent phenomena. It might be advanced against this that a relaxation oscilation similar to every other periodic phenomenon can be formally compounded from various harmonic motions by means of a Fourier series. But in contradistinction to a harmonic motion, the most characteristic property of a relaxation oscillation is, indeed, not the periodicity of the process. In our example we saw how a typical aperiodic process, viz, the charging of a condenser, can be continually repeated, linked up by interposed intervals of discharging of the condenser. The rhythm in which these sequential operations take place is determined by the rate of supply from the energy source E through the resistance R; by disconnecting the source E we can interrupt the charging process at any desirable moment and then again continue it from the same point at any subsequent time. This system of oscillation therefore exhibits no preference for any characteristic frequency, which latter can be readily influenced by extraneous factors. On the other hand, the amplitude of the relaxation oscillation is fixed; the reversal from charging to discharge of the condenser and inversely always takes place at the ignition voltage or at the extinction voltage of the discharge tube, the system continually fluctuates between these two voltages.

Application of Relaxation Oscillations for Maintaining Harmonic Oscillations

Let us now consider the conversion of energy which takes place with a relaxation oscillation and with a harmonic oscillation respectively. In the example of a relaxation oscillation discussed above, we had an energy accumulator (the condenser) to which energy was supplied from a constant source (the battery). The system also contained a unit (the discharge tube) which at a certain high "tension" of the energy accumulator suddenly commences to dissipate energy (converting it to heat) until the potential of the accumulator has dropped to a specific low value: the dissipation of energy then ceases and the same cycle commences afresh. The net result is, therefore, that the system absorbs and dissipates a definite quantity of energy from a constant energy source, and this process can be continued indefinitely.

In a system of harmonic vibrations, we always have two energy accumulators, e.g. a mass m in which kinetic energy can be accumulated and a spiral spring c in which potential energy can be stored (*fig. 3a*), or a condenser C for electrical energy and a self-induction L for magnetic energy (*fig. 3b*). During the motion energy is transformed periodically from the one form to the other. A dissipation of energy, which occurs in all practical cases (friction, electrical resistance), results in the gradual decay of the oscillation. Hence to obtain a sinusoidal vibration lasting a long time, we must make up the energy lost. But here the striking fact must be considered that from a source of constant energy we cannot directly apply energy to a system of harmonic oscillations in order to maintain the vibratory motion. This may be readily seen with the aid of the differential equation for harmonic motion, e.g. in the mechanical system (fig. 3a):

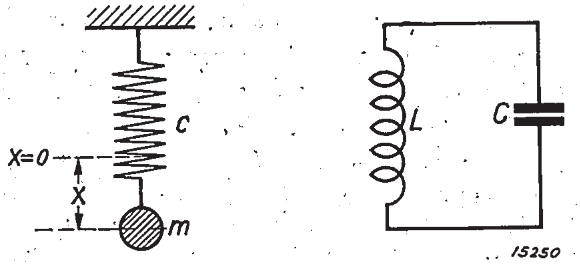

Fig. 3. Examples of systems carrying out harmonic vibrations.
a) Mechanical system consisting af a mass m attached to a spring with a retracting force c.
b) Electrical system comprising a condenser C and a self-induction L connected in series.

$$m\frac{d^2x}{dt^2}+a\frac{dx}{dt}+cx=0 \quad . \quad . \quad . \quad (1)$$

where x is the deviation of the system from its position of rest (i.e. the amplitude) and the three terms give in the order shown the inertia (accumulator m or L), the friction (dissipation of energy) and the retracting force (accumulator c or C), which at every instant of time are in dynamic equilibrium. If for the moment we neglect damping, the solution of (1) is a sine function (*fig. 4*) whose frequency is fixed, but whose phase and amplitude can have any values, being only governed by the initial conditions (the magnitudes of x and dx/dt at time $t=0$). If a constant external force K is applied to the system, equation (1) becomes:

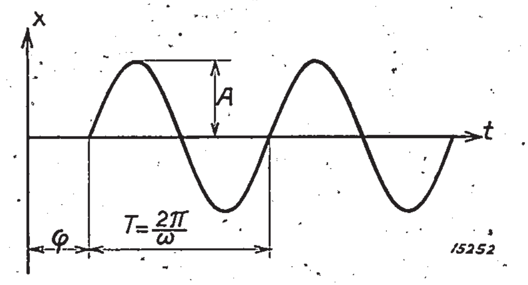

Fig. 4. Undamped harmonic oscillation (sine function). The period $T = 2\pi/\omega$ is determined by the magnitude of the components of the system. The phase φ and the amplitude A are arbitrary (i.e. only determined by the initial conditions of the differential equation (1)).

$$m\frac{d^2x}{dt^2}+a\frac{dx}{dt}+cx=K \quad . \quad . \quad . \quad (1a)$$

The energy imparted to the system by this means is determined by the integral of the force over the path traversed:

$$\textit{Work done} = \int K\,dx = K\int dx$$

But if we substitute for x the sine function expressing the oscillation to be maintained, the integral is equal to zero over each complete period of the sine [2]). In order that the value of the integral shall not become zero, i.e. energy is actually supplied to the system, we must apply a force which is not constant but is an arbitrary function of the time, provided only that this function contains a component synchronising with x (e.g. to be determined by Fourier analysis), i.e. a sinusoidal function similar to x. In the majority of cases the sources of energy available furnish constant forces: for instance, gravity, wind pressure or a current of water, the E.M.F. of a battery, etc. In order to introduce the requisite sinusoidal component here, we must intercept the constant time function of the force at regular intervals, so that the influx of energy is alternately free and blocked. But this is just what relaxation oscillations are able to do. We can therefore place between the constant energy source and the damped system of harmonic vibrations a system of relaxation oscillations in order to supply the requisite energy in fractions as required.

This principle is indeed actually employed in practice. The simplest example of maintained harmonic oscillations which suggests itself is the mechanism of a clock. Being constrained to a definite frequency, harmonic oscillations are ideal for time measurement; thus, a pendulum (in a wall clock) or a balance wheel (in a watch) or a piezoelectric quartz lamina (in some modern astronomical clocks) is allowed to oscillate and the time measured by counting the number of oscillations. To maintain these oscillations, so that as a result of damping they do not rapidly decay and cease altogether, we provide a source of constant energy, e.g. the wound spring in a watch. Through the lever A

---

[2]) For the constant force merely causes a displacement of the position of rest about which the system oscillates; this follows from the differential equation (1a) which on making the substitution $x' = x - K/c$ can be written as:

$$m\frac{d^2x'}{dt^2}+a\frac{dx'}{dt}+cx'=0.$$

This is again the same equation as (1), except that the position of rest is now $x'=0$, i.e. $x=K/c$, instead of $x=0$.

(anchor) of the escapement (*fig. 5*) the balance wheel O is given a fresh impulse at the end of each half-period of its oscillation by the driving spring uncoiling a very little way, i. e. a small part of its potential energy is transmitted as twist to the gear mechanism and the anchor. The lever A of the escapement performs a typical movement of the relaxation oscillation type; it moves to and fro between two fixed terminal positions to the right and left (stops s), the reversal in direction in this case being produced itself through the coupling with the harmonic oscillation [3]).

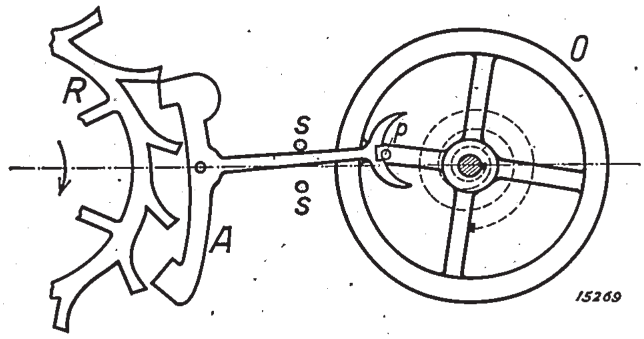

Fig. 5. Escapement of a watch. The harmonic vibrations of the balance wheel O are maintained by a periodic supply of energy through the anchor A which performs a relaxation oscillation. In detail this process is as follows: As soon as the balance wheel during oscillation approaches its middle position (maximum velocity), the pin p coming from above strikes against the fork of the anchor A, which up to this moment rested against the upper pin s. The anchor is turned slightly, and its upper claw slides along the tooth of the escapement wheel R against which it rested; when the tooth has been released (this instant is shown in the figure), the scape wheel turns through the space of one tooth, under the tension of the driving spring, in the direction of the arrow (being again immediately engaged by the lower claw of the anchor) and now accelerates the motion of the anchor by means of the lifting "surface" at the top of the tooth in such a way that the anchor tilts into its opposite terminal position (the lower stop s), its fork at the same time giving a push to the pin p of the balance wheel in the direction of its oscillation. Hence, in this moment energy is imparted to the harmonic system by the spring. The anchor remains in its lower terminal position until the balance, after passing through half a swing, again initiates the same operations in the opposite direction.

A further example is a tuning fork whose harmonic oscillations are maintained by a similar mechanism as used in the electric bell: this is also a relaxation oscillation (the energy accumulator charged and discharged being here the magnet coil) [4]).

The sound in an organ pipe is also produced in a similar way: the column of air in the pipe performs a harmonic oscillation, which is created and maintained by a current of air blown over a tongue. Air eddies are produced behind the tongue which grow to a certain size, then become unstable and release the tongue. This is repeated periodically and is another example of a relaxation oscillation which maintains a harmonic oscillation.

The Synchronising of Relaxation Oscillations

In the above we have seen the important practical difference in behaviour between systems of harmonic and relaxation oscillations with respect to a constant force. We shall now see how these two systems would react to a periodic, e.g. sinusoidal, external force.

Under the action of an external periodic force, a harmonic system becomes subject to what are called forced vibrations, with a frequency equal to that of the external force, but with an amplitude which is very small if there is a great difference between the forced and natural frequencies; if, however, the forced vibration frequency approaches the value of the natural frequency, the amplitude of the system becomes large, i.e. "resonance" is obtained.

A system of relaxation oscillations does not exhibit a similar resonance phenomenon. The amplitude is here fixed by the difference between the "potentials" of the energy accumulator at which a reversal of the controlling unit (in our first example the discharge tube) takes place. The external force, however, determines the moment reversal takes place: without appreciably altering the amplitude of the relaxation oscillations it influences its frequency within certain limits.

This is very aptly shown in frequency demultiplication [5]). In the system in fig. 1 a periodic voltage $e \sin \omega t$ (*fig. 6*) is applied in series with the discharge tube. We then find that the time between two ignitions, i.e. a period of relaxation oscillation, favours an integral multiple n (n = 1, 2, 3, ...) of the periods of the applied voltage: the frequency of the relaxation oscillation becomes synchronised with the n-th part (1/n = 1/1, 1/2, 1/3, ...) of the applied frequency, viz, that fraction whose value is nearest to the frequency of the "free" (unconstrained) relaxation oscillation. If in fig. 6 the "free" frequency is gradually altered by varying the capacity of the condenser, the frequency of the "forced" vibrations initially remains unchanged, i.e. in step with the fraction of the extraneous frequency with which it has been synchronised; as the deviation becomes greater the frequency jumps to the next fraction to which the "free" relaxation frequency has now approached more closely. In this way van der Pol and van der Mark, (loc. cit.) have succeeded in synchronising relaxation oscillations with 1/200 of the frequency of an applied oscillation.

---

[3]) That the escapement through the scapement wheel R at the same time sets in operation a counting mechanism which enables us to read the time on the dial, is of no importance for our considerations. By the way, the "relaxation system" (anchor) could not in this case perform independent oscillations without being coupled to the harmonic system.

[4]) For musical purposes, Niaudet has constructed a clock in which a tuning fork with a frequency of 64 cycles acting as regulator is driven by an escapement (the scapement wheel here makes a complete revolution per second). If this clock loses a second per day, the frequency of the tuning fork is only 63.99926 cycles, as may be readily calculated. With this instrument extremely accurate measurement of pitch is possible by the method of beats.

[5]) B. van der Pol and J. van der Mark, Nature **120**, 363, 1927.

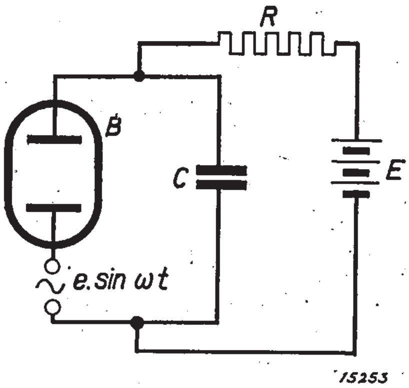

Fig. 6. The same system of relaxation oscillations as shown in fig. 1 (intermittent glow discharge), but here with the addition of a periodic voltage $e \sin \omega t$ which affects the times of ignition and extinction.

Further Examples and Technical Applications of Relaxation Oscillations

We have seen above that in the case of harmonic oscillations a special mechanism is required for the periodic addition of fresh energy. Relaxation oscillations do not require a similar provision. Hence nature and technology provide us with many examples of systems of relaxation oscillations which continue indefinitely in vibration without any special demand being made on the energy source for the maintenance of the motion. In addition no harmonic oscillation is required to control reversal as, for instance, in the case of the clock. We have already met with a typical example in the swelling and self-generating air eddies in a continuous current of air when discussing the organ pipe; the same process is also responsible for the musical sounds of the Aeolian harp and the humming of telegraph wires in the wind. The period of the note produced (pitch) is determined by the duration of growth of an eddy to the unstable size, i.e. by the velocity of the wind and the diameter of the wire, but does not depend on the length and tension of the wires (as with the harmonic vibration of strings, in for example the violin and piano). Many other well-known sounds are also due to relaxation vibrations; the grating of a knife on a plate, the fluttering of a flag, the hammering or singing of a water pipe, etc.

In the biological world, there are probably also many phenomena which can be interpreted as relaxation oscillations, e.g. the beat of the heart. In this periodic process the fact that the heart "beats" already enables us to deduce that it does not perform a sinusoidal vibration but a relaxation oscillation. Actually in the heart three systems of relaxation oscillations are coupled in a specific manner. Van der Pol and van der Mark[6]) by coupling in a similar way three electrical systems of relaxation vibrations have succeeded in reproducing in a most striking manner electrocardiograms as obtained with healthy and diseased hearts.

The opening and closing of blossoms is also frequently a relaxation oscillation which the plants continue to carry out with a definite periodicity when they are removed from all external influences (such as light, heat, etc.) and which can then be synchronised with new light stimuli.

In electro-technology, relaxation oscillations have perhaps been investigated most exhaustively of all branches of science. Apart from the example of the intermittent glow discharge and the electric bell, there is the Wehnelt interrupter, further the combination of a series-wound dynamo which feeds a motor with independent field-excitation, the dynamo commutating periodically; furthermore there is the multi-vibrator of Abraham and Bloch, as well as other circuits with electron tubes with specific characteristics.

Particularly the last-named electrical relaxation oscillations are widely employed in technology (cf. for instance the above-mentioned descriptions already published in the first issue of this Review). Other applications deserving of mention are the use of bi-metal switches for luminous advertising signs and other purposes (the relaxation period is here the time required for heating), the motion of windscreen wipers on motor cars which are driven pneumatically by a type of escapement, and finally the automatic flushing of water closets by cisterns which periodically are filled slowly and then rapidly discharged by means of a syphon.

---

[6]) B. van der Pol and J. van der Mark, Phil. Mag. 6 763, 1928.

Mathematical Representation of Relaxation Oscillations

In a previous section we have used the differential equation (1) of harmonic motion. The question arises whether we can also represent relaxation oscillations mathematically, i.e. deduce their properties from the solutions of certain differential equations.

Consider again our first example of the intermittent glow discharge in fig. 1. During the charging of the condenser C from the battery with potential E through the resistance R, the discharge tube has an infinitely high resistance; the condition of equilibrium between the voltages gives us the following differential equation for the condenser current i_1 at this point:

$$Ri_1 + \frac{1}{C}\int i_1\,dt = E \quad . \quad . \quad . \quad (2a)$$

The solution of this equation is

$$i_1 = \frac{E}{R}\,e^{-\frac{t}{RC}}$$

For the condenser potential $V = E - i_1 R$ we thus get:

$$V = E\,(1 - e^{-\frac{t}{RC}})$$

This represents the first portion of the curve shown in fig. 2: V increases with a velocity which is determined by the "relaxation time" RC in the exponential function. But as soon as V becomes greater than the ignition voltage V_1 of the tube, its resistance jumps from infinity to the value r. From this instant onwards the discharge current of the condenser i_2 in the opposite direction is defined by the following differential equation (neglecting the small term r/R with respect to unity):

$$r\,\frac{di_2}{dt} + \frac{1}{C}\,i_2 = 0 \quad . \quad . \quad . \quad . \quad (2b)$$

which gives for the potential of the condenser

$$V = V_1\,e^{-\frac{t}{rC}}$$

We have now arrived at the next portion of the curve in fig. 2, the one with a negative slope, until the extinction potential V_2 is reached; the velocity with which this point is reached is again determined by a relaxation period, which is here rC. The total duration of the process, which is continually repeated, is the sum of the two components of which each one is proportional to a relaxation period [7].

---

[7] It is readily found that the charging period is

$$T_1 = RC \cdot \ln \frac{E - V_2}{E - V_1}$$

and the discharging period

$$T_2 = r\,C \cdot \ln \frac{V_1}{V_2}$$

The whole period is $T = T_1 + T_2$.

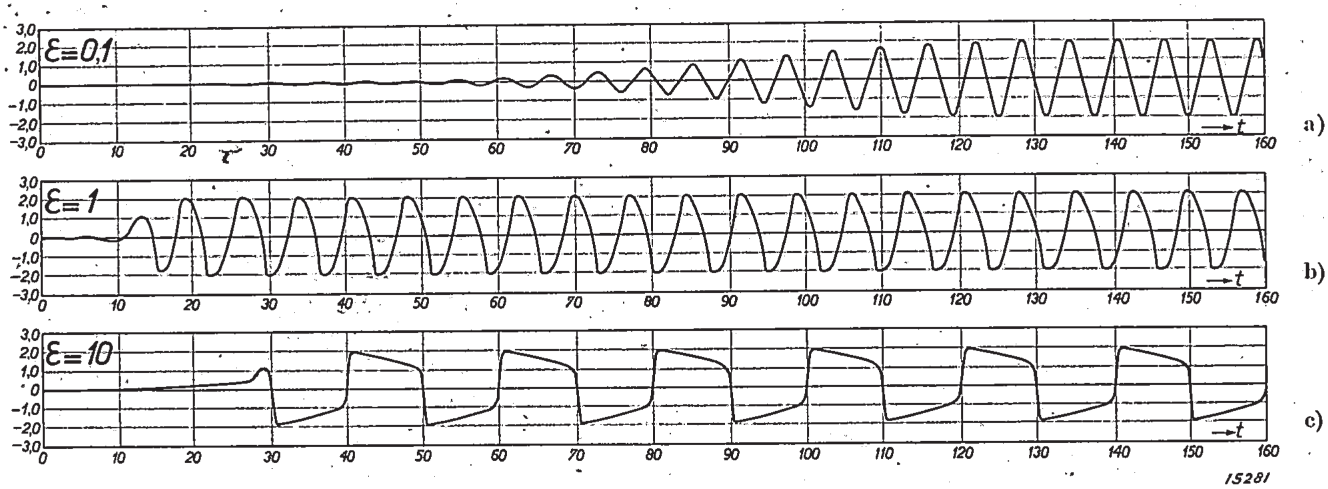

Fig. 7. Graphically found solutions of the differential equation (3) for three different values of the parameter ε.

a) For $\varepsilon << 1$ the solution is a gradually-developing sinusoidal vibration with a terminal amplitude of 2.

b) For $\varepsilon = 1$ we get a distinctly distorted vibration, which more rapidly reaches the terminal amplitude.

c) For $\varepsilon >> 1$ the solution brings out the typical properties of a relaxation oscillation. A to and fro movement between two terminal positions is shown, neither such positions nor the zero position being stable themselves. On closer analysis it is found that the period is proportional to a magnitude physically equivalent to a relaxation period.

Corresponding to the two entirely different processes of which it is made up, the relaxation oscillation is here represented by two differential equations (2a and 2b) which have alternate application.

B. van der Pol has succeeded in deducing mathematically from a single differential equation the behaviour of the multi-vibrator and other systems, which perform relaxation oscillations and were referred to above under technical applications. This equation after certain simplifying transformations can always be written in the form:

$$\frac{d^2x}{dt^2} - \varepsilon\,(1 - x^2)\,\frac{dx}{dt} + x = 0 \quad \ldots (3)$$

Compared to differential equation (1) for harmonic vibrations, equation (3) differs in respect to the non-linear "damping" term containing the coefficient ε. The solution of (3) (which is obtained by a graphical method) proves to be closely dependent on the magnitude of ε (cf. *figs. 7a, b and c*). If $\varepsilon << 1$, e.g. $\varepsilon = 0.1$ (fig. 7a) we obtain an almost sinusoidal vibration with a gradually increasing amplitude. At $\varepsilon = 1$ (fig. 7b) the sine function has become distinctly distorted and the final amplitude is attained much quicker. At $\varepsilon >> 1$, e.g. $\varepsilon = 10$ (fig. 7c), a vibration is obtained whose essential properties agree with those of what we have defined as a "relaxation oscillation" in fig. 2. We have an amplitude determined by two fixed terminal positions (independent of the energy consumption), as well as the typical discontinuities (the attainment of instability); also the period (numerically approximately equal to ε) can be shown to be determined by a magnitude which is essentially a relaxation period. The symmetrical form of the function with respect to the abscissa (fig. 7c) is only due to the simple form of the damping term; if we add to it an asymmetrical term so that the damping term becomes

$$\varepsilon\,(1 - \beta x - x^2)\,\frac{dx}{dt}$$

the solution also becomes asymmetric, resembling still more fig. 2.

This far-reaching concordance between the behaviour of the general type of relaxation oscillation discussed above and the properties of the solution of equation (3) for $\varepsilon >> 1$ makes it not unjustifiable to regard equation (3) as the mathematical expression of the phenomenon of the "relaxation oscillation". From it the essential characteristics of systems of relaxation oscillations can be deduced and predicted, although care must be taken that conclusions of further import are not drawn. For those cases for which the differential equation (3) has been deduced physically (multivibrator, etc.) it has been observed that a continuous transition to sinusoidal vibrations is possible; and these transition forms have actually been realised experimentally in the cases in question. From the equation (3), however, no direct conclusions can be drawn regarding the behaviour of, for instance, the intermittent glow discharge with respect to these transition forms.

Compiled by S. GRADSTEIN.

OPTICAL MODEL EXPERIMENTS FOR STUDYING THE ACOUSTICS OF THEATRES

By R. VERMEULEN and J. DE BOER.

Summary. In the auditoriums of theatres where one of the primary considerations is the perfect audibility and intelligibility of the spoken word, a short period of reverberation is essential; this, however, should not cause too great a reduction in the "useful sound intensity". The distribution of loudness is examined in this paper with the aid of optical model experiments, in which the source of sound is replaced by a small lamp and the walls of the theatre simulated in a three-dimensional model by walls with a suitable coefficient of reflection. This method was applied on the occasion of the rebuilding of the assembly hall in Philips "Ontspanningsgebouw" (Philips Theatre).

To gain an idea of the acoustics of a hall or theatre during a concert or a theatrical production requires no special knowledge or auxiliary means. On the contrary, the opinions of the uninitiated audience witnessing the show here act as a yardstick. If the audience is not satisfied, it is the business of the expert to establish the cause of such dissatisfaction. But he must also be in a position to determine the potential acoustic characteristics of a hall even before it is built, merely from a study of the plans. In both cases he must make use of measurements and experience with existing halls and from these deduce with the aid of calculations and designs the information required. In addition, the behaviour of the sound waves in the structure in question can also be determined by means of a small scale model of the hall. A new method will be described here for carrying out such experiments with models, which has been applied in the Philips Laboratory, inter alia, to assist in the reconstruction of the assembly hall in Philips "Ontspanningsgebouw" (Theatre) at Eindhoven.

Acoustic Properties of a Hall

The acoustic characteristics of a hall or theatre are almost completely determined by the reflection of the sound waves at the walls. The sound which becomes audible to the audience can be resolved into various components, viz:

1) The direct sound, i.e. the sound waves reaching the audience without reflection at one of the walls or other surface;
2) The "useful" sound, which in addition to the direct sound also includes every sound wave striking the ear within $^1/_{15}$ of a second after the arrival of the direct sound. Useful sound has been so named because it has been found that all these contributed sounds aid in making the spoken word audible and intelligible, and in practice cannot be distinguished from the direct sound.
3) Reverberation, which includes all sound persisting after the emission from the sound source has ceased. Reverberation thus embraces the "useful" sound and all contributed sound waves which reach the ear after $^1/_{15}$ of a second.
4) For the sake of completion echoes will also be included here. An echo comprises a reflected sound wave which, owing to the peculiar shape of a part of the reflecting walls, predominates above the reverberation and can be distinguished separately because of its high intensity.

The reverberation period is defined as the time taken by the intensity of sound in a sound-filled space to decay to a millionth part of its initial intensity after emission from the sound source has ceased. In the case of musical productions it has been found that there is an optimum value of the reverberation period at which the music is heard to the best effect. For the spoken word, specific reverberation periods also give optimum results, signifying that at these values maximum intelligibility is obtained. That an optimum is actually obtained here is due to the fact that the useful sound constitutes a part of the reverberation, so that with too short a reverberation period the useful sound intensity becomes too weak; if, on the other hand, the reverberation period becomes too long the successive syllables overlap and the intelligibility again deteriorates.

In the ideal theatre the whole sound radiated from the source would reach the audience as useful sound. Except for the case where the speaker stands in a suitable spot and is surrounded by a sound reflector, this acoustic ideal cannot be even approximately realised. A certain quantity of sound will always be "wasted", reaching the audience only after many reflections, i.e. after a long delay, and in the form of reverberation will only have an adverse effect on intelligibility. Even if for a particular theatre the useful sound intensity has been found to be sufficiently large, it is still necessary to keep the reverberation period within reasonable limits by the provision of sound-absorbing materials.

Optical Model Experiments

The hall of Philips Theatre was primarily intended for theatrical performances for which it was essential to obtain a sufficient intensity of useful sound. On reconstruction of the auditorium it appeared desirable to obtain an insight into the magnitude and distribution of the useful sound intensity in the old theatre and in the new one for which plans had been drawn up. For this purpose model experiments were carried out in which the source of sound was replaced by a light-source and the resulting light intensity determined directly for different parts of the auditorium.

The model of the hall is made of sheet aluminium (see *figs. 1a and b*), and a small lamp is used as a "sound-source" which can be placed in different positions. About 50 per cent of the light-rays impinging on the aluminium walls is reflected so that after three reflections the intensity of a light-ray is already reduced to about 10 per cent of its initial value and thus will no longer contribute much to the total intensity. The luminous intensity at each point in the model is, therefore, determined by the interaction of only a few reflected rays,

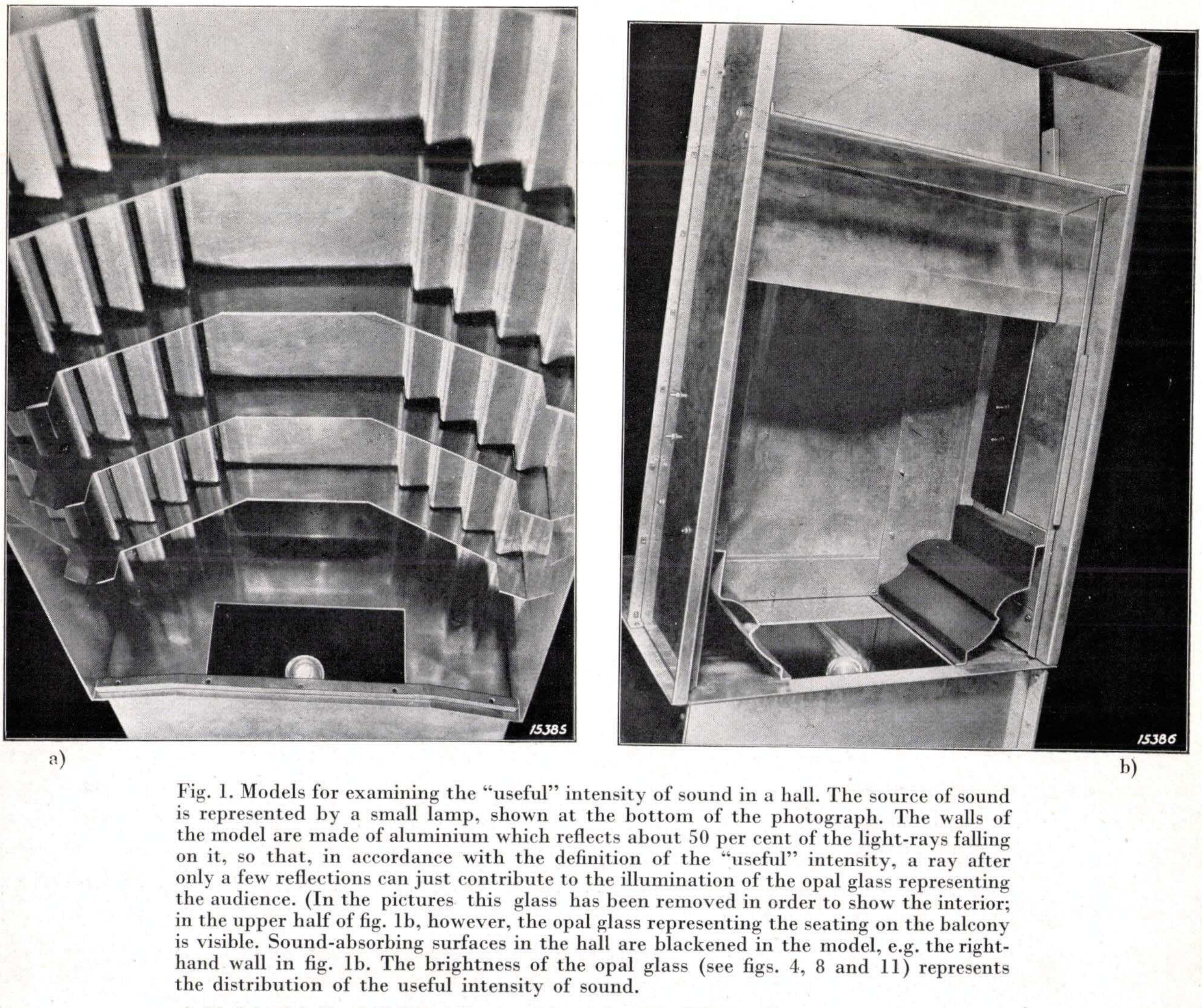

a) b)

Fig. 1. Models for examining the "useful" intensity of sound in a hall. The source of sound is represented by a small lamp, shown at the bottom of the photograph. The walls of the model are made of aluminium which reflects about 50 per cent of the light-rays falling on it, so that, in accordance with the definition of the "useful" intensity, a ray after only a few reflections can just contribute to the illumination of the opal glass representing the audience. (In the pictures this glass has been removed in order to show the interior; in the upper half of fig. 1b, however, the opal glass representing the seating on the balcony is visible. Sound-absorbing surfaces in the hall are blackened in the model, e.g. the right-hand wall in fig. 1b. The brightness of the opal glass (see figs. 4, 8 and 11) represents the distribution of the useful intensity of sound.

a) Model of hall of Philips "Ontspanningsgebouw" (Theatre) before reconstruction.

b) Model of the same hall after reconstruction on the plans of Prof. Witzmann, Vienna.

i.e. the resultant luminous intensity is actually a measure of the useful sound intensity. In the model the area occupied by the audience was represented by an opal glass plate with a low reflecting power [1]). The brightness of this plate which may be observed and photographed from the outside, gives a picture of the distribution of sound intensity over its area.

How far is our assumption that an analogy exists between sound and light waves justified? We all know from experience that sound waves per se exhibit an entirely different behaviour to light waves. Light is propagated rectilinearly, undergoes simple reflection and casts deep shadows. From a superficial glance, none of these properties appears to be shared by sound waves. Sound travels round corners, does not throw deep shadows and on the whole does not appear to obey the laws of simple reflection to any extent (except in the case of echoes) but always seems to undergo scattered reflection. This difference in behaviour is due to the difference in wave-length; visible light is made up of (ether) waves with a wave-length from 0.4 to 0.76 μ, while audible sound consists of atmospheric waves with a wave-length from 6 cm to 6 m, i.e. 100,000 to 10 million times longer. Waves which strike an obstruction will behave similarly if the dimensions of the obstruction are the same relative to the wave-length. Thus sound waves are reflected at surfaces in exactly the same way as light waves, if the dimensions of the surface are large as compared with the wave-length, although surface inequalities which just permit a true reflection of sound waves may be far greater for these waves than for light waves. It is, therefore, necessary to use a perfectly smooth surface for light, while sound can still exhibit true reflection at fairly rough-finished walls. We can therefore assume that sound in an auditorium is reflected in the same way as the light-rays in our models. It is true this no longer applies to low-frequency sounds, as a hall usually contains many surfaces which are not very large in comparison to these (long) wave-lengths. But the intelligibility of the spoken word depends in a large measure on just the higher socalled characteristic frequencies (thus whispered words in which the low tones in particular are absent can be heard almost equally as well as loudly-spoken words). These frequencies are in the neighbourhood of 1,000 cycles, corresponding to a wave-length of 30 cm. For these important speech frequencies the light model can, therefore, be definitely employed.

Application of the Method

Firstly a model was built of the hall before reconstruction (*figs. 1a, 2 and 3*). The length of the hall was 34 m, its width 16 m and the greatest height 9 m. At an earlier period the rear wall had been completely covered with Akusti-celotex to suppress echoes. The floor sloped a little upwards. The roof was supported by framework trusses and was of stepped construction with the vertical sections of glass, which were closed by roller shutters during performances. The trusses were completely covered by a panelling and thus formed transverse walls 1.8 m high.

On making a closer examination of the distribution of brightness on the opal glass of the model (*fig. 4*), a feature which strikes one immediately is the abundance of light close to the stage, representing the direct sound. Perhaps more striking still is the fact that this intensity diminishes so rapidly to the rear, much more rapidly in fact than should follow from the quadratic diminution in intensity with distance for a point source of light. The

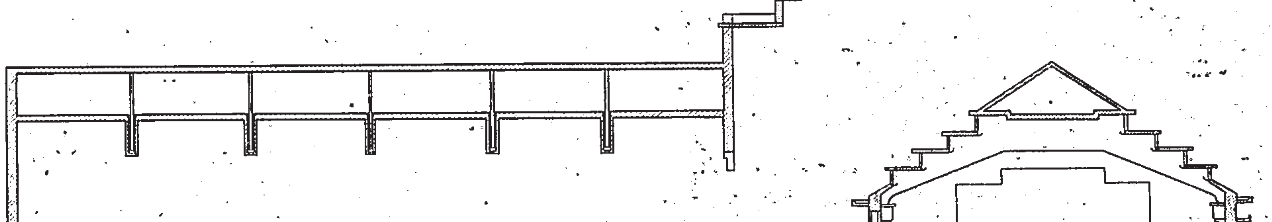

Fig. 2. Longitudinal and transverse sections through the hall of the Theatre before reconstruction. The hall was very low compared to its length. Note the transverse partitions in the roof which are formed by the roof trusses.

---

[1]) The coefficient of absorption of the audience is taken as 0.90 to 0.95.

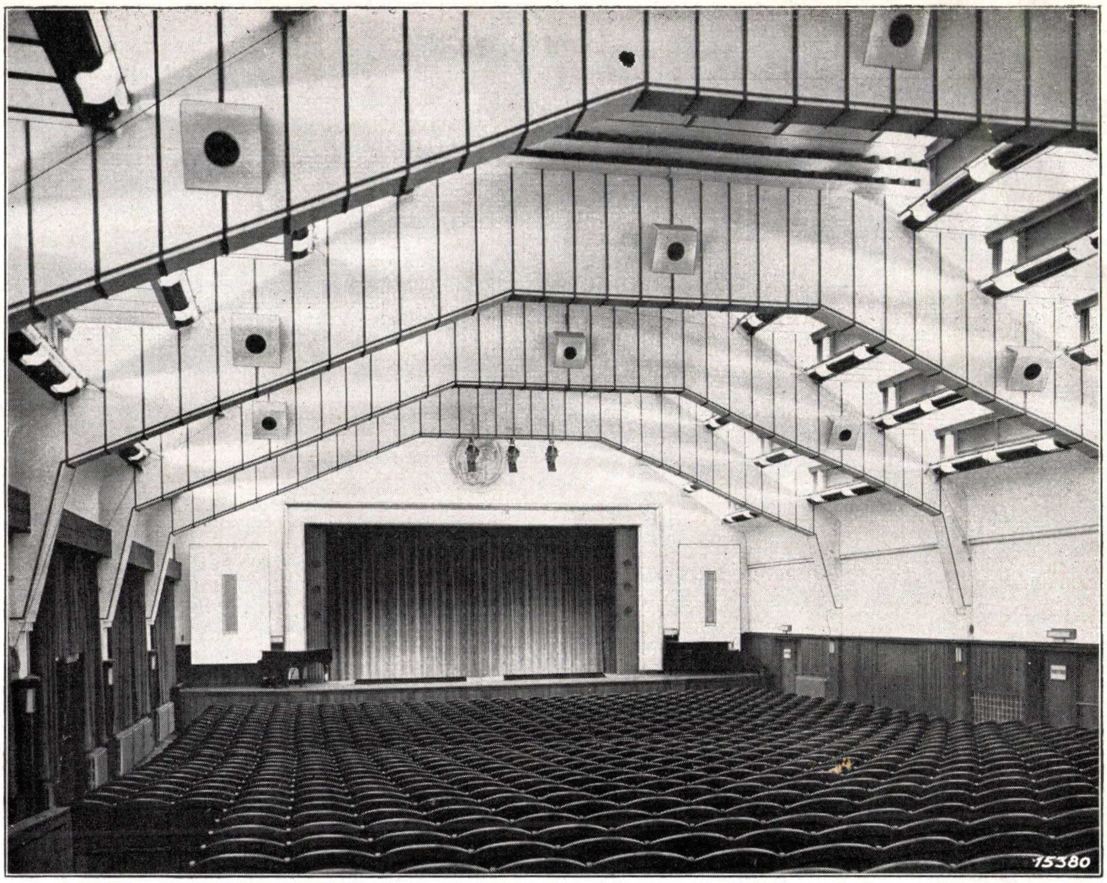

Fig. 3. Auditorium of the "Ontspanningsgebouw" (Theatre) before reconstruction.

reflection at the ceiling, however, which is shown as a trapezoidal area of light in the foreground, has a very high intensity, much greater than that of the direct sound, although the distance from the source of sound along the reflected ray is much greater and in reflection a certain amount of absorption has taken place.

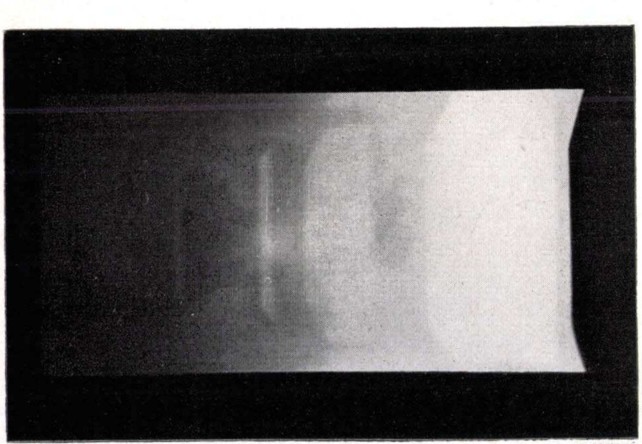

Fig. 4. Photograph of the opal glass in the model of the old hall (fig. 1a). The stage is on the right-hand side. The rapid diminution in illumination intensity towards the left may be noted: at the rear of the hall the useful sound intensity was far too small. The bright trapezoidal spot near the stage is due to reflection at the forepart of the ceiling (see text) which was not screened by the transverse roof trusses.

And yet this phenomenon is easy to account for. The brightness of the opal glass is determined by the quantity of light falling on unit area. The source radiates light with an equal intensity in all directions, so that the intensity of illumination is determined by the solid angle which the unit of surface subtends at the source. As the height of the source above the audience is not very great and the floor slopes only slightly, this solid angle diminishes very rapidly towards the back (*fig. 5*).

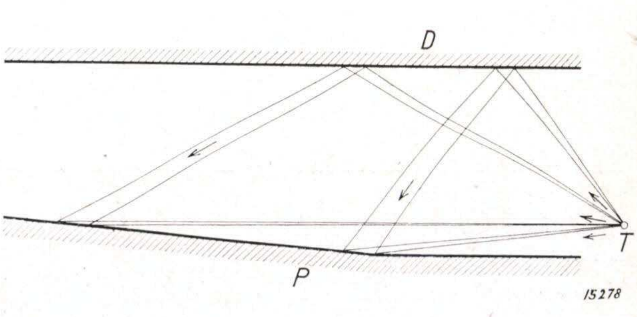

Fig. 5. Effect of reflection at the ceiling. In the normal case of a slightly sloping floor (auditorium P) the solid angle subtended by the audience at the sound source T decreases rapidly towards the rear of the hall. On the other hand, the solid angle subtended by the audience at the mirror image of the sound source above the ceiling D diminishes much more slowly: Reflection at the ceiling contributes more to the sound intensity than the direct sound waves.

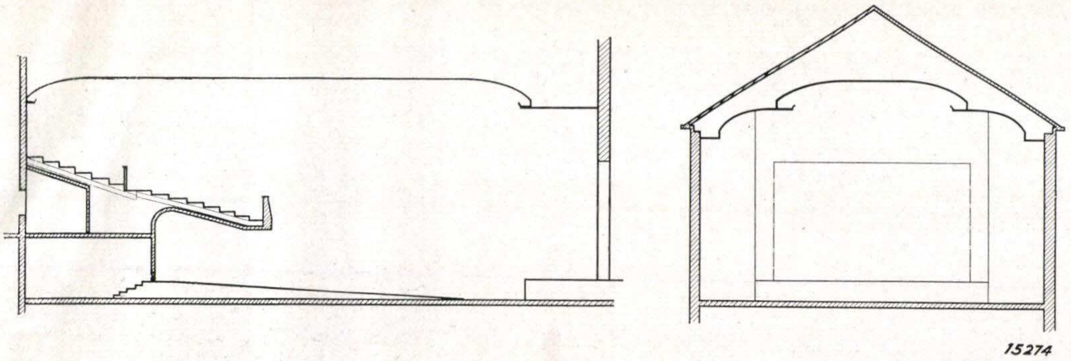

Fig. 6. Longitudinal and transverse sections of the hall in the Theatre after reconstruction on the plans of Prof. Witzmann. The auditorium has been made shorter and higher (cf. fig. 2), and a balcony has been added, the seating accomodation being practically the same as in the old hall.

On the other hand, the solid angle which the unit of surface (in the auditorium) subtends at the mirror image of the source above the ceiling is much greater in spite of the greater distance these are apart. It is thus clear that the audience receives far more energy fro[illegible]eflected ray than from the direct ray [2]).

The roof trusses prevent the sound reaching the back parts of the hall by reflection at the ceiling, so that in that area only the weak direct sound is received. The rear wall of the hall reflects the sound,

---

[2]) It may be argued against this that the sound receiver in the auditorium (the head of a person in the audience) is vertical and the solid angle it subtends at the stage must not be compared with a surface of the same area located on the sloping floor. It could thus be deduced that the sound intensity received by reflection at the ceiling could in no case be greater than the direct sound. This explanation would, however, not be correct: the seating and the audience, particularly in the projection perpendicular to the direction of the direct sound, in their parts have measurements of the order of magnitude of the sound wave-lengths and thus act as a single absorbing surface; or, expressed in other words, the seats or the heads of the audience screen off the sound by their diffraction effect, although one can see optically across the elements of this diffraction "grating". Cf. Békésy, Z. f. techn. Phys. **14**, 6, 1933, and Brillouin, Rev. acoust. **4**, 113, 1935.

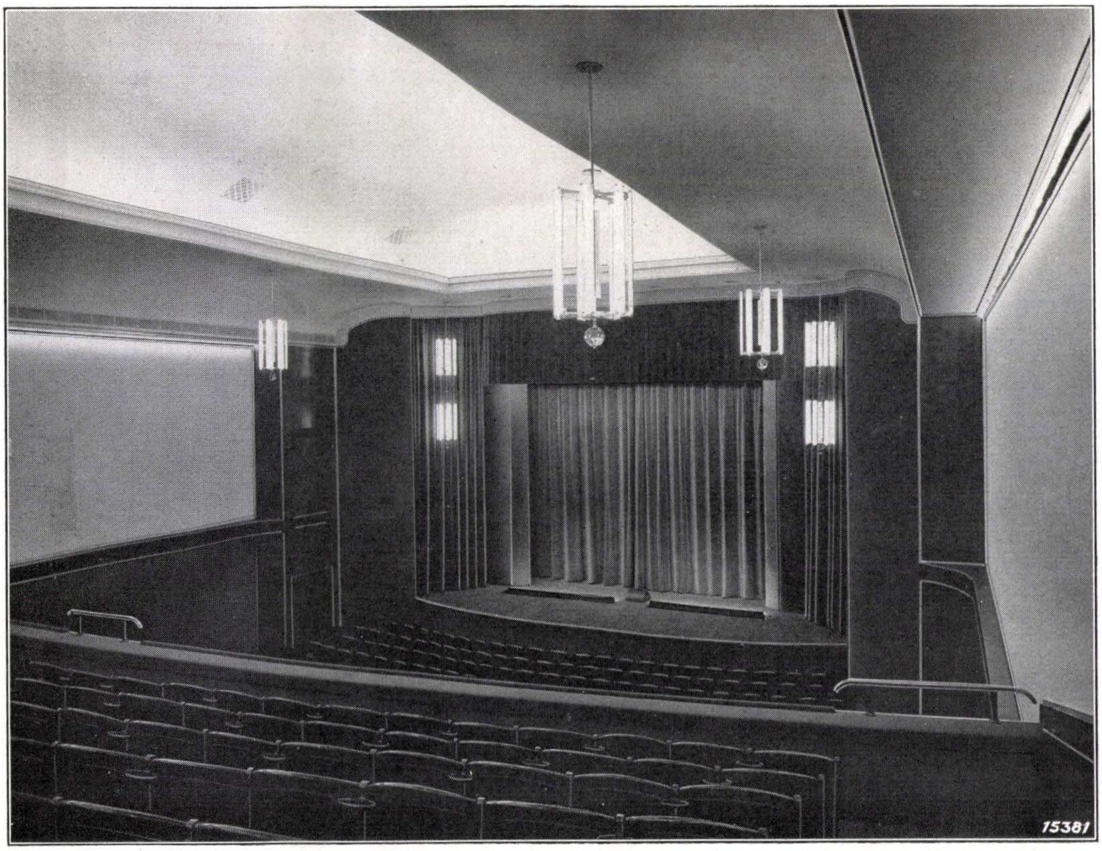

Fig. 7. Auditorium of the Theatre after reconstruction, as seen from the balcony.

not towards the audience, but also towards the ceiling, or rather to the roof trusses, so that this sound is also lost and only becomes audible after a large number of reflections as reverberation. It was, therefore, correct in this case to make the rear wall sound-absorbing.

This model shows in a most convincing manner that in general the largest part of the audible sound comes from the roof, provided the latter is of suitable design. Further confirmation of this is the fact that in open-air theatres the spoken word is much less audible. To remedy this drawback, the benches are arranged on a steep slope or amphitheatre, and it is clear that as a result thereof the available solid angle through which sound is received is considerably increased.

The second model made was of the same hall reconstructed on the plans of Prof. Witzmann of Vienna (*figs. 1b, 6 and 7*). The whole roof has been raised and a ceiling fixed under the trusses. The hall has also been made shorter and a balcony added, which runs further back than the lower part of the hall. The new dimensions are: Width 16 m, height 11 m, length 22 m, and length with balcony 28 m. The seating accomodation has been left practically unchanged. The improved distribution of sound was immediately revealed by the new model (*fig. 8*). The forepart of the auditorium again receives a large percentage of direct sound, and from the middle of the hall reflection at the ceiling comes into play and transmits a satisfactory intensity of sound to the balcony also. The space under the balcony naturally receives no part of this reflected sound and is therefore shown in the model as much darker. How this drawback has been remedied is outlined below.

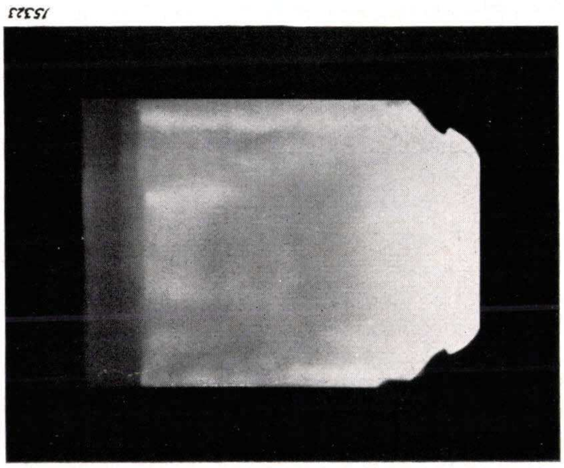

Fig. 8. Photograph of the opal glass in the model of the new hall (fig. 1b). The stage is again on the right-hand side. The distribution of illumination (useful sound intensity) is much more uniform than in fig. 4. The rear part of the hall under the balcony is still fairly dark (see text and fig. 11).

The side walls are panelled and hence absorb sound to some extent. The model and experiments in a "ripple tank" [3]) (*fig. 9*) had already demonstrated that the sound falling on the walls of the auditorium did not have much opportunity to reach the audience as useful sound. After repeated reflection between the walls the bulk of this sound contributes to reverberation. The side-walls thus appeared to be the most suitable places for fixing the panelling, which was necessary to reduce the reverberation period to the desired value (for this purpose a certain degree of absorption at the walls is necessary).

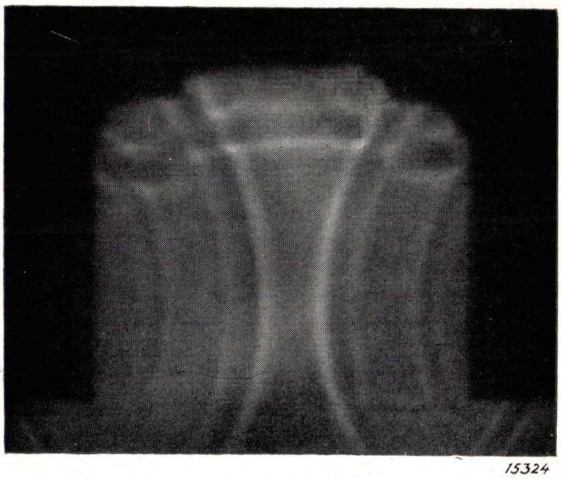

Fig. 9. Registration of waves in a ripple tank model of the cross-section of the new hall. By this means the effect of reflection at the side walls was investigated. It is seen that the waves are in the main reflected to and fro between the walls, so that they do not contribute much to the useful sound intensity but only increase reverberation.

In this way the requirement has been met as far as practicable that the sound shall reach the audience either directly or after one or two reflections (with the largest possible solid angle) and then be absorbed. All other sound has to be absorbed to such an extent that the hall does not possess too small a reverberation period. The hall can therefore also be used for concerts for which a greater blending of sound is required, i.e. the sound-waves also after several reflections must reach the audience with sufficient intensity.

It must still be outlined how the audibility under the balcony was improved. After the optical models had shown that the intensity there was too small, the area in question was examined in greater detail

---

[3]) In these experiments a reduced section of the hall is filled with water and the propagation of small artificial water waves is studied.

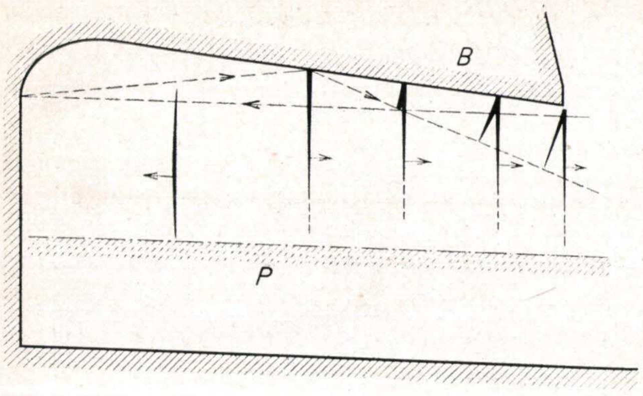

Fig. 10a. Path of a sound wave entering the space under the balcony B and reflected at the vertical rear wall. The wave is so to speak folded back by reflection at the underside of the balcony and again leaves this space without reaching the audience P.

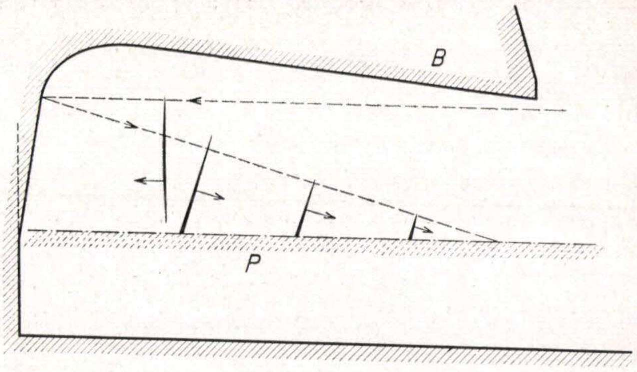

Fig. 10b. The same wave as shown in fig. 10a, but with a wall sloping slightly forward in place of the vertical wall. The entering wave is now immediately reflected to the audience.

in the ripple tank. It was then found that the rear wall reflected an intense wave to the underside of the balcony, but which impinged against the latter at such a small angle of incidence that it was not reflected to the seats under the balcony (*fig. 10a*). The wave was as it were folded up and left the space as a concentrated packet of waves, passing just under the edge of the balcony. This difficulty was very easily remedied: If the rear wall is given a slight slope forward the sound waves are reflected directly to the audience in this part of the hall (*fig. 10b*). Naturally in doing this care must be taken that only the back rows are reached by the wave so that not too long an interval intervenes between the arrival of the direct sound and that of the sound reflected at the wall (echo). In the model the effect of the sloping rear wall was clearly demonstrated (*fig. 11*).

Already during the inaugural performances in the new hall on October 11, 12, and 13, 1935, audibility was found to be very good in all parts of the auditorium; later performances confirmed that at all points of the hall, also under the balcony, the words spoken on the stage were now clearly intelligible and no effort in listening was required whatsoever.

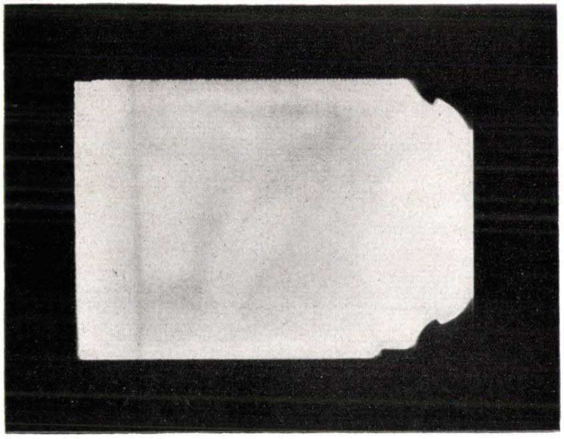

Fig. 11. Photograph of the opal glass in the model, as in fig. 8, but now with the rear wall under the balcony sloping slightly forward. The space under the balcony now also receives a satisfactory intensity of sound.

A HIGH-FREQUENCY FURNACE WITH VALVE GENERATOR

Summary. An induction furnace employed in the foundry of Philips works especially for melting charges of scrap is described. Alternating current of high frequency is required as a power supply for the furnace and is generated with the aid of a transmitting valve which has a useful output of 250 kW.

To be of service to other finishing branches of its works, Philips have for some years been operating their own melting shop and foundry, which for example produces a chrome-iron alloy that can be fused with glass to give a vacuum-tight joint and in view of this property is employed in a large number of apparatus. One of the commonest functions of the melting shop is to melt comparatively small quantities of material under conditions guaranteeing a prescribed analysis within narrow limits of composition. In this work great difficulty is usually experienced with alloying constituents which burn in air, such as the carbon in ferro-alloys, or are very volatile, such as zinc and cadmium in copper alloys. The electric arc furnace, which was originally used for all melting operations, did not conform with the increasingly severe requirements in this direction, since a marked volatilisation of the volatile constituents was found to occur at the electrodes whose temperature was about 4000 deg C. It thus became necessary to build a new melting furnace, which had to meet the following requirements:

1) The furnace must take a charge of 50 kg of iron, and also enable scrap and other waste materials to be utilised;
2) The melting charge must be kept free from all impurities; any contact with combustion gases or electrodes was therefore undesirable.
3) To reduce the volatilisation of volatile constituents, temperatures above the casting temperature must be avoided as far as possible. For the same reason the melting time must not exceed 15 minutes.

To meet these requirements, the method of eddy-current heating was adopted, i.e. the heating of the melting charge by electrical eddy currents which are produced in the charge itself by alternating magnetic fields.

In this process the melting charge does not in fact come in contact with either combustion gases or electrodes. In addition, the fusing metal constitutes the hottest part of the furnace so that no temperatures higher than the melting temperature occur.

The first attempts at utilising eddy current heating for practical purposes were made some 30 years ago (Soc. Schneider, Creuzot and O. Zander, 1905). Fundamental theoretical investigations of the induction furnace were carried out by Northrup [1]), Ribeaud [2]), Wever and Fischer [3]), Burch and Davis [4]), Strutt [5]) and others. Details about the general behaviour of an induction furnace will be given below in connection with the description of the Philips melting plant. It has been found that the efficiency of inductive heating in general increases with the frequency. The smaller the pieces making up the charge, the higher are the frequencies required. If pieces of metal a few centimetres in diameter are to be melted with a satisfactory efficiency, frequencies from 5000 to 10000 cycles are found to be necessary.

A voltage of this high frequency cannot be readily and easily produced with ordinary generators. A transmitting valve was therefore employed, viz, Philips TA 20/250 valve which on correct adaptation can furnish a useful output of 250 kW ($V_{\mathrm{eff}} =$ rms 14000 volts, $I_{\mathrm{eff}} = 18$ amps). This output is greater than that required for melting the charge in 15 minutes.

---

[1]) Northrup, J. Frankl. Inst. **20**, 240, 1926.

[2]) M. G. Ribeaud, La technique moderne, **19**, No. 8-9, 1929.

[3]) F. Wever and W. Fischer, Inst. f. Eisenforsch. **8**, 149, 1926.

[4]) C. K. Burch and N. R. Davis, Arch. f. El. **20**, 211, 1928.

[5]) M. J. O. Strutt, Ann. d. Phys. **82**, 605, 1927; Arch. f. El. **19**, 424, 1928.

Description of the Induction Furnace

The melting throughput of the plant was required to be 200 kg of steel per hour, for which about 250 kW are drawn from the mains supply. The furnace plant can take a load of 300 kW so that it has an ample rating. The capacity of the melting crucible is 12.5 litres (diameter 20 cm and height 40 cm) which when half charged represent 50 kg of steel. If material is added during the melting process, the total charge can be increased to 100 kg. As the time taken for the settling and removal of the slag and for casting is roughly the same as that required for melting alone, two furnaces have been installed which are connected alternately with the same electrical supply. The latter is therefore in constant service.

The furnaces are so small and easy to manipulate that no casting ladles are required. The charges are poured directly into the moulds placed below the furnaces. In this way operations are continuous and regular, while with larger furnace charges the casting metal, after requiring a longer period for melting, must be distributed through one or more intermediate ladles to the various moulds and in fact with great speed, as otherwise the melt is too hot at the start or too cold at the end of casting.

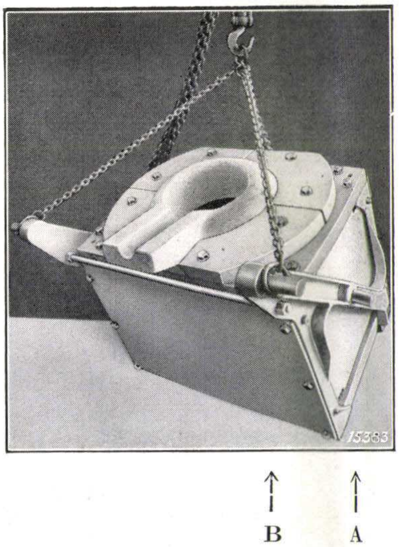

Fig. 1. Induction furnace. On the right-hand wall are the trunnions A and B which support the furnace during service. During heating the furnace rests in A and during casting in B.

Figs. 1 and *2* show the furnace installed ready for use and with the side walls removed. The base and cover plates of the furnace are made of insulating material and are joined together with brass angles. These plates support the fireproof crucible which is surrounded by an induction coil, being insulated from the latter by an earthenware jacket and a layer of asbestos. The self-induction of the coil is 0.125 millihenry; it is of single-lay and consists of 20 windings of rectangular copper tube, 12.5 by 25 mm, through which cooling water is passed during service. The diameter and height are each 40 cm. In the construction of the furnace, mutual insulation of the metal parts was provided, in order to avoid any short circuits in which powerful eddy currents could be formed. Owing to these precautions the brass units only become hand-warm. Iron which offers a much greater resistance to eddy currents would become red-hot under the same conditions.

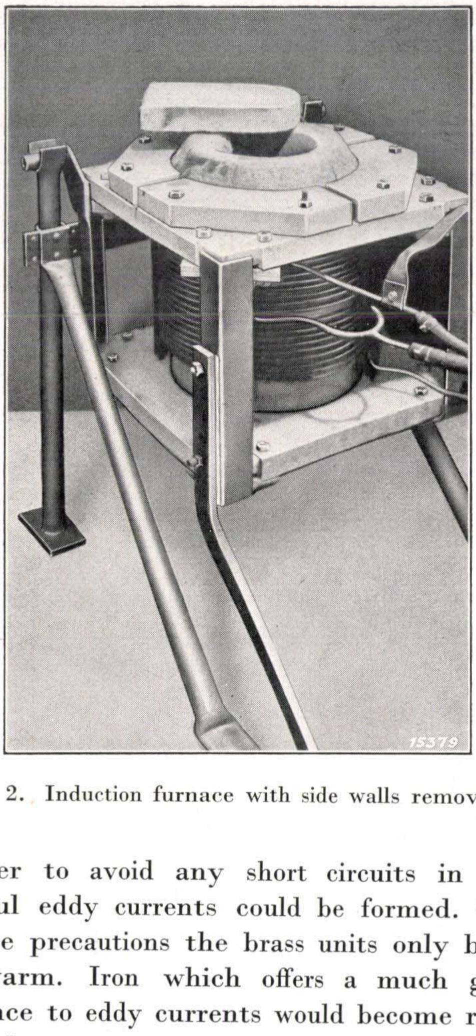

Fig. 2. Induction furnace with side walls removed.

Fig. 3 is a general view of the furnace platform and shows the suspension of the furnace during the heating period (left) and during casting (right). During the heating period the furnace is supported by two axle bolts (one of which is visible in fig. 1) which are located just above the centre of gravity, thus enabling the furnace to be easily turned. When pouring the charge, the furnace is turned by the tension of a wire rope. The mouth then moves in a circle forwards and downwards until two other axle bolts, fixed in line with the axis through the mouth, drop into the corresponding bearings.

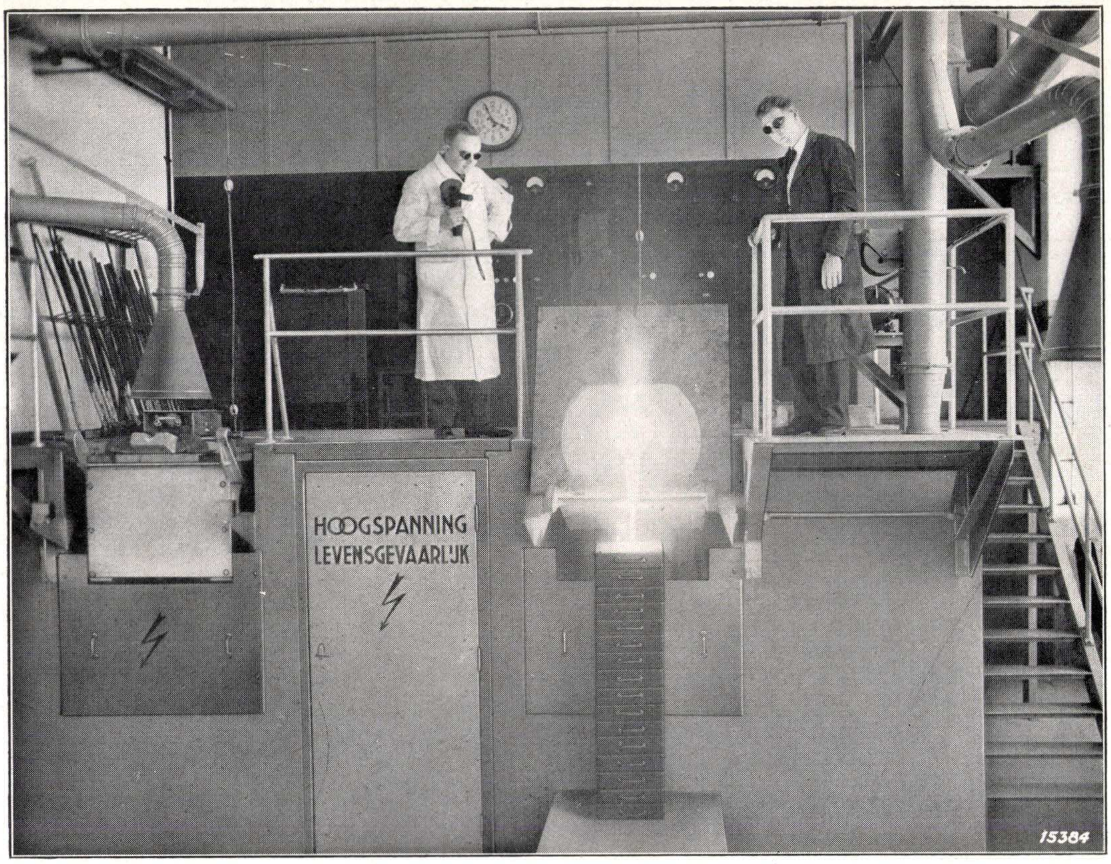

Fig. 3. General view of the melting plant. Behind the furnace is the switchboard for the electrical plant which heats the two furnaces alternatively. The door marked "Hoogspanning" is the entrance to the transformer room.

This position has been reached by the right-hand furnace in fig. 3. With continued tension on the rope, the furnace turns about its mouth so that the stream of poured metal remains in one position and it is unnecessary to move the mould during casting.

The Electrical Plant

Fig. 4 shows the general lay-out of the electrical plant. The latter is made up of a high-frequency generator, an air-core transformer which reduces the voltage from 12500 $\text{volts}_{\text{eff}}$ to 5000 $\text{volts}_{\text{eff}}$, and the condenser C, which takes up the wattless current of the furnace coil. The self-induction of the furnace is represented by L and the non-reactive resistance by R. This non-reactive resistance is made up of the eddy current losses in the charge, the ohmic losses in the coil and the dielectric losses in the condenser. As the oscillating circuit of the valve generator is formed by the furnace coil L and the condenser C themselves, it always operates with the natural frequency of the L-C-circuit. At this frequency the impedance at the poles of the generator is a true non-reactive resistance, thus avoiding an unnecessary loading with reactive currents. The resistance is determined by the type and temperature of the charge, but can also be altered by varying the capacity C[6]).

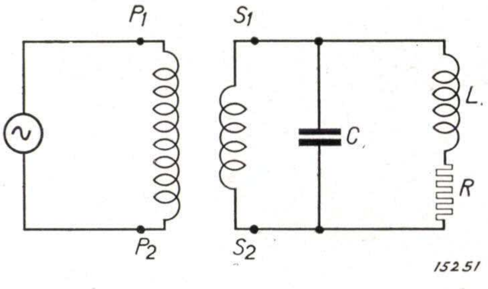

Fig. 4. Electrical lay-out of the melting plant.

This method is employed to maintain the loading resistance of the generator practically constant during the heating of the crucible.

---

[6]) This naturally also alters the frequency of the alternating voltage applied to the furnace coil.

Owing to the variability of the loading resistance, the transmitting valve constitutes a marked advance over the mechanical generator. To derive the full output from a current generator the loading resistance must have a definite value. With a mechanical generator, however, the loading resistance cannot be varied in the manner described above because the frequency is generally fixed. It would therefore be necessary to alter the capacity C and the self-induction L simultaneously in such a way that the natural frequency

$$f = \frac{1}{2\pi\sqrt{LC}}$$

of the oscillating circuit maintains exactly the same value as the frequency of the mechanical generator.

Fig. 3 shows the switchboard of the transmitting-valve plant located at the rear of the platform. The door marked "Hoogspanning" is the entrance to the transformer room which also accomodates a large battery of condensers. *Fig. 5* shows a view of this room as seen from the door, while *fig. 6* shows half of the condenser battery. This battery is made up of 72 separate condensers, each of 0.083 μF, which can be interconnected in four different ways. In the four positions of the switch drum, the following capacities are obtained:

0.75 μF, 1.5 μF, 4.5 μF and 6 μF.

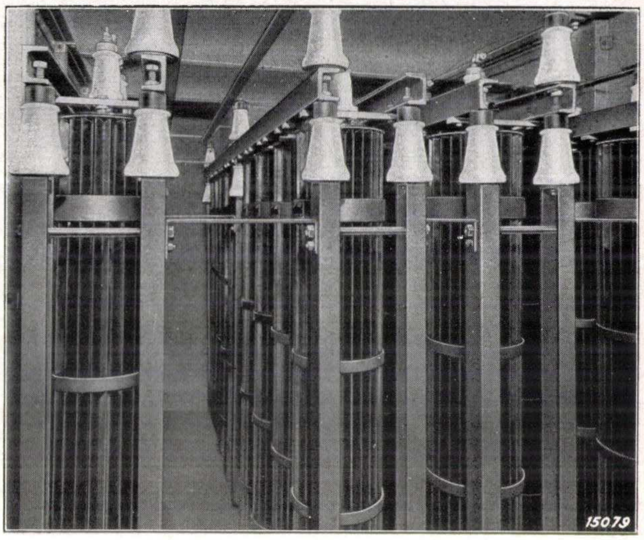

Fig. 6. Half of the battery of condensers. The 72 condensers, each of 0.083 μF, are arranged in 8 series.

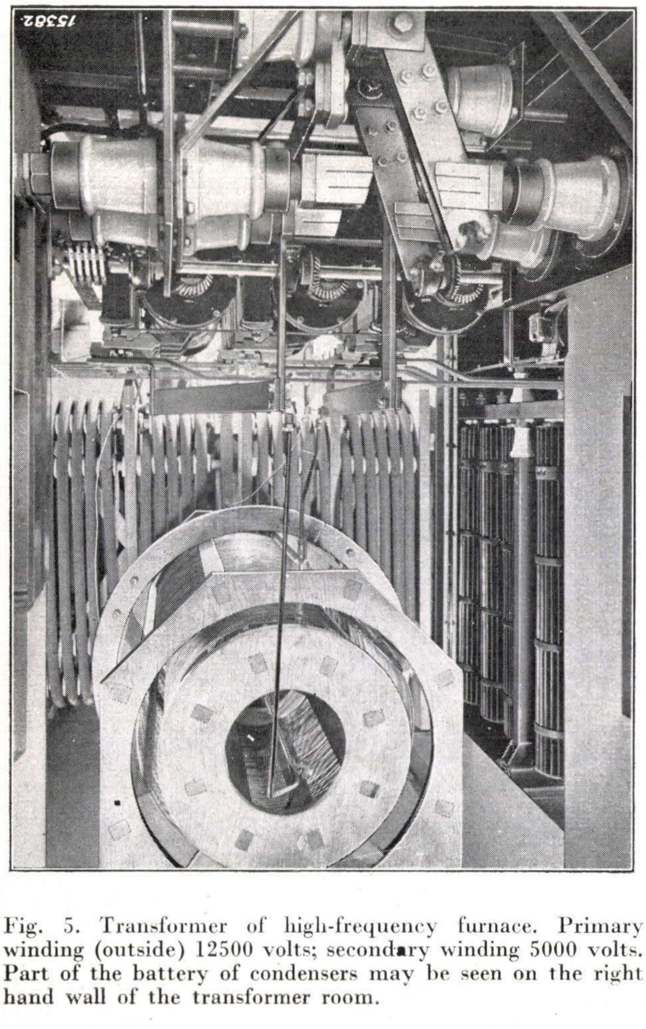

Fig. 5. Transformer of high-frequency furnace. Primary winding (outside) 12500 volts; secondary winding 5000 volts. Part of the battery of condensers may be seen on the right hand wall of the transformer room.

The phase difference of the condensers is given by $tg\ \delta = 0.007$. In consequence of the high voltage and frequency of the current the dielectric losses are quite considerable. The dielectric losses N of a condenser are given by:

$$N = \omega C \cdot V_{eff}^{2}\, tg\ \delta = \sqrt{\frac{C}{L}}\, V_{eff}^{2}\, tg\ \delta$$ rms

Substituting the respective numerical values: $V_{eff} = 5000$ volts, $C = 6$ μF and $L = 0.09$ millihenry, one obtains as a maximum value of the losses

$$N = 45 \text{ kW}.$$

Table I collates the principal data relating to the high-frequency furnace.

Table I. Operating data, relating to the high-frequency furnace.

Capacity of condenser C	Frequency of alternating current
0.75 μF	16300 to 18000 cycles
1.5 μF	11600 to 12800 cycles
4.5 μF	6700 to 7400 cycles
6.0 μF	5800 to 6400 cycles

Self-induction of coil: 0.09 to 0.125 millihenry (depending on the charge).

Voltage applied to furnace coil: . . .	5000 volts eff r.m
Apparent power	Max. 6400 kVA
Effective power	Max. 200 kW
Useful power in charge:	Max. 130 kW

The required rate of heating is readily attained with the furnace. With a loss of 30 per cent as a result of thermal conduction and radiation, about 18 kW-hrs. are required for melting 50 kg of iron. As under the most favourable conditions of adaptation about 130 kW are furnished to the charge, the time required for melting is found to be 8.3 minutes. The actual time taken is of course longer, but even with the most difficult charge in the crucible only 10 to 15 minutes are required.

In the case of metals with a higher conductivity than iron, the proportion of the total power supplied which is absorbed by the charge is naturally smaller. Nevertheless aluminium, silver and copper can also be melted in this high-frequency furnace. At a first glance this appears surprising, since for instance a charge of copper shavings can in no case be heated to a higher temperature than the copper induction coil itself, if the diameter of the shavings is not greater than that of the copper tube of which the coil is made. This shows quite clearly that water cooling is imperative. Cooling keeps the resistance of the induction coil low, while the resistance of the charge rises as a result of heating to about 4 times its initial value.

Discussion of the Method of Operation of the High-Frequency Furnace

Omitting all consideration of the processes in the high-frequency furnace itself, we can regard it as a loading impedance with an inductance L and a resistance R. For the plant in question we thus obtained the diagram shown in fig. 4. At the resonance frequency, the secondary terminals S_1 and S_2, of the transformer are loaded with a non-reactive resistance W, which in the case of a sufficiently small damping resistance R [7]) of the oscillating circuit, is given approximately by:

$$W = \frac{L}{CR}$$

As already pointed out, the commutable capacity C is so adjusted that the resistance W approaches as close as possible to a specific optimum value W_S. In this case W_S is 127 ohms. The resistance across the primary terminals of the transformer is then $W_P = W_S$ times squared transformation ratio $= 127 \times 6.25 = 720$ ohms.

It is thus equal to the internal resistance of the transmitting valve.

A somewhat closer insight into the process of heat evolution in the furnace is obtained by regarding the furnace coil as the primary winding of a transformer whose secondary winding constitutes the path of the current in the charge. This is shown in the diagram in *fig.* 7 where the indices 1 relate to the furnace coil and the indices 2 to the current path through the charge.

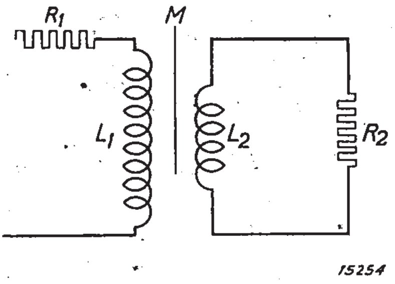

Fig. 7. Substitution diagram for high-frequency furnace. L_1 and R_1 are the self-induction and resistance of the furnace coil. L_2 and R_2 are the self-induction and resistance of the charge. The mutual induction is represented by M.

Owing to the mutual inductance M the resistance of the charge is imparted to the primary coil. In order to obtain a satisfactory efficiency, this resistance R_K which is coupled to the input side must be as large as possible compared with the input resistance R_1. The power input is

$$N = I_{\mathrm{eff}}^2 \, (R_1 + R_K)$$

and the efficiency

$$\eta = \frac{R_K}{R_1 + R_K}$$

If ω is the frequency of the alternating current expressed in circular measure, one obtains by a simple calculation

$$R_K = \frac{R_2 \; M^2 \; \omega^2}{\omega^2 \; L_2^2 + R_2^2} \quad . \quad . \quad . \quad (1)$$

Equation (1) is derived from the transformer equations:

$$I_1 \, (R_1 + j \, \omega \, L_1) + I_2 \, j \, \omega \, M = U_1$$
$$I_1 \, j \, \omega \, M + I_2 \, (j \, \omega \, L_2 + R_2) = 0,$$

which express the relationship between the primary voltage U_1 and the primary and secondary currents I_1 and I_2. Eliminating I_2 from these equations, one obtains:

$$U_1 = I_1 \left[R_1 + j\omega L_1 + \frac{R_2 \cdot \omega^2 M^2}{\omega^2 L_2^2 + R_2^2} - \frac{j\omega L_2 \cdot \omega^2 M^2}{\omega^2 L_2^2 + R_2^2} \right]$$

The third and fourth terms in this expression give the additional resistance R_K and a corresponding (negative) additional inductance.

---

[7]) "Small damping" signifies $\frac{R^2 C}{L} \ll 1$.

The variation of R_K with respect to ω is shown in *fig. 8.* This diagram shows (R_K/R_2). (L_2^2/M^2) plotted against $(\omega L_2/R_2)$.

It is seen from the curve that R_K at first rises quickly with the frequency, eventually to become asymptotic to the limiting value: $R_K \rightarrow R_2\, M^2/L_2^2$.

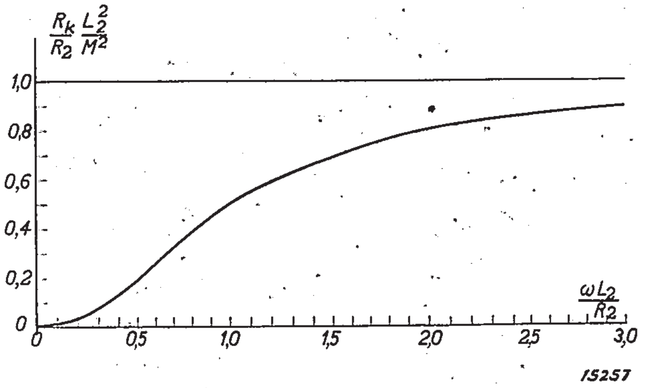

Fig. 8. Coupling resistance R_K plotted against the frequency. When $\omega\, L_2/R_2 = 3$, R_K assumes 90 per cent of its asymptotic limiting value.

As already stated, a high coupling resistance is required in order to obtain a satisfactory efficiency. The frequency must therefore be made so high that the limiting value is almost obtained. On the other hand, it is desirable to keep the frequency as low as possible since at a given output the losses exterior to the furnace as a rule increase with the frequency. We shall therefore stipulate a coupling resistance of only 90 per cent of the limiting value, which according to the graph (8) corresponds to the condition that:

$$\frac{\omega L_2}{R_2} > 3 \quad . \quad . \quad . \quad . \quad (2)$$

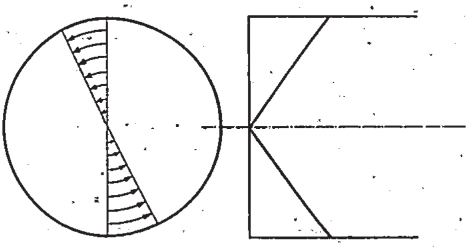

Fig. 9. Intensity of eddy currents produced in a metal cylinder by a homogeneous magnetic field in the direction of the axis. The arrows indicate the direction of the eddy currents.

A further increase in the frequency (in radians) would result in very little improvement of the efficiency.

The substitution of a self-induction L_2 and a resistance R_2 for the electrical properties of the charge asks for a further comment. The distribution of the eddy currents in the charge depends on the frequency of the magnetic field, and as a result L_2 and R_2 also vary with the frequency.

In order to visualise the distribution of the eddy currents, consider firstly the limiting cases at very low and very high frequencies. Consider a cylinder whose axis is parallel to the magnetic field (*fig. 9*). It is well known that the induction currents are in such directions that within the metal they weaken the magnetic field. If the frequency is sufficiently low, the induced voltages and currents are, however, so small that the weakening of the field can be neglected. In this case the distribution of current shown in fig. 9 is obtained. The current density is zero along the axis and increases in proportion to the radius.

The higher the frequency, the greater will be the weakening of the magnetic field in the interior of the cylinder. At the same time the eddy currents in the interior also become weaker and with rising frequency we get in succession the current distribution curves II, III and IV shown in *fig. 10.* In the limiting case of a very high frequency the current flows merely through a thin layer at the surface.

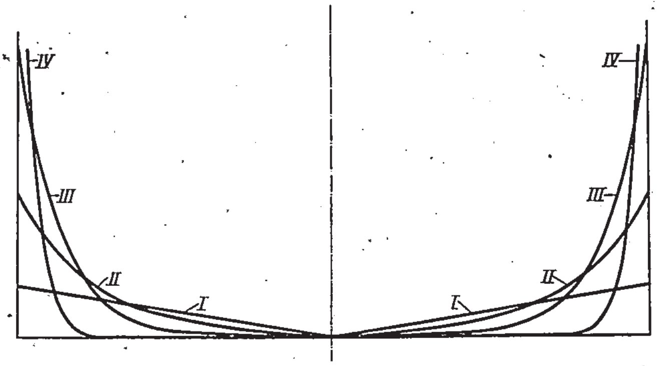

Fig. 10. Intensity of the eddy currents produced in a cylinder at different frequencies. Owing to the natural magnetic field of the eddy currents, the total field is not homogeneous, but greater at the walls than in the interior. With rising frequency the current distribution is altered from I (see also fig. 9) to II, III and IV.

We shall reserve the opportunity of returning to these interesting phenomena in greater detail in a subsequent issue of this periodical. Closer investigation shows that the condition $\omega L_2/R_2 > 3$ in every case leads to such a high frequency that the displacement of the magnetic field from the interior of the pieces making up the charge already becomes very pronounced. The current flows through a layer at the surface, whose thickness at a given frequency is only slightly dependent on the sizes of the pieces. In this case the fraction of the self-induction value L_2 due to a single piece (e.g. of spherical shape) will increase with the volume, while the resistance R_2 will be practically independent of the size of the piece. As a result the ratio L_2/R_2 will increase with the size modulus. The smaller the pieces making up the charge, the higher therefore will be the frequency required in order to make $\omega L_2/R_2$ sufficiently large.

With the frequencies of 6000 to 7000 cycles used here, the condition $\omega L_2/R_2 > 3$ is still met with pieces a few centimetres in size. In general the policy will be not to use the frequencies higher than are absolutely necessary, as the generation of high-frequency alternating currents with a satisfactory efficiency becomes progressively more difficult as the frequency is raised (e.g. owing to the increase in the dielectric losses).

Convection Currents in the Melt

A particularly valuable characteristic of the induction furnace is the production of convection currents in the melt by the action of electromagnetic forces, which promote a rapid and uniform intermixing of the alloying constituents. The magnetic field acts on the conductor of eddy currents with a gravitational force directed inwards (the eddy currents are in a direction opposite to the current through the coil). The pressure in the fluid mass therefore increases towards the centre. *Fig. 11* shows diagrammatically the distribution of pressure in the melting crucible, which curve can also be regarded as a contour of the free surface. As near the surface of the melt the magnetic field is not homogeneous, the pressure caused by the magnetic forces will vary with the height. This leads to the formation of convection currents, which are marked qualitatively in fig. 11. With eddy currents of a given intensity, the pressure causing the convection currents is proportional to the magnetic field. In a practical sense this signifies that convection decreases with rising frequency, for the greater the frequency, the weaker are the magnetic fields required to generate the requisite eddy currents.

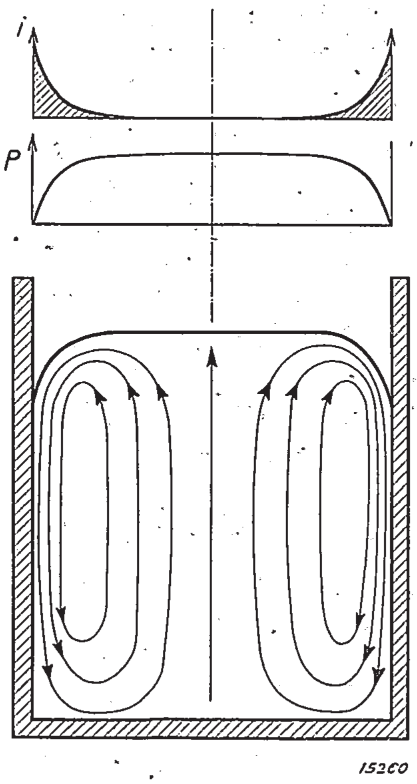

Fig. 11. Convection currents in the molten metal. Above: first curve, current distribution i; second curve: pressure P, produced by magnetic forces.

Compiled by G. HELLER.

PRACTICAL APPLICATIONS OF X-RAYS FOR THE EXAMINATION OF MATERIALS

II.

By W. G. BURGERS.

Two examples are given here of the examination of materials by means of X-rays in which the difference in the properties of the preparations examined is not due to a difference in chemical composition, but to a difference in texture, i.e. in the arrangement of the crystals of which the substances are built up.

The "scattering" of X-rays by crystals may be visualised as a reflection of the rays at the planes which are formed by the atoms in the crystal; from this it may be deduced that a substance in which the crystallites do not assume a preferred orientation gives rise to lines in the X-ray pattern which are uniformly black throughout their whole length. If, on the other hand, the crystallites have a certain preferred orientation (as is always found for instance in worked metals and also in many natural substances), the rays are reflected more strongly in certain directions than in others, and hence the blackening of the X-ray lines varies along their length.

In the limiting case where the rays impinge on only one crystal, this effect may be so pronounced that the lines are resolved into discrete points, whose arrangement then corresponds to that of the planes in the crystal lattice, i.e. to the symmetry of the crystal (Laue-photograph).

3. Quality Tests on Soapstone before Firing ¹).

Soapstone is a soft material which can be worked to exact dimensions. After suitable shaping it can be converted by firing (heating to about 1200 deg. C. during which about 6 per cent of water is given off) into a compact, hard and heat-resisting stone. During firing it frequently happens that certain places swell and as a result cracks appear which make the product useless. It is desirable to be able to detect and reject these pieces before firing, and as it appeared probable that the cracking was associated in some way with certain structural characteristics, examination by means of X-rays was indicated as offering a possible solution.

Fig. 1a shows a radiograph of that part of the raw material which did not swell on subsequent firing, while *fig. 1b* is a similar exposure of another part where swelling actually took place later.

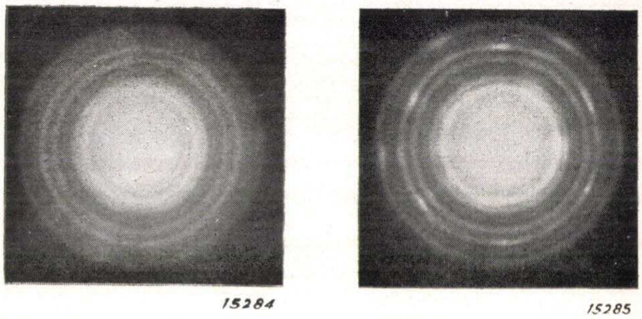

a) b)

Fig. 1. Radiographs of steatite before firing:
a) of a place which did not swell on subsequent firing, and
b) of a place which later swelled on firing.

An examination of these exposures reveals the same system of interference rings ²) in both. But there is a fundamental difference in that the intensity distribution is uniform round the periphery of the rings in exposure 1a, but varying in 1b, where certain intensity maxima appear round the circumference. This enables us to conclude that while there is no essential difference in composition at swelling and non-swelling places (identical systems of rings are obtained) there is yet a difference in texture: the places swelling on subsequent firing reveal that the crystallites favour a pronounced directional configuration (fibro-crystalline structure). Thus without entering into an analysis why this difference in structure causes a swelling during firing, we have evolved a method for testing the quality of soapstone before the firing process.

4. Differentiation between Natural and Cultured Pearls

A natural pearl is built up of concentric layers of calcium carbonate (mother-of-pearl) which have

---

¹) W. G. Burgers and J. Hoekstra, Polytech. Weekblad **29**, 443, 1935.

²) That here complete circles appear, while in the reproductions included in the first article (cf. this Review **1**, 29, 1936) the lines consisted only of circular arcs, is due to the method of registration. If it is only required to determine the relative positions of the rings, it is sufficient to use a narrow strip of film cut along a diameter of the circles.

been deposited by the oyster round any available nucleus (e.g. a grain of sand). Each layer consists of crystallites with a sixfold symmetry, the axis of each crystallite being perpendicular to the layer. This structure is shown schematically in *fig. 2a*.

A "cultured" (or Japanese) pearl is obtained by inserting in the oyster a bead of mother-of-pearl cut from an oyster shell. This shell is built up of plane layers of mother-of-pearl with the sixfold axis of symmetry of the individual crystallites again arranged perpendicular to the layer. The nucleus of a cultured pearl therefore has a structure as shown schematically by the horizontally shaded section in *fig. 2b*. Round this "nucleus" the oyster deposits several thin concentric layers so that in external appearance the finished cultured pearl cannot be distinguished from a natural pearl.

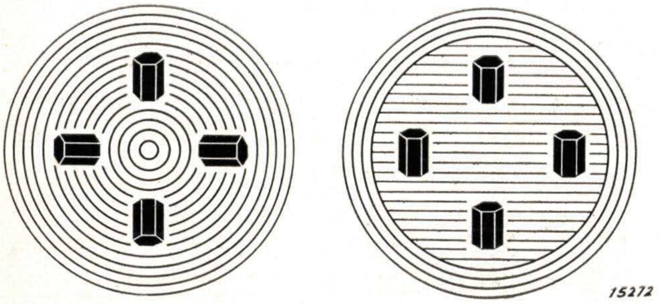

a) b)

Fig. 2. Diagrammatic representation of the structure of a natural and a cultured pearl.
a) The natural pearl is made up of concentric layers of mother-of-pearl (crystallites of calcium carbonate).
b) The cultured pearl consists of a nucleus of plane layers of mother-of-pearl, on the outside of which several thin concentric layers have become secreted.

If now a narrow beam of X-rays is brought to impinge on a natural pearl in any direction, the rays will always be perpendicular to the layers, i.e. parallel to the axis of the hexagonal crystals of calcium carbonate. On the other hand with a cultured pearl, the rays will as a rule not coincide with the direction of the crystal axis [3]) (the external concentric layers are so thin that compared to the pearl as a whole their effect can be neglected).

From the connection between the symmetry of the crystals and the X-ray pattern (which is produced by reflection of the rays at the crystal lattice planes) referred to at the beginning, it follows that the patterns obtained with a natural pearl must always exhibit an arrangement of dots with a sixfold symmetry, which latter cannot be obtained with a cultured pearl. *Figs. 3a and 3b* confirm this conclusion, and show that it is indeed possible to distinguish between natural and cultured pearls by means of X-rays [4]).

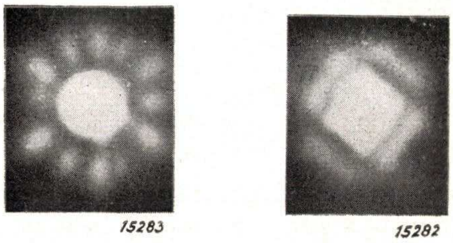

a) b)

Fig. 3. a) The diffraction pattern of a natural pearl always exhibits a sixfold symmetry.
b) A cultured pearl gives another type of pattern.

This method, together with other (e.g. optical) methods, is employed in practice by jewellers. For this purpose a special apparatus has been developed, which is shown in *fig. 4*.

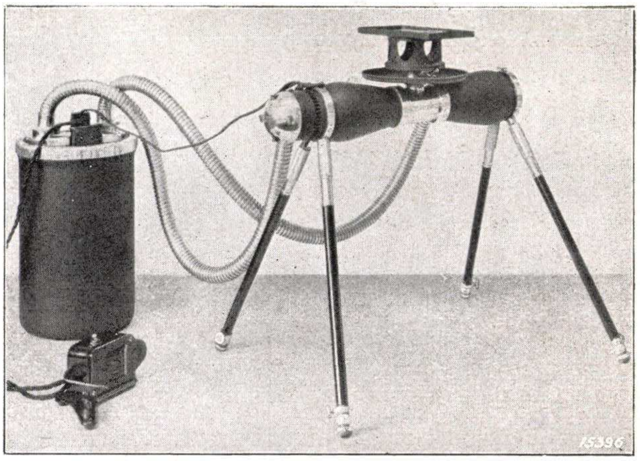

Fig. 4. The Philips pearl-testing apparatus. On the right hand is the "Metalix" X-ray tube mounted horizontally on four legs. On the tube the camera is fixed containing the support for the pearls to be examined. At the rear on the left is the high-tension transformer, in front of it the switch.

---

[3]) Such coincidence would only be obtained if the X-rays accidentally impinged on the pearl in a vertical direction in the figure. A second exposure made after slightly turning the pearl would, however, soon bring this to light.

[4]) The principle of this method has been indicated by J. Galibourg and F. Ryziger, Revue d'Optique **6**, 97, 1927.

SHORT NOTICES

Dosage control in X-ray Laboratories and Works

X-rays can exercise a healing action on diseased tissues as well as cause serious injury to healthy tissues. In both cases a specific "dosage" of rays is necessary before the respective effects are produced. Originally the dosage of X-rays was indeed defined on the basis of their biological action, an exposure to the radiation being taken as a unit dose, viz, 1 HED, when it just sufficed to produce an erythema (sunburn) on the human skin. Today this biological definition of dosage has been replaced by a physical one which is more accurately reproducible and which is based on the ionisation action of the X-rays (air being rendered an electrical conductor). This physical unit is the "Röntgen" (abbreviated "r"), and is equivalent to 1/600 HED.

Where a person working with X-rays is exposed to accidental (stray) radiation, it has been laid down that the dosage of exposure must not exceed 0.2 r per day. Experience has shown that when a person is exposed to this maximum radiation even over a long period no ill effects need be feared. In modern X-ray tubes, such as the Philips "Metalix" tube, care has been taken that outside the useful beam of rays the dosage is always below this limiting or tolerable dose. There is thus no danger whatsoever outside the actual X-ray beam in the use of all permanent X-ray installations designed for specific purposes, such as diagnosis, therapy or the radiographic examination of materials. But in laboratories and in works making X-ray apparatus fairly frequent exposure of the research worker or the workman to the action of the rays cannot be avoided. Naturally in these cases one must not wait until the exposed person begins to show the symptoms of harmful exposure to the rays before providing some form of special protection: it is essential to test continually whether those working in such exposed positions are being exposed to a daily dosage below the tolerable maximum of 0.2 r or not.

In the Philips X-ray laboratory and works, this is done by providing each person with a small cassette containing an X-ray film, which is always carried in the pocket. Every week this film is developed and the intensity of blackening measured photometrically, from which is calculated the X-ray dosage which has fallen on the film and to which therefore the person carrying the film has been exposed. The blackening of the film is not fully determined by the dosage, but is also dependent on the hardness (wave-length) of the X-rays; this can be taken into consideration in a simple way.

In many occupations it is natural that not the whole body of the exposed person receives the same dosage. Thus, in the case of a physician who frequently must place his hands in the useful beam of X-rays, these will be exposed to the action of the rays far more than any other part of the body. In this case a small film is carried on the hand or wherever the greatest exposure to the rays may be expected.

Brightness greater than on the sun

Brightnesses greater than those on the sun were recently produced in the Philips Laboratory by further increasing the wattage of the water-cooled super-high-pressure mercury vapour lamp described by Bol (De Ingenieur **50**, E 91, 1935). Theoretical considerations of Elenbaas indicated that by reducing the diameter the brightness would be increased, and a lamp was therefore constructed with an internal diameter of 1 mm and an external diameter of $3^1/_2$ mm, which with electrodes 10 mm apart and an 805-volt alternating current took a load of 1400 watts. The luminous intensity with this load was 11,000 candle-power and the pressure about 200 atmos. Along the axis of the discharge the brightness was 1,160,000 candle-power per sq. in.; this was measured by passing a photo-electric cell with a small slit parallel to the axis of the discharge tube across an enlarged image of the lamp.

Seen from the earth, the brightness at the surface of the sun is only 1,065,000 candle-power per sq. in. (according to the International Critical Tables).

ABSTRACTS OF RECENT SCIENTIFIC PUBLICATIONS OF THE N.V. PHILIPS' GLOEILAMPENFABRIEKEN

No. 1036: Balth. van der Pol, Interaction of radio waves, II (T. Ned. Radio Genootsch. 7, 93-97, Sept. 1935).

This report contains the conclusions drawn from 1823 observations of the interference produced in the modulation of radio waves reflected by the Heaviside layer. These observations which were made by 30 radio workers in different parts of the world relate primarily to the interference with reception of a number of European radio stations caused by a Morse signal specially radiated for this purpose by the Luxemburg transmitter. It is found that the effects produced by a station with a long wave-length on transmitters of long and medium wave-lengths are of the same order of magnitude. The effect has a monotonic decrement as the distance increases between the interfering station and a point midway between the station searched for and the observer. If this distance exceeds 600 km, interference is practically negligible. The observations made show that interference is due to the non-linear conductivity of the ionosphere, and also give a closer insight into the manner radio waves are reflected at the ionosphere.

No. 1037: J. A. M. van Liempt, Die Berechnung der Auflockerungswärme der Metalle aus Rekristallisationsdaten (Z. Phys. 96, 534-541, Sept. 1935).

A formula is derived for calculating the energy required for disintegrating the crystal lattice of metals from recrystallisation data. This energy expressed in cals. per gram-atom is approximately 4.6 times the socalled recrystallisation constant; more roughly still, this energy is proportional to the melting point, the factor of proportionality being 32 cals. per degree. This relationship is in close agreement with observation. In conclusion the author discusses Langmuir's and his own diffusion formulae, referring inter alia to various still obscure diffusion phenomena.

No. 1038*): J. G. C. Stegwee: Het harden van snelstaal met hoog kobaltgehalte (Metaalbewerking 2, 341-343, Sept. 1935).

A practical method for hardening a high-speed tool steel containing 18 per cent tungsten and 15 to 18 per cent cobalt is described. It was found, inter alia, that in tools which have been hardened in oil from temperatures above 1300 deg. C, fracture immediately took place as a result of hardening cracks. This was avoided by hardening in compressed air. In order to obtain adequate hardening, it is essential to anneal twice at 620 to 630 deg. C for 15 to 30 minutes each time. A single annealing for a longer period is not sufficient.

No. 1039: E. J. W. Verwey: The structure of the electrolytical oxide layer on aluminium (Z. Kristallogr. A 91, 317-320, Sept. 1935).

A structure is proposed for cubic γ'-Al_2O_3 obtained by electrolytic oxidation of aluminium. The elementary cell according to this structure contains 4 negative O ions in a space-centred configuration. Of the positive Al^{3+} ions $2^2/_3$ are present in each elementary cell, i.e. they are distributed statistically over all the spaces between the O^{2-} ions, and in such a way that 70 per cent of the Al^{3+} ions have the co-ordination number 6 with respect to oxygen and 30 per cent the co-ordination number 4. The modifications γ'-Al_2O_3 and γ-Al_2O_3 represent intermediate cases between the amorphous state and that with a complete atomic arrangement.

No. 1040: E. J. W. Verwey: Incomplete atomic arrangement in crystals (J. chem. Phys. 3, 592-593, Sept. 1935).

With respect to their positive ions, γ-Fe_2O_3, γ-Al_2O_3 and γ'-Al_2O_3, which is produced on electrolytic oxidation of Al, possess a structure which can only be defined statistically. The two modifications of γ and γ' have indeed the same oxygen lattice, although they differ in the incompleteness of the arrangement of the negative ions. These structures represent transition stages between the amorphous state and the complete atomic arrangement.

---

*) A sufficient number of reprints for purposes of distribution is not available of those publications marked with an asterisk (*). Reprints of other publications may be obtained on application from Philips Laboratory, Eindhoven, Holland.

No. 1041: J. A. M. van Liempt: De wet voor overeenstemmende toestanden van roosterherstel (Chem. Wbl. **32**, 546-550, Sept. 1935).

If a piece of metal which has been worked or shaped is heated to a sufficiently high temperature for some time, a "recovery" of its lattice takes place. On heating for different periods (*t* secs.) to different temperatures (*T* deg. abs.) "corresponding states" of lattice recovery are obtained, if $T\ (13.5 + \log t)$ is a constant. This formula is in satisfactory agreement, for instance in the case of brass and pure copper, with practical experience.

No. 1042: P. G. Cath: Het gedrag van metaaldraadlampen bij het branden op wisselstroom (Ingenieur **50**, E 101-104, Aug. 1935).

The temperature of the metal filament fluctuates when electric lamps are run from an alternating current supply. These fluctuations are calculated in this paper and represented in a diagram. In addition it is stated for a certain mean temperature how many times the vaporisation, the luminous intensity and thermal emission of electrons from the filament is greater with alternating current than the corresponding values for direct current.

No. 1043: K. F. Niessen: Erweiterung einer früheren Formel für die Erdabsorption in der drahtlosen Telegraphie (Ann. Physik **24**, 31-48, Sept. 1935).

The author calculates the absorption by the earth of radiated wireless waves for various types of surface strata (sea water, fresh water, wet and dry soil) and for various dipole levels above the surface of the ground, the latter within certain limits. It is shown that the wave-lengths may also assume values in which the densities of the displacement and conduction currents in the earth are in any arbitrary ratio.

No. 1044: J. Sack: A new method for the investigation of the transfer of material through the welding arc (Symposium on the welding of iron and steel, organised by the Iron and Steel Institute, London, May 1935, vol. **2**, 553-559).

The drop transfer from the welding electrode to the work-piece is registered by means of the slow-motion camera. For this purpose the welding process is illuminated with X-rays. Compared to exposures with ordinary light, these rays offer the advantage that the formation of metal drops within the coating of the electrode can be recorded. In addition, the definition of the pictures is not adversely affected by the clouds of gas and vapour surrounding the welding arc. (See the short article on this subject in No. 1 of this Review, p. 26).

No. 1045: J. A. M. van Liempt and J. A. de Vriend: Eine einfache Methode zur Bestimmung der Farbtemperatur von Blitzlichtern (Z. wiss. Photogr. **34**, 237-240, Oct. 1935).

The colour-scale temperature of flashlights cannot be determined by the ordinary spectro-photometric method, as their duration is too short. It is therefore necessary to employ exposures of Lagorio's colour scale on panchromatic plates, obtained with both flashlights and different light-sources of known colour-scale temperature. A colour-scale temperature of approx. 4000 deg. abs. is found for magnesium, aluminium and alloys of these two metals burning in oxygen.

VOL. 1 No. 3 MARCH 1936

Philips Technical Review

DEALING WITH TECHNICAL PROBLEMS
RELATING TO THE PRODUCTS, PROCESSES AND INVESTIGATIONS OF
N.V. PHILIPS' GLOEILAMPENFABRIEKEN

EDITED BY THE RESEARCH LABORATORY OF N.V. PHILIPS' GLOEILAMPENFABRIEKEN, EINDHOVEN, HOLLAND

A NEW METAL RECTIFYING VALVE WITH MERCURY CATHODE

By J. G. W. MULDER.

Summary. The new type of rectifying valve with mercury cathode described in this article has a cathode chamber which is made of metal and is water-cooled. Owing to the use of chrome-steel the pump which has hitherto been necessary with metal rectifier chambers has been dispensed with. The valve is of the single-phase type, whereby its construction has been much simplified and at the same time its dimensions considerably reduced. The new type of rectifier is designed for medium and high powers corresponding to current intensities of about 50 to several hundred amps per unit.

Introduction

For the rectification of high powers, rectifying valves with a mercury cathode[1]) are particularly suitable, owing inter alia to their ability to withstand overloading. The development of these rectifying valves has resulted in the production of two main types, the glass valve and the metal valve.

Where high powers have to be rectified the main difficulty in the design of rectifying valves, as in many other branches of electrical technology, has been the dissipation of the heat generated. This problem is dealt with by introducing a system of artificial cooling, a current of water being the most efficient. Water cooling is most suitably carried out with a metal valve body and has led to the construction of mercury cathode rectifiers with iron jackets for currents above 1000 amps, which are equipped with a water-cooling system and a high-vacuum pump. The latter was essential in this class of rectifier, as hydrogen ions present in the water diffuse through the iron walls. But the need for high-vacuum pumps in order to employ water cooling had many disabilities, since the presence of the pump, in spite of the use of automatic regulating devices, called for more careful supervision of these rectifiers than was required with sealed rectifier valves.

For this and other reasons metal rectifier valves were not constructed for currents below 1000 amps. In the glass valves which were used for these ratings, the dimensions had to be very large in order to provide for the necessary dissipation of the heat generated. But there is naturally an upper limit in dimensions to which glass bulbs can be manufactured. So that if with the maximum practical dimensions the valve was still unable to dissipate all the heat generated, it became imperative to adopt more intensive air cooling.

At the Philips Works a new type of metal single-phase rectifying valve with mercury cathode has now been evolved which, like glass valves, is used in a sealed condition. In this valve which is intended for a power range at present catered for by glass mercury-cathode rectifying valves (and even for still higher powers) the same advantages are offered as by the iron types rated for high powers, while the pump necessary in the latter has been dispended with in the new rectifiers. This new type of rectifying valve is described in the present paper [2]).

---

[1]) This term appears to us more suitable than that in common use hitherto, viz, "mercury rectifying valve", as thermionic rectifying valves nowadays also frequently contain an atmosphere of mercury vapour.

Construction of the New Type of Valve

A diagrammatic section through the valve is shown in *fig. 1*. The cathode is a pool of mercury K contained in a chrome-steel chamber. The latter is cooled by a current of water which circulates between the wall of the valve and a metal cooler which is screwed on to the outside for this purpose. The use of chrome-steel enables the valve to be sealed without raising any difficulties regarding the maintenance of a vacuum, since no hydrogen diffuses through chrome-steel into the valve as was known in this laboratory from the experience with water-cooled transmitting valves. The general design is, however, here the exact reverse to that adopted with transmitting valves, for in the latter the chamber acts as the anode, while here it is the cathode. The chamber is pressed from a single piece of sheet metal.

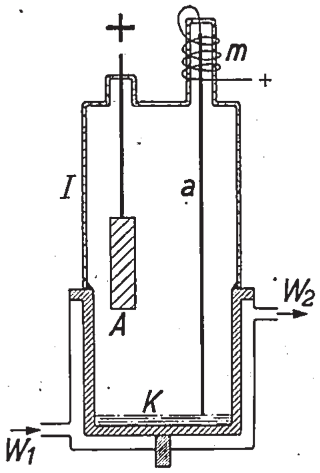

Fig. 1. Section through new type of mercury-cathode rectifying valve (schematic). The cathode K is a pool of mercury in a chrome-steel chamber, and the anode A a graphite block. The chrome-steel chamber and the glass anode insulator I form a hermetic seal. The chamber is cooled with water which flows in at W_1 and flows out at W_2. An auxiliary anode a with a magnetising coil m provides ignition.

A partition has been fitted inside the cooler to avoid water remaining at rest in "dead" ends. The chamber is as a result uniformly and effectively cooled, and the greater part of the discharge takes place in this highly-cooled metal system.

The glass anode insulator I forms a hermetic seal with the edge of the cathode chamber. The head of the cathode insulator with the two cylinders mounted on it is pressed in one piece. The two welded joints are produced by machine.

The anode A is a graphite block. The valve is started in the usual way by an auxiliary anode a, which can be moved up and down through a short distance. At the beginning an auxiliary direct current which has been rectified independently flows through the auxiliary anode and a magnetising coil m connected in series with it, which then draws the auxiliary anode out of the mercury. The arc generated in this way ignites the actual discharge.

The temperature of the anode insulator I must be kept below a specific maximum in order to avoid damage, while on the other hand it must not fall below a certain minimum in order to prevent mercury condensing on the inner wall during the running of the valve. All mercury which is volatilised from the cathode spot must become deposited on the metal walls before it can reach the anode; if there is mercury on the anode back-firing may occur.

The design of valve shown in fig. 1 is suitable for low voltages. For higher voltages special cooling and de-ionisation walls must be introduced in the usual way in the discharge path of the valve. One or more of these walls may be suitably insulated and then act as a control grid. In their place, however, the auxiliary anode a can also be replaced by an ignition unit permitting the ignition time to be displaced, as required, with respect to the phase of the anode voltage.

The complete valve mounted in its cooler is shown in *fig. 2*.

Single-phase or Polyphase Valves

Hitherto rectifying valves with mercury cathodes have always been of polyphase construction, i.e. with an anode for each phase of the polyphase alternating current and a single common cathode for all phases. There are various reasons for this policy. In the first place the polyphase mercury-cathode rectifying valve is more stable in service, as the anodes assist each other when starting up. The generation and maintenance of the cathode spot is indeed the weakness in all designs of this type of rectifier [3]). Secondly, in a polyphase valve a single common auxiliary ignition-system can be used for starting up in all phases. This system consists of an ignition anode and two auxiliary anodes for which an auxiliary current of several amps is independently rectified and smoothed. There is still another important reason for building mercury-cathode rectifying valves always on the polyphase principle. Each valve must, even if it were built on single-phase lines, be provided with a spacious condensing chamber for the purpose of condensing so much of the mercury volatilised that the pressure in front of the anodes remains low. In a polyphase design this domed chamber, which at any rate must be provided, is employed far more efficiently.

---

[2]) In the design and testing of the new valve, valuable assistance was rendered by Mr. Lems.

[3]) Thermionic rectifiers are certainly more convenient in this connection, where the heated cathode is always ready for emitting electrons. Directly-heated or indirectly-heated hot-cathodes for emission currents of several hundred amps are indeed feasible, but introduce a number of practical difficulties.

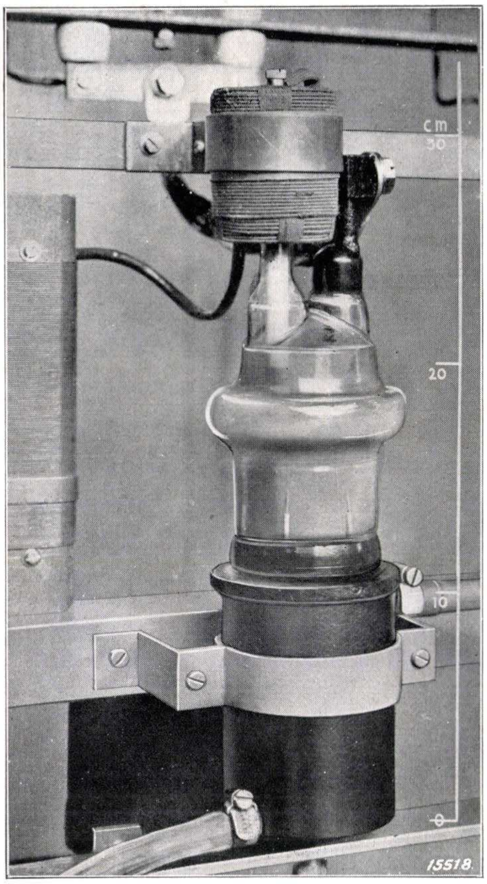

Fig. 2. Construction of the single-phase metal rectifying valve shown diagrammatically in fig. 2.

In the new type of valve this chamber has become superfluous owing to the vigorous cooling action of the metal walls. For this reason a single-phase design is more practical [4]) in the present case. It offers important advantages which more than completely outweigh the above-mentioned drawback that adequate provision for satisfactory ignition must be made for each valve individually. General construction is thus considerably simplified, and permits complete mechanical manufacture, so that six single-phase metal valves are better productions than a single glass valve rated for a sixfold current. The dimensions can be kept small, since in the negative phase no anode is affected by the ionisation produced by the current flowing to one of the other anodes. (This phenomenon would again occasion large dimensions in the case of polyphase valves, so that the advantages due to watercooling would not be entirely utilised. See also footnote [4])). Erection and transport are extremely simple with the single-phase metal valves. In service it is, moreover, important that when using single-phase valves a spare for only a fraction of the total power of the plant need be provided. In addition, the liability to defects which usually occur only at leading-through points and welded joints is still lower with the simple single-phase valves than with one corresponding polyphase valve. Finally, if a valve fails the rectifying plant does not cease operating as a whole since the remaining valves continue to run.

Characteristics of the New Type of Valve

The valve shown in fig. 2 is rated for a medium current of 75 amps and a peak current of 500 amps. Like other mercury-cathode rectifying valves this valve can without trouble carry heavy overloads for short periods. The only damage which overloads could do would be to produce too high a temperature rise, which, however, requires a certain time. The valve can sustain a 50 per cent overload for 5 minutes and a 100 per cent overload for 30 seconds. The quantity of cooling water required is comparatively low, as on full load only about 1150 watts are converted to heat in the valve. Each valve requires about 1 litre of water per minute, the temperature of the water rising by 16 deg. C.

The ignition voltage has been reduced to less than 22 volts by the auxiliary current of 2.5 amps already referred to and which flows through *a* (fig. 1). Auxiliary ignition must be furnished separately for each valve in view of the single-phase design adopted. It has, however, been found possible to avoid using three auxiliary anodes in each valve (one for ignition and two for maintaining the cathode spot). A single anode *a* performs both functions since it is fed with direct current. The direct current is furnished for all phases (valves) in common from a specially-provided rectifier rated for a low voltage and low power. This auxiliary rectifier operates through a thermionic valve.

---

[4]) Actually only the single-phase design has made it possible to do away with the condensation chamber; in a six-phase valve of small volume constructed on corresponding lines to the type described here (with mercury cathode in a chrome-steel chamber) it would not have been so easy to localise the discharge within the cooled metal portion of the valve.

The voltage-drop depends on the current intensity and the temperature, and varies between 10.5 and about 18 volts, with an average of 15 volts. In the case of new valves, or where the cathode spot is not sufficiently stable, it may be slightly higher (up to 25 volts). *Fig. 3* shows the variation of the voltage-drop in relation to the load.

The back-firing voltage in the case of the valve shown in fig. 2 is about 500 volts. The valve operates with 100 per cent reliability up to 250 volts.

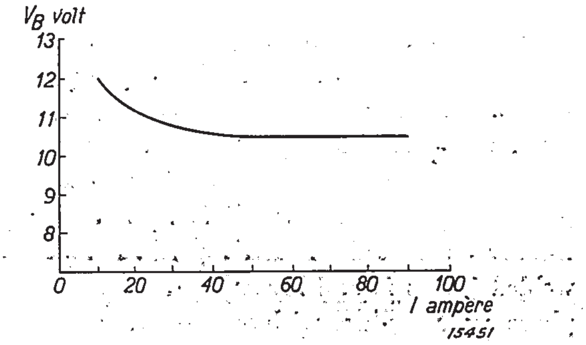

Fig. 3. The voltage-drop V_B plotted as a function of the load I for the new rectifying valve, measured with direct current.

The efficiency depends on the rectified power. The total losses in the valve at full load are 1150 watts, including the consumption for auxiliary ignition. The efficiency at 220 volts and 75 amps is therefore 93 per cent and at 120 volts and 75 amps 88 per cent.

Regarding the life of these valves no numerical data can yet be furnished, as up to the present not a single one of the valves (which have been under test for more than a year) has failed. The life therefore amounts in any case to many thousands of hours.

Use of the Valve in a Rectifying Unit.

Fig. 4 gives the circuit lay-out and *fig. 5* a photograph of a 58-kilowatt (450 amps, 130 volts) rectifying unit erected in one of the power stations of the Philips Works. The direct current circuits of the factory shops are designed for this voltage and are fed at different points from the power stations.

Hitherto rotary converters have been used for this purpose and owing to the impulsive loads (e.g. for feeding lathes, etc.) each of these had

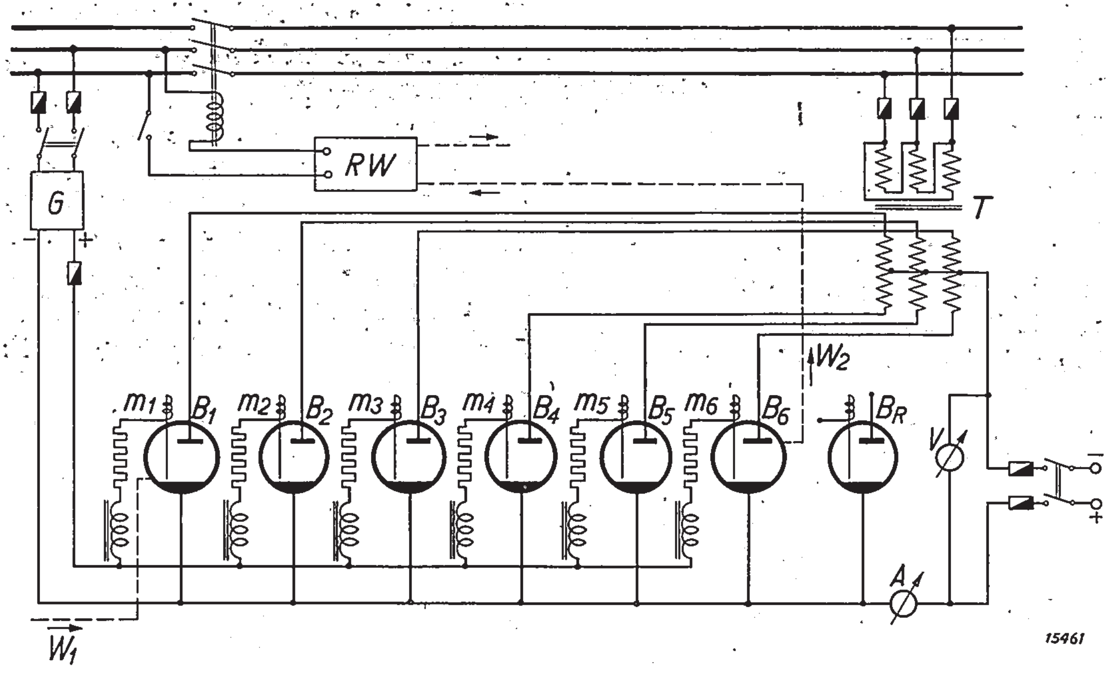

Fig. 4. Circuit connections of a rectifying unit rated for 130 volts and 450 amps. This unit is equipped with six sealed mercury-cathode metal rectifying valves B_1 to B_6. B_R is a spare valve. Each valve is ignited by means of its own auxiliary anode and a magnetising coil (m_1 to m_6). The auxiliary anodes are fed from a common and independent thermionic rectifier G. For water cooling, the valves are divided into two groups, of three valves each. Each group has a water-actuated relay RW which switches off the unit on any interruption of the water supply. (In this diagram only one water-actuated relay is shown and the water pipes are only indicated at the inlet of the first and the outlet of the sixth valve).

to be liberally rated. Thus under normal conditions they are run at loads considerably below their ratings and hence with a low efficiency. The rectifiers described here are much better suited for this purpose. Their efficiency remains satisfactory even with loads far below their ratings, and impulsive loads can be handled without inconvenience.

Brief reference must be made to some of the principal features of the rectifying unit. The water cooling systems of the six valves are divided into two groups, each of three valves connected in series, so that the water consumption of the whole unit is not greater than that required for two of the valves. A water-actuated relay *RW* has been introduced into the water supply (fig. 4) which cuts off the whole unit if the circulation is interrupted for any reason.

The auxiliary ignition is fed from a rectifier *G*, whose power consumption is the product of the D.C. voltage of 30 volts and the sum of the auxiliary currents. The auxiliary currents for all six auxiliary anodes are smoothed separately. Each auxiliary current draws its own auxiliary anode *a* out of the mercury by means of the magnetising coils m_1, m_2, etc. If the arc in any valve breaks the valve is thus re-ignited automatically.

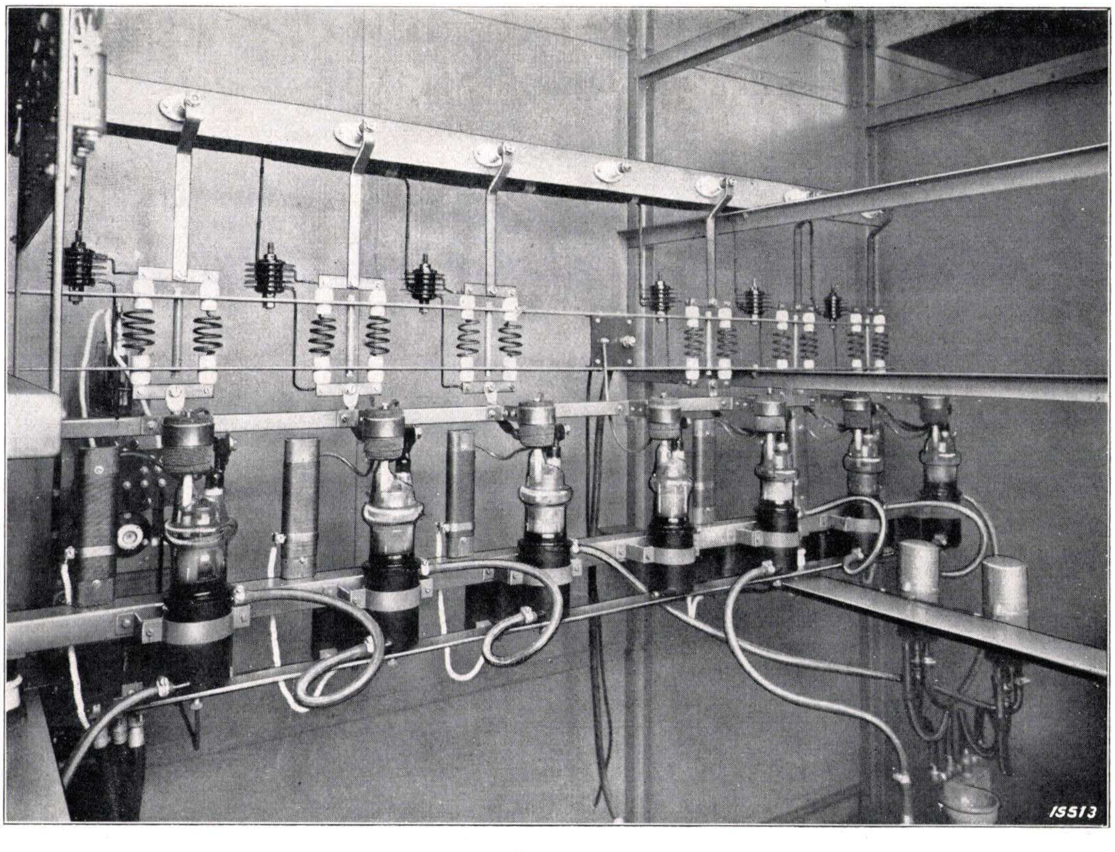

Fig. 5. Photograph of the unit shown in fig. 4. The middle valve of the seven shown is the spare valve which is not connected in the operating circuit. On the extreme righthand side the two water-actuated relays for the two cooling circuits are shown. On the left is the thermionic rectifier for the auxiliary direct current (ignition). A back-firing relay, which is not included in fig. 4, is to be seen fixed above each valve.

COMPARISON BETWEEN DISCHARGE PHENOMENA IN SODIUM AND MERCURY VAPOUR LAMPS

II.

Summary. An analysis of certain fundamental phenomena in the mechanism of discharges through gases gives important conclusions regarding the properties of sodium and mercury vapour lamps. Use is made in this article of the characteristics of excitation and ionisation of sodium and mercury discussed in a previous issue of this Review [1]). Discussion is here limited to the middle portion of a long discharge column.

Conduction of Electricity through Gases

In its simplest form a gaseous discharge takes place in a vessel with two electrodes C_1 and C_2 (*fig. 1*) which are fused through the walls and connected to a source of current through a resistance R, necessary for limiting the current flowing. The current from C_1 to C_2 is conveyed by ions and electrons. The electrons travel towards the positive pole (C_1) where they are absorbed, while the ions travel to the negative pole (C_2) and combine with the electrons emitted from this electrode to form neutral atoms. Thus at both plates the carriers of the charge are destroyed, while other carriers are lost through recombination at the walls of the vessel or in the gas space.

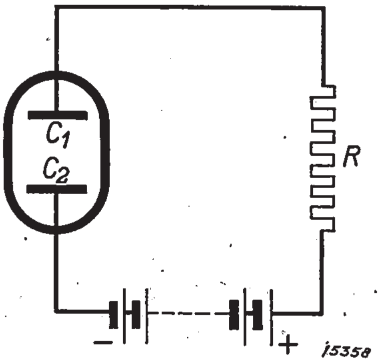

Fig. 1. Circuit diagram of a gas-discharge.

To maintain a continuous flow of electricity through gases it is necessary that under suitable conditions the gas of itself attains a state such that the generation of ions (ionisation) exactly balances the rate of recombination. If ionisation is greater than the rate of recombination, the strength of the current will increase. As a result the voltage-drop at the resistance R will rise and the voltage across the poles C_1 and C_2 will drop. In response to these changes ionisation will also in general decrease and the discharge tends towards a stationary state. But the external resistance R is an essential sine qua non for the attainment of this equilibrium.

In the middle portion of a long column, to which for the sake of simplicity the present discussion will be limited, the stationary state is determined by the equilibrium between the ionisation in the gas space and the recombination of ions and electrons at the walls. The emission of light, which as regards practical applications is of main interest to us, depends on other phenomena which were described in part I of this paper and which are of secondary importance in the mechanism of electrical conduction.

The obscurity in which the mechanism of gaseous discharges is shrouded is mainly due to the vast multiplicity of the types of particles present even in a simple atomic gas (i. e. a gas in which the atoms have not combined to form molecules). In addition to atoms in the fundamental state, electrons, atoms in different states of excitation and light quanta of different frequencies also occur. The state of equilibrium referred to above is determined by the mutual interaction of all these various particles.

An insight into the complex phenomena ruling is best obtained by a consideration of the limiting cases:

1. Low current-density,
   low vapour-pressure.
2. High current-density,
   high vapour-pressure.

As shown in the first part of this article already published the limiting case 1 is represented by the sodium vapour lamp, the limiting case 2 by the mercury vapour lamp. The point of view adopted here is therefore particularly suitable for an analysis of the discharge characteristics in these two types of lamp.

---

[1]) Philips techn. Rev. **1**, 2, 1936.

Low pressure discharge. Motion of Ions and Electrons

In the column of gas discharges, electrons and ions occur with the same space-charge density, but owing to their greater mobility, the electrons carry practically the whole of the current. The energy imparted to them per cub.cm, viz: Energy per cm^3 = Current density × longitudinal field-strength (gradient) is transmitted by various processes to the atoms in the gas or to the walls of the containing vessel and is finally radiated in the form of light and heat.

The smallness of the kinetic energy transmitted from the electrons to the atoms, which is related to the large difference in the masses m and M of the electrons and atoms respectively has a very important bearing on the motion of the electrons. The maximum energy E imparted to an atom at rest by a single elastic collision is:

$$E = \frac{4m}{M}\,\varepsilon \quad . \; . \; . \; . \; . \quad (1)$$

where ε is the energy of the electron. According to equation (1) at most 1/10,000th part of the energy of the electron is given up on a single elastic collision in the case of sodium vapour, and at most 1/100,000th part in the case of mercury vapour. On the other hand by ionisation or excitation, the electron can impart its whole kinetic energy to an atom. Appreciable transmission of energy to the gas atoms therefore is only initiated when the electrons have derived sufficient energy from the electric field to produce atomic excitation. A state is therefore established in which the mean kinetic energy of the electrons is comparable with the energy of excitation, whilst the mean energy of the atoms does not assume a greater value than that corresponding to the temperature of the vapour. The temperature of the sodium vapour at the wall of the tube is approximately 280° C. In the axis of the discharge column the temperature is about 50 degree higher. The mean kinetic energy of the free electrons is of the order of 2 electron-volts [2]). Such a high mean energy would only be acquired by the atoms at a temperature of 15000 °K. This fact is sometimes stated by saying that the „temperature of electrons" is 15000 °K. *Table I* gives electron temperatures such as are met with in sodium lamps at different vapour pressures.

Equation (1) is derived from the equations of energy and momentum. The maximum energy is transmitted from an electron to an atom on central collision (*fig. 2*). Denoting the velocity of atom and electron before collision as V and v and after collision as V' and v' respectively and assuming the atom to be at rest before the impact ($V = 0$) the following equations are obtained:

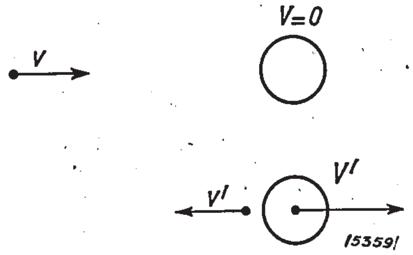

Fig. 2.

Conservation of energy:

$$\frac{m}{2}\,v^2 = \frac{m}{2}\,v'^2 + \frac{M}{2}\,V'^2$$

Conservation of momentum:

$$mv = mv' + MV'$$

Eliminating v' one obtains:

$$V' = \frac{2\,m\,v}{M - m}$$

which on substituting the kinetic energies:

$$E = \frac{M}{2}\,V'^2$$

$$\varepsilon = \frac{m}{2}\,v^2$$

leads to the result:

$$E = \frac{4\,mM}{(M+m)^2}\,\varepsilon$$

or approximately

$$E = \frac{4m}{M}\,\varepsilon$$

The assumption that the atoms are at rest before collision is justified by the very marked difference in the mean kinetic energies of atoms and electrons. Owing to their higher velocity more electrons than ions impinge on the wall of the discharge tube, which thus become negatively charged. As a result subsequent electrons are repelled and ions attracted, so that the ionic current at the wall becomes just as great as the electronic current. The wall, however, always remains negatively charged. The path described by the ions is shown diagrammatically in *fig. 3*. It is seen that ions which are produced in the discharge soon terminate at the walls after traversing a short path. There they recombine with electrons of the wall charge to form neutral atoms and give up the ionisation energy liberated to the walls in the form of heat.

---

[2]) The unit electron-volt (eV) is the energy which an electron must expend in order to overcome a voltage drop of 1 volt. $1\ eV = 1.59\ 10^{-19}$ watt-sec.

Excitation and Ionisation Processes dependent on Pressure and Current Density

In very rarefied gases and with small current-densities the frequency of excitation and ionisation reactions is proportional to the product of the concentrations of electrons and atoms in the fundamental state. The number of excited atoms is then relatively small and has no influence on the reactions taking place. The probability of excitation is closely governed by the velocities of the free electrons and by the properties of the individual atoms. In general excitation of the resonance state is particularly favoured. Thus, Krefft, Reger and Rompe[3]) found that in sodium vapour at a pressure of 0.005 mm and a current density of 0.05 A per sq.cm 95 percent of the energy of the electrons is utilised for excitation and emission of resonance light.

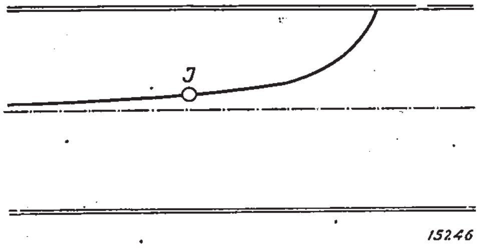

Fig. 3. Path of the ions J in a discharge through gases.

In the sodium lamp somewhat higher pressures and current densities are in general used than in the experiments of Krefft, Reger and Rompe, whereby owing to the intervention of secondary processes, the excitation processes become extraordinarily complex.

However, in a qualitative sense, it can be readily conceived that the intensity of the resonance light will become diminished as compared with the intensity of the higher transitions and that the concentration of the ions will increase to a greater degree than the concentration of the excited atoms. Responsible for this transformation are self-absorption, collisions of the second kind and cumulative excitation.

Self-absorption and Secondary Processes

Light quanta of the resonance line become absorbed, after traversing a short path S, by an atom in the fundamental state, resulting in the latter's excitation to the resonance state, and are re-emitted in no particular direction by the excited atom. These quanta thus describe a very long wandering path if the density of the gas is not too small, which with a tube of radius R is made up of

$$Z = (R/S)^2$$

absorptions and re-emissions before a particular quantum of light escapes from the tube. As the number of absorptions Z increases, there is a greater probability that one of the atoms will be excited from the resonance state to a higher energy level by electron impact (cumulative excitation) or inversely transfer its energy to the colliding electron thus returning to the fundamental state without emission (collision of the second kind). Both these processes produce a weakening of the resonance radiation. The calculation of Z is rendered very difficult by the heterogeneity of the radiation, which latter does not possess a single well-defined wave-length, but an intensity distribution covering some hundredths of an Ångström unit and giving a spectral line of finite width. The wings are subject to much less absorption than the core. The calculation of the free path S thus stipulates a knowledge of the shape of the spectral line, which in turn undergoes marked alteration owing to self-absorption. (See *fig. 4*). These processes have been investigated theoretically by de Groot[4]) and Kenty[5]). Under average operating conditions, the value of Z for sodium lamps is estimated to be of the order of 1000 to 10000. Self-absorption reduces the concentration of the atoms in the fundamental state and intensifies excitation to higher levels including the ionized state. At a given velocity distribution for the electrons, the secon-

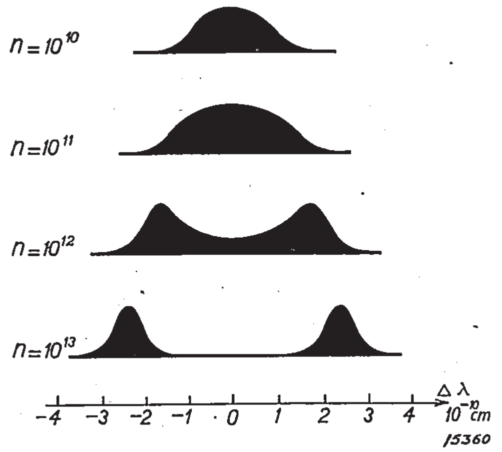

Fig. 4. Spectral distribution of resonance radiation at various concentrations of the sodium vapour. The curves are calculated for a layer thickness of 2 cm. n is the number of atoms per cub. cm. (Reproduced from W. de Groot, Physica **12**, 289, 1932).

---

[3]) H. Krefft, M. Reger en R. Rompe, Z. f. techn. Phys. **14**, 242, 1933. M. J. Druyvesteyn, Phys. Z. **33**, 822, 1932.

[4]) W. de Groot, Physica **12**, 289, 1932; **13**, 41, 1933.

[5]) Carl Kenty, Phys. Rev. **40**, 633, 1932; **41**, 390, 1932; **42**, 823, 1932.

dary processes thus produce an augmentation of ionization greater than in proportion to the concentration of the electrons and the atoms. This has an important bearing on the interpretation of the characteristics of discharges in gas tubes.

Effect of Pressure and Current Density on the Voltage Gradient

At a constant pressure the recombination of ions and electrons occurring at the walls is proportional to the current density. As no excess of ions can be produced, the same also applies to ionisation. With a constant velocity distribution of the electrons, however, as shown in the preceeding chapter, ionisation would increase more than the relative increase in current density. Hence, in view of the stability of the discharge referred to at the outset, it may be expected that as a result of a drop in the voltage gradient the velocities of the electrons will diminish and the ionisation will be restored to the correct measure. The decrease of the gradient with rising current density is known as the negative resistance of the discharge. For stability to be obtained it is necessary for the external resistance to be sufficiently great to make the total resistance positive. Also if the current strength is constant and the pressure increased, the mean kinetic energy of electrons will fall and thus compensate the increasing influence of cumulative processes. *Table I* gives details of measurements taken of sodium tubes by Druyvesteyn and Warmoltz[6]) which confirm this interpretation.

Table I

Vapour pressure	Current	Gradient	Energy of electrons	
mm	Ampere	Volt per cm	Volt	Temp. °K
$2 \cdot 10^{-3}$	0.2	0.432	4,00	30900
	1.0	0.398	2.48	19200
$8 \cdot 10^{-3}$	0.2	1.082	3.80	29400
	1.0	0.668	1.24	9600

The table gives data of the voltage gradients and the temperature of the electrons at two vapour pressures ($2 \cdot 10^{-3}$ mm and $8 \cdot 10^{-3}$ mm), which correspond to wall temperatures of 255 and 287 deg. C. On increasing the current from 0.2 A to 1 A, the voltage gradient and the energy of the electrons decrease for both vapour pressures. Furthermore, the energy of the electrons also decreases at constant current density and increase in the vapour pressure, so that the "electron temperature" T_e and the temperature of the vapour T_g converge.

Transition to the high-pressure Discharge

The variation in the electron temperature at constant current density and rising vapour pressures has been studied over a wider range with discharges through mercury vapour than with discharges through sodium vapour. With mercury vapour also, T_e and T_g approach each other as the pressure rises. As shown in *fig. 5*, these two temperatures are practically equal at pressures above 30 mm. At these vapour pressures a thermal equilibrium between the electrons and atoms has been attained. The thermal equilibrium is a characteristic feature of the high-pressure discharge.

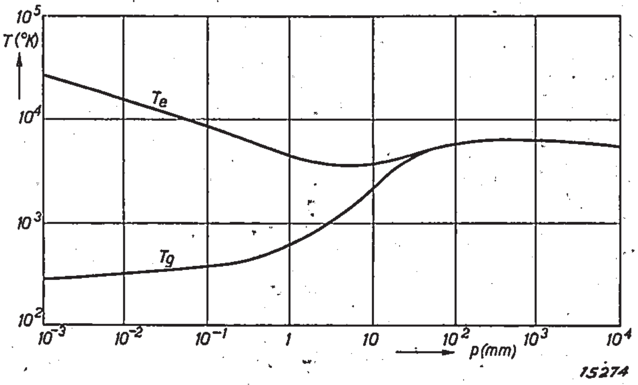

Fig. 5. Electron temperature T_e and vapour temperature T_g at constant current strength and different vapour pressures. (Diagrammatic.) Reproduced from W. Elenbaas, Ingenieur **50**, E 83, 1935.

High-pressure Discharge

Whilst the transition processes between the limiting cases are very complex, the high-pressure discharge itself can be described more easily.

At thermal equilibrium the degrees of excitation and ionisation can be deduced from statistical considerations without any knowledge of the atomic mechanism. For the density n_a (per cub.cm) of the excited atoms, the Boltzmann equation applies:

$$n_a/n_o = e^{-\frac{\varepsilon_a}{kT}} \quad . \quad . \quad . \quad . \quad . \quad (2)$$

where n_o is the density of the atoms in the fundamental state ε_a the excitation energy, k the molecular gas constant of Boltzmann[7]).

---

[6]) M. J. Druyvesteyn and N. Warmoltz, Phys. Z. **33**, 822, 1932; Phil. Mag. **17**, 1, 1934.

[7]) The molecular gas constant k is related to the molar gas constant R by the formula: $R = k \cdot N$ where N is the number of molecules per gram-molecule. ($N = 6.06\ 10^{23}$, $k = 1.37\ 10^{-16}$ erg per degree.)

The density of excited atoms determines the intensity of radiation in the corresponding wavelengths.

Ionisation may be regarded as dissociation of the gaseous atoms into ions and electrons. The degree of ionisation α can be calculated from the equilibrium condition between ions and electrons and neutral atoms by means of the law of mass action. The dissociation equilibria are thus given by the equation:

$$\frac{\alpha^2 n_o}{1-\alpha} = C\,(T) \quad . \ . \ . \ . \quad (3)$$

where C is a function of the temperature containing the energy ε of ionisation in the Boltzmann factor $exp\,(-\,\varepsilon_i/kT)$. Saha [8]), calculating the value of the constant C for ionisation equilibria in ideal gases, found:

$$C = \frac{(8\,\pi\, m\, kT)^{3/2}}{2\,h^3}\; e^{-\frac{\varepsilon_i}{kT}}$$

whereby $h = 6.55 \cdot 10^{-27}$ ergsec (Cf. Nr. 1, p. 3 of this journal). Introducing the concentration n_i of excited atoms: $n_i = \alpha\, n_o$, one computes from equation (3) with the numerical values of m, k and h:

$$\frac{n_i^{\,2}}{n_o - n_i} = 0{,}98 \cdot 10^{-16}\, T^{3/2}\, e^{-\frac{\varepsilon_i}{kT}}\ \mathrm{cm}^{-3} \ . \ (4)$$

This expression determines the concentration of ions as a function of the temperature.

Mechanism of Discharge at Thermal Equilibrium.

At thermal equilibrium the conditions of discharge are completely described by the temperature T in the cylindrical discharge tube as a function of the radius r. Knowing the temperature distribution, one can compute as a function of the radius:

1) The concentration n_i of thermal ionised atoms and thus the current density, given by

$$j = n_i\,(\beta_i + \beta_e)\,G$$

where G means the gradient, β_i and β_e the mobilities of ions and electrons.

2) The concentration n_a of thermal excited atoms and thus the intensity of radiation in the different wavelengths.

3) The power $j \cdot G$, supplied per cub.cm and thus, after subtraction of the radiation power, the heat development Q per cub.cm and sec.

The temperature distribution is given by the laws of thermal conduction. The heat flow is proportional to the temperature-gradient and for a cylindrical surface of radius r is:

$$q = 2\pi\, r\, \frac{dT}{d\,r}\,\sigma \ . \ . \ . \ . \ . \ . \ . \quad (5)$$

where σ means the coefficient of thermal conduction and is a function of the temperature. From equation (5) it is simple to derive a differential equation for the temperature distribution. Consider a cylindrical volume element with a thickness dr. The difference dq between the heat influx and heat efflux is equal to the amount of heat generated in the element of volume per second. This is $2\,\pi\, r\, dr.\ Q\,(r)$, where $Q(r)$ is the amount of heat developed per cub. cm per sec. Thus:

$$\frac{dq}{dr} = 2\,\pi\, r\, Q(r)$$

or substituting for q from equation (5):

$$\frac{d}{dr}\left[\,2\,\pi\, r\, \frac{dT}{dr}\,\sigma\right] = 2\,\pi\, r\, Q(r) \ \ldots\ldots \ (6)$$

As shown above, the heat development Q can be calculated as a function of the temperature. Substituting this function in equation (6), one obtains a differential equation for the temperature which contains no arbitrary coefficient. This equation was analysed by Elenbaas [9]) for discharges through high-pressure mercury vapour and for a particular case (vapour pressure P = 1 atmos., power input N = 40 watts per cm of the discharge column) gives the temperature distribution shown in *fig. 6*. The temperature at the middle of the discharge path is above 6000 deg.

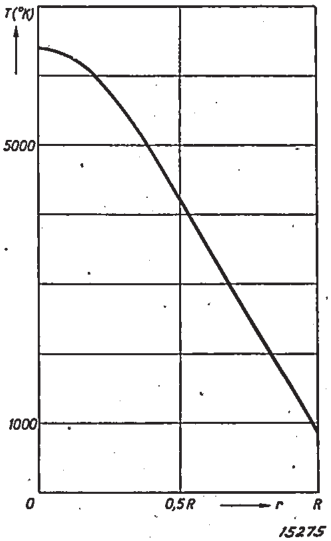

Fig. 6. Temperature in a mercury vapour discharge (in deg. abs.) as a function of the distance r from the axis of the discharge tube. Vapour pressure 1 atmos., power input 40 watts per cm, diameter of tube 2cm. Reproduced from W. Elenbaas, Ingenieur **50**, E83, 1935.

---

[8]) M. N. Saha, Phil. Mag. **40**, 472, 1920; Z. f. Phys. **6**, 40, 1921.

[9]) W. Elenbaas, Physica **1**, 673, 1934.

abs. Concordance between the calculated current density and the measured values was satisfactory. The differential equation can, however, not be strictly correct as the transfer of energy by radiation as compared with thermal conduction has been neglected.

Contraction of the Column

The constriction of the path of the discharge is the visible indication of the transition from the mechanism of electronic collision to the thermal form of discharge. This phenomenon is readily explained from the temperature distribution shown in fig. 5. At the hottest part, i.e. along the centre, ionisation and hence the current density has the greatest value. *Fig. 7* shows as a function of the radius:

a) The current density (theoretical)

b) The intensity of the yellow mercury lines (experimental measurement).

Curves a) and b) show qualitatively the same trend, but curve b) is wider. This is chiefly due to the fact that in the external zones of the discharge where, in consequence of the lower temperature, practically no more ionisation takes place, there is still a slight emission of light, owing to absorption and re-emission of light quanta emanating from the hot internal zone. This phenomenon is treated more in detail in part I of the article. (See this periodical, page 4, Januari 1936).

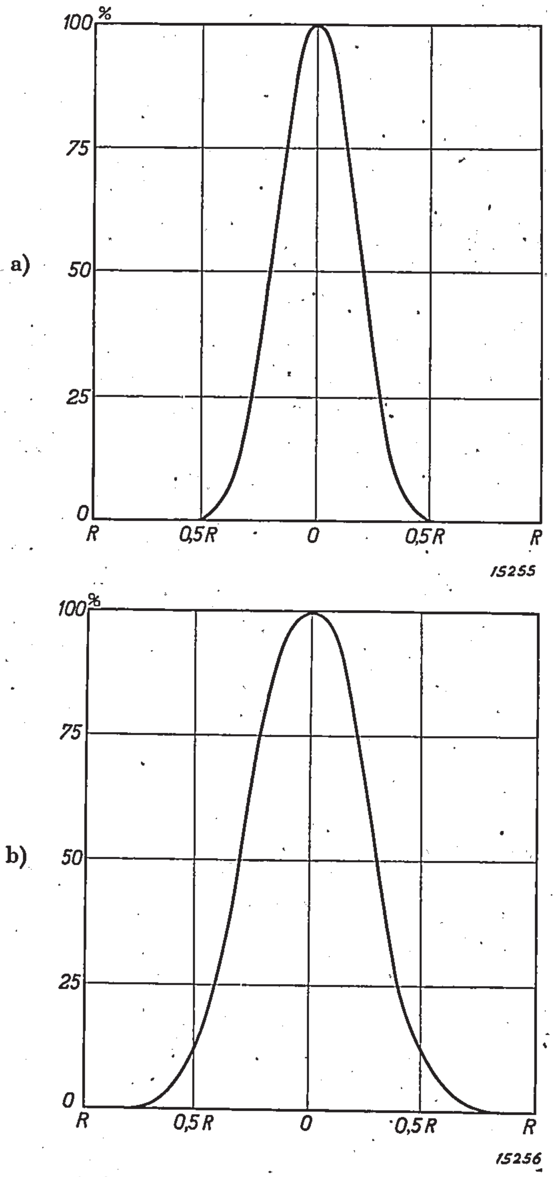

Fig. 7. a) Calculated current strength.
b) Measured intensity of the yellow lines at 5770/90 Å as a function of the distance r from the axis of the tube for a mercury-vapour discharge at a pressure $P = 1$ atmos and a power $N = 40$ Watt per cm. (Relative units).

Conclusions to Parts I and II

The visible light of the sodium lamp chiefly comes from resonance radiation. Radiation corresponding to higher transitions is generally infra-red. On the other hand the visible light from the mercury vapour lamp is due to transitions between higher levels; the resonance lines are ultra-violet.

Resonance light is principally radiated at low current densities and gas pressures. Excitation then takes place owing to electron impact upon atoms being in the fundamental state. Transitions between higher excited levels are favoured at high current strengths and pressures. Resonance light is then weakened by self-absorption and collisions of the second kind; the excitation of higher states is promoted by cumulative processes.

By such considerations one is led to run sodium lamps from which a marked resonance radiation is desirable with the lowest possible current densities and pressures. A limit is here set by the fact that the heat evolved must give a sufficiently high operating temperature (280 deg. C) with suitable types of insulation. On the other hand, mercury vapour lamps give the highest efficiency at very high current strengths and pressures, and are therefore designed in the form of high-pressure discharges. The limits are here set by the pressures and temperatures which can be maintained technically.

At the practical limits sodium vapour and mercury vapour radiate their characteristic luminous rays with approximately the same efficiency.

Compiled by G. HELLER.

DEMONSTRATION MODEL ILLUSTRATING SUPERHETERODYNE RECEPTION

Introduction

At the World Exhibition held in Brussels last year, a demonstration model was exhibited which illustrated in the most elementary manner the method of operation of modern radio receivers. It is of course generally known that in radio transmission a carrier wave of high frequency is employed and the much lower audio-frequencies are transmitted as a modulation of the amplitude of this carrier wave. The function of the rectifying stage in the receiver is to separate these low audio-frequencies from the high frequency of the carrier wave. Perhaps less well known is the sequence of operations which actually take place in a superheterodyne receiver in which an "oscillator", a "converter valve" and an "intermediate frequency" are used. The main object of the demonstration model described in the present article is therefore to illustrate the principles underlying superheterodyne reception.

The Superheterodyne Principle

In superheterodyne receivers, not only is the incoming high-frequency carrier wave appropriately dealt with, but provision is also made for the simultaneous generation of an additional oscillation by means of an oscillator, the frequency of this local oscillation differing by a specific number of cycles per second from the frequency of the carrier wave. The function of the converter valve is to reduce modulation to a new carrier wave of lower frequency. This is done by producing a periodic fluctuation in the amplification of the incoming wave in synchronism with the self-generated auxiliary oscillation of the oscillator. The alternating current I_a in the anode circuit of the converter valve is given by the product of the gradient S of its characteristic and the amplitude V_g of the alternating current component of the grid potential, thus:

$$I_a = S\,V_g \quad \dots\dots\dots\dots\dots\dots (1)$$

The gradient S is now varied with the angular frequency ω_h of the auxiliary oscillation, while the grid potential V_g varies with the angular frequency ω_i of the incoming carrier wave. For the sake of convenience we shall express the conditions obtaining simply as sine functions:

$$S = S_o + \alpha \cos\omega_h t \quad \dots\dots\dots\dots (2)$$

$$V_g = \beta \cos\omega_i t \quad \dots\dots\dots\dots\dots (3)$$

In the expression for the anode current I_a we then have the term:

$$\alpha\,\beta\,\cos\omega_h t\,\cos\omega_i t$$

which can be resolved into two terms containing the sum and the difference respectively of the frequency of the carrier wave and of the auxiliary oscillation, thus:

$$I_a = \dots + \frac{\alpha\beta}{2}\left\{\cos(\omega_h + \omega_i)\,t + \cos(\omega_h - \omega_i)\,t\right\} \dots (4)$$

The differential frequency $(\omega_h - \omega_i)$, which is also termed the intermediate frequency, is then filtered out in the receiver. The differential-frequency circuits are very accurately tuned to an intermediate frequency-band at 125 kilo-cycles, which from now on acts in the receiver as the new carrier wave of the audio-frequency modulation. For if β in equation (3) is not constant, but varies with the audio-frequencies to be transmitted, then according to equation (4) the amplitude of I_a also will fluctuate with the same frequency. After suitable amplification, the intermediate-frequency carrier wave is separated in the usual way in the rectifying section of the receiver from the low-frequency modulation, which it is required to render audible in the loudspeaker.

The chief advantage of superheterodyne reception as compared with direct amplification and elimination of the high-frequency carrier wave is that the tuning of the intermediate-frequency circuits by the reception of stations operating with very different high-frequency carrier waves can always be very accurately maintained at the individual intermediate-frequency bands. Particularly the desire to make receiving apparatus capable of receiving, in addition to ordinary radio waves, also very short wave lengths, has been responsible for the adoption of the superheterodyne principle in radio reception.

The Octode

To generate the auxiliary oscillation and to modulate it on the incoming oscillation a special converter valve, the octode, is used in Philips superheterodyne receivers. This valve may be regarded as a triode and a pentode, connected in series, in which the triode serves for the generation of the auxiliary oscillation, while the pentode further handles the alternating current generated in the triode.

In the diagrammatic sketch in *fig. 1* the grids are marked from *1* to *6*. The indirectly-heated cathode together with the control grid *1* and the auxiliary anode *2* constitute the triode. The control grid *1* is connected to the oscillating circuit L_1C_1 which is tuned to the auxiliary frequency. L_2 is a reaction coil connected to the auxiliary anode *2*, while a third grid serves for screening the triode against the pentode. In the latter, *4* is the control grid, *5* the screen-grid and *6* the interceptor grid connected to the cathode, which prevents the secondary electrons emitted from the various grids and the anode from contributing to the anode current. The control grid *4* is in circuit with the tuned aerial circuit L_3C_3.

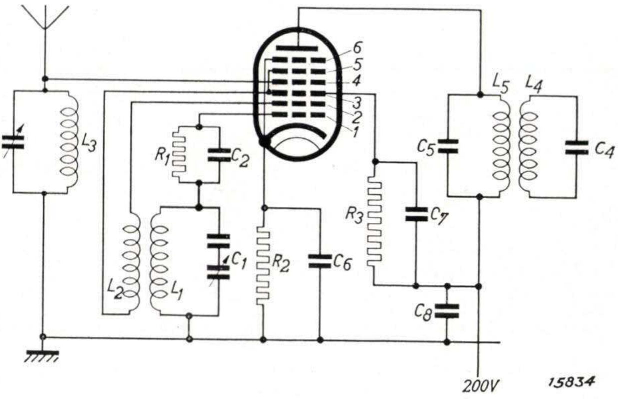

Fig. 1. Circuit diagram of the octode. The circuit L_1C_1 is tuned to the auxiliary oscillation, L_3C_3 to the incoming signals, L_5C_5 and L_4C_4 to the intermediate frequency.
1 = Control grid
2 = Auxiliary anode
3 = Screen-grid
4 = Control grid
5 = Screen-grid
6 = Intercepter grid

The potential applied to grid *1* varies in synchronism with the auxiliary frequency. As a result the electrons emitted from the cathode can only intermittently pass through the control grid *1*. An electron stream is therefore obtained in the pentode whose intensity varies with the auxiliary frequency. The amplification factor in the pentode of the converter valve will thus also vary periodically with the auxiliary frequency according to equation (2). The incoming oscillation, which has to be amplified, is applied to the control grid *4* of the pentode. This grid will therefore allow a more or less free passage to the electron stream in synchronism with the frequency of the incoming carrier wave, since its potential varies according to equation (3). In the anode circuit, resultant currents will therefore be obtained with either the additive or differential frequency of the auxiliary oscillation and the carrier wave, as expressed by equation (4). The connected circuits of the receiver, L_5C_5 and L_4C_4, are accurately tuned to the differential frequency, which is filtered out here and then passed to the rectifying stage as described above.

Mechanical representation with the aid of sand figures

Electrical oscillations are usually represented diagrammatically by means of a sinusoidal or similar type of wavy line. It appeared therefore that these oscillations, which are usually drawn with chalk on a blackboard, could be usefully reproduced mechanically for general exhibition by means of a sand figure on a slowly-moving belt. This would enable a practical demonstration of the principles of reception and the properties and uses of the carrier wave. In the demonstration model which was evolved for this purpose, the utilisation of the actual carrier wave is also demonstrated by means of a number of cathode ray tubes, which produce a visible trace of the electrical oscillations on their fluorescent screens.

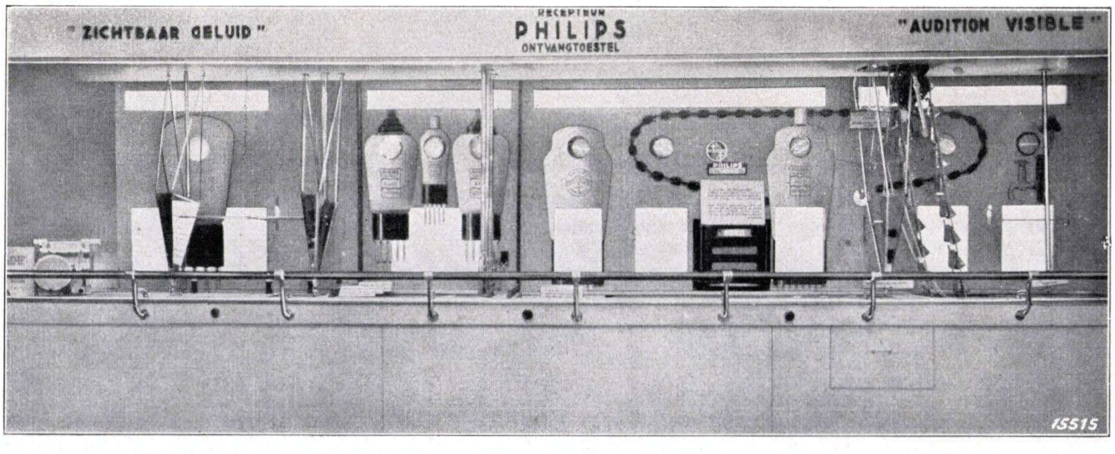

Fig. 2. Front view of model demonstrating superheterodyne reception, as shown at the Brussels 1935 World Exhibition.

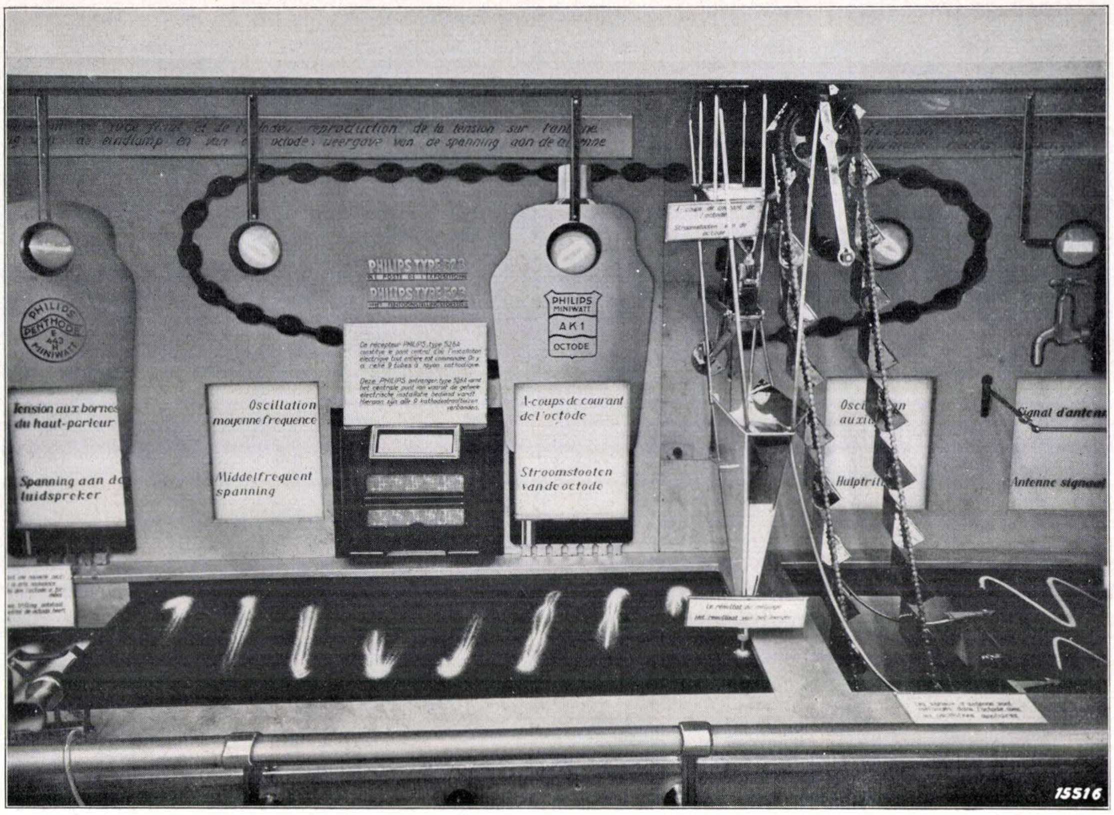
PHILIPS PENTHODE MINIWATT
Tension aux bornes du haut-parleur
Spanning aan de luidspreker
Oscillation moyenne frequence
Middelfrequent spanning
PHILIPS TYPE 528
PHILIPS MINIWATT
AK1
OCTODE
I-coups de courant de l'octode
Stroomstooten van de octode
Hulptril
Signal d'antenne
Antenne signaal
15516

Fig. 3. Sand figures demonstrating the anode current of the octode.

In *fig. 2* the apparatus is shown which was exhibited on the Philips stand at Brussels. The graphing of the various oscillations occurring in radio receivers in the form of sand figures is performed on a moving belt which moves in a horizontal direction from right to left. The belt is only just visible in this picture, but is more clearly shown in *fig. 3*. The feed tubes for the sand and the pendulums fitted with funnels which swing to and fro from back to front and thus produce the sand figures, can be picked out in fig. 1. *Fig. 4* is a diagrammatic sketch of the arrangement. The conveyer belts running from right to left are shown dotted in fig. 4b (*I*, *II*, ...). Above them are the funnel-shaped and tubular sand distributors (*1*, *2*, ...). Fig. 4a depicts the sand figures as they are produced on the horizontal moving belts.

The carrier waves of the incoming oscillations is shown in fig. 4a by curve *A*; the sand distributor *1* swings to and fro, while at the same time the belt *I* moves from right to left so that a sinusoidal or wavy line is traced. The modulation of the carrier wave has not been taken into consideration here as even with a very high musical note of for instance 5000 cycles, modulated on a 200-metre (1500-kilocycle) carrier wave, no less than 300 carrier-wave periods are required to reproduce a single modulation period. The variation in amplitude after only a few periods would therefore be too small on the belt to be distinctly visible. The curve *B* depicts the local oscillation which is generated by the octode in the receiver. It is traced on the belt by funnel *2*.

The superposition of the carrier wave and the local oscillation is represented by means of the sand figures in the following way. The two sand figures *A* and *B* drop into a mixing box at the end of the moving belt *I* and are then transferred to funnel *3* by means of an elevator, this funnel then tracing the striking figures *C* on the second belt. These figures symbolise the current in the anode circuit of the octode. The *C* figures are traced in the following manner:

Pendulum *3* always swings in phase with pendulum *1* which traces curve *A* (incoming carrier wave), but its flow of sand is not continuous, being regulated by means of a flap which opens and closes in phase with the motion of pendulum *2*. This intermittent release of sand gives a trace of the electron stream in the triode in phase with the auxiliary oscillation. The magnitude of the anode current varies in synchronism with the incoming carrier wave, which in the demonstration model is simulated by phase equality in the motions of pendulum *3*. If the ends of the sand figures *C* are visualised as connected by an envelope, a curve is obtained which slowly fluctuates up and down

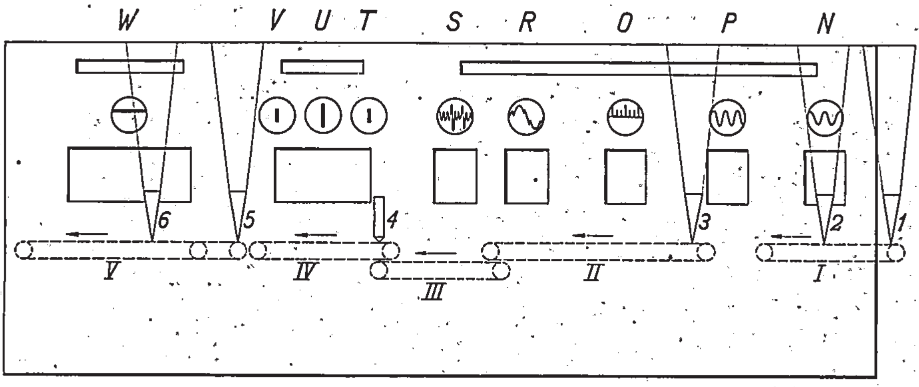

b

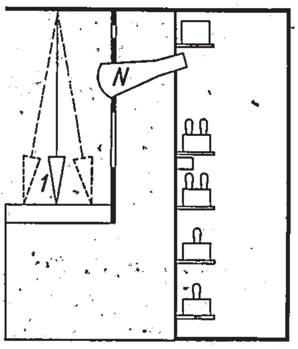

c

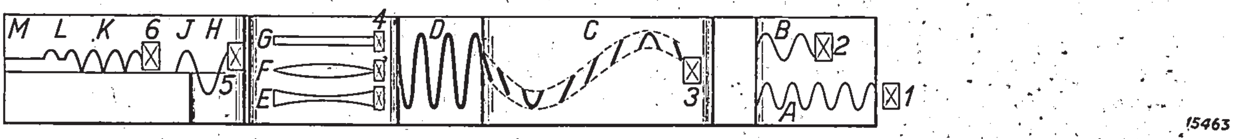

a

Fig. 4a. The belts moving from right to left on which the sand figures are traced.

A = Incoming signal
B = Auxiliary oscillation
C = Anode current of the octode
D = Intermediate-frequency oscillation
E = Variable magnitude of incoming signals
F = Amplification
G = Loudspeaker current, practically constant

E, *F*, *G* represent the automatic volume control.
H, *J*, *K*, *L* and *M* represent the methode of operation of the mains-fedd component of the receiver.

Fig. 4b. Diagrammatic front view of the demonstration model. *I* to *V* are the belts moving from right to left, on which the pendulums *1* to *6* trace the sand figures. *N* to *W* are the fluorescent screens of the cathode ray oscillographs on which the following voltages and currents are depicted.

N = Incoming signals from the aerial.
P = Auxiliary oscillation generated by the octode.
O = Variation of the anode current of the octode.
R = Voltage at the intermediate-frequency transformer.
S = Low-frequency voltage at the loudspeaker poles.
T = Portion of the signal voltage in first circuit of the receiver.
U = Amplication factor to which the receiver is automatically controlled.
V = Portion of the voltage at the loudspeaker terminals.
W = Variation of the rectified voltage.

Fig. 4c. Side view of model.

and represents the oscillation of the intermediate frequency. This behaviour can be observed in fig. 3.

In the intermediate-frequency circuits, the intermediate-frequency oscillation is filtered out from the current impulses leaving the converter valve. It then acts as a new carrier wave for audio-frequency modulation, which is what is required as it constitutes the sound emitted from the loudspeaker. As in this representation by means of sand figures modulation of the high-frequency carrier wave (pendulum *1*) has not been taken into account the converter valve of the demonstration model furnishes only an unmodulated intermediate frequency for the carrier wave. In view of the absence of modulation, rectification of the radio signals also has not been considered in the present model.

In the demonstration model, the sand figures on reaching the end of belt *II* are allowed to slide down a short inclined plane, which causes a more uniform distribution of the sand particles before the lower moving belt *III* is reached. This belt moves at a slower speed so that the sand particles falling on it produce a closed wavy curve *D* with a shorter wave-length (see fig. 4a). This curve represents the filtered oscillation of intermediate frequency as a function of a slower time parameter; thus for the sake of clearness the time axis of the sine curves, which are of principal interest here, has been slightly compressed on belt *III*.

Representation of other factors in reception

The radio receiver also incorporates a self-regulating fading eliminator or automatic volume control whose operation is based on the following principle. The fluctuation in the unidirectional voltage, which occurs on a variation in the amplitude of the intermediate-frequency carrier wave behind the rectifying stage, is led back to the preceding valves, whereby these valves receive a greater or smaller negative grid bias. As the incoming signals fade this bias is reduced and the amplification is increased. The method of volume control is represented by the sand figures *E*, *F* and *G* (fig. 4a). *E* represents the variable intensity of the incoming carrier wave, *F* the amplification which is maintained automatically in the receiver, and *G* the voltage fed to the loudspeaker and which is practi-

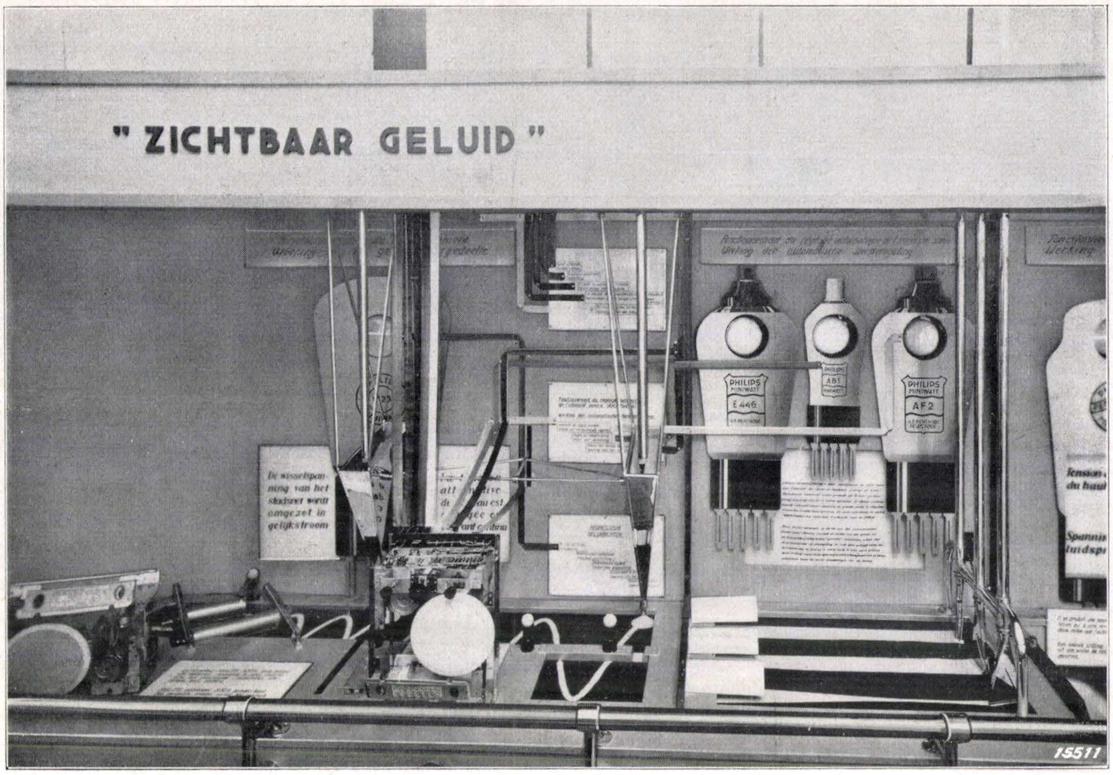

Fig. 5. Representation of automatic volume control and rectification of mains supply.

cally unaffected by the fading effect. These sand figures are traced by means of three funnels with flattened extremities from which the sand runs out (see the right half of *fig. 5*). The first two funnels can be turned about their longitudinal axis, but are coupled together in such a way that their relative positions differ by a fixed angle of 90°. If the first funnel traces a very thin line (corresponding to a very weak incoming signal) the second funnel traces a line of maximum breadth (corresponding to maximum amplification). The third funnel traces a curve of practically constant breadth. Only when the line traced by the first funnel becomes very thin (very extreme fading) is the third funnel turned a little, so that its trace also becomes somewhat narrower.

Finally, on the last belt (*V* in fig. 4b) the operation of the two-way rectifier is represented, which furnishes the anode voltage required for the receiving valves. A pendulum *5* traces sine curves which represent the transformer voltage, where *H* is one half and *J* the other half of the wave. The rectifying valve allows current to flow through it in one direction only. An arrangement has therefore been employed here which dispenses with *H* and retains only *J*. Two-way rectification may be regarded as the combination of two separate rectifiers which operate alternately, so that each of the half-waves is rectified. To represent this a second pendulum *6* is allowed to trace a sine curve in phase opposition to the first pendulum funnel, and which traces the voltage of the other half of the transformer. After two-way rectification a pulsating rectified current is produced which is represented in sand figure *K*. The first condenser of the smoothing circuit reduces the non-uniformity of the rectified current. This is simulated in the sand figures by means of a small revolving brush which sweeps the sand towards the middle, so that figure *L* is produced. Further smoothing makes the current completely uniform and steady; thus a second brush removes the slight remaining waviness and traces figure *M* (see on the left of fig. 5).

The sand dropping off the ends of the belt is collected and is returned to the storage box by means of an elevator which is not visible to the public; at the same time it is dried to prevent the sand particles adhering to the belts.

Demonstration with Cathode Ray Tubes

In addition to this highly slowed down representation of the processus occurring in the superheterodyne receiver, the various electrical phenomena have also been rendered visible by a series of nine cathode ray tubes whose fluorescent screens are shown in fig. 2. The alternating voltages at nine different points of the receiver are magnified by amplifiers to such values that their fluctuation can be demonstrated with the aid of the cathode ray tubes. Each amplifier has its own rectifier so that no disturbing coupling actions can be produced.

The amplified voltages are applied to the deflection plates of the cathode ray oscillographs which deflect the electron beam in a vertical direction. By means of a horizontal time-base deflection [1]) of suitable frequency the alternating current figures are traced on the fluorescent screens. The period of the time-base can be adjusted as required, but it must be a whole multiple of the alternating voltage represented.

In fig. 4b the screens of the tubes are indicated by the letters *N* to *W*. The suffixes indicate the nature of the trace on each screen. By applying more or less quickly varying saw-tooth voltages, sinusoidal figures were obtained on the screen which showed more or fewer oscillations as indicated in fig. 4.

In place of the saw-tooth voltage variation of the time-base a sinusoidal voltage of mains frequency can also be applied to the horizontal deflecting system or to both systems. In the first case the so-called Lissajous curves are obtained and in the second case ellipses, which may be seen on the screens in figs. 2 and 3.

Fig. 4c shows a section through the electrical portion of the demonstration model, which consists of a radio receiver with 53 auxiliary units. This part (see *fig. 6*) is enclosed in a metal chamber which effectively screens off the action of surrounding disturbing fields. (A tramway line with heavy traffic passed directly under the Philips stand at the exhibition.) As the sand figures require a considerable amount of space and the cathode ray tubes must also not be placed too close to each other, the whole model is 7.5 metres long and is thus probably the largest radio receiver in the world. The demonstration model was constructed in the Research Laboratory on designs of R. P. Wirix.

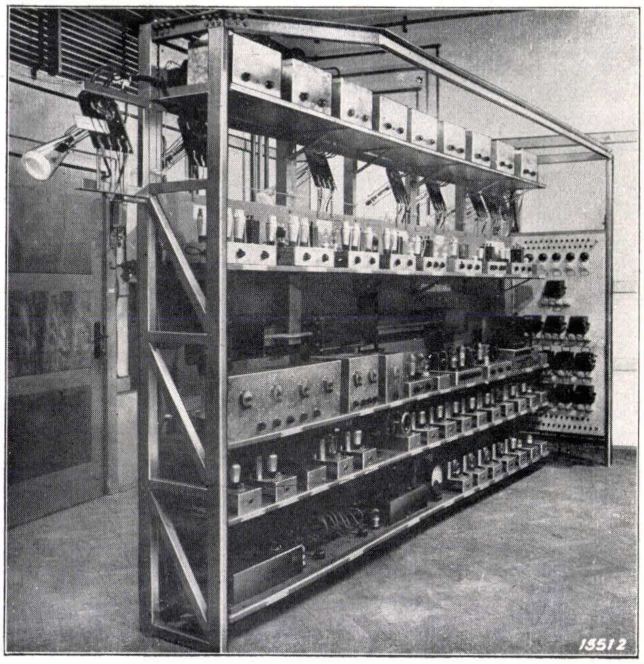

Fig. 6. Rear view of model.

Compiled by H. J. J. BOUMAN.

---

[1]) For the time-base deflection the saw-tooth variation of a special type of relaxation oscillations is employed. For further details see: Philips techn. Rev. **1**, 16, 1936.

ABSOLUTE SOUND-PRESSURE MEASUREMENTS

By J. DE BOER.

Summary. The paper discusses two methods for the measurement of sound pressures, by both of which a microphone is calibrated. The difference of the results is within the limits of discrimination of the ear.

Introduction

To determine the sensitivity of a loudspeaker or a microphone it is necessary to measure two magnitudes of different quality, an electrical magnitude (e.g. the current passing through the coil of the loudspeaker or the voltage at the output terminals of the microphone) and an acoustic magnitude (e.g. the sound output of the loudspeaker or the sound pressure at the location of the microphone). The first two sections of this article describe two methods for measuring sound pressures. In the first Raleigh's disc is used and in the second the condenser microphone. In the concluding section details are given of the results of a calibration carried out by these two methods.

Raleigh's Disc

Raleigh's disc is a thin circular plate suspended from a torsion wire (*fig. 1*). If a disc of this type hangs vertically in a uniform or periodic stream of gas or fluid, it will sustain a torque which will tend to turn its surface in a direction perpendicular to the direction of flow. The magnitude of this torque M is determined by the mean velocity v of the vibrating air particles. If M is known then the velocity and hence also the sound pressure can be calculated. Rayleigh was the first to investigate these phenomena. König [I]) has calculated the torque M on the basis of the following assumptions:

a) An incompressible fluid,
b) uniform rate of flow, and
c) total absence of friction and viscosity.

He obtained the expression:

$$M = \frac{4}{3}\,\varrho\, a^3\, v^2 \sin 2\vartheta \qquad (1)$$

where ϱ is the density of the fluid, v the velocity of flow, ϑ the angle between the vertical to the disc and the direction of flow, and a the radius of the disc.

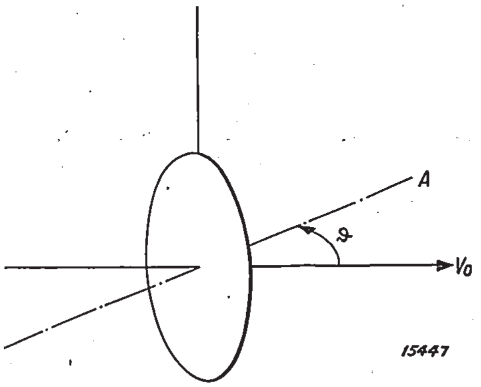

Fig. 1. Rayleigh's disc. The atmospheric vibrations in the field of sound exercise a torque on the disc such that its axis A tends to turn into the direction of propagation v_0 of the sound. The torque has its greatest value when the angle ϑ between A and v_0 is 45 deg.

With the aid of the streamline diagram reproduced qualitatively in *fig.* 2, an idea may be gained of the action of the flowing medium on the disc. With a current flowing in a horizontal direction without eddies, the following relationship connects the pressure p and velocity v:

Pressure energy + kinetic energy = constant.

Applying the theorem to 1 cm³ of the fluid gives Bernoulli's equation:

$$p + \frac{\varrho}{2}\, v^2 = \text{constant.}$$

The highest excess pressure p_m is obtained at the condensation points P_1 and P_2 in fig. 1, where the velocity of flow is zero. The peak values of the pressure on the back and front of the disc are obviously displaced with respect to each other and produce a torque which tends to turn the disc perpendicular to the direction of flow. If the pressure distribution on the front and rear of the disc is in each case replaced by the resultant K, one obtains *fig.* 3. It is clear that

the pressure p is proportional to $^1/_2\, \varrho\, v_0^2$,

the force K is proportional to $^1/_2\, \varrho\, v_0^2\, \pi\, a^2$,

The torque M is proportional to $^1/_2\, \varrho\, v_0^2\, \pi\, a^2\, a$.

This result is in agreement with equation (1). Furthermore it is obvious from conditions of symmetry that the torque must disappear if the angle between the disc and the direction of flow is either zero or 90 deg. This is expressed by the term $\sin 2\vartheta$ in equation (1).

For the purpose of König's calculation it is not absolutely essential to assume that the flow is uniform. Equation (1) also applies to periodically-variable conditions of flow provided the wave-length is sufficiently great compared with the dimensions of the disc. The mean value of the torque is therefore:

$$\overline{M} = \frac{4}{3}\,\varrho\, a^3\, \overline{v}^2 \sin 2\vartheta \qquad (2)$$

where $\overline{v}^2$ is the mean square of the velocity. $\overline{M}$ represents the torque produced by a sound field[1]. As owing to its inertia Raleigh's disc cannot respond to acoustic vibrations, the average torque alone is of practical interest. From equation (2) one gets:

$$\overline{v} = \sqrt{\frac{3\,\overline{M}}{4\,a^3\,\varrho \sin 2\vartheta}} \qquad (3)$$

By carrying out a measurement of $\overline{M}$, $\overline{v}$ can be calculated from this equation, i.e. the square root of the mean square velocity of the vibration. The relationship between $\overline{v}$ and the corresponding sound pressure $\overline{p}$ depends on the type of sound waves under consideration.

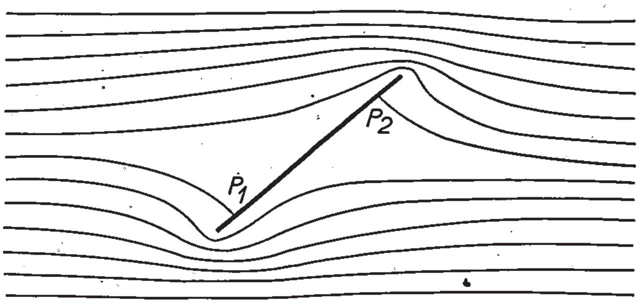

Fig. 2. Streamlines around an infinitely long strip arranged perpendicular to the plane of the paper. The diagram also applies qualitatively for the conditions of flow round a circular disc. The hydrodynamical pressure is greatest at the condensation points P_1 and P_2.

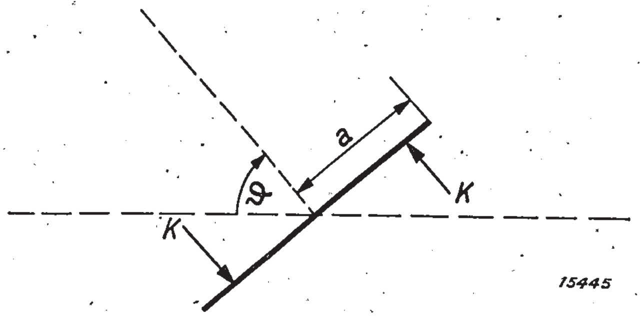

Fig. 3. Hydrodynamical forces. The resultants K of the component pressures on the rear and front sides of the disc are displaced with respect to each other (corresponding to the positions of the condensation points) and produce a torque. The arm on which this torque acts is proportional to the radius a of the disc; the force K is proportional to the surface area πa^2 of the disc.

With plane waves, this relationship is expressed by $p = \varrho \cdot c \cdot v$, where c is the velocity of sound. If c is measured in cm per sec, we get for air at 1 atmospere pressure and a temperature of 20 deg. C numerically:

$$\overline{p} = 42{,}6\ \overline{v}\ \text{bar (see footnote } ^{2})) \qquad (4)$$

In the case of spherical waves emitted from a point source of sound, the relationship between the sound pressure and the velocity of the vibrating particles is by no means so simple. For a sound with a frequency ν and a wave number k (i.e. k wave-lengths per unit of length) the laws ruling p and v take the form:

$$p = A \sin 2\pi(\nu t - kr)$$

$$v = A\cdot\varrho\cdot c\left[\sin 2\pi(\nu t - kr) - \frac{\cos 2\pi(\nu t - kr)}{2\pi kr}\right]$$

These expressions indicate that equation (4) is applicable also to spherical waves with an accuracy of 1 ‰, if the distance r from the source of sound is at least 3.5 wavelengths of the sound under consideration (e.g. 120 cm with 1000 cycles).

Deviations from König's theory occur, when the length of the sound waves becomes comparable with the diameter of the disc. If the disc has a diameter of 1 cm, the correction required at 10,000 cycles is in the neighbourhood of 10 per cent.

Measurement of the Torque

The torque $\overline{M}$ given by equation (2) will turn the disc through an angle α, which will have such a magnitude that the elastic strain of the torsion wire will balance the torque ($\overline{M} = D\,\alpha$). The angular deflection α of the reflecting disc is determined by the reflected beam method, which consists in viewing through a telescope the image of a scale reflected by the disc (see fig. 4). The directing torque D is obtained from the time of oscillation T of the disc when swinging freely and from its known moment of inertia Q, thus:

$$D = \frac{4\pi^2 Q}{T^2};\quad M = \frac{4\pi^2 Q}{T^2}\,\alpha \qquad (5)$$

Substituting M in equation (3), we get the average velocity:

$$\overline{v} = \frac{\pi}{T}\sqrt{\frac{3\,Q\,\alpha}{\varrho\, a^3 \sin 2\vartheta}} = \frac{5{,}44}{T}\sqrt{\frac{Q\,\alpha}{\varrho\, a^3 \sin 2\vartheta}} \qquad (6)$$

---

[1] The medium of the sound-waves does not correspond with the assumption of an incompressible frictionless fluid as made by König in his calculations. Nevertheless, as King[II]) has shown, König's result as summarised in equation (1) also applies to sound-waves.

[2] 1 bar = 1 dyne/sq.cm. = 0.75 10^{-3} mm Hg.

Equation (6) expresses the velocity $\overline{v}$ of the sound vibrations as a function of the angular deflection α of **Raleigh**'s disc. All other terms in the equation are known.

It suggests itself that these measurements could be suitably carried out in the open air where no reflected sound would be a source of disturbance. This, however, has proved impossible as **Raleigh**'s disc responds, not only to audio-frequency sound waves, but also to slowly-variable air currents which always occur with measurements in the open and seriously disturb measurements, due to the long oscillation time of the disc. For this reason the disc was suspended in a room surrounded by walls having a high sound-absorption factor (*fig.* 4). The wall opposite the sound-source was left open as it is the sound-wave reflected from this wall which constitutes the most serious source of error. The higher the frequency, the lower is the interference due to reflected waves, since the absorption coefficient of the walls increases with the frequency and since, moreover, if a loudspeaker is the source of sound, the beam of sound becomes increasingly directional with rising frequency.

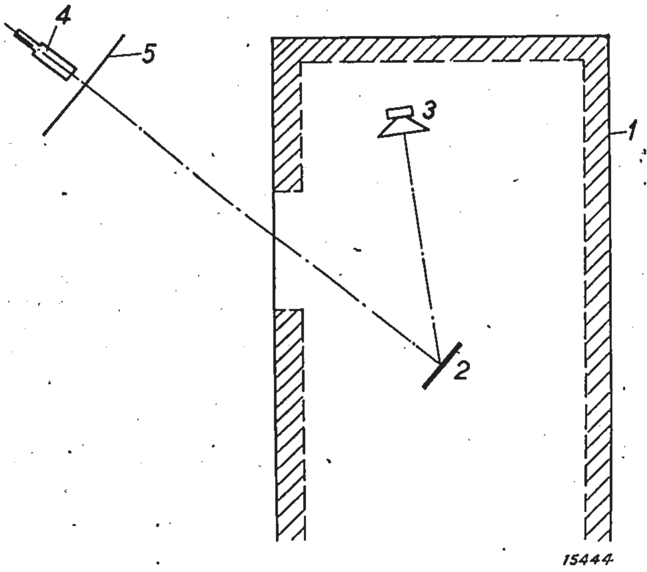

Fig. 4. Room with sound-absorbing walls suitable for measurements with Rayleigh's disc.
1. Wall covering
2. **Rayleigh**'s disc
3. Loudspeaker
4. Telescope
5. Scale.

The Condenser Mikrophone

The responsive element of the condenser microphone is a diaphragm conducting electricity **1** (e.g. of aluminium 20 μ in thickness), stretched directly in front of an electrode **2**. This diaphragm vibrates under the action of the sound-waves in exact response to the fluctuations in pressure. The capacity of the condenser composed of the electrodes **1** and **2** is thus subject to a periodic fluctuation. As the condenser is charged, the fluctuations in capacity become converted into fluctuations in voltage, which are measured by means of an amplifying voltmeter. The circuit of the condenser microphone and its connection with the first valve of the voltmeter is shown in *fig.* 5.

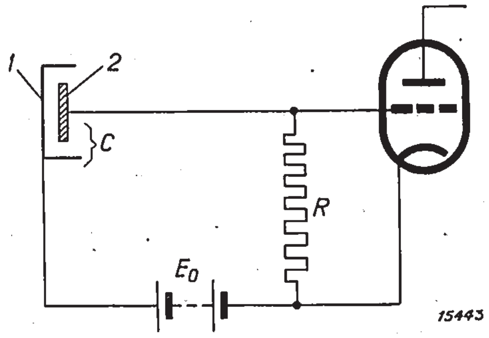

Fig. 5. Diagrammatic sketch of a condenser microphone.
1 = Diaphragm
2 = Contra-electrode
R = Resistance leak
E_0 = Battery.
The varying sound-pressure acting on the diaphragm **1** produces changes in the capacity C. As a result the voltage of the condenser fluctuates, since the charge cannot flow with sufficient speed from or to the condenser via the resistance R.

If ω is the angular frequency of the sound, the distance between the electrodes **1** and **2** can be expressed by:

$$d = d_0 - d_1 \sin \omega t$$

where d_o is the mean value of the distance between the plates and d_1 is the amplitude of oscillation. The capacity C of the condenser is also subject to periodic variation:

$$C = \frac{Surface\ of\ plates}{4\,\pi \cdot gap} = \frac{O}{4\,\pi\,(d_0 - d_1 \sin \omega\, t)}$$

At a sufficiently low frequency, a quantity of electricity would flow either to or from the condenser through the resistance R such that the E.M.F. of the condenser would remain constant, viz, equal to the battery voltage E_0. At sufficiently high frequencies (time of oscillation small as compared with the relaxation time RC of the condenser [3])) the charge q of the condenser may, however, be regarded as invariable ($q = OE_0/4\,\pi\,d_0$). The E.M.F. of the condenser then becomes:

$$U_C = \frac{q}{C} = \frac{q}{O}\,4\pi\ (d_0 - d_1 \sin \omega\, t)$$

---

[3] The period of discharge of a condenser C through a resistance R is given by the product RC (cf. the article dealing with relaxation oscillations, this journal **1**, 44, 1936).

The potential difference U_R across the terminals of R is:

$$U_R = E_0 - U_C = \frac{4\pi q}{O} d_1 \sin \omega t$$

$$= E_0 \frac{d_1}{d_0} \sin \omega t \qquad (7)$$

As stated above, equation (7) applies when

$$RC \gg \frac{1}{\omega} \text{ or } RC\omega \gg 1.$$

In order to draw conclusions regarding the sound pressure from the amplified alternating voltage, the elastic characteristics of the diaphragm must be known and in addition all other magnitudes in the electrical amplifier. The very tedious work of determining the numerical value of each factor can, however, be dispensed with, since the whole system can be calibrated by applying a known pressure, generated electrically. This pressure is generated by means of an electrode placed in front of the diaphragm. Applying to the fronting electrode the sum of a D.C. voltage and an A.C. voltage of audio-frequency, the diaphragm will be attracted by alternating forces which can be casily calculated.

The tension on the plate of a condenser is:

$$p = \frac{E^2}{8\pi}$$

where E is the electrical field-strength. In the case in question (*fig.* 6) $E = E_1 + E_2 \sin \omega t$ and hence

$$p = \frac{1}{8\pi}\left[E_1^2 + 2 E_1 E_2 \sin\omega t + \tfrac{1}{2} E_2^2 (1 - \cos 2\omega t)\right] \qquad (8)$$

The pressure expression contains a constant term, a term which varies with the angular frequency ω and a term varying with 2ω. It is therefore not purely harmonic, but also includes a second overtone. This latter can, however, be neglected if the amplitude E_2 of the A.C. voltage is sufficiently small with respect to E_1. If E_1 is zero, only the overtone is obtained, i.e. a purely harmonic oscillation of double the frequency.

The fronting electrode (fig. 6) is designed as a latticed bar. If a solid plate were used an enclosed air-space would be produced between 1 and 3, and as a result the diaphragm would acquire an additionall stiffness during calibration which would be absent in ordinary sound-pressure measurements. As the above calculation of the sound pressure applies to a flat electrode, equation (8) is not strictly correct, and there should be included a correction factor independent of the frequency III).

In measurements with the condenser microphone two further corrections must still be taken into account, for the microphone measures the sound-pressure at the location of the diaphragm, while actually information is required of the pressure at the same point in the absence of the microphone. For two reasons the pressure is not the same in the absence and presence of the microphone:

a) Owing to refraction of the sound-waves around the microphone, a phenomenon which increases the sound pressure. The smaller the wave-length of the sound, the greater will be this correction. If the sound-waves are small compared with the diameter of the diaphragm, the sound-pressure will be doubled. The requisite correction can be calculated if the design and dimensions of the microphone are known IV).

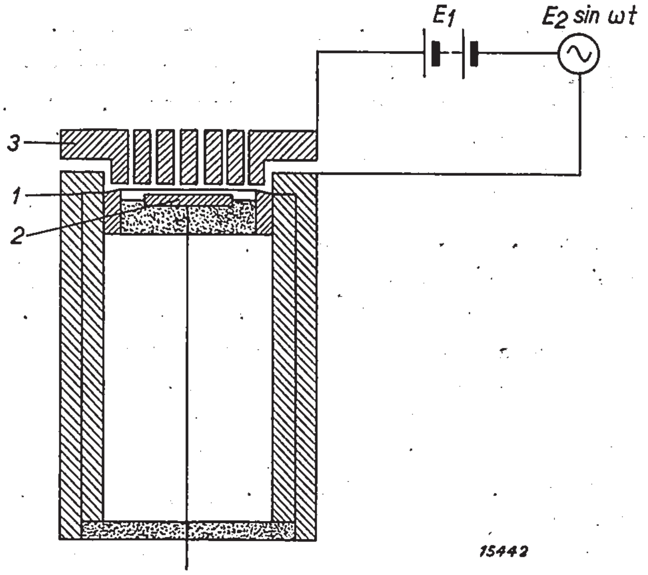

Fig. 6. Section through a condenser microphone with electrode placed in front of it.

1 = Diaphragm
2 = Contra-electrode
3 = Fronting electrode.

By means of a D.C voltage (E_1) and an A.C. voltage ($E_2 \sin \omega t$), connected in series to the fronting electrode, a pressure of known magnitude and frequency is applied to the diaphragm. Bij this means the whole system can be calibrated.

b) Owing to the shape of the housing. The microphone is designed in such a way that the diaphragm

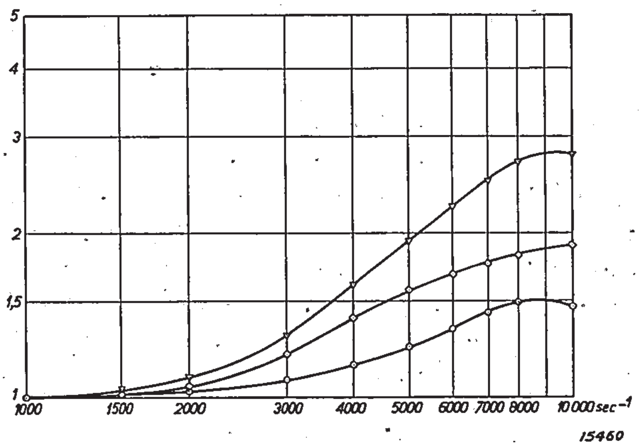

Fig. 7. Correction factors for the condenser microphone. Lower curve: Correction for resonance of the extension, mean curve: Refraction correction, upper curve: Total correction.

With sound-frequencies of 10,000 cycles the pressure on the diaphragm is nearly 3 times as great as the pressure at the corresponding point in space in the absence of the microphone At frequencies below 1000 cycles no corrections need be made.

constitutes the rear of a short cylindrical extension tube. The pressure on the diaphragm is not exactly equal to the pressure on the front surface of the extension. **Ballantine** and **West** have calculated the ratio of the two pressures V)). In *fig. 7* in addition to the correction for refraction, computed for a microphone of 25 mm diameter, the correction due to the resonance of the extension tube is also shown as a function of the frequency for an extension 3 mm long, and a diaphragm 18 mm in diameter. The upper curve in this figure represents the aggregate correction taking into consideration these two factors.

Measurements with the Condenser Microphone

As already pointed out, the voltage of the microphone is amplified. The amplifier must not be placed too close to the microphone as otherwise it will interfere with the field of sound. On the other hand the leads from the microphone to the amplifier must not be too long, since otherwise the capacity of the leads becomes too high.

The method is particularly suitable for use in the open air. The effect of uniform air currents can be neglected, and although sudden air impulses do affect the deflection, these can be readily detected, since the voltmeter operates with practically no lag.

Comparison of the Two Methods

A **Raleigh** disc was suspended in front of a loudspeaker at a distance of 1 m. The loudspeaker current was adjusted for different frequencies such that the disc indicated a sound-pressure of 1 bar. A condenser microphone was then substituted for the **Raleigh** disc and the voltage at the output terminals of the microphone amplifier was measured with exactly the same frequencies and current intensities through the loudspeaker coil. The calibration curve for the microphone obtained in this way was compared with electrostatic calibration results, allowing for the corrections discussed above. The result obtained is shown in *fig. 8*.

The degree of concordance between the two methods is entirely satisfactory. Throughout the whole frequency-range up to 8000 cycles the results differ by less than 7 per cent (i.e. by less than 0.6 db 4))). At very low frequencies the **Rayleigh** disc is perhaps slightly less reliable, for the effect of the reflected waves is difficult to eliminate in these circumstances. On the other hand, at the highest frequencies less credence must be put on the indications of the condenser microphone, as the corrections for refraction are then very large (e.g. at 8000 cycles almost equal to a factor 3). The maximum difference of 7 per cent between the two methods is below that which can be detected by the human ear. The degree of accuracy thus conforms with all practical requirements.

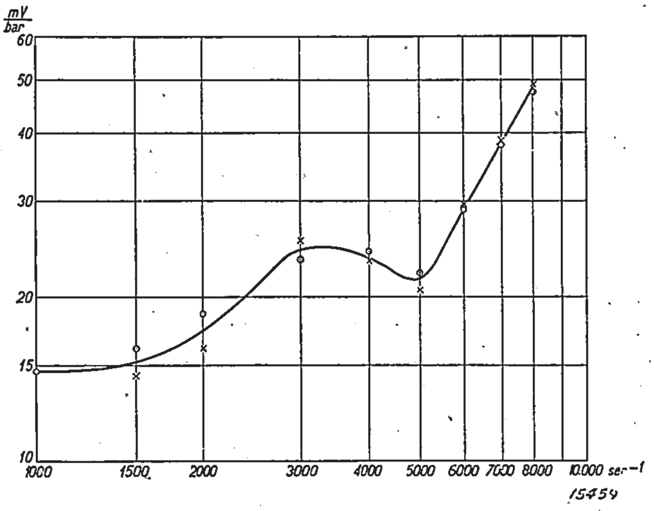

Fig. 8. Calibration of a condenser microphone. Sensitivity of the microphone in millivolts per bar plotted as a function of the frequency.
× Calibration by means of the fronting electrode
⊙ Calibration by means of **Rayleigh**'s disc.

LITERATUUR

I) W. **König**, Wied. Ann. **43**, 43, 1891.
II) L. v. **King**, Proc. Roy Soc. A. **153**, 17, 1935.
III) S. **Ballantine**, Journ. Ac. Soc. Am. **3**, 352, 1932.
IV) S. **Ballantine**, Journ. Ac. Soc. Am. **3**, 319, 1932.
V) S. **Ballantine**, Proc. I.R.E. **18**, 1206, 1930.
W. **West**, Proc. Inst. Electr. Eng. **5**, 145, 1930.

---

4) The difference ΔI of two sound-intensities corresponding to the sound-pressures P_1 and P_2, is defined by $\Delta I = 20 \, log_{10} \, P_1/P_2$ decibel. The ear cannot discriminate differences below 1 decibel, i.e. of 12 per cent of the sound-pressure.

HIGH-FREQUENCY OSCILLATIONS IN SODIUM LAMPS

By L. BLOK.

Summary. In addition to the high-frequency oscillations occurring on ignition with all discharge tubes fed with alternating current, permanent high-frequency oscillations can also be present in the discharge in sodium lamps, and in certain circumstances, if no suitable precautions are taken, these can interfere with radio reception. The investigation of these oscillations in direct-current lamps has resulted in the recognition of two types of oscillations, A and B, which differ from each other in their external characteristics and in their response to several factors. Type A oscillations are apparently due to oscillations of positive ions, and type B to oscillations of electrons. With current designs of lighting equipment, in which each lamp is fed via its own auto-transformer (with secondary winding split into two parts symmetrically connected to the lamp), the oscillations normally do not react on the mains supply. In special cases where interference with radio reception may occur, a small and simple interference suppressor will be found adequate to remove all interference.

Introduction

It is well known that in discharges through gases high-frequency oscillations may occur, which by radiation or transmission along conductors may cause interference with radio receiving apparatus in the neighbourhood. The propagation of these oscillations to the mains supply is nowadays in the case of sodium lamps avoided very simply by a suitable design and circuit for the supply transformer. In order to find out what precautious would be suitable for avoiding interferences, it was desirable to obtain a closer insight into the production and nature of these oscillations.

A distinction must here be drawn between high-frequency oscillations generated during the burning of the lamp and those generated during ignition. The latter type is a well-known cause of radio interference; it may occur with practically all A.C.-fed discharge tubes, such as the neon tubes used in luminous signs, rectifying valves, etc., which are started up and extinguished again twice in each period. In many cases this kind of interference is absent altogether; when it occurs, however, it is similar to the interference caused by sparking at switches and electric motors. An analysis of this type of oscillation offers no new information and will therefore not be discussed here, the more so since these oscillations are rendered harmless by interference suppressors at the same time as the oscillation of the gas discharge per se.

In the case of interference from direct-current discharges it is evident that only the permanent high-frequency oscillations can be responsible, for ignition only takes place once here, viz, on switching on. That the permanent oscillations may in certain circumstances interfere with radio reception was seen on adopting sodium lamps (which were originally of the D.C. type) for street lighting. This gave the impetus to a closer investigation of the problem, the results of which are briefly outlined in this article 1)).

Measurement of the High-Frequency Oscillations

At the outset an arrangement was evolved for measuring the high-frequency oscillations. The apparatus used for outdoor measurements consisted of a transportable receiver with aerial, the high-frequency oscillation being reproduced in the loudspeaker as a radio interference, while at the same time the rectified voltage was measured with an

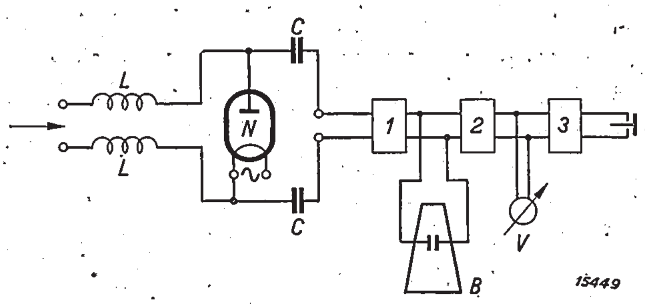

Fig. 1. Measuring apparatus for investigating high-frequency oscillations in sodium lamps. The lamp N is fed with direct current. Two chokes L prevent the transmission of the high-frequency oscillations to the network, and two condensers C shut off the unidirectional voltage from the actual measuring apparatus. 1 is a high-frequency amplifier, behind which the cathode-ray tube B is connected. In 2 the high-frequency oscillations are rectified and in the amplifying voltmeter V connected after it the high-frequency voltage is measured. 3 is a low-frequency amplifier which renders the oscillations audible in the loudspeaker as radio interference.

---

1) Although, in the meantime, the Philips Works have for various reasons changed over to the production of sodium lamps for alternating current, the observations made on direct-current lamps are still of interest.

amplifying voltmeter. In measurements in the laboratory the high-frequency voltage was in addition rendered visible by means of a cathode-ray tube. For this purpose, however, the high-frequency oscillation was tapped directly from the lamp. The experimental apparatus used is shown in *fig. 1.*

By means of a band-pass filter in the high-frequency amplifier, various wave-bands from 200 to 2000 m could be adjusted for determining the frequency range of the oscillations. The fluorescent spot on the screen of the cathode-ray tube was expanded to a luminous line of adjustable length (time axis), by means of a "saw-tooth" deflection voltage [2]). The (amplified) high-frequency voltage broadened this line to a band (*fig. 2*) whose width was a direct measure of the amplitude of this voltage. In subsequent measurements with A.C. lamps the time-deflection frequency was synchronised with the frequency of the A.C. mains supply or with a fraction of this frequency; in this way information was also obtained of the distribution of the oscillations throughout the period of the A.C. supply.

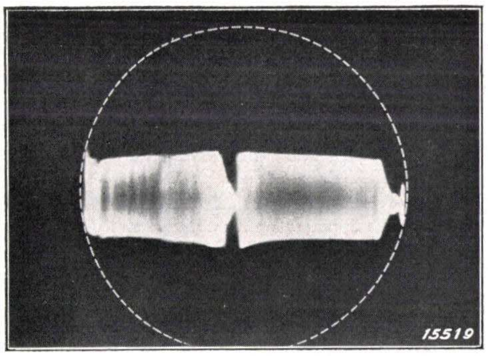

Fig. 2. Fluctuation of the high-frequency voltage of an alternating current sodium lamp ("Philora" type SO 100) during a single period of the mains alternating current. The fluorescent spot on the screen of the cathode-ray tube is elongated to a (horizontal) luminous line, the time-axis, by a "saw-tooth" voltage. The high-frequency voltage deflects the electron beam in a direction perpendicular to the time axis, and the luminous line of the fluorescent screen is broadened to the band photographed here. The width of the band is a measure of the amplitude of the high-frequency voltage. The time-deflection frequency is synchronised with the frequency of the A.C. mains supply. If conditions are exactly the same in each period, a stationary image is obtained. Exposure time of this picture was about 10 periods (approximately $^1/_5$ sec).

The majority of the measurements made were carried out with sodium lamps of the low-voltage arc type. These lamps were fed with 24 volts unidirectional current (the voltage drop was approximately 14 volts). The arc intensity i_b was 5 to 12 amps, the cathode was heated by an alternating current i_f of about 10 amps.

Two Types of Oscillation

The oscillations obtained with different lamps were never of exactly the same type. Yet it was soon established that two essentially different types of oscillation A and B were present, providing criteria by which almost all lamps could be classified according to their behaviour.

Type A oscillations contain components with frequencies from about $1.5 \cdot 10^6$ to $0.5 \cdot 10^6$ cycles corresponding to wave-lengths λ of 200 to 600 m. The components are found to be at certain fairly well-defined wave-lengths in this range. In many cases the frequency difference between several successive components was constant, and these may therefore be regarded as harmonics of an oscillation of much lower frequency (i.e. equal to the frequency difference in question, with λ up to 30,000 m), whose existence was proved indirectly in this manner. Type A oscillation is modulated to a marked degree with the frequency of the heating current (50 cycles).

Type B oscillations are also situated in the range of wavelengths from 200 to 600 m, but cover a more continuous frequency band. They are much weaker than A and cannot therefore be detected by the oscillograph; they are modulated to a lesser degree or not at all. The striking observation was made that in suppressing radio interference due to the B type of oscillation (but not of the A type) by means of a condenser connected in parallel (see below), the length of the connecting leads played an important part. It may be concluded from this that the B oscillations also contain an ultra-short wave component.

More striking still than the difference in the characteristics of these types of oscillations is their difference in response to conditions under which the lamp is run. The determining factors here are the arc intensity i_b and the intensity of the heating current i_f; i_b determines the concentration of the ions in the discharge and i_f the emission of electrons from the cathode [3]). If a lamp generates type A oscillations, oscillation increases as i_b is raised and/or i_f is reduced. If on the other hand the lamp is subject to B oscillations, its behaviour is the exact converse: oscillation increases as i_b is reduced and/or i_f is increased. In very many lamps a transition from type A to type B could in fact be obtained by altering i_b and i_f. In a lamp with A oscillations, by reducing i_b and raising i_f, the amplitude of the high-frequency voltage (read on the amplifying voltmeter) was progressively reduced, and eventually disappeared altogether at certain values of i_b and i_f; on a further alteration of i_b and i_f in the same sense, type B oscillations then made their appearance with a gradually increasing amplitude. In principle this could provide a means for eliminating a possible radio interference, viz, by suitable regulation of the arc and heating currents of the lamps. In practice, however, this method of suppression is not suitable. Even if the working conditions of the lamp were not already fixed by other considerations, and the transition from type A to type B could be effected in all lamps via an intermediate state devoid of oscillation (which is definitely not the case), a single regulation of each lamp would not in fact suffice, since the oscillatory behaviour of the lamps varies considerably with increasing age. Moreover, the oscillations can be rendered harmless by much simpler means, as is shown below.

---

[2]) See e.g. Philips techn. Rev. **1**, 19, 1936.

[3]) Actually the emission of electrons is also determined by i_b, as the ions may pull out extra electrons from the cathode and also may heat the cathode by their bombardment. On a variation of i_b, there is thus a change in the concentration of the ions as well as in the emission of electrons.

As already pointed out, type A oscillations are promoted by an increase in the ion concentration and reduced emission of electrons, while type B oscillations are promoted by just the opposite, viz, an increase in emission and a reduced ion concentration. These facts suggest that in the case of type A oscillations the oscillations of positive ions in the discharge play a part, while with type B on the other hand the oscillations of electrons are the governing factor. Oscillations of ions and electrons in gases have in fact been known for some time. The frequencies which have been deduced theoretically for the oscillations of ions are also of the same order of magnitude as those found here. The oscillation of electrons may perhaps be regarded as a Barkhausen-Kurz oscillation [4]) in which the positive space-charge cloud hovering behind the cathode fall assumes the rôle of the positive grid [5]).

Suppression of Oscillations

Investigation of the high-frequency oscillations obtained with various street-lighting systems confirmed the results of laboratory work. In particular it was found that an overhead feeder system with a number of sodium lamps connected in series selected from the wide frequency-band of the lamps' oscillations the particular frequency to which it was "tuned". Along the feeder stationary waves are produced, whose nodes and antinodes may be readily located by moving the transportable measuring equipment along the feeder. Hence from the point of view of the feeder promoting interference, a lighting system fed through a buried cable is more suitable than an overhead feeder owing to the smaller amount of radiation due to the cable. With the latter an ordinary interference filter may prove sufficient to prevent the propagation of the high-frequency oscillations to other sections of the supply.

At the present day, however, it is more common practice to connect the lamps in parallel than in series. In these systems interference is suppressed in the following way. Each lamp is connected in parallel to the supply via its own auto-transformer (*fig. 3*). For both lamp terminals a portion of the secondary winding of the transformer acts as a choke, which prevents the propagation of the high-frequency oscillations. All interferences are avoided by this arrangement, provided the transformer is placed directly next to the lamp. Where this is not possible, for instance in cases where the lamp and transformer are separated by a section of the overhead feeder (acting as an aerial), each lamp must be supplemented by its own suppression units. This is done in the usual way by the addition of condensers and self-induction coils.

For direct-current lamps, a small condenser of about 2 μF rating is in general sufficient for suppressing the high-frequency oscillations. To ascertain whether a lamp is oscillating or not, a simple method was available here. The voltage-drop across the lamp is measured, the condenser being paralleled during measurement. If high-frequency

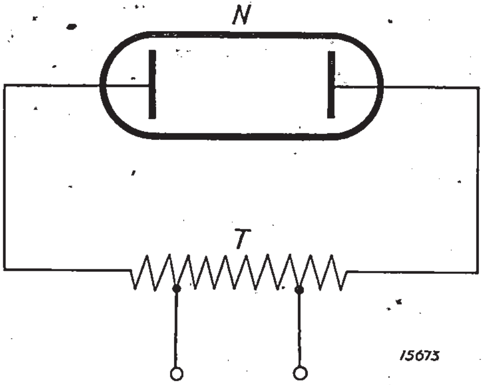

Fig. 3. Current method of interconnection of lamps for suppressing high-frequency oscillations. Each lamp N is connected in parallel to the mains with its own auto-transformer T, in such a way that a portion of the secondary winding of the transformer acts on the two poles of the lamp as a high-frequency choke, thus preventing the propagation of the high-frequency oscillations to the network. The magnetic characteristics of the transformer, which for the sake of simplicity have not been shown here, are in fact of essential importance in the high-frequency choke-action.

---

[4]) These are oscillations of very high frequency ($\lambda = 10$ to 100 cm) which may occur in a radio valve if the grid is given a high positive voltage with respect to the anode.

[5]) See F. M. Penning, Physica **6**, 241, 1926.

oscillations of type A are being generated this voltage-drop will increase a little at the instant the condenser is connected up, i.e. at the moment the oscillations cease. As a result of these oscillations the requisite number of ions is apparently already generated at a somewhat lower average voltage. If the high-frequency voltage fluctuations disappear owing to the elimination of the oscillation, a higher (now constant) working voltage must be attained to reproduce the same number of ions. Type B oscillations cannot be detected by means of this effect. But experience has shown that direct-current lamps, which at the moment give type B oscillations or do not oscillate at all, steadily pass over to type A oscillation with increasing age [6].

In the case of alternating-current lamps it is not permissible to connect a condenser of the rating indicated in parallel with the lamp, as the impulses in the discharge resulting therefrom would increase flickering; moreover, the working life of the tubes would be reduced owing to the high instantaneous values of the current densities. In these lamps, therefore, in order to render the external effect of the high-frequency alternating voltage E harmless, a self-inductance L of about 4 millihenries and a condenser C of approximately 0.01 μF rating are provided in the manner shown in *fig. 4*. With the chosen values of L and C we have $\omega L >> 1/\omega C$, so that the high-frequency current in the LC circuit is approximately $i = E/\omega L$ and the interference voltage reacting on the rest of the system (being equal to the potential of the condenser) is $e = E/\omega^2 LC$. The interference-suppression factor obtained in this way is therefore $E/e = \omega^2 LC$ (for the smallest frequencies coming into question E/e is approximately equal to 30).

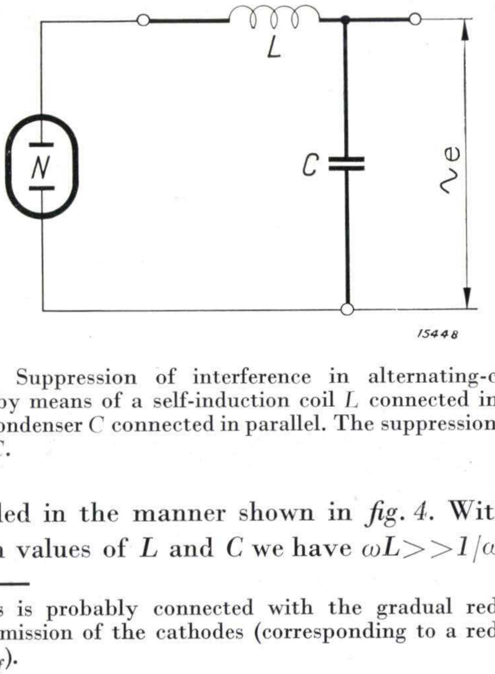

Fig. 4. Suppression of interference in alternating-current lamps by means of a self-induction coil L connected in series and a condenser C connected in parallel. The suppression factor is $\omega^2 LC$.

Fig. 5 reproduces a photograph of the interference-suppression unit in which the condenser and the self-induction coil are combined; it can be connected without preliminary alterations to any lamp where suppression is considered desirable. *Fig. 6* shows a lighting fitting with the suppressor unit incorporated.

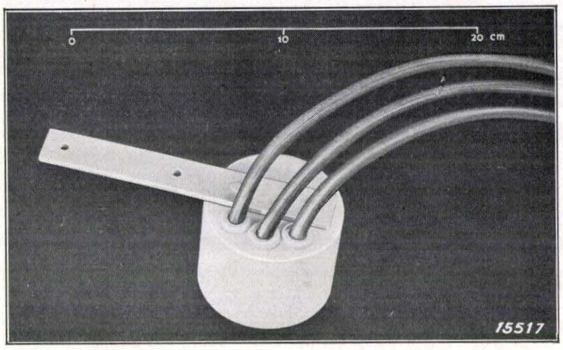

Fig. 5. Photograph of the small interference-suppression unit. The three wires are connected up in the manner shown in fig. 3.

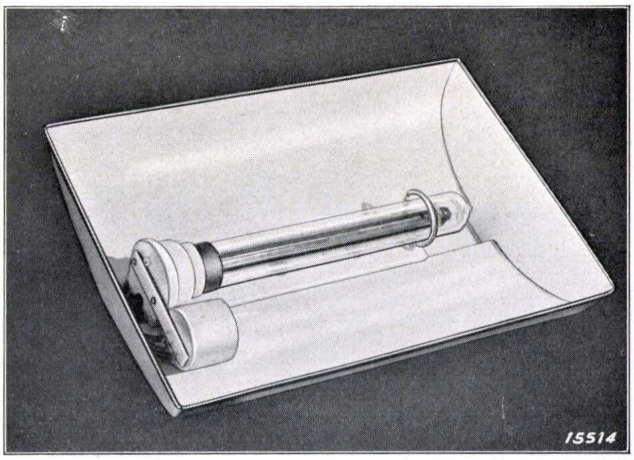

Fig. 6. Lighting unit with interference-suppression unit (left) incorporated.

---

[6] This is probably connected with the gradual reduction in emission of the cathodes (corresponding to a reduction in i_f).

CONTROL OF THE BEAM INTENSITY IN CATHODE RAY TUBES

Summary. A survey is given of the principal methods which have been devised for the control of the current intensity in cathode ray tubes. Characteristics of the Philips cathode ray tubes 3951/3952 are discussed.

Introduction

In the preceding issue of this Review[1]) the production of high-definition fluorescent spots in cathode ray tubes was discussed, but the brightness of the light-spot on the fluorescent screen was not then dealt with in detail. In general it is unnecessary to regulate the intensity of the beam in cathode ray oscillographs, but where these oscillographs are used for television reception, fluctuation in the brightness of the picture spots due to variations in the beam intensity has a considerable bearing on the definition of the picture [2]). For sound-films a procedure (Lignose-Breusing) is elaborated in which a cathode ray tube is used where the electron beam is not deflected but only varied in intensity. The fluorescent spot on the screen is photographed on the film and its varying brightness is used in this manner for registration of the sound. In the present article the principal methods for controlling the beam intensity will be discussed in some detail.

The brilliancy of the bright spot on the screen is determined by the current density of the electrons which produce the spot, and by their velocity. When it is required to alter the intrinsic brilliance of the spot, but without in any way affecting its size and position on the screen, it is sufficient to change the velocity of the electrons by varying the accelerating field (voltage modulation) while keeping the current intensity constant. In television receivers it is imperative that a change in intensity does not produce any alteration whatsoever in the size of the picture spot or its position on the screen. As this condition is extremely difficult to be satisfied by voltage modulation, the usual method employed in cathode ray tubes for television reception is to vary the current intensity of the electron beam, but to leave unchanged the voltages for accelerating and deflecting the beam (so-called current or intensity modulation). The intrinsic brilliance of the fluorescent spot is proportional to the current intensity within the range of current densities employed in television reveivers.

The deflection response of the electron beam is not affected by intensity modulation. The spontaneous concentration of the beam in gasfilled tubes due to the space-charge of the positive ions is, however, dependent on the current intensity. As already indicated in the previous issue [3]), gasfilled cathode ray tubes have only a limited application for television purposes for this very reason.

Current or Intensity Modulation

Since the intensity of the electron beam must frequently be altered very rapidly, it is not possible to vary the current intensity by regulating the heating current of the cathode. The emission temperature, and hence also the emission current, is too slowly built-up for this method to be of use. Mechanical control of the current (e.g. by means of an adjustable screen) would also possess too great an inertia (in television apparatus modulation frequencies of the order of 10^6 cycles are met with).

There are nevertheless available two fundamentally different methods of electrical current modulation which operate with a sufficiently low inertia.

1. A variable part of the electron beam is passed through a screen, by imparting to the beam in front of the screen a small variable deflection.
2. A variable portion of the electrons emitted is forced back to the cathode by applying a variable opposing field in the immediate neighbourhood of the cathode.

Current Modulation with Screen

The electron beam is pre-concentrated by means of a Wehnelt cylinder. As long as no potential is applied to the plates P and P' almost all the electrons pass through the small aperture in the centre of the anode A. The shape of the beam where P and P' have a positive bias with respect to the anode is shown in *fig. 1*. A portion of the beam which increases as the voltage is raised is cut off by the edge of the screen. The deflections of the electron beam produced by the plates P and P' balance each other, so that the spot is not appreciably displaced on altering the intensity.

---

[1]) Philips techn. Rev. **1**, 33, 1936.

[2]) See J. van der Mark, Philips techn. Rev. **1**, 16, 1936. In addition to intensity control, velocity regulation is also employed for television purposes and consists in passing an electron beam of constant intensity over the various parts of the picture at a high speed varying with the latter's brightness. Space does not permit this method to be discussed in detail in this article.

[3]) Philips techn. Rev. **1**, 38, 1936.

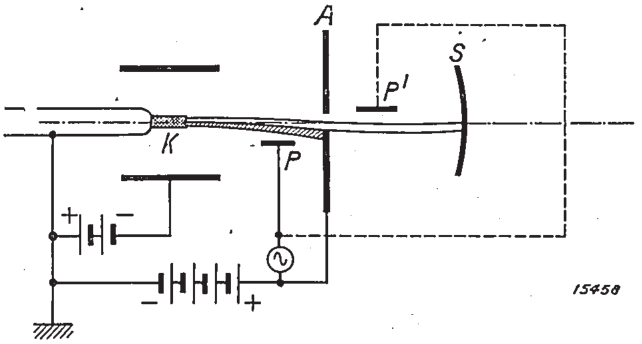

Fig. 1. Current modulation by deflection of the ray, using the electrode P. The electrode P' compensates the deflection so that the light-spot is not displaced on the screen.

Instead of unilateral screening of the electron beam by the edge of the aperture, the ray can also be symmetrically screened off on all sides. An arrangement for doing this is illustrated in *fig. 2*. By applying an alternating potential between the cathode and the cylinder C, the focussing action of the cylinder can be varied in such a way that a variable fraction of the electron beam passes through the aperture in the screen. This arrangement has the disadvantage that the definition of the spot is influenced by modulation, since the distance of the cathode image varies with the potential applied to C, but can be avoided by throwing on the fluorescent screen not an image of the cathode but an image of the screen aperture at A.

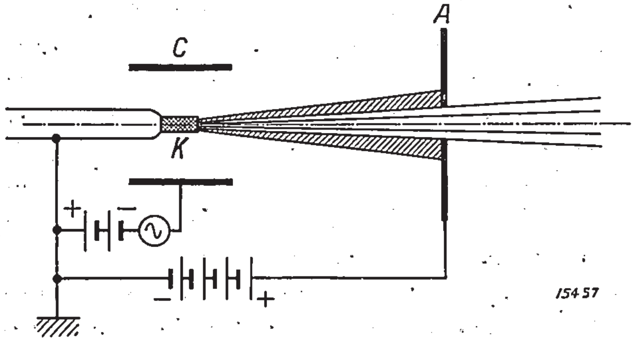

Fig. 2. Current modulation by modulation of the concentrating action of the Wehnelt cylinder.

Where the cathode beam is focussed by electromagnetic means, current modulation can be employed to similar purpose. The gradient of the helical paths described by the electrons [4]) is approximately equal to the distance between the cathode and anode and for control purposes is altered in synchronism with modulation. The cathode image thus alters its distance from the screen aperture so that a variable portion of the beam passes through the aperture.

Current Modulation by means of the Space Charge

If the cylinder C (fig. 2) has a negative bias with respect to the cathode, a very powerful negative space charge is produced in the cathode space. Since the majority of the electrical lines of force pass between the anode and the highly-negative cylinder and practically no lines of force penetrate the interior of the cathode space, it is very difficult for the electrons to leave the cathode. On altering the potential of the cylinder, the current intensity is altered without a screen being required at all. The Wehnelt cylinder, which was originally used for the purpose of promoting spontaneous focussing in gasfilled tubes, here serves an altogether different purpose, and when used as such it will be referred to below as the control cylinder.

According to the magnitude of the negative bias of the control cylinder, more or less electrons will be able to leave their storage chamber, the cathode space. If the temperature of the cathode is sufficiently high to cause the continuous emission of excess electrons, it will not affect the intensity of the cathode ray, which is determined solely by the voltages of the control cylinder and the anode.

The storage chamber of the electrons can be regarded as a condenser of specific capacity. In other words, the charge accumulated in it, and hence also the charge density, is proportional to the potential V applied to it. The intensity of the current flowing out of the storage chamber is proportional to the product of the charge density and the velocity of the electrons. As the charge density increases in proportion to the potential, and the velocity is proportional to the square root of the potential, the current intensity as long as it is determined by the space charge alone is proportional to $V^{3/2}$. The current-voltage curves of cathode ray tubes reproduced in fig. 5 show in fact that the current increases according to the 3/2 power of the control voltage.

The control cylinder of high-vacuum cathode-ray tubes serves the same purpose as the control grid in wireless valves. The control electrode is a cylinder closed at the front, which surrounds the cathode. The front wall is situated very close in front of the emitting surface of the cathode and has a small aperture at the centre. The current intensity of the cathode ray is determined not only by the control voltage, but also by the surface area of that part of the cathode participating in emission. In *fig. 3* the variation of the electric field between the cathode and the control electrode is represented diagrammatically. The greater the opposing voltage of the control electrode, the smaller will be the effective area of the cathode, which in fig. 3 is bounded by the points *a* and *b*. At the highest permissible currents of about 100 µA the diameter of the emitting surface is about 0.5 mm. With a diameter of 0.1 mm the electron current is only 1 µA.

---

[4]) Philips techn. Rev. 1, 36, 1936.

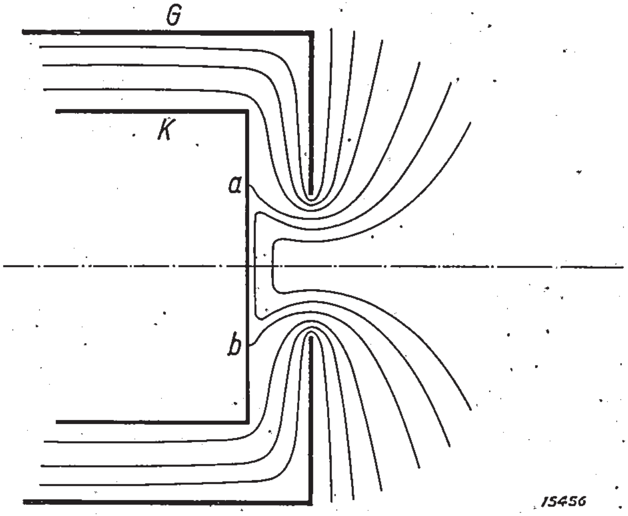

Fig. 3. Current modulation by means of a control electrode *G* placed very close to the surface of the cathode *K*. Diagrammatic sketch of the field with a cold cathode.

Only that portion of the emitting surface of the cathode between *a* and *b* participates in generating the cathode ray, as here the field applied at the cathode accelerates the electrons. Beyond the boundary points *a* and *b* the electrons are retarded by the external field and driven back to the cathode. The greater the negative potential applied to the control cylinder, the smaller becomes the distance between *a* and *b*. Finally *a* and *b* will coincide along the central line so that the portion of the cathode surface contributing to emission will become zero.

The arrangement of the electrodes in a Philips cathode ray tube designed for television purposes is shown in *fig. 4*. In addition to the negative control electrode G_1, these tubes are also provided with a positive screen-grid G_2, which screens off the fields of the electronic lenses A_1 and A_2 against the variable field of the control electrode. In the arrangement illustrated here potentials of about 10 volts are sufficient to control the electron beam intensity over a wide range. These small modulation potentials have practically no influence on the paths of the electrons, so that the definition of the fluorescent spot remains unaltered. The high sensitivity of this arrangement is due to its very compact construction from small components. A construction of this type requires a very homogeneous cathode material and an exact centring of the individual components.

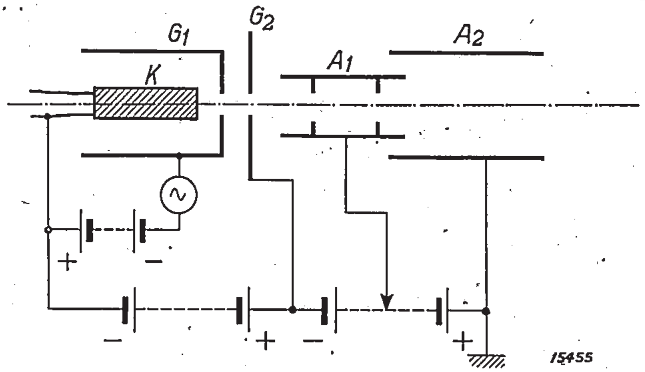

Fig. 4. Circuit diagram of a Philips cathode ray tube for television purposes.
G_1 = Control electrode. G_2 = Screen grid. A_1 and A_2 are anodes which serve for both the acceleration of the electrons and electron-optical focussing.

Current-Voltage Curves of Intensity Modulation

In order to gain some idea of what can be achieved by current modulation, it is necessary to know for each anode potential V_a how the current I_a varies with the potential V_g of the control electrode. In this direction the arrangement corresponds completely to a radio valve equipped with a control grid. Accordingly the slope of the curve in which I_a is plotted against V_g may be taken as the gradient S of the characteristic.

As indicated above, the anode current may be regarded as a function of a control potential V applied to the supply chamber, which is principally determined by the potential V_g of the control cylinder, although the anode potential also has a subsidiary influence, thus:

$$V = V_g + \frac{1}{g} V_a \quad . \; . \; . \; . \; . \quad (1)$$

$$\text{and } I_a = f(V) = f\left(V_g + \frac{1}{g} V_a\right) \quad . \; . \quad (2)$$

The amplification factor g indicates to how much larger extent the potential V_g of the control cylinder determines the anode current than the anode potential V_a does. Equation (2) brings out the fact that the ratio g of the effects produced by the potentials of the control electrode and the anode is independent of V_a and V_g. This equation is useful if the characteristics $I_a = f(V_g)$ produced at different potentials V_a can be brought to coincide by displacement in the direction of the V_g-axis. The ratio of the difference ΔV_a of the anode potentials of the two curves to the displacement ΔV_g is then the amplication factor g.

The characteristics of Philips 3951 and 3952 high-vacuum cathode-ray tubes for potentials of 1000 and 2000 volts at the anode A_2 (anode A_1 is at a potential of 200 and 400 volts respectively) are shown in *fig. 5*. It is observed that the curves have an almost uniform displacement of about 10 volts in the direction of the V_g-axis. The amplification factor of the tubes is thus $g = \Delta V_a / \Delta_g V = 1000/10 = 100$. With an anode potential of 1000 volts, the anode current can be regulated between 0 and 150 μA by altering the potential of the control cylinder between —25 volts and zero. With an anode potential of 2000 volts, the anode current can be regulated between zero and almost 300 μA. The modulation potential in this case must be varied between —35 volts and zero. The heating current is about 1 amp. The capacity of the control cylinder with respect to the other electrodes is 10 μμF.

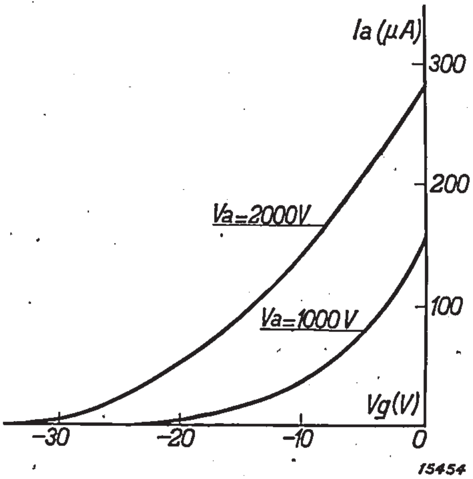

Fig. 5. Current-voltage curves for the Philips 3951 and 3952 cathode-ray tubes for anode potentials of 1000 and 2000 volts.

Voltage Modulation

As stated at the outset, the intrinsic brilliance of the spot can also be controlled when keeping the current intensity constant, viz, by modulating the voltage of the fluorescent screen. A great disadvantage of voltage modulation is that the faster electrons are less influenced by the deflecting system than the slower ones. This may be avoided by stretching a large wire gauze directly in front of the screen and imparting to it a fixed potential difference as against the other electrodes, while the control voltage is applied between the wire gauze and the fluorescent screen (*fig. 6*). If the field of the screen has only a slight through-pull across the wire gauze, the deflection of the electrons is independent of the velocity with which they arrive at the pick-up screen.

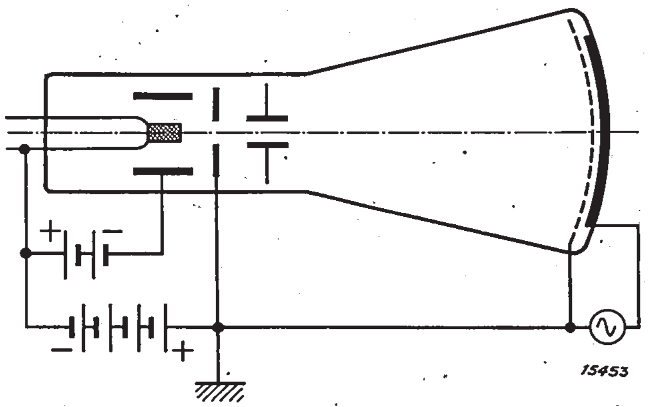

Fig. 6. Voltage modulation with a wire gauze placed in front of the pick-up screen.

However, every type of voltage modulation has the inherent disadvantage that, in order to obtain a sufficiently high control of the luminous intensity, control potentials of several thousand volts are required, while with current modulation potentials of the order of 10 volts are adequate.

Compiled by G. P. ITTMANN.

PRACTICAL APPLICATIONS OF X-RAYS FOR THE EXAMINATION OF MATERIALS

III.

By W. G. BURGERS.

The following example of X-ray analysis is of the same type as the two applications, Nos. 3 and 4, described in the previous part (II) of this section. Here again the preparations investigated differ only in texture, i.e. in the arrangement of the crystallites, and not in their chemical composition.

5. Texture of Electrolytically-Deposited Nickel Coatings

Electrolytically-deposited metal coatings may differ in many properties such as lustre, hardness, internal stresses, etc., according to the conditions of deposition employed, e.g. the composition of the plating bath, the current density, etc.

X-ray examination shows that in certain cases an alteration in the conditions of electrolysis may result in an alteration of the texture of the deposited coatings. Moreover, one and the same coating may be built up of zones with a different texture[1]).

Fig. 1 reproduces an X-ray photograph of a nickel coating, 15 μ in thickness and having a metallic lustre, which was deposited on a copper rod in an industrial nickel plating bath. From the fairly uniform blackening on the whole circumference of the interference rings it may be deduced that the crystallites in the nickel coating are haphazardly positioned.

Fig. 2a is a photograph of a much thicker coating (150 μ) which has a matt surface. This picture reveals very marked intensity maxima round the periphery of the rings. The crystallites must therefore, at least in the outer zone of the nickel coating, possess a perfectly well-defined orientation. *Figs. 2b-d* are photographs of the same coating after etching to various depths. It is seen that the blackening of the rings becomes more and more uniform: in fig. 2d nearly the same picture is obtained as shown in fig. 1. The layer deposited first thus had no well-defined texture at all, the texture only having been developed as the coating was built up.

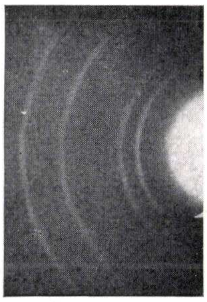

Fig. 1.

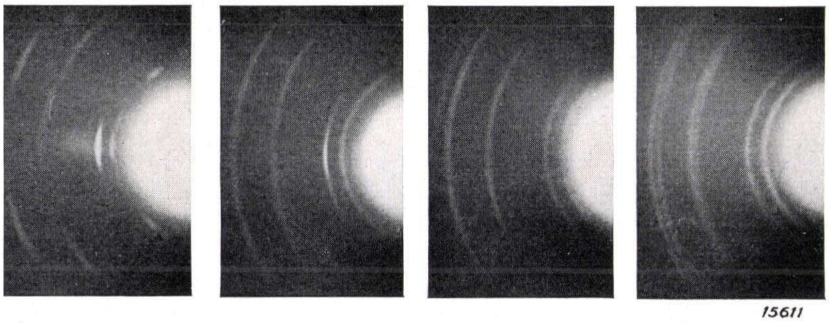

Fig. 2 a) b) c) d)

Fig. 1. X-ray photograph of an electrolytically-deposited nickel coating, 15 μ in thickness, possessing a metallic lustre.
Fig. 2. Zonal structure of an electrolytically-deposited nickel coating, 150 μ in thickness, with a matt surface.
a) The surface.
b)—d) After etching to depths of 100, 130 and 140 μ.
These photographs have been obtained by radiation grazing the nickel surface[2]). In fig. 2d the nickel coating is so thin that the interference lines of the substratum of copper also commence to become visible.

---

[1]) W. G. Burgers and W. Elenbaas, Naturwiss. **21,** 465, 1933.

[2]) Cf. fig. 4 in this section, part I, Philips Techn. Rev. **1,** 31, 1936.

ABSTRACTS OF RECENT SCIENTIFIC PUBLICATIONS OF THE N.V. PHILIPS' GLOEILAMPENFABRIEKEN

No. 1046: P. J. Boumá: Verblinding (Polytechn. Wbl. **29**, 625-629, Oct. 1935).

A distinction is drawn between direct and indirect glare according as the rays producing glare do or do not fall on those parts of the retina whose reduction in sensitivity is observed. Furthermore a distinction is also made between simultaneous and successive glare. The former is a reduction in sensitivity during exposure to glare, and the latter that persisting some time after exposure. In this paper the effect of glare on the contrast sensitivity is investigated in relation to the position, dimensions, brightness and colour of the light-source. In general the results of the measurements made agree with those of Holladay; some small discrepancies appearing are discussed. A comparison is made between the glare effect with uniocular and binocular vision, and the question is studied how exposure to glare of one eye reacts on the contrast sensitivity of the other eye. Finally the author describes further measurements of the velocity with which the contrast sensitivity is restored, and measurements of the time during which white, sodium and mercury-vapour light continue to produce after-images on the yellow spot of the retina. (We shall revert to this subject in a subsequent issue of this Review).

No. 1047: W. Uyterhoeven and C. Verburg: Effets de la variation périodique de la concentration des atomes neutres de la vapeur dans une lampe à courant alternatif au sodium (C. R. Acad. Sci., Paris, **201**, 647-649, Oct. 1935).

For a 50-cycle alternating-current sodium lamp, oscillograms are obtained of the current, voltage and intensity of the yellow sodium light. The current varies almost sinusoidally, while the fluctuations of voltage and luminous intensity are on the other hand much more irregular. This is ascribed to the variable degree of ionisation of the sodium and the finite time separating ionisation, recombination at the walls and vaporisation. Actually the phase displacement between the current and the intensity maxima increases at higher frequencies. At a constant temperature the distortion of the voltage and intensity curves become still more marked if the current density is increased. The distortion is reduced if, at constant current, the temperature, and hence also the pressure of the sodium vapour, are raised. The intensity distribution in the sodium lines was found to be dependent on the time to some extent, as was to be expected from the periodic variation in concentration of the neutral sodium atoms.

No. 1048*: J. L. Snoek: Apparaat ter demonstratie van het ontstaan van ferromagnetische hysteresis (Faraday **5**, 141-144, May 1935).

Becker's theory of ferromagnetic hysteresis is illustrated by means of a mechanical model. A revolving arrow, which represents the direction of magnetisation, is positively connected to a tube ellipsoidally bent to give a total enclosure which is partly filled with mercury. The equilibrium positions of this tube represent the states with minimum magnetic energy. If in a magnetic material the preferred direction of magnetisation is everywhere the same and if an external magnetic field is applied perpendicular to this preferred direction, no hysteresis losses occur. Magnetisation is reversible, which can also be shown by the mechanical model.

No. 1049: W. G. Burgers and J. J. A. Ploos van Amstel: Cinematographic record of the $\alpha \rightleftarrows \gamma$ iron transition as seen by the electron-microscope (Nature, **136**, 721, Nov. 1935).

By careful volatilisation of barium and strontium oxides, the authors have succeeded in increasing the emission of electrons from an iron lamella to such an extent that emission was already sufficient at the transition temperature of about 900 deg. C to permit the recrystallisation process to be followed with the electron-microscope. On raising the temperature slowly above the transition point, it is possible to obtain complete recrystallisation in 5 to 10 mins. During this period an exposure of the electronic image was made every 4 secs. In this way a microfilm has been obtained which shows distinctly the growth of the α-crystals in the γ-phase and the inverse.

---

*) A sufficient number of reprints for purposes of distribution is not available of those publications marked with an asterisk (*). Reprints of other publications may on application be obtained from Philips Laboratory, Kastanjelaan, Eindhoven, Holland.

VOL. 1 No. 4 APRIL 1936

Philips Technical Review

DEALING WITH TECHNICAL PROBLEMS
RELATING TO THE PRODUCTS, PROCESSES AND INVESTIGATIONS OF
N.V. PHILIPS' GLOEILAMPENFABRIEKEN

EDITED BY THE RESEARCH LABORATORY OF N.V. PHILIPS' GLOEILAMPENFABRIEKEN, EINDHOVEN, HOLLAND

THE DEVELOPMENT OF THE COILED-COIL LAMP

By W. GEISS.

Summary. The coiled-coil filament, while emitting the same luminous energy, transmits less heat to the surrounding gas envelope than the single-coil filament. As a result coiled coils give a marked increase in efficiency, especially with lamps of low rating.

One of the primary aims of the electric lamp industry is to produce sources of light which will convert electrical energy into useful light with the maximum efficiency. In the pursuit of this goal two different methods of approach have been followed during the last ten years. On the one hand entirely new sources of light have been evolved, such as gaseous discharge lamps, in reference to which several articles have already appeared in this Review. On the other hand, systematic investigations have been carried out into all possible means for improving the efficiency of existing types of electric lamp. In this direction also, considerable progress has been made, for instance by the production of the coiled-coil lamp, which was placed on the market about two years ago. Some details of the investigations which led to the design and manufacture of this new lamp are described below.

The efficiency of an electric incandescent lamp increases with the temperature of its filament, but this gain is obtained at the cost of the life of the lamp since the rate of volatilisation of the filament also increases considerably with the temperature. In endeavouring to obtain a high efficiency it is of primary importance to keep the rate of volatilisation as low as possible, or, what comes to the same thing, to obtain the highest temperature for a given rate of volatilisation. This end may be attained in two ways:

1) By the discovery of a substance which volatilises very slowly, and
2) By the introduction of a gas filling.

The original material used for lamp filaments was carbon (carbonised bamboo fibre), which was later replaced by graphite. A further increase in temperature was made possible by the adoption of metals with high fusion points, viz, osmium, tantalum and tungsten. Developments in this direction have now provisionally terminated with the general use of tungsten, but it is not impossible that certain metallic oxides and nitrides volatilise still more slowly than tungsten, although up to the present no success has attended the attempts to produce sufficiently homogeneous filaments from these substances. Tungsten thus remains without dispute the best material for lamp filaments.

The most important properties of tungsten filaments are collated in *Table I.* If a life of 1000 hours is required, an efficiency of about 10 lumens per watt may be obtained with a filament 0.01 mm thick. With a filament 0.1 mm in thickness an efficiency of about 13 lumens per watt can be obtained under equivalent conditions. These values apply to straight filaments in vacuo.

Table I. Life of an incandescent straight-wire tungsten filament as a function of the temperature. The mean life is related to the rate of volatilisation by the experimental fact that during the normal mean life 10 per cent of the mass of the filament volatilises. (Taken from C. Zwikker, Physica 5, 252, 1925.)

Absolute temperature	Efficiency	Rate of volatilization	Life of a filament 0.01 mm in diameter	Life of a filament 0.01 mm in diameter
°K	lumens/watt	gr/cm² sec.	hours	hours
2000	2.93	$15.5 \cdot 10^{-15}$	$1.04 \cdot 10^{7}$	$1.04 \cdot 10^{8}$
2200	5.71	$22.4 \cdot 10^{-13}$	$7.20 \cdot 10^{4}$	$7.20 \cdot 10^{5}$
2400	9.77	$13.8 \cdot 10^{-11}$	$1.17 \cdot 10^{3}$	$1.17 \cdot 10^{4}$
2600	14.8	$41.7 \cdot 10^{-10}$	38.6	386
2800	20.9	$83.3 \cdot 10^{-9}$	1.9	19
3000	27.8	$10.5 \cdot 10^{-7}$	0.15	1.5

The effect of a gas filling on the rate of volatilisation may be discussed from *fig. 1.* Consider the filament to the left of the vertical line. A tungsten atom on volatilising will in the first place move towards the right. After a few collisions with the gas molecules the atom will have lost its initial energy, and it will then depend on fortuitous circumstances whether the atom will now turn back in its path or continue to travel away from the filament. Half the atoms will do the one thing and the other half the reverse. In consequence of further collisions with gas molecules this alternative will repeat, when the tungsten atom has travelled a certain path. It is seen from *fig. 1* that only a small fraction of the atoms reach the opposite wall. In the case illustrated with two plane walls at a distance of five of these paths apart, the rate of volatilisation will be reduced to a fifth. *Fig. 2* gives a diagram of the reduction of volatilisation which is obtained with a tungsten filament 75 μ in diameter. It is seen that the rate of volatilisation decreases to a few per cent of its original value by a filling of argon or nitrogen at 50 to 100 cm pressure.

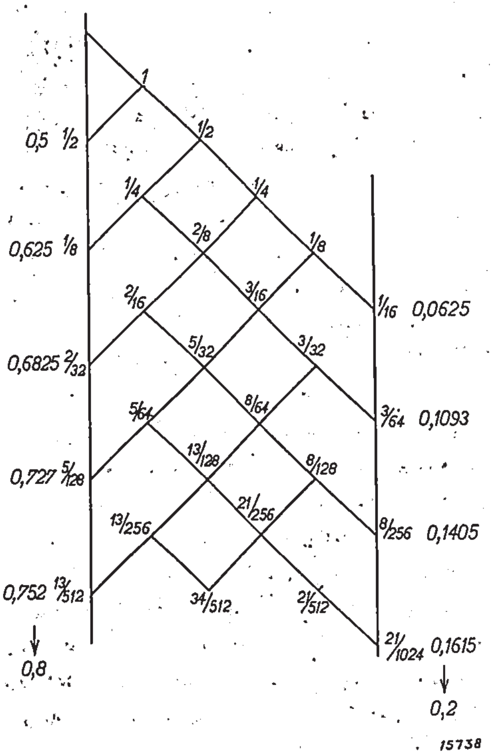

Fig. 1. Diagrammatic representation of the diffusion of atoms through a gas. In consequence of collisions with the gas molecules the atoms emitted from the plate at the left are able, after a certain path, to choose a direction either to the right or to the left. With the plates at a distance of five of these paths apart, only a fifth of the atoms emitted reaches the right-hand plate.

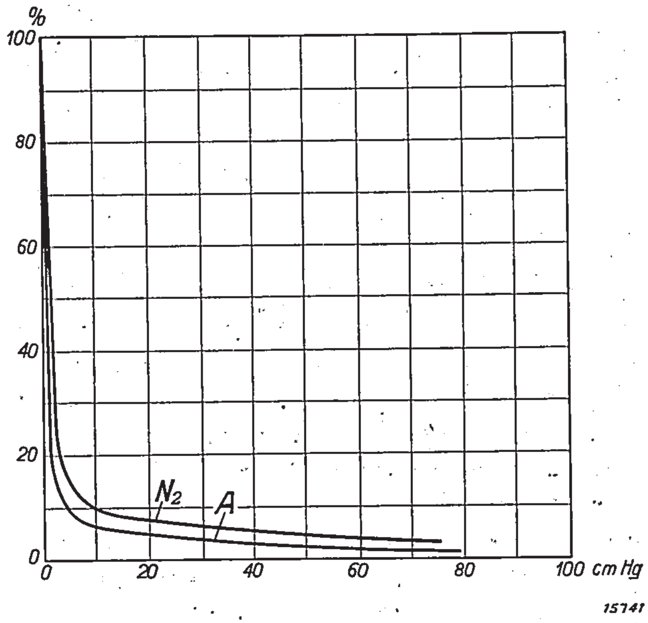

Fig. 2. Rate of volatilisation of incandescent tungsten filaments in atmospheres of nitrogen and argon respectively, plotted against the gas pressure.

Unfortunately a gas filling also introduces a disadvantage, for the thermal conduction and convection of the gas causes additional losses which in the case of thin straight filaments may in fact be greater than the gain obtained by the increase in temperature. Thick filaments in this respect give much more satisfactory values than thin ones. Experience has shown that the loss of heat due to the presence of the gas increases but little with increase in filament diameter, while radiation is proportional to the diameter. In other words, at a given radiation output the losses due to thermal conduction increase almost proportionally to the length of the filament. Langmuir, who was the first to call attention to this remarkable phenomenon, advanced the following explanation. Convection currents are set up in the hot gas surrounding the filament. The latter is itself, however, surrounded by a film of gas, which remains at rest since its viscosity owing to its high temperature is very high (cf. *fig. 3*). The thickness of the stationary film is determined by convection currents along the outer wall of the cylinder and is only slightly dependent on the diameter and temperature of the very much thinner filament.

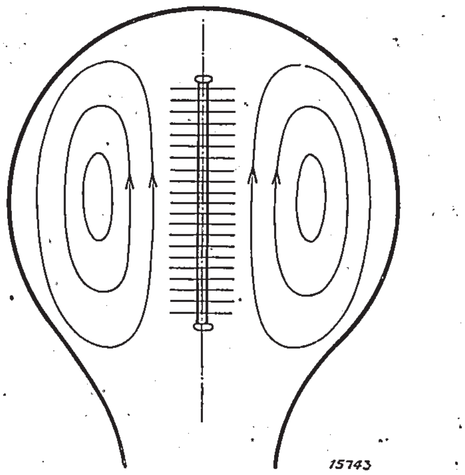

Fig. 3. The incandescent filament is surrounded by a stationary film several millimetres in diameter. Outside this layer the convection currents in the gas ensure uniform temperature distribution. The heat dissipated is, however, restricted by the thermal conductivity of the layer of stationary gas.

The energy losses are due to thermal conduction through the film of stationary gas and with a constant thickness of the layer they are proportional to the length of the filament.

In former years investigations have been proceeding at this laboratory with respect to the thermal conduction of incandescent filaments, and these investigations have shown very clearly the action of the stationary layer. Two similar incandescent tungsten filaments were suspended side by side in an atmosphere of argon at 60 cm pressure, using a holder by means of which the distance between the wires could be altered at will. Curves S and C in *fig. 4* show the heat losses due to radiation and conduction as a function of the distance between the filaments, the temperature being constant. While radiation is practically constant, the conduction factor diminishes very considerably as soon as the stationary films of the two filaments overlap. At a very small distance apart, conduction (curve *C*) is only half the initial value, while the radiation loss (curve *S*) has barely altered. The two filaments are then surrounded by a common layer of stationary gas so that the effective length of the filament is reduced to half.

The heat losses through conduction are particularly important in the case of small lamps. The lower the rating of the lamp the thinner are the tungsten filaments, and hence the smaller the radiation emitted per unit of length as compared with the heat losses.

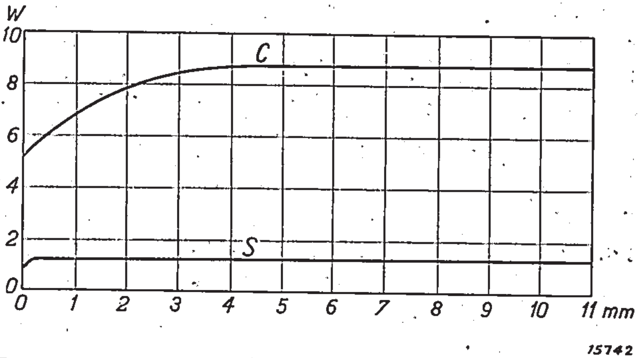

Fig. 4. Heat losses from two incandescent filaments as a function of their distance apart.

S By radiation.

C By conduction and convection of the gas filling. The heat transfer to the gas is considerably diminished when the filaments are brought so close together that the stationary layers overlap. On the other hand radiation is practically independent of the distance between the filaments.

An important advance was made in the design of small lamps, by the introduction of the coiled-coil filament. If a long thin filament is wound in the form of a spiral or coil, its total heat losses are of the same order as for a filament with the same length and cross-section as the coil. In this way the effective overall length of the filament can be considerably reduced, the reduction becoming the greater the greater the diameter of the coil.

The diameter of the coil cannot, however, be indefinitely increased, for with increasing diameter the resistance to deformation of the coil diminishes to such an extent that there is a danger of short circuits occurring between the turns when exposed to unavoidable shocks and vibrations. Nevertheless it has been possible to reduce the effective length of the coil still further by winding the coil itself round a core and thus arriving at a coiled-coil arrangement.

The first attempts to use coiled coils were already carried out about 20 years ago, but these failed owing to the inadequate processes for manufacturing the coiled-coil filament. The incandescent elements made at that time possessed the undesirable property of expanding during service so that the coil of an old lamp showed a marked sag.

Extensive research on tungsten wires and filaments which were worked cold and hot by various processes, showed that the sag f of the filaments could be expressed as a function of the time t, as follows:

$$f = a_1 + a_2\, t^b \quad . \; . \; . \; . \; . \quad (1)$$

The initial sag a_1 is produced when the filament is firstly raised to its incandescent temperature and is largely independent of the pre-treatment of the coil. By suitable pre-treatment it is, however, possible to reduce the value of the exponent b very considerably. Finally the initial sag a_1 can be widely reduced, by submitting the finished coil to prolonged heat treatment at a high temperature so that it assumes a suitable crystal structure. To prevent expansion of the filament already during this heat treatment it has been found necessary to use for the core a material with a high melting point. The primary and secondary coils are wound on molybdenum cores, which after heat treatment are removed from the coils by chemical means. *Fig. 5* showing the filaments of a modern lamp and of an old one (both after about 1000 hours' burning) indicates the progress which has been made in the course of the last few years in stiffening the coils. This improvement is also shown quantitatively in *fig. 6*. These illustrations show clearly that it is now no longer possible to estimate the age of a lamp from the sag of the filament, even in lamps with single coils which have also shared in the advances made in filament-finishing processes.

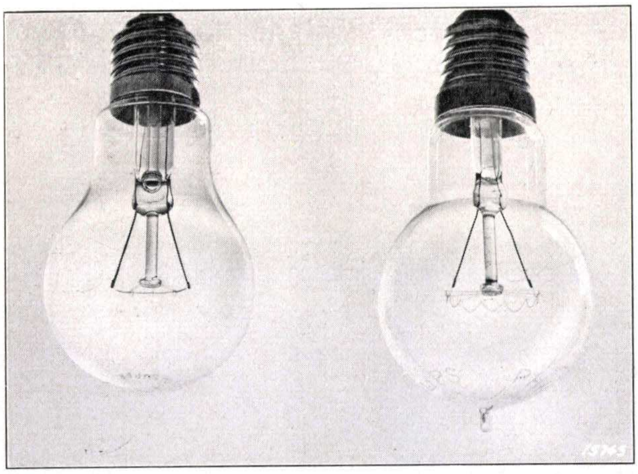

Fig. 5. A lamp with non-sagging coiled-coil and another with a sagging single coil, both after about 1000 hours' burning. It is clear that nowadays no conclusion can be drawn from the sag as regards the age of the lamp.

A mixture of argon and nitrogen has been used for filling coiled-coil lamps as was employed for single-coil lamps also. As both the heat losses and the rate of volatilisation diminish with increasing atomic weight of the filling gas, an examination of the properties of the heavier rare gases suggested itself. This work has only been made possible in recent years after technical methods had been evolved for isolating krypton and xenon in such quantity and of such purity as to permit comprehensive experiments on a technical scale [1]).

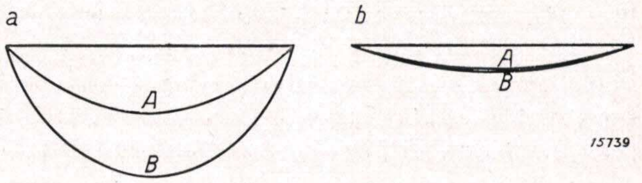

Fig. 6. The depth of sag f is related to the hours of burning by the equation: $f = a_1 + a_2\, t^b$. The figure shows the sag: A after 1 hour, B after 500 hours.

a) Sagging filament:
$a_1 = 0.08$
$a_2 = 0.08$
$b = 0.150$

b) Non-sagging filament:
$a_1 = 0.00$
$a_2 = 0.08$
$b = 0.005$

A marked diminution in the factors investigated was actually found with these gases, the rate of volatilisation in krypton being only half that in argon under the practical conditions in question here. The heat losses were also much lower, as may be seen from the example quoted in *Table II*.

Table II. Heat losses due to gas Filling.

Gas	Per cent Heat losses
Argon filling	100
Krypton filling	68
Xenon filling	53

In spite of these advantages, the substitution of an expensive krypton filling for argon does not at the present time appear practicable. Whether such substitution may be possible in the future depends on what progress is made in the isolation of the rare gases.

A further novelty of the coiled-coil lamp is that each lamp is supplied with its own self-contained fuse. This has been done because the break-spark produced when the lamp blows may strike an electric arc between the electrodes. The internal fuse then blows and thus protects the mains fuses.

---

[1]) Krypton and xenon are constituents of the atmosphere. 1 cub.m of air contains about 10 ccm of krypton and 1 ccm of xenon.

The semi-frosting frequently used hitherto has been replaced by internal frosting in the coiled-coil lamp, since it has been possible to reduce the absorption of light with the latter to below that with semi-frosting; the light loss is now only 0.5 to 1 per cent as compared with 2 per cent for semi-frosting. Moreover, from the point of view of illuminating engineering semi-frosting is incorrect, since it acts as a reflector so that 60 per cent of the light is reflected upwards and only 40 per cent is thrown downwards. In the diagram of flux distribution (*fig. 7)* the difference between these two methods of frosting in clearly shown.

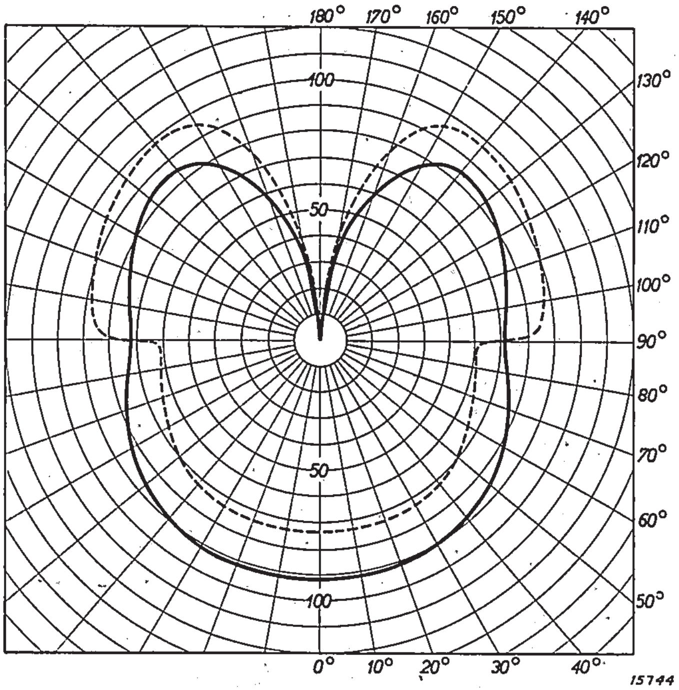

Fig. 7. Diagram of light distribution for a internally-frosted lamp (continous line) and a semi-frosted lamp (broken line). The semi-frosting acts as a reflector, which reflects upwards part of the light radiated downwards.

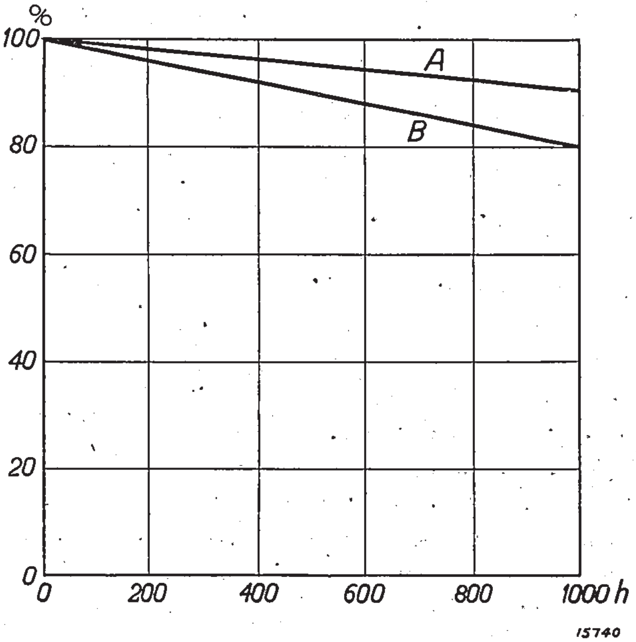

Fig. 8. Diminution in the efficiency of a lamp with use.
A Single-coil lamp.
B Coiled-coil lamp.

In conclusion, it may be stated that the substitution of the coiled-coil for the single-coil has resulted in a saving in power of 7 to 10 watts, the initial luminous flux of the two types being the same. Considering the whole life of the lamp, a better illumination is also obtained, for, as shown in *fig. 8*, the decline in luminous efficiency with the age of the lamp is much less with the coiled-coil than with the single-coil filament.

CHARACTERISTICS OF THE EYE WITH SPECIAL REFERENCE TO ROAD LIGHTING

By P. J. BOUMA.

Summary. Following a brief discussion on the way in which objects are seen on artificially-illuminated highways, the circumstances in which the eye is likely to fail are studied. The efficient or imperfect functioning of the eye is determined mainly by the visual acuity, the contrast sensibility, the richness of contrast and the speed of vision. The interconnection of these phenomena is discussed in reference to the following characteristics of the eye: Accommodation, diameter of pupil, chromatic and spherical aberration, astigmatism, adaptation, glare and the Purkinje phenomenon.

When the question is asked: "What constitutes really good road lighting?" the extreme complexity of the problem entailed must be adequately realised. The solution of this problem can only be arrived at by the closest collaboration between the most divergent branches of science, while considerable practical experience is also imperative. It must be borne in mind that particularly in the interests of safety on the road the conditions of lighting must be such as to afford distinct vision. Apart from a host of technical and physical factors (such as the distribution of brightness, the physical composition of light, etc.), the conditions of vision are in large measure determined by the intrinsic characteristics of the human eye itself. A detailed study of these characteristics is hence indispensable in dealing with the problem of road lighting.

The eye is one of the most remarkable organs with which Nature has endowed us; remarkable for the many divergent functions which it can fulfil, for its enormous sensibility, and finally for the wide variety of conditions under which it operates as an efficient instrument.

On the other hand, in studying the properties of the eye with reference to road lighting, we shall frequently have to consider the defects and shortcomings of this remarkable organ, since to ensure safety of the highway it is essential to know when and under what conditions the eye is likely to fail in the discharge of its duty; for this failure is the cause of many accidents which could be avoided by better lighting.

To determine which characteristics of the eye are the most important in this connection, we must first establish exactly in what way objects are seen on highroads. We perceive an object in the street because it stands out from its background, i.e. because usually its brightness differs from that of the background. (Differences in colour may also play a part, although usually only a subsidiary one, in creating this contrast.) When we have perceived the object, we must also recognise it, i.e. distinguish its from and distance. It is also of the greatest importance that this recognition take place rapidly; sometimes an object only remains a short time in a position suitable for its recognition and frequently rapid recognition is necessary in order to take timely measures to prevent an accident.

From the above it follows that the principal causes for the failure of the eye to perform its due functions may be classified in three groups:

1) The impossibility of perceiving very weak contrasts: when the contrast is very small, the object will not be perceived at all.
2) The image of the object impressed on the retina is not sufficiently well defined: the object is not recognised.
3) The eye functions too sluggishly: the object is not perceived or recognised quickly enough.

The second cause is the simplest to discuss, and in this respect there is a considerable similarity between the eye and a photographic camera. Exactly as the camera lens throws an image of an object on the photographic plate, so does the lens of the eye impress an image of the object viewed on the retina. The focal length of the lens of the eye can be altered by the contraction of certain muscles. This alteration is termed accommodation, and it enables us to form sharply-defined images of objects at very different distances from the eye on the retina successively. Accommodation can be obtained consciously and voluntarily; usually it is, however, created involuntarily by force of habit. Furthermore, the eye is also equipped with a variable diaphragm by means of which the effective diameter of the lens — and hence the quantity of light falling on the eye as well as the quality of the image — can be varied. This adjustment of the diameter of the pupil takes place quite involuntarily and is a reflex action caused by external influences.

The lens of the eye is subject to the same optical defects in the production of images as ordinary lenses. Those defects which only cause a distortion of the image are usually not disturbing in the case of the eye, for in spite of this distortion the brain is capable of visualising the correct shape and form of the actual object. The clearest proof of this is the fact that the inverted image on the retina presents no difficulties, and that it is possible by the use of an optical system which turns the image through a right angle (i.e. turns it on to its side) to see "normally" again after a time. On the other hand, those defects of the eye may prove very troublesome which cause rays emanating from a point of the object not to meet at the same point on the retina. The principal defects of this type, which all adversely affect the "definition" or "sharpness" of the image on the retina and hence also the visual acuity are:

1) Lack of accomodation, which may be due to two causes:
   a. Because the object is situated at a distance to which the eye cannot be sharply focussed, the normal eye can be sharply focussed to distances between about 12 to 15 cm and infinity; with short-sighted and long-sighted eyes this range is smaller.
   b. Because the object emits light of different wavelengths and the focal length of the eye lens depends on the wavelength (see *fig. 1*). Fig. 1 shows for example that an eye which is sharply focussed for a wavelength of λ = 5550 Å possesses a myopia (short-sightedness) of 3.5 diopter at 4000 Å and a hypermetropia (long-sightedness) of 1.8 diopter at 7000 Å 1). This phenomenon — chromatic aberration — can only be avoided by using monochromatic light.

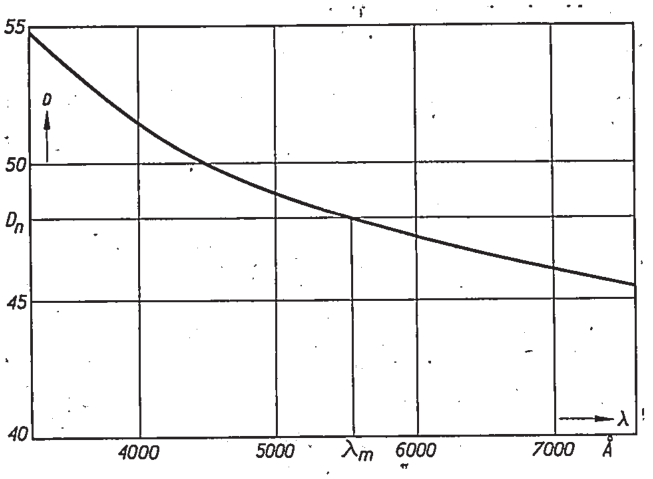

Fig. 1. Refractive power in diopter D of the normal or emmetropic eye at rest a sa function of the wavelenght λ. At the wavelenght λ = 5550 (maximum of the visibility curve of the eye), the refractive power of the normal eye is approx. $D_n = 48$. As may be seen from the graph the eye is myopic with reference to blue light and hypermetropic with reference to red light.

2) The phenomenon that monochromatic rays emanating from a point are not focussed at a point. This defect — spherical aberration — which is shared by every normal eye, can be avoided by a stronger curtaining of the eye lens (either by involuntary contraction of the pupil of the eye or by placing an artificial pupil in front of the eye).
3) Astigmatism: The rays emanating from a point and travelling in a horizontal plane have another focus than those rays lying in a vertical plane. This asymmetry of the eye is of common occurrence, frequently in conjunction with myopia and hypermetropia; it is dependent on the wavelength (*fig. 2*).

These three defects all affect the visual acuity and hence render the recognition of objects at a great distance more difficult.

To investigate in further detail the first-mentioned cause of defective vision (the impossibility of perceiving small differences in brightness), we must regard the eye as a measuring instrument capable of measuring brightness values. In such an instrument the first point to consider is the magnitude of the measuring range, in other words the range of brightness over which the eye is still a serviceable instrument. This range is much greater with the eye than with most physical

---

1) The number of diopter (*D*) of a lens is the reciprocal of the focal length in metres. For the normal eye in a position of rest D^n is approximately 48.

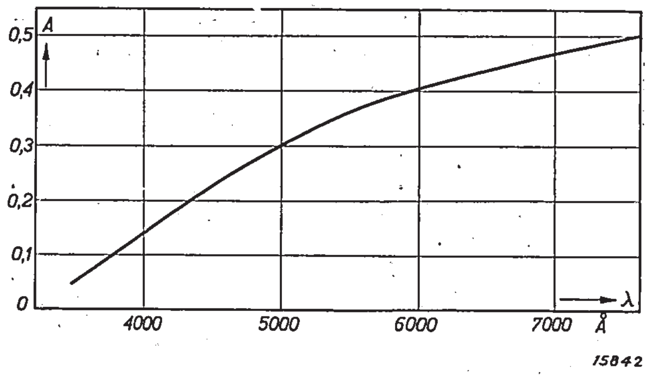

Fig. 2. Astigmatism A of a myopic eye in diopter (i.e. $1/f_1 - 1/f_2$, where f_1 and f_2 are the focal lengths for light beams in the horizontal and vertical planes respectively) for the myopic eye of the author at different wavelengths λ.

measuring instruments, for the eye can function well at brightness levels differing by a factor of 10^8 or 10^{10}. In a technical instrument, for instance an ammeter, the measuring range can be increased by attaching shunts, and for a specific range of the magnitude under measurement the sensitivity of the instrument is then adapted to the values to be measured. The sensibility of the eye can be similarly altered by a process here termed adaptation, viz, by making two different adjustments, which both take place involuntarily when the eye is exposed for a time to a certain brightness level:

1) By altering the diameter of the pupil, the latter becoming smaller the greater the brightness [2]) of the field of view *(fig. 3)*; this alteration does not take place instantaneously, and actually occupies a time interval of the order of 1 second.
2) By changes in the properties of the retina with the illumination intensity; if for instance the eye is first exposed to a high and then to a low brightness, the retinal sensitivity will increase for these low intensities after a time. The change is very slow; for while the eye adapts itself to a high intensity in a few minutes, adaptation to very low brightness levels may sometimes take several hours.

It requires no detailed explanation to show that the speed and degree of adaptation has an important bearing on road-lighting problems, particularly where considerable fluctuations in the illumination falling on the eye may take place, for the capacity of the eye depends in a large measure on its state of adaptation.

In addition to the measuring range of a measuring instrument we are also interested in its sensibility, which is determined by the smallest still just detectable difference in the magnitude under measurement. The tendency is frequently therefore to make the sensibility throughout the whole measuring range roughly the same, i.e. to design the instrument on such lines that the percentage changes just detectable are the same throughout the range.

In the case of the eye this requirement is fulfilled over a wide range of brightness values, and including practically all brightness values covered by daylight; at very low and very high intensities the sensibility of the eye diminishes. If a brightness of $H + \Delta H$ can still just be distinguished from a brightness H, the ratio $H/\Delta H$ is termed the contrast sensibility (see *fig. 4)*. It is nearly constant over a wide range of brightness values (Weber-Fechner law). In road lighting, on the other hand, we are always concerned with a range in which a reduction in brightness results in a diminution in the contrast sensibility. As the perception of an object depends on the contrast between it and its background, it is evident that the contrast sensibility is here an important factor. Fig. 4 shows for instance that with a

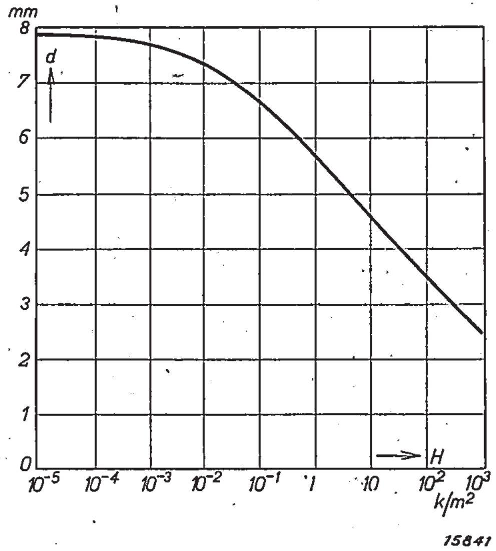

Fig. 3. Diameter of pupil d as a function of the adaptation brightness H; with increasing brightness the pupil contracts from 8 to $2^1/_2$ mm (Reeves). The unit of brightness is the candle per sq.m. = 10^{-4} stilb = 0.092 foot candle.

---

[2]) Brightness values are always expressed in candles per sq.m. (1 candle per sq.m. is equal to 10^{-4} stilb = 0.292 foot candle). To visualise the order of magnitude of this brightness unit, it should be noted that a surface which is illuminated with 1 lux (0.093 foot candle) and by which the whole of the incident light is perfectly diffusedly reflected has a brightness of $1/\pi$ candles per sq. m. The concept of brightness cannot be discussed in detail in this article, but will be dealt with comprehensively in a subsequent article.

brightness of 0.3 candle per sq. m. (= 0.028 candle per sq. ft.) on the surface of the highway an object whose brightness differs by less than 4 per cent from that of the highway, i.e. $H/\Delta H > 25$, cannot be perceived even under the most favourable conditions.

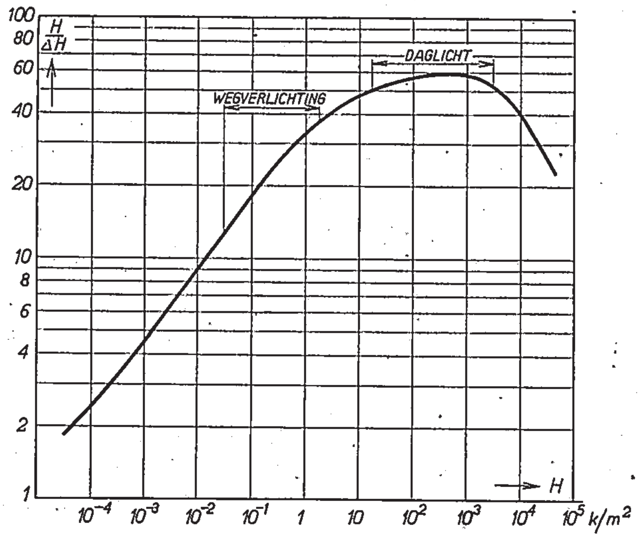

Fig. 4. The contrast sensibility $H/\Delta H$ for white light as a function of the brightness H is practically constant in daylight (Weber-Fechner), but varies strongly with the brightness in the case of road lighting (König).

A third cause for the defective functioning of the eye may lie in its sluggish operation. This rate of operation — the speed of vision — depends inter alia on the following factors:

1) The time of exposure or illumination which is necessary to produce a satisfactory image on the retina.
2) The time required for the construction of an image on the retina. (Construction of the image may in certain circumstances persist even after exposure.)
3) The time elapsing before the image is impressed on the brain.

The first time-element depends on the sensibility of the eye, the second on a chemical reaction time and the third on a psychical reaction time. The complexity of this mechanism is thus obvious. In general it may be assumed that the speed of vision increases with brightness (see *fig. 5)*.

If the road-lighting system is so devised that in normal circumstances the visual acuity, the contrast sensibility and the speed of vision suffice for distinct vision, these magnitudes may still drop below their critical values as a result of one part of the retina (not necessarily that part on which the image is impressed) being exposed to a much greater brightness than the rest of the retina. Glare is then experienced. Both during the presence in the field of vision of a light source causing glare and after the disappearance of such source, the visual acuity, the contrast sensibility and the speed of vision are reduced. Frequently glare may be regarded as the production of an unsatisfactory state of adaption.

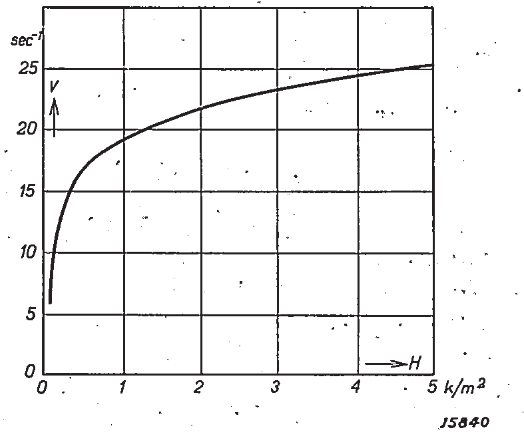

Fig. 5. Speed of vision V (reciprocal of the time of illumination of a specific object which is required just to perceive it) as a function of the brightness H (Weigel).

Finally, a factor must be referred to which — in particular with low brightness values — has a marked effect on the measurement and interpretation of brightnesses, viz, the fact that individual parts of the retina have intirely different structures. The retina contains two types of elements sensitive to light stimuli, the cones and the rods. In the centre of the retina is a nearly circular yellow spot (macula lutea) with a diameter of approximately 2 mm. Outside this yellow spot the retina is composed almost exclusively of rods. In the yellow spot the number of rods per sq. mm. diminishes progressively from the edges to the centre, while the number of cones rapidly increases. At the centre of the yellow spot (fovea centralis, diameter about 0.25 mm) no rods occur at all, whilst the cones are packed closely together. The cones and rods behave very differently in the following respects:

1) The rods give us an impression where all objects have the same colour (a bluish grey), while the cones are able to perceive colour differences.
2) At very low brightness levels only the rods register a sensation, and at high intensities practically only the cones; in the intervening transition range both types of elements func-

tion. The brightness values obtained with road-lighting systems are generally situated in the upper part of this transition range.

3) The sensibility of the rods to light-rays depends on the wavelength in an altogether different way to that of the cones (see *fig. 6*).

These differences result in a group of phenomena which are included under the name of the Purkinje phenomenon and may play an important part on comparing lights of different colours.

In particular, these phenomena affect the brightness ratios of the various parts of the field of vision, i.e. the richness of contrast. This richness of contrast is also an important magnitude with regard to the perception of objects. Also when the contrast is already considerably greater than the value required in view of the contrast sensibility, an object is perceived with still greater certainty and more quickly the more pronounced the contrasts are, i.e. the greather the richness of contrast.

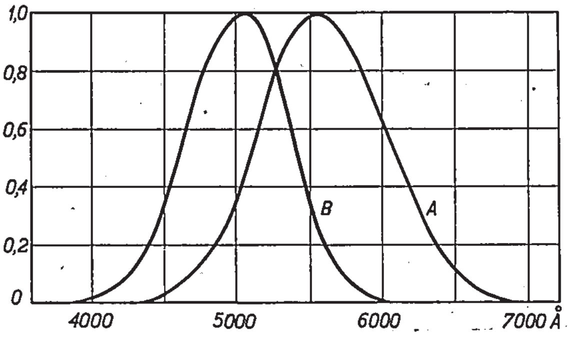

Fig. 6. Visibility curves of the eye (relative reciprocal values of the energy required to obtain a uniform "impression of brightness" as a function of the wavelength λ):
A) For the cones (valid for brightnesses exceeding 3 candles per sq.m. = 0.28 candle per sq. ft.).
B) For the rods (valid for brightnesses in the neighbourhood of the absolute threshold value of the eye).

In a series of further articles we shall enter in greater detail into the concepts mentioned here.

THE PHILIPS-MILLER SYSTEM OF SOUND RECORDING

By R. VERMEULEN.

Contents. On the ordinary disc sound is recorded and reproduced mechanically; in the photographic method of sound recording, both recording and reproduction are carried out by optical means. Mechanical reproduction on the one hand and optical recording on the other hand possess certain inherent disadvantages. The Philips-Miller system of sound-recording, whose principles are discussed in this article, avoids these disadvantages, in that the sound-track is recorded on the film by mechanical means and is then optically reproduced.

The art of recording music and speech with high fidelity — it is impossible to conceive of modern life existing without it — has been employed in a host of directions. It is the medium for bringing music into the homes of all, it has proved useful in the teaching of languages, it is employed for producing ethnographical and cultural documents and records, in ordinary office work (in the form of the dictaphone), and on a more magnificient scale for producing sound-films and for broadcasting purposes. Particulary the latter two fields of application have made very specific demands, not always easy to fulfil, on the methods employed for recording sound.

In the oldest form of sound-recording apparatus, the Edison phonograph, the recorded sound-track was inscribed on a wax cylinder. Where no copies of the sound-track are required and the quality of the sound does not have to satisfy special requirements, as for instance in the dictaphone, this earliest method of recording is still employed to the present day. In later methods a magnetisable steel wire, a wax disc, or a strip of film or paper chart were, or are still being, used for recording a sound-track.

For reproducing music in the home, the classical method of sound-recording continues to be employed, viz, the gramophone disc. It is evident therefore that in making the first sound-films the gramophone disc was also selected to carry the recorded sound. Certain difficulties were, however, soon found to be inherent in sound-tracks on discs, as for instance the difficulty of synchronising the sound after "cutting" and "splicing" the film, and the frequent changing of the discs which was necessary owing to their short playing time, etc. For this and other reasons another method of recording sound was adopted in sound-film work, viz, the production of a sound-track on the film strip itself. The sound-track was inscribed by optical means, the blackening produced by a narrow beam of light on the photographic surface being made to vary in synchronism with the sound vibrations either in dimensions (variable width) or in intensity (variable density) (see figs. 5 and 6). Various inconveniences inherent in this method, such as the time lost for developing the film, a weakening of the higher notes, etc., were temporarily tolerated or complicated means were evolved for remedying them.

In the Philips Laboratory a new method for recording sound has been evolved in the last few years, which is based on a principle proposed by J. A. Miller. A description of this Philips-Miller system, which has now reached a high stage of perfection, is given below. In this article it is proposed to describe in the main the principle employed and to compare this new method with those in use hitherto. The technical development of the basic principle of the Philips-Miller system introduced a number of special problems, the solution of which will be discussed in a series of articles in this Review.

---

[1] "Splicing" is the operation of joining together a number of pieces of film in the required order to produce the final sound film or news reel.

Basic Principle of the Philips-Miller Method

In the Philips-Miller method as in the photographic sound-film processes a sound-track is recorded on a strip of film. However, this is not done by optical means as hitherto but by mechanical means. The film material, the "Philimil" tape, consists of a celluloid base, which in place of the usual photographic emulsion is coated with an ordinary translucent layer of gelatine about 60 μ in thickness, on which a very thin opaque surface layer about 3 μ in thickness is affixed. Perpendicular to the tape, a cutter or stylus shaped like an obtuse wedge as shown in *fig. 1* moves in synchronism with the sound vibrations to be recorded. This cutter removes a shaving from the gelatine layer which is displaced below it at a uniform speed.

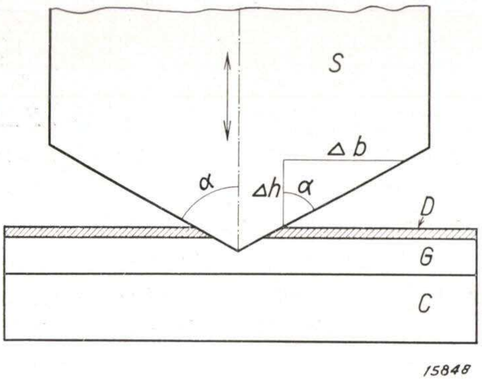

Fig. 1. Section through the wedge-shaped cutter *S* and the "Philimil" tape. The latter consists of a celluloid base *C*, a transparent layer of gelatine *G* and a very thin opaque coating *D*. The cutter shaves a groove from the tape which is moved under the cutter. The coating *D* thus being removed along this groove, a transparent track on an opaque background is obtained. By making the cutter in the form of an obtuse wedge, small elevations and depressions Δh of the cutter produce marked changes in width $2\Delta b$ of the inscribed track; with a semi-apical angle of the wedge α the "magnification" is $2 \tan \alpha$. In practice α is made 87 deg, hence $2 \tan \alpha =$ about 40.

If the cutter remains stationary, it cuts a groove of uniform width $2b$ in the film below it. Along this groove the thin top coating (and a part of the gelatine layer) is removed, so that a transparent trace is obtained on an opaque background. If the cutter is now brought deeper into the film by a distance Δh, the groove cut will become wider by a small amount $2\Delta b$ (cf. *fig. 2*) and if α is half the apical angle of the wedge (fig. 1) the relationship

$$2\,\Delta b = \Delta h \cdot 2 \tan \alpha$$

will apply. At $\alpha = 90$ deg, *tan* α will be infinity; it is thus seen that if α is nearly 90 deg a slight displacement Δh of the cutter will produce a marked alteration $2\Delta b$ in the width of the recorded trace. With 87 deg, the angle of the wedge used in practise, the "magnification" obtained will be $2\Delta b/\Delta h = 2 \tan 87$ *deg*, i.e. about 40.

Now if the cutter moves up and down in synchronism with the sound vibrations to be recorded (perpendicular to the tape), a transparent track on an opaque background will be produced on the moving tape whose width will vary in synchronism with the sound vibrations *(fig. 3)*. To obtain a maximum width of trace of $2b = 2$ mm, as commonly used in sound-film recording practice, the displacement of the cutter need only have a double amplitude Δh of $2000/40 = 50\ \mu$. The principal characteristic of the whole method is this small magnitude required for the cutter amplitude.

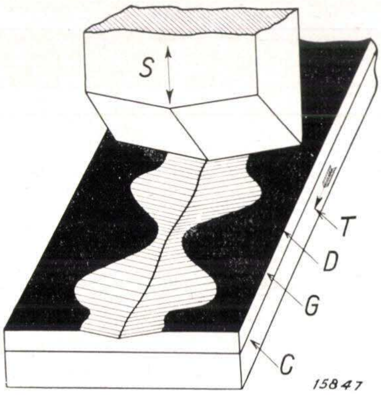

Fig. 3. The cutter *S* moves up and down in synchronism with the sound vibrations to be recorded (perpendicular to the plane of the tape). *D*, *G* and *C* represent the same as in fig. 1. A transparent sound-track on an opaque background is produced on the "Philimil" tape which moves under the cutter in the direction *T*.

The recorded sound is reproduced by the usual method employed in optical sound-film technology. The film carrying the sound-track is moved between a photo-electric cell and a small, brightly

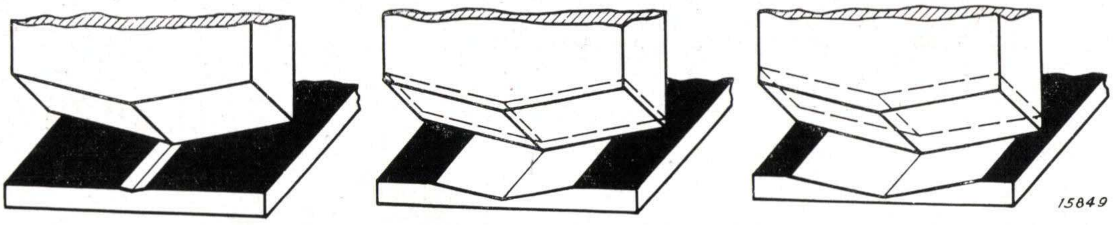

Fig. 2. The width of the track inscribed in the tape for three different positions of the cutter.

illuminated slit (transversal to the direction of motion of the film). The intensity of the light falling on the photo-electric cell thus varies with the variable width of the sound-track, and the resulting current fluctuations in the photo-electric cell are amplified and passed to a loudspeaker.

The Philips-Miller system is thus a combination of a mechanical recording method with an optical method of reproduction. This unique association offers distinct advantages over the methods hitherto in use, as will be evident from the discussion below.

Mechanical Sound Recording and Reproduction on Discs

Sound is recorded on the gramophone disc by mechanical means: an oscillating cutter (scribing stylus) cuts an undulating groove in a wax disc *(fig. 4)*. Reproduction is also performed mechanically, the gramophone needle (reproducing stylus) being made to follow the undulation of the groove. The disc is manifolded with the aid of a mould produced by electro-deposition. This process is very suitable for producing large numbers of a record and will therefore not be easily superseded by any other process. Yet it possesses certain general disadvantages in in addition to those already referred to and which are particularly undesirable for sound-film work, viz, the short playing time of a disc and the difficulty of excising part of the sound-track. As a result of mechanical playing back the disc is subject to considerable wear; even if the needle is changed each time the disc is played, the quality of reproduction is still noticeably reduced already after playing the disc 20 times. Moreover, the resistance to motion produced by the needle on the revolution of the disc depends on the intensity of modulation in the sound-groove, so that in a loud passage (particularly of pianoforte music) the disc may be retarded, with the production of the well-known undesirable booming effect [2]).

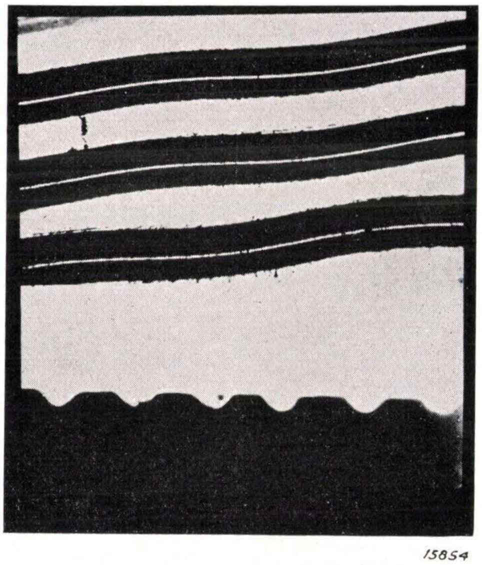

Fig. 4. Undulating grooves of a gramophone disc. View from above and in section.

Above all the method of reproduction introduces an unavoidable falling-off in the higher notes. The wear and resistance to motion of the disc are due to the needle on travelling through the groove sustaining considerable accelerations, i.e. great forces, at all highly curved points. In fact with too great a curvature in the groove the needle may even stick or break down the walls of the groove. It follows, therefore, that the curvature of the groove must not exceed a certain value (as may be readily seen, the radius of curvature must not become smaller than the width of the groove). The groove has an undulating form expressed by the equation $A \sin \omega x$, where A is the amplitude, and ω the frequency of the recorded sound; the maximum curvature and hence also the force is then proportional to $\omega^2 A$. It would, therefore, if A were constant, assume high values at the high frequencies. On prescribing that the forces must for the high frequencies remain the same as for the low ones, provision must be made in sound-recording such that the (fully-modulated) amplitude A diminishes in proportion to $1/\omega^2$. This would, however, result in such small amplitudes at the higher frequencies, that they would become indistinguishable from the ever-present small surface inequalities of the material, with the result that the higher notes would be submerged in the ground noise (surface noise) of the disc itself. Moreover, for the lower notes the amplitudes obtained would be too great, so that the distance between the grooves would have to be made very large and the discs thus become most cumbersome (or the playing time become undesirably short). In practice, therefore, a recording method is adopted in which, at full modulation, an amplitude is recorded proportional to $1/\omega$ (instead of to $1/\omega^2$) [3]). Such a frequency characteristic is in fact also very suitable for electromagnetic reproduction. The needle is connected with an armature or a coil which moves in a magnetic field. The voltage produced by displacement of the armature, which latter for instance may be represented by $A \sin \omega t$, is proportional to the velocity $\omega A \cos \omega t$ of this displacement, i.e. proportional to the product ωA of the frequency and the amplitude. Since according to the above method of recording the inscribed amplitude A of the groove is proportional to $1/\omega$, ωA remains constant, so that we obtain directly the required constant (frequency-independent) output voltage which is passed to the valve amplifier. However, with this frequency characteristic (A proportional to $1/\omega$ instead of to $1/\omega^2$), the amplitudes of the lower notes and the curvature of the groove for the higher notes would still become too great, so that at both ends of the frequency range the amplitudes must be reduced (see footnote [3]). This loss can be compensated at the lower frequencies by selecting a suitable characteristic for the valve amplifier, but at the higher frequencies such compensation would at the same time result in a more marked ground noise.

---

[2]) During recording the load on the driving motor naturally also varies according to the intensity of modulation. This fluctuation in load can be conveniently taken up here by a fly-wheel. The addition of a massive fly-wheel to a gramophone for the home would, however, not be a very satisfactory solution.

[3]) At the lowest frequencies, the amplitudes are even made independent of the frequency.

All these disadvantages; wear, retardation of the disc, and degeneration of the high frequencies, are as we see only due to mechanical reproduction and not to mechanical registration.

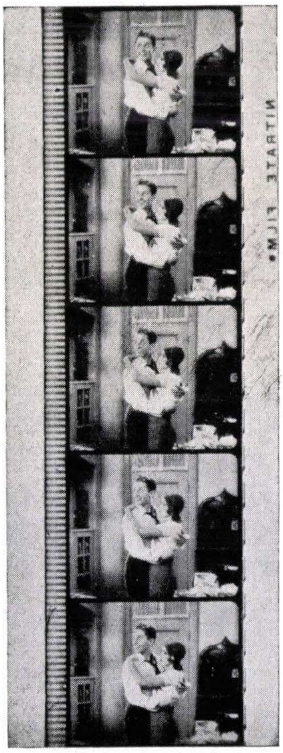

Fig. 5

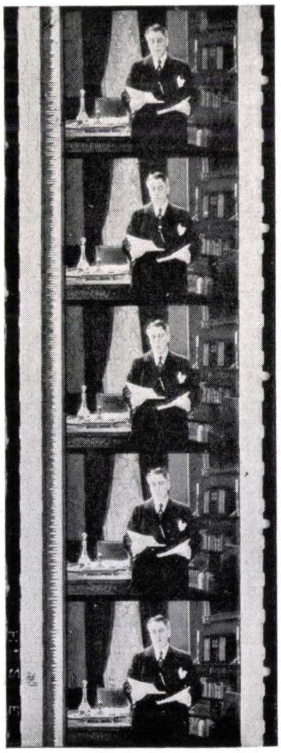

Fig. 6

Fig. 5. Sound-film strip with variable-density sound-track. The sound-track is produced by illuminating the film through a slit situated transverse to the direction of motion of the film, the intensity of illumination (or the width of the slit) being varied by the sound vibrations.

Fig. 6. Sound-film strip with variable-width sound-track. This sound-track is produced by varying the length of the illuminated slit in synchronism with the sound vibrations, see fig. 7.

Optical Sound Recording and Reproduction from Sound-Film Tracks

Optical registration of the sound-track on a film strip represented a marked advance in sound-film technology. The playing time was now made much longer, being the same as for the picture itself. Synchronising vision and sound, and film cutting and splicing were also much simplified. Wear resulting from (optical) reproduction no longer occurred, nor a fluctuating load placed on the motor which pulls the film through the reproduction machine. Optical reproduction thus offered a very satisfactory solution of the problem. Also manifolding is very simple since as many copies as required can be obtained by photographic means.

Certain drawbacks of the optical method are, however, inherent in the method of recording the sound track. The film is exposed by an illuminated slit of varying intensity (variable-density record, *fig. 5*) or of varying length (variable-width record, *figs. 6* and *7*). The illuminated slit always has a definite width, e.g. $25\ \mu$. With a film speed of 50 cm per sec $= 20000 \cdot 25\ \mu$ per sec, each part of the film is therefore in front of the slit for a period of $1/20000$ sec. With a vibration of 5000-

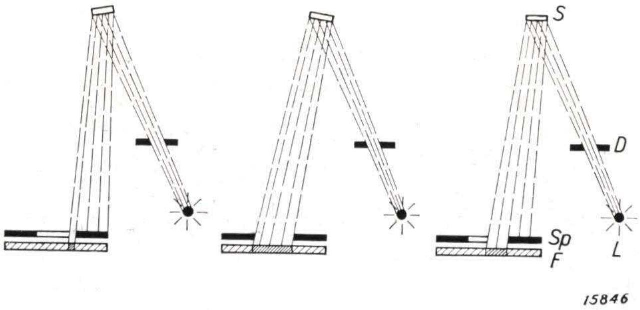

Fig. 7. Arrangement for the photographic recording of a variable-width sound-track. From the light emitted from the constant light source L a beam is passing through the diaphragm D. The mirror S mounted on a sensitive oscillograph throws the beam of light on to the slit Sp, under which the film F is moved (perpendicular to the plane of the paper). When the mirror S commences to swing under the action of the sound to be recorded, the sharply-focussed beam of light oscillates to and fro over the slit Sp and produces a blackened band of varying width on the film (see fig. 6). The path of the rays is shown for three different positions of the mirror.

cycle frequency, the brightness of the slit with a variable-density record or the length of the slit with a variable-width record varies quite considerably already in this period of time, so that the modulation recorded on the film decreases in intensity in favour of an increasing uniform blackening over the whole width (or, with the variable-width method: part of the width) of the film.

The finite width of the slit thus results in a certain degeneration in reproduction of the high notes [4]). The same effect is also produced by the unavoidable grain and halation due to dispersion and reflexion of light (cf. *fig. 8*) in the photographic material; the grains and the lack of definition at the edges of the sound-track produce a murmur on reproduction, which again affects especially the high notes.

In fact the use of photographic material is not very satisfactory. After the sound has been recorded it is necessary to wait until the film has been developed, which frequently results in much inconvenience owing to loss of time (it is usually necessary to wait until the next day). It is true developing can be accelerated but speed is only obtained at the expense of quality. The blackening produced on the film must depend in a definite way on the exposure in order to obtain undistorted reproduction [5]), and to satisfy this requirement it is essential to exercise considerable care in developing.

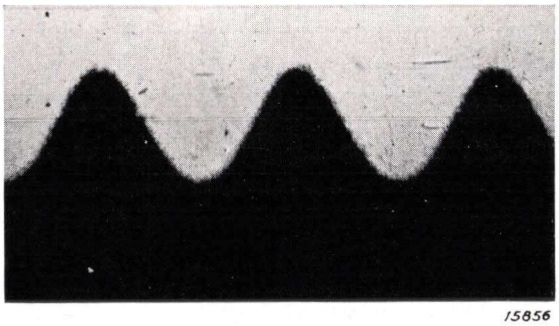

Fig. 8. Microphotograph of a variable-width record of a 1000-cycle note. Owing to the grain and dispersion of light in the emulsion the track is not wholly sharp. Magnification approx. 50 times.

We thus see that in the optical method the disadvantages (loss of time and also deterioration of the high frequencies) are due mainly to optical recording on the photographic material, and not to the method of optical reproduction.

Mechanical Sound Recording on a Tape

In the Philips-Miller method the disadvantages of mechanical reproduction as well as those of photographic recording are avoided, since reproduction is effected by optical means and registration on the film by mechanical means. Already before Miller, various other methods had been evolved to the same end, but all proved unsuccessful as the mechanical recording of sound on the film had to face insuperable obstacles. Some details of these difficulties will be discussed here.

In optical reproduction of the sound-track, the fluctuations in light, i.e. the modulation of the track width on the "Philimil" tape are converted directly into voltage fluctuations. In contrast to the method of reproduction with discs where, in agreement with the insertion of the electromagnetic system, the recorded amplitude was made to diminish with increasing frequency, in the optical method of reproduction the recorded amplitude is made independent of the frequency, in order to obtain an output voltage independent of frequency. *Fig. 9* shows in a striking manner the difference in sound-recording with both these types of amplitude-frequency relationship. One and the same sound vibration has been recorded on the

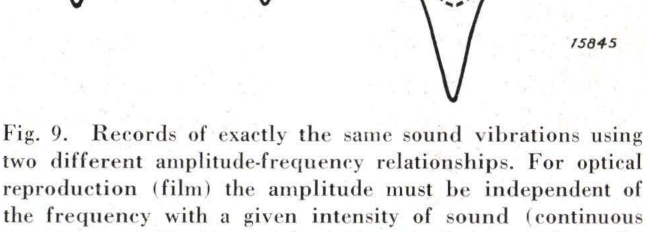

Fig. 9. Records of exactly the same sound vibrations using two different amplitude-frequency relationships. For optical reproduction (film) the amplitude must be independent of the frequency with a given intensity of sound (continuous sound curve *F*). For mechanical reproduction (disc), the amplitude must be inversely proportional to the frequency (dotted sound curve *G*). It is seen that in the first case (continuous sound curve) the higher frequencies are much more pronounced in the sound-track.

---

[4]) This effect of course is also obtained in the (optical) method of reproduction, but if it only occurs during reproduction it is not yet so troublesome as when it occurs twice, viz, during both recording and reproduction.

[5]) This condition is also due to the finite width of the slit. With an infinitely narrow slit, the law of blackening can have any arbitrary from in the variable-width method where the length of the illuminated slit is varied, but not so with a finite slit, owing to the half shadows produced at the edges (in variable-density recording where the intensity of blackening is varied, still more severe requirements must be met as regards accurate maintenance of the prescribed relationship between blackening and the incident amount of light).

basis of each frequency relationship. It is seen that on the film (amplitude for optical reproduction being independent of the frequency) the high frequencies are much more distinctly recorded than on the disc (where the amplitude diminishes with the frequency), and are hence also situated higher above the interference level. The normal width of the sound-track on the sound-film is 2 mm. The sound-recording machine must therefore record an amplitude of 1 mm.

How must a system be designed for mechanically recording sound? Let the stylus or cutter be attached to a spring-controlled armature, which for instance may be driven electromagnetically by the amplified microphone currents. The mechanism can be visualised as a mechanical oscillator of mass m (armature with cutter), a directional force c (spring control) and a certain damping constant r. If the system is set in motion by a force $k \sin \omega t$, it will oscillate with an amplitude:

$$A = \frac{k}{\sqrt{(c - m\,\omega^2)^2 + (r\,\omega)^2}} \quad \ldots \quad (1)$$

This equation can be reduced to the form:

$$\frac{A}{k/c} = \frac{1}{\sqrt{[1 - (\omega/\omega_0)^2]^2 + \delta^2\,(\omega/\omega_0)^2}} \quad \ldots \quad (1a)$$

where $\omega_0 = \sqrt{c/m}$ is 2π times the natural frequency of the undamped system and $\delta = r/\sqrt{mc}$ is the only parameter contained in this expression. *Fig. 10* shows $A/(k/c)$ plotted against ω/ω_0 for various values δ of the parameter. If the damping is not too high ($\delta < 1$), resonance is obtained in the neighbourhood of $\omega/\omega_0 = 1$, i.e. when the driving frequency ω is close to the natural frequency ω_0. The curves show that it is essential to remain below the resonance frequency if an amplitude sufficiently independent of the frequency is to be realised, or alternatively, since the frequency range of sound registration is fixed (up to approx. 8000 cycles) the driving system (sound recorder) must be so dimensioned that its natural frequency $\omega_0 = \sqrt{c/m}$ lies within the range of the highest frequencies to be recorded. For this purpose it is evident that the controlling force c must be made large and the mass m small. The diminution possible in the mass of the armature is, however, limited by the dimensions which it must have in order to obtain the requisite driving force to overcome the resistance of the tape and inertia of the cutter. We are therefore constrained to make the directional force (of the spring) c of the system very large, but this in its turn results in the amplitude A, with which the system responds to one and the same force k, becoming undesirably small; this follows from equation (1). This drawback cannot be remedied, either, by increasing k arbitrarily, since this will lead to an increase in the stress on the material and soon exceed the permissible limiting load.

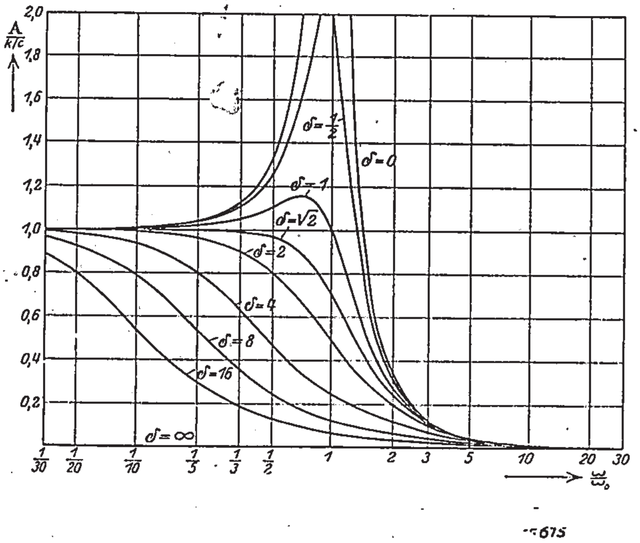

Fig. 10. Resonance curves of an oscillating system (spring controlling force c, mass m, damping r) set in motion by a force $k \sin \omega t$. The frequency ratio ω/ω_0 ($\omega_0 = 2\pi$ times natural frequency) is plotted along the abscissa (which for convenience' sake is divided logarithmically), and the ratio of the amplitudes $A/(k/c)$ (A = amplitude with which the system responds to excitation) along the ordinate. The resonance curve if plotted in these dimensionless variables is completely determined by the similarly dimensionless parameter $\lambda = r/\sqrt{mc}$. In working out the dimensions of the sound recorder the form of the resonance curve is the primary factor; δ ought to be made equal to about unity. In addition A/k should be as large as possible. (Reproduced from B. D. H. Tellegen, Arch. Elektrotechn. 22, 62, 129.)

The conclusion must therefore be drawn that a high natural frequency and a considerable amplitude independent of the frequency cannot be realised simultaneously[6]). Miller provides a way out of the difficulty: By giving the cutter the shape of an obtuse wedge (fig. 1) the sound-track is recorded with a large amplitude (= half-width of track = 1 mm at complete modulation), while the amplitude of the mechanical oscillating system serving as sound recorder need only be comparatively small, viz, a maximum of 25 μ. These values can just be attained by most careful construction. In a following article the whole problem involved here will be discussed in greater detail. *Fig. 11* gives the frequency characteristic of the sound recorder which has been attained at present.

---

[6]) In the mechanical recording of sound on discs, conditions are much simpler in this respect as only at the lower frequencies is a pronounced amplitude required, but with the high frequencies a lower amplitude is needed; this kind of frequency characteristic is readily to be obtained from the ordinary form of resonance curves, see fig. 10.

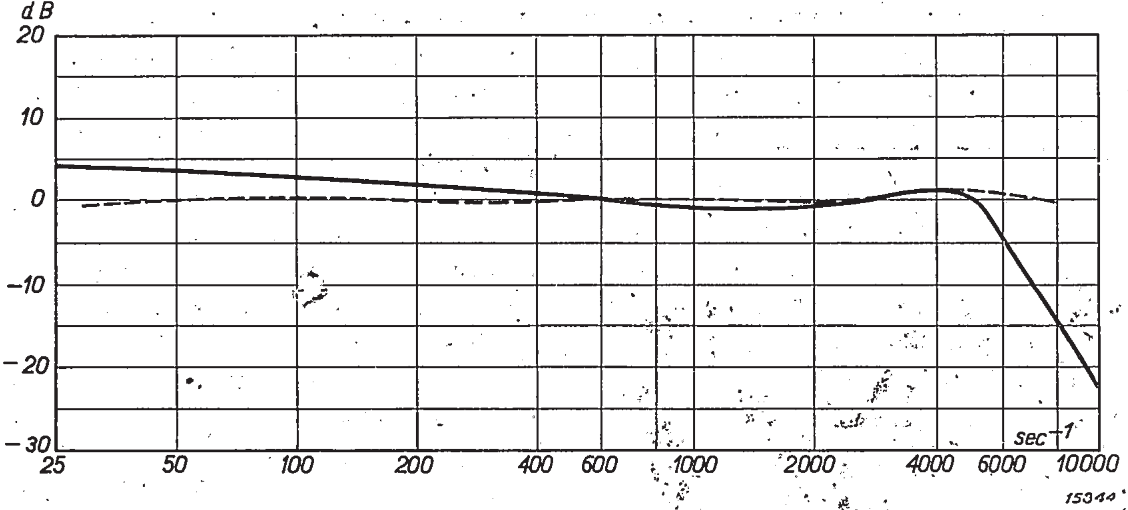

Fig. 11. Characteristic of the sound recorder (continuous curve) as at present constructed. The sound frequencies in cycles are plotted logarithmically along the abscissa and the amplitude differences in decibels along the ordinate. (A difference of m decibels between two amplitudes A_1 and A_2 ($A_1 > A_2$) signifies that the squares of the amplitudes A_1^2 and A_2^2 are in a ratio of $10^{0.1m} : 1$). It is seen that the amplitude between 20 and 6000 cycles is practically independent of the frequency. The dotted line gives the characteristic of the whole recording and reproducing apparatus; by suitably designing the amplifier the characteristic is still further improved with respect to the continuous line; the differences in the range between 20 and 8000 cycles do not now exceed 2 decibels, which is hardly to be heard. Reproduction is thus free from (linear) distortion.

The high magnification with the wedge-shaped cutter called for the solution of a number of practical problems. The slightest change in the distance between the cutter and the tape, as a result for instance of a slight eccentricity of the roller carrying the tape or the presence of a particle of dust between the roller and tape, or a slight variation in the thickness of the tape, is able to cause immediately an audible distortion of the sound-track. The recording apparatus must therefore be constructed with the greatest precision, while in the manufacture of the tape every care must be taken to obtain maximum uniformity and purity of the material. This latter precaution is also necessary in order to prevent the very heavily-stressed cutter becoming damaged by particles of dust or traces of impurities in the gelatine layer.

It is also most essential to have an absolutely uniform motion of the tape. The resistance applied by the tape to the cutter, however, varies with the width of track from 0 to 2 kg, this rendering the uniform motion very difficult to be obtained. The fluctuation in load cannot be taken up by the perforation taken over from the picture film and by the driving sprocket wheel, without producing undesirable vibrations in the tape motion. A new driving method has brought the remedy here.

The recorded tape can be copied photographically in the same way as an ordinary variable-density or variable-width sound-film, but as the sound-track possesses a modulation not only in its width but also in its density, it acts on a beam of light passing through it as if it were a prism. The fluctuations in the light resulting herefrom do not cause interference, and in any case can be rendered innocuous by simple means.

Characteristics and Applications of the Philips-Miller System

The sound-track on the "Philimil" tape has the same desirable characteristics as the ordinary film: A longer playing time (30 tot 60 minutes), the possibility of cutting and splicing, and the production of copies photographically. In addition all disadvantages of the photographic material have been avoided. All operations with the film strip can now be carried out in daylight. The sound-track is more sharply recorded since no granulation and dispersion of light in the photographic emulsion occur here, see *fig. 12.* Moreover, owing to the almost complete absence of granulation in the material the ground noise has been considerably reduced. High frequencies are recorded with more fidelity; the cutter can be made so sharp that it does not alter the frequency characteristics, as was the case in the optical method of recording by the width of the light-slit.

The most important and most striking advantage offered by this method is that the sound-track can be reproduced immediately the recording process has been completed (e.g. after 1/5 of a second). This property is of the greatest importance and value when recording sound-films. The producer has now no longer to wait for the development of the light-sensitive film in order to decide whether the sound record conforms with his requirements. After each scene has been recorded he can listen in to the playback of the sound-track immediately and decide on the spot of the sound-track for documentary and other repeated.

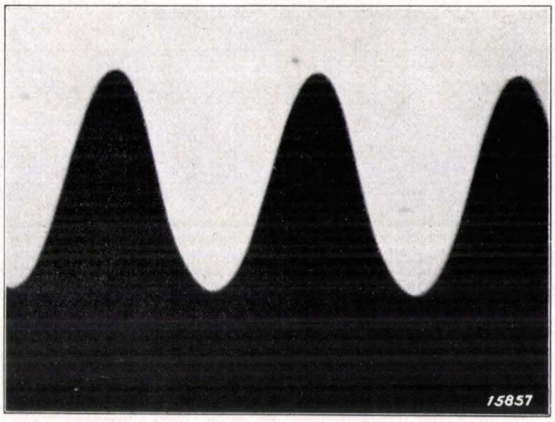

Fig. 12. Microphotograph of the sound-track of a 1000-cycle note on the "Philimil" tape, with the same magnification as in fig. 8. The coating is devoid of all grains and the edges of the sound-track are sharply defined. The ground noise is therefore much reduced.

For broadcasting purposes also, the immediate reproducibility of the sound-track is of the greatest utility. The exchange of programmes between stations, the postponement of the transmission of current items of news (races, speeches, etc.) to a more suitable time of the day, the production of radio plays, all these are much facilitated by the Philips-Miller system, while the tonal quality exceeds that obtainable with the wax disc. The high fidelity of reproduction also offers a method of copying sound-records which in certain circumstances may be very convenient, viz, by making a new record of the reproduced sound track on a second "Philimil" tape. This "mechanical" copying can be carried out at the same time as reproduction, so that a direct duplicate can be obtained of the sound-track for documentary and other purposes.

THE V.R. 18 TRANSMITTING AND RECEIVING EQUIPMENT

By C. ROMEYN.

Introduction

With the progressing development of commercial flying, the need for some means of intercommunication between an aircraft in flight and the airport very soon became apparent, and the first passenger and commercial airplanes, although still very small, were already equipped with wireless apparatus. With the steady and radical improvements in technical methods and apparatus during the last ten years both flying and wireless technology have made rapid strides. The importance of wireless intercommunication during flight has progressively increased and at the present day it is impossible to conceive of a passenger or commercial aircraft being without wireless apparatus. Reports of weather conditions along the aircraft route, landing instructions, direction-finding signals, etc., have become indispensable to the pilot.

It is the task of the wireless industry to provide suitable apparatus capable of meeting the special requirements for use in modern aircraft. That an aircraft radio equipment in many respects must differ fundamentally from a permanent and stationary ground equipment is obvious. In the present article the V. R. 18 aircraft transmitting-receiving equipment designed by Philips is described. This equipment has been specially evolved to meet the various requirements for use aboard aircraft, yet in its design attention has, moreover, been given to certain specialised needs considering the application of this equipment for the Douglas air liners operating on the Netherlands East Indies route of the K.L.M. air services.

General Characteristics of a Wireless Equipment for Aircraft Use

The V.R. 18 equipment (see *fig. 1*) consists in the main of the transmitter, receiver, aerial and requisite sources of power, as well as a series of auxiliary components such as the control box, the aerial lead-through, etc. In both electrical and mechanical characteristics, all components have to be designed to meet special requirements. Thus all parts must be as light as possible and take up the minimum of space without constituting an obstruction. Furthermore, the equipment must be installed in such a way that it is not exposed to serious vibration or hard jolts. To permit the interior to be tested readily and quickly, easy dismantling of both the transmitter and the receiver is moreover desirable.

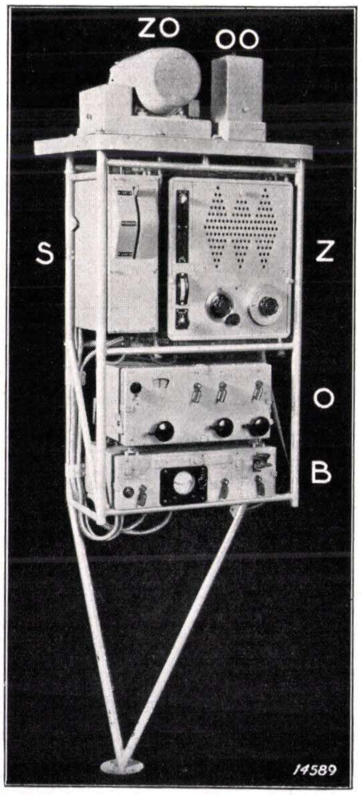

Fig. 1. Complete wireless equipment V.R. 18 for aircraft. (In the Douglas machines the various components are mounted in different places.) Z = Transmitter. O = Receiver. B = Control box. ZO = Converter furnishing anode voltage of transmitter. OO = Converter furnishing anode voltage of receiver. S = Switch for changing over from trailing aerial to fixed aerial.

Intercommunication between aircraft and airport is nowadays performed almost exclusively by telegraphic means. In this connection it is interesting to review briefly the historical development of the methods employed. During the early years of flying intercommunication with aircraft was carried out solely by means of the telephone. This instrument alone could be used at that time, since the pilot who had to operate the wireless apparatus already had both hands fully occupied in controlling the flight of the machine and it was thus impossible for him to work a Morse key. The disadvantages of using telephony became, however, steadily more apparent. In the first place, to cover the same range a telephone transmitter has to have a greater power than a telegraph transmitter; yet the most serious drawback of telephony is that it requires a wider frequency band, since, owing to modulation, an additional side band is transmitted at both sides of the carrier-wave frequency. In view of the increasing number of transmitting stations, which were concentrated in a comparatively small geographical area, the few frequency bands available were soon taken up. The only practical means for avoiding intensive mutual interference of stations was to adopt the telegraphic method of intercommunication. This made it necessary to provide a wireless operator for each aircraft in addition to the pilot. This addition to the crew would, however, have become necessary for other reasons, even without changing over from the telephone to the Morse key. The greater demands made on the pilot by the more complex problems associated with navigation (flying at night and through fog) were already making the care of the telephone an onerous additional responsibility, while on the other hand wireless intercommunication for the self-same reason, viz, the much-increased number of reports required for safe navigation, itself demanded closer attention. Moreover, it had become practicable to carry a special operator, as larger aircraft were being built in which more room was provided in the pilot's cabin.

Intercommunication between aircraft and airports is thus at the present time almost exclusively based on telegraphy. By international agreement the wave-lengths of 600, 944, 918 and 932 m have been allocated for wireless aircraft transmitters, of which the 600-m wave-length is only allowed for transoceanic flights.

The Transmitter

The transmitter of the V.R. 18 equipment is constructed for continuous-wave and tonic-train telegraphy. In the former a high-frequency oscillation is radiated at intervals corresponding to the Morse signals. These oscillations are generated by a control stage *S* (see *fig. 2*) containing an oscillating valve (called the control valve) and a tuning-circuit. The oscillations generated are amplified by an amplifying stage *V* comprising two valves connected in parallel. In the anode circuit of this stage the amplified energy is fed to the transmitting aerial *A*. This method of wiring ensures a very constant frequency, as aerial reaction on the oscillator (control stage) is very small. For frequency adjustment the tuning-curcuit of the control stage is provided with a variable condenser, which by a snap action can be fixed in four standard positions. These four settings corespond to the above-mentioned standard international wave-lengths, but can be altered to conform to any subsequent alteration in the agreed wave-lengths.

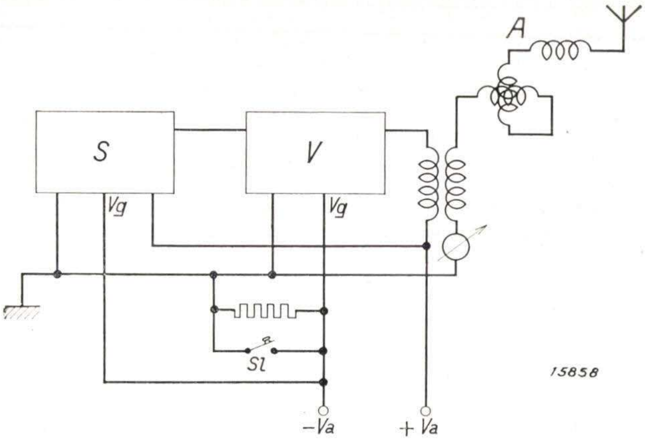

Fig. 2. Simplified circuit diagram of the transmitter V.Z. 18. *S* is the control stage, which generates the desired frequency, *V* the amplifying stage containing two valves in parallel, *A* the aerial circuit with aerial reaction, tuning variometer and ammeter. The voltage-drop at the resistance in parallel with the Morse key *Sl* is applied as negative grid bias *Vg* to all valves and inhibits transmission. By means of the Morse key this resistance is shorted and, as a result, the transmitter enabled to transmit in synchronism with the Morse signals.

A high negative bias *V* is applied to the grids of the control and amplifying valves, which inhibits the oscillation. During transmission this negative bias is removed in synchronism with the Morse signals (see fig. 2).

By means of a rotary interrupter, which is in series with the Morse key, the radiated high-frequency oscillation can, moreover, be interrupted 1000 times per second. This method of transmission, tonic-train telegraphy, is used for making the connection with some station. Owing to the greater width of the frequency band as a result of modulation with the 1000-cycle frequency, tuning is rendered more simple. But as soon as the connection has been set up, the wireless operator changes over to continuous-wave telegraphy, since the latter causes less interference owing to the absence of side bands.

The Douglas air liners on the East Indies route of the K.L.M. have to cross regions in Asia where airports are few and far between. In order to keep in communication with at least one airpost a powerful transmitter is required, and for this reason the power output of the V.R. 18 equipment in the aerial circuit has been rated at 75 watts. The range when using a trailing aerial (see below) is then at least 600 km for continuous-wave telegraphy and 300 km for tonic-train telegraphy. In certain circumstances the range may be considerably greater and on several occasions this equipment has been able to transmit over distances exceeding 6000 km. During flights in the European zone, where a large number of well-equipped airports are situated close to each other, a fairly small transmitting power is, on the other hand, sufficient for efficient intercommunication, provided atmospheric disturbances are not too serious. In fact, a transmitter with an excessive power output is undesirable for this zone, since it may interfere with the wireless signals being transmitted simultaneously from an airport to other aircraft in flight. The transmitting power of the equipment can therefore be regulated, the aerial power being reducible to either a half or a quarter by increasing the negative bias of the amplifying valves.

The interior of the transmitter, with the chassis pulled out, is shown in *fig. 3*.

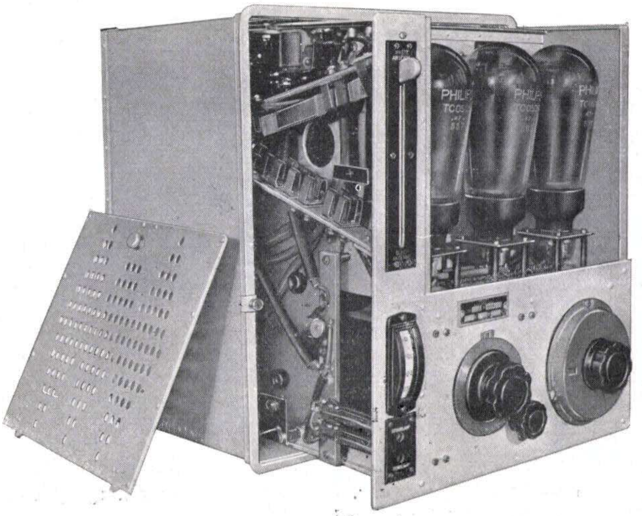

Fig. 3. V.Z. 18 transmitter with chassis drawn out and front wall removed. The housing and chassis are made of duralumin.

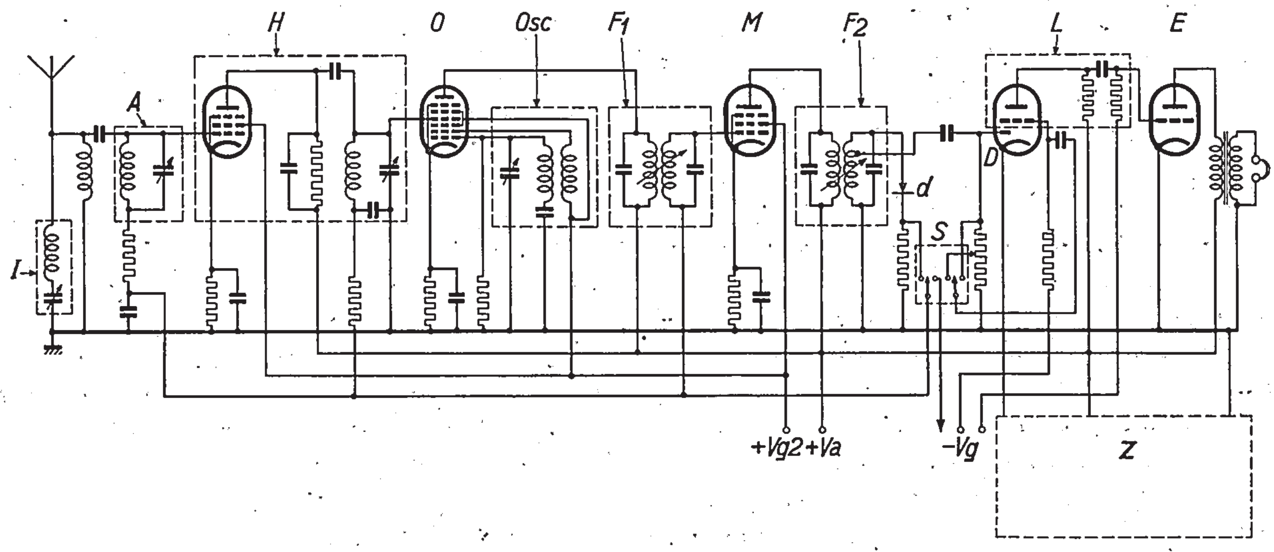

Fig. 4. Simplified circuit diagram of receiver V.O. 18. The circuit shown is that of a five-valve superheterodyne receiver, where *A* is the first tuning circuit, *H* the high-frequency amplifying stage, *O* the modulating and oscillating valve, *Osc* the oscillating circuit, which is tuned to an oscillation with a frequency differing by an almost constant amount (differential or intermediate frequency) from the tuning frequency of *A* and *H*. The three variable condensers of these three stages are mounted on a common shaft. F_1 is the first and F_2 the second intermediate-frequency band filter; by means of a variable coupling the band width passing through these filters can be varied. The intermediate-frequency amplifying stage *M* is situated between the two filters. The intermediate-frequency alternating voltages are applied to the diode *D*, which also contains in the same glass-body the three-electrode valve of the low-frequency amplifying stage *L*. *Z* is the beat oscillator which generates an oscillation differing from the intermediate frequency by a specific (variable) frequency (usually 1000 cycles). The oscillation of the beat oscillator is also applied to *D*, so that at the exit of the rectifying stage an oscillation with the differential frequency (1000 cycles) is to be heard. *E* is the terminal stage with the output transformer.
The oscillating circuit *I* is tuned to the intermediate frequency and hence short-circuits any (disturbing) carrier wave emanating from a long-wave transmitter with a frequency equal to the intermediate frequency. By means of the switch *S* the automatic volume control reacting on all preceding valves *H*, *O* and *M*, can be switched on (left position) or replaced by manual control (right position). To generate the rectified output voltage for the automatic volume control a special detector *d* is provided. This is necessary because the diode *D*, being coupled to the beat oscillator *Z*, already furnishes an output voltage when no signal at all is received at the receiver, and would thus in this case already reduce the sensitivity of the receiver.

The Receiver

When crossing those areas of Asia sparsely provided with airports an aircraft must needs be equipped with a very sensitive receiver. The superheterodyne method adopted in the V.R. 18 equipment is particularly suitable for obtaining the high sensitivity required. A lay-out of the circuit employed (simplified) is shown in *fig. 4*. An octode (*O*) serves as a converter valve. It is preceded by a high-frequency amplifying stage (*H*). The intermediate frequency generated in the converter valve is again amplified (in *M*), then rectified (in *D*) and amplified once more in the low-frequency stage (*L*). A small beat oscillator (*Z*) is provided to render the continuous-wave signals audible, (since no audible frequencies per se are obtained from these signals after the rectifying stage). This oscillator generates oscillations with a frequency which differs only slightly from the intermediate frequency. If this frequency together with the intermediate-frequency signals is passed to the rectifying stage, the Morse signals become audible on the differential frequency between the two. The frequency of the beat oscillator can be regulated, so that the pitch of the Morse signals can be adjusted as required. This simplifies the separation of stations operating on wave-lengths close together. The receiver is rated for wave-lengths between 520 and 1300 m.

The apparatus, on a wave-length of 600 m, furnishes a power output of 10 milliwatts with a 0.75 μ-volt amplitude of the incoming signal[1]). This is roughly the maximum sensitivity which can be attained at present.

The sensitivity of the receiver can be regulated by hand, or an automatic volume control (see *S* in fig. 4) may be put into action with the aid of which the receiver adjusts itself continuously to a fairly constant output power and the volume can then be adjusted by hand to the required value. Volume control is particularly useful when approaching radio beacons, as without it the volume has to be continually readjusted.

---

[1]) Measured in accordance with the usual definition of sensitivity.

A further requirement which has to be met in the receiving apparatus is the possession of a high selectivity. This feature is necessary to set up a reliable channel of communication in areas where air traffic is heavy, and is also of great value for flying in the tropics in order to reduce the effects of atmospheric interference. The circuit of the superheterodyne receiver permits a very high selectivity to be obtained in a very simple manner, for the intermediate frequency is constant so that a large number of invariable oscillating circuits can be tuned to it (see F_1 and F_2 in fig. 4). In some cases, however, a high selectivity is undesirable, particularly during wireless telephone reception (by cutting off the side bands, speech becomes distorted or even unintelligible) and particularly when picking up stations; in this case the wireless operator listens whether he is being called by any airport and must therefore listen as it were to all stations at the same time. To permit this to be done the selectivity of the apparatus is variable; the band width can be adjusted to 3.8, 5.5 and 7.5 kilocycles. The smallest band width is used for receiving continuous-wave telegraph transmitters, the medium width for telephony and tonic-train telegraphy, and the largest for picking up stations.

A photograph of the receiver with the chassis pulled out is reproduced in *fig. 5*.

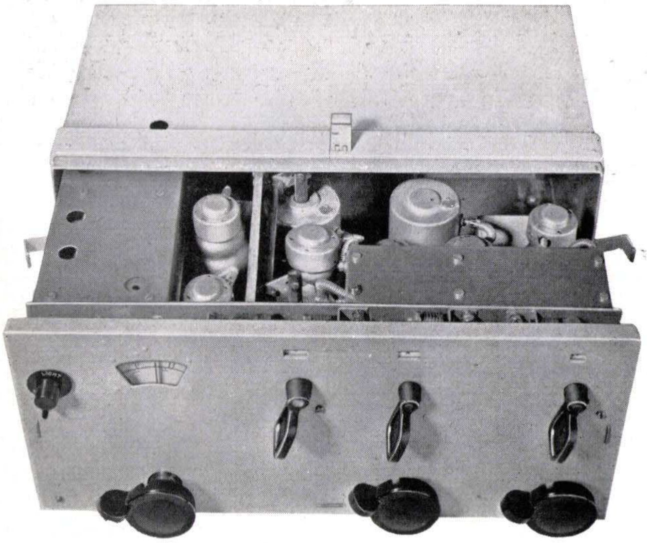

Fig. 5. V.O. 18 receiver with chassis pulled out. The housing and chassis are made of duralumin.

The Aerials

The Douglas air liners are equipped with a trailing aerial, i.e. a wire 60 m long which is loaded with a weight at the lower end and can be paid out during flight through a lead-through in the body of the aircraft. The paying-out and winding-in of the aerial is performed by a winch. An electrical counterpoise is provided by the metal fuselage of the aircraft.

In many cases a trailing aerial cannot be used. The time required to fly from one airport to another at a small distance, e.g. from Schiphol to Waalhaven, is only a few minutes at the high speeds attained by the Douglas machines. This time is not sufficient for paying out the aerial. Nevertheless, unbroken radio communication is necessary, for the aircraft must receive its landing instructions from the airport during flights. Moreover, it is desirable when landing to take in the aerial in good time and yet remain in communication with the airpost up to the last minute. For this purpose each machine is equipped with an additional aerial which is fixed permanently above the body. This is also naturally the only means whereby landing can be controlled from radio-beacons.

The Douglas air liners must be capable of flying in all weathers. Should they fly through storm clouds, a long trailing aerial will increase the danger of being struck by lightning. The aerial is therefore taken in and transmission and reception must then be maintained with the aid of the fixed aerial. To keep in communication with the airport, which in this case may be at a greater distance, and in spite of the lower radiation of the fixed aerial, which has only one quarter of the "effective height" of the trailing aerial, every care has been taken that the maximum possible portion of the available energy is radiated. In view of this, not only the trailing aerial but also the fixed aerial has, therefore, been carefully adapted to the amplifying stage, by introducing a special aerial-loading inductance and aerial coupling. A single manual movement of the switch provided is all that is required to change over from the trailing aerial to the fixed aerial.

Power Supply

Perhaps the nature of the power supply best brings out how far improvements in aircraft design have had a fundamental influence on the design of the aircraft wireless equipment. In the past an outboard generator was used with an auto-regulating air-screw (the anode voltage and the filament voltage had to be kept constant; in other words, the speed of the air-screw had to be independent of the "wind" velocity over a wide range, i.e. of the flying speed). As the flying speed was increased, which was achieved mainly by giving all and even the smallest components of the aircraft a stream-line design, the use of an outboard generator was no longer permissible in view of its high air resistance.

To act as a source of power for the whole equipment, the 12-volt starting battery is now used with the V.R. 18 set. The filaments are fed directly from the battery. The anode voltages for the transmitting and receiving valves are furnished by two converters which are driven from the battery. The anode voltage of the receiving valves must be properly smoothed and any interference eliminated. Formerly the necessary supply was therefore furnished by a dry battery; the converter now used for this purpose is of special design with a very low interference from the commutator brushes and in which all causes of interference have been most carefully eliminated by means of condensers and chokes.

The converter for the transmitting valves furnishes a uni-directional voltage of 500 volts at 300 milliamps and the converter for the receiving valves 200 volts at 40 milliamps. The starting battery is recharged during flight by a dynamo, which is driven from the aero-engines. Compared with the outboard generator, the battery offers the additional advantage that the machine can for some time continue to send out wireless messages from the ground, for instance after a forced landing.

Installation of Equipment

The transmitter with the associated converter is accommodated in a corner of the luggage cabin. It is suspended by shock-absorbing cables and is thus adequately protected against jolts and vibration. The receiver is set up on spring rubber supports in front of the operator's seat (*fig. 6*), together with the control box, on which are arranged, among other items, the Morse keys, various switches and the aerial ammeter. For night flying, dial illumination is provided, being capable of regulation and so placed that it does not interfere with the pilot's field of vision. The components of the transmitter and receiver are mounted on special chassis, which can be taken out separately. Like the boxes and the converter housings, these chassis are made of duralumin or aluminium in order to keep the weight as low as possible. The whole equipment (transmitter, receiver, two converters, winch and aerial lead-through, control box, switches, cable and telephone) weighs about 92 lbs.

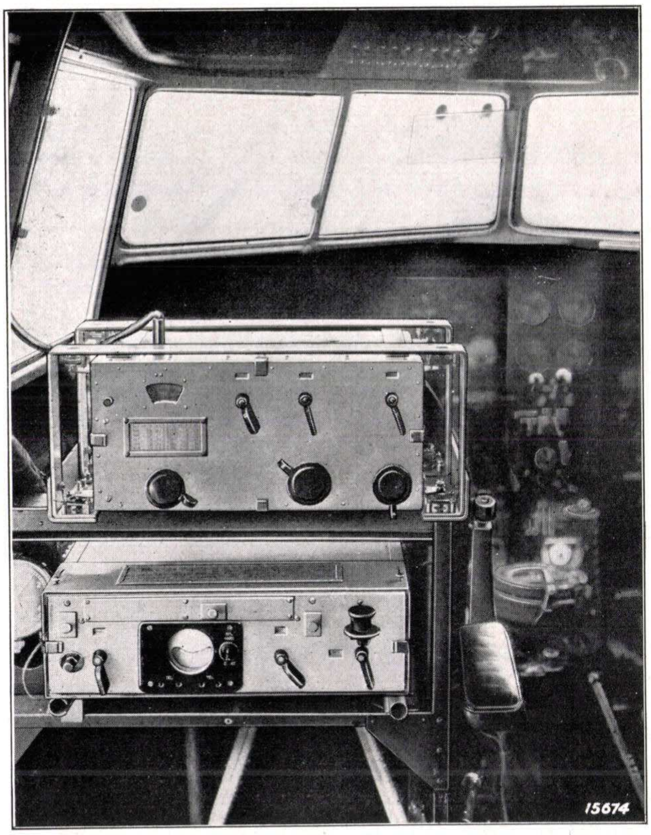

Fig. 6. Installation of the receiver (above) and the control box (below) in front of the wireless operator in the pilot's cabin of a Douglas air liner.

THE PHOTOMETRY OF METAL VAPOUR LAMPS

Summary. Following a discussion of the principles of photometry with regard to coloured light sources, an arrangement is described by means of which the luminous flux of gaseous discharge lamps are measured in this laboratory. Some results obtained in the photometric investigation of sodium and mercury vapour lamps with this apparatus are discussed in detail. The fundamental difficulties in the photometry of light-sources whose spectral intensity distribution does not correspond to that obtained with the standard, appear to be partiularly pronounced in measurements on the mercury vapour lamp. In conclusion, investigations are discussed which are being made in order to overcome the difficulties of heterochromatic photometry.

Introduction

As gaseous discharge lamps and in particular metal vapour lamps have become more widely employed, the photometric investigation of colourd light sources (heterochromatic photometry) became an urgent technical problem. An account is given below as to how the luminous flux of coloured light sources is measured in this laboratory, together with some special results obtained in measurements on sodium and mercury vapour lamps.

Before entering into details of these measurements, some of the principles of heterochromatic photometry will be briefly discussed.

Every photometric measurement is based on the comparison of brightness values. The particular difficulties encountered in photometric measurements on coloured light sources are due to the fact that the equality of brightness of two surfaces of different colour is determined by physiological means and therefore cannot naturally be reduced to a pure physical basis. Such determination depends entirely on the characteristics of the human eye. Particularly with very great difference in colour is it difficult to decide whether two surfaces A and B are equally bright. Various criteria of equivalent brightness are feasible and are indeed employd in practice as may be gathered from the following.

Direct Comparison of Brightness (Equality of Brightness Method)

Two light sources of different colour illuminate the two comparison fields of a photometer, viz, fields$A$ and B. The positions of the light sources are so adjusted that the observer "sees" both fields illuminated equally bright. The criterion employed here yields a definite result only if the difference in colour is sufficiently small.

Step by step Method

If the difference in colour is so marked that a direct comparison is difficult, it is advantageous to introduce a series of intermediate stages, viz, the auxiliary fields $A_1, A_2 \dots A_n$, which respective to their neighbours show such slight changes in colour that a direct comparison of brightness is possible between A and A_1, between A_1 and A_2, and so on, up to between A_n and B.

Application of the Flicker Photometer

In the flicker photometer, two illuminated surfaces whose brightness values have to be compared with each other, are projected into the field of vision alternately with a specified frequency. At a low frequency the field of vision appears to flicker in intensity as well as in colour. Beyond a certain frequency the colours merge into a composite colour, while with unequal intensities of the two surfaces a flicker in the brightness persists. At the lowest frequency at which the colour flicker has just disappeared, there exists a sharply defined adjustments of intensities at which the brightness flicker ceases also. The disappearance of brightness flicker may be considered to be a criterion for equality of brightness of the two surfaces.

It is important that, under the specific experimental conditions laid down by Ives [1]), the judgments regarding equality of brightness conforms to the following laws:

1) If brightness h_1 is equal to brightness h_2 and h_2 is equal to h_3, then $h_1 = h_3$ (transitive law).
2) If $h_1 = h_3$ and $h_2 = h_4$, then $h_1 + h_2 = h_3 + h_4$ (additive law). $h_1 + h_2$ is the sensation due to the sum of radiations yielding the sensations h_1 and h_2 respectively.

---

[1]) H. E. Ives, Phil. Mag. **24**, 149, 352 and 853, 1912. The angle of vision of the photometer field must be about 2 deg., corresponding roughly to the yellow spot of the retina. This point will be discussed again later on. Furthermore, the brightness must be at least 1 candle per sq. foot (at lower brightness values the Purkinje phenomenon is obtained owing to a displacement of the spectral distribution of ocular sensitivity). On the other hand it must not be too high, in order to avoid glare.

The transitive law is an inherent need, if it is desired to characterize a certain brightness by a single numerical value. But it is the additive law which offers a fundamentally simple method for a photometry, which is objective, i.e. independent of the eye of the observer.

Ocular Sensitivity Curves and Physical Definition of Brightness

The eye responds most sensitively to rays with a wave-length of approx. 5550 Å, so that of all radiations which produce an equal sensation of brightness a monochromatic (green) radiation of 5550 Å has the least energy. The ratio of the energy E_{5550} of this radiation to the energy of an equally bright radiation with a wave-length λ is a measure of the relative ocular sensitivity or luminosity factor V for the wave length λ:

$$V(\lambda) = \frac{E_{5550}}{E(\lambda)}$$

Various investigators have determined the spectral distribution of relative ocular sensitivity for a large number of observers [2]). An average of these results has been accepted as the international ocular sensitivity curve [3]).

By utilizing the additive law and the international ocular sensitivity curve an objective measure H can be introduced to represent the brightness of a radiation with arbitrary spectral distribution. The brightness of a radiation composed of light of different wave lengths λ_1, λ_2 ... can by the additive law be put proportional to the sum of the products of the luminosity factors $V(\lambda_1)$, $V(\lambda_2)$ ... and the corresponding radiation energies $E(\lambda_1)$, $E(\lambda_2)$ ... In practical units the definition of brightness so obtained is expressed as follows:

$$H = 621\, \Sigma V(\lambda_n)\, E_n \text{ lumens per sq. foot and solid angle unit.}$$

Here E is expressed in watts per sq. foot and solid angle unit (1 lumen per sq. foot and solid angle unit is equal to 1 candle per sq. foot).

In general the intensity is continually distributed throughout the spectrum, then the sum must be replaced by the integral:

$$H = 621 \int_0^\infty V(\lambda)\, E(\lambda)\, d\lambda \text{ candles per sq. foot} \quad (1)$$

Measurement of Brightness

For brightness measurements an observer should be required whose sensitivity curve coincides reasonably with the international curve. Experience has shown, however, that this condition is practically never fulfilled. A simple method has therefore been sought for selecting a small group of observers whose average results are of sufficient reliability. To do this it is absolutely essential to be able to determine in some way the difference between the sensitivity curve of an observer and the international sensitivity curve. The method proposed by Ives and Kingsbury [4]) for this purpose consists in determining the transmission factor of a yellow and a blue solution (aqueous solutions of potassium bichromate and copper sulphate of specified concentrations in vessels with an internal diameter of exactly 1 cm) for the light from a carbon filament lamp of specific temperature. The solution filters are so selected that their transmission factors are equal as measured with reference to the "international eye". The "yellow-blue ratio"

$$R_{yb} = \frac{\text{transmission of yellow filter}}{\text{transmission of blue filter}}$$

for an observer is then considered to be a measure for the deviation of his ocular sensitivity curve from the international curve. If the observers are so chosen that the average value of all "yellow-blue ratios" is unity, then, according to Ives, even with a comparatively small number of observers the average value of the results obtained will be in satisfactory accord with the values which would be obtained on the basis of the international luminosity curve. It must, however, be borne in mind that this method, which up to the present has only been employed in photometric measurements on incandescent filament lamps in which the differences in colour are small, cannot be applied without reservation to metal-vapour lamps.

Description of the Photometric Apparatus

The apparatus [5]), which has been used for some years in this laboratory, has been designed specifically for the measurement of the luminous flux of direct-current and alternating-current gaseous discharge lamps. An integrating sphere is used in this apparatus which has been previously calibrated with a lamp giving a known flux. The arrangement of the apparatus is shown in *fig. 1*, the inscriptions below indicating some details of the design. The use of the flicker photometer for measurements with the sphere did not appear desirable at the outset, as in measurements with alternating-current lamps difficulties were anticipated as a result of interferences between the alternating-current and the flicker frequency. For this reason the equality of brightnes method was adopted and the chromatic difference kept as low as possible by equalising the colour of the comparison surface to that of the gaseous discharge by means of a filter[6]). The flicker photometer cannot, however, be dispensed with when using this arrangement, but serves for determining the transmission factor of the filter. Determination of the luminous flux of a gaseous discharge lamp thus requires three separate measurements, of which I and II need in principle only be carried out once for each type of lamp; these three are:

---

[2]) K. S. Gibson and E. P. T. Tyndall, Bur. Stand. Scient. Papers, Nr. 475, p. 131, 1923.

[3]) Proc. International Commission of Illumination, 6th Meeting, Geneva, July 1925, pp. 67 and 232. Cf. also D. Judd, J. O. S. A. 21, 267, 1931.

[4]) H. E. Ives and E. P. Kingsbury, Trans. Ill. Eng. Soc. 9, 795, 1914; 10, 195, 1915.

[5]) P. Clausing, Physica, 2, 731, 1935.

I) Calibration of the filter,
II) Calibration of the integrating sphere with a lamp of known luminous flux, and
III) Measurement of the luminous flux of a gaseous discharge lamp with the sphere by the filter method.

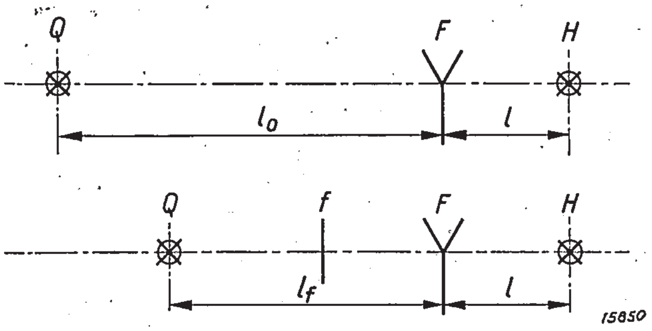

Fig. 2. Photometric arrangement for determining the transmission factor of the filter f.
Q = Standard lamp,
H = Auxiliary lamp for photometric comparison,
f = Filter,
F = Flicker photometer.

Calibration of Filter

Using a flicker photometer F (*scheme 2*) the

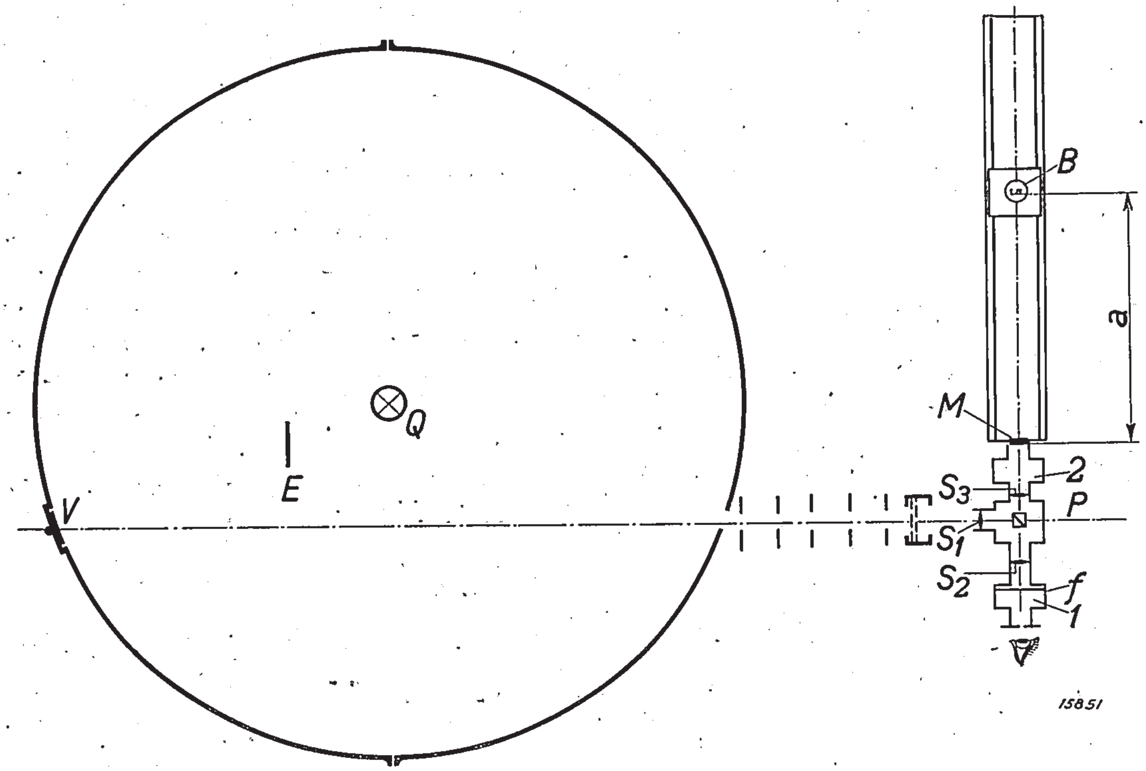

Fig. 1. Design of integrating sphere. The inner surface of the sphere is painted with a neutral grey colour, i.e. a colour whose coefficient of reflection is approximately independent of the wave length. Q = Standard lamp, V = Measured field of the sphere, E = Opaque, white screen, M = Opal glass, B = Band lamp for photometric comparison, P = Photometer cube, S_1 = Lens for obtaining an image of V on the focal point of S_2, S_3 = Lens for obtaining an image of M on the focal point of S_2, 1 and 2 = Filter boxes, f = Filter. The measurement of luminous flux by means of the integrating sphere is based on the fact that the illumination of every part of the surface which is screened against direct rays of the lamp (such as the measuring surface V here) is proportional to the total luminous flux. The illumination of V is determined by photometric comparison with the illumination of the opal glass M.

---

[6]) Similar methods have also been employed by other laboratories, cf. e.g. G. T. Winch, E. H. Palmers, C. F. Machin, B. P. Dudding, G.E.C.Journal **5**, No. 3, August 1934. H. Buckley, Ill. Eng. **27**, 118 and 148, 1934.

horizontal candle power of an incandescent lamp Q with a known luminous flux L is measured on a photometer bench, the lamp being later used for calibrating the integrating sphere. This measurement is carried out twice, viz, with and without the filter f in the path of the light from Q. The transmission factor of the filter is calculated from the adjustments l_f and l_0 obtained, thus:

$$D = \left(\frac{l_f}{l_0}\right)^2$$

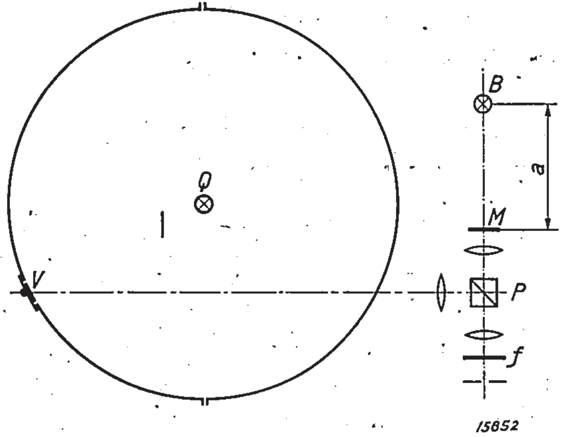

Fig. 3. Sketch of apparatus for calibrating the integrating sphere. The filter f is so placed that both the radiations from Q and B have to pass through the filter.

Calibration of the Integrating Sphere

The standard lamp Q is submitted to photometric measurement with the integrating sphere as shown in *fig. 3*. The distance a between the opal glass window M and the comparison lamp B is determined at which the surfaces of the Lummer-Brodhun photometer head, both viewed through the filter f, appear equally bright. (The comparison lamp B is a tungsten band-lamp.)

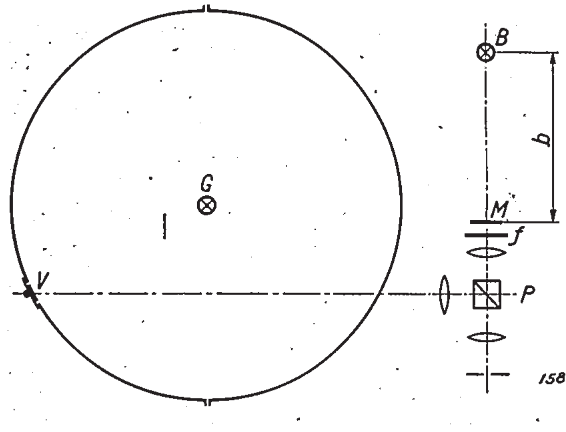

Fig. 4. Sketch of apparatus for measuring luminous flux. The filter f is so placed that only the light from B is filtered.

Measurement of Luminous Flux of Gaseous Discharge Lamps

The gaseous discharge lamp G is set up in the arrangement shown in *fig. 4* and compared photometrically with the comparison lamp B. The filter f is in a position different from that during calibration; it is so placed that the light from the integrating sphere does not pass through the filter. If the adjustment of equality of brightness yields a distance b between M and V the luminous flux of the gaseous discharge lamp is given by:

$$L_G = L \cdot D \cdot \frac{a^2}{b^2} = L \cdot \left(\frac{l_f}{l_0}\,\frac{a}{b}\right)^2 \text{ lumens.}$$

Filters

Filters of coloured gelatine are used, viz, Wratten filters. The best combinations found for various types of light are shown in *Table I*.

Table I. Best combinations of Wratten filters for adapting the radiations of a tungsten band lamp to various types of light.

Type of Light	Principal wave lengths in Å	Combinations of Wratten filters Nos.
Sodium light	5890 and 5896	23 A + 57
Mercury light	5461, 5770, 5790, 4358	38 + 51
Green mercury line	5461	62
Yellow mercury line	5770 and 5790	61 + 22

Table I also gives the filters used for measuring the luminous flux of individual mercury lines alone. In this case the mercury light must naturally also be filtered. The arrangement shown in fig. 3 (rather than that shown in fig. 4) must therefore be used in these measurements. The absorption of the yellow or green mercury line by the filter is determined in a separate measurement, using a photo-electric cell [7]).

Results

The adaptation of the filtered radiation of the comparison lamp to the colour and spectral distribution of the sodium vapour lamp is in general very satisfactory. Photometric measurements of mercury vapour lamps are, however, more difficult, mainly because the colour of the light, emitted from these lamps varied considerably during the rapid technical progress which has been made in these lamps in the course of the last few years. In addition the avalable filters for adapting the spectral distribution of the comparison lamp to that of the mercury lamp are not so suitable as that for the sodium lamp.

---

[7]) The determination of the absorption coefficients with the photo-electric cell is of course only permissible when the radiation undergoes no change in spectral distribution as a result of absorption. This condition is fulfilled for instance on filtering monochromatic light.

To test the reliability of measurements, the luminous flux of the yellow and green lines was separately determined for a number of mercury lamps in addition to the total flux. The sum of the values obtained for yellow and green radiation should agree to within a small percentage with the total flux, as the blue radiation contributes very little to the total light. *Table II* gives some results which appear quite satisfactory.

Table II. Luminous flux (lumens) of green and yellow lines separately and total flux of mercury lamps.

Lamp	Green line	Yellow line	Green + yellow	Total	Difference per cent
1)	9085	10350	19435	20600	—5.6
2)	3530	3456	6986	7187	—2.8
3)	2075	2190	4265	4320	—1.3
4)	5285	5640	10925	11030	—1.0
5)	3195	3214	6409	6575	—2.5
6)	7948	9209	17157	12800	—3.6
7)	3300	3310	6610	6850	—3.5
8)	5010	5275	10590	10590	—2.5
9)	6610	6610	13220	13800	—4.3

More protracted measurements and a change in the group of observers have, however, shown that photometric measurements were not always reproducible owing to the inadequate chromatic adaption. *Table III* shows that measurements made by the two observers R and K, which were in satisfactory agreement in February, were subject to a marked deviation in August. The second column gives the results obtained by the same observers when using a flicker photometer instead of the equality of brightness method. In this case there is no abrupt difference in the results obtained by the different observers. From this it may be concluded that the sudden anomaly is not due to a change in the properties of one observers' eye.

Table III. Luminous flux (lumens) of mercury lamps, measured by two observers in February and August.

Lamp	Date	Observer	Filter method	Difference %	Flicker method	Difference %
I	February	R	7940	1.0	7000	1.7
		K	7860		6860	
II	August	R	9140	8.4	8290	1.2
		K	8370		8190	

The results obtained by the two observers using the filter method are in very good agreement in February, but differ considerably in August. Moreover, except for observer K in August, there is a marked difference between the results obtained by the filter method and with the flicker photometer.

Investigations are being prosecuted in three directions with the goal of improving the reproducibility of the measurements.

Reduction of the Photometer Field

As Ives (cf. footnote 1)) has shown, the results obtained with the flicker photometer are only reliable when the angle of vision does not exceed 2 deg. With direct comparison also a systematic difference is observed between the results obtained with angles of vision of 6 deg. and 2 deg. respectively. As to be expected, on reducing this angle the difference between the equality of brightness method and the flicker photometer diminishes. *Table IV* gives the results of measurements carried out all on the same lamp with angles of vision of 6 deg. and 2 deg., and with an equality of brightness photometer and a flicker photometer respectively.

Table IV. Luminous flux (lumens) of three mercury lamps, measured by the flicker method and the equality of brightness method with angles of vision of 2 deg. and 6 deg.

Lamp	Observer	Flicker method Angle of field 8)		%age difference	Equality of brightness method Angle of field		%age difference
		2 deg.	6 deg.		2 deg.	6 deg.	
A	V	6875	6745	+1.9	7140	7850	+9.9
	R	6955	7000	+0.6	7475	7940	+6.2
	K	6925	6860	—0.9	7440	7860	+5.6
B	V	8245	8245	0.0	8635	9385	+8.7
	R	8550	8280	—3.1	8965	9615	+7.2
	K	8300	8220	—1.0	8830	9320	+5.5
C	V	8195	8175	—2.4	8675	9485	+9.3
	R	8475	8375	—1.2	9130	9595	+5.1
	K	8290	8320	+0.4	8940	9440	+5.6

On using the equality of brightness method, it was found that a decrease of the field of vision from 6 deg. to 2 deg. causes a considerable reduction in the observed values of luminous flux (particularly with observer V). With the flicker photometer the influence of the angle of vision is less marked. The difference between the results obtained with the flicker photometer and the equality of brightness method is certainly reduced by diminishing the angle of the photometer field, but is not entirely eliminated.

---

8) The flicker photometer with 6 deg. angle of vision (Bechstein type) has a divided field; the inner field of 2 deg. flickers in opposition to the outer field. The observation that (contrary to the statement of Ives) the results obtained with the 2 deg. and 6 deg. fields are practically the same is perhaps due to the fact that the eye of the observer is fixed on the inner field only.

Application of the Flicker Photometer also to A.C. Lamps

In spite of interferences between the brightness fluctuations of A.C. lamps and the flicker frequency, the measurements with the flicker photometer were found reproducible beyond all expectations (see *Table V*). Since, however, as indicated in Table III, three of the four measurements using the equality of brightness method yielded higher brightness values for the mercury lamp than the flicker photometer, the question arose as to whether systematic errors occurred in measurements on A.C. lamps when using the flicker photometer. This point was investigated by means of a light-source flickering with a 100-cycle frequency, which was produced by rotating a sector disc in front of a direct-current lamp. It was found that between the photometrically measured transmission factor of the sector disc and the value calculated from the dimensions, non-systematic errors not exceeding 4 per cent occurred, so that in this respect there is no serious objection to the use of the flicker photometer.

Table V. Reproducibility of measurements on alternating-current lamps with the flicker photometer.

Date of measurement	Sodium Lamp 70 watts	Sodium Lamp 50 watts	Mercury Lamp 500 watts	Mercury Lamp 400 watts
	lumens	lumens	lumens	lumens
11.10.35	—	—	23400	15580
15.10.35	—	—	23400	15600
4.11.35	3400	2020	—	15650
16.11.35	—	2080	—	—
30.11.35	3450	2110	23670	15940
4.1.36	—	—	23510	—
14.1.36	3410	2015	—	15690
24.1.36	—	—	—	15020
26.2.36	—	—	23300	—

The values for the luminous flux of one and the same lamp obtained on different days agree within the limits of the accuracy of measurement, which is a few per cent.

Physical Measurement of the Luminous Flux

The luminous flux is defined on a physical basis by equation (1), indicating that it is fundamentally possible to determine the value of this magnitude by purely physical means. For this purpose a light-sensitive apparatus is required which reacts to radiation of the wave length proportional to $E(\lambda)\ V(\lambda)$ (e.g. electrically). Furthermore, the reactions to raditions of different wave lenghts must be additive. The construction of such an apparatus using a photo-electrical cell and filters has been described in detail by König[9]). The practical application of this objective method is undoubtedly highly desirable because with every subjective method it is very difficult to determine in how far results obtained by a limited number of observers conform to the results based of international luminosity curve. There are, however, certain technical difficulties, since severe requirements have to be met as regards the absolute constancy of the properties of the photoelectric cell and the filters. It may, however, be expected that these difficulties will be overcome enabling the physical measurement to be regarded as the most suitable method of the future.

Compiled by G. HELLER.

---

[9]) H. König, Helvetica Physica Acta 4, 427 and 433, 1934.

A very sensitive spring balance

It has been known since ancient times that forces and in particular weights, can be measured by the elongation they produce in a spiral spring. Spring balances based on this principle offer various advantages, such as extreme simplicity of construction, the possibility of taking continuous readings, etc. Moreover, by making the spiral spring of very thin quartz wire (quartz being very suitable on account of its small elastic after-effect and its chemical inertness) it is possible to obtain very high sensitivities, as a result of which these spiral springs can be employed for numerous purposes and particularly for micro-investigations [1]). Spring balances of the type described below are used technically, for instance, in gas analysis, for checking the liberation of gas from metals in high-vacuum tubes. They may futhermore serve for testing the amount of moisture absorbed by textiles and paper, for testing the spread of lubricants, and in general for measuring very small forces or weights.

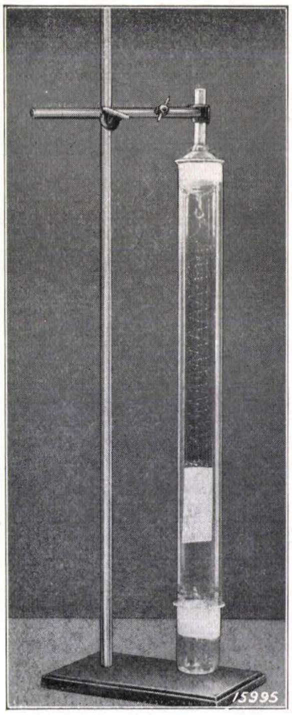

For the study of gases one frequently makes use of the adsorption phenomenon whereby the gas adheres to the surface of a suitable solid substance. When this adsorptive substance is suspended from the quartz spring in a space into which the gas is introduced, the increase of weight of the adsorbing medium resulting from the adsorption of a certain quantity of gas causes an elongation of the coil which can be read accurately to within 0.01 mm by means of a cathetometer.

The sensitivity of a spring balance of this type, i.e. the elongation per unit weight suspended from it (cm per mg) increases with the thinness of the quartz wire, the width of the spiral and the number of turns it possesses. With a thickness of wire of 70μ, a spiral of 2.5 cm diameter and 10 turns, a sensitivity of 1 cm per mg (and over) has been obtained here. The minimum elongation of 0.01 mm measurable with the cathetometer thus corresponds to a weight of 1/1000 mg.

In order to be able to utilise this high sensitivity, however, care must be taken that the initial load on the quartz coil (i.e. the total weight suspended from the coil) is made very small. In similar apparatus used elsewhere the initial load ranged from 500 to 1000 mg, so that a coil with a sensitivity 1 cm per mg would become extended by from 5 to 10 metres as a result of this load! For this reason a new method has been elaborated in which a few milligrams (this small amount being sufficient) of the adsorbing medium is deposited by volatilisation on a mica foil 5 μ in thickness and $4 \times 6 = 24$ sq. cm in area. Deposited layers of this type have an active surface which is many times (e.g. 50 times) larger than the geometrical surface. The mica foil with the deposited surface-layer is suspended from the quartz coil (see fig.), and as it weighs only about 25 mg the initial elongation is 25 cm.

One particular problem in making the balance is the manner of preparing the quartz coils. This operation is performed automatically on a coiling machine in which a quartz cylinder is used as a core. If wires are used whose thickness does not vary by more than 5%, very uniform coils free from stresses can be obtained by this method. The quartz wires are prepared by a special process and their thickness is checked with the microscope.

C. J. Dippel.

---

1) See for instance J. W. MacBain and A. M. Bakr, J. Am. chem. Soc. **48**, 690, 1926.

ABSTRACTS OF RECENT SCIENTIFIC PUBLICATIONS OF THE N.V. PHILIPS' GLOEILAMPENFABRIEKEN [1]

No. 1050: J. H. de Boer and C. F. Veenemans: Adsorption of alkali metals on metal surfaces. VI — The selective photo-electric effect (Physica **2**, 915-922, Nov. 1935).

Alkali atoms are primarily adsorbed at metal surfaces in the form of ions. From a covering fraction Θ upwards, atoms are adsorbed and these take up positions immediately adjoining an ion. At covering fractions $\geqq \Theta_m$ atoms are also adsorbed which are not linked directly to an ion but to other alkali atoms. The authors in this paper investigate the adsorption of sodium by tungsten. With low covering fractions, ordinary photo-electric emission of the tungsten takes place which is intensified by the electrical double-layer formed by the sodium ions. At higher covering fractions ($> \Theta_i$) selective photo-electric emission of the adsorbed ions forms an appreciable part of the photo-current. Those atoms which are bound next to the ions ($\Theta_i < \Theta < \Theta_m$) emit electrons only at comparatively short wave-lengths in the ultra-violet. But as soon as $\Theta > \Theta_m$ a selective photo-electric effect occurs at higher wave-lengths. This is due to the adsorbed atoms which are located near other atoms and are less loosely linked in such positions, but on transition to ions by photo-ionisation become more firmly bound than in the neighbourhood of another ion. At the end of the paper a summary is given of parts I tot VI.

No. 1051: J. A. M. van Liempt: Die Dampfdrucke der Metalle und ihre Verdampfungsgeschwindigkeit im Vakuum (Rec. Trav. chim. Pays-Bas **54**, 847-852, Nov. 1935).

For regular crystals formulae are deduced expressing the rate of vaporisation in vacuo as a function of the temperature, for the vapour pressure as a function of the temperature, and for the heat of vaporisation at the temperature of vaporisation. The rates of vaporisation and vapour pressures for different metals are in satisfactory agreement with the values calculated from these formulae.

No. 1052: J. van Niekerk: Changes in the sensitivity of rachitic rats for vitamin D (Arch. néerl. de physiologie de l'homme et des animaux **20**, 477-480, Oct. 1935).

The anti-rachitic dose of a vitamin D preparation of Reerink and van Wyk determined by the author before the introduction of standard preparations, appeared very small to van Harreveld compared with the activity of the same preparation in international units estimated subsequently by the author. The latter now explains this difference as being due to a diminution of sensitivity of his strain of experimental animals; this diminution was concluded from a long series of control calibrations with international standard preparations.

No. 1053: E. J. W. Verwey and M. G. van Bruggen: Structure of solid solutions of Fe_2O_3 in Mn_3O_4 (Z. Kristallogr. **92**, 136-138, Oct. 1935).

By means of X-rays the authors have investigated the crystal structure of a series of solid solutions of Fe_2O_3 in Mn_3O_4. It was found that the tetragonal structure of Mn_3O_4 (Hausmannite) with increasing Fe_2O_3 content gradually passes over into the cubic spinel structure. The axial ratio, which is 1.16 with M_3O_4, assumes a value of 1.0 with an atomic ratio of $Mn : Fe = 3 : 2$, so that from this composition onwards the structure can no longer be distinguished from one with cubic symmetry.

No. 1054: J. A. M. van Liempt and J. A. de Vriend: Die Schmelzzeit von Schmelzsicherungen II (Z. Phys. **98**, 133-140, Nov. 1935).

By means of a high-vacuum cathode-ray oscillograph, the times of fusion of a number of fusible cut-outs were determined at different short-circuit current values, which were up to 20 times the limiting current ratings of the fuses. In the case of 2-25 amp fuses, it was found in accordance with previous investigations that the product of the time of melting and the square of the applied short-circuit current was fairly constant for each type of fuse. The constant is in satisfactory agreement with the values calculated theoretically. Finally 6-amp fuses were loaded with the limiting current of 6 amps for half an hour and in this pre-heated state the short-circuit current was applied. The time of fusion was then found to be reduced to half the initial value.

---

[1] Reprints of these papers may be obtained on application from Philips Laboratory, Kastanjelaan, Eindhoven, Holland.

No. 1055: E. J. W. Verwey: Electrolytic conduction of a solid insulator at high fields. The formation of the anodic oxide film on aluminium (Physica **2**, 1059-1063, Dec. 1935).

To account for the formation of the crystalline oxide film during the electrolytic oxidation of aluminium, the author suggests the following mechanism: Under the action of the powerful field, Al ions are drawn into the initially formed surface oxide film composed of close-packed oxygen ions, wherein electrolytic conduction then takes place. As the author has already shown the product obtained is γ'-Al_2O_3, a cubic face-centred oxygen-ion lattice in which the Al^{3+} ions are distributed statistically, viz, 70 per cent at the octahedral positions and 30 per cent at the tetrahedral positions. The unoccupied positions then serve as "intermediate lattice positions" in the sense of Frenkel's theory of electrolytic conduction in a solid. The electrical conductivity calculated is of the same order of magnitude as the measured values.

No. 1056: W. G. Burgers and J. L. Snoek: Lattice distortion and coercive force in single crystals of nickel-iron-aluminium (Physica **2**, 1064—1074, Dec. 1935).

The phenomenon of hardening as a result of the tendency for the precipitation of molecules from the super-saturated solid solution is investigated by X-rays and magnetically on single crystals of Ni-Fe-Al alloys, obtained by unilateral cooling. The γ-phase which should be precipitated, does not occur under normal conditions of hardening but only on heating to above 1000 deg. C. During hardening characteristic changes in the X-ray diffraction lines of the α-phase are observed. The authors assume that in the original crystal lattice nuclei of varying composition are formed which possess a different lattice distance and hence produce stresses in their environment. On increasing or enlarging these nuclei, the coercivity increases to a maximum, after which it diminishes again. This may be explained either by a plastic deformation of the stressed material which in this way regains its structure or by the assumption that the precipitation of the γ-phase does actually take place, the unstressed lattice then being re-established during transformation.

No. 1057: E. J. W. Verwey: Eenige vlakkengecentreerde roosters met onvolledig gerangschikte kationen (Chem. Wbl. **32**, 721-726, Dec. 1935).

The structure of many crystal lattices is determined by the anions which are considerably greater than the cations. In the case of the crystals under consideration here the anions form a regular face-centred lattice; on the other hand the cations are distributed statistically over the available tetrahedral and octahedral positions. The various types of these "intermediate structures" differ in the degree of random arrangement of the cations owing to their thermal mobility, or in the presence or absence of unoccupied positions in the statistical distribution (cf. also Nos. 1039 and 1040).

No. 1058: A. Bouwers: Die Leistungsfrage bei Röntgenaufnahmen (Röntgenpraxis **7**, 779-780, Nov. 1935).

In this paper the commonly-held opinion is opposed that in order to improve the definition of the X-ray pictures the power of X-ray tubes must be raised. This raise at the present could only be achieved by enlarging the radiating focus whereby the geometrical lack of definition U_g of the radiograph would increase. Though the lack of definition caused by the motion of the object, U_b, would diminish (the increased power enabling a shorter time of exposure), the definition would not be much improved; since the optimum definition in a radiograph is always obtained when $U_b = U_g$, From these considerations the author concludes that by shortening the time of exposure the definition of the picture will only be increased, when this shortening is possible (owing to more sensitive photographic material) with a reduced power of the X-ray tube.

VOL. 1 No. 5 MAY 1936

Philips Technical Review

DEALING WITH TECHNICAL PROBLEMS
RELATING TO THE PRODUCTS, PROCESSES AND INVESTIGATIONS OF
N.V. PHILIPS' GLOEILAMPENFABRIEKEN

EDITED BY THE RESEARCH LABORATORY OF N.V. PHILIPS' GLOEILAMPENFABRIEKEN, EINDHOVEN, HOLLAND

M.F. 1936 pp. 129-160.

THE MERCURY VAPOUR LAMP HP 300

Contents. Electrical discharges through mercury vapour at high vapour pressures constitute light-sources with a high luminous efficiency coupled with small overall dimensions. The new mercury vapour lamp "Philora" HP 300, which is designed for connection to alternating current mains, has roughly the same size and shape as an incandescent lamp of the same rating (75 watts) but gives three times the luminous flux. The present article discusses the electrical and illumination characteristics of this lamp, with special reference to the importance and the function of the current-limiting unit (series or leak transformer) and the spectral composition of the emitted radiation.

Introduction

In the history of the technical application of electricity for illumination purposes various periods of development can be distinguished. Neglecting consideration of the arc lamps, the first period may be regarded as starting from the time Edison demonstrated his first carbon-filament lamps and lasting to the beginning of the present century, during which these carbon filament lamps completely held the field. About 1900 there appeared the first Nernst lamps and a variety of metal-filament lamps, first merely as negligible competitors, but later gaining such ground that by about 1912 they had practically ousted the carbon-filament lamp. And today when the field has been held almost exclusively by the tungsten-filament lamp for a period of nearly 25 years, gas-discharge lamps are steadily encroaching on its preserves. In a variety of important directions sodium and mercury lamps have already been adopted on a large scale for practical purposes, principally for street and road lighting and for illuminating shunting-yards and workshops.

In the new "Philora" lamp HP 300 Philips have added a small mercury-vapour lamp, which possesses an exceptionally high efficiency, the output of light being about three times that of a tungsten lamp of the same rating. In the long run, will this lamp be capable of displacing the tungsten lamp in the same way as the latter has completely superseded the carbon-filament lamp?

No, this cannot be anticipated, since the tungsten lamp possesses certain desirable characteristics which are lacking in the new lamp. Thus the tungsten lamp burns at its full brilliancy the moment it is switched on, whilst in the new lamp several minutes must elapse before this state is reached. Moreover, the colour of the mercury light differs from that which one has become accustomed to with the incandescent lamp.

But what may be expected from the new lamp? Wherever the level of illumination is low, a marked increase in this level can be obtained with a lamp of this type for a small extra current consumption. By mixing the mercury light with that of the incandescent lamp a very pleasing tone coupled with a high luminous efficiency is obtained. Thus if tungsten lamps of 200 watts are supplemented by a 75-watt mercury-lamp, the luminous flux is practically doubled, and all colours appear very nearly the same as in ordinary daylight. This mixed light thus offers advantages as compared with the light obtained from each source separately.

Although the carbon-filament lamp during the early years of lighting by electricity made a very important contribution to the development of this branch of electrical engineering, it yet remained to the much more efficient tungsten lamp to popularise the use of electric lighting to a degree which a decade previously no one would have dared to prophecy. In less than 50 years the annual consumption of incandescent lamps has grown to more than a thousand million, accounting for the consumption of about $25 \cdot 10^9$ kWh of electricity per annum. Electric lighting has introduced electricity into practically every household.

We are now again on the threshold of an important advance in the increased efficiency of electric lighting. In view of the fact that the level of illumination in practically all applications of electric lighting still is kept very low for economic reasons, it appears that the new lamp will also open up a number of new avenues of application for electric illumination which have hitherto not been accessible to it.

Characteristics of the New Mercury Lamp

Fig. 1 shows the mercury vapour lamp in its natural size. The discharge tube is of quartz, with the liquid mercury contained in the small cupules which surround the electrodes. During operation the pressure of the mercury vapour rises to 20 atmos. The external dimensions of the glass bulb are similar to those of an incandescent lamp of the same rating. The principal electrical and illumination data for this lamp are collected in *table I*.

TABLE I. Characteristics of the mercury lamp HP 300 in stationary operation.

Voltage-drop across the lamp	230 volts
Current intensity	0.4 amp
Consumption of lamp	75 watts
Losses in connected transformer 5450 G/86	15 watts
Power factor	0.55
Luminous flux	3000 lumens
Net yield of light	33 lumens per watt
Diameter of discharge tube	ab. 4 mm
Distance between electrodes	18 mm
Mean luminous density	420 candles/sq. cm
Luminous density along axis	ab. 1150 candles/sq. cm

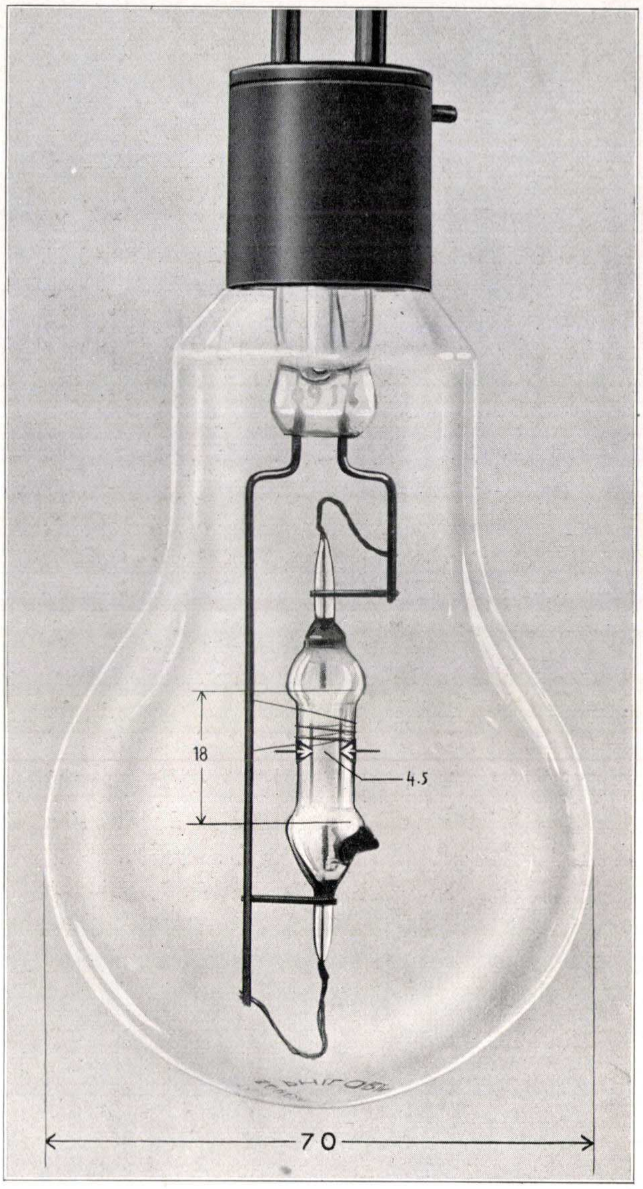

Fig. 1. Mercury vapour lamp "Philora" HP 300 rated for 75 watts and 3000 lumens in natural size.

The lamp is designed for running from an alternating-current mains supply. As with all other gas-discharge lamps, the new mercury vapour lamp also may not be connected directly to the mains, but must be connected in series with a resistance, condenser or a self-induction coil, in order to limit the current. The use of resistances is naturally avoided as far as possible in order to guard against supplementary power-losses. A strikingly simple solution of this problem is offered by the use of a transformer with a high leakage which serves both as a voltage source and as an inductive series resistance. The leak transformer (type No. 5450 G/86) provided for the new lamp is so rated that on the secondary side an inductive resistance of suitable magnitude is obtained and on connecting to a 220-volt mains supply the open-circuit voltage of 410 volts(eff.) for starting up and running the lamp is furnished.

To obtain a closer insight into the operation of this current-limiting unit, oscillograms were registered of the voltage drop U_E across the discharge and U_L across the unit in question, as well as of the total voltage U and the current intensity I (*fig. 2*). These curves show that the total tension is practically of sinusoidal form. On the other hand the voltage-drop U_E at the discharge when represented as a function of the time is roughly of rectangular form. The magnitude of the voltage-drop is thus almost independent of the current intensity, and we will call it the running voltage E_B. The direction of the voltage-drop, however, suddenly reverses when the direction of the current is reserved. The instant after reversal the voltage-drop rises to a higher value E_D, which we will term the re-ignition voltage, as this voltage is necessary to re-ignite the lamp when it becomes extinguished each time after reversing the current. The voltage U_L at the series transformer is equal to the difference between U and U_E. It is therefore not sinusoidal but, as shown in the figure, has a fairly complex form. As the series transformer has an inductive resistance, the following relationship holds between the current intensity I and the voltage U_L:

$$U_L = L\frac{dI}{dt}.$$

This expression indicates in accordance with fig. 2 that the current attains its highest value when the voltage U_L changes sign. Only when this has occurred does the current commence to drop. It is thus found that the current lags behind the feed voltage U, which was to be expected owing to the inductive character of the series transformer, although the currents in question here are not sinusoidal. When the current intensity becomes equal to zero, the voltage-source is already furnishing an appreciable reverse voltage. The magnitude of the re-ignition voltage E_D now determines whether this reverse voltage is sufficient to re-ignite the lamp immediately in the opposite direction after it has been extinguished. This is definitely possible if the ignition voltage is sufficiently low, as in the case shown in fig. 2. But under certain working conditions the lamp remains dead for a finite period, the so-called dark pause, before the current changes direction and before the tension has again reached such a value that re-ignition of the discharge takes place. *Fig. 3* shows the calculated fluctuation of the voltages and the current intensity assuming a sinusoidal total voltage, a rectilinear voltage-drop at the lamp and a purely inductive resistance at the series transformer. The agreement with the oscillograms is very satisfactory.

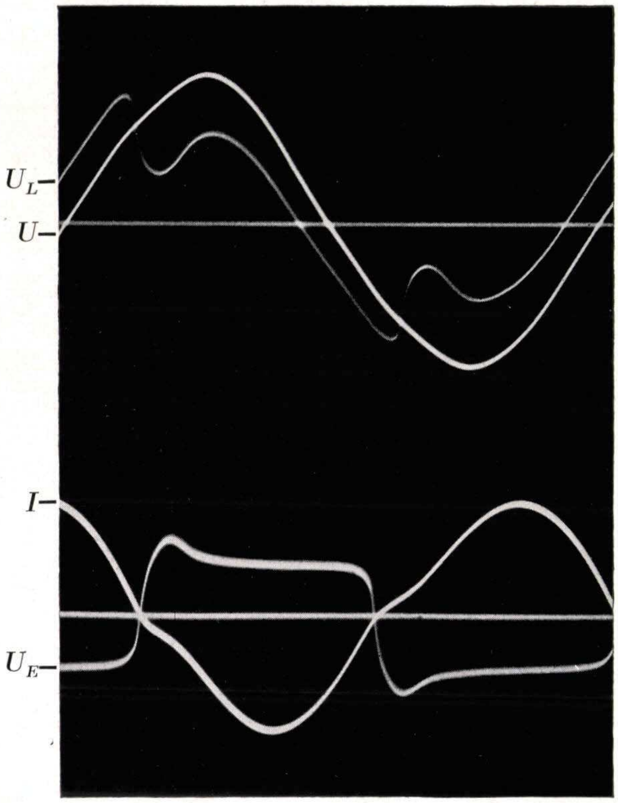

Fig. 2. Oscillograms of mercury vapour lamp HP 300 under normal running conditions. U_E = discharge voltage; U_L = voltage at series unit; U = total voltage; I = current intensity.

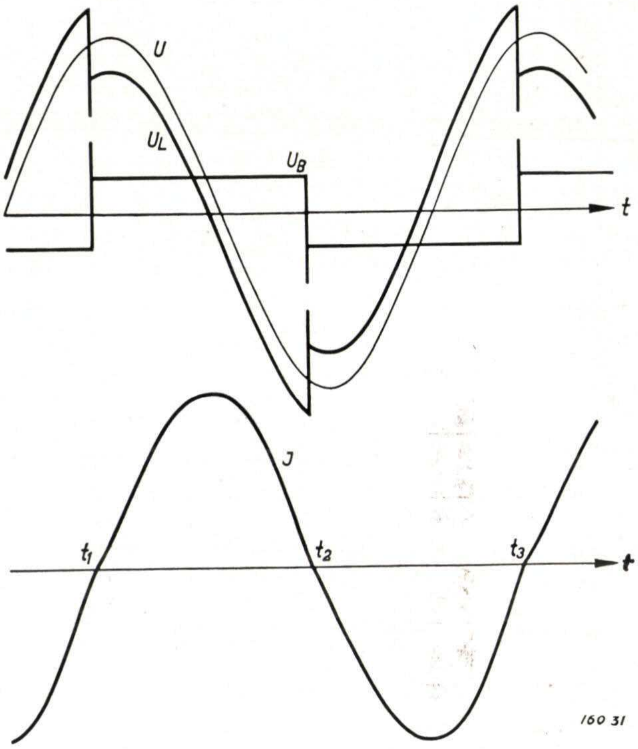

Fig. 3. Calculated current and voltages of the gas discharge and the series unit assuming simplified characteristics for the lamp. The concordance with the oscillograms is very satisfactory.

Shortness of the dark pause is not only advantageous from considerations of better illumination (less flickering) but also enables the lamp to be run with the minimum feed voltages. The re-ignition voltage E_D is indeed not constant but increases during the dark pause, and as a result the running of a lamp with a resistance in series requires higher peak voltages than when using chokes in series.

Heating-up and Stability

The voltage-drop E_B and the power output W of the mercury-vapour discharge both increase with the vapour pressure. If W is represented as a function of E_B, nearly a straight line as shown in *fig. 4* is obtained for the HP 300 mercury lamp. The curves N_1, N_2 and N_3 give the inputs of the lamp fed through the series unit, also as a function of the voltage drop, for an opencircuit voltage U

of 410 volts$_{\text{eff}}$ and various settings of the leak transformer. Expressed as a function of the voltage-drop the power input has a maximum value. This may be readily understood, for at $E_B = 0$ the voltage-drop disappears and at $E_B = 580$ the current disappears. Actually the curve already breaks off at $E_B = 350$ volts, as the re-ignition voltage then exceeds the maximum open circuit voltage (580 V).

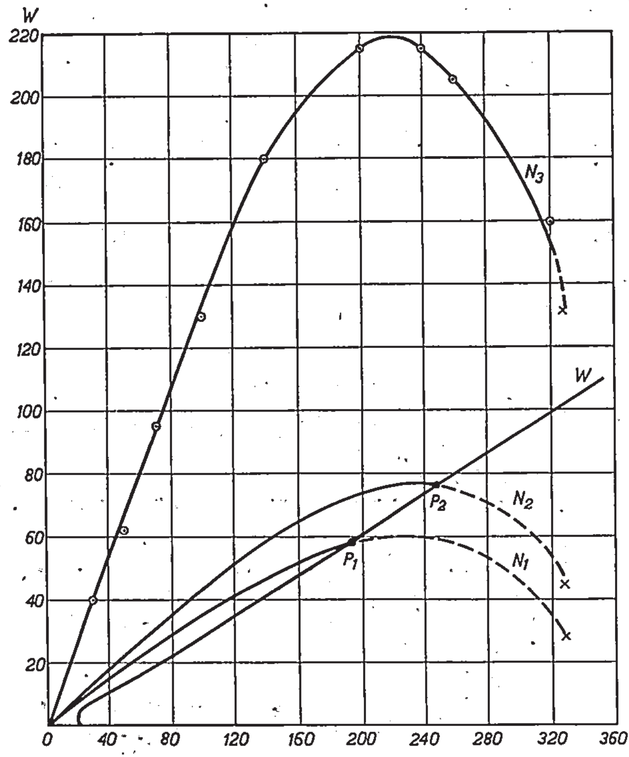

Fig. 4. The power output W of the mercury lamp HP 300 plotted as a function of the voltage-drop E_B under normal cooling conditions. The curves N_1, N_2 and N_3 show the inputs of the lamp with a total voltage of 410 volts$_{\text{eff}}$ and various settings of the leak transformer. The points P_1 and P_2 correspond to stable working states of the lamp. If the energy input is that corresponding to the top curve N_3 no stable working point is obtained. The lamp becomes heated and goes out as soon as the re-ignition voltage rises above the maximum voltage applied to the lamp.

On switching on the cold lamp, the input power N is initially greater than the total output W. As a result the lamp heats up, whereupon its voltage-drop E_B, and hence also the power output W according to fig. 4 increases. The input power expressed as a function of E_B is represented by the curve N_2 for a load slightly higher than normal. In this case the heating-up stage terminates at $E_B = 250$ volts in the stationary working state P_2, in which the energy input N_2 and the radiation emitted W are equal.

Consider now the heating-stage curve N_3 which was obtained with a lamp running on a heavy overload. The output in this case too follows the curve W. As the input of energy is always in excess, the temperature as well as the re-ignition voltage rises until (at $E_B = 350$ volts) the maximum feed voltage is insufficient to ignite the lamp. The discharge is then extinguished, the temperature drops, the lamp is re-ignited after the elapse of a short interval and so on.

When the lamp is running on a subnormal load (heating-stage curve N_1) no abnormal behaviour is observed. The difference between the heat input N_1 and the output W is, however, very small as shown in the diagram, so that the time taken to reach the stationary state on reducing the power input increases very considerably. Moreover, owing to the small angle between the curves N_1 and W the position of the working point P_1 (stationary state) is very susceptible to slight displacement of these curves, i.e. small changes in the working conditions.

Under certain operating conditions (intense cooling and subnormal load), it may even happen that a lamp will not become heated to the normal working state. Such a case is shown in *fig. 5*. The stationary working point is P with a voltage E_B,

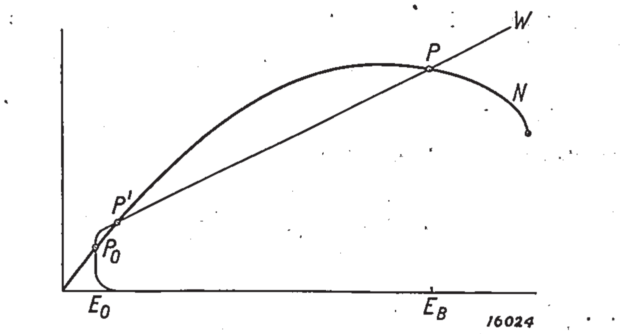

Fig. 5. The same as fig. 4, but with abnormally high cooling and insufficient energy input (diagrammatic). The stable working point P is not attained, as the input N and the output W are already in equilibrium at the point P_0.

but this working level is not attained. During heating, the lamp does not get beyond the first point of intersection P_0 of the curves N and W, so that at the very low running voltage E_0 it remains at the stage corresponding to a low-pressure discharge. To get it into a proper working condition, the vapour pressure must be raised by suitable means, e.g. by external heating, to such a level that the running voltage rises above the second point of intersection P' of the curves W and N. In this case the input energy will again exceed the output energy, so that the lamp will continue to heat itself and tend to attain its stable end state.

It can thus be generally concluded that the normal load of the lamp is fixed within certain limits. With a subnormal load the temperature rises too slowly, whilst with a very heavy overload no stable working point is obtained. The mean heating curve is obtained when using the leak transformer 5450 G/86 for an output of 75 watts in the end state. The curves in *fig. 6* show the heating process as a function of the time.

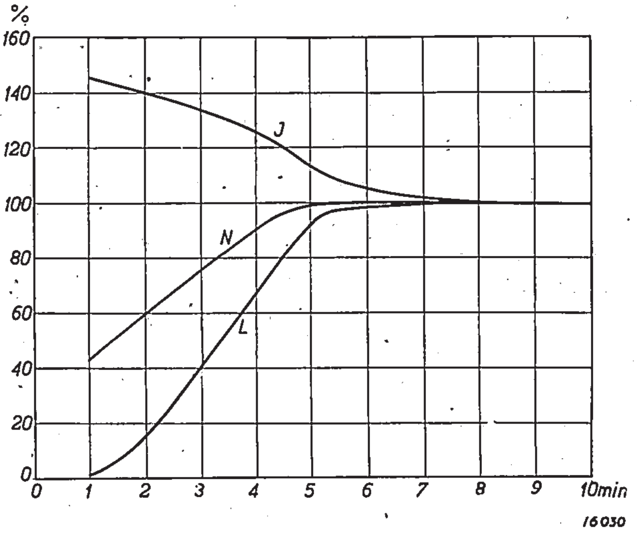

Fig. 6. Current intensity I, power N and luminous flux L of the mercury lamp HP 300 expressed in percentages of their end values and plotted as a function of the time after switching on. After the elapse of about 5 minutes the lamp gives about 90 per cent of its total luminous flux.

Illumination Characteristics

The luminous flux of the new mercury vapour lamp on a normal load is 3000 lumens. As the current-limiting unit itself absorbs about 15 watts, the light yield is 33 lumens per watt [1]). The spatial distribution of the light emitted by a lamp suspended vertically and with an opal globe is shown in *fig.* 7. A detailed discussion of the spectrum of the mercury-vapour discharge has already been published in a previous issue of Philips techn. Rev. (**1**, 5, 1936), where it was indicated that the distribution of spectral intensity was determined by the vapour pressure of the mercury. In general it may be assumed that the higher the vapour pressure the richer will be the spectrum in long-wave (red and infra-red) radiation, and hence the stronger will the ultra-violet lines be absorbed by the vapour. In addition the lines are broadened to an increasing extent and a continuous background appears between the lines especially in the visible region. *Fig. 8* shows the intensity distribution of the new mercury-vapour lamp in the visible spectrum. The figures at the peaks of the curves indicate the percentage contribution of the corresponding lines to the total luminous flux. As could be expected, this lamp already has a definite continuous background as well as an appreciable proportion of red light. Nevertheless the spectral distribution still deviates very considerably from that of daylight and the light given by incandescent lamps.

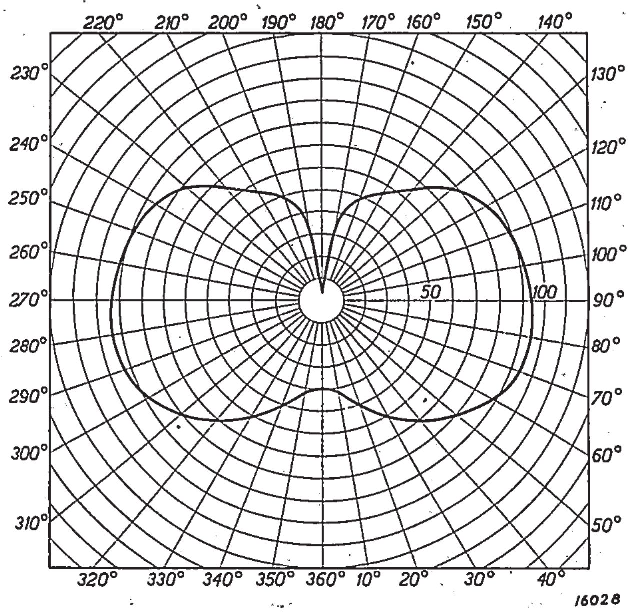

Fig. 7. Spatial distribution of the luminous flux of the new mercury lamp with opal globe.

To obtain a convenient survey of the spectral distribution the scale of wave-lengths has been subdivided in *table II* into four ranges, these ranges being of such extent that they contribute equal proportions of luminous flux in the case of a spectrum of constant intensity in the wave-length scale (so-called equal energy spectrum). As indicated by table II, solar radiation is distributed almost uniformly over the different ranges selected. The

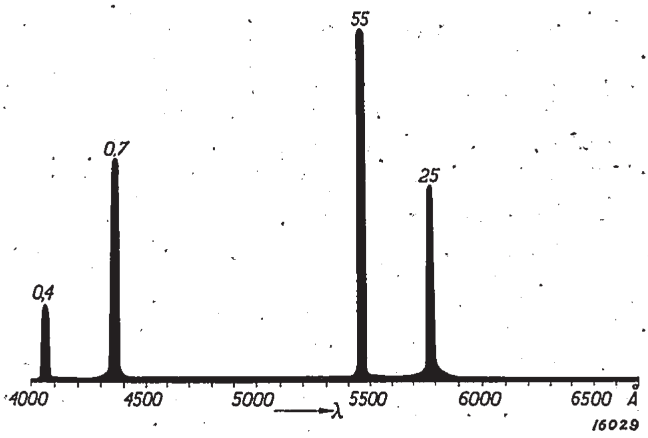

Fig. 8. Intensity distribution of the radiation of the new mercury lamp in the visible spectrum. The figures at the peaks of the intensity curve represent the percentage contribution of the respective spectral lines to the total luminous flux.

---

[1]) With the same power, the efficiency of an incandescent lamp is approximately 13 lumens/watt.

TABLE II. Distribution of luminous flux of various light-sources over four spectral ranges of visible light expressed as a percentage of the total light output.

Range of wave-lengths Å	Equal energy spectrum	Sun	Incand. lamp	Mercury vapour lamp HP 300	Mixed light. G and H denote the luminous flux of the incand. lamp and the mercury vapour lamp resp.	
					$G/H = 1/1$	$G/H = 2/1$
	%	%	%	%	%	%
4000—5300	25	26	14	8	10	12
5300—5580	25	26	22	58	40	34
5580—5880	25	25	28	31	30	29
5880—7000	25	23	36	3	20	25

incandescent lamp contains a higher proportion of long-wave radiation and a less proportion of short-wave. The mercury-vapour discharge is made up mainly of yellow and green light. The blue lines, owing to their very short wave-length (4358 Å and 4047 Å), contribute only very little to the total luminous flux. Although long-wave radiation ($\lambda =$ above 5880 Å) is indeed present as a continuous background it is by no means sufficient to produce a natural impression.

Control of the Spectral Composition of the Light

Experiments have shown that the impression given by coloured surfaces on illumination with mercury vapour lamps can be considerably improved by the admixture of red radiation. This may be done in various ways, e.g. the use of red-fluorescing reflectors or the addition of light from incandescent lamps, which as we have seen has an excess of red radiation as compared with daylight. In order to give a numerical instance of the degree of adaptation, two cases of mixed illumination are included in Table II. Favourable adaptation appears to be obtained when about $^{2}/_{3}$ of the light is furnished by incandescent lamps and $^{1}/_{3}$ by the mercury vapour lamp. In this case the proportions of yellow and red radiation compare favourably with those of sunlight, although there is an excess of green and a corresponding lack of blue radiation. Perfect adaptation to the spectral intensity distribution of sunlight can naturally not be achieved and is possibly not desirable at all. It is indeed, quite probable that the eye requires a different distribution of spectral intensity with artificial light than with daylight owing to the necessarily lower brightness. The best mixture of glowlamplight and mercury vapour light can therefore only be determined by experiment.

Compiled by G. HELLER.

THE SOUND RECORDER OF THE PHILIPS-MILLER SYSTEM

by A. TH. VAN URK.

Summary. In this article the connection between the resonance frequency and the attainable amplitude is discussed for various constructions. It is shown that the attainable amplitudes are very small in all cases (of the order of 0.1 mm) and only by a marked magnification of the amplitude by means of the special shape of the cutter can a sound track of normal width (1,8 mm) be recorded. The magnetic driving system finally evolved and its operating characteristics are discussed in detail.

In the previous issue of this Review the basic principle of the Philips-Miller system of sound recording was described and a comparison made with those methods in use hitherto [1]). Attention was called to certain difficulties which had to be overcome at the outset in developing the new method. In particular it was indicated that the construction of the apparatus for recording sound by mechanical means, i.e. the sound recorder, constituted the nucleus of the method.

The fundamental principle of the method is as follows. Under a stylus or cutter S a tape is displaced which is composed of a celluloid base C covered with a simple transparent layer of gelatine G which is itself coated with a very thin opaque coating D (*fig. 1*). The cutter is a wide-angled wedge as shown in fig. 1. On its displacement in response to the sound vibrations, this cutter moves in a direction perpendicular to the tape and cuts a strip of varying width out of the top coating of the film, thus giving a transparent sound-track on an opaque background. The sound-track, produced mechanically in this way is used for sound reproduction by optical means.

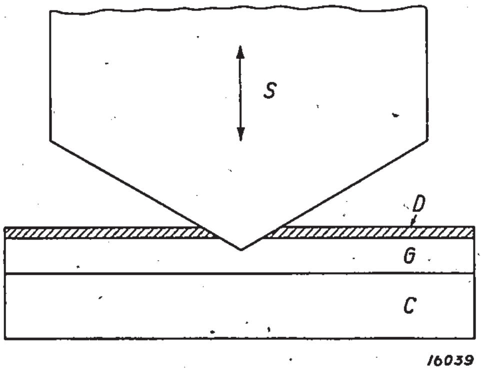

Fig. 1. Principle of the Philips-Miller system. S = Wedge-shaped cutter. C = Celluloid base G = Transparent gelatine surface. D = Opaque coating of "Philimil" strip on which the sound-track is produced.

It was pointed out earlier that by combining mechanical recording with optical reproduction a number of important advantages are obtained. The method had, however, one difficulty, viz, that in order to produce an equivalent sound amplitude, the amplitude to be recorded must be much greater at high frequencies than in older systems of mechanical recording (gramophone discs). The mechanical vibrating system, composed of the driving system of the cutter, must have a very high resonance frequency in order to obtain an amplitude independent of the frequency in the frequency range embracing musical sounds [2]).

This condition cannot be combined with a large amplitude [3]). By the wedgeshaped form with the obtuse angle of about 174° of the cutter adopted by Miller and the magnification of 40 obtained thereby, it has been possible to work with a cutter amplitude of 25 μ. Yet even this apparently minute amplitude is just at the practical limit — at the high resonance frequency in question [4]).

Amplitude and Natural Frequency of the Sound Recorder

If the sound recorder is designed with a high natural frequency the vibrating system becomes comparatively insensitive; it responds only with small amplitudes and powerful driving forces must be provided in order to obtain an adequate amplitude. The actual increase in these forces is however limited by the permissible stresses which can be applied to the material. It is important to note that this limit is independent of the dimensions of the sound recorder and is determined solely by the mechanical properties of the material. This may readily be seen from a simple example, as shown below:

---

[1]) R. Vermeulen: The Philips-Miller System of Sound Recording, Philips techn. Rev. 1, 107, 1936.

[2]) Philips techn. Rev. 1, 107-114, 1936. See here equation (1) and fig. 10 on p. 112.

[3]) The maximum amplitude of the sound track has been standardised to 1·8 mm. (Here and elsewhere in the computations 2 mm are adopted for the reason of simplicity).

[4]) For comparison it may be mentioned that the diaphragm of a powerful loudspeaker oscillates with an amplitude of some tenths of a μ at the highest frequencies.

Consider the case of a rod of circular section which is firmly secured at one end (*fig. 2*). The minimum natural frequency n of the transverse vibrations is:

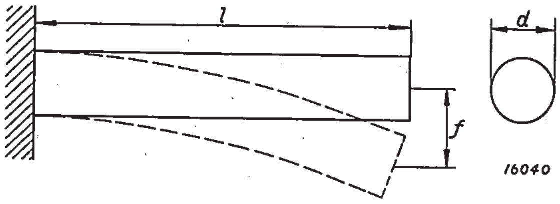

Fig. 2. Bar of circular section clamped at one end to form a simple mechanical oscillating system. Length of bar l, sectional diameter d, flexure f.

$$n = 0.140\ d\ c/l^2, \quad \dots\dots \quad (1)$$

where d and l are the dimensions of the rod as shown in fig. 2 and c is the velocity of sound through the material of the rod. On the other hand the amplitude f of the end of the rod with an oscillation corresponding to the lowest natural frequency is:

$$f = {}^2/_3 \cdot \frac{\sigma_{max}}{E} \cdot \frac{l^2}{d}, \quad \dots\dots \quad (2)$$

where E is the modulus of elasticity and σ_{max} the maximum stress in the rod. Multiplying these two equations together, we get

$$nf = 0{,}0935\ \sigma_{max}\ c/E \quad \dots\dots \quad (3)$$

The dimensions of the rod l and d are now no longer contained in this expression. The same result could also be deduced for other types of vibrating systems. If we substitute in (3) the values for iron $c = 5.10^5$ cm. per sec and $E = 2.10^6$ kg per sq cm, and put $f = 25\mu$ and $\sigma_{max} = 1300$ kg per sq. cm (i.e. approx. the maximum stress), we get

$$n = 12000 \text{ cycles/sec}$$

We thus see that the limiting natural frequency calculated in this way is still sufficiently above the audio-frequencies.

Driving System

For a given natural frequency of the recorder, the attainable amplitude is limited not only by the proportionality limit of the material, but also by the forces available for driving the mechanical vibrating system. There are in the main two types of drive which can be employed, viz, the electrodynamic and the electromagnetic. In the electrodynamic drive a coil through which a fluctuating current I (in amperes) flows is situated in a constant magnetic field H (see *fig. 3*). A force $0.1 \cdot H \cdot l \cdot I$ then acts on the coil, where l is the length of wire on the coil. If furthermore its mass is m and it is so fixed that the resonance frequency is $\omega/2\pi$, the amplitude of the coil will be:

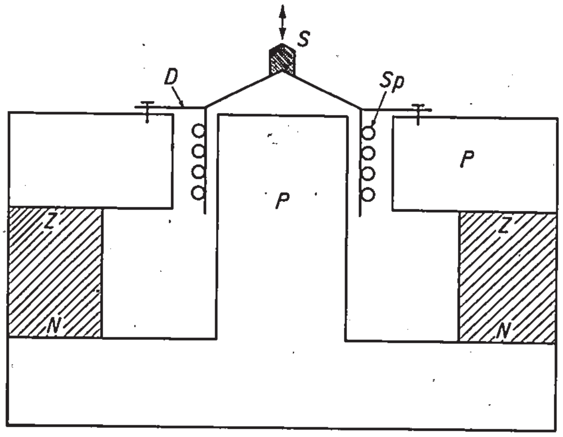

Fig. 3. Electrodynamic drive. Coil S_p, through which the microphone currents pass, moves between the pole-pieces P in the permanent magnetic field generated by the magnets ZN. The coil is represented as held in position by a flat spring D. The cutter must be attached at S, motion being in the direction of the double arrow.

$$a = \frac{0.1\ H l I}{m\ \omega^2} \quad \dots\dots \quad (4)$$

Introducing the cross-sectional area q and the density ϱ of the coil wire, as well as the current density i, we can substitute $I = iq$ and $m = lq\varrho$ [5]), and thus obtain for the amplitude of the coil the expression:

$$a = 0.1\ \frac{H\,i}{\varrho\,\omega^2} \quad \dots\dots \quad (5)$$

Again all dimensions of the system are absent in the result. To obtain a great amplitude at the given resonance frequency $\omega/2\pi$, H and i must be made large and ϱ made small. In practice the maximum values which can be obtained are: a field strength H of 15000 gauss, a maximum current density i of 10 A per sq.mm and a minimum density ϱ of 3 gr. per cub. cm. (alumnnium). With the very low resonance frequency of 3500 cycles ($\omega = 2\,\pi \cdot 3500$) one computes from (5) that the attainable amplitude is $a = 10\ \mu$, which is insufficient for a full modulation of the sound track. Further progress cannot be made in this direction as a limit is set by the properties of the material.

---

[5]) The small mass of the body of the coil has been neglected here.

For this reason the electromagnetic driving system has been preferred, as shown diagrammatically in *fig. 4*. Contrary to an electromagnetic system the attainable amplitude with the electromagnetic system is determined by the dimensions of the system. The amplitude is found to be:

$$a = k \frac{H_o \, \Delta H}{\varrho \, \omega^2} \quad . \; . \; . \; . \; . \; . \quad (6)$$

where ΔH is the alternating field in the armature A and H_o the field in the air gap L due to the permanent magnet P; k is a factor of the dimension of a reciprocal length and is inversely proportional to the dimensions of the system. By reducing the size of the recorder its amplitude can be increased, although there is an upper limit to this increase due, inter alia, to the fact that the air gap L must remain appreciably larger than the amplitude a of the vibrating armature. At a resonance frequency of approx. 5000 cycles, an amplitude of about 30μ was cut with the driving system shown in *fig. 5*.

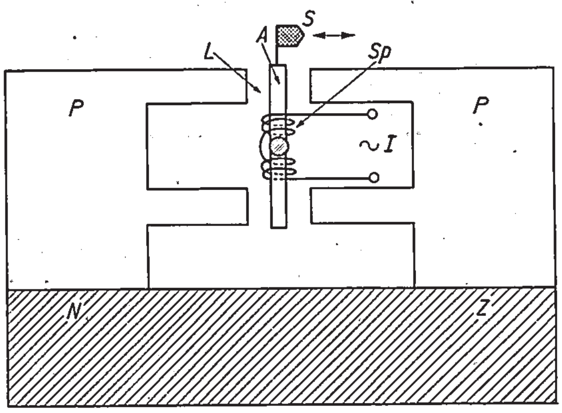

Fig. 4. Electromagnetic drive. The armature A which is energised by the coil Sp (microphone current I) moves in the air gap L between the pole-pieces P. The cutter is attached at S and moves in the direction of the double arrow.

Description of the Sound Recorder

The interior of the sound recorder is shown diagrammatically in *fig. 6*. *Fig. 7* shows the armature component separately. The armature is connected with the two clamping plates *Pl* by a pair of short bridge stays *T* which provide a torsion axis. In designing the sound recorder, the first requirement to be met was that air gap (*L* in fig. 4), in which the armature moves, must be made large compared with the armature amplitude, as otherwise the dispacement of the armature would not be proportional to the force. On the other hand the air gap must be kept small in order that the magnetic resistance of the magnetic circuit does not become too large. The air gap is only 0.12 mm, accurate adjustment to this value being obtained in the following way. The armature is made in one piece with the clamping plates *Pl* and the torsion stays, and is ground quite flat. Similarly the upper pole-piece together with the top part of the brass frame *R* in which it is countersunk, and the lower pole-piece with the lower section of the frame are also ground flat on the front surfaces. When clamping the armature thin spacing sheets *Zb* (figs. 6), exactly 0.12 mm in thickness, are inserted between the end surfaces of the frame and the clamping plates *Pl*. This arrangement gives the required dimension for the air gap between the pole-pieces and the armature. The

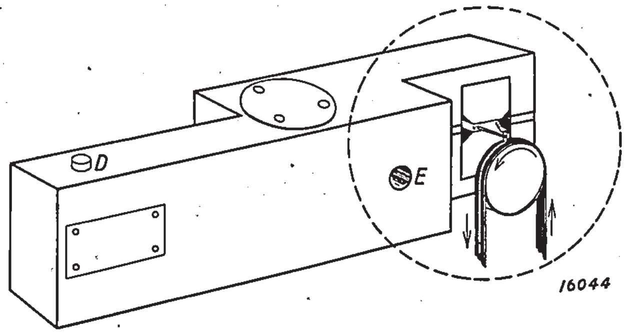

Fig. 5. Diagrammatic sketch of the sound recorder. To regulate the depth of the track in the film, the sound recorder can be turned about the axis E by means of the adjustable stop D. The part enclosed in the dotted circle is reproduced on an enlarged scale in fig. 6.

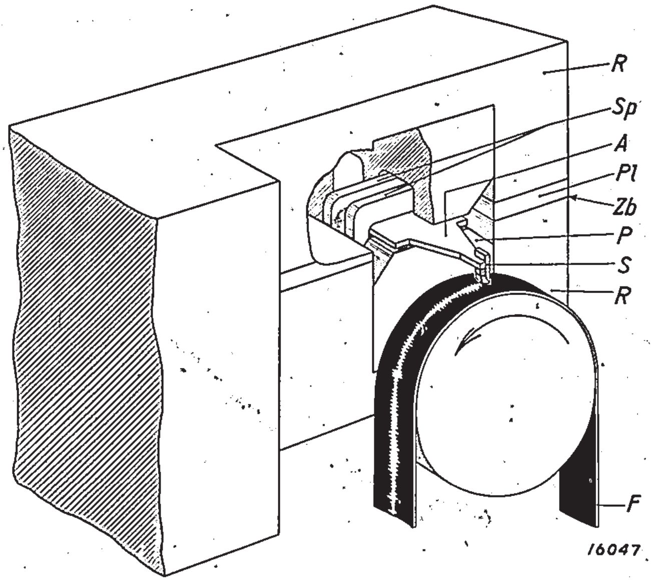

Fig. 6. View of the interior of the driving system, showing the pole-pieces P (Z = south pole, N = north pole) countersunk in the brass frame R, between which the armature A oscillates. The energising coils Sp enclose the armature A which is clamped between the upper and lower halves of the frame by means of the clamping plates Pl, the spacing plates Zb serving for accurately adjusting the required air gap between A and P. To a lug on the armature A is attached the cutter S which engraves the sound-track in the film F when the latter moves in the direction of the arrow.

marked torsional rigidity of the short stays with which the armature is secured in position, provides the necessary powerful controlling force and hence the high resonance frequency of the armature vibrations frequently referred to above.

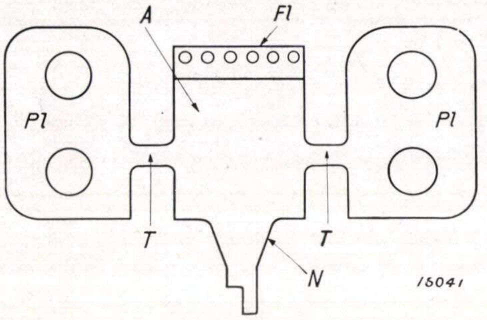

Fig. 7. The flat armature component consists of the armature proper *A*, the links *T* providing a torsion axis, and the clamping plates *Pl*. The armature is provided with a lug *N* for attaching the cutter and a vane *Fl* for providing additional damping, see page 141.

To obtain the high field-strengths H_0 and ΔH which are required here (equation (6)), provision must be made for a low magnetic resistance in the iron circuit, in addition to a small air gap. The pole-pieces have therefore been given a large section and are made of a nickel-iron alloy, a material with a high permeability and a high magnetic saturation. The electrical conductivity of this material is small so that eddy current and hysteresis losses are slight. In view of the limited mechanical strength of this alloy it was, however, not suitable for the armature. This is made of a silicon-iron (4 percent Si) having practically the same magnetic and electrical properties as the nickel-iron alloy; it is, however, very much harder and more brittle. The brittleness is here not a disturbing factor as the armature unit requires only very simple machining and finishing. In *fig. 8* the sound recorder is depicted, mounted on the desk of the recording machine.

Frequency Characteristics of the Sound Recorder

Determination of the frequency characteristic of the sound recorder in the no-load condition, i.e. without the cutter making a trace on the film, gives a resonance curve of the type shown in the family of resonance curves in fig. 10 on page 112 of the previous issue of this Review, which relate to a simple mechanical vibrating system. This characteristic is reproduced in *fig. 9*, curve *A*.

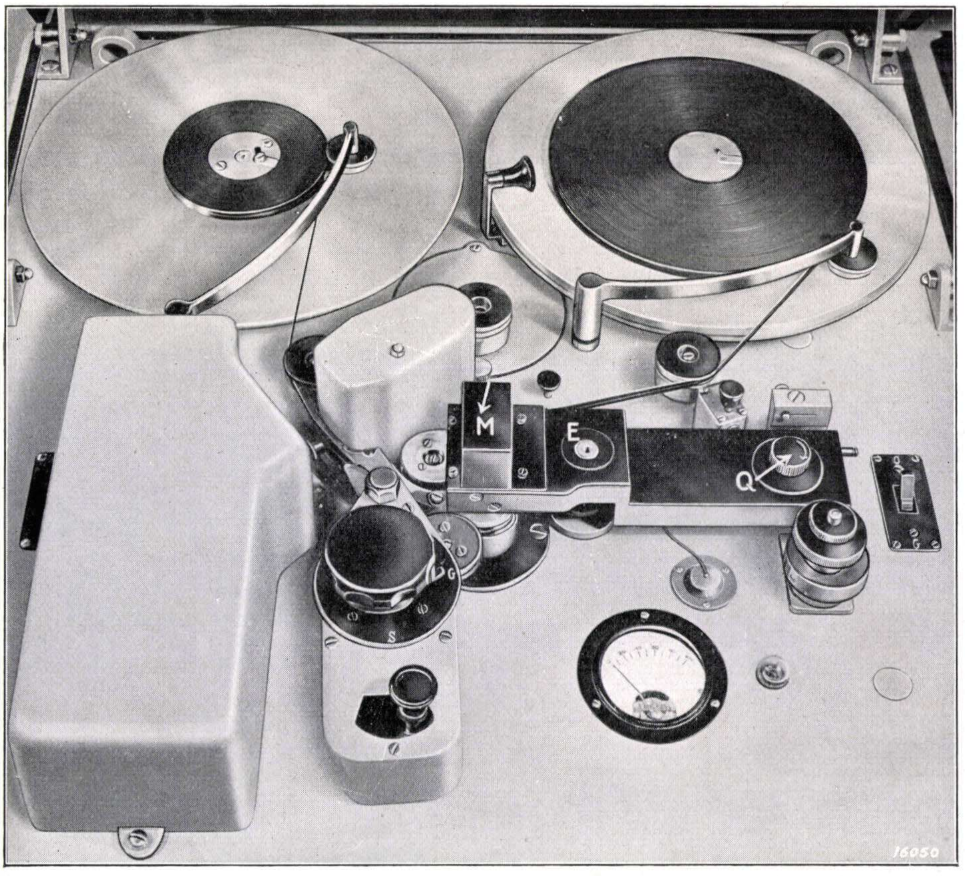

Fig. 8. The sound recorder mounted on the desk of the recording machine. By means of the micrometer screw *Q* which displaces a stop (not visible here, see *D* in fig. 5) the whole recording unit can be turned about the pin *E* for adjusting the depth of tracing of the cutter.

On graphing the corresponding characteristic for the sound recorder on load[6], i.e. during the tracing of the sound-track, the shape and the absolute height of the resonance curve are found to be altered (fig. 9, curve *B*). The flattening of the resonance peak is due to the damping action exercised by the film on the vibratuon of the armature. At the same time there is also a lateral displacement in the position of the resonance maximum which is due to the fact that the film not only applies a damping force (which only absorbs energy) to the cutter, but as already mentioned also has an elastic force which increases the directional force of the whole vibrating system. As a result there is an increase in the resonance frequency. In addition the sensitivity of the system is reduced, which tends to lower the position of the whole curve. By appropriately dimensioning the clamping arrangements of the armature, the potential increase in the resonance frequency has already been taken into consideration; when running freely the resonance frequency is at about 3500 cycles/sec, being increased during normal operation by the directional force caused by the film to about 5000 cycles (cf. curves *A* and *B* in fig. 9). The drop in the characteristic curve in the range between 100 and 1000 cycles/sec is due to the iron losses which increase with the frequency.

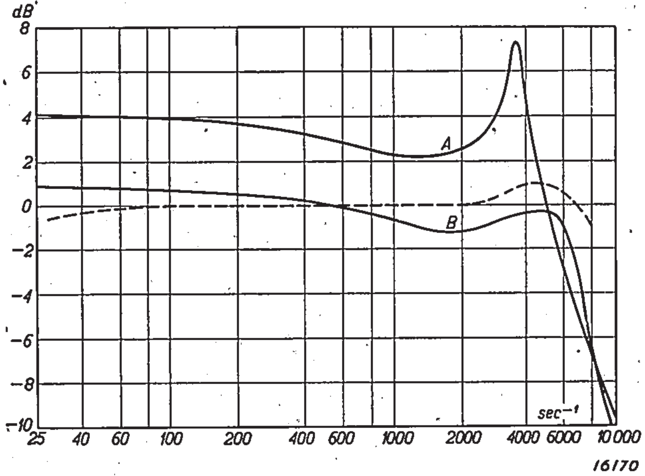

Fig. 9. Frequency characteristics of the sound recorder: *A* in the no load condition with the cutter oscillating freely, the resonance point is here about 3500 cycles; *B* during normal running with the cutter engraving a sound-track, where, owing to the additinal directional force due to the film, the resonance point has been displaced to about 5000 cycles and the sensitivity of the system, i.e. the amplitude at an equivalent energising current has dropped by about 3 dB (3 decibels corresponding to a factor $10^{0.3} = 2$); the damping due to the film has here caused a marked flattening of the resonance peak. The deviations from the horizontal still present in curve *B* are eventually largely compensated by choosing a suitable characteristic for the amplifier. The dotted curve *C* shows the frequency characteristic of the whole apparatus used for sound recording and reproduction.

Possible Causes of Distortion

In the reproduction of music the principal aim is to reproduce the mixture of component sound vibrations without any distortion. To achieve this the intensity ratio of all component notes must be maintained, in other words the frequency characteristic for the whole apparatus must be as closely horizontal as possible. Slight deviations from the horizontal are not very disturbing, and only appreciable differences actually become apparent as variations in timbre. Moreover, such deviations of the frequency characteristic from the horizontal which occur in one part of the apparatus, e. g. in the sound recorder as in curve *B* of fig. 9, can be readily compensated in other parts of the apparatus, e.g. in the valve amplifier. Thus the broken curve *C* in fig. 9 which represents the frequency characteristic of the whole sound-recording and reproducing apparatus is almost horizontal.

In addition to variations in timbre, a further type of distortion is that due to the formation of new notes with frequencies which were not originally present in the incoming sound vibrations. This form of distortion makes its appearance when the output amplitude (for each individual frequency) is not absolutely proportional to the input amplitude; it is therefore termed "non-linear distortion".

Thus, in the case of the sound recorder, the recorded amplitude A must be proportional to the intensity of the energising current I in the armature coil, i.e. $A = f(I)$ must be a linear function. If this is not the case, and if the function contains for instance a quadratic term, on substituting for I a vibration $I_0 \sin \omega t$ we get $f(I)$ containing an extra term $\sin^2 \omega t$, i.e. a term $\cos 2 \omega t$[7]. Hence A contains in addition to the initial frequency ω also a second harmonic 2ω. If the deviation of function $f(I)$ from linearity is still more marked, a whole series of harmonics of each individual note in the frequency mixture of the incoming musical vibrations can occur. If, furthermore, we substitute for I the sum of several sinusoidal vibrations (which corresponds to the case occurring in practice), e.g. $I_1 \cdot \sin \omega_1 t + I_2 \cdot \sin \omega_2 t$, A will contain, among others, also a term of frequency ($\omega_1 - \omega_2$) and another of frequency ($\omega_1 + \omega_2$). In addition to the harmonics (overtones) already referred to, summation and differential tones are thus also obtained. These contribute a sound which stands, in view of harmonics, entirely apart from the original music to be recorded and hence may considerably harm the music when reproduced.

---

[6] In measurements made to obtain these characteristics a constant current with a continuously increased frequency is passed through the energising coil of the sound recorder and the cutter allowed to trace the corresponding track. Measurement of the amplitudes of this sound-track by means of a microscope gives the characteristic directly (amplitude as a function of the frequency). The sound recorder thus traces its own characteristic on the film.

[7] Since $\sin^2 a = {}^1/_2 \, (1 - \cos 2 a)$.

A "non-linear" distortion is thus more disturbing to the ear than a distortion due to the frequency characteristic not being quite horizontal (variation in timbre alone, see above). Moreover, it is practically impossible to compensate a non-linear amplitude characteristic of one component of the transmission circuit in one of the succeeding components, such as can be done with a non-horizontal frequency curve. It is essential, therefore, that every trace of non-linearity is as far as possible eliminated in each component separately.

Various causes might be thought of in the Philips-Miller sound recorder, for a deviation from the linear relationship between the recorded amplitude and the energising current. In the main, three points require consideration. Firstly, such deviation may be caused by the magnetic conditions. In order to make the amplitude a of the armature proportional to the energising current I, the alternating field ΔH generated by I in the air gap must, as follows from equation (6), be proportional to I. But the connection between the intensity of this alternating field in the air gap and the energising current is determined by the whole magnetic circuit, which is composed of the air gap and the iron components. In a magnetic circuit through air alone the required proportionality would always be maintained, as air has a constant permeability or, in other words, a constant magnetic resistance to the passage of the magnetic flux. In iron, however, this magnetic resistance is well known not to be constant; it depends on the field strength, so that in a magnetic circuit through iron alone the connection between the alternating field and the energising current will deviate more or less from linearity according to which part of the magnetisation curve is under consideration. As the magnetic resistance of the circuit as a whole is arrived at by compounding the "linear" resistance in the air gap and the "non-linear" resistance in the iron, it is evident that the required linearity can be approached by making the magnetic resistance of the iron component small compared with the resistance in the air gap. This is achieved by selecting a type of iron with a high alternating-current permeability [8]) and by making the iron component of ample cross-section, particularly the pole-pieces. To ensure high permeability through the iron it is naturally necessary to work sufficiently below the saturation range on the magnetisation curve, i.e. with field strengths at which the permeability is still very large.

A second possible cause of non-linear distortion is that the various parts of the mechanical vibrating system subject to torsion and transverse bending may, during vibration, become deformed beyond the limit of proportionality. As this is most liable to occur at sharp corners and edges where the stresses may attain high peak values, all edges and corners (particularly on the torsion axis and clamping units of the armature) have been carefully rounded off. Experimental tests by loading the armature with weights (up to 2 kg) and measuring with the microscope the bending produced, have shown that Hooke's law is satisfied within reasonable limits up to the highest forces which may occur in practice.

Finally, non-linear distortion may also be produced by the damping due to the film not being linear, i.e. the resistance applied by the film is not strictly proportional to the velocity of the cutter [9]). There were indeed certain indications that a slight distortion during recording was actually due to this cause, since it was found on recording a vibration with a frequency of a half or a third of the resonance frequency that a suggestion of the latter was also present in the recorded track. Thus, up to a point the second and third harmonics of the oscillations to be recorded were also generated in the sound recorder (as already pointed out, this is in fact the nature of a non-linear distortion). To eliminate this undesirable effect of non-linear damping due to the film, the vibrating system was given an additional (linear) damping, so that the damping due to the film constituted only a fraction of the total damping, and its non-linearity no longer had a disturbing effect. The extra damping was applied by providing the armature with a type of vane (*Fl*) on the side opposite to the lug, this vane during oscillation of the armature moving in a plastic medium (R). The arrangement of the vane and the damping medium in the chamber formed by the pole-pieces and the magnet block is shown in *fig. 10*; to increase the adhesion between the damping medium and the vane the latter is given a number of perforations.

---

[8]) In the case of the nickel-iron alloy chosen, μ is > 600 when the induction in the iron (pole-pieces), which is numerically roughly equal to the field strength in the air gap, (dispersion not being taken into account), is about 10000.

[9]) E. g. it might also depend on the depth of the track.

Fig. 11 shows the relationship between the current intensity I in milliamperes (at a frequency of 200 cycles) in the armature coil (1200 turns) and the amplitude a in millimetres, which the sound recorder traces at different current intensities on the "Philimil" strip.

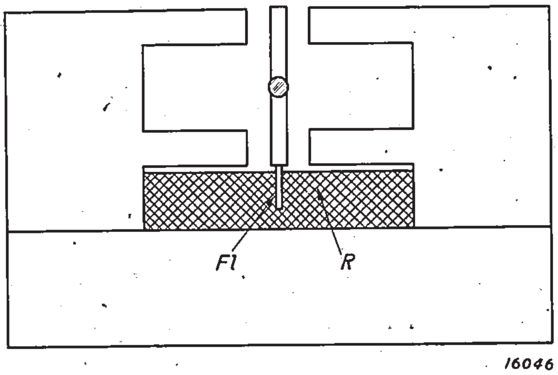

Fig. 10. Application of additional damping force to reduce the effect of a non-linear damping due to the resistance produced by the film. To the armature a vane Fl (see also fig. 7) is attached moving in a demping medium R which has been specially evolved for this purpose and with which the chamber formed by the pole-pieces and the magnet is filled.

It is seen that by adopting the various measures described, viz, reducing the share of the iron in the total resistance of the magnetic circuit, avoiding peak stresses in components exposed to torsion, and reducing the effect of non-linear damping due to the film, true linear recording of the sound waves is obtained.

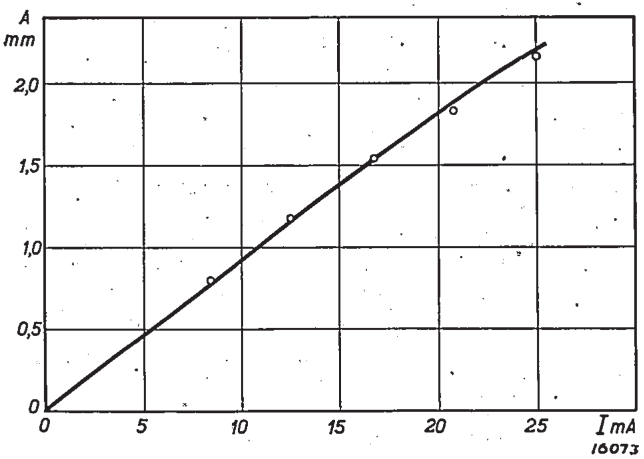

Fig. 11. Relationship between the amplitude A (in mm) traced by the sound recorder and the current intensity I (in milliamps) through the energising coil at a frequency of 200 cycles/sec. This line is nearly a straight line, thus, the required proportionality is satisfactorily fulfilled.

THE DEFINITIONS OF BRIGHTNESS AND APPARENT BRIGHTNESS AND THEIR IMPORTANCE IN ROAD LIGHTING AND PHOTOMETRY

By P. J. BOUMA.

Summary. In illumination technology brightness is defined as the magnitude $H = C \int E(\lambda)\, V(\lambda)\, d\lambda$, where C is a constant, $E(\lambda)$ the relative spectral distribution and $V(\lambda)$ the international standard visibility curve. In the investigation of various problems in physiological optics and particularly problems relating to road lighting it has, however, been found necessary to introduce another quantity, the so-called apparent brightness h, which is more closely related to the sensation of brightness which the eye experiences. The apparent brightness h is defined as follows: If two surfaces appear to the eye to be "equally bright" we assume that they have the same h value. At high brightness levels (daylight) the two quantities are identical, but at low brightnesses (at the level of road lighting and lower) there are considerable differences between them. The significance of these differences in photometry, physiology and road lighting are briefly discussed.

In dealing with problems of road lighting, the concepts of brightness and apparent brightness are of paramount importance. It is therefore necessary to define these two quantities as accurately as possible, particularly as considerable misapprehension and contradiction in the literature relating to this subject exist due to the insufficient differentiation between these two terms.

What does direct experience teach us? If in the first place we limit ourselves to light of a specific spectral composition (i.e. of a specific colour), the eye can establish whether two surfaces which radiate this light are equally bright; if this is not the case we can state which of the two surfaces is the brighter. Direct observation cannot give us more information, and in particular the eye is unable to assign by mere inspection a quantitative ratio to two unequal sensations of brightness. We cannot say: "This surface is six times brighter than that one", although we can state: "This surface is brighter than that one". Experience further informs us that a particular surface is the brighter the more energy it emits of the type of light in question.

From this it follows that we can represent the "brightness" numerically, without contradicting our direct experience of the sensation of brightness, by a magnitude H which is proportional to the energy E which the surface radiates per second from each unit of surface and in each unit of solid angle, thus:

$$H = k\,E \quad \ldots\ldots\ldots \quad (1)$$

The constant k is as yet still quite arbitrary [1].

The matter becomes much more complicated when we have to compare the luminosities of two surfaces which radiate light of different spectral composition (different colour).

From measurements on the optical bench it can readily be established that the eye can determine without difficulty which of two surfaces with considerable differences in brightness is the brighter; if the photometer is adjusted in such a way that the difference in brightness is very small, comparison is rendered very difficult by the difference in colour. But after a little practice it is possible to adjust sufficiently accurately two surfaces with different colours to equivalent brightness values. Now what are the results on making such "heterochromatic" adjustments to obtain an equivalent brightness?

Restricting ourselves in the first place to the spectral colours and determining for the various wavelengths λ the energies $E(\lambda)$ which are required to obtain the same sensation of brightness, we find that the minimum amount of energy required for this purpose is for the yellowish green (5550 Å), whilst considerably more energy is required at the two ends of the spectrum. In other words the eye responds most sensitively to yellowish-green light; it is least sensitive to red, blue and violet, and is quite unresponsive to wavelengths outside the range between 3100 and 7600 Å. A good measure for ocular sensitivity or visibility can be assumed to be the ratio $1/E(\lambda)$, i.e. the reciprocal of the energy which must be utilised to obtain a specific sensation of brightness. Generally these magnitudes are multiplied by such a constant as will make the maximum value of the sensitivity of the eye exactly equal to unity. *Fig. 1* shows the ocular sensitivity $V(\lambda)$ obtained in this way, plotted as a function of λ. (Cf. curve A in fig. 6, Philips techn. Rev. **1**, 106, 1936.)

---

[1] Theoretically we could have equally well selected other definitions for the brightness, e.g. $H = k \log E$. Such definitions are frequently found in physiological and opthalmological literature. The advantages of the definition adopted by us (which is that in general technical use) are purely of a practical nature as the calculations are much simplified by it.

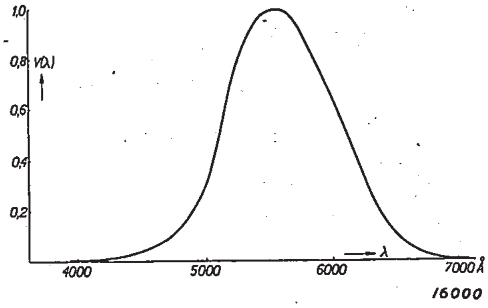

Fig. 1. The standard visibility or sensitivity curve of the eye. $V(\lambda)$ is, except for a constant factor, the reciprocal of the energy required at different wavelengths to produce an equal brightness.

The curve has now been determined for a specific sensation of brightness. If we repeat these measurements for other brightness levels a striking fact emerges, viz., that over a wide range of brightness values (which inter alia includes the whole range of daylight) the same curve is always obtained, in other words the visibility ratio of the eye is constant for various wavelenghts over a wide range of brightness. The visibility curve obtained for this range — which we shall term the standard visibility curve — has been determined with great accuracy by Gibson, Tyndall and others and has been taken as the international standard.

On this standard curve $V(\lambda)$ the definition for "brightness" is based on the following:

For a spectral colour of wavelength λ_0 the luminosity is

$$H = C\ V(\lambda_0)\ E(\lambda_0) \quad \ldots \quad (2a)$$

for composite colours made up of a number of spectral colours (line spectra, e.g. of gaseous discharge lamps):

$$H = C \sum_k V(\lambda_k)\ E(\lambda_k) \quad \ldots \quad (2b)$$

and for continuous spectra (sunlight, incandescent lamps):

$$H = C \int V(\lambda)\ E(\lambda)\ d\lambda \quad \ldots \quad (2c)$$

Here $E(\lambda_k)$ is the energy of wavelength λ_k which is radiated per second from unit surface and in unit solid angle in the direction of the eye, $E(\lambda)\ d\lambda$ the energy which is radiated in the range of wavelengths $\lambda \rightarrow \lambda + d\lambda$, and C is a universal constant whose magnitude depends only on the choice of unit for the brightness and for the energy.

The most common brightness units are the candle per sq. metre, the candle per sq. cm (stilb), apostilb, milli-lambert and the candle per sq. ft., which are inter-regulated as shown in the following table:

Table I

	candles per sq. metre	candles per sq. cm	apostilb	milli-lambert	candles per sq. ft.
1 candle per sq. metre =	1	10^{-4}	π	$\frac{\pi}{10}$	0.0929
1 candle per sq. cm =	10^4	1	$\pi.10^4$	$\pi.10^3$	929
1 apostilb =	$\frac{1}{\pi}$	$\frac{1}{\pi}10^{-4}$	1	1/10	0.0296
1 milli-lambert =	$\frac{10}{\pi}$	$\frac{10^{-3}}{\pi}$	10	1	0.296
1 candle per sq. ft. =	10.76	$1.076 \cdot 10^{-3}$	33.8	3.38	1

If H is expressed in candles per sq. cm and E in watts per sq. cm per unit solid angle, C becomes 621 (this figure is termed the mechanical equivalent of light, and represents the brightness of a surface which from each sq. cm of surface and in each unit of solid angle radiates in the direction of the eye 1 watt of monochromatic light with the wavelength of maximum visibility).

Now experiments have shown that in the range of brightnesses in which the standard visibility curve applies, the definitions of brightness (2) are in no wise in contradiction with our subjective sensation of brightness, i. e. two surfaces to which on the basis of (2) we ascribe the same brightness impress the eye as being "equally bright" ²). In what way is the "range of brightness" frequently mentioned above limited? And what deviations occur outside this range?

In an upward direction the range is limited by the range where the brightnesses are so great that their glaring effect prevents the eye from making a comparison of brightness values.

Of more importance to us is the lower limit of the range as it lies in the neighbourhood of the brightnesses obtained with road lighting systems. It is indeed found that at brightnesses below approx. 3 candles per sq. metre visibility curves are obtained of a different type to that shown in fig. 1; the

---

²) This general statement embraces various characteristics of the eye as regards the comparison and addition of brightnesses, an aspect which we cannot enter into at the present juncture.

visibility curve becomes displaced at diminishing brightnesses towards the blue, at first slowly, then more rapidly. The principal part of the displacement takes place in the brightness range between 0.3 and 10^{-3} candles per sq. metre. At still lower brightnesses a further slight displacement occurs, and finally the curve assumes a constant shape again at about 3.10^{-5} candles per sq. metre (*fig. 2*)[3]. The maximum becomes displaced from 5550 Å to 5050 Å. If we remember how a visibility curve is obtained experimentally, we see that this displacement of the curve signifies that the ratio of the energies which must be utilised by different colours in order to obtain a visual sensation of equivalent brightness is dependent on the brightness level (thus, for instance, the same amount of energy is required for the wavelengths 5300 and 5800 for a specific high brightness, whilst for an extremely low brightness twelve times more energy is required for the second wavelength than for the first).

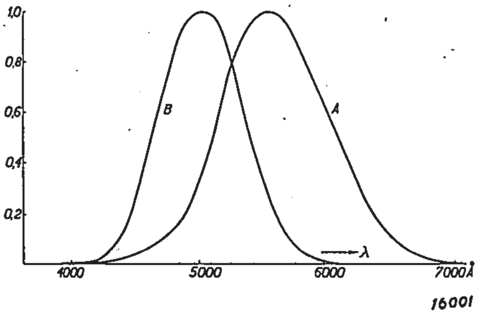

Fig. 2. Various visibility curves:
A. for high brightness levels (standard curve),
B. for extremely low brightnesses.
For intermediate brightness levels (road lighting) an intermediate curve applies.

This extremely important fact, which is termed the Purkinje effect, can be expressed in various other ways, e.g.:

Two surfaces emitting light of different colours and appearing to be equally bright do not retain this appearance of equivalence when both energies are divided by the same factor, or:

If two surfaces have the same numerical value for the brightness according to definition (2), they need not always produce the same brightness impression, and hence:

The interpretation of brightness according to definition (2) no longer coincides, outside the range of validity of the standard visibility curve, with the concept of brightness deduced from everyday experience.

It thus follows that to avoid a loose interpretation we must adopt two different concepts, viz., brightness and apparent brightness.

Brightness *H* is defined — for every range of brightness — as the numerical value given by definition (2). This definition has already been adopted as the international standard. Our first requirement as regards the apparent brightness *h* is that two surfaces which produce the sensation of equivalent brightness must also have the same value of *h*. It follows from this that the plotting of the visibility curve by the method described above constitutes in all cases a measurement of energies, which must be radiated at different wavelengths in order to create the same apparent brightness.

This "definition of equality" (which answers the question: When have two surfaces the same apparent brightness ?) is already adequate in itself for dealing with a large number of problems. In other cases it will be, however, of great advantage if we can also assign a definite numerical value to the apparent brightness, i.e. obtain a "quantitative definition" answering the question: How great is the apparent brightness of this surface ? Exactly as when assigning numerical values to the brightness (see footnote [1]) there is a certain latitude in choosing this "quantitative definition". We select the following definition:

The apparent brightness of a surface which radiates light of any arbitrary colour has assigned to it the same numerical value as the brightness of a surface which emits monochromatic light of wavelength 5350 Å[4]) which gives the same brightness-impression as the surface under investigation (König, Bouma).

We can express this complete concept of apparent brightness also in somewhat different terms, viz., as follows:

For monochromatic light of 5350 Å the brightness and the apparent brightness have according to definition the same numerical value. The values for light of different colours are determined by the rule: Two surfaces have the same apparent brightness if they appear to the eye to be "equally bright".

Expressed in this way it is seen immediately that in the range above 3 candles per sq. metre two surfaces which have the same brightness also have the same apparent brightness, and that hence above 3 candles per sq. metre the brightness and the apparent brightness completely coincide. The very marked difference which can occur in these two factors at low brightness levels is shown by *fig. 3*, where the lines of equal apparent brightness h are plotted graphically with the wavelength λ along the abcissa and the brightness H along the ordinate. It is seen for example that to obtain the same apparent brightness $h = 3.10^{-4}$ candles per sq. metre a luminous density is required for red light (6500 Å) about 140 times greater than for blue light (4500 Å).

---

[3]) These curves have also already been published in Philips techn. Rev. 1, 106, 1936.

[4]) This wavelength of 5350 Å has been chosen to facilitate correlation with König's measurements.

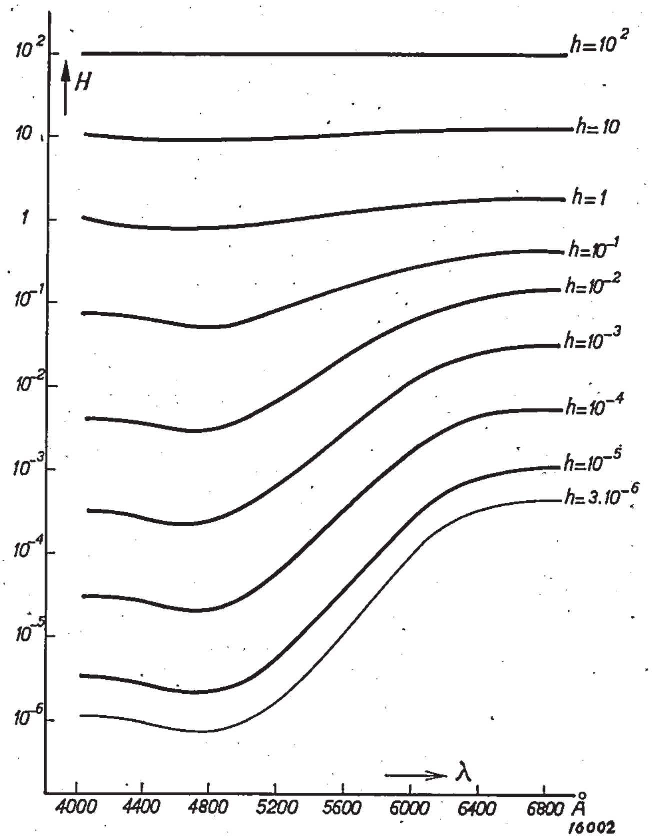

Fig. 3. The relationship between brightness (H) and apparent brightness (h) for monochromatic light: in an H-λ diagram the lines of constant apparent brightness are drawn; the curvature of these lines indicates the occurrence of the Purkinje effect. Both H and h are given in candles per sq. metre. The line $h = 3.10^{-6}$ candles per sq. metre represents approximately the absolute threshold value.

The physiological cause of the Purkinje effect is very probably to be sought in the functioning of the two different light-sensitive elements of the eye, the cones and rods (cf. also the article in Philips techn. Rev. **1**, 102, 1936). Above 3 candles per sq. metre vision is due practically solely to the cones which give us the standard visibility curve (A in fig. 2); below about 3.10^{-5} candles per sq. metre only the rods are functioning and these give the visibility curve B in fig. 2. At intermediate brightness levels there is a combined functioning of both elements, cones and rods, to produce vision, and the visibility curve obtained for this range is therefore situated between curves A and B in fig. 2. As the rods and cones are irregularly distributed over the retina, it is evident that for the accurate definition of apparent brightness it is in fact also necessary to state the size and shape of the field of vision, and for this purpose we choose two semicircles in contact with each other with an angular diameter of at least 6 deg. (a smaller diameter would partially exclude the rods, whilst an increase in the diameter would not affect the results of measurement).

We cannot conclude this discussion without indicating the practical value of the concepts of brightness and apparent brightness in certain branches of science and engineering.

1. Photometry. The principal purpose of photometry is the measurement of brightnesses and the calculation of other technical light magnitudes (candle power, luminous flux, etc.) from the measured brightnesses. The methods of measurements [5]) employed are divided into two groups:

a) Those methods in which the eye is used as a measuring instrument, as in the flicker photometer. True brightnesses are only obtained by these methods when the values are above 3 candles per sq. metre. At lower brightness levels values are found which in general agree with neither the brightness nor the apparent brightness.

b) Those methods in which the eye is not used directly for measuring purposes, e.g. in adapting a photo-electric cell to the standard visibility curve. Accurate brightness values are obtained with these methods also below 3 candles per sq. metre.

2. Physiology, the description of the characteristics of the eye. Many physiological properties (contrast sensibility, diameter of pupil, state of adaptation, etc.) are determined principally by the apparent brightness and not by the brightness. Thus if we plot the contrast sensibility as a function of the brightness we get very different curves for various colours; but if we plot the apparent brightness along the abcissa the curves agree fairly closely. We thus see that here, by introducing the notion of apparent brightness, we obtain a more comprehensive survey of the results of measurements and means for simplifying the laws regarding the behaviour of the eye.

3. Road lighting. In this connection the two concepts discussed are of importance in various directions. The brightness levels obtained with road lighting systems are of the order of 0.06 to 1.5 candles per sq. metre i.e. they are in a range in which the Purkinje displacement becomes appreciable. As an example showing how the

---

[5]) Cf. Philips techn. Rev. 1, 120, 1936.

quality of road lighting can be affected by this factor, we can compare sodium light and white light (from an ordinary incandescent lamp). The result of the Purkinje effect is as follows:

If two roads are illuminated with the same and sufficiently high brightness, one with sodium light and the other with white light, it is found that vision is better on the road illuminated with sodium light. Now if the levels of illumination of the two roads are reduced by the same factor, vision deteriorates much more quickly in the road illuminated with sodium light than in that illuminated with white light. The reason for this is that although the brightnesses in the two roads remain the same, the apparent brightness of the "sodium road" diminishes more rapidly than that of the "white road". We conclude from this that the illumination in the sodium road is only better when the brightness remains above a certain lower limit (about 3 candles per sq. metre).

This same phenomenon of "more rapid darkening" of the sodium road causes dark objects in the sodium road to stand out more clearly from the bright background than is the case in the white road, in other words the appearance of greater richness of contrast with the sodium light is also explained by the Purkinje effect and the difference between apparent brightness and brightness connected with it. We shall discuss this phenomenon in greater detail in a later article.

BIBLIOGRAPHY

König, Ann. Physik **45**, 604, 1892 (Visibility curves at different brightness levels).

Nutting, Bur. Stand. Bull. **7**, 235, 1911, (contains, inter alia, the fully-evaluated measurements made by König).

Teichmuller, E. T. Z. **38**, 296 and 308, 1917 (here for the first time the need is emphasised for two different concepts of brightness in street lighting problems).

Bertling, Licht und Lampe **23**, 82, 130, 207 and 227, 1934; **24**, 77, 1935.

Bertling, Das Licht **4**, 98, 1934.

Reeb and Richter, Das Licht **4**, 59 and 100, 1934.

Reeb, Licht und Lampe **24**, 50, 1935.

Dziobek, Das Licht **5**, 9, 1935.

Bouma, Licht und Lampe **24**, 217, 1935.

(These articles contain a detailed discussion of the concepts of brightness and apparent brightness.)

Gibson and Tyndall, Bur. Stand. Bull. **19**, 131, 1923. (The determination of the standard visibility curve; the figures of Gibson and Tyndall are to be found in a large number of physical, photometric and illumination works).

AN OSCILLOGRAPH APPARATUS

Summary. A cathode-ray oscillograph which has been constructed by Philips is described, by means of which the fluctuations of voltages from 5 millivolts upwards can be studied in a frequency range from 10 to 500000 cycles.

Introduction

An electrical oscillograph can be usefully employed for rendering visible the fluctuations of a specific voltage. As already indicated in previous issues of this Review [1]) the cathode-ray oscillograph has now been developed to a useful technical apparatus. In this article, a description is given of an oscillograph (type G.M. 3150) evolved by Philips.

This oscillograph contains an amplifier by means of which the voltage under investigation is raised to the value required for feeding to the deflector plates V of the cathode-ray tube (*fig. 1*). The apparatus also incorporates a time-deflection (or relaxation voltage) unit, which furnishes the saw-tooth voltage [2]) for the plates H for periodically deflecting the cathode ray in a horizontal direction. In place of the saw-tooth voltage, a voltage from an external source can also be applied to the plates H. The saw-tooth voltage can be synchronised with the signal transmitted by the amplifier or with a signal transmitted from any external source or also with the alternating current mains supply. Two anode rectifiers are also incorporated in the apparatus for furnishing the direct voltages for the cathode-ray tube, for the amplifier and for the relaxation voltage (time-deflection) unit. With this oscillograph, time diagrams can be produced, with practically no distortion, of voltages from 5 millivolts upwards and with frequencies from 10 to 500000 cycles.

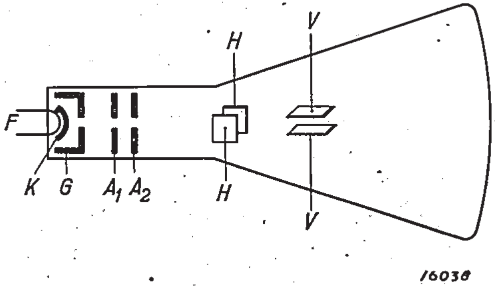

Fig. 1. Diagram of cathode-ray tube. K = cathode; F = filament; G = control electrode; A_1 and A_2 = first and second anode; H and V = pairs of plates which can impart horizontal and vertical deflections respectively to the cathode ray.

Feed Circuit for the Cathode-Ray Tube

Fig. 1 shows the circuit connections of the cathode-ray tube (type No. 3957) which is employed in the oscillograph. The various direct voltages, which must be applied to the control electrode and the anodes, are furnished by a rectifying valve L_2 (*fig. 2*) with smoothing condenser C, and can be tapped with the required magnitudes from a resistance (R_1, R_4). The circuit (fig. 2) is so arranged that the second anode A_2 is earthed and the indirectly-heated cathode K has a negative bias of about 12000 volts compared with the second anode. The potential of the control electrode G, which is slightly lower than that of the cathode K, and the potential applied to the first anode A_1 can be regulated. By altering the tapping on R_4 the intensity of the electron beam which the control electrode G allows to pass is altered, whilst by means of R_1 the definition of the fluorescent spot can be adjusted. In addition to the usual deflecting voltages an adjustable bias is also applied to the pairs of plates H and V, by means of which the spot can be adjusted to the centre of the fluorescent screen. The front panel of the oscillograph housing (*figs. 3a* and *3b*) contains inter alia the knobs R_1 and R_4 by means of which the definition and the brightness respectively of the spot can be altered. Knob R_4 also operates the switch S_5 with which the primary winding of the feed transformer is switched on and off, i.e. the whole apparatus is connected up to or disconnected from the supply.

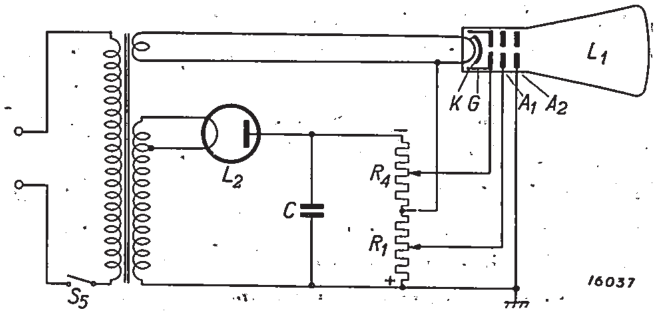

Fig. 2. Simplified feed circuit of cathode-ray tube. By means of R_4 and R_1 the brightness and sharpness respectively of the fluorescent spot can be varied.

Time Deflection

The electrical voltage, whose time diagram is to be reproduced on the fluorescent screen, is applied to the plates V (fig. 1) which deflect the cathode ray in a vertical direction. To achieve this a voltage must at the same time be applied to the plates H which deflect the cathode ray in a horizontal direction; this voltage must vary linearly with the time and, after the elapse of an integral number of periods of the voltage under investigation, must return rapidly to its original value, and then again increase linearly with the time in exactly the same way. This so-called "saw-tooth voltage" for the plates H is furnished by the relaxation voltage (or time-deflection) unit.

---

[1]) Philips techn. Rev. 1, 33 and 91, 1936.

[2]) Cf. Philips techn. Rev. 1, 16, 1936.

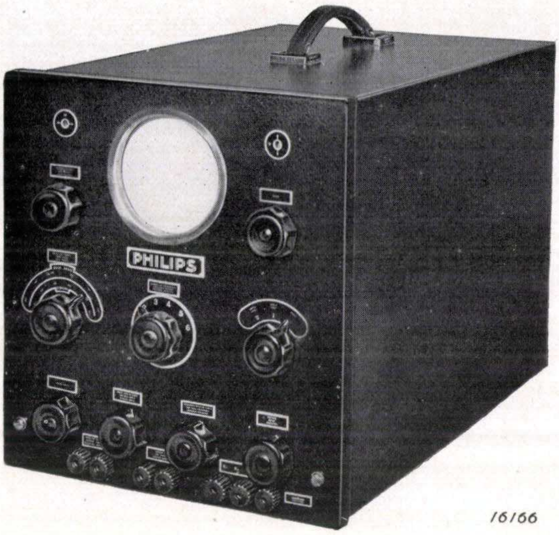

Fig. 3a. General view of the oscillograph unit.

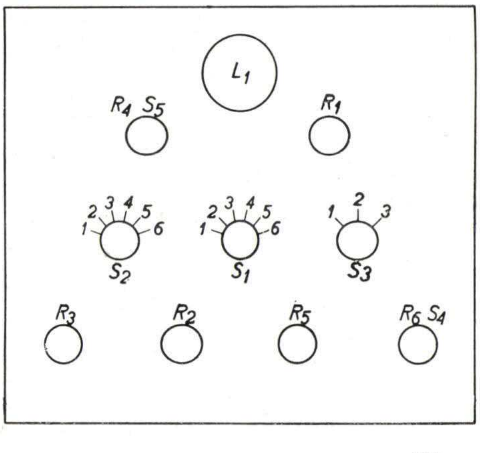

Fig. 3b. Front view of oscillograph unit.
R_1 controls the sharpness of the fluorescent spot.
R_2 controls the width of the time diagram.
R_3 controls the intensity of the synchronising signal.
R_4 controls the brightness of the fluorescent spot.
R_5 controls the frequency of the saw-tooth voltage.
R_6 controls the amplification of the voltage under investigation.
S_1 serves for rough regulation of the frequency of the saw-tooth voltage.
S_2 determines what voltage is applied to the deflector plates H.
S_3 determines which method of amplification is used.
S_4 changes over the amplification.
S_5 connects up the feed transformer.

The main details of the circuit in the relaxation voltage unit are shown in *fig. 4*. An anode rectifier furnishes a direct voltage of about 400 volts across the terminals A and B of the relaxation voltage unit. Across the terminals C and D a saw-tooth voltage as far as possible of rectilinear form is required. To do this the potential at the condenser V_F must increase linearly with the time. This cannot be done by charging the condenser V_F through a resistance, since owing to the increase in voltage at the condenser the charging current would drop during charging. One characteristic of a pentode, however, is that the anode current is practically independent of the anode voltage over a wide range. This property is employed in the relaxation voltage unit. At the beginning of a period the condenser V_F is uncharged, whilst the anode voltage is applied to V_G. No voltage is then applied to the pentode L_7, so that it passes no current, although pentodes L_8 and L_9 do so. The condenser V_F is charged with a constant current intensity through L_8. The voltage V_F across the terminals B and D thus increases linearly with the time (*fig. 5*) and this is the voltage which is applied to valve L_7. When this voltage has increased to a certain value an anode current will also flow through L_7, but at the same time the screen grid S of this valve will be carrying a current which can flow away through r_1. As a result a voltage-drop occurs at r_1 which causes a diminution of the voltage at the two plates of the condenser V_G charged to the anode voltage. The potential at the negative plate of V_G thus drops below the voltage of the common negative conductor AC. A current will then flow through r_3 which will discharge the condenser V_G, whilst the control grid of the pentode L_9 will acquire a negative potential (V_9 in fig. 5). The ratings of the apparatus have been so chosen that this voltage-drop at the control grid of L_9 is large enough to reduce the passage of current through L_9 to practically zero (I_9 in fig. 5). The anode of L_9 and hence the control grid of the pentode L_7 are thus reduced to nearly the same voltage as the anode of L_7. This pentode is thus rendered a very good conductor and the condenser V_F will become rapidly discharged through it (L_7 in fig. 5). Hence as soon as the condenser V_F commences to become discharged through L_7, the circuit provided with the pentode L_9 will ensure that this discharge takes place very rapidly, after which the whole process recommences from the beginning.

The voltage of the anode of L_8 is passed through terminal D to one of the deflector plates H of the cathode-ray tube. It has the requisite saw-tooth characteristic for this purpose as it is the difference between the direct voltage at the terminals A and B and the voltage V_F in fig. 5. The other plate H receives a specific adjustable potential difference

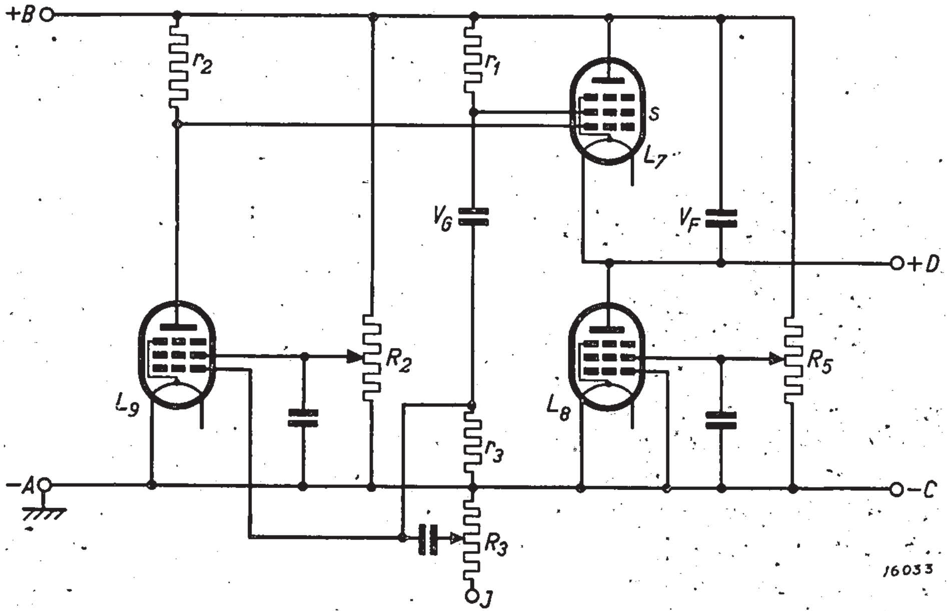

Fig. 4. Circuit details of the time-base unit. A constant direct voltage of about 400 volts is applied across terminals AB and a synchronising signal to terminal J. The saw-tooth voltage for the deflector plates H is taken from terminals CD. L_7 is a pentode AL4 Pentodes AF7 are used for L_8 and L_9.

with respect to terminal C such that the fluorescent spot travels to and fro over the required area of the screen. If the screen-grid voltage for L_9 is tapped at various points of R_2, the anode current I_9 of L_9 will assume different values, whereby the screen grid of L_7 will receive different voltages. This will also alter the voltage at which the condenser V_F becomes discharged through L_7. Using R_2, regulation is thus obtained of the voltage fluctuations at D and hence of the magnitude of the horizontal deflections of the cathode ray in the cathode-ray tube. Knob R_2 in fig. 3 serves for adjusting the width of the time diagram on the screen. The time taken for the condenser V_F to become once charged depends on its capacity. The frequency of the relaxation voltage is therefore easy to adjust in this unit by merely inserting condensers of different capacity for V_F. This is done by means of switch S_1 which has six different settings, as shown in fig. 3b. Naturally in this way only rough regulation of the frequency of the saw-tooth voltage can be obtained, and must be followed by fine regulation which is carried out by tapping from different points of resistance R_5 the voltage for the screen grid of L_8 by means of which the charging current of the condenser V_F is regulated.

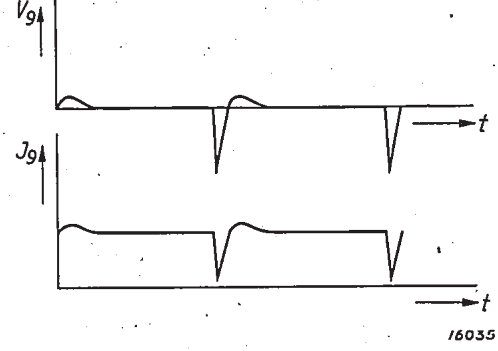

Fig. 5. Time diagrams of voltage at condenser V_F, of the anode current I_7 of pentode L_7, of the voltage V_9 at the control grid of L_9 and of the anode current I_9 of the pentode L_9.

To ensure that at different frequencies of the saw-tooth voltage the ratio between the charging and the discharging periods remains practically constant, S_1 alters not only the capacity of V_F but also alters that of V_G at the same time. In this way the lability of the circuit by means of which the condenser V_F can be discharged at such a rapid rate (I_7 in fig. 5), is maintained even after altering the capacity of V_F. In this circuit the function of the pentode L_9 is therefore to make the resistance of the pentode L_7, which is in parallel with the condenser V_F, suddenly very small, so that condenser V_F becomes very rapidly discharged through the pentode L_7 which practically shorts the condenser. The instant this sudden discharge takes place is very easily affected [3]) in this circuit by small changes which may for instance occur in the voltage at certain points of the circuit. We can regulate the moment at which the discharge current I_7 commences to flow by applying a voltage over terminal J (fig. 4) to the control grid of L_9, which makes V_9 sufficiently negative either slightly earlier or later[3]) so that the anode current I_9 is reduced practically to zero (fig. 5). The voltage applied to J, which is drawn from the amplifier or the mains or an external supply provided for this purpose, thus determines the correct instant at which the condenser F becomes very rapidly discharged; it thus serves as a so-called synchronising signal, in other words it ensures that the saw-tooth voltage is always synchronised with either the magnitude under investigation, or the alternating-current mains or a periodic current applied from an external source. The required intensity of the synchronising signal is regulated by means of R_3.

---

[3]) Cf. D. M. Duinker, Philips techn. Rev. 1, 14, 1936.

Fig. 6 shows how, with the aid of switch S_2, different potentials can be applied to the deflector plates H and various synchronising signals can be applied to the terminal J (cf. fig. 4).

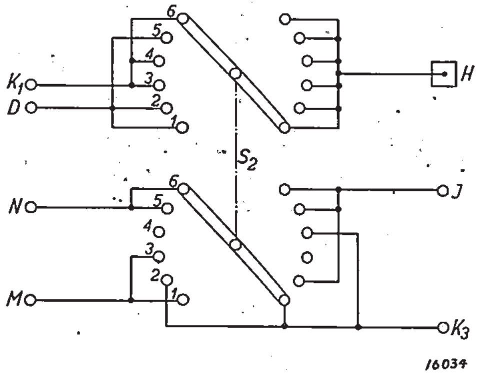

Fig. 6. Diagram of the six different combinations between the deflection settings of the cathode ray and the synchronising settings which can be obtained with the switch S_2. J is the terminal over which the synchronising signal is passed to the time-base unit, and H is the plate which imparts a horizontal deflection to the cathode ray. To terminals D, N and M are applied respectively the saw-tooth voltage, a voltage in phase with the a.c. mains and a synchronising signal from the amplifier. Through terminals K_1 and K_3 a deflection voltage or a synchronising signal from an external source can be passed in or out.

Position 1: Saw-tooth voltage (D) applied to the deflecting plate (H); synchronising signal (J) taken from the amplifier (M). This is the normal setting.

Position 2: Saw-tooth voltage (D) applied to the deflecting plate (H); external synchronising signal (J) applied over terminal K_3. This setting is used to synchronise with a specific frequency, when for instance the signal under investigation consists of a combination of different vibrations.

Position 3: External deflecting voltage (H) applied through terminal K_1; synchronising signal from the amplifier (M) passed outwards over terminal K_3. By this means a different relaxation voltage unit to that incorporated in the apparatus can be put in circuit.

Position 4: External deflecting voltage (H) applied over terminal K_1; synchronising signal (J) cut out to prevent this signal causing distortion.

Position 5: Saw-tooth voltage (D) applied to deflector plate (H); synchronising signal (J) taken from the alternating current supply (N), thus synchronising with 50 cycles.

Position 6: External deflecting voltage (H) applied through terminal K_1; synchronising signal from the a.c. mains (N) passed outwards over terminal K_3. This setting differs from setting *5* only in that the built-in time-base unit is replaced by another.

Amplifier

Fig. 7 shows a simplified diagram of the various circuits by which the signal to be plotted by the oscillograph is applied to the plates V of the cathode-ray tube; these plates have to produce a vertical deflection of the electron beam. The same anode rectifier which feeds the time-base unit also furnishes the amplifier with a direct voltage of about 400 volts across the terminals A and B, of which A is earthed. The signal under investigation is applied across the terminals K_5 and K_7, of which the latter is earthed. If switch S_3 is moved into position *1*, a signal for feeding to the amplifier can be taken from the resistance R_6. When a current flows through R_6, which causes pronounced distortion of the signal voltage under examination, the signal must be applied across K_6 and K_7 so that it reaches the control grid of the pentode L_2 directly through the condenser C_1. The regulating knob of R_6 (cf. fig. 3) is then turned to the left, whereupon S_4 is switched off and R_6 no longer carries current either. Normally the voltage tapped from R_6 passes to the control grid of L_2 through C_1. The screen grid has a specific potential difference with respect to the cathode, whilst the collecting grid is directly connected to it.

The alternating voltage generated at resistance r_4 by the anode current of L_2 is now an amplification of the signal and at position *1* of S_3 is applied to the control grid of pentode L_3 through the condenser C_2. If the original signal is powerful enough it can also be applied directly to C_2 by moving S_3 into position *2*, the first amplifying stage with the valve L_2 being cut out. At settings *1* and *2* of S_3 the anode of L_3 is connected through condenser C_4 to terminal *M*, from which the voltage is tapped for one of the plates *V* of the cathode-ray tube which deflect the cathode ray in a vertical direction. Furthermore, at positions *1* and *3* of switch S_2 (cf. fig. 6) the synchronising signal *J* for the time-base unit (cf. fig. 4) is also drawn from *M*. To ensure that the potentials applied to the pair of plates *H* are symmetrical, the pentodes L_3 and L_4 are connected in such a way that the anode of L_4 gives through condenser C_6 a voltage form at the terminal *O* which is similar to that at terminal *M* but has an opposite sign. The ratio of the resistances r_7 and r_8 is so chosen that the anode alternating voltages of L_3 and L_4 have the same absolute value. The voltage at terminal *O* is then applied to the other pair of deflecting plates *V*.

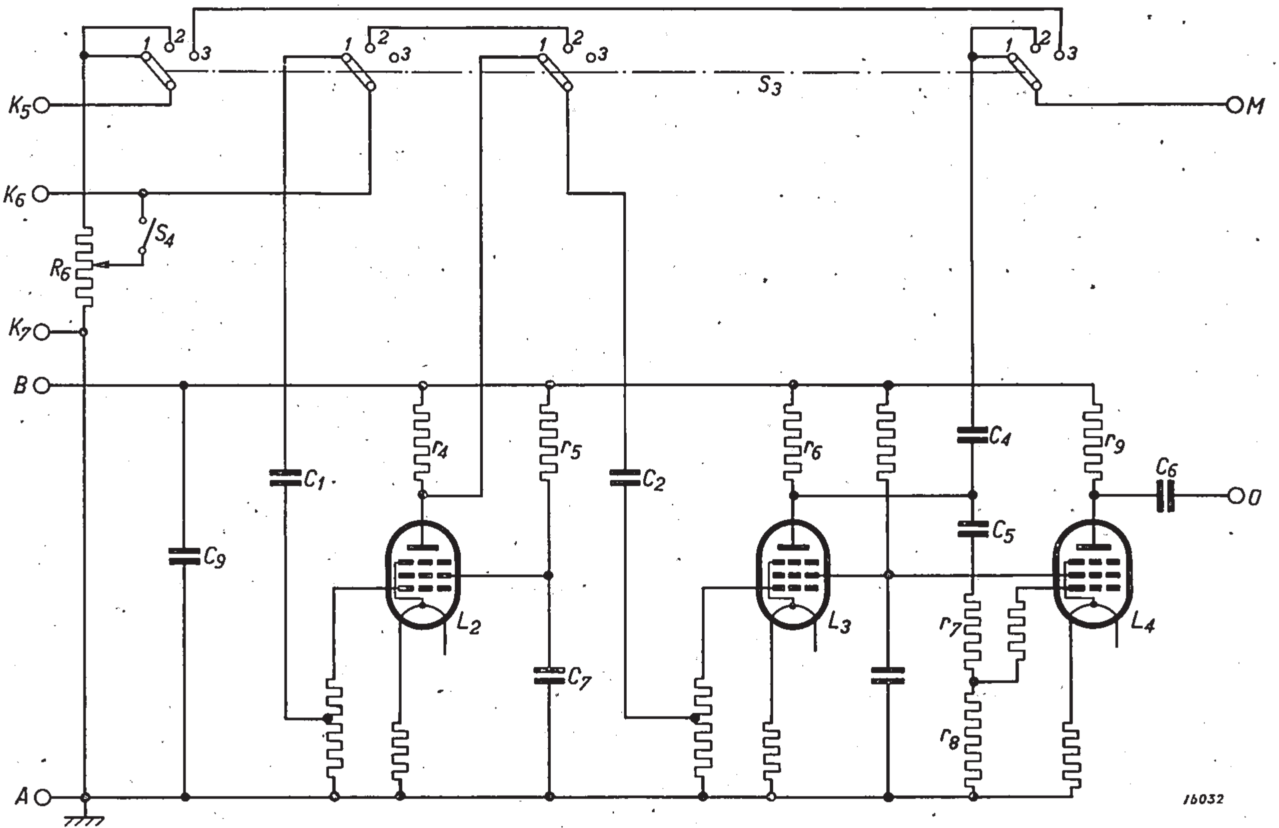

Fig. 7. Simplified circuit of the amplifier for the signal under investigation. A direct voltage of about 400 volts is applied across terminals *A* and *B*. The incoming signal is applied across K_5 and K_7 (or K_6 and K_7). By means of switch S_3 different types of amplification can be selected. The amplified or unamplified signal is then applied through terminals *M* and *O* to the plates *V* which impart a vertical deflection to the cathode ray (cf. fig. 1). For L_2 a pentode AF7 is used and for L_3 and L_4 pentodes AL4.

If the signal to be represented by the oscillograph possesses a sufficient intensity, it can also be applied directly to the deflector plates *V* of the cathode-ray tube by cutting out the amplifier altogether by putting switch S_3 into position *3*. The maximum intensity of the signals which can be applied by using the amplifier across K_5 and K_7 is 45 volts, when a power of 0.2 watt is converted in the resistance R_6. If only the valves L_3 and L_4 are used for amplification, a standard image 6 cm in size is obtained with a voltage of 0.5 volt across the terminals; when using the whole amplifier the same size of image may be obtained with signals of only 0.05 volt. As a 6-cm image is quite adequate, voltages from 5 millivolts upwards may be investigated. Care must be taken that at the deflector plates, both at *V* and at *H*, no voltages exceeding 90 volts are applied. The apparatus is suitable for frequencies from 10 to 500000 cycles; at the highest frequency the amplification ratio has not yet dropped 10 per cent.

Compiled by G. P. ITTMANN.

OPTICAL TELEPHONY

By J. W. L. KÖHLER

Summary. In the apparatus for optical telephony described in this article, a modulated ray of light is generated by feeding an incandescent lamp simultaneously with a direct current and with an alternating current from a microphone amplifier. The characteristics of this lamp are discussed. The range of transmission of this method is limited by the noise interference produced at the receiving apparatus. The means for suppressing this interference as far as possible are outlined. The apparatus described has a transmission range of 4.5 km when using white light and of 3 km with red light.

Introduction

The term optical telephony has been applied to the method of telephonic intercommunication by means of light rays, and is thus an extension of the principle of the ordinary signalling lamp by means of which telegraphic signals are transmitted. In the latter method an incandescent lamp fitted with a reflector is provided as a transmitter at each of the two points of intercommunication and by means of these a parallel beam of light is transmitted to the opposite receiving point. Each lamp is connected in circuit with a Morse key and, with the aid of the two beams of light employed, Morse signals can be transmitted and thus a channel of intercommunication established.

This system of telegraphic intercommunication occasions a considerable loss of time which in many cases has proved a serious obstacle to its use. This difficulty has been avoided in optical telephony, where the intensity of a beam of light is also varied periodically, not by Morse signals but by the speech frequencies which are used for intensity modulation. Reception is therefore not possible with the naked eye as with Morse signals, but requires the use of a photo-sensitive cell with an amplifier and telephone.

The complete equipment for optical telephony comprises the following components (see *fig. 1*). At the transmitting station there are provided a lamp L which is fed with direct current and is located at the focus of the reflector R, as well as a microphone M and an amplifier V_Z which amplifies the microphone current for modulating the beam of light. With this arrangement an image of the incandescent lamp filament is obtained at a great distance. The size b of this image is determined by the distance a between transmitter and receiver, the focal length f of the mirror and the size v of the filament, according to the expression:

$$b = \frac{v \cdot a}{f}$$

If, for instance, $a = 1$ km, $v = 0.1$ mm and $f = 75$ mm, then $b = 130$ cm. If this image is thrown on a parabolic reflector R' a portion of the image can be directed on to the photo-electric cell F situated at the focus. The receiving end is also equipped with a photo-electric amplifier V_0 and a telephone T.

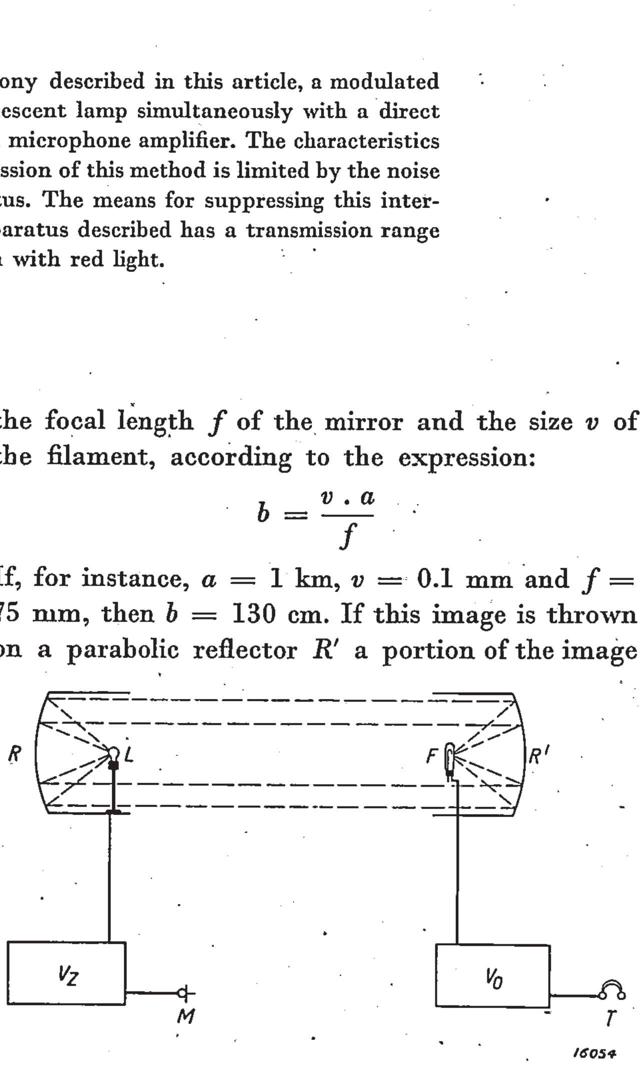

Fig. 1. Diagrammatic sketch of intercommunication by optical telephony. R and R' are the transmitting and receiving mirrors. L is the incandescent lamp. The lamp is modulated by the microphone M and the transmitter amplifier V_Z. At the focus of the receiving mirror the photo-electric cell F is situated which converts the light fluctuations into alternating currents: after amplification by the receiving amplifier V_0 these alternating currents become audible in the telephone T.

Transmitter

Simple consideration of the various methods by which the intensity of a beam of light can be modulated with speech frequencies indicates that several of these methods cannot be employed in the present case, since with them the position of the image varies. Thus, for example (see *fig. 2*) an image of the lamp filament can be obtained by means of a supplementary lens L_1 and the image periodically covered with a screen S which is controlled by an electro-magnetic system M. The total flux of the beam will then certainly vary, but at the receiving mirror, where an image of the filament is reproduced, it is not the intensity of the image that will vary but merely the size of the image; part of the image will in fact be covered. This method can thus only be employed where the image is small compared with the receiving apparatus, while in practice the very reverse is actually the case. It is therefore essential for the image to be maintained as a whole at the receiving station, but to have a fluctuating intensity. This may be achieved in various ways, viz:

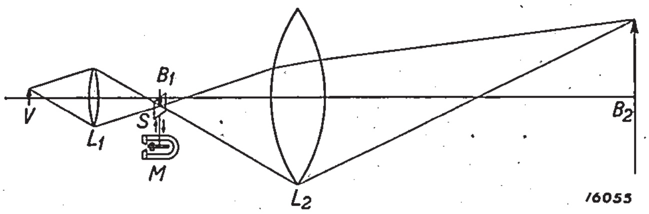

Fig. 2. Modulation of light with a screen. V is the source of light of which the lens L_1 produces the image B_1. This image is situated at the focus of the lens L_2, which throws an image B_2 to infinity. At the position of B_1 the screen S is placed which is moved up and down by the electromagnetic system. In this way the image B_2 is covered to varying degrees.

1. The beam of light is screened off by a screen placed in the immediate vicinity of the lens.
2. The beam of light is passed through a medium with a variable transmissibility.
3. The temperature of the incandescent filament is varied.

The first method requires only brief consideration. Since the transmitting mirror always has a fairly large diameter (e.g. about 20 cm), it is evident that the diaphragm or screen must be of the same size. But it is very difficult to vary the size of a diaphragm of these dimensions with a frequency of 2000 cycles per second.

An example of the second method is the Kerr cell (*fig. 3*). This cell is a condenser K with a liquid dielectric which has the property of being double-refracting in an electric field. The two light components, whose electric fields vibrate parallel and perpendicular to the field, are propagated with different velocities in the double-refracting medium. This phenomenon is utilised in the following way for modulating the light radiated. The light from the incandescent lamp becomes polarised linearly by the nicol N_1, which is so arranged that it only allows light to pass through whose plane of vibration makes an angle of 45° with the direction of the electric field in the plane perpendicular to the direction of propagation. This direction is indicated by the arrow in the plane sketched below the figure. In the electric field of the Kerr cell K the equal vertical and horizontal field components of this vibration are propagated at different velocities. The two components then pass through the nicol N_2, which is so arranged that it only allows light to pass whose electric field vibrates in a direction perpendicular to the direction of transmission of N_1. Of the light waves with electric vectors vibrating in vertical and horizontal planes which issue from the Kerr cell, only those components pass through the second nicol which vibrate in the plane of transmission of N_2. This is also shown by arrows in fig. 3. If no potential difference is applied to the condenser of the Kerr cell, then, as may readily be seen from the figure, these two equal and opposite components just balance each other. In these circumstances, as is well known, no light passes through the crossed nicols N_1 and N_2. But if a potential is applied to the Kerr cell, then the two components which pass through N_2 suffer a phase displacement owing to the difference in their velocities of propagation in the double-refracting medium. They are in this case no longer equal and opposite at every instant and thus do not balance each other, so that light passes through with the same periodicity as the frequency of the potential applied to the Kerr cell. An advantage of this method is the complete absence of inertia, although on the other hand the nicols and the rest of the system absorb a considerable amount of light and thus make the method uneconomical.

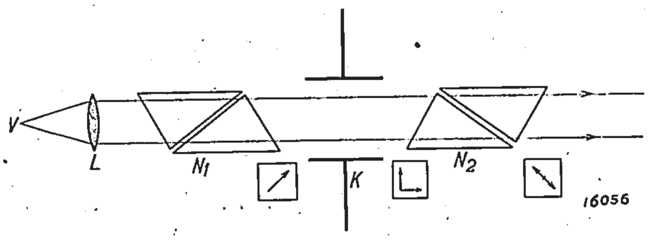

Fig. 3. Light modulation with the Kerr cell. The light from the light-source V is rendered parallel by the lens L. The beam of light then passes through the nicol N_1 by which it is linearly polarised (the arrow marked below denotes the direction of polarisation in the plane perpendicular to the direction of propagation). When the light has then passed through the double refracting medium of the Kerr cell, the phases of the vertical and horizontal components are displaced with respect to each other. The second nicol N_2 is crossed with respect to the first. If no potential is applied to the plates of the Kerr cell, the two transmitted components will just balance each other beyond N_2. Owing to the displacement in phase sustained by the components in the double refracting medium light will, however, pass through N_2.

A third method which starts with an incandescent lamp fed with direct current, has been evolved at the Philips Laboratory. This direct current has superposed on it the alternating current furnished by the microphone amplifier (*fig. 4*), so that the temperature of the hot filament varies with the frequency of the alternating current. To visualise this, consider the energy fed to the filament by the direct and alternating currents. If a is the amplitude of the direct current, b that of the alternating current (peak value), r the resistance of the filament regarded as independent of the temperature, ω the frequency of the alternating current and w the power input, we have:

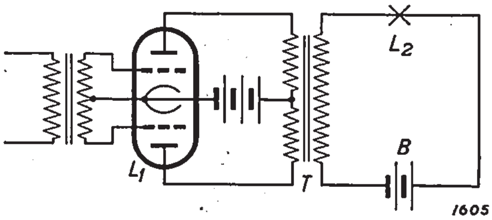

Fig. 4. Modulation of the incandescent lamp. The lamp N_2 is fed from the battery B. This circuit contains the secondary winding of the output transformer T of the transmitting amplifier. L_1 is the power valve of the amplifier, viz, Philips KDD 1 valve.

$$w = r\,(a + b \sin \omega t)^2 = r\,a^2\,(1 + m \sin \omega t)^2 \quad . \quad (1)$$

where $b/a = m$ is the degree of modulation. We thus get:

$$w = r\,(a^2 + 2\,ab \sin \omega t + {}^1/_2\, b^2 - {}^1/_2\, b^2 \cos 2\omega t) =$$
$$= r\,a^2\,(1 + 2\,m \sin \omega t + \frac{m^2}{2} - \frac{m^2}{2} \cos 2\omega t) \quad . \quad . \quad (2)$$

This expression contains a constant part and a variable part. The first term of the alternating energy, which is the determining factor, is $2ra^2m \sin \omega t$, and this has the same frequency as the alternating current; the second term has double this frequency. Naturally this second term is undesirable. On complete modulation, i.e. $m = 1$, its energy is $^1/_4$ of that of the fundamental wave. The potential difference at the photo-electric cell is proportional to the light energy and so in this case has a distortion of 25 per cent.

The result desired is that the intensity of the light shall vary with the fundamental frequency. Since small temperature fluctuations at the filament cause variations in the luminous intensity which to a first approximation are proportional to the temperature fluctuations, the temperature must fluctuate with the fundamental frequency. With a definite rate of a.c. input per second the magnitude of these temperature fluctuations is determined mainly by the thermal capacity of the filament and by the frequency.

Simple calculation shows how the energy input should be regulated in order to obtain a temperature

$$T = T_0 + A \sin \omega t \quad . \quad . \quad . \quad . \quad (3)$$

which fluctuates sinusoidally with the time t. The energy input ($E\,dt$) per element of time dt is dissipated partly by radiation ($W\,dt$), whilst the remainder ($C\,dt$) is imparted to the filament, whose thermal capacity is C, to produce a temperature rise dT:

$$E\,dt - W dt = C\,dT \quad . \quad . \quad . \quad . \quad (4)$$

The energy W dissipated per unit of time can be approximately represented by:

$$W = W_0 + a\,(T - T_0) \quad . \quad . \quad . \quad (5)$$

where W_0 is the mean energy dissipation in unit time. Hence the energy input (E) per unit of time required at each instant is given by:

$$E = W_0 + a\,A \sin \omega t + C\,A\,\omega \cos \omega t \quad . \quad (6)$$

If the frequency ω is sufficiently high, the last term in equation (6) will have the largest value, so that the expression for the input energy required E—W_0 may be approximated as follows:

$$E - W_0 = C\,A\,\omega \cos \omega t \quad . \quad . \quad . \quad . \quad (7)$$

The following conclusions may be drawn from this expression:

1. If a specific a.c. power is fed to a given filament in each second, the product $A\,\omega$ is determined. The amplitude A of the temperature fluctuations will then be inversely proportional to the frequency ω.
2. But if we have filaments of different diameters and employ a constant frequency, the constant energy which must be supplied to the filaments to maintain them at a specific temperature will be proportional to the diameter d of the filament. This energy is radiated by the surface of the filament, and will therefore be proportional to the surface area, and hence proportional to the filament diameter. Now if the input energy is made to vary with a definite modulation coefficient, then the a.c. power according to equation (2) will be proportional to the constant energy component and hence also proportional to the diameter of the filament. We thus find that in equation (7) the a.c. power $E - W_0$ is proportional to the diameter d of the filament, whilst the thermal capacity C of the filament is naturally proportional to its volume, i. e. to d^2. It thus follows that the amplitude A of the temperature fluctuations is inversely proportional to the diameter d of the filament.

Measurements have confirmed this conclusion, at least for frequencies at not too low a level. But the amplitude of the temperature variations is very small in the case of a lamp with a filament burning in vacuo.

In this respect gas-filled lamps are more suitable than vacuum lamps for the following reasons. Equation (6) also applies to gas-filled lamps, but W_0 and a are then much greater in value. If the frequency is made sufficiently high, equation (6) can again be reduced to the form of expression in (7). The presence of the gas-filling has therefore not altered the relationship between temperature variation and the a.c. power input. The amplitude of the temperature fluctuations is thus independent of the gas filling when the a.c. input, filament diameter and frequency are constant. But, owing to the much greater thermal conductivity of the gas, a much greater stationary power is now required to maintain the filament at a definite temperature than in the absence of the filling. At the same degree of modulation m, the possible alternating power is thereby also increased in the same ratio, and in accordance with equation (7) also the amplitude of the temperature variations. For example, the temperature fluctuations of the filament are three times greater with a nitrogen filling, and even ten times greater with hydrogen, than in vacuo.

A high temperature is desirable because the variation produced in the amount of light radiated by a specific temperature change is greater at a higher mean temperature. But there is a limit in this direction as the life of the lamp becomes rapidly shortened with increase in the temperature.

Receiver

The arrangements at the receiving terminal follow directly from the above considerations. The photo-electric cell converts the intensity fluctuations of the light into alternating currents which are amplified and passed to the telephone (*fig.* 5). But the intensity of the beam of light decreases with the square of the distance, and still more so as a result of absorption and dispersion in the atmosphere. Thus, in order to obtain a sufficient intensity at the telephone a high amplification must be employed, which determines the practicable range of transmission with this apparatus. It is well known that the amplification cannot be infinitely increased, as noise interference in the amplifier becomes heavily intensified at the same time. The sources of these noises may be classified into three groups as follows:

1. The first amplifying valve;
2. The coupling resistance coupling the photo-electric cell with the amplifier, and
3. The photo-electric cell itself.

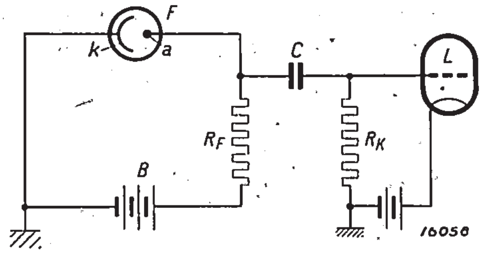

Fig. 5. Connection of photo-electric cell with receiving amplifier. The battery B furnishes the voltage for the photo-electric cell F. The alternating currents, which are produced by variable illumination of the cell, generate an alternating voltage at the resistance R_F. This voltage is passed through the condenser C and the resistance R_K to the grid of the input valve L of the amplifier.

Space does not permit of a detailed discussion of the interference due to the amplifier, although a few of the more important points may be dealt with.

Noises due to the Amplifying Valves

These interfering noises are due to the electric current, here the anode current, not being a continuous current, but a stream of electrons which are detached from the cathode in a haphazard fashion. These small current fluctuations produce a noise in the telephone. There is thus a natural limit set to reception, for if the amplitude of the variation in anode current produced by the signal is smaller than the current variation due to the inherent noises the signal will no longer be detectable. The only remedy here is to use a valve which gives a minimum of noise and to adjust it as accurately as possible.

Noises due to the Grid-Circuit Resistances

Owing to the Brownian movement of the electrons in the resistance slight voltage fluctuations are produced in it which cannot be eliminated in any way. But the various ratings can be so adjusted that interference is reduced to a minimum. The amplitude of the noise voltage at the resistance is proportional to the root of the resistance rating. At a specific illumination the photo-electric cell gives a definite current. The voltage-drop produced at the coupling resistance by this current is proportional to the resistance. Hence if we double this resistance, the signal voltage at this unit will also be doubled, whilst the noise voltage will be $\sqrt{2}$ times greater. We have thus reduced the ratio of signal voltage to noise voltage by $\sqrt{2}$. Although a greater resistance increases the noise, a higher coupling resistance is nevertheless of advantage here. On the other hand this resistance must not be made too large, owing to the input capacity of the valves connected in parallel to it, the capacities of the photo-electric cell and the leads which for high frequencies short the resistance.

Noises in the Photo-electric Cell

This noise is due to the same radical cause as the noise produced in the amplifying valves. In addition to the beam of light directed on to the photo-electric cell, the latter is also exposed to daylight, which generates a direct-current component in the photo-electric current. This component, similar to the anode current, is also subject to fluctuations owing to electronic conditions, such variations being responsible for the noises. In addition the illumination itself can also fluctuate and constitute a new source of disturbance. The only remedy here is to screen off daylight as far as possible. At the focus of the receiving mirror an image of the transmitting lamp and its surroundings is produced. If a screen is therefore set up with the same size as the image produced by the receiving mirror from the transmitting mirror, daylight will practically be completely cut off (*fig. 6*). But this is only the case with an ideal mirror. With ordinary mirrors with a short focus parallel beams of light are not focussed to a mathematical point but to a spot about 1 mm in diameter. If we therefore make the aperture of the diaphragm or screen less than 1 mm, more daylight will be cut out but at the same time also a part of the useful light from the transmitter, so that no advantage will be gained. A much better method is to increase the focal length, whilst lenses can be used to advantage instead of mirrors. With ordinary lenses the focus is still 1 mm in size, although now, owing to the greater focal length, the image of the transmitting mirror is also larger, so that only a smaller part of the surroundings is visible through the diaphragm aperture of 1 mm.

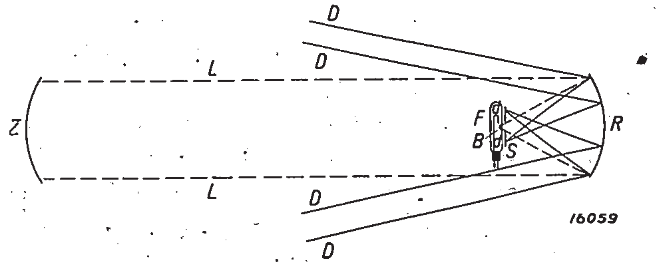

Fig. 6. Screening off daylight. At the focus of the receiving mirror *R* the image *B* of the incandescent lamp is produced which is set up at the focus of the mirror *Z*. Daylight rays (*D*) from the vicinity of the transmitting lamp are focussed at the points *d*. The screen *S* prevents access of these rays to the photo-electric cell *F*.

In this way very good results have been achieved with a lens of 40 cm focal length. It is evident that with the smaller diaphragm aperture it is more difficult to direct the receiver on to the transmitter, yet with the dimensions selected this difficulty has remained within reasonable limits.

There is also a general method which may be employed for suppressing interfering noises. These noises cover a frequency band, and the aggregate noise voltage increases with the square root of the width of the frequency band in question. If provision is made that the amplifier does not amplify those frequencies which are not absolutely essential for telephonic communication, the noise may be considerably reduced. The receiver has therefore been designed on such lines that frequencies above 2500 cycles are not amplified.

General Remarks

It has already been indicated that owing to the thermal capacity of the hot filament the amplitude of the luminous fluctuations decreases considerably with rising frequency. To ensure intelligible intercommunication it is naturally necessary for the frequency characteristics from the microphone to the telephone to be as near horizontal as possible for speech frequencies between 300 and 2500 cycles. For this reason a suitable correction must be made. The most practicable method for doing this appears to be to give the transmitter a characteristic which rises with the frequency, for if this means is employed in the receiving amplifier, interfering noise would become intensified. As long as the current through the lamp is only weakly modulated, no difficulties are encountered in this direction. With a constant input power for all frequencies at the transmitting amplifier the degree of modulation of the current through the lamp will, however, be greater for the higher frequencies than for the lower ones; this will not constitute a disadvantage as long as the degree of modulation for the higher frequencies does not attain 100 per cent. Upon further increase in the input voltage the current at the highest frequencies will at a given instant be fully modulated, so that amplification may not be further increased. But the current is then by no means fully modulated in the lower frequencies, so that the transmitter is apparently being run at a very low efficiency. In practice, however, entirely different conditions prevail since the human voice contains a far lower proportion of the higher frequencies than of the lower ones. When speaking into the microphone the current through the incandescent lamp is almost equally modulated by the different frequencies, provided the transmitting amplifier is given such a characteristic that, with an input signal having an intensity independent of frequency, the amplitude of the temperature fluctuations is similarly independent of frequency.

Since an apparatus for optical telephony must be readily portable, it is desirable for all amplifiers to be fed with current from anode batteries. The output power of the amplifier is therefore limited. Now with a specific modulation the a.c. energy absorbed by the lamp is proportional to the direct-current energy. The latter must therefore be kept low, which may be arrived at by making the filament short. From these considerations a lamp has been evolved which requires a 3-watt direct-current supply in order to burn at the correct temperature. At full modulation $1^1/_2$ watts is therefore sufficient. This energy can be controlled by the Philips KDD 1 valve, a double triode, the lamps of which are used in the neighbourhood of the zero of the characteristic (*B*-connection). This arrangement has the advantage that the anode battery does not have to furnish a current in the absence of modulation. The use of a small filament is furthermore useful since it gives a very narrow beam of light; the dispersion with a focal length of 75 mm is only about $1^1/_2$ per cent of the range of transmission.

Practical Results.

The efficiency and reliability of intercommunication depend inter alia on the wave-length of the light used, since the photo-electric cell has a different sensitivity for different wave-lengths, whilst moreover atmospheric absorption may also vary for different wave-lengths. Standard caesium photo-electric cells have a maximum sensitivity in the infra-red region of the spectrum, but also respond to visible light. Red light is less dispersed by air than violet light; nevertheless the intensity still decreases considerably if, in place of white light, dark red or even infra-red light is used by introducing a filter. The range of transmission is then reduced by at least 30 per cent.

With the apparatus built in the laboratory, satisfactory inter-communication was maintained over a distance of 4.5 km with white light and over 3 km with red light. The transmitting and receiving mirrors were each 130 mm in diameter. It should be mentioned in this connection that the range of transmission is proportional to the diameter of each of the reflectors. The data given here apply for good visibility, but it is quite possible to maintain intercommunication over a medium distance also through fog when once established, although to set up the required channel of communication is very difficult under these circumstances.

Compared with other methods of intercommunication, optical telephony has the disadvantages of being dependent on atmospheric conditions and of offering only a restricted range of transmission. On the other hand it has certain advantages; thus, compared with signalling lamps, messages can be transmitted with much greater speed, which applies in fact as regards all methods of telegraphic transmission. In regard to short-wave spark telegraphy there is, moreover, the added advantage of secrecy. Owing to the extremely small dispersion of the ray it is impossible to detect the position of the transmitter during the day, even when using white light; messages therefore cannot be tapped. For the same reasons intercommunication is also proof against malicious interference.

PRACTICAL APPLICATIONS OF X-RAYS FOR THE EXAMINATION OF MATERIALS

IV.

By W. G. BURGERS.

Perhaps the most fruitful application of X-rays for practical purposes is in those cases where the presence of certain compounds has to be established in a mixture or a chemical reaction product, or a chemical product has to be identified. Every crystalline body possesses its own characteristic crystal structure and hence gives a specific X-ray pattern. A given mixture can therefore in most instances be analysed directly by comparing its X-ray photograph with the patterns obtained for those compounds whose presence is suspected in the product under examination. Naturally, for the application of this method it is essential to have at hand a series of standard X-ray photographs relating to the comparison substances in question. These radiographic standards can usually be obtained without difficulty.

To enable the detection of an impurity or admixture in a given substance by means of X-rays, the impurity must generally be present in at least a certain percentage in order that the diffraction pattern given by it can be recognised besides that of the principal constituent. In this respect the X-ray method is subject to a certain limitation [1]) as compared with chemical analysis. Nevertheless, chemical analysis is only able to identify the nature of the atoms (or the ions) present, whilst the X-ray method directly indicates the compounds present; thus, by means of X-rays it is possible to distinguish for instance between a mixture of NaCl + KBr and another containing KCl + NaBr (see example No. 7). It is evident that the two methods of analysis supplement each other to a marked degree, since they afford information on different matters.

In view of the multiplicity of these special applications of the radiographic examination of structure (i.e. for identification), practical examples of this kind will frequently be encountered.

6. Diagnosis of Renal Calculus

For the successful treatment of patients suffering from renal calculus it is, inter alia, essential to know whether the calculi consist of oxalate or phosphate. In general this can be easily established by chemical means. But in many cases (where the calculi are small) it may be desirable not to sacrifice any part of the stone for chemical analysis, and just in these instances a radiograph will prove of great value. *Fig. 1a* shows an X-ray diffraction pattern which was obtained from a small quantity of a powdered calculus, whilst *fig. 1b* reproduces an X-ray diffraction pattern of calcium oxalate. From the identity of the arrangement of the various lines in the two radiographs it may be concluded that the calculus under examination was composed largely of calcium oxalate.

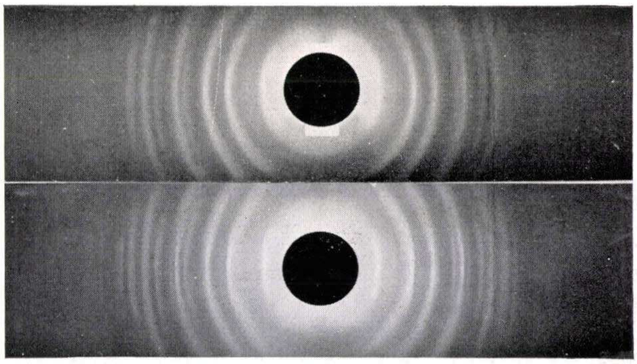

Fig. 1. Diagnosis of renal calculus.
a) Powder of a renal calculus
b) Calcium oxalate

7. Detection of Compounds in a Mixture

By pounding the powdered substances in a mortar, mixtures were produced of (a) NaCl + K Br, and (b) KCl + NaBr, equivalent molecular quantities being taken of each substance.

Figs. 2a and *b* reproduce the radiographs of the two mixtures side by side, and the difference between them may be clearly seen. From *figs. 3a-c*

---

[1]) In the case where mixed crystals or solid solutions are formed by which the crystal lattice is altered, the presence of admixtures can often be indirectly detected even in much smaller quantities.

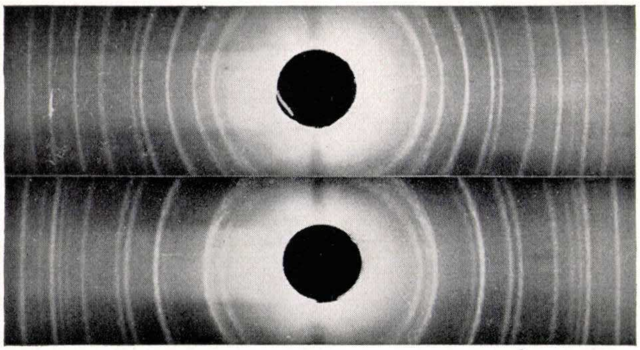

Fig. 2. Mixture of chemical compounds.
a) $NaCl + KBr$
b) $KCl + NaBr$

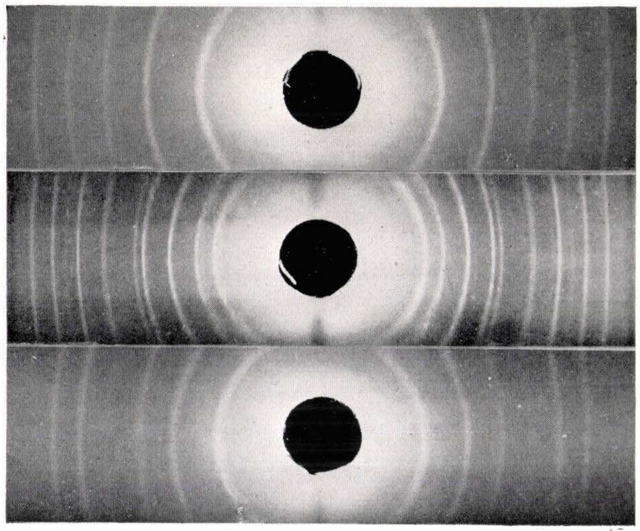

Fig. 3. Identification of compounds in the mixture in fig. 2a.
a) $NaCl$
b) $NaCl + KBr$ (= fig. 2a)
c) KBr

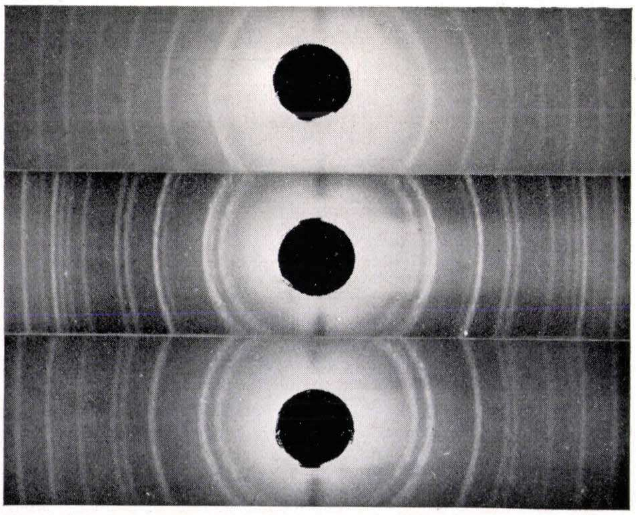

Fig. 4. Identification of compounds in the mixture in fig. 2b.
a) KCl
b) $KCl + NaBr$ (= fig. 2b)
c) $NaBr$

and *4a-c*, which reproduce not only the radiographs of the mixtures but also those of the constituents, the composition of the mixtures may be deduced.

Ordinary chemical analysis would have shown the same atomic (or ionic) composition for both mixtures (2) and would thus have given no information as to which metal was present as chloride and which as bromide.

8. Identification of Aluminium Oxide

Aluminium oxide is employed in the manufacture of incandescent lamps. There are various modifications of it, including the corundum modification, which occurs in natural crystals. This modification is formed for instance by heating aluminium hydroxide to a very high temperature, in the neighbourhood of 1200 deg. C. For the technical product used in manufacture it was essential to know whether this corundum modification was actually present, as otherwise heating to a very high temperature might have caused a conversion undesirable for various reasons. This point is very difficult to establish by chemical means, but a comparison of radiographs of the powder, which the works had submitted for examination (*fig. 5a*), and of pulverised natural corundum (*fig. 5b*) showed that both substances had the same arrangement of lines. It follows from this that at least 90 per cent of the aluminium oxide is present as the corundum modification. From the presence of individual dots on the lines in fig. 5a (see the second article in this section, in No. 2 of this Review, p. 60) it may be furthermore concluded that the crystals of aluminium oxide in the technical product are at least in part greater than 10 μ.

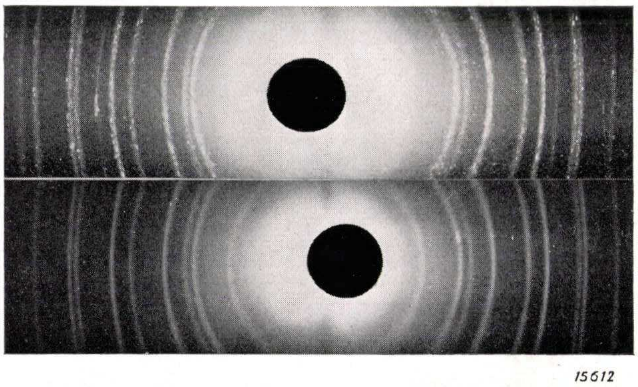

Fig. 5. Identification of a modification of aluminium oxide as corundum.
a) Aluminium oxide (initially of unknown modification)
b) Pulverised natural corundum

---

[2] The above example is not of a practical nature, but has been included here merely to bring out the fundamental difference between the potentialities of X-ray and chemical analysis.

ABSTRACTS OF RECENT SCIENTIFIC PUBLICATIONS OF THE N.V. PHILIPS' GLOEILAMPENFABRIEKEN

No. 1059: M. J. O. **Strutt** and A. **van der Ziel**: Messungen der charakteristischen Eigenschaften von Hochfrequenz-Empfangsröhren (Elektr. Nachr.-Techn. **12**, 347-354, Nov. 1935).

For a variety of commercial and other high-frequency penthode valves the authors have measured the input and output impedances, the slope and the reaction of the anode on the grid in the short-wave range. In this range the damping at the input and output is inversely proportional to the square of the frequencies. Up to a frequency of approximately 60 megacycles, the slope is still roughly equal to its statical value. The reaction of the anode on the grid can be represented by a capacity which with long waves roughly agrees with its static value. On shortening the wavelength the reaction diminishes and many in fact change its sign. At very high frequencies its absolute value increases in proportion to the square of the frequency. It appears that the pentodes (type AF 3) investigated are quite suitable for high-frequency amplification up to wavelengths op 7m as used for television purposes.

No. 1060: J. **van Niekerk**: Evaluation of the relative toxic effects of large doses of Calciferol and the crystalline antirachitic preparation substance L (Arch. néerl. de physiologie de l'homme et des animaux **20**, 559-561, Dec. 1935).

It was found that the ratio of the toxic to the antirachitic dose with **Reerink** and **van Wijk**'s preparation is almost the same as with Calciferol. For the smallest toxic dose the author has obtained roughly the same value as other investigators.

No. 1061*): M. J. **Druyvesteyn**: Der positive Ionenstrom zur Glühkathode einer Gasentladung (Phys. Z. Sowjetunion **8**, 579-581, Nov. 1935).

Various investigators have measured the positive ionic current in discharges through gases with a cold probe-electrode. They have also determined the electronic emission of the heated probe-electrode, which is raised e.g. to a potential about 7 volts lower than the surrounding plasma. If it was then found that the discharge was not affected by electronic radiation at a certain distance from the cathode, some investigators assumed that the ionic current flowing towards a heated cathode was the same as that to a cold one. The author points out that this assumtion is untenable and from measurements made by **Gvosdover** concludes that the ionic current flowing to a heater electrode is roughly double that flowing to a cold one. For the ratio between the electronic and ionic currents using a hot cathode the author obtains the value 200, which is in better accord with the plasma theory of **Langmuir** than the value of 400 which **Gvosdover** deduces himself from his measurements.

No. 1062: K. F. **Niessen**: A contribution to the symbolic calculus (Phil. Mag. **20**, 977-997, Suppl. Nov. 1935).

New methods are given for deriving from a function and its operational transformation certain new functions which are inter-related as "original" and "operational image". For certain "images" of simple form this method enables the original to be deduced. The new operational relationships finally give new mathematical relationships.

No. 1063: J. M. A. **van Liempt**: Eine Beziehung zwischen Umwandlungswärme und Umwandlungspunkt bei enantiotropen Modifikationen (Rec. Trav. chim. Pays-Bas **54**, 934-936, Dec. 1935).

On the basis of the equality of the sublimation velocities of two enantiotropic modifications at the transition temperature, a formula is deduced for the relationship between the heat of transformation and the transition temperature. This formula was tested for tin and suphur. Sufficient data regarding the specific heats of these elements as a function of the temperature are, however, lacking and preclude a thorough test of the formulae derived. It appears, however, that values of the correct order of magnitude are obtained on calculation of the above relationship.

---

*) A sufficient number of reprints for purposes of distribution is not available of those articles marked with an asterisk (*). Reprints of other papers may be obtained on application from Philips Laboratory, Kastanjelaan, Eindhoven, Holland.

VOL. 1 No. 6 JUNE 1936

Philips Technical Review

DEALING WITH TECHNICAL PROBLEMS
RELATING TO THE PRODUCTS, PROCESSES AND INVESTIGATIONS OF
N.V. PHILIPS' GLOEILAMPENFABRIEKEN

EDITED BY THE RESEARCH LABORATORY OF N.V. PHILIPS' GLOEILAMPENFABRIEKEN, EINDHOVEN, HOLLAND

A CONTROLLABLE RECTIFIER UNIT FOR 20 000 VOLTS/18 AMPERES

By J. G. W. MULDER and H. L. VAN DER HORST.

Summary. The use of relay valves enables the construction of highly-efficient controllable rectifier units. In this article a controllable rectifier unit for 20 000 volts / 18 amperes is described for feeding the transmitting valve of a high-frequency furnace with valve generator.

Introduction

Gas-filled rectifying valves are particularly suitable for rectifying high powers. They differ from the high-vacuum valves, which have been given preference in the past, by their much lower internal resistance and correspondingly higher efficiency. At the same time the whole unit is of simple construction, since the cooling arrangements which become very cumbersome with high-vacuum valves for high tensions (dissipation) can be dispensed with.

The relay valves represent an important advance in the design of gas rectifiers. These are gas-filled rectifying valves which, in addition to the cathode and anode, also have a control grid with the aid of which the ignition voltage of the valve can be regulated within wide limits with a very small power consumption (low grid voltages and small

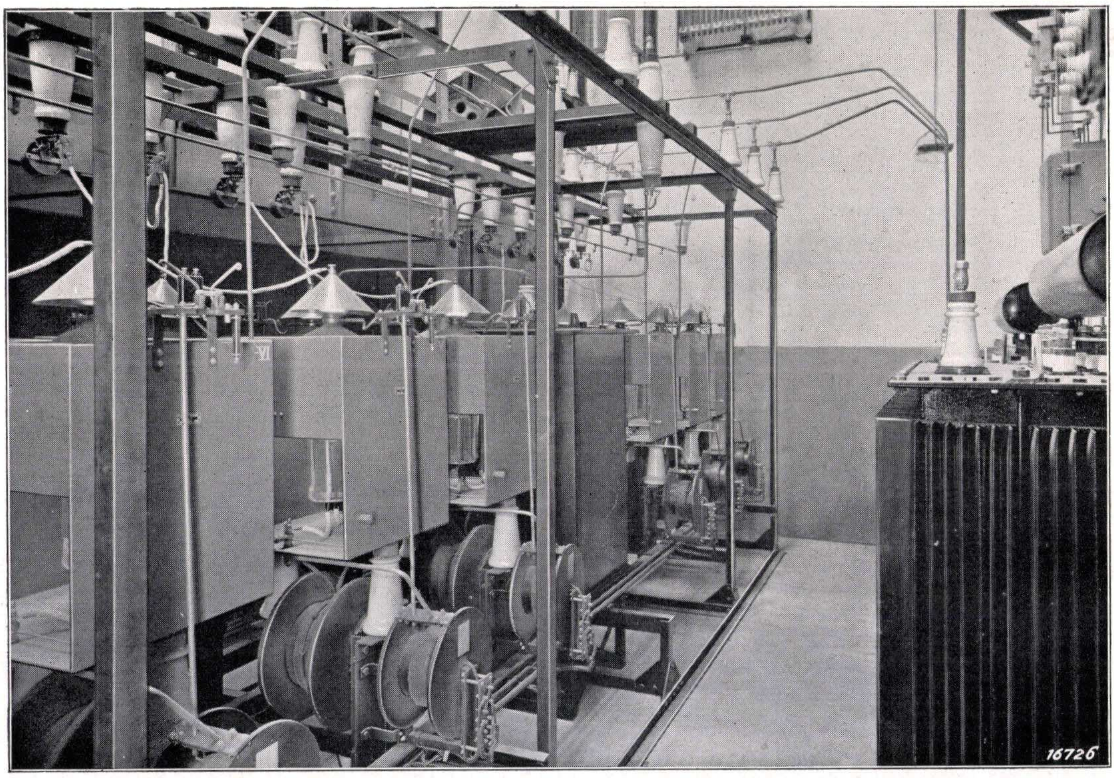

Fig. 1. General view of the 20-kilovolt, 18-ampere rectifier unit. On the right is one of the two high-tension transformers furnishing the anode voltage. On the left are the rectifying valves, which are screened by metal walls against electric fields. The anodes are shown above. Below are the heating current transformers (left coils) and the grid voltage transformers (right coils).

grid currents). By means of these relay valves the continuous voltage furnished by the unit can be controlled and regulated in a very simple manner, without the need for opening or closing any contacts whatsoever in the high-tension circuit.

A description is given below of a rectifying unit equipped with relay valves (*fig. 1*), which feeds the transmitting valve of a high-frequency furnace with valve generator already described in this Review [1]). On its full load of 20 amps this unit furnishes a D.C. potential of 20 000 volts, which can, however, be adjusted to any desirable lower value merely by turning a phase regulator.

Lay-out of the Rectifying Unit

The lay-out of the rectifying unit is shown diagrammatically in *fig. 2*. It is seen, that the plant is made up of two similar components, each of which furnishes half the voltage and can also be used separately. Each unit is connected to a transformer (T_1, T_2) and contains six rectifying valves, which provide six-phase rectification on a circuit described by Graetz, the current in each phase passing through a pair of valves connected in series.

The transformer primaries are connected in delta (380 volts) and the secondaries in a star circuit, 7400 volts against the neutral. These circuits are both of exactly identical design, although the secondaries carry different voltages against earth. This offers the advantage, that only one transformer of half the capacity of the whole unit is sufficient as a spare.

The pulsating direct current charges the 2μF condenser C, which at the same time is discharged through the transmitting valve Z connected in parallel. The anode current of the transmitting valve must also pass through the 100-millihenry choke coil L_2, which protects the rectifier against the high-frequency alternating voltage of approximately 7000 cycles generated at the transmitting valve. The large choke coil L_1 (1 henry) serves for smoothing the current which charges condenser C and hence also the D.C. potential applied to the transmitting valve. The resistance $R = 50$ ohms, which is in series with L_1, limits the anode current in the event of any transient irregularities at the transmitting valve.

The rectifying valves B_1 — B_{12} can each furnish a mean D.C. of 6 amps, so that the whole unit can carry a load of 18 amps. These valves are shown only diagrammatically in the circuit diagram by arrows. The detailed drawings of the valves B_3 and B_6 show the indirect heating of the cathode by means of a separate filament transformer for each valve, as well as the supply of an alternating voltage to the control grid through the transformers t_3, t_6 and the phase-shifters F_1, F_2.

These phase-shifters used, consist of a stator and a rotor, which are adjusted and secured by means of a worm transmission. The rotating field generated by the stator intersects the rotor windings earlier or later, according to the position of the rotor with reference to the stator. By altering the position of the rotor, the phase displacement of the rotor voltage against the stator voltage can thus be altered.

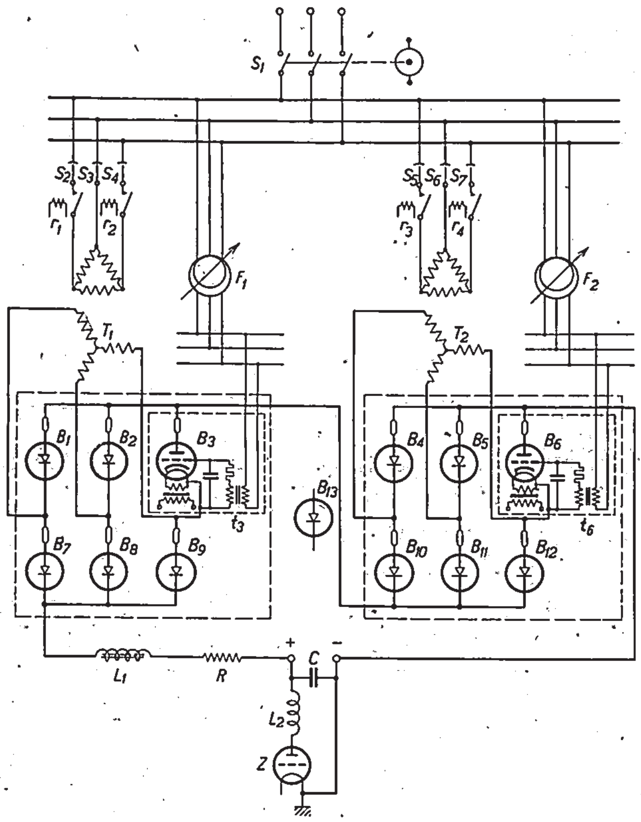

Fig. 2. Electrical lay-out of the rectifying unit. The unit consists of two 10-kilovolt, 18-ampere components, which are connected in series. The rectifying valves B_1 to B_{12} (type DCG 5/30) serve as relay valves. The grid voltage is taken from the phase-shifters F_1 and F_2 through the transformers t_1 to t_{12}. (In the circuit diagram only t_3 and t_6 are shown, since the remaining valves are indicated only diagrammatically). The choke coil L_1 and the condenser C serve for smoothing the D.C. potential furnished. The choke coil L_2 protects the rectifying unit against high-frequency oscillations from the transmitting valve.

The voltage systems of the stator and rotor are both three-phase. The grids of the rectifying valves are connected to the rotor in such a way that the grid voltage of all the valves has the same phase displacement against the corresponding anode voltage.

---

[1]) Philips techn. Rev. 1, 53, 1936.

The action of the phase of the grid voltage in regulating the voltage of the rectifier is discussed in detail in the section dealing with this matter.

Construction of the Rectifying Valves

The rectifying valves used are Philips relay valves type DCG 5/30 with hot cathode and with mercury vapour as a gas filling, whose main electrical characteristics have already been described in a separate article in this Review [2]). The valve, which is shown in *figs. 3* and *4*, is made up of two glass bulbs b_1 and b_2, which are fused to the much narrower chrome-iron ring r. The top bulb b_2 contains the anode a, and the lower bulb b_1 the indirectly-heated hot cathode k. The lower bulb terminates in a cylindrical neck h containing liquid mercury, the temperature of which is only slightly above the ambient temperature. The vapour pressure of the mercury in the cold state is a few thousandths of a millimetre. The ring r serves as a control grid, its voltage differing from that of the cathode by not more than a few hundred volts. In addition the presence of this ring increases the back-firing voltage of the valve. For this purpose a funnel-shaped extension t is provided, which is shaped to conform with the conical anode a. The distance between the funnel and the anode is roughly the same at all points, the optimum distance to obtain a high back-firing voltage being fairly critical, for in the negative phase practically the whole reverse voltage is applied across the funnel and the anode. If this distance is too large, back-firing may occur since the electrons in the gas-space are given every opportunity to ionise, whilst with too small a distance the field strength and

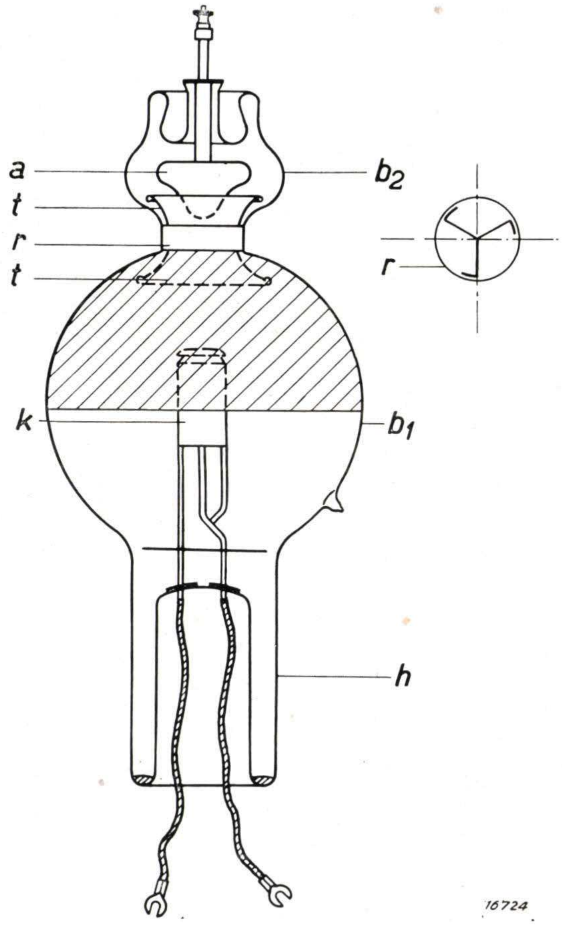

Fig. 3. Relay valve type DCG 5/30 with mercury vapour discharge. a is the graphite anode, k the indirectly-heated cathode, and r the control grid subdivided by partitions, with the funnel-shaped extension t. The upper half of the bulb b_1, is covered on the inner side with a conductive coating which is connected to the control grid. The liquid mercury is in the neck h at the bottom.

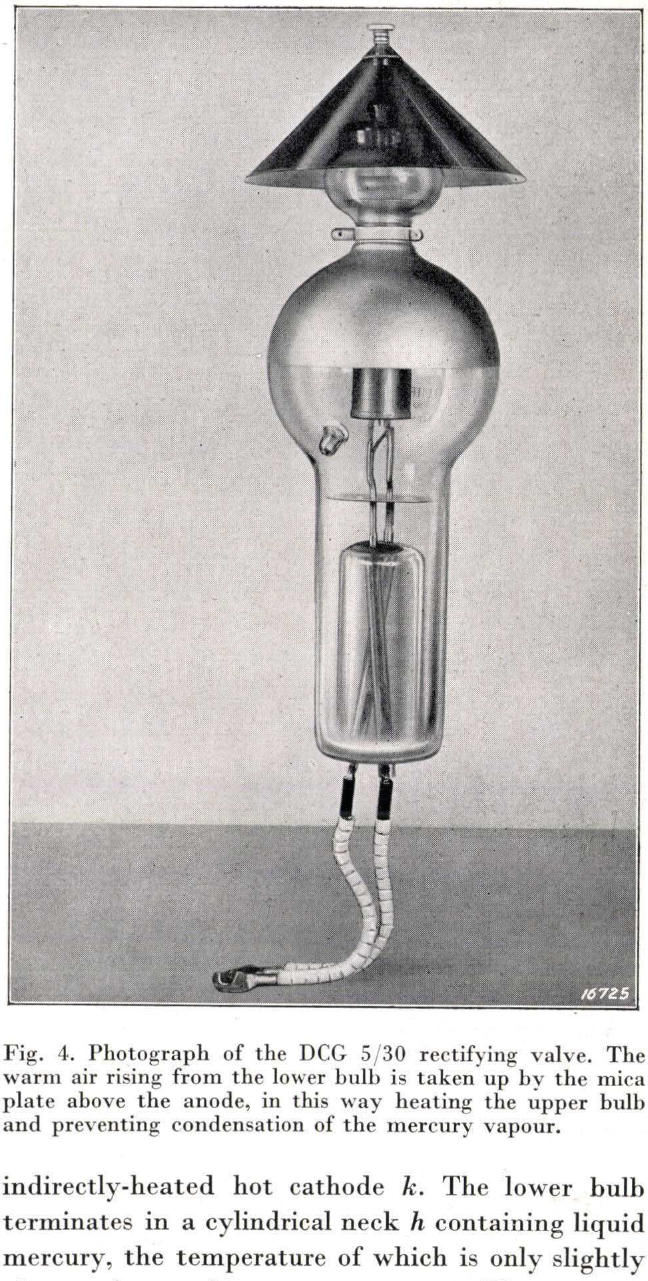

Fig. 4. Photograph of the DCG 5/30 rectifying valve. The warm air rising from the lower bulb is taken up by the mica plate above the anode, in this way heating the upper bulb and preventing condensation of the mercury vapour.

---

[2]) Relay valves as timing devices in seam-welding practice, D. M. Duinker, Philips techn. Rev. **1**, 11, 1936. Since the publication of this article the construction of the DCG 5/30 valves has been slightly altered. The inside wall of the bulb enclosing the cathode has been coated with a conductive layer, which is connected to the control grid. Owing to this change the characteristic (ignition voltage plotted as a function of the grid voltage) is no longer identical with that shown in fig. 1 of the article cited above. The grid voltage required for ignition in the modified valve is approximately 18 volts and is practically independent of the anode voltage.

hence the danger of auto-electronic emission from the anode are considerably enhanced.

The temperature of the ring is determined mainly by the radiation of heat from the hot cathode and by the anode current. To avoid excessive heating, when the valve is running on full load, the width of the ring has had to be made larger, than appeared desirable, to make sure of suppressing back-firing between the anode and cathode. It was therefore found advantageous to subdivide the aperture of the ring as shown in fig. 3, so that in place of an open ring there are three parallel, narrow tubes.

Electrical Characteristics

The permissible mean working current of the relay valve DCG 5/30 is 6 amps. The voltage-drop at the discharge is about 16 volts and is practically independent of the current intensity. The ignition voltage is not appreciably greater with a sufficiently high potential at the control ring. If, on the other hand, the grid voltage is reduced below 18 volts, the ignition voltage will rise abruptly to more than 10 000 volts, so that with the available transformer voltage ignition is no longer obtained. When, however, ignition has once taken place the discharge cannot be extinguished by merely reducing the control voltage. The discharge is only extinguished, when the alternating voltage at the anode passes through zero.

Voltage Regulation

The phase displacement of the grid voltage V_g of the relay valve with respect to the anode voltage V_a determines the moment of ignition in each positive phase of V_a and hence the average value of the output voltage of the cycle. This is due to the fact that, as already stated, ignition is only obtained when the grid voltage exceeds a certain critical value V_c (of about 18 volts).

Fig. 5 shows the action of the phase-shifter in the case of one single valve V_a is the anode voltage, V_g the alternating grid voltage, V_c the critical grid voltage, and α the phase-lag of the grid voltage against the anode voltage. In case (1) V_g and V_a are in-phase. The discharge is obtained when V_c exceeds the critical value ($\omega t = \varphi$). To fix satisfactorily the moment of ignition, also with small fluctuations of V_c, the alternating grid voltage should be several times greater than the

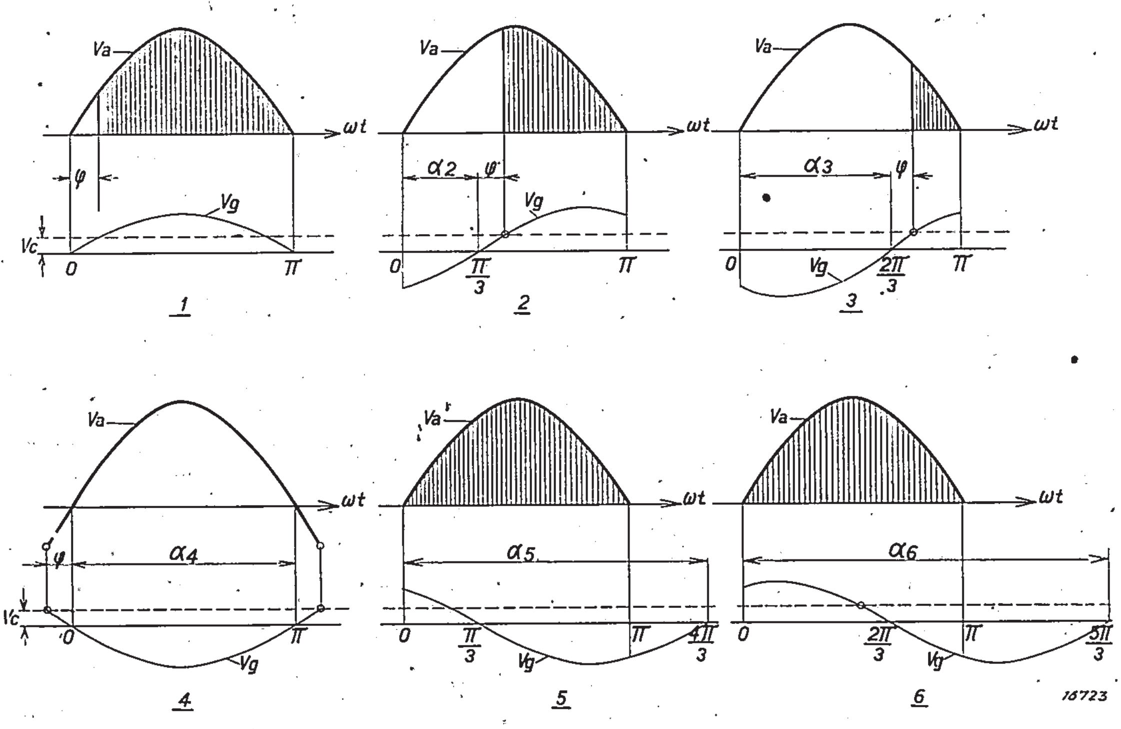

Fig. 5. Ignition sequence of a relay valve with the alternating anode voltage V_a and the alternating grid voltage V_g. V_c is the critical grid voltage. α is the phase lag of the grid voltage with respect to the anode voltage.

1) $\alpha_1 = 0$ Current passes almost during the whole positive phase from $\omega t = \varphi$ onwards.
2) $\alpha_2 = \pi/3$ Current passes from $\omega t = \pi/3 + \varphi$ onwards.
3) $\alpha_3 = 2\pi/3$ Current passes from $\omega t = 2\pi/3 + \varphi$ onwards.
4) $\alpha_4 = \pi$ Grid voltage in opposing phase. No current passes.
5) $\alpha_5 = 4\pi/3$
6) $\alpha_6 = 5\pi/3$ } Current passes throughout the positive phase.

critical voltage (e.g. 100 volts). The current passes during the greater part of the positive phase of the anode voltage, as indicated by the shading. As the phase retardation increases ($\alpha_2 = \pi/3$, $\alpha_3 = 2\pi/3$) the portion of the period during which current passes is reduced. If V_g and V_a are in counter phase ($\alpha_4 = \pi$) no current at all flows. If the phase retardation is further increased, then at $\alpha = \pi + \varphi$ the current suddenly commences to pass with its maximum value; it continues to flow during the whole positive half of the cycle of the anode voltage, although the grid voltage has in the meantime dropped below the critical value and even become zero. When ionisation has once taken place, the grid is inactive. In *fig. 6* the average D.C. potential V_0 furnished by a single valve is plotted as a function of the phase retardation α. The points *1* to *6* correspond to the cases represented in fig. 5.

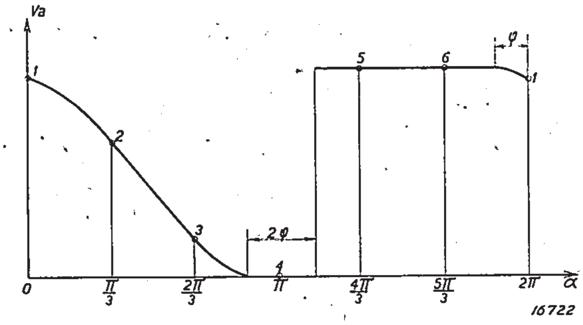

Fig. 6. Average D.C. potential V_0 plotted as a function of the angle of lag α between the alternating grid voltage and the alternating anode voltage. Points *1* to *6* correspond to the special cases of fig. 5.

Safety Precautions in the Rectifying Unit

The operation of the fairly extensive plant of high-tension transformers, rectifying valves, transmitting valve, high-frequency oscillating circuits and melting furnaces has been considerably simplified by the adoption of suitable safety precautions and the provision of automatic auxiliary equipment. In addition these protect the transformers, the rectifying valves and the transmitting valve against overloads, which might result, when the switches are operated in the wrong order.

The protection of the high-tension transformers against overloads is afforded by the adjustable maximum-current relays (r_1—r_4, fig. 2), which are inserted in two of the three primary conductors. If one of the maximum-current relays operates the main switch is tripped.

The rectifying valves must be protected against anode voltage, being applied before the cathode having reached operating temperature. For this purpose a slow-acting relay is provided, which is connected in parallel with the heating transformers. The main switch can only be closed after this relay has been under tension for 6 minutes. In cold situations it is advisable to extend this time from 10 to 15 minutes. Although after 6 minutes the cathode has been sufficiently heated, the vapour pressure of the mercury is still very low. With too low a vapour pressure the arc voltage is too high, and as this might adversely affect the cathode, it is desirable to wait before switching on the anode voltage until the whole bulb, as well as the mercury in the neck at the bottom, has become sufficiently heated to raise the vapour pressure of the mercury to the required value.

The transmitting valve is protected against overheating by means of a so-called "water lock" which prevents the heating current or the anode current from being applied, if the flow of cooling water is not adequate. Moreover, the heating current can only be switched on, when the regulating device is adjusted to the minimum voltage. The anode is protected in a similar way. The anode voltage can only be switched on, when the phase-shifter for voltage control is at its minimum setting. Regulating the output voltage to its maximum value by turning the phase-shifter takes only a few seconds. The anode is also protected against overloads, which might occur if the anode voltage is applied before the valve can oscillate. This is, for instance, the case when the electrical connection with the furnace is broken, which takes place automatically when the furnace is tilted from its vertical position for casting operations.

THE PERCEPTION OF BRIGHTNESS CONTRASTS IN ROAD LIGHTING

By P. J. BOUMA.

Summary. The two essential factors in the perception of brightness contrasts are:

1) Contrast sensibility, which determines the smallest still perceptible contrasts and depends on the brightness; at equivalent apparent brightnesses it is practically the same for all colours.
2) Richness of contrast (the relative intensity of stronger contrasts). It is shown, that the marked differences existing between the various types of light are related to the Purkinje phenomenon, which accounts, inter alia, for the marked richness of contrast with sodium light at the brightness levels commonly obtained in road lighting. After introducing a measure R for the richness of contrast, the lines of equal R are plotted in a brightness-wavelength diagram (*fig.* 5).

The perception of an object on the highway is always fundamentally the perception of contrast: The object is seen, because it has a brightness, different from that of the road surface against which it stands out. In addition to this contrast in brightness, colour contrast may also play a part, the object and the background having different colours. This factor is, however, of secondary importance for the following two reasons:

1) Because most objects (just as the road surface itself) usually possess very unsaturated (not very pronounced) colours on illumination with non-monochromatic light;
2) Because the low brightnesses, possessed by most dark objects standing out dark against the road surface, cause the colours to appear paler still (in addition to the photopic (or cone) vision which differentiates between colours, the non-chromatic scotopic (or rod) vision already plays a part).

In the present article, we shall consider only brightness contrasts and must therefore discuss the conditions under which the eye can still perceive a brightness contrast and when it is liable to fail in fulfilling this function. This failure may be due to two different causes:

1) Because the existing contrast is too small, i.e. the two brightness values differ by so little, that even with keen and prolonged focussing the eye is unable to perceive the object in question; in this case the contrast sensibility of the eye is obviously not great enough to observe the object.
2) Because the contrast, although much greater than the minimum value required for perception of the object by keen and prolonged focussing, is still so low that the object escapes observation altogether or is not perceived in time, because the perception requires a certain time, a fairly accurate focussing and a certain measure of concentration. In this case we say that the richness of contrast is insufficient for satisfactory and quick perception.

In this first case, we are thus dealing with a minimum contrast, which the eye can still just perceive under favourable conditions, whilst in the second case we are concerned with the more or less pronounced occurrence of stronger contrasts.

Both cases have an important bearing on road lighting and we shall therefore discuss them in turn.

The contrast sensibility at a specific brightness H is defined as follows: If a brightness $H + \Delta H$ can still be just differentiated from H, the ratio $H/\Delta H$ is termed the contrast sensibility (K). This contrast sensibility is determined by a large number of factors, of which the principal are the following:

1) The brightness H.
2) The colour of the light.
3) Size and shape of the two fields under comparison.
4) Use of an artificial or natural pupil (viewing through a small diaphragm placed before the eye or with the naked eye).
5) Individual differences.
6) Method of measurement.
7) Disturbing factors, such as incorrect adaptation, presence of dazzling sources of light in the field of view, after-images, etc.

In the case of 3) above, we assume, that the fields are taken so large that practically the whole retina is adapted to the brightness H; where use is made of an artificial pupil 4) specific mention is made in every case. Regarding the method of measurement 6), the following should be noted: The usual measurement made is the determination of what additional brightness ΔH must be impressed on a part of the field of view, in order to make this portion appear just a little brighter than the surrounding areas, which have a brightness H (direct method). In some cases the mean error in photometric adjustment is taken as a measure of the contrast sensibility (indirect method). The results obtained with these two methods may differ considerably; we always employ the direct method ourselves.

It is assumed, that the disturbing factors enumerated under 7) (which may be referred to by the general term of "glare") do not occur and therefore do not require consideration.

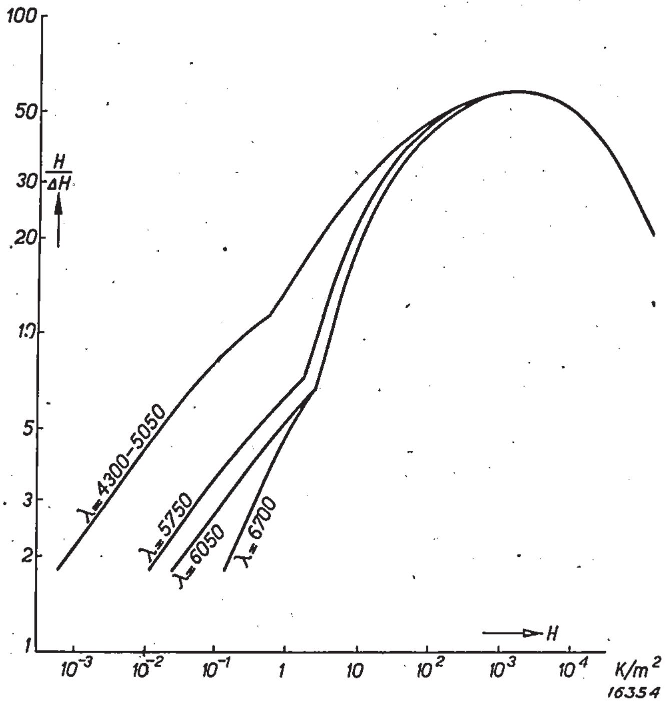

Fig. 1. Contrast sensibility $H/\Delta H$ plotted as a function of the brightness H in candles per sq. m, for monochromatic light of different wavelengths λ (König).

Fig. 1 based on measurements made by König indicates the general variation of contrast sensibility with the brightness and its relation to the colour of the light. In this figure $log(H/\Delta H)$ is plotted as a function of $log\ H$ for monochromatic light of different wavelengths. H is expressed in candles per sq. m; an artificial pupil of 1 sq. mm was used in these measurements. The following characteristics are deducible from the curve:

1) There is an area, where $H/\Delta H$ varies only slightly with the brightness (only in this range does the Weber-Fechner law apply).
2) Both at lower and at very high brightness values the contrast sensibility diminishes.
3) The curves are made up of two parts, which meet at an angle. This is probably due to the fact, that below this point the rods have the greater contrast sensibility and hence are mainly responsible for vision, whilst above this point the cones are mainly operative.
4) At high brightness values the contrast sensibility K is independent of the colour, whilst at low brightnesses a much greater brightness of red rays than of blue rays is required, in order to obtain the same K.

A greater brightness of red light than of blue light [1]) is also necessary for obtaining an equivalent apparent-brightness in this range (Purkinje phenomenon), and so it appears interesting to examine, what trend the curves would have if K were plotted as a function not of the brightness H but of the apparent brightness h. This is done in *fig. 2*. (In this figure the conversion has also been made from the artificial to the natural eye-pupil, so that fig. 2 relates to the perceptions obtained with the eye proper). All curves in fig. 1 are now reduced to a single curve, of which individual measurements in no case differ by more than 20 per cent, i.e. the contrast sensibility at a specific apparent brightness is practically independent of the colour of the light. The causes of small deviations which might occur will be discussed in more detail below.

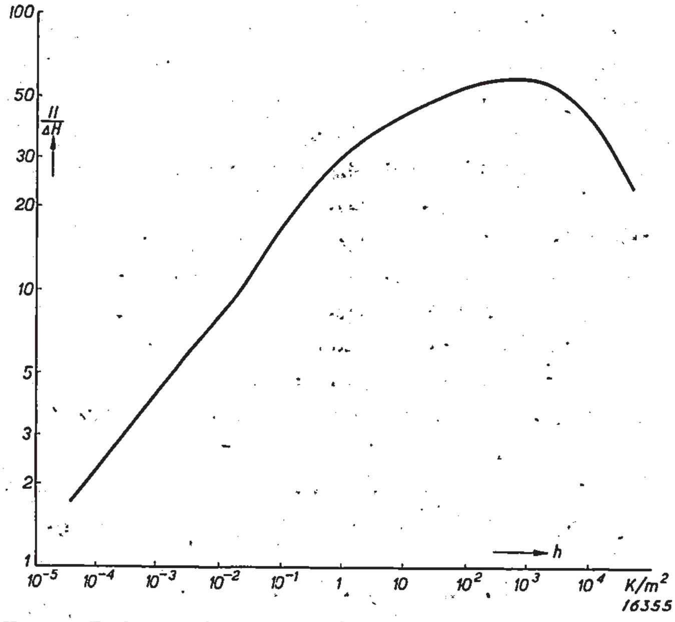

Fig. 2. Richness of contrast $H/\Delta H$ plotted as a function of the apparent brightness h in candles per sq. m; this curve applies within close approximation to all types of light.

A large number of recent measurements with very different types of light (monochromatic light, incandescent lamp light, mercury vapour light, etc.) on correct conversion [1]) are also in very satisfactory accord with fig. 2.

---

[1]) Regarding the definition of brightness H and apparent brightness h and the quantitative connection between these two magnitudes cf. Philips techn. Rev. **1**, 144, 1936.

From the above the following conclusions of a practical nature may be deduced:

1) Since in road lighting we are always dealing with a range of illumination in which K is still closely dependent on h, every increase in the level of apparent brightness will permit an increase of K and hence an improved perception of low-contrasting objects.
2) As long as the apparent brightness of the road surface does not drop below 0.3 candle per sq.m, practically the same h and hence almost the same K is obtained for lights of different colours with the same H, i.e. there are no marked differences in contrast sensibility at equivalent values of H for different coloured rays.

In considering the second point, the richness of contrast, we have to compare much greater contrasts than the above, and we must consider the question:

If the same road is illuminated in succession with two different types of light having equal intensities, can the contrasts in the one case be still more pronounced than in the other?

It is found, that this is indeed the case and as an example, illumination with sodium light and with white incandescent lamp light may be considered. In the first case we see dark objects stand out blacker from the road surface than with the second type of illumination. How can this be explained from the characteristics of the eye? The most obvious explanation would be, that the coefficients of reflection of dark objects on the highway are much lower with sodium light than with white light; at equivalent intensities of illumination objects would thus have a much lower brightness in sodium light. Extensive measurements of the coefficients of reflection, with different types of light, have however shown that such differences do not in fact exist. We must therefore assume that the brightness of dark objects is about the same in both cases; yet we see them darker with sodium lighting, i.e. the apparent brightness is in this case smaller. This interpretation suggets immediately a relationship with the Purkinje phenomenon [2]).

For a more precise investigation we must know the relationship between the brightness H, the apparent brightness h and the wavelength λ for monochromatic light (see *fig. 3* based on measurements by König and showing the lines of equivalent apparent brightness h drawn in an H-λ diagram).

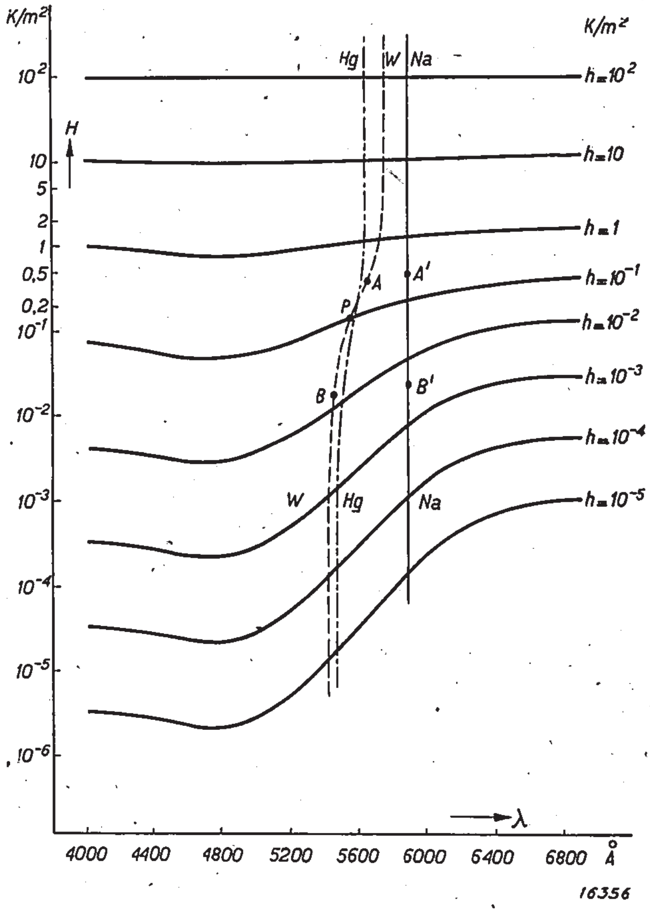

Fig. 3. Relationship between brightness (H) and apparent brightness (h) for incandescent lamp light (W — — —), mercury light (Hg — · — · —) and monochromatic light, inter alia sodium light (Na —).

From the measurements of König, there can also be deduced the apparent brightness h corresponding to every brightness H for a composite type of light, e.g. incandescent lamp light, which may be assumed to have a black body temperature of 2700 deg.K. Each pair of values of h and H determines a point in the diagram shown in fig.3 (that a brightness of 0.13 candle per sq. m of white light corresponds to an apparent brightness of 0.10 candle per sq. m gives for instance the point P). By connecting all points determined in this way by a curve, a line(— — —) is obtained indicating the behaviour of white light (W). The second line (— · — · —) showing the corresponding conditions for mercury light (*Hg*) was obtained in the same way. In general a composite source of light is indicated in our diagram by a curved line and a monochromatic light by a vertical line.

---

[2]) The contrasts may here also be influenced by another effect, though one of secondary importance only, viz, the fact, that blue light is dispersed in the eye to a slightly greater degree than other light-rays. This may result in small dark objects being veiled by dispersed light, when illuminated with white light; with sodium light this effect is much less pronounced.

[3]) The wavelength λ determined by this point signifies in a physical sense that white light behaves, as regards the ratio h/H, in exactly the same manner as monochromatic light of this wavelength λ.

To explain from the diagram the better contrasts obtained with sodium light, consider the following simple experiment (*fig. 4*). Two semicircular spots of light are projected on a sheet of white paper, the left half (AB) of white light and the right hal, ($A'B'$) of sodium light. The intensities of illumination are so adjusted, that the two apparent brightnesses are the same, e.g. 0.3 candle per sq. m. Now place on the lower half (BB') a piece of black cloth, whose coefficient of reflection is for example 20 times smaller than that of the paper. A remarkable result is then observed, viz, that whilst A and A' appear equally bright, the quadrant B' appears much darker than the quadrant B, in other words the "sodium contrast" $A'B'$ is much more pronounced than the "white contrast" AB.

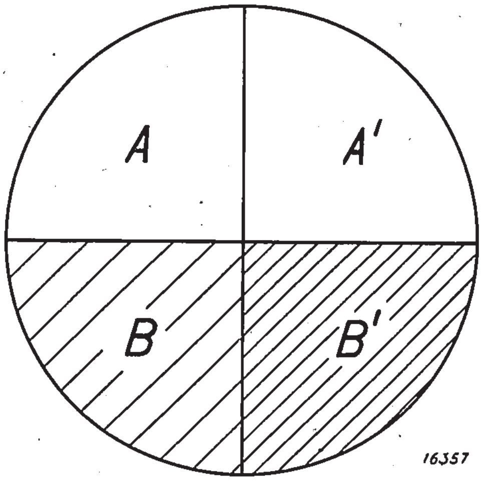

Fig. 4. Demonstration of the greater richness of contrast with sodium light:

AB	white light	$A'B'$	sodium light
AA'	white paper	BB'	black cloth.

If A' is as bright as A then B' appears much darker than B.

This phenomenon can be directly explained from fig. 3, in which the four points are indicated showing the conditions in the quadrants $ABA'B'$. The two points A and A' both lie on the curve $h = 0.3$ candle per sq. m, and correspond to brightnesses $H = 0.390$ and 0.474 candle per sq. m respectively. The points B and B' should have a brightness 20 times smaller, viz, $H = 0.0195$ and 0.0237 respectively (the vertical distance between A and B on a logarithmic scale is thus equal to that between A' and B' in the diagram). It is seen that an apparent brightness $h = 0.0138$ corresponds to the point B and a value $h \doteq 0.0036$ to the point B'. It is actually found that the apparent brightness of the quadrant B' is much lower than that of B.

In exactly the same way the better contrast obtained on sodium-lighted roads can also be explained. The two road surfaces then correspond to the quadrants A and A', and the dark objects to quadrants B and B'; the object B' stands out much more strongly from road A' than object B from road A.

Since this phenomenon is fundamentally due to the displacement of the visibility curve of the eye, it follows that it will only occur when at least one of the two brightnesses is situated in the range in which such displacement takes place. This effect thus disappears at both high and very low brightnesses. In road lighting we are in a very favourable range, for the brightness of the road is of the order of 0.3 candle per sq. m and is thus near the top of the displacement range, whilst that of the object is usually much lower in the transition region. Between these two brightnesses there is an appreciable Purkinje displacement, which intensifies the contrasts when using sodium light.

A still closer insight into these conditions is obtained by introducing a measure for the richness of contrast, and for this purpose we have again drawn the function connecting H, h and λ in *fig.5*. How can we obtain a physiologically correct measure for the contrast between, say the points P and Q, which both represent a definite brightness with light of 5350 Å? Neither the difference in energy nor the energy ratio (the length PQ in fig. 5) is a measure of the contrast which can claim physiological accuracy; the best measure for the contrast between P and Q is the number of steps of just perceptible difference in apparent brightness between P and Q. Thus, on the line $\lambda = 5350$ Å we must locate the points, which are separated by one step (in the figure each tenth point is marked), and assume that through all these points the curves of equivalent apparent brightness have been drawn [4]). Each curve is given a number n (numbering commencing from $n = 0$ for the absolute threshold value); these numbers have been inserted on the left-hand side of the curves.

We thus establish the fact, that the contrast between two points of the diagram applying to the same type of light is $n_1 - n_2$, when the curve with number n_1 passes through one point and the curve with number n_2 through the other point.

The contrast between P and Q in fig. 5 is thus 20, that between $h = 0.878$ and $h = 0.0239$ is 80 for every type of light, and those between A and B

---

[4]) These curves thus belong to the family of curves shown in fig. 3.

and between A' and B' in fig. 3 are 55 and 67 respectively. The definition is in agreement with the requirement: Two contrasts PQ and $P'Q'$ are equal, when P and P' and also Q and Q' each have the same apparent brightness.

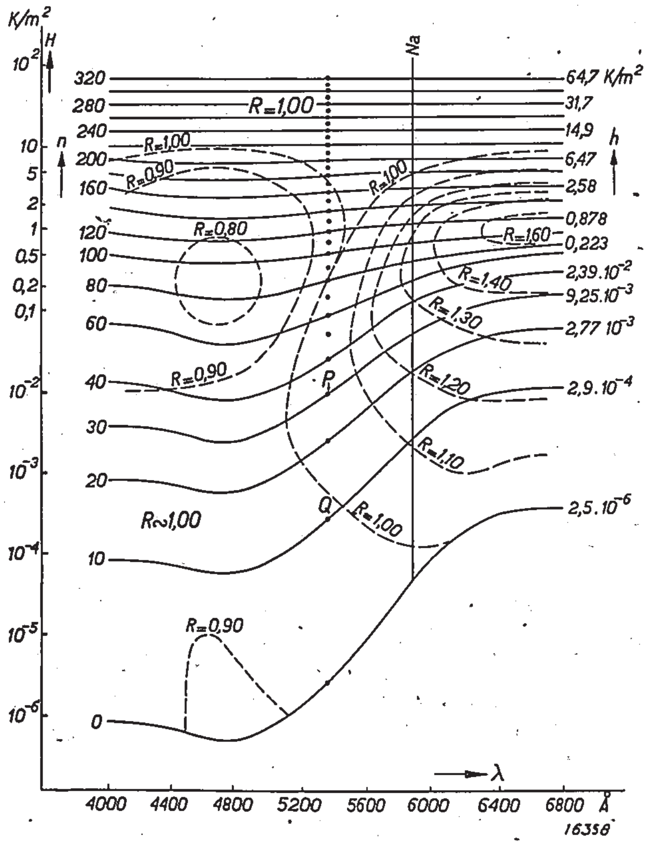

Fig. 5. H-λ diagram with lines of equivalent apparent brightness h (——) and lines of equal richness of contrast R (- - -). For sodium light the maximum value of R (1.33) is at $H = 0.3$ candle per sq. m, whilst for white light R is everywhere equal to unity.

The richness of contrast R of a specific type of light with a given apparent brightness h_0 is defined as the quotient of the contrast obtained by reducing the brightness by a factor 5, and the contrast with white light between the apparent brightness h_0 and the apparent brightness obtained when again the brightness is reduced five times. (The factor 5 is a common ratio of brightness on highways).

Thus, for every point in the diagram we can determine in this way the richness of contrast R and plot the curves for equivalent R, as has been done in fig. 5. The following is noted:

1) For very low and high brightnesses, the richness of contrast is practically equal to unity, i.e. it is the same for all colours as for white.
2) The maximum richness of contrast is obtained at the greatest wavelengths (red) at apparent brightnesses of 0.3 to 0.6 candle per sq. m.
3) The richness of contrast is lowest at the short wavelengths (blue) for an apparent brightness of approximately 0.3 candle per sq. m.
4) For sodium light the richness of contrast assumes its greatest value at a brightness of about 0.3 candle per sq. m., i.e. just at those brightness values, which occur most frequently on road surfaces.

The richness of contrast for white light is according to definition always equal to unity; the richness of contrast for mercury light is nearly the same since the mercury curve (Hg) and the curve for white light (W) in fig. 3 differ very little from each other. Actually in practice the use of mercury light does not improve the contrast obtained. Too much importance must not be attached to the marked richness of contrast in the extreme red, because the reduced sensitivity of the eye in this range of wavelengths makes the use of this kind of light of little use in practice.

In conclusion, it may be noted, that it is reasonable to expect that at a specific apparent brightness a greater richness of contrast is accompanied by a somewhat greater contrast sensibility. This phenomenon has indeed been observed on comparing sodium light and white light: In the region of the Purkinje displacement the contrast sensibility is slightly higher for sodium light, than for white light, at equivalent apparent brightnesses. At equivalent brightnesses no marked differences are observable.

BIBLIOGRAPHY.

Contrast Sensibility:

König, Brodhun, Sitz Ak. Berl. 1888, p. 917 (Gesammelte Abhandl. p. 115). (Contrast sensibility at different brightnesses and wavelengths).

Nutting, Bur. Stand. Bull. **3,** 59, 1907; **5,** 261, 1908. (Contains, inter alia, the evaluated measurements of König).

Stiles, Crawford, Proc. Roy. Soc. B **113,** 496, 1933; **116,** 55, 1934; Nature **132,** 759, 1933. (Contrast-sensibility measurements under very divergent conditions).

Blanchard, Phys. Rev. **11,** 81, 1918. (Measurements of König, supplemented by the author's own measurements).

Houston, Phil. Mag. **12,** 538, 1931. (Comparison of direct and indirect methods of measurement).

Cobb, Trans. Ill. Eng. Soc. **8,** 292, 1913; **11,** 372, 1916. (Effect of brightness of the surrounding area).

Klein, Licht und Lampe 23, 168, 1934; Das Licht 4, 81, 1934. (Comparison between white light and sodium light).

Hecht, Nat. Acad. Sc. Proc. 20, 644, 1934. (Interpretation on the basis of photochemical reactions).

Weigel, Das Licht 5, 211, 1935. (Comparison between the light from incandescent lamps, sodium and mercury lamps).

Bouma, Ingenieur 49, A 290, 1934. (Comparison between white light and sodium light; relationship with the richness of contrast).

Richness of Contrast:

Bouma, Ingenieur 49, A 290, 1934; Licht und Lampe 24, 217, 1935. (Relationship between the richness of contrast and the Purkinje phenomenon).

SOME CHARACTERISTICS OF RECEIVING VALVES IN SHORT-WAVE RECEPTION

By C. J. BAKKER.

Summary. Phenomena are discussed which relate *a*) to the space-charge of electrons in the spaces between the electrodes of a receiving valve, and *b*) to the finite time of transit of the electrons between the different electrodes. On the input side of the valve *a*) causes detuning and *b*) a damping in the input circuit. These effects must be considered particularly with short waves.

A new method of amplification is described, which is based on the induced charge produced by the electrons on an "anode" with negative bias. With short waves this new method is under certain circumstances superior to the standard method of amplification using a "positive" anode.

Introduction

At the present time there is a pronounced tendency to include short waves in the range of wave lengths used for broadcasting. In the following the term short waves is used for all waves with a wave length under 15 m, and in this connection it may be recalled, that waves of approximately 7 m and even shorter are now being employed for television purposes.

In this article a number of the most important characteristics of these short waves are discussed, which must be taken into consideration when using the receiving valves in the short-wave range.

The present discussion will be restricted in the main to three-electrode valves or triodes, but can easily be extended to tubes with more electrodes. The operation of a valve of this type is governed by the laws connecting the alternating currents in the input circuit i_g and the output circuit i_a with the voltages e_g and e_a on the input and output sides. The input circuit is defined here as the circuit connected to the cathode and the control grid, whilst the output circuit is connected to the cathode and the anode. If the alternating voltage e_g and e_a are sufficiently small, then the relationship between the voltages and the currents is linear, i.e. equations of the following form apply:

$$i_a = A\,e_g + B\,e_a$$
$$i_g = C\,e_g + D\,e_a$$

A, B, C and D in these equations are determined by the characteristics of the receiving valve and by the d.c. voltages applied to the anode and the grid.

The coefficient A is the slope or characteristic of the valve, and is a measure of the degree to which the anode current i_a is controlled by the grid potential e_g.

B indicates, which alternating current passes to the anode as a result of an alternating anode voltage e_a. $1/B$ is termed the output impedance of the valve.

The coefficient C determines the alternating current, which flows between the cathode and the grid when the latter is fed with alternating voltage. $1/C$ is termed the input impedance. If the bias of the grid is negative, no direct current can pass from the cathode to the grid. The passage of alternating current is, however, not zero, since the input voltage e_g generates a capacity current between the grid and the cathode. We shall see later, that in spite of a negative bias and particularly at high frequencies a resistance term also appears in the expression for the input impedance in addition to a capacity term.

The coefficient D gives the "reaction", i.e. the action of the anode potential on the grid current.

The current in a receiving valve is conveyed by electrons, which are emitted from the hot cathode. This signifies that electrons are always present in the space between the cathode, grid and anode, and that their density is the greater the larger the number emitted from the cathode per second and the slower the speed at which they move. The effects associated with these electrons existing in the vacuous space (space-charge) and having a finite velocity of translation are of paramount importance, when dealing with ultra-short waves and form the subject of this article.

An important property of the space-charge is its influence on the mutual capacity of the electrodes between which the charge is generated. These capacity variations and their effects are discussed in detail in the section: Variations in Tuning, and in the first part of the theoretical section.

Those phenomena are also dealt with, which are due to the fact, that the electrons in the valve require a short yet finite time-interval to pass from one electrode to another. This signifies, inter alia, that the phase of the anode current will be behind that of the control voltage, the angle of lag increasing with the frequency of the alternating control voltage. The results of these effects are discussed in the section: Damping Effects, and in the second part of the theoretical section.

The influence of both the space-charge and the time of transit of the electrons will be discussed mainly in reference to the input side of the receiving valve. Our investigations will therefore relate exclusively to the coefficient C. It is useful to note that both these effects are more marked here than on the output side. Between the cathode and the control grid the electrons have very much lower velocities than between the other electrodes, owing to the low acceleration voltage (the bias of the control grid is negative). In consequence the space-charge is of greatest density in this area and for the same reason the time of transit from the cathode to the first control grid is large compared with the time of transit between the other electrodes.

Finally, in the section: Induction Effect we shall consider an induction effect produced by the space-charge, which has an important result in six-electrode mixing valves and also in octodes. On this induction effect is based an entirely new method of amplification applicable to ultra-short waves and which will be dealt with in the last section.

Variations in Tuning

As the simplest example consider the circuit of a triode given in *fig. 1.* The following discussion can, however, be applied *pari passu* to multi-grid amplifying valves. The electrode condensers C_{gk} and C_{ga} are in parallel with the condenser of the connected oscillating circuit and hence reduce the natural frequency of the latter. Since the capacity C_{gk} is governed by the space-charge between the cathode and grid which fluctuates with the anode current its effect on the tuning is not constant, and on theoretical analysis it is found, that this space-charge raises the capacity C_{gk}. The increase ΔC_{gk} of the capacity is greatest, when the current is determined by the so-called space-charge equilibrium, i.e. when the filament emits an excess of electrons, so that part of the electrons are forced back to the cathode owing to repulsion sustained from electrons in the intervening space. In this case ΔC_{gk} is independent of the current intensity. In all other working conditions of the valve ΔC_{gk} is smaller.

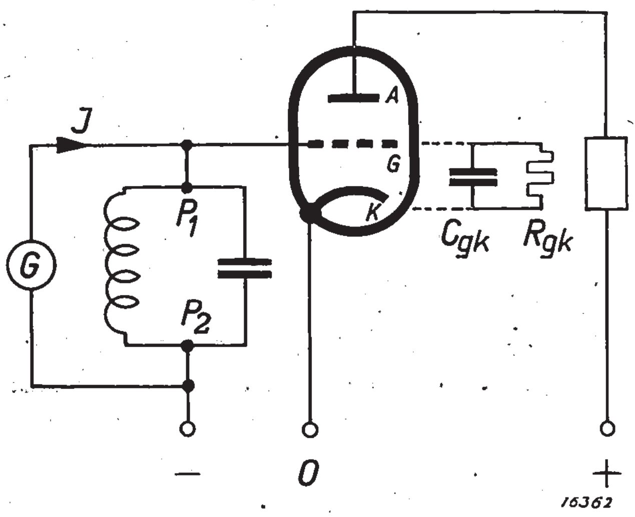

Fig. 1. The input circuit consisting of a self-induction and a condenser is connected with the grid of the triode. The inter-electrode capacity C_{gk} is raised by the space-charge between G and K. As C_{gk} is in parallel with the external capacity, the space-charge affects the tuning of the input circuit. The resistance R_{gk} which bridges the capacity C_{gk} is produced as a result of the finite time of transit of the electrons between K and G. R_{gk} causes a damping of the input circuit which is proportional to the square of the frequency.

Variations in tuning are particularly marked in receivers equipped with automatic volume control, since the latter is so designed that as the aerial signals become more powerful the amplification of the control valves is reduced by increasing the negative bias of the control grid. The control valve has a control grid with a wire winding of variable slope. On raising the negative bias the current is first suppressed at those points of the cathode most closely covered by the winding, which results in a shortening of the emitting cathode and hence in a reduction of the supplementary space-charge capacity, thus producing an alteration in the tuning. The capacity variations ΔC_{gk} in question are of the order of 1 μμF in valves of normal dimensions. They are naturally the greater the smaller the capacity C of the oscillating circuit. In general the capacities used are the smaller the higher the frequency to be picked up. The effect of capacity fluctuations is therefore particularly marked in short-wave reception.

The capacity fluctuations in the receiving valve become the more apparent, the greater the sharpness of tuning of the oscillating circuit, which is detuned by the change in capacity.

Consider the circuit shown in fig. 1. To obtain the maximum alternating voltage e_g at the terminals P_1 and P_2 (i.e. between the grid and the cathode) for a given current intensity I of the generator the impedance R of the oscillating circuit must be as high as possible 1)). The impedance and the sharpness of tuning of an oscillating circuit are, however, closely related to each other, viz, by the equation:

$$R = \frac{1}{2\pi\nu\Delta C}$$

where ν is the natural frequency of the oscillating circuit and ΔC that alteration in capacity in the tuned oscillating circuit which reduces the potential difference between P_1 and P_2 to 70 per cent (more accurately $\sqrt{1/2}$) of its maximum value. With wave lengths exceeding 20 m an impedance $R = 20\,000$ ohms can be readily obtained. Taking this impedance value in a concrete example, and requiring a flatness in tuning $\Delta C \geqslant 1\ \mu\mu F$ (the deviation must be at least this value in order that capacity fluctuations shall not cause detuning), one obtains an upper limit for the frequency:

$$\nu \leqslant \frac{1}{2\pi R\Delta C} = 8 \cdot 10^6\ \text{sec}^{-1}$$

which corresponds to the wave length:

$$\lambda \geqslant 38\ \text{metres}.$$

Thus, in the example considered here, the effect of capacity fluctuations is felt in reception of wave lengths below 40 m.

Damping effects

The finite time of transit of the electrons from the cathode to the control grid, as discussed in more detail in the theoretical section, causes a damping in one of the oscillating circuits connected to these two electrodes. It is found, that when the voltage of the generator G is kept constant, the effective power taken from it is greater with the valve in circuit than when the valve is cut out. (This valve can be cut out, for instance, by making the negative grid bias V_g so high that no anode current passes.) This damping is equivalent electrically to a resistance R_{gk}, which bridges the capacity C_{gk}. Contrary to the capacity fluctuations ΔC_{gk} which are independent of the frequency, R_{gk} is inversely proportional to the square of the frequency. *Table I* gives a selection of experimental data for the high-frequency pentode AF 7. *Fig. 2* shows logarithmically the measured values of R_{gk} for various frequencies ω (in radians); these points lie on a straight line with a gradient of —2 in accord with theoretical requirements. The damping, which increases with the frequency, causes a marked reduction in the attainable amplification with ultra-short waves. In the theoretical appendix it is shown, that the period of oscillation of the shortest waves which can be amplified must be 1.4 times greater, than the time of transit of the electrons between the cathode and the grid. For the valve

Table I. Input capacity and input damping of the AF 7 receiving valve at different wave lengths.

	Input capacity		Input damping		
λ	$C_{i_a=0}$	$C_{i_a=3\,mA}$	$R_{i_a=0}$	$R_{i_a=3\,mA}$	R_{gk}
m	μμF	μμF	MΩ	MΩ	MΩ
200	6·5	8·0	5	3	8
40	6·5	8·0	3	0·28	0·31
20	6·5	8·0	1·5	0·074	0·078
10	6·5	8·0	0·6	0·0185	0·019
4	6·5	8·0	0·1	0·0029	0·003

The effect of the space-charge on the input capacity is independent of the wave length ($\Delta C_{gk} = 1.5\ \mu\mu F$). On the other hand the input damping is inversely proportional to the square of the wave length owing to the time of transit of the electrons ($1/R_{gk} = 1/R_{i_a=3\,mA} - 1/R_{i_a=0}$).

---

1) The impedance is defined experimentally by the quotient $R = e_g/I$ of the tuned circuit.

AF 7 calculation gives a shortest wave length of 85 cm.

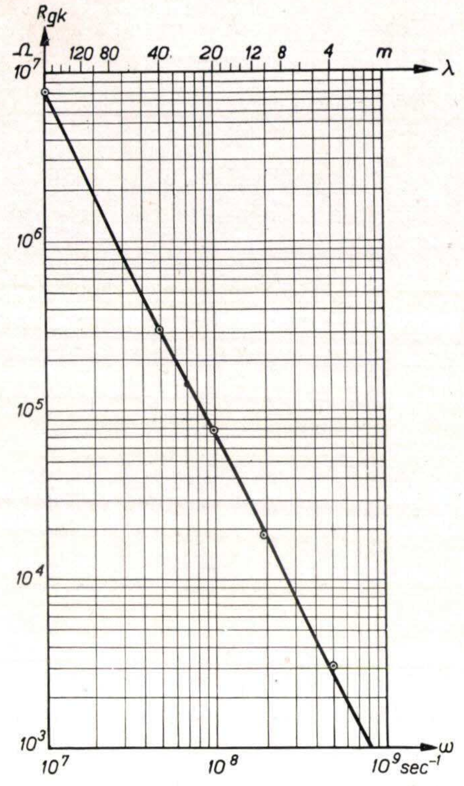

Fig. 2. The resistance R_{gk}, produced as a result of the finite time of transit of the electrons between the cathode and grid, is plotted along the ordinate, and the logarithm of the frequency in circular measure along the abscissa. The values measured with the high-frequency pentode AF7 lie on a straight line with a slope of -2. This is in agreement with theory, which states that R_{gk} must be inversely proportional to ω^2.

Both the capacities of the electrodes and the times of transit of the electrons are proportional to the dimensions of the valve with a specific arrangement of electrodes and given voltages. An immediate method for controlling ultra-short waves is therefore to reduce the external dimensions of the valves. *Fig. 3* shows the evolution of high-frequency amplifying valves for short-wave reception. The two valves on the left are used in modern sets for normal wave ranges, whilst the smallest type on the right can still be used at a wave-length of 50 cm. The input capacity C_{gk} has been reduced from about 6 μμF to 2.5 μμF. The cathode-grid distance has been reduced from 0.4 mm to 0.1 mm and the times of transit of the electrons from the cathode to the control grid have been reduced from $2 \cdot 10^{-9}$ sec to $0.5 \cdot 10^{-9}$ sec.

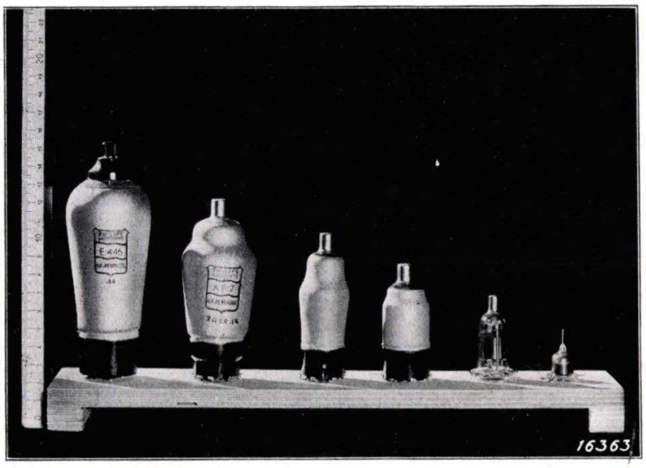

Fig. 3. The picture depicts the evolution of the high-frequency amplifying valves (pentodes) for short-wave reception. The second valve on the left (AF7) is used in modern radio receivers. The smallest pentode on the right, which is a little more than 1 cm high can still be used at a wave length of 50 cm.

Induction Effects

In multi-grid valves it may occur, that the voltage at one pair of electrodes (e.g. across grid and cathode) affects the space-charge between two other electrodes. A circuit in which this effect is produced is shown in *fig. 4*. The grids *1* and *3* have a small negative bias, and the anode a still higher potential. Owing to the retardation of the electrons by grid *2* a rather high space-charge density will be present between grid *2* and *3*. This charge will fluctuate in phase with the alternating tension of grid *1* provided by generator *G*. The fluctuation in space-charge will induce a fluctuating charge on grid *3*, so that an alternating current will pass in the outer circuit between the grid *3* and the cathode. If this circuit contains impedance the potential of grid *3* will fluctuate in synchronism with the generator voltage.

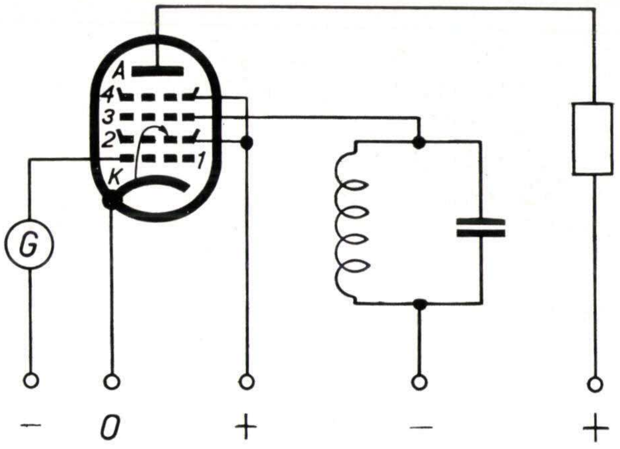

Fig. 4. Part of the electrons which pass through grid 2 are turned back from grid 3 so that between grids 2 and 3 a large space-charge is produced, which varies with the frequency of the alternating voltage at grid *1* furnished by the generator G. The varying space-charge between grids 2 and 3 induces a variable charge on grid 3 so that an alternating current passes through the circuit connected to grid 3. Owing to the "inductive forces" of the electrons, alternating voltages with the generator frequency are produced in the circuit of grid 3. According to the phase of these voltages the slope is either increased or reduced.

The characteristics of the impedance between the grid to the cathode will thus determine the phase relationship between the two voltages. If the voltages are in phase, induction will intensify the effect of the grid potential on the anode current and increase the slope. If, however, the potential at grid *3* is in phase opposite to the anode current, induction will reduce the effect of the grid voltage on the anode current, i.e. the slope. Which of these two results will obtain, depends on the natural frequency of the *L-C*-circuit. If the free oscillation ν of the circuit has a higher natural frequency than the oscillation ν_o produced by the generator *G*, the slope will be increased. If on the other hand $\nu < \nu_o$ the slope will be reduced. The effect of the induction on the slope is clearly apparent with octodes, when used as mixing valves in heterodyne receivers.

A New Amplifying Method

As shown already in the previous section, the induction forces of the space-charge can result in an increase of the amplification factor of a valve if a suitable circuit is used. An arrangement will be described below, which for short waves is just as efficient as the standard amplification circuit, in some cases even better, and in which amplification is due entirely to induction. Consider the tetrode in *fig. 5*. The "screen grid" *2* has a high positive bias, e.g. 100 volts, whilst control grid *1* and anode *A* have a small negative bias.

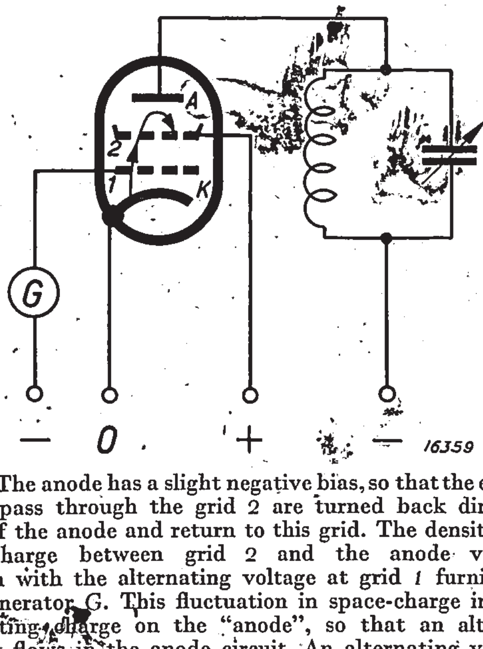

Fig. 5. The anode has a slight negative bias, so that the electrons which pass through the grid 2 are turned back directly in front of the anode and return to this grid. The density of the space-charge between grid 2 and the anode varies in rhythm with the alternating voltage at grid *1* furnished by the generator G. This fluctuation in space-charge induces a fluctuating charge on the "anode", so that an alternating current flows in the anode circuit. An alternating voltage is thus produced in the anode circuit, which may be several times greater, than the alternating voltage at grid *1*. With short waves this circuit with a "negative" anode gives a greater amplification than a normal circuit with a "positive" anode.

Part of the electrons emitted from the cathode passes through the meshes in the screen grid, is repelled by the anode and finally ends at the screen grid itself. The density of electrons is very great at the point where they reverse direction. The negative charge between the screen grid and the anode induces a positive inductive charge Q on the anode. If the control grid is given a small alternating voltage with a frequency in radians of ω, the space-charge density in front of the anode will be altered and hence also the inductive charge Q. The anode current is $i_a = dQ/dt$. From this it follows, that the anode current has the following characteristics:

a) its frequency in radians is ω;
b) its amplitude is proportional to ω;
c) with a pure ohmic resistance R in the anode circuit it is in phase quadrature with the potential at the control grid.

The ratio of the voltage fluctuations at the resistance R to the corresponding voltage fluctuations at the control grid can as usual be taken as the amplification. By suitably rating the resistance R a higher amplification factor can be obtained for short waves by this method, than by the usual method using a high positive anode potential. The amplification does not, however, rise with increasing frequency in this wave range, but falls, since, owing to the finite time of transit of the electrons between the screen grid and the anode, damping effects are produced on the anode side which, like the input damping, increase with the square of the frequency.

Upon closer examination of the induction process it is found, that the new method of amplification offers advantages only at frequencies at which the time of transit of the electrons already causes appreciable damping. The slope S of induction amplification is:

$$S = \frac{2}{3}\, s\omega\tau \quad \ldots\ldots\ldots \quad (1)$$

where s is the natural slope, ω the frequency in radians and τ the time of transit of the electrons from the screen grid up to near the anode and back. S will be of the same order of magnitude as the static slope s if $\omega\tau$ is of the order of unity, i.e. in the same frequency range in which damping is considerable.

To interpret equation (1) it must be remembered that the order of magnitude of the induced charge is represented by the product of the current i_a passing through the meshes of the screen grid and the time of transit τ (up to near the anode and back to the screen grid).

$$Q = \beta \cdot i_a \cdot \tau = \beta \tau \cdot s\, e_g \sin \omega t$$

The induction current to the anode is therefore:

$$\frac{dQ}{dt} = \beta\, s\, \omega\tau\, e_g \cos \omega t = i_{infl} \cos \omega t$$

and hence the slope of induction-amplification:

$$S = \frac{i_{infl}}{e_g} = \beta\, s\, \omega\tau$$

in agreement with equation (1) if for β the numerical value $^2/_3$ is inserted as deduced by more detailed analysis [2]).

In experimental work on the new method of amplification a 40-fold amplification was obtained with a 50-m wave and a 10-fold with a 5-m wave. In the standard amplification circuit the corresponding factors were 75 and 7. The new method is thus superior at a wave-length of 5 m.

In conclusion it should be mentioned, that good results have been obtained in the construction of a complete radio receiver with three-stage high-frequency amplification and operating on the new method. In interconnecting the various amplifying stages it was found particularly advantageous that the anode and control grid have the same direct voltages. The anode of the preceding valve can therefore be connected directly with the grid of the next valve, without the aid of a coupling unit consisting of a condenser and grid-leak as is usually necessary.

Some Theoretical Considerations

Detuning. Consider the simple case of a three-element valve with flat electrodes (*fig. 6*) whose surface area is large compared with the space between the electrodes. The broken lines indicate the potential distribution obtained in the absence of space-charge in the valve (i.e. with a cold cathode). The space-charge affects the potential field mainly between the cathode and grid. If the electrode potentials are kept constant and the anode current is increased by heating the filament up to the limiting value of the space-charge equilibrium, the potential distribution represented by the continuous lines is obtained. In the absence of a space-charge the capacity of the grid relative to the cathode is:

$$C_{gk} = \frac{f}{4\pi a}$$

where a is the distance between the grid and cathode and f the area of the surface.

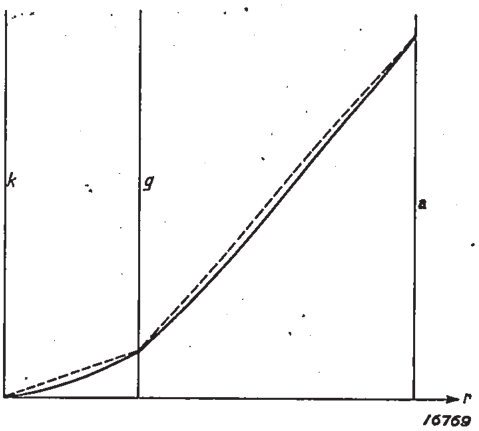

Fig. 6. The broken lines indicate the potential distribution without a space-charge in the valve (i.e. with a cold cathode). The continuous lines show the potential distribution with the space-charge. At the cathode the tangent to the potential curve is horizontal so that at the cathode the field strength is zero.

The variation in capacity due to the space-charge can be readily calculated if the alteration in the field strength at the location of the grid is known. Langmuir has given the following equation for the potential distribution as affected by the space-charge:

$$V = V_s \left(\frac{x}{a}\right)^{4/3} \quad \ldots\ldots \quad (2)$$

V_s is here the effective potential at the surface of the control grid, termed the control voltage or potential. This potential is determined primarily by the potential V_g of the grid wires, the anode voltage V_a having a much less effect. To a satisfactory approximation we may put:

$$V_s = V_g + \frac{1}{g} V_a$$

where $1/g$ is a small number, g is termed the amplification factor. If the anode voltage is constant, as is assumed below, the alternating control voltage is equal to the alternating grid voltage. The field strength at the grid is, according to equation (2):

$$E = \left(\frac{\partial V}{\partial x}\right)_{x=a} = \left[\frac{4}{3}\frac{V_s}{a}\left(\frac{x}{a}\right)^{1/3}\right]_{x=a} = \frac{4}{3}\frac{V_s}{a}$$

The charge per unit surface of the grid is $Q = (E/4\pi) f$, where f is the area of the grid; with the aid of the relationship:

charge = capacity × voltage ($Q = C\, V_s$)

we get the capacity:

$$C = \frac{4}{3}\frac{f}{4\pi a}$$

whilst in the absence of the space-charge:

$$C_{gk} = \frac{f}{4\pi a}$$

would be obtained. The capacity thus increases by a third of its value.

With a grid and cathode of cylindrical form a similar calculation gives the relative variations in capacity $\Delta C_{gk}/C_{gk}$, which are determined by the ratio r_g/r_k of the radii of the grid and cathode and in general are greater than with flat electrodes. In *fig. 7* the relative increase in capacity has been plotted as a function of r_g/r_k.

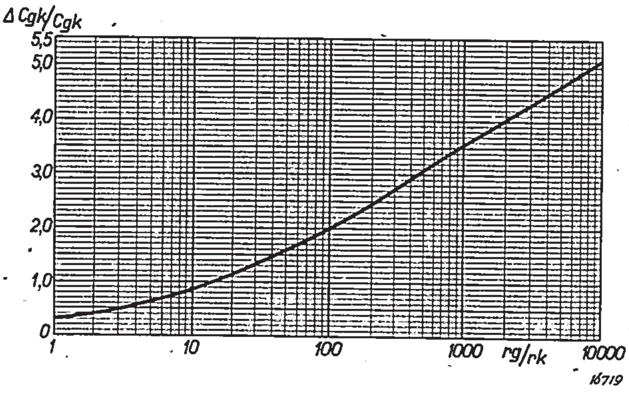

Fig. 7. In a cylindrical valve the variation ΔC_{gk} in the inter-electrode capacity C_{gk} due to the space-charge is a function of the ratio r_g/r_k of the radii of the grid and cathode. The figure shows the shape of this function.

---

[2]) C. J. Bakker and G. de Vries, Physica 1, 1045, 1934.

Input impedance. To calculate the input damping, flat electrodes are again considered. The alternating grid voltage in the circuit in fig. 1 is $e_g \sin \omega t$. The capacity current to the grid at low frequencies, at which the time of transit is short compared with the period of oscillation, is:

I = capacity × differential quotient of the voltage with respect to time

$$I = \frac{4}{3} C_{gk}\, e_g\, \omega \cos \omega t \quad \ldots\ldots \quad (3)$$

At high frequencies, owing to the finite time of transit of the electrons, the current phase will lag considerably behind the value given by equation (3); the lag is proportional to the time of transit τ and the frequency ω in radians. If the proportionality factor is α, we have:

$$I = \frac{4}{3}\, \omega\, C_{gk}\, e_g \left[\cos (\omega t - \alpha\, \omega\, \tau)\right]$$

or since even with ultra-short waves $\alpha\, \omega\, \tau \ll 1$:

$$I = \frac{4}{3}\, \omega\, C_{gk}\, e_g \left[\cos \omega t + \alpha\, \omega \tau \sin \omega \tau\right] \quad \ldots \quad (4)$$

Accurate calculation[3]) gives $\alpha = 0.075$. From equation (4) it is seen that the current receives a component which is in phase with the voltage. Energy is thus dissipated, which is the direct cause of the damping of the associated oscillating circuit.

The damping expressed in equation (4) corresponds to a bridging of the grid-cathode capacity by a conductor:

$$\frac{1}{R_{gk}} = \frac{4}{3}\, \alpha\, C_{gk}\, \omega^2\, \tau$$

If in place of C_{gk} we introduce the usually better known slope s of the valve, according to the equation:

$$C_{gk} = \frac{s\,.\,\tau}{2} \quad \ldots\ldots\ldots \quad (5)$$

we get:

$$\frac{1}{R_{gk}} = \frac{2}{3}\, \alpha\, s\, \omega^2 \tau^2 = \frac{1}{20}\, s\, \omega^2 \tau^2 \quad \ldots\ldots \quad (6)$$

Equation (5) follows from the known law of the space-charge current:

$$i_a = const.\ V_s^{3/2}$$

The slope is:

$$s = \frac{d\, i_a}{d\, V_s} = \frac{3}{2}\, \frac{i_a}{V_s} \quad \ldots\ldots \quad (7)$$

The anode current i_a is equal to the space-charge Q between the grid and cathode, divided by the time of transit ($i_a = Q/\tau$). In the case of the space-charge equilibrium under consideration here the field strength at the cathode is equal to zero[4]). As a result no inductive charge is generated on the cathode. The inductive charge on the grid is then equal to the space-charge Q between the cathode and grid with the sign changed. If for Q we insert the product of the grid voltage V_g and the grid-cathode capacity $4/3\ C_{gk}$ we get:

$$i_a = 4/3\ C_{gk}\, \frac{V_s}{\tau},$$

and thus equation (7) becomes

$$s = \frac{3}{2} \cdot \frac{4}{3}\, \frac{C_{gk}}{\tau}$$

hence

$$C_{gk} = \frac{s\,.\,\tau}{2} \text{ in accord with equation (5).}$$

From equation (6) it may be deduced, that an input signal whose period of oscillation is shorter than the time of transit of the electrons can no longer be amplified; this signifies that it is then no longer possible to obtain an alternating voltage in the anode circuit greater than the alternating grid voltage e_g. The alternating anode voltage e_a is equal to the product of the anode alternating current i_a and the resistance R_a in the anode circuit. This resistance is, however, limited if the alternating voltage generated at it is passed to the grid of the succeeding valve. For, as already indicated, grid and cathode are bridged by a resistance R_{gk} which decreases with rising frequency. If we assume that this resistance determines the anode resistance, we get:

$$e_a = i_a\, R_{gk} = s\,.\,e_g\, R_{gk}$$

and hence the amplification obtained with the valve is:

$$f = \frac{e_a}{e_g} = s\, R_{gk} = \frac{20}{\omega^2 \tau^2} \quad \ldots\ldots \quad (8)$$

The last part of equation (8) is really only another way of writing equation (6).

If we insert the time of oscillation $T = 2\ \pi/\omega$, we get:

$$f \sim 0.5 \left(\frac{T}{\tau}\right)^2$$

To obtain amplification ($f > 1$) the time of oscillation T of the incoming wave must be greater than $1.4\,\tau$.

With the high-frequency pentode AF 7, τ is for example $2{\cdot}10^{-9}$ sec. Hence the limit of amplification is $T = 2.8{\cdot}10^{-9}$ sec, corresponding to a wave length $\lambda = 85$ cm.

---

[3]) C. J. Bakker and G. de Vries, Physica 2, 683, 1935.

[4]) It is assumed here that the electrons are emitted from the cathode with zero velocity.

HEAVY-CURRENT CONDENSERS

Summary. A short survey is given of the reasons responsible for the extensive use of heavy-current condensers as phase-shifters. This is followed by a discussion of the internal construction, the electrical characteristics and the testing, the life and finally the external design of these condensers. Further applications (other than for power factor improvement) are also briefly referred to.

Introduction

Extensive use has been made of heavy-current condensers as phase-shifters which are generally employed for this purpose for reactive powers up to approximately 1000 kVA. During recent years these condensers have also superseded rotary phase-shifters for still higher powers. The principal reasons responsible for these developments are:

a) The almost complete absence of loss in these condensers.

b) Their simple and economical divisibility which enables their distribution throughout a whole network. In so far as other practical considerations permit, the reactive power can be generated close to the point of consumption and thus relieve both lines and transformers of reactive currents. The following advantages accrue: Reduction in transmission losses, improvement in voltage regulation and, in new plants and systems, marked economies in installation costs for the line network.

c) A battery of condensers can be economically expanded to any desired proportions, so that the capacity of the plant can be adapted to the current demand without incurring unnecessary installation costs and losses.

d) As the condensers contain no moving parts, no special attendance is required.

About ten years ago the general adoption of heavy current condensers was limited by their life in service not always being satisfactory. Moreover, at that time experience was lacking regarding the interconnection of large batteries of condensers and the means for avoiding resonance effects. Since these difficulties have now been overcome, the use of rotary phase-shifters appears to be justified only in cases, where they have a second duty to perform, viz, where large synchronous motors are used simultaneously for driving machinery and for generating reactive power.

Internal Construction

Heavy-current condensers are built up of reels made on reeling machines from aluminium foil with several intermediate layers of thin paper (*fig. 1*). These reels are rated for a capacity of 0.5 to 2.5 μF and for voltages from 220 to 900 volts. At a 50-cycle frequency their reactive power is 30 to 100 VA. For higher capacities the individual reels required are connected in parallel, and for higher voltages they are series-connected in groups. In the case of low-voltage condensers the reels in parallel are connected to the bus-bar by thin silver wire which also acts as a fuse. These reels are fixed in a frame and then evacuated in an impregnating tank; after being impregnated with oil they are finally placed in a casing which is hermetically sealed (figs. 3 and 4).

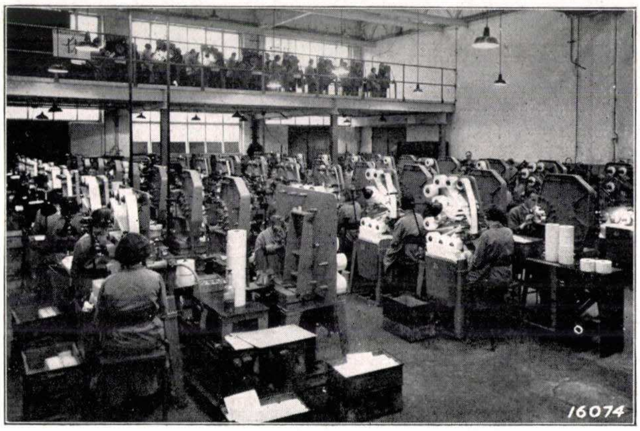

Fig. 1. Condenser reeling machine.

The dielectric composed of oil-impregnated paper sheets determines the efficiency and reliability of the condenser. As the capacity of a condenser is inversely proportional to the thickness of the dielectric, it is desirable to use the thinnest possible dielectric in order to save both cost and weight. At the present time a rating of 0.5 to 1 kVA has been obtained per cub. dm (at 50 cycles). A reduction in dielectric losses has gone hand in hand with an increase in the permissible voltage loading of the dielectric. These improvements and advances have been responsible for the rapid development of the condensers during the last decade. Condenser paper of satisfactory uniform texture can now be made with a thickness of only 7μ, and with very low dielectric losses, which do not increase with temperature rise in the range of heating experienced with these condensers. At a working temperature of 50 to 60 deg. C. the losses of the finished dielectric are a minimum. The dielectric, which is usually only a few hundredths of a millimetre thick, is built up of several layers of this thin paper, so that the unavoidable slight defects of the single layers cannot cause trouble. Rag paper is in most cases more suitable than cellulose paper, since it can be made thinner and with lower losses. For impregnation highly refined mineral oils are used, whose chemical and electrical properties have to comply with severe standards.

In the manufacture of these condensers evacuation and impregnation are the two most important operations. Before evacuation the paper contains 5 to 8 per cent moisture, and 20 to 40 per cent of the total volume is occupied by air. The extent to which moisture and occluded air can be removed, the correct handling of the material during manufacture and the retention of the initial conditions during service are the main factors determining the losses, efficiency and life of the condenser. Water and air are removed from the oil by atomising it on spraying into the evacuated impregnating tank. By using flat reels and making them of the most suitable dimensions, adverse mechanical stresses in the condenser reels are avoided and the dielectric can be compressed to a standard size, thus ensuring uniform impregnation. The reels are made fairly small in order to ensure adequate removal of air and moisture from the interior. The subdivision of the condenser into small elements also permits simple and reliable control of every stage in manufacture.

The surface area of the dielectric is already of the order of 1000 sq. m with a 50 kVA condenser. Such a large surface of the thin dielectric can only be obtained with satisfactory precision by extremely careful supervision of the raw materials used and of every step in the manufacturing processes. The paper is tested before use for tenacity, folding coefficient, elongation, freedom from acid, dielectric losses and conductive places. The acid value, insulation resistance, disruptive voltage and viscosity of the oil are also continually tested.

Electrical Characteristics and Testing

An effective pressure of 10 to 20 kilovolts can be applied per mm of the dielectric without endangering the efficiency and life of the condenser. If the condenser is used mainly for direct current, as for instance in voltage smoothing in rectifier units, an effective pressure up to 80 kilovolts per mm may be applied, according to the ripple of the voltage and the duration of loading. The disruptive voltage found in D.C. tests is as high as 240 kilovolts per mm. With a 50-cycle alternating current applied for 1 minute, the disruptive voltage is roughly 120 kilovolts per mm. If the A.C. test voltage is applied for longer periods the disruptive voltage first diminishes rapidly, then more slowly, and after a time attains practically a constant value in the neighbourhood of 40 kilovolts$_{\text{eff}}$ per mm. The test specified in current standards in which 2 to 3 times the working voltage is applied for the period of a minute does not therefore give an adequate insight into the behaviour of the condenser during continuous service, and it is only suitable for bringing out the more serious defects. It is, however, not advisable to increase the test voltage, as there is then the danger that the life of the condenser will be impaired. A closer insight into the operating characteristics of the condenser is gained by measuring what is termed the phase displacement δ 1).

Fig. 2 shows the connection between *tan* δ and the voltage per mm thickness of the dielectric. In addition to the absolute value of *tan* δ at the working voltage it is particularly important to

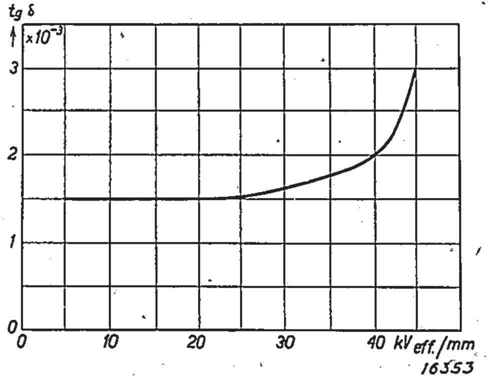

Fig. 2. Tangent of the phase displacement (*tan* δ) as a function of the voltage per mm at 50 cycles.

---

1) If the current taken from the condenser differed by exactly 90 deg. in phase from the voltage, the condenser would operate without loss. In condensers the dielectric losses are only very small as compared with their reactive power. They cause a small deviation from 90 deg. in the phase lag between current and voltage, such deviation being represented by the phase difference δ. The tangent of this angle (*tan* δ) is therefore the quotient of the watt losses of the condenser and its reactive power.

know its variation as the voltage rises. The curve given here was obtained in measurements, in which the voltage was gradually increased at the rate of 5 kilovolts per mm per hour. It is seen that at the outset *tan* δ remains constant up to a certain applied pressure. It then begins to increase slowly, probably owing to the ionisation of the dielectric. Later *tan* δ increases very rapidly and indicates the imminence of rupture. In current production a standard value of 0.002 is obtained for *tan* δ, i.e. the losses total only 2 per 1000 of the reactive power of the condenser, which is at most 1/20 of the operating losses with rotating phase-shifter. From practical considerations, it would indeed not be a disadvantage for the losses to have been a little higher; the smallness of the losses and particularly their constancy over a wide voltage range are, however, reliable criteria showing the efficiency of the condenser [2]).

Life

At international technical congresses the life of power current condensers was stated in 1927 to be only 3 years, but by 1933 their accredited life has already increased to 30 years. The first-mentioned figure applied to condensers with a solid impregnation, which are no longer adapted for heavy-current purposes. Although the latter figure cannot be borne out by experience for obvious reasons, it is nevertheless based on reasonable evidence. The last and determining stage in the advances made has been due to research on certain chemical changes in the impregnation oil during long service, such changes being first observed on cables and later also in the interior of condenser reels. These changes probably take place owing to the traces of residual oxygen in the dielectric and their ionisation in powerful electric fields. Accompanied by the evolution of gas the oil is then converted to higher molecular compounds of a wax-like nature. The voltage at which this transformation takes place has therefore been termed the "gas voltage". By, inter alia, more complete evacuation at the outset and by employing an oil less liable to undergo such transformation, it is possible to raise the gas voltage far above the working voltage range and thus eliminate the direct causes of aging. This has been confirmed by accelerated aging tests with voltages higher than the normal working level.

External Construction

A high condenser capacity can be accommodated either in a single enclosure or built up of a number of separate small elements. The second method results in a higher efficiency and has therefore been favoured by Philips. Large batteries of condensers are built up from units rated from 10 to 60 kVA, either of single-phase or three-phase design. This method of battery assembly offers moreover the following advantages:

The large cooling surface relative to the volume obtained in smaller units, coupled with the low losses, results in a temperature rise of only about 5 deg. C. The thermal expansion is therefore small, enabling hermetically-sealed enclosures to be used which completely exclude access of moisture and air during service. The rise in temperature is, moreover, so slight that the phase difference and disruptive strength remain practically constant. The time during which the impregnated reels are in contact with the air before hermetic enclosure in the condenser chamber has been reduced to a harmless minimum. In practice the subdivision of a battery of condensers into any number of groups to meet specific requirements or an alteration of the grouping to satisfy a new distribution of the load involves no difficulty whatsoever. In the most common cases where the mains voltage is altered, the condensers can be adapted to the new voltage quite readily by modifying the arrangement of the circuits (delta, star and series circuits). Erection of the condensers on site is quite simple and does not require a crane, whilst they can also be readily adapted to the available space.

A battery of condensers for low-voltage circuits composed of six units each of 10 kVA, which is set up in a simple iron frame, is shown in *fig. 3*. The condenser chamber of each unit is a welded sheet-iron structure with pressed-in strengthening ribs. The cover of the chamber has two connecting terminals of moulded insulating material and an earthing terminal. In the interior of the chamber there is a discharge resistance, which lowerst he charge of the condenser to 1/10 of its working voltage within 30 secs. after disconnection. Tinned copper strips connect the units in a delta circuit. The earthing terminals of the units are screwed to the frame, which is itself earthed.

High-tension condensers for phase-shifting and for mains voltages up to 30,000 volts are made as cylindrical units (*fig. 4*). The leading-out insulator of each unit constitutes one electrical pole, and the iron casing the second pole. The top frame of the iron rack, to which the units are suspended, connects the chambers in a star circuit and constitutes their neutral. In assemblies with insulated neutral point the rack is supported on insulators.

---

[2]) The standardisation of a dielectric by measurement of its dielectric losses was first adopted in Holland in 1925 in the regulations laid down for tests on high-tension cables, on the basis of investigations by C. F. Proos: Eenige beschouwingen omtrent dielectrische verliezen van hoogspanningskabels (v. Kampen, Amsterdam 1921). Similar testing regulations appear applicable to condensers also.

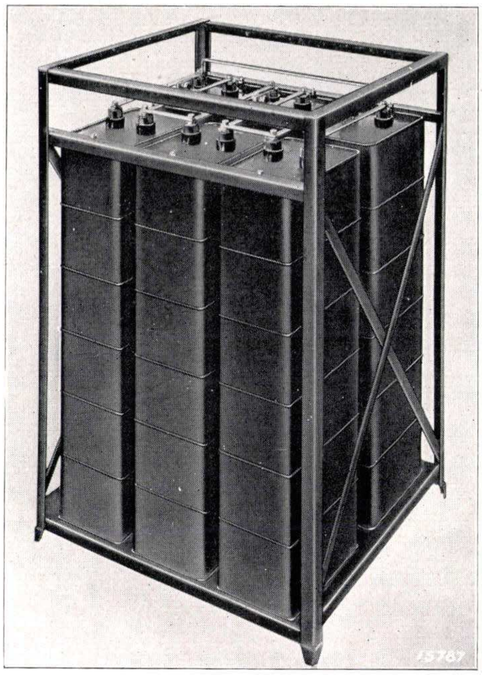

Fig. 3. Low-voltage condensor-battery 60 kVA for phase-shifting.

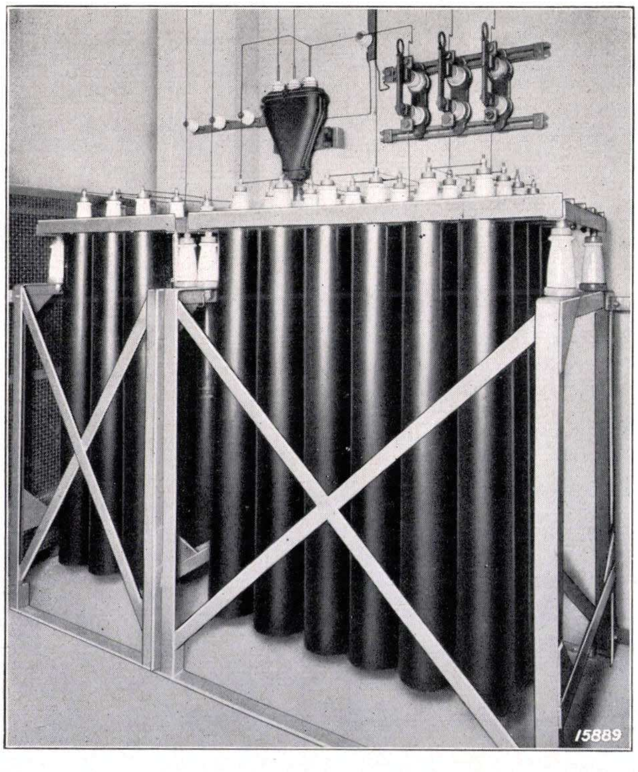

Fig. 4. High-voltage condensor-battery 360 kVA for phase-shifting.

The production of phase-shifting condensers for mains voltages over 30 000 volts by series interconnection of the reels appears to present no difficulty, but at the present time there is no demand for such assemblies. High-tension condensers are, however, employed for other purposes, of which a few examples will be given here.

Further Applications

After it was demonstrated, that condensers could be built to satisfy all requirements imposed for use in heavy-current circuits their employment made rapid strides. In addition to their use for power factor improvement, these condensers have also been employed in heavy-current equipments for the following purposes:

a) Starting of single-phase asynchronous motors.

b) Voltage smoothing in rectifier equipment.

c) Over-voltage protection (protection against surges produced by electric shadow, leakage and storms.

d) In oscillating circuits of high-frequency furnaces.

e) Coupling of high-tension lines with high-frequency telephone circuits.

f) For the protection of radio receivers against interference from consumers connected to the power mains.

Brief reference to various types of heavy-current condensers used for the above purposes may prove interesting.

For coupling high-tension lines with high-frequency telephone, tele-metering and remote-control circuits, the condensers are incorporated in porcelain insulators. The insulator shown in *fig. 5* contains a capacity of 0.001 μF at a working voltage of 150 kV, which corresponds to a reactive power of 7 kVA. Condensers for over-voltage protection are of similar design.

For X-ray apparatus and impulsive voltage apparatus, the reels are accommodated in rings of insulating material, each rated for 0.05 μF at 50 kV. Any high voltages can be obtained by mounting the requisite number of rings one above the other. *Fig. 6* shows a 400-kV X-ray equipment with the condenser rings in the pillars standing against the wall. From the same rings an impulsive voltage generator for 2 millions of volts, has been built which will be described in a later issue of this journal. The same type of condensers is used in the high-voltage equipment described in this Review **1**, 6, 1936 (s. fig. 3).

A further type of heavy-current condenser operating in the oscillatory circuit of a high-frequency induction furnace has also already been described in a previous issue of this Review [3]). The battery of condensers, shown in that article, was rated for 6000 kVA at 7000 cycles and 5000 volts. It is made up of 72 units, each of 83 kVA, which have been provided with cooling ribs to dissipate the heat generated by the specific powers and losses which increase with the frequency.

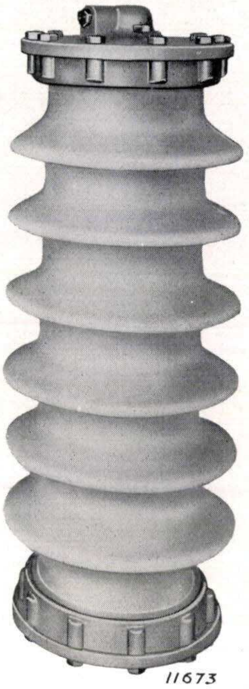

Fig. 5. Condenser for connecting high-frequency telephone-sets with high voltage conductors.

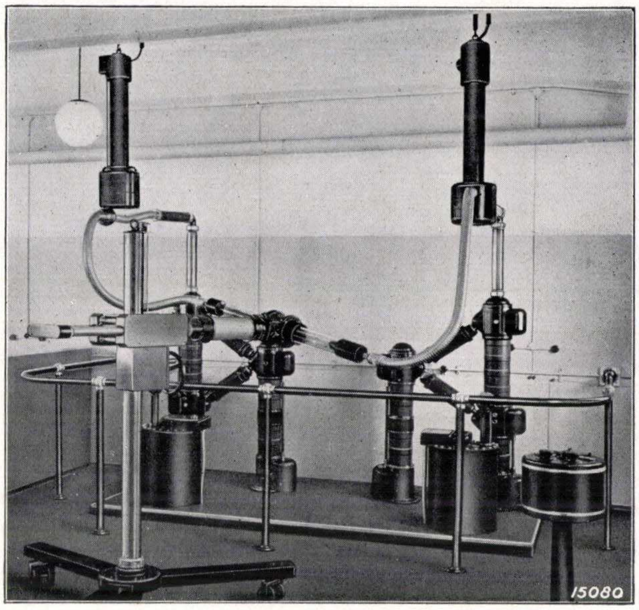

Fig. 6. A 400 kV X-ray equipment.

Compiled by H. EHRNREICH.

---

[3]) Philips techn. Rev. **1**, 56, 1936.

Rectification: On page 157, in the May issue of this Review (article "Optical Telephony") the dispersion of the beam of light is estimated to $1\,^1/_2$ per cent. This value must be replaced by $1\,^1/_2$ per mille.

A SPEED-INCREMENT TEST AS A SHORT-TIME TESTING METHOD FOR ESTIMATING THE MACHINABILITY OF STEELS

Summary. Cutting tests on lathes, in which the cutting speed increases proportionally to the time (speed-increment tests), are suitable for estimating the machinability of different kinds of steel and the wearing properties of lathe tools made of high-speed steel. It is found, that the results obtained in cutting tests with a constant cutting speed (Taylor tests) can be deduced from the results of tests in which the face of a disk is turned with radial feed, beginning at the centre.

Introduction

The materials required by the N.V. Philips' Gloeilampenfabrieken for its products and their manufacture are supplied according to strict testing standards. The supervision of all materials received is in the hands of the material-testing department, which is itself a section of the material-investigating department of the research laboratory. This investigation department develops the specifications on which the testing procedure is based and is also engaged in research work on various problems, such as the choice of material, the working out of the best methods of treatment and the elimination of practical difficulties in manufacturing processes. We propose to describe such material investigations from time to time in this Review and will commence with a description of an investigation directed towards an improvement of certain testing methods as well as towards the choice of materials and their optimum treatment.

The consumer is always faced with serious difficulties in the testing of metals as soon as specific information is required of their machinability. These difficulties lie mainly in the considerable amount of time and comparatively high expense due to extensive machinability tests. As a result users endeavour to obtain a guarantee for satisfactory machinability by stipulating specific requirements for certain other properties, e.g. in respect of hardness and chemical composition. It has, however, been amply demonstrated that this policy does not give the desired result. Therefore it is unquestionably one of the most important problems of the metal-industry to develop some kind of short-time test for machinability, which can form the basis of practical testing procedure. Restricting ourselves in the following to the machinability of steel in turning round bars in a lathe, a good impression is obtained by measuring at different cutting speeds the time during which a standardized tool holds (i.e. the time until the tool breaks down through wear and chipping), when making a cut of definite dimensions. The reliability of the results obtained in practice with these Taylor tests (as they are called) will be the greater the more closely the conditions of test agree with those met with in actual practice. This signifies, inter alia, that the duration of the tests must be of the order of at least 30 or 60 minutes. However, the unavoidable large diversity in the results of such tests renders it necessary, that each test be repeated several times in order to obtain a reliable mean value.

This tedious and wasteful method has naturally given rise to a desire for a short-time testing method. Such a method is that, in which the cutting speed is progressively increased ¹). Fundamentally this method consists in increasing the cutting speed at such a rate, that in spite of a low initial speed the tool becomes blunted very quickly (usually after no more than a few minutes). Tests based on this principle can be carried out in two different ways. Firstly, in turning a round bar the angular speed of the lathe can be gradually increased, the size of the chip automatically remaining unaltered. Secondly, keeping the angular speed of the lathe constant, the face of a short thick bar or a disc can be cut, beginning at the centre towards the outside (see fig. 3). In this case the cutting speed increases proportionally to the distance of the tool from the axis of the disc. In this paper we will mainly deal with this second method, which will be referred to below as the "disk-test" ²).

---

¹) Cf. Werkstoff-Handbuch Stahl und Eisen, E 41, Düsseldorf, 1927.

²) Compared with the first-mentioned method the disk-test offers the advantage, that it can be applied on any lathe without a special arrangement (such as a D.C. motor with regulator) for gradually increasing the speed of the lathe. However, a disadvantage is that the disk-test generally requires materials with a larger diameter, than is necessary in other tests, which not only limits the application of the method but also introduces a certain degree of uncertainty owing to the unavoidable difference between thin and thick material and a more or less marked irregularity over the cross-section of the thick material.

Where machinability tests have been referred to above, it has always been assumed that the turning tools were all identical. Only the bars to be cut were considered to be made from different materials.

Conversely, the cutting qualities of various high-speed steels can be compared with each other by carrying out Taylor-tests and/or disk-tests on one definite kind of steel with tools of a standard model. Moreover, a comparison can also be made between lathe tools from one and the same high-speed steel which has been submitted to different heat treatments. Systematic experiments on these lines were performed in this Laboratory by W. F. Brandsma[3]), and aimed primarily at establishing the best process for hardening and tempering modern high-speed steels. These steels in fact require an exceptional heat-treatment to endow them with optimum cutting properties.

Other series of experiments have been performed to demonstrate that the disk-test is very suitable as a short life-test for determining the optimum tool angles and for obtaining a criterion of the machinability [4]).

Principle of the Taylor test

The arrangement used in the Taylor tests is shown diagramatically in *fig. 1*.

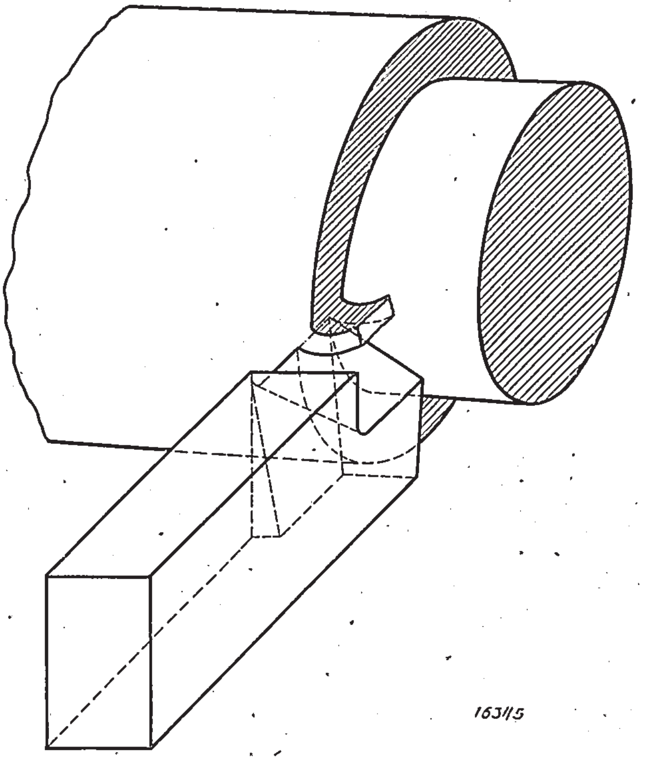

Fig. 1. Normal Taylor test. A cylindrical layer is cut from the bar, which revolves at constant angular speed. Thus the cutting speed v is constant throughout the test and a definite tool-life T (i.e. the time elapsing before the tool completely breaks down) is found for every value of v.

F. W. Taylor [5]) was the first who called attention to the simple formula:

$$T = \left(\frac{C}{v}\right)^n \quad . \; . \; . \; . \; . \quad (1)$$

which represents to a fair degree of approximation the relation between the tool-life T and the linear cutting speed v, when throughout a series of tests all other factors, such as the material being cut, the material and angles of the tool, the dimensions of the chip, the lubrication, etc., are kept the same and only the cutting speed is varied. C and n are constants, which depend only on the factors mentioned. If the cutting speed is expressed in meters per minute and the tool-life in minutes, then C varies, according to circumstances, between 10 and 500 and n between roughly 6 and 20. The straight line by which equation (1) is represented in a double logarithmic diagram facilitates the determination of the speeds v_T (e.g. v_{30} and v_{60}) corresponding to definite values of the tool-life (e.g. T = 30 and 60 min) from a small number of tests made with several suitable cutting speeds.

Fig. 2 shows a double logarithmic v-T-diagram for one of the kinds of steel, which have been examined.

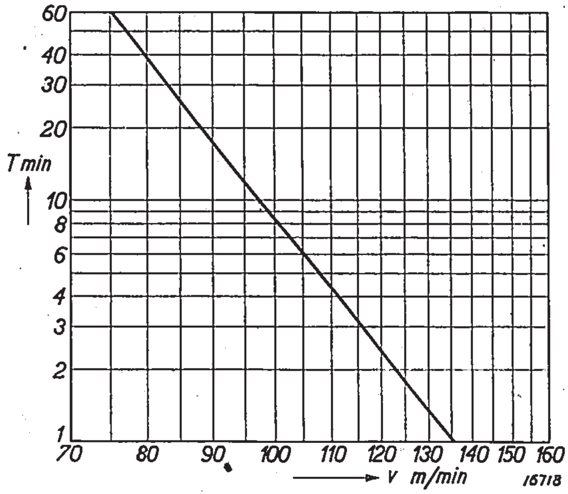

Fig. 2. Results of Taylor tests with a particular kind of steel. The tool-lives T have been determined for different cutting speeds v and are plotted in a double-logarithmic diagram. In agreement with Taylor's equation (1) these points lie on a straight line from which the values of the constants C and n for the particular steel can be deduced.

We have assumed, that the speed v_{30}, i.e. the cutting speed corresponding to a tool-life of 30 minutes (other conditions being equal) has a greater practical significance than v_{60}. This is more readily understood, when it is remembered that on the whole the lathes in workshops do not allow the cutting speed to be varied continously. Generally that speed will be used, which is as close as possible to v_{30} and is smaller than v_{30}. If one keeps v equal to or smaller than v_{30} and it is assumed that the lathe-speeds, which can be successively adjusted are roughly in a ratio of $1 : \sqrt{2}$, the time between two grindings (e.g. for $n = 8$) will occasionally turn out to be $(\sqrt{2})^8 \times 30$ min $= 8$ hours; the mean time being about 2 hours.

---

[3]) W. F. Brandsma, Metaalbewerking **2**, 541, 1936.

[4]) J. R. J. van Dongen and J. G. C. Stegwee, Metaalbewerking **3**, 1 and 49, 1936.

[5]) Taylor, "On the art of cutting metals" 1907. A considerable amount of data and an extensive bibliography are given in E. Brödner, „Zerspanung und Werkstoff", Berlin, 1934.

As a tool is blunted, its face becomes gradually grooved and scored by the chip travelling across it. At the start this wear of the tool has very little effect on the power consumption of the lathe and on the state of the worked surface, but during the last stage of blunting, when a more or less wide bright-polished zone appears on the bar being cut, the temperature and hence the wear of the edge and the power consumption increase more and more rapidly until the cutting edge becomes so hot, that the tool breaks down. The bright-polished zone results from the blunt tool rubbing harder and harder against the surface. The last stage during which the cutting action of the tool is no longer normal is always of such short duration, that it can safely be neglected in determining the life of the tool.

Principle of the disk-test

In a disk-test, a disk of the material being tested is clamped to the lathe chuck and a hole is bored at the centre. The tool to be used in the test is now fixed at centre level, started at the surface of the central hole and fed towards the periphery of the disk, the lathe operating at constant angular speed. *Fig. 3* shows the principle of the arrangement.

Fundamentally in disk-tests the tool is subject to similar changes in face-lathe work as in Taylor-tests, except that owing to the steady increase of the linear cutting speed these changes take place more and more rapidly. The result is, that the last stage of blunting, now limited to a much shorter period, becomes apparent by no more than a bright edge at the end of the worked surface. Again the cutting edge becomes hot and breaks down.

During the test the lathe runs at a constant angular speed of N r.p.m. The diameter D_m of

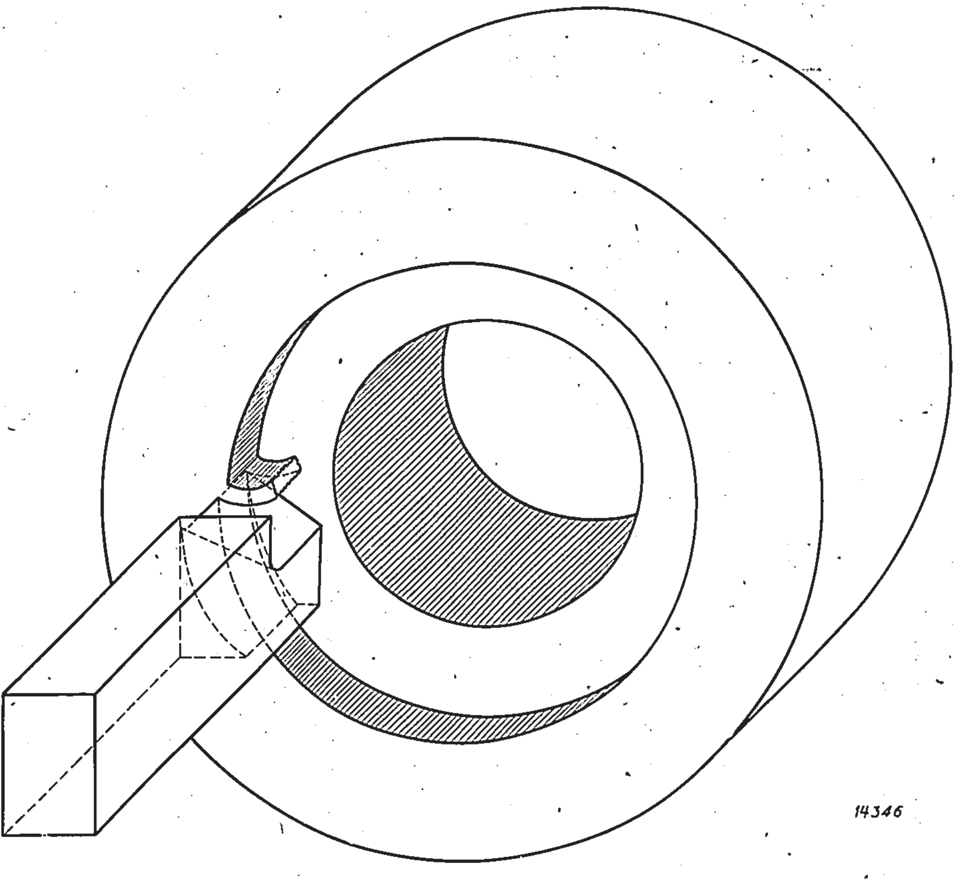

Fig. 3. Normal disk-test. The disk which revolves at a constant speed, is cut from the centre outwards. The cutting speed v now increases during the test up to a definite value v_m at which the tool completely breaks down.

---

[6] As a matter of fact from equation (1) we get $T_1/T_2 = (v_2/v_1)^n$. Hence a ratio $v_1/v_2 = 1/\sqrt{2}$ for two cutting speeds gives $T_1/T_2 = (\sqrt{2})^n$ for the ratio of the corresponding tool-lives (e.g. $(\sqrt{2})^n = 16$ for $n = 8$).

the disk, at which the failure of the tool has occurred is measured in mm. The maximum obtained cutting speed v_m expressed in meters per minute, corresponding to D_m, is given by the expression

$$v_m = \frac{\pi N D_m}{1000} \quad . \quad . \quad . \quad . \quad . \quad (2)$$

In accordance with formula (1) the tool will, with a smaller N, not break down at the same D_m as at first, for over the same cutting length the speed has been lower during the whole time. As a result the tool cuts on further to a larger D_m. On the other hand, with the smaller N only a smaller v_m will be obtained on account of the longer cutting length. *Fig. 4* shows the relationship found experimentally between v_m and N for the same steel as considered in fig. 2.

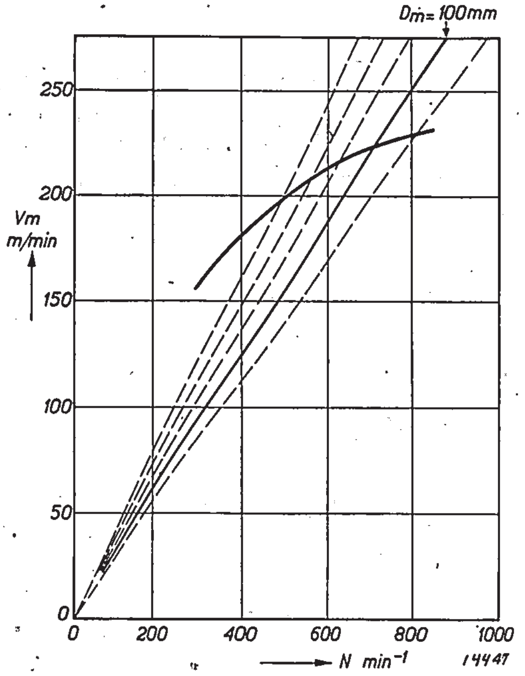

Fig. 4. If a disk-test is repeated with a lower number of revolutions N, a lower maximum cutting speed v_m is found, which, however, then corresponds to a greater cutting length (and a greater D_m). The curve shows the relation found experimentally between N and v_m for the same steel as in fig. 2. By keeping D_m constant the formula (2) between N and v_m is represented by a straight line. A series of these straight lines for different values of D_m are also plotted in this figure; they allow those values of v_m to be found, which correspond to definite values of D_m, e.g. to D_m = 100 mm.

The simplest method would of course be, to keep N the same in all tests, in which case the values of v_m would be directly comparable with each other. If, however, the investigation includes a widely different range of steels, this method cannot be adopted, at any rate if very large disk diameters are to be avoided in testing the better machinable steels. Van Dongen and Stegwee [4]), taking this difficulty into consideration, have measured for each of these different steels v_m as a function of N, and by interpolation found those values of v_m for each steel at which D_m have definite values. This enables a comparison on the basis of equal D_m, which seems as justified as a comparison with a constant lathe speed, moreover, in practice we have the advantage that equal values of D_m enable a fixed size of disk to be used.

According to equation (2), the interpolation referred to is made by drawing in the N-v_m diagram the lines corresponding to the given values of D_m and by determining their intersections with the N-v_m curve. In fig. 4 this interpolation has been made for five values of D_m and special attention is called in this diagram to the line for $D_m = 100$ mm, the cutting speed $v_m = v_m^{(100)}$ for this D_m being taken as the characteristic value of v_m for the material being tested.

Relation between Taylor tests and speed-increment tests

We have assumed above, that under comparable conditions of cutting, the progress of the wear of a cutting tool in disk-tests and in Taylor tests is analogous. However, this does not hold good in all respects. Thus, a comparison of blunt tools with each other reveals the fact, that in Taylor tests of long duration the top surfaces of the tools are excavated by the chip, whilst in the short disk-tests (and also in very short Taylor tests) there is no time for this to occur. To this excavation corresponds a change in the amount of frictional work and in the energy of deformation of the chip and in consequence the heating of the tool is altered. It is reasonable to assume, however, that the differences in the frictional and machining work in the two methods of test are small compared with the total energy applied to the tool. Although, on closer examination of the blunted edge, differences may also be found in other respects, one may ask whether the results of the two methods are in any way related. This is indeed found to be the case.

The equation of Taylor already referred to, for the tests named after him:

$$T = \left(\frac{C}{v}\right)^n \quad . \quad . \quad . \quad . \quad . \quad (1)$$

gives the relationship between the cutting speed v which remains constant during a test and the time T which elapses before the tool breaks down. We can write equation (1) also in the following form:

$$T \cdot v^n = C^n \quad . \quad . \quad . \quad . \quad . \quad . \quad (1a)$$

Assuming, that the reduction in the cutting capacity of a tool in all the Taylor tests (with different cutting speeds) is given by the same function of the time expressed in the time T as unit, one can derive the following equation for cutting tests with variable speeds:

$$\int_0^{T_m} [v(t)]^n \, dt = C^n \quad . \; . \; . \; . \; (3)$$

Here the speed $v(t)$ can still be an arbitrary function of the time, whilst T_m is the time, in which the tool completely breaks down. This formula, which for $v =$ constant is reduced to Taylor's expression (1), shows that in every cutting test, no matter how the speed is varied, there is a relationship between the generalised tool-life T_m and the constants C and n of Taylor's equation.

Of course the nature of this relation will depend on the procedure of the test, i.e. on the variation of the cutting speed v with the time. In order to be able to apply (3), we must know the function $v(t)$. For disk-tests this function can be readily deduced. If N is the (constant) angular lathe-speed, a the radial feed and D_0 the diameter of the hole in the disk (the cutting speed at the start of the experiment thus being $v_0 = \pi N D_0$), then the cutting speed $v(t)$ at time t will be given by the expression

$$v(t) = \pi N (D_0 + 2a Nt) = v_0 + 2 \pi N^2 at,$$

if it is remembered that the diameter of the cut increases by $2a$ after each revolution. Substituting in equation (3), we get:

$$C^n = \int_0^{T_m} (v_0 + 2 \pi N^2 at)^n \, dt =$$

$$= \frac{1}{2 \pi (n+1) N^2 a} (v_m^{n+1} - v_0^{n+1}),$$

v_m being the maximum speed found in the disk-test. We now get the following expression for the required relation between the Taylor tests and the disk tests:

$$v_m^{n+1} - v_0^{n+1} = 2 \pi (n+1) \, a \, N^2 \, C^n \quad . \; (4)$$

By substituting the values v_{m1} and v_{m2} for two disk-tests carried out with different lathe speeds N_1 and N_2 we get two equations of the form of (4), from which C and n can be readily calculated. Thus, for $T = 30$, v_{30} can be directly calculated by inserting these values in (1).

If n is already known, the normal cutting speed v_T corresponding to the tool-life T can be deduced from a single test on a disk, for by eliminating C from (4) and (1) and neglecting v_0^{n+1} against v_m^{n+1} [7]) we get:

$$v_T = v_m \sqrt[n]{\frac{v_m}{2 \pi (n+1) N^2 a T}}$$

To obtain the simplest expression, we substitute $v_m = \pi N D_m$ (equation (2)) under the radical sign. If further the cutting speed is expressed in meters per minute, the feed a in mm per revolution, the diameter D_m in mm, the lathe speed N in r.p.m. and the time T in mins, so we finally get:

$$v_{30} = v_m \sqrt[n]{\frac{D_m}{60 (n+1) N^2 a}}, \quad . \; . \; (5)$$

By this expression the normal cutting speed v_{30} for a tool-life of 30 min can be calculated from the values of v_m and D_m obtained in a single disk-test.

Equation (5) has been very satisfactorily confirmed by actual tests. For a number of steels submitted to Taylor tests and to disk-tests, v_{30} was determined in the Taylor tests by interpolation in the v-T diagrams and in the disk-tests by the use of equation (5). The measured and calculated values of v_{30} are plotted in *fig. 5*. Each point marked corresponds to a particular kind of steel. If the assumptions made were rigorously valid, all points should lie on the drawn 45-degree line.

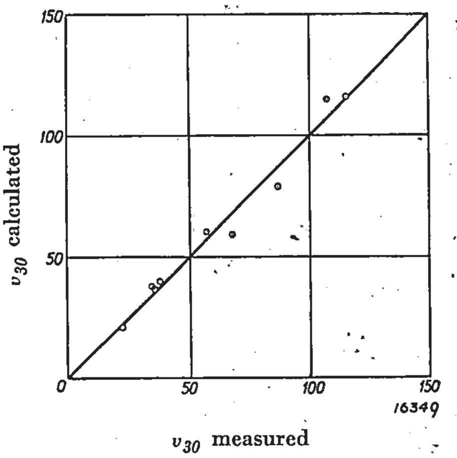

Fig. 5. Relation between the measured and calculated values of v_{30}. Each point shown corresponds to a particular steel. The measured value of v_{30} is derived from a v-T diagram such as in fig. 2 and is thus the result of a series of Taylor tests; the calculated value of v_m has been deduced from equation (5) with values of v_m and D_m found in a disk-test. As the diagram shows, the agreement between these two sets of values is very satisfactory.

In view of the low degree of reproducibility inherent in cutting tests of this type, it is evident that the deviations found are rather small. The scattering of the points about the 45-degree line is, moreover, such as to indicate accidental deviations, so that on the whole the results may be considered satisfactory.

(To be continued.) Compiled by P. CLAUSING.

---

[7]) With $n = 6$, the smallest value occurring in practice, the error due to this neglect is still less than 1 per cent, if the diameter D_0 of the hole in the plate is less than $D_m/2$.

PRACTICAL APPLICATIONS OF X-RAYS FOR THE EXAMINATION OF MATERIALS

V.

By W. G. BURGERS.

As already indicated in the previous article in this series, the possibility of detecting by radiographic means the presence of specific chemical compounds in a mixture or a chemical reaction product leads to numerous applications of the X-ray method for investigation. Some more examples of these applications (identifications) are given in the present issue.

9. Metallic Deposition in the Formation of Metallic Carbides [1])

Metallic carbides, i.e. the compounds composed of carbon and metals, such as *titanium*, *zirconium*, *tantalum*, etc., are characterised by a high melting point, which in certain cases, e.g. tantalum carbide, is even higher than that for tungsten. In consequence the formation and properties of these compounds have been closely investigated in the light of their potential use for incandescent bodies.

One method of preparing these carbides consists in strongly heating a carbon filament in the vapour of a volatile compound of the metal in question (usually a halogen compound), with or without an admixture of hydrogen. The formation of the carbide may then be represented by an equation of the type:

$$\mathrm{M\,X_n + C \rightarrow M\,C + n\,X}$$

(M = metal, X = halogen), the halogen liberated either being evacuated or combining with the hydrogen.

The carbide filaments obtained, which have a metallic appearance, are difficult to analyse by chemical means, as they are highly resistive to all reagents. Owing to their simple crystal structure they can, however, be quite conveniently identified by radiographic means. *Fig. 1a* shows an X-ray photograph of zirconium carbide ZrC. The discontinuous character of the lines indicates, that the wire is composed of comparatively large crystals (> 10 μ) (cf. the introduction to section II in this Review **1**, 60, 1936).

In certain cases (depending on the temperature at which the above reaction takes place) wires are obtained, having a colour differing from the normal colour. An X-ray photograph of a wire of this type is shown in *fig. 1b*, which in addition to the ZrC lines found in *fig. 1a* also contains a number of lines coinciding with those in *fig. 1c*. This latter photograph was obtained with a wire of metallic zirconium. Thus it is shown that, in fig. 1b, in addition to the formation of carbide a deposition of metal has also taken place. A similar result was also observed in the case of tantalum carbide, where moreover it was found that two different carbides could be formed, viz, TaC and Ta_2C, each having a different crystal structure.

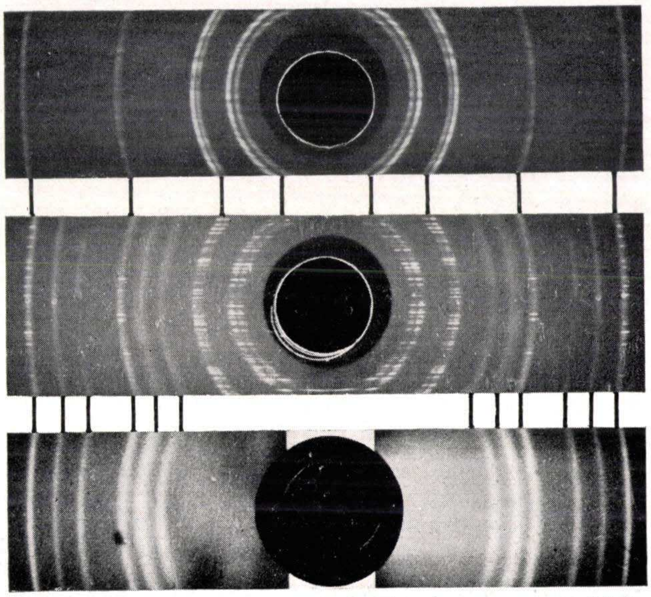

Fig. 1. Metallic deposition in the formation of metallic carbides.
a) Zirconium carbide,
b) "Zirconium carbide" wire obtained by heating a carbon filament in an atmosphere of zirconium halide,
c) Metallic zirconium.

10. Detection of Thorium Oxide and Metallic Thorium in Tungsten Wire [2])

Various properties of drawn tungsten wires, such as crystal growth, recrystallisation ability, electronic emission, etc., depend on the presence of certain admixtures of which one of the commonest is thorium. Tungsten containing thorium is obtained by adding thorium nitrate or hydroxide to the tungsten oxide which is to be reduced. For electronic emission it is of paramount importance, whether the thorium occurs in the metallic state (Th) or as oxide (ThO_2) in the reduced tungsten which is made into wire.

---

[1]) W. G. Burgers and J. C. M. Basart, Z. anorg. allg. Chem. **216**, 209, 1934.

[2]) W. G. Burgers and J. A. M. van Liempt, Z. anorg. allg. Chem. **193**, 144, 1930.

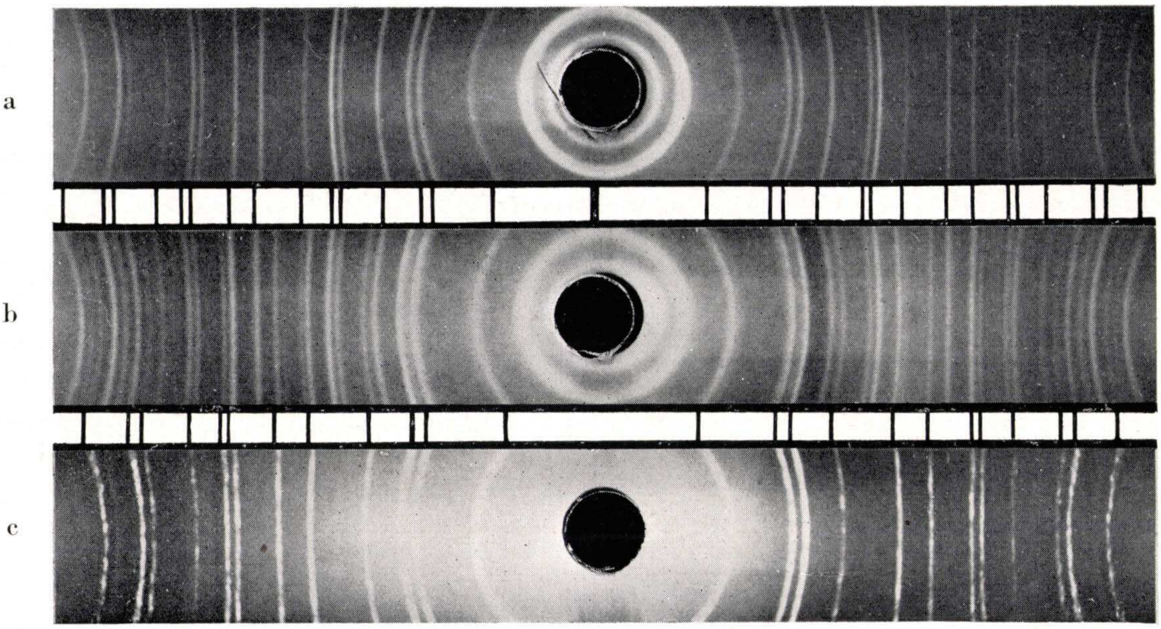

Fig. 2. Thorium oxide and metallic thorium in tungsten wire.
a) Thorium oxide (ThO_2),
b) Mixture of thorium oxide and metallic thorium,
c) Metallic thorium.

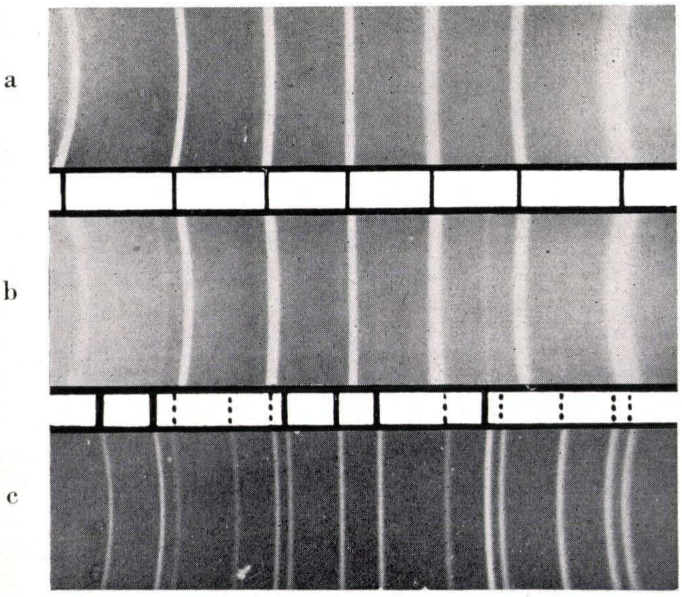

Fig. 3. Thorium oxide in tungsten wire before heating.
a) Pure tungsten (drawn wire),
b) Tungsten + 3 per cent thorium oxide (drawn wire),
c) Thorium oxide (= left part of fig. 2a).
The dotted lines between figs. b and c indicate diffraction lines, which were too weak in photograph b to be sufficiently clear for reproduction by printing.

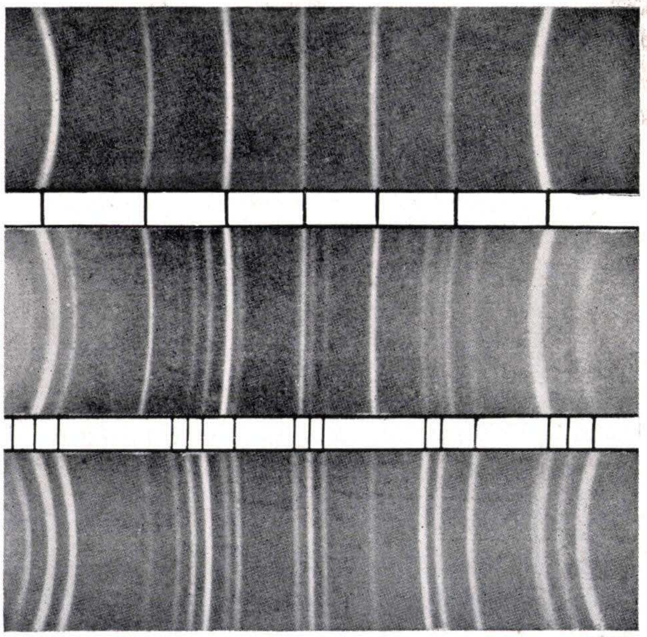

Fig. 4. Electrolytic deposition of β- with α-tungsten.
a) α-tungsten (= fig. 3a),
b) Electrolytic product from a ternary melt of tungstates,
c) β-tungsten obtained from a phosphate melt.

It is generally assumed, that the thorium compounds mentioned (nitrate and hydroxide) are not themselves reduced during the reduction of the tungsten oxide, but are converted to oxides and are thus present in the wire as such before heating or on heating to a comparatively low temperature. According to the current theory partial reduction of the thorium oxide to metallic thorium is assumed to occur only on raising the wires to a high temperature (about 3000 deg. C); the metallic thorium thus formed may then produce an enhanced electronic emission according to Langmuir.

It is difficult to determine definitely by chemical means, in how far these conclusions are justified. Though it is possible, to dissolve away the metallic tungsten with special solvents which attack neither metallic thorium nor thorium oxide (a mixture of concentric hydrofluoric acid and nitric acid) [3]), leaving a white residue in the case of an unheated wire and a grey residue in the case of a strongly heated wire, the quantity of these residues is usually too small for accurate quantitative chemical analysis (normally a total of $^3/_4$ per cent of thorium oxide is contained in tungsten wire). This quantity is, however, amply sufficient for X-ray analysis. It is found, that a radiograph for the white residue is identical with that for ThO_2, while that for the grey residue contains, in addition to the ThO_2 lines, other lines corresponding to those of metallic thorium. A comparison of the photographs reproduced in *figs. 2a, b* and *c* shows clearly, how these differences can be determined, and thus demonstrates quite definitely, that the unheated tungsten wire contains the added thorium as oxide whilst the strongly-heated wire contains metallic thorium.

Even without chemical treatment, the X-ray method can be employed to detect directly the presence of thorium oxide in tungsten wires before heating, provided the tungsten used initially contained an extra large amount of the admixed thorium compound, to give for instance a ThO_2 content of 3 per cent. *Fig. 3b* is a radiograph obtained with such a wire, together with a comparison photograph for pure tungsten (*a*) and for thorium oxide (*c*). A comparison of these photographs shows, that the wire radiograph contains, in addition to the very intensive (strongly overexposed) lines of tungsten itself (cf. with *a*), also a few weaker lines, which coincide with the ThO_2 lines in *c*.

11. Electrolytic Deposition of β- with α-Tungsten [4])

Metallic tungsten can be deposited by the electrolysis of fused alkaline tungstates [5]). By means of X-rays it can be shown, that when the temperature of the melt is kept below 700 deg. C in addition to the normal α-tungsten another modification, β-tungsten, is deposited. According to the discoverers of this phenomenon, this only occurs, when tungstate phosphate melts are used.

It was important to demonstrate, that β-tungsten was also formed in the absence of phosphoric acid, provided only the temperature of the melt was kept below the upper limit mentioned above.

This is indeed shown to be the case by the radiographs reproduced in *fig. 4*. Fig. *4b* relates to an electrolytic product obtained at 500 deg. C from a ternary melt of potassium, sodium and lithium tungstates; *a* is the photograph for pure α-tungsten and *c* the radiograph [7]) of β-tungsten obtained from a phosphate melt. A comparison of *b* with *a* and *c* shows that the metal obtained from the phosphate-free melt contained both modifications; a study of *c* moreover shows, that conversely the β-tungsten obtained from the phosphate also contains a certain amount of α-tungsten.

---

[3]) J. A. M. van Liempt, Rec. Trav. chim. Pays-Bas **45**, 512, 1926.

[4]) W. G. Burgers and J. A. M. van Liempt, Rec. Trav. chim. Pays-Bas **50**, 1050, 1931.

[5]) J. A. M. van Liempt, Z. Elektrochem. **31**, 249, 1925.

[6]) H. Hartmann, F. Ebert and O. Bretschneider. Z. anorg. allg. Chem. **198**, 116, 1931.

[7]) This radiograph was made by Dr. H. Hartmann.

ABSTRACTS OF RECENT SCIENTIFIC PUBLICATIONS OF THE N.V. PHILIPS' GLOEILAMPENFABRIEKEN*)

No. 1064: J. H. de Boer and J. D. Fast: Die Diffusion von Wasserdampf durch Kupfer (Rec. Trav. chim. Pays-Bas **54**, 970-974, Dec. 1935).

At temperatures of approximately 800 deg. C. steam diffuses very easily through copper. Hydrogen diffuses much quicker through this metal, whilst nitrogen does not diffuse through it at all. With respect to ferro-chrome, nitrogen and steam exhibit opposite behaviours: Steam does not diffuse through ferro-chrome, while nitrogen diffuses very readily.

---

*) A sufficient number of reprints for purposes of distribution is not available of those articles marked with an asterik (*). Reprints of other papers may be obtained on application from Philips Laboratory, Kastanjelaan, Eindhoven, Holland.

No. 1064A: J. H. de Boer: Verandering van de ionisatie-energie van een alkali-atoom door binding (Ned. T. Natuurk. **2**, 273-288, Dec. 1935).

A simple description is given, showing how the binding energy of an electron to an ion decreases under the influence of an external electric field. This concept is then expanded, to describe the reduction in the ionisation energy of an alkali atom which is adsorbed at the surface. Potential curves for the adsorptiou of caesium in various states to a salt surface are given. Various phenomena are discussed in their relation to adsorption.

No. 1065: G. Heller: Dynamical similarity laws of the mercury high-pressure discharge (Physica **6**, 389-394, Dec. 1935).

According to Elenbaas the properties of electric discharges through mercury vapour at a high pressure are determined by the quantity of mercury vapour (m) and the energy consumption (L) per cm of the tube length. It is investigated, how m and L must be altered simultaneously in order to obtain corresponding states. Thermal equilibrium is assumed in this analysis. Self-absorption and the effect of differences in the temperature of the walls are not considered. Experiments show, that the laws derived are applicable in practice.

No. 1066: M. Ziegler: Shot effect of secondary emission. I. (Physica **3**, 1-11, Jan. 1936).

The author assumes, that the impact of a primary electron on a metal surface and the emission of the n secondary electrons, which are liberated by such impact, take place practically simultaneously, so that the primary and the n secondary electrons together give a single current impulse. As not all primary electrons liberate the same number of secondary electrons, the secondary electron current is not made up of equal impulses. It can however be resolved into components composed of equal impulses. Since the primary collisions are independent of each other, it is possible by means of the theory of the shot effect, to calculate the quadratic variations of secondary electron currents. The author has carried out this calculation for a triode, in which the grid and anode are positive and secondary electrons can be emitted. It is found, that there must be a certain relationship between the quadratic fluctuations of the anode current and those of the grid current. This relationship is confirmed by accurate measurements indicating the correctness of the assumption, on which the calculation was based.

No. 1067: W. Elenbaas: Dynamische Charakteristiken des Quecksilberbogens (Physica **3**, 12-30, Jan. 1936).

Alternating currents with frequencies from 50 to 1400 cycles were superimposed on the D.C. through a discharge tube containing mercury vapour at a pressure of 1/6 to 100 atmos. On raising the frequency from 60 to 14000 cycles the phase angle between the voltage and current diminished from 150 deg. to 25 deg. The ratio of A.C. to D.C. conductivities first increased and then diminished again, and at very high frequencies probably approaches unity. For a frequency of 50 cycles the curve for the emitted luminous radiation was measured by taking an oscillogram of the amplified current of a potassium photo-electric cell; the modulation of the luminous intensity at this frequency is greater than that of the current or the energy consumed. On the assumption of a temperature equilibrium and Boltzmann's distribution the radiation curve was calculated from the current and voltage curve using Saha's formula. The calculated modulation is then about double the value measured; this is probably due to neglecting the absorption which is greater at maximum luminous intensity than at minimum. By striking an energy balance for the discharge and applying Saha's ionisation theory the characteristics for the discharge can be deduced when only the shape of the current curve is given. The relationship between temperature and phase found in this way is in very good accord with the values calculated by the first-mentioned method. The calculated voltage curve is in satisfactory coincidence with the results of measurement.

No. 1068: J. A. M. van Liempt: Die Verdampfungsgeschwindigkeit der Metalle in einer Gasatmosphäre (Rec. Trav. chim. Pays-Bas **55**, 1-6, Jan. 1936).

In continuation of paper No. 1051, where the volatilisation of a metal surface in vacuo was studied, this paper is devoted to a discussion of the influence of the gas molecules in the surrounding atmosphere on the volatilisation of a metal filament. The number of atoms, which at a specific temperature leave the surface of an incandescent filament is independent of the surrounding gaseous atmosphere. Owing to the collisions with gas atoms a part of the metal atoms may, however, drop back to the surface of the filament, as a result of which the rate of volatilisation in a gaseous atmosphere of pressure is reduced in a definite ratio as compared with the ratio in vacuo. The author obtains an expression for this ratio, which at the limit $p = 0$ tends to unity. The formula of Sophus Weber according to which this ratio is inversely proportional to the square root of the gas pressure does not satisfy this limiting condition and cannot therefore have a strict validity. For pressures which are not too low the two formulae agree fairly well with each other as well as with the experimental results. At higher pressures deviations are observed which are probably due to the fact, that the free path of the atoms then has an order of magnitude comparable to the irregularities in the surface of the filament.

No. 1069: M. J. Druyvesteyn: Calculation of Townsend's α for Ne (Physica **3**, 65-74, Febr. 1936).

For electrons which diffuse through a rare gas under the action of a homogeneous electric field the stationary distribution of velocity is calculated from a consideration of elastic collisions, excitation and ionisation. It is assumed in this calculation that the probabilities of excitation and ionisation are linear functions of the energy of the electron. A number of physical properties can be calculated from the velocity distribution. For ratios between the electric field strength and the pressure between 5 and 30 volts per cm and per mm gas pressure, the ionisation coefficient α of Townsend was calculated and found to be in good agreement with experimental measurements. The energy loss due to elastic collision can in this case be neglected without affecting the result.

No. 1070: J. L. Snoek: Magnetic powder experiments on rolled nickel-iron. I. (Physica **3**, 118-124, Febr. 1936).

The so-called Bitter striae were registered for rolled nickel-iron in a more or less pronounced anisotropic state. The striae always run parallel to the direction of easiest magnetisation. With highly anisotropic material the system of lines is less clear than with a low anisotropy; it can in fact only be clearly seen when the lines of force issue perpendicularly. According to the author this is probably due to the fact that in a highly anisotropic sheet the internal stresses are weaker. Reheated material shows no striae. With coarse-crystalline sheets striae are found which correspond to those observed by Bitter and Akulov with stress-relieved single crystals. Intersecting systems of lines are found and sometimes also a second system parallel to the first, but with a much greater period.

No. 1071: J. H. de Boer: The influence of Van der Waals' forces and primary bonds on binding energy, strength and orientation, with special reference to some artificial resins (Trans. Faraday Soc. **32**, 10-37, Jan. 1936).

This paper commences with a discussion of the mutual orientation of the molecules under the influence of Van der Waals' forces. The tendency of the atoms to be in contact with as many other atoms as possible generally predominates over the anisotropy with respect to polarisability. Neglecting the repulsive forces, satisfactory results are obtained for the energy in the equilibrium state by means of the approximation formulae of London or of Kirkwood and Slater. As is well known, a much greater tensile strength is calculated for a theoretical crystal than that found by actual measurement of ordinary crystals. If the Van der Waals' forces are taken into consideration in such calculations then the tensile strength of the crystals would be found higher still. By assuming a mosaic structure of the type suggested by Zwicky much lower tensile strengths are obtained, but these are still much higher than the measured values. According to Smekal the low tensile strengths are due to structural defects in the crystal lattice. These suggestions made with regard to salt crystals are applied by the author to artificial resins of the phenol-formaldehyde and m-cresol-formaldehyde types. For the theoretical structure the tensile strength is found to be about 4000 kg per sq. mm, whilst in a mosaic structure with Van der Waals' forces this value would be reduced to 35 kg per sq. mm, which, is however, still much higher than the measured value of 7.8 kg per sq. mm for the tensile strength of phenol-formaldehyde. This may probably be due to inhomogeneities of the substance. With a theoretical structure, values for the tensile strength can indeed be obtained in this way which are of the correct order of magnitude. Young's modulus for artificial resin does not depend on Van der Waals' forces (cf. No. 1072 by R. Houwink). The potential curve of the linkage between two benzene molecules was also investigated on the basis of the mutual forces acting between the individual CH groups. Regarding the orientation of the benzene rings in a substance, such as polystyrene, it was found that the benzene ring assumes a preferential position with its plane vertical to the direction of the aliphatic carbon chain of this substance. The negative double refraction caused by flow in the case of polystyrene is thus explained.

VOL. 1 No. 7 JULY 1936

Philips Technical Review

DEALING WITH TECHNICAL PROBLEMS
RELATING TO THE PRODUCTS, PROCESSES AND INVESTIGATIONS OF
N.V. PHILIPS' GLOEILAMPENFABRIEKEN

EDITED BY THE RESEARCH LABORATORY OF N.V. PHILIPS' GLOEILAMPENFABRIEKEN, EINDHOVEN, HOLLAND

IRRADIATION OF PLANTS WITH NEON LIGHT

By J. W. M. ROODENBURG and G. ZECHER.

Summary. Owing to the want of light the growth and development of plants during the winter becomes considerably arrested. This check may be completely or partly counterbalanced by irradiating the plants with artificial light. Owing to its favourable spectral distribution neon light is particularly suitable for this purpose. The technical development of neon light sources for plant irradiation and the irradiation conditions laid down by Roodenburg on the basis of extensive experimental work now permit the commercial grower and the amateur horticulturist to promote the growth of their plants by irradiation.

After decades of abortive experiments in the Netherlands and elsewhere on the artificial irradiation of plants, an appreciable measure of success has recently been achieved in this direction. That light is one of the principal factors in the growth of plants has been realised for many years, and the idea has long been entertained of attempting to influence the growth and development of plants by irradiation with artificial light. But only with the technical development of the requisite sources of light has a fundamental investigation of this problem been made possible and enabled the market grower and amateur horticulturist to employ irradiation methods on a practical scale.

Composition of light for the irradiation of plants

The life and growth of plants are intimately connected with certain chemical processes. One of the chief of these is the assimilation of carbon dioxide, in the course of which the plants absorb carbon dioxide from the air and the carbohydrates from the water of which plants are principally built up. Carbon dioxide assimilation takes place only when a light stimulus is provided, the light being absorbed by the green colouring matter of the leaves, viz, chlorophyll. If the light available for the plant drops below a specific level, e.g. during the short days of winter, growth is practically static, even though all other conditions for their growth are adequately met, as for instance by placing in heated and moist greenhouses and by the addition of suitable fertilisers.

By augmenting the natural light with an auxiliary source of illumination, it has now been possible to promote the growth of plants even during the darkest winter months.

Carbon dioxide assimilation is most active in red light, which is absorbed to a high degree by chlorophyll. Hence, in providing auxiliary irradiation for plants, it is essential to utilise a source of light containing a sufficient concentration of red rays. At an early date it was therefore proposed to employ neon light for this purpose [1]). *Fig. 1* shows the spectrum of a neon light source and the assimilation curve, the latter indicating the amount of carbohydrate formed on irradiation with an equivalent light energy of each wavelength. Neon has the most intense lines just in that region in which the effect of light on carbon dioxide assimilation is greatest. The same figure also gives the spectrum for an ordinary glowlamp. The greater part of the radiation from the glowlamp consists of infra-red (invisible) rays and only 8 per cent of its radiation is situated in the visible spectrum, whilst about 20 per cent of the total energy radiated from the neon tube lies in this region. But since glowlamp light is much easier to generate and to manipulate than neon light, experiments have also been carried out on the irradiation of plants with glowlamp light. In the first place it is necessary to produce an adequate intensity of red light. This can be readily obtained with high-power glowlamps, although at the same time an immeasurably greater amount of energy is also radiated in the undesirable region of the spectrum.

---

[1]) G. Höstermann: Experiments with neon light. Bericht Königl. Gärtnerlehranstalt Dahlem, 1916-17, p. 76.

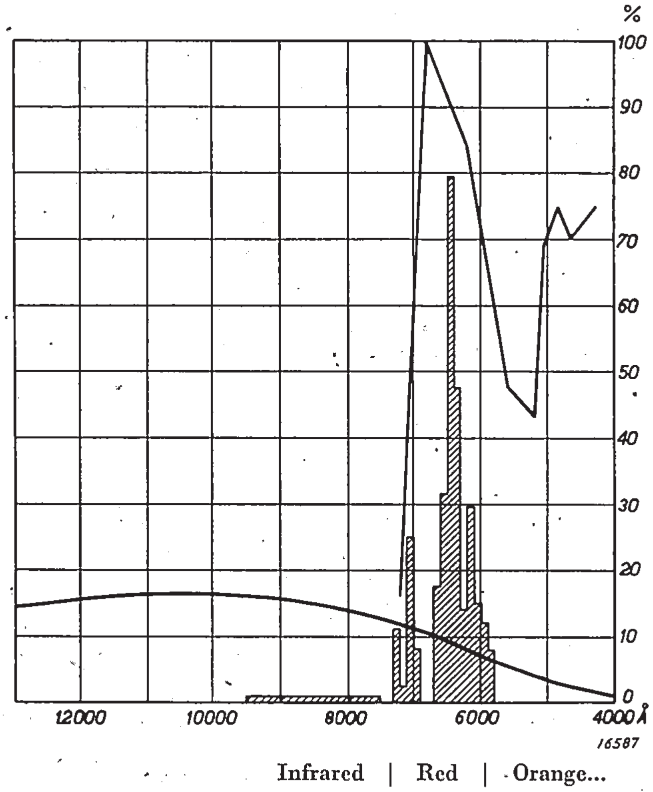

Fig. 1. Assimilation curve of plants, giving the relative amount of carbonhydrate formed on irradiation with a specific light energy at each wave length. The spectra for a neon light source and an ordinary glowlamp are also included. The strongest neon lines are situated exactly in that region of the spectrum of principal importance to assimilation, whilst maximum radiation from the glowlamp is obtained at much higher wave lengths, viz. in the infra-red.

Investigations made by Roodenberg [2]) gave a fresh insight into this problem in so far as they demonstrated that excess infra-red rays were not only superfluous but even deleterious to the plants. Nearly all investigators have found with glowlamp light that, although the growth of the leaves was promoted in the irradiated plants, the general quality of the plants suffered, as the stems and stalks grew too "leggy". This "legginess" is due to the high percentage of infra-red heat rays given out by glowlamps [3]).

As we have already seen, neon light also contains infra-red radiation, although there is here not the same disproportion between the infra-red and the red rays as found with the glowlamp. Moreover, the distribution of the radiated energy over the various parts of the infra-red region is here quite different, as is shown in *fig. 2*. The "infra-red" has here been divided up into three almost arbitrary ranges, viz. from a wave length of 0.8 to 1.3 μ, from 1.3 to 3 μ, and above 3 μ. The "visible" wave lengths extend from 0.4 to 0.8. Neon light radiates an adequate amount of energy in the first (visible) range, almost none at all in the second and third ranges and a very large proportion in the last range (above 3 μ). A glowlamp, on the other hand, which in the visible spectrum gives the same amount of radiation energy as the neon tube, radiates light rays principally in the two ranges of 0.8 to 1.3 and up to 3 μ. It is, moreover, probable, although not yet confirmed by experiments, that the infra-red radiation in the range from 0.8 to 3 μ causes more "legginess" in plants than the very long wave radiation 3 μ. For the latter radiation is already radiated to a considerable extent by the heating arrangements provided in greenhouses and living rooms.

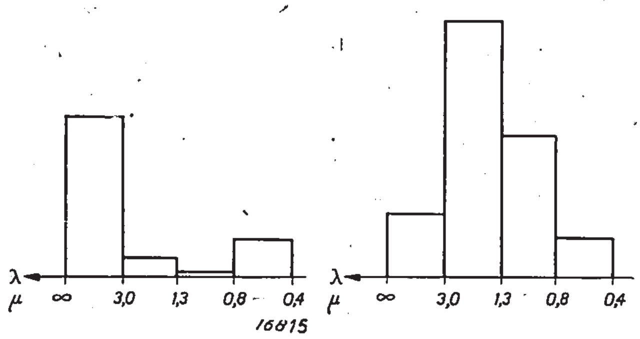

(a) (b)

Fig. 2. Infra-red radiation in neon light (*a*) and in glowlamp light (*b*). The infra-red range is divided into three fairly arbitrary parts. The ratio of visible to infra-red radiation is much less favourable with the glowlamp than with the neon tube. At the same time radiation between 0.8 and 3 μ, which probably is mainly responsible for the unwanted "legginess" of plants, is almost completely absent in the neon light, whilst it constitutes the greater part of radiation from the glowlamp.

The points outlined above have been confirmed by a large number of experiments on a wide variety of plants, in which the neon light was found exceptionally suitable for plant irradiation. In *figs. 3* to *6* a few of the results arrived at in these experiments are reproduced. The general observation may be made that apart from more rapid growth larger leaves are also formed, which owing to the greater amount of chlorophyll formed are coloured a dark green [4]), the stems are thicker, the roots are stronger, and frequently the formation of fruit and blooms is also much promoted.

---

[2]) J. W. M. Roodenburg: Kunstlichtcultuur, October, 1930 and December, 1932. Meded. Landbouwhoogeschool Wageningen, vol. **34**, No. 8 and vol. **36**, No. 2. (Published by R. Veenman, Wageningen.)

[3]) In some cases it is mainly a question of rapid growth, as in the germination of seeds and bulb culture, etc. No carbohydrates need be formed in these instances, their formation taking place at the cost of reserve bodies which have been accumulated in the bulb. With these plants, growth may be equally well promoted merely by increasing the temperature; "light" is of no specific value here.

Dosage of irradiation

Similar to the procedure dictated in irradiation treatment for medical purposes, the application of the correct dosage is also a most important factor in the irradiation of plants if successful results are to be obtained. The correct dosage can also be established by actual experiments, and is determined by two factors: The radiation intensity to be used and the time during which the plants are exposed to irradiation. Important experimental data have already been collected regarding this question, particularly by the Agricultural College at Wageningen. It is evident that in these experiments the "efficiency" of irradiation has also had to be given consideration in view of the practical adoption of the method by market growers: The costs of irradiation must be in reasonable proportion to the extra return which well-developed plants will fetch.

As regards the requisite intensity of irradiation, the experiments have shown that with the majority of plants very good results can be obtained with an illumination intensity of 500 to 1000 lux. For purposes of comparison it may be stated that the mean illumination on a December day at about 3 o'clock in the afternoon is roughly 3000 lux and during the evening on a sufficiently illuminated desk about 200 lux.

Turning to the irradiation times, it is possible to regulate the "light diet" of the plants in a variety of ways. Consideration must be given to the stage of growth at which the plants are irradiated, furthermore for how many weeks or months irradiation is to be applied and how many hours each night. In general an irradiation period of 8 hours nightly is recommended, e.g. from 10 p.m. to 6 a.m. It does not lie within the scope of this article to set forth full instructions for irradiating plants, such as have been worked out on the basis of the research carried out at Wageningen referred to above, particularly as the instructions vary according to the genus of the plants.

The irradiation of Star of Bethlehem (Campanula isophylla) may, however, serve as an example. This plant, which is slipped and potted in spring and is disbudded as much as possible during the summer, is usually transferred to the forcing house about the first of September. About the middle of November irradiation with neon light is commenced (at a forcing house temperature of 15 °C.). During the first few weeks little result is to be seen, although the irradiated plants very soon acquire a fine dark-green colour. During December the growth of the plants is rapid and large leaves and stout stems are formed. At the end of January, when the plants have borne a host of buds, irradiation can be terminated. Irradiation is therefore only applied during the budding period. As early as the beginning of February the first buds will open on the irradiated plants (see the photograph in fig. 3).

Plant irradiation equipment. Neon tubes

At the time neon lights were introduced for the irradiation of plants, they had already been employed for several years for luminous advertisements. The neon light sources used for these purposes consisted of a long glass tube, into the ends of which two iron electrodes were fused, and containing a neon filling at a pressure of approx. 10 mm. They were run on high tension (e.g. 3000 volts) and emitted a comparatively small luminous flux per metre of tube length (160 lumens per m). The use of high tension in damp forcing houses for the irradiation of plants met with serious objection as well as the low brightness of the high-tension tubes. To obtain the requisite illumination of at least 500 lux

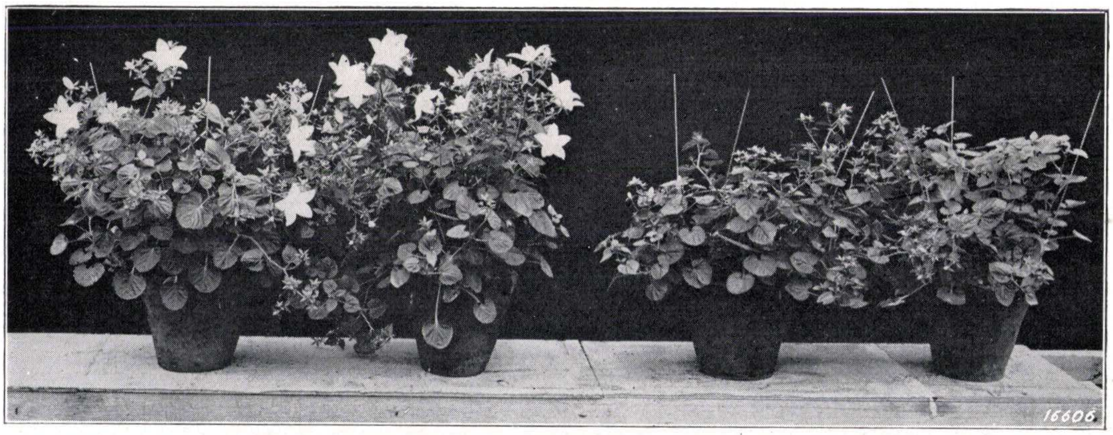

Fig. 3. Star of Bethlehem (Campanula isophylla). Picture taken on February 5, 1934. Left: Irradiated with neon light, 600 lux, each night from 10 p.m. to 6 a.m. from November 2, 1933, to January 25, 1934. Right: plants non-irradiated.

---

[4] This result is frequently observed after only a few nights' irradiation.

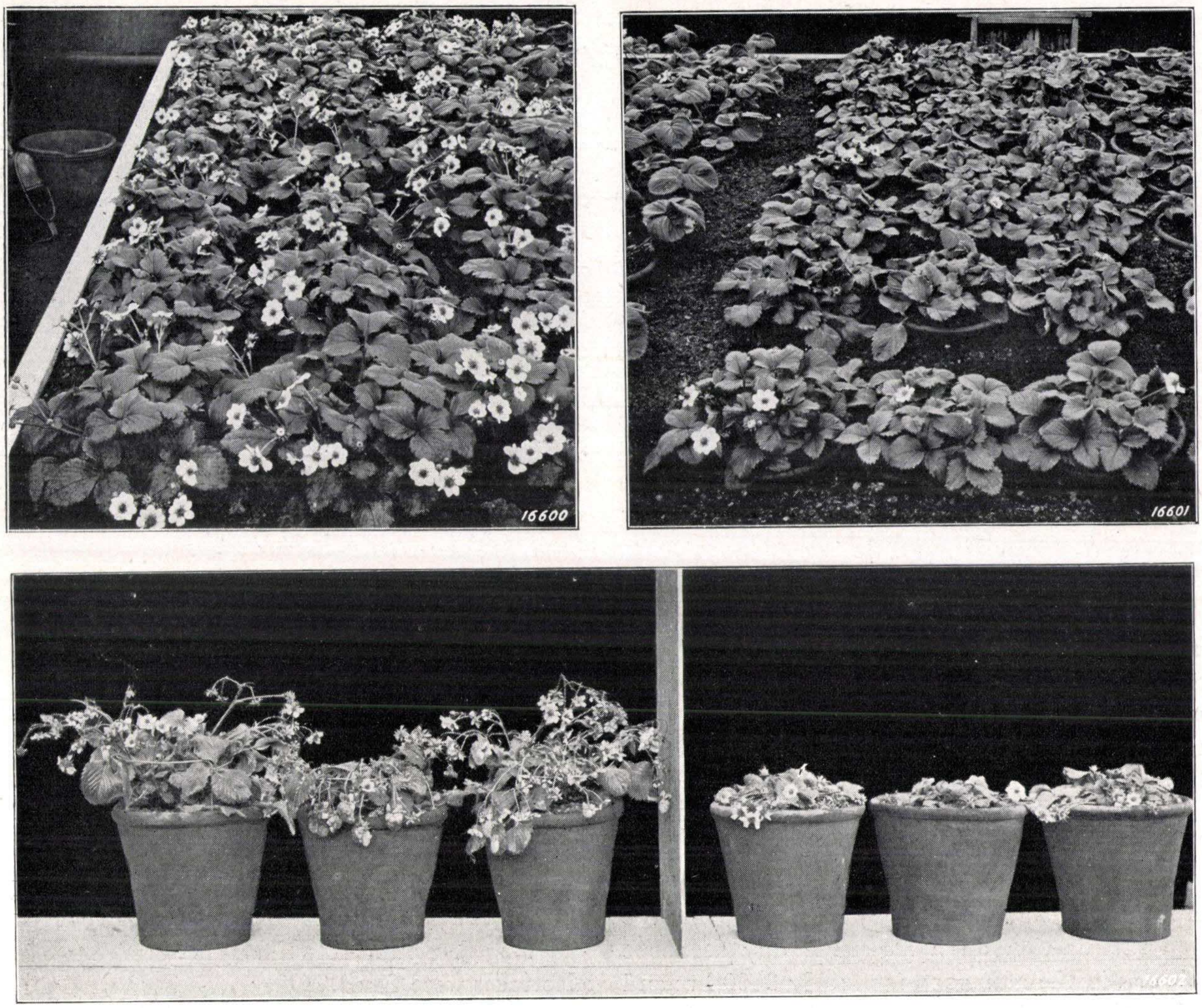

Fig. 4. Strawberry, var. "Deutsch Evern." Potted in the open, July 19, 1935; transferred to forcing house October 2.

a) Picture taken on December 7, 1935. Left: Irradiated with neon light, approx. 450 lux, nightly 10 p.m. to 6 a.m. Right: Non-irradiated plants.

b) Picture taken February 28, 1936 (towards the end of the crop). Left: Irradiated as at (a). Right: Non-irradiated plants.

a tube already about 5 m long was required for 1 sq. m of radiation surface.

The illumination intensity could only be increased at that time by raising the current intensity, but with the then normal pressure (10 mm) of the neon filling this had a very adverse effect on the efficiency and the life of the tubes. A satisfactory efficiency could only be achieved with a pressure of 1 mm and below, or by increasing the current density in the tubes ten times. This lower pressure, however, led to a pronounced disintegration of the iron electrodes due to ionic bombardment resulting from the high voltage drop at the cathode in this range (approx. 300 volts); the life of a low-pressure neon tube was thus reduced to a few hours. Amelioration was afforded by the use of hot cathodes, which owing to their electronic emission reduced the cathode fall to a few volts and enabled the tubes to be run on low-tension. Modern gas-discharge lamps for highway lighting are also constructed on this principle. Compact high-power units are thus obtained, operating with currents of a few amperes instead of for instance 25 milliamps in the case of high-tension tubes. A selection of early and

Table I. Dimensions and Data of a High-tension Neon Tube (*H*) and Three Low-Tension Neon Tubes (Type Nos. 4307, 4309, 4311).

Tube	Running voltage volts	Overall diameter mm	Length of light column m	Tube current amps	Consumption watts	Light output lumens	Gross light yield lumens per watt
H		13—14	2	0.025	36	320	9
4307	380	40—43	1.5	3.0	500	8750	17.5*)
4309	220	45—48	1	4.5	450	6300	14
4311	220	16—18	0.35	0.95	90	1200	14

*) The light yield of the neon column after substracting the losses in the input unit and at the electrodes is in this case 26.5 lumens per watt.

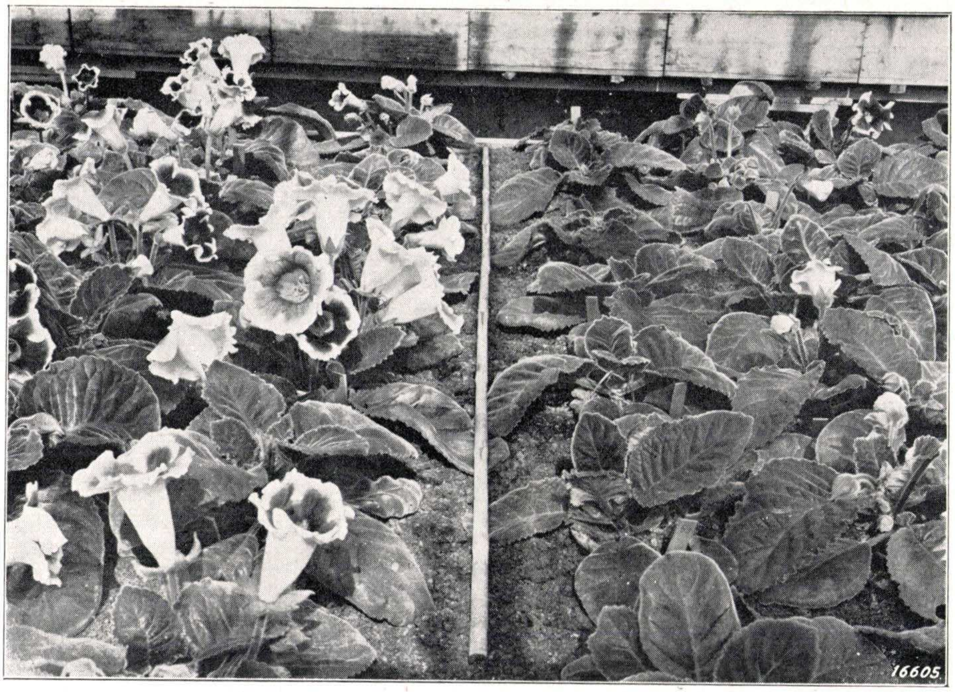

Fig. 5. Gloxinia, var. Kaiser Friedrich. Bulbs planted Nov. 11, 1932. Picture taken on April 3, 1933, i.e. one month after end of irradiation period. Left: Irradiated with neon light, approx. 800 lux, 8 hrs. nightly, until the end of February. Right: Non-irradiated plants.

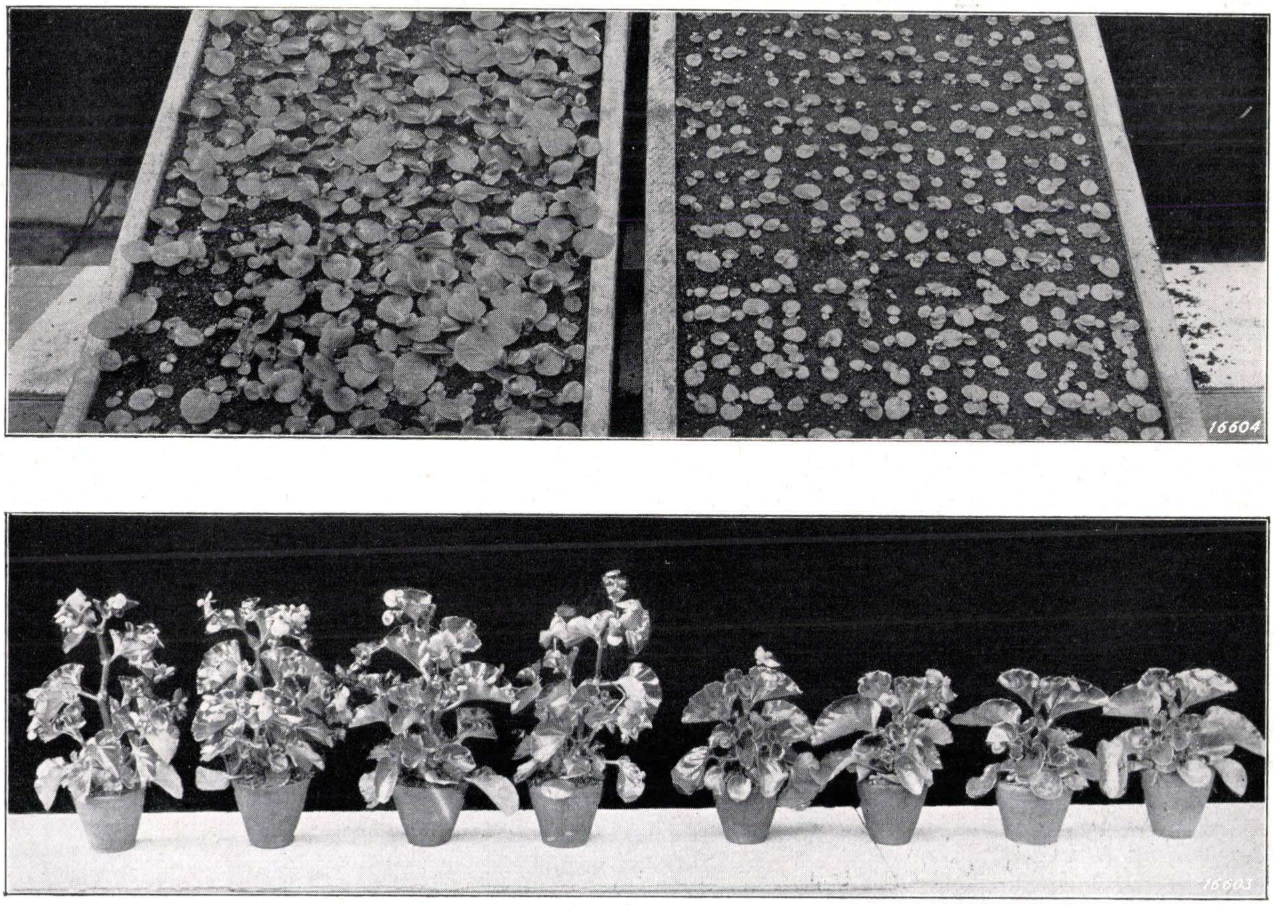

Fig. 6. Begonia gracilis luminosa. Sown November 3, 1934.

a) Picture taken on January 2, 1935. Left: Irradiated with neon light, approx. 600 lux, 10 p.m. to 6 a.m. nightly, from November 21. Right: Non-irradiated plants.
b) Picture taken on April 6, 1935, the same plants as shown in (a). Left: Irradiated till February 15, 1935. Right: Non-irradiated plants.

The second picture, which was taken seven weeks after the end of irradiation, shows very clearly the after-effects of irradiation.

modern types of tube are shown in *fig. 7*. A summary of the dimensions, applications and light outputs of these tubes is given in *Table I*.

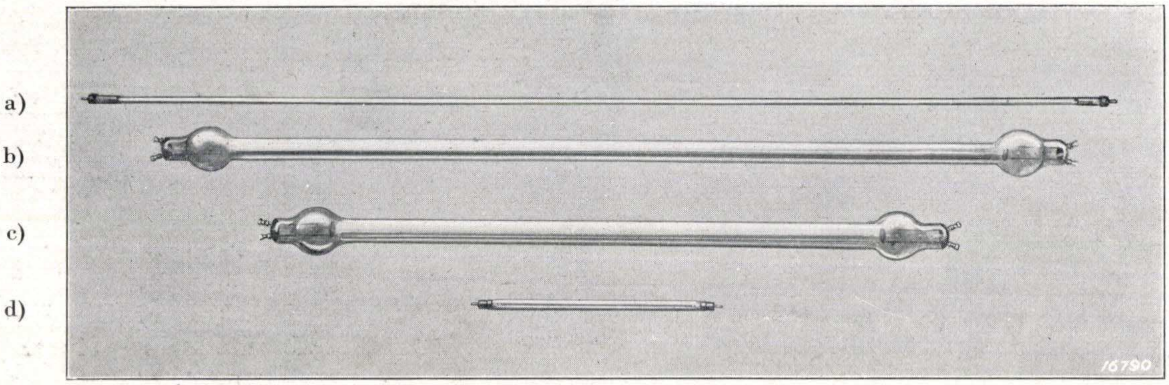

Fig. 7. Some early high-tension neon tubes (*a*) and various modern low-tension neon tubes (*b* to *d*). The electrical and illumination characteristics of these tubes are collated in Table I. Tube (*b*) emits practically 30 times as much light as (*a*) with approximately double the light yield; the small tube (*d*) gives almost four times the light obtained from (*a*).

The hot cathode is that component of the tube which ultimately determines the life of the tube, since the emitting substance (barium-strontium oxide) on the heated coil is steadily consumed. During the burning of the lamp the cathode suffers practically no disintegration at all and the light output of the tube remains uniform. Only after 2000 running hours does the consumption of the radiating substance become noticeable, the voltage-drop at the cathode increases, the cathode commences to be atomised, and in its neighbourhood a black deposit forms on the glass wall ⁵), which adsorbs gas, as a result of which the cathode voltage-drop increases considerably until it becomes impossible to run the tube off the mains voltage and the tube must be replaced. The long life of 2000 running hours of the tube is due, *inter alia*, to the fact that in front of each cathode a plate is located (see fig. 7) which in the positive phase of the alternating voltage serves as anode and in this way protects the heated coil from excessive heating during the anode phase.

Circuit details and construction of plant irradiators

The neon tubes with hot cathodes are connected directly to 220 or 380 volts mains supply through a series-connected choke coil. In contrast to high-tension tubes special provision must be made here for starting up the tube, since the running voltage is too low to initiate the first electric discharge through the low-pressure neon gas. The extra-tension impulse which is obtained at the terminals of the series-connected choke on shorting the neon tube is utilised for this purpose. After the first discharge has taken place adequate residual ionisation is retained in the tube for re-ignition to be regularly obtained with a 50-cycle A.C. on reversing the polarity, even with a voltage which is too low for initiating the first discharge.

The circuit details of the large plant irradiators (types 4308, 4310 with tubes 4307, 4309) which have been designed for market growers, are shown in *fig. 8*. *T* is the heating transformer for the heated coils *K* which are run on 2 volts and 18 amps. *S* is the series choke coil. The heating coil *R* and the bimetallic strip *B* constitute a slow-acting relay, which connects up the initially-shorted tube *L* only after the coils *K* have become sufficiently heated. The tube is thus started up automatically by the slow-acting relay. If the first attempt at starting up fails owing to the phase of the supply being temporarily unfavourable at the instant the relay operates, the starting procedure is immediately repeated. The condenser *C* connected in parallel with the tube facilitates re-ignition, thus reducing

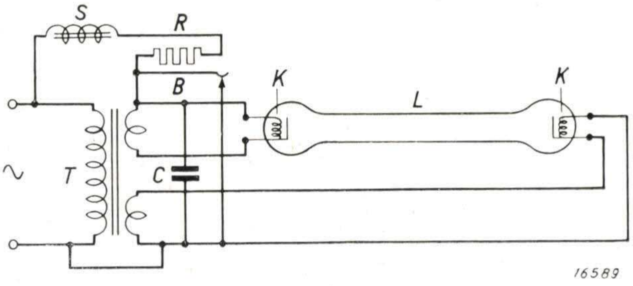

Fig. 8. Circuit details of the plant irradiator 4308 and 4310. The tube *L* is connected to the A.C. mains through a series-connected choking coil *S*. A bimetallic slow-acting relay *R* and *B* control signition. The cathodes *K* are heated through their own heating transformer *T*.

---

⁵) The black deposit is always restricted to the neighbourhood of the cathodes; the whole tube is never covered with a black deposit.

the mains voltage required and at the same time suppressing radio interference.

For small-scale operations and to meet the requirements of amateur horticulturists for conservatories and indoor use, a lower-power irradiator (rated for 90 watts) has been designed of which circuit details are given in *fig. 9*. By omitting the automatic starting device the circuit has been much simplified, whilst it has also been found possible to dispense with a heating current for the cathodes. When the cathodes have been once raised to the requisite temperature at the beginning of the discharge, they are kept suitably hot by the discharge itself. By introducing a special circuit the series choke coil is used as a heating transformer for heating the cathodes at the start of the discharge: After connecting the irradiator to the mains the two-pole switch *S* is pushed in, so that the choke now acts as an auto-transformer and the hot cathodes heat up. After releasing the switch the tube fires and the original circuit is re-established.

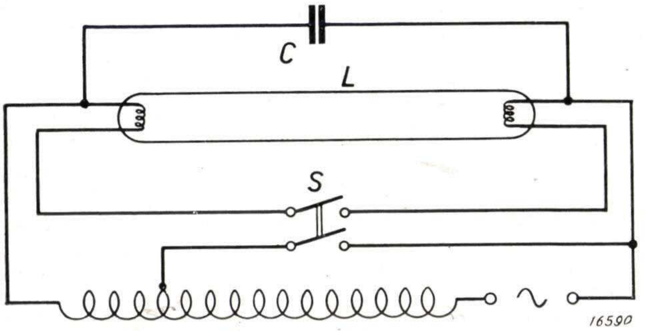

Fig. 9. Circuit diagram of the small plant irradiator 4312. By dispensing with the automatic ignition device the circuit has been much simplified; the choke coil also acts as a heating transformer.

The light-yield of this small tube is 14 lumens per watt (taking into consideration all losses); it has a life of 1000 running hours.

Installation of irradiation units

The neon tubes are mounted in reflectors, which considerably increase the efficiency of irradiation. These reflectors are flat and fairly small, so as not to take up too much space in the usually low forcing and greenhouses and particularly so that they do not cast a wide shadow during the day. The live ends of the tube are protected in the reflectors. The large irradiation units 4308 and 4310 (see *fig. 10*) are connected up through cables to a watertight cast-iron box containing the transformer, choking coil and relay. In the case of the small irradiator 4312 the input unit (choke, condenser and switch) is incorporated with the tube in the radiator, thus making a very simple arrangement which can be directly connected to a 220-volt A.C. mains plug (*fig. 11*). With this unit an area of 10 sq. ft. can be adequately irradiated from a distance of 20 to 24 in.; the larger irradiator 4308 is sufficient for irradiating an area of about 100 sq. ft. The large units are suspended above the plants at a height of 3 to 5 ft. When suspending a series of irradiators in a forcing house a space equal to the length of the irradiator is usually left between consecutive units, this arrangement permitting an efficient and comparatively uniform irradiation of the plants.

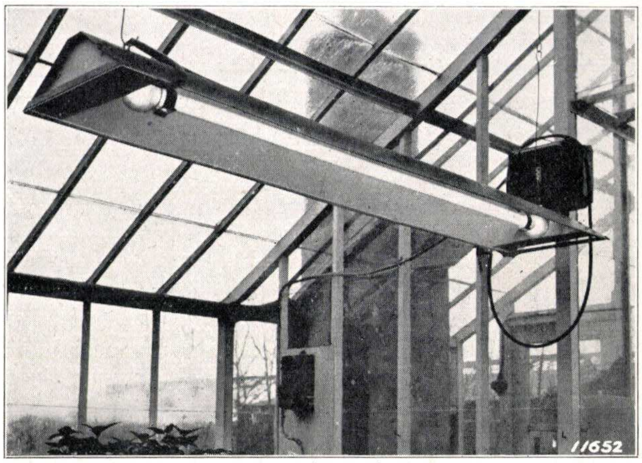

Fig. 10. The large plant irradiator 4310 installed for use. The input unit (*T*, *B*, *R*, *C* and *S* in fig. 8) is enclosed in the watertight cast-iron box on the right, to which the tubes mounted in the reflector are connected by a cable.

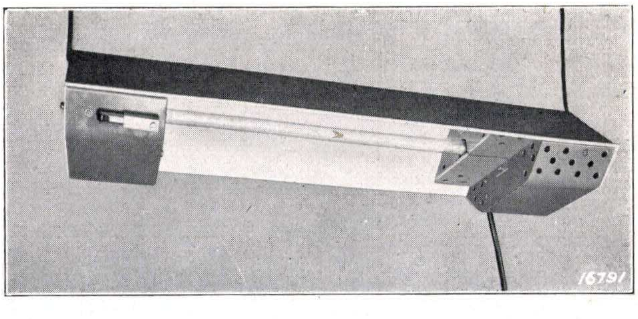

Fig. 11. The small plant irradiator 4312. The input unit is here incorporated with the tube in the reflector, thus giving a very simple arrangement.

THE DISK TEST AS A RAPID METHOD FOR ESTIMATING THE MACHINABILITY OF STEEL

(Continued from p. 187)

In the first part of this paper the general procedure adopted in the Taylor test and the disk test was discussed and the relation between these two methods of test analysed. In the present section the experiments carried out here and the results arrived at are reviewed.

General Experimental Details

Materials Used. To facilitate a discussion of the test made, full details of all types of steel used in these investigations are given in *Table I.*

Cooling agents. In accordance with the experimental work carried out by other investigators no cooling agents or lubricants were used in the present work. Although the absence of a cooling agent considerably reduces the cutting efficiency of cutting tools, the advantage gained is that the experiments are more closely reproducible.

Shapes of Cutting Tools Used. In his experiments Brandsma employed tools with straight sides, and in later work adopted knife-edge cutters of the type already illustrated in figs. 1 and 3. The shape of these tools is shown more clearly in *figs.* 6 and 7. In fig. 6 the sizes of all angles are given. It is seen from the last but one column in Table I that the cutting angle was not taken the same for all steels; in fact the most suitable angle for each particular steel was selected. The only difference between the cutting tools used in the disk tests (see figs. 3 and 7) and those used in the Taylor tests (see fig. 1) was that in the former the back of the tool was ground down so that the cutting edge alone was in contact with the test disk. The cutting properties of the steels are probably very little influenced by this modification.

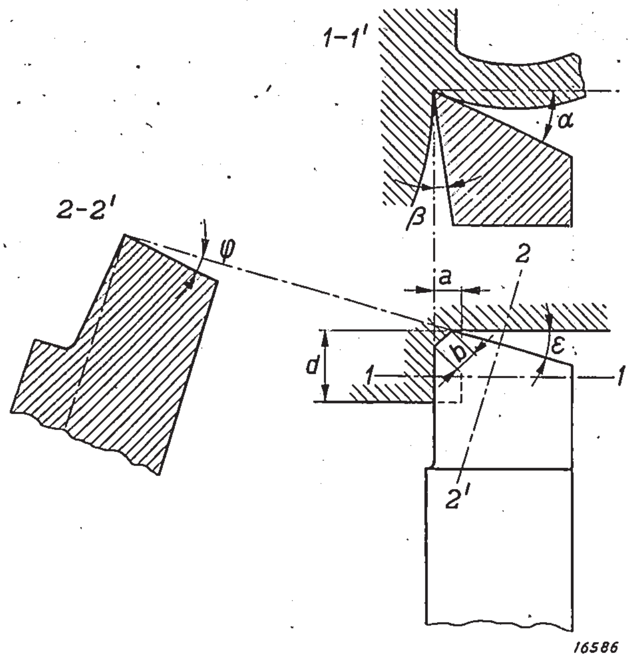

Fig. 6. Cutting tool (cutter angle 90 deg.) with horizontal edge. α = Cutting angle. β = Principal angle of clearance. ε = Secondary cutter angle. φ = Secondary angle of clearance. b = Blunting width. d = Depth of cut. a = Width of cut. The various cutting angles used for the different types of steel are given in Table I. With all steels, α, β and φ were each equal to 30° and b was 0·5 mm.

Table I. Survey of all the steels investigated.

Type	Approx. percentage composition of components other than Fe											State in which used	Angle of cut	Brinnell hardness (10/3000/30)
	Carbon	Silicon	Phosphorus	Sulphur	Vanadium	Chromium	Manganese	Cobalt	Nickel	Molybdenum	Tungsten			
Carbon Steel I	0.08	<0.5	0.08	0.15	—	—	<0.8	—	—	—	—	Forged	25°	116
Carbon Steel II	0.15	<0.35	<0.04	<0.04	—	—	<0.4	—	—	—	—	"Normalised"	25°	121
Carbon Steel III	0.45	<0.35	<0.03	<0.03	—	—	<0.8	—	—	—	—	"Normalised"	20°	174
Chromium steel	0.12	<0.35	<0.03	<0.03	—	0.4	<0.4	—	—	—	—	Soft annealed	25°	107
Nickel-chromium steel I	0.14	<0.35	<0.03	<0.03	—	0.75	<0.5	—	3.5	—	—	Soft annealed	20°	175
Nickel-chromium steel II	0.30	<0.35	<0.03	<0.03	—	1.0	0.6	—	3.5	0.4	—	Heat-refined	15°	311
Nickel-chromium steel III	0.35	<0.35	<0.03	<0.03	—	1.2	<0.6	—	4.5	—	—	Soft-annealed	15°	263
Tool steel I	1.1	0.3	<0.03	<0.03	—	1.0	1.0	—	—	—	1.0	Soft-annealed	15°	216
Tool steel II	2.2	0.6	<0.03	<0.03	—	1.2	0.25	—	—	—	—	Soft-annealed	15°	241
Cobalt high-speed steel	0.7	<0.35			1.5	5	<0.25	16	—	—	20	Hardened and twice annealed		
Vanadium high-speed steel	1.2				3.5	5		—	—	0.7	15	Hardened as delivered		

Lathes Used. The first disk tests were carried out on a lathe with a maximum speed of 600 r.p.m.

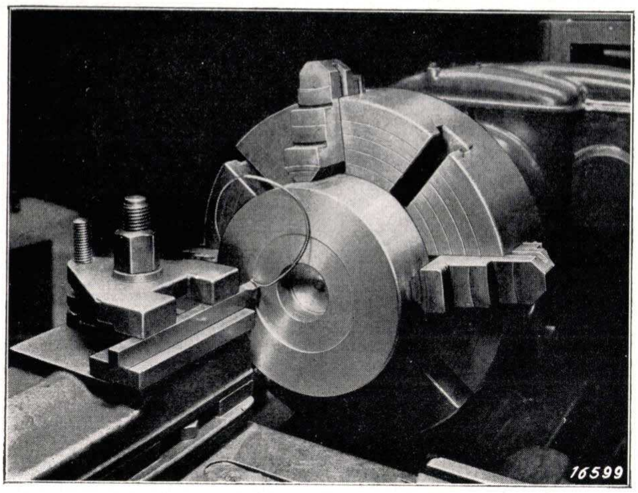

Fig. 7. View of lathe as used for carrying out a disk test.

and driven by a 4 h.p. motor. Subsequently these tests were carried out on the same lathe as used for the Taylor tests. This lathe had a maximum speed of 1500 r.p.m. and was driven by a variable-speed 7.5 h.p. D.C. motor. The cutting speed was kept as constant as possible during the tests with the aid of a tachometer.

Disk Test for Examining the Heat Treatment of High-Speed Steels

The high-cobalt high-speed steel shown in Table I was used in these tests, and tools ground from square bars of 12-mm side. After annealing, the tools were reheated once or twice. Very important factors in heat treatment are the annealing temperature, the rate of cooling and the number of times re-heating is applied.

In investigating the influence of these factors, all cutters were tested on disks of a very homogeneous and pure plain carbon steel which, apart from a somewhat higher manganese content, was similar to carbon steel II shown in Table I. The width of cut was 0.125 mm and the depth of cut 1.0 mm in all cases.

Effect of the Annealing Temperature. In those experiments designed to establish the influence of the annealing temperature, all tools were reheated twice. This characteristic twofold reheating with intermediate cooling is particularly recommended for high-cobalt high-speed steels in order to obtain a high hardness value (cf. Table II).

The results obtained in disk tests carried out on two cutting tools to estimate the effect of the annealing temperature are given in *Table II*, which shows, firstly, that the tests are satisfactorily reproducible and, secondly, that the maximum cutting speed v_m is the greater the higher the temperature of annealing.

Table II. Maximum cutting speed in disk test (v_m in m per min) in relation to the annealing temperature of the cutting tool in deg. C.

Annealing temperature	v_m	v_m after re-grinding	Average value of v_m
1280	220 211	217 221	217
1300	224 227	223 223	224
1320	225 225	243 234	232
1340	244 241	258 246	247

Influence of the Number of Re-Heatings. The results of tests performed to examine this question are collated in *Table III*, which also gives the corresponding "Rockwell hardness on the C-scale" in column *H*. It should be noted that twofold annealing results in an improvement only at the higher annealing temperatures, whilst on the other hand a third annealing process has a marked adverse effect on the cutting properties of the steels.

It may be quite definitely concluded from the table that the hardness is in many cases an unreliable measure of the cutting properties of a steel. On twofold annealing a greater hardness corresponds to better cutting properties as measured in the disk test, in other words a greater hardness is equivalent to a higher cutting speed v_m. On comparing the steels which have been annealed twice and three times, it should follow from the hardness values that treble annealing would be more advantageous, although disk tests show that the cutting properties of the steel are then less satisfactory than after a single annealing process.

Effect of the Rate of Cooling in Annealing. In the case of high-cobalt high-speed steels very

Table III. Rockwell hardness on scale C (*H*), and maximum cutting speed in the disk test (v_m in m per min) in relation to the annealing temperature in deg. C on reheating 1 to 3 times.

Annealing temperature	After no reheating	After reheating once		After reheating twice		After reheating three times	
	H	*H*	v_m	*H*	v_m	*H*	v_m
1280	60	63.5	211	62.5	209	62.5	182
1300	55.5	61	221	64	217	63	185
1320	52.5	60.5	214	65	220	63.5	190
1340	51	59.5	218	66	241	65.5	230

---

[8] W. F. Brandsma, Metaalbewerking **2**, 541, 1936.

rapid cooling is not desirable in view of the risk of hardness cracks appearing and of the premature crumbling of the cutting edge on the lathe. The effect of cooling was studied by cooling in compressed air, slower cooling in the fairly quiescent hot air of a furnace and still slower cooling in a very highly-insulating kieselguhr. As it was intended to detect particularly any brittleness developing, a groove 13 mm wide was cut radially in the disk in such a manner, that the cutting was interrupted once during each revolution. The results of these experiments are given in *Table IV*, where it is shown that the cutting ability increases with the rate of cooling and that it is barely affected by periodic interruption. Whether the brittleness can be evaluated in this way, therefore appears very doubtful, although some information on this point was furnished by a number of works tests and a metallographic examination of the structure. On the basis of these experiments and the results of the disk tests described above, the optimum heat treatment required for the steels was established.

Table IV. Rockwell hardness on scale C (H), and maximum cutting speed in the disk test (v_m in m per min) in relation to the annealing temperature in deg. C. and the rate of cooling during annealing.

Annealing temperature	Cooling in	Rate of cooling	H	v_m	v_m after regrinding	Average value of v_m
1300	Compressed air	Fairly slow	63.5	*)	214	214
	Furnace	Slow	64	199	200	200
	Kieselguhr	Very slow	60.5	185	185	185
1320	Compressed air	Fairly slow	64.5	223	237	230
	Furnace	Slow	63.5	220	207	213
	Kieselguhr	Very slow	62	196	199	197
1340	Furnace	Slow	64	226	220	223
	Kieselguhr	Very slow	63.5	217	157	187

*) Gradually became useless.

Disk Test for Testing and Classifying Steels according to their Machinability [9])

To determine whether the results obtained in disk tests are in concordance with those found by the Taylor test, a large number of experiments were carried out with the first nine steels enumerated in Table I. In these tests those cutting tools were used which had been found best suited for both the Taylor and disk tests, i.e. the exact instant at which the edge crumbled could be readily observed in each case, this not being always the case with other forms of cutting tools. All steels used in the investigation described below were made from high-speed vanadium steel (delivered hardened) given in Table I.

In both the Taylor and the disk tests the depth of cut d and the width of cut a were 1.00 and 0.26 mm respectively. With each of the steels studied, the material for both the Taylor and the disk tests was taken from the same bar; only with tool steel II was this not possible as the available bar diameter for carrying out the disk test was too small. But disks of sufficiently large diameter were available. The diameter D_0 of the hole in the disc was again 50 mm in all tests.

In all Taylor tests, always the same three cutting tools were used in a continuous series of measurements for plotting the complete v-T curve with all types of steel [10]), so that the final results given below

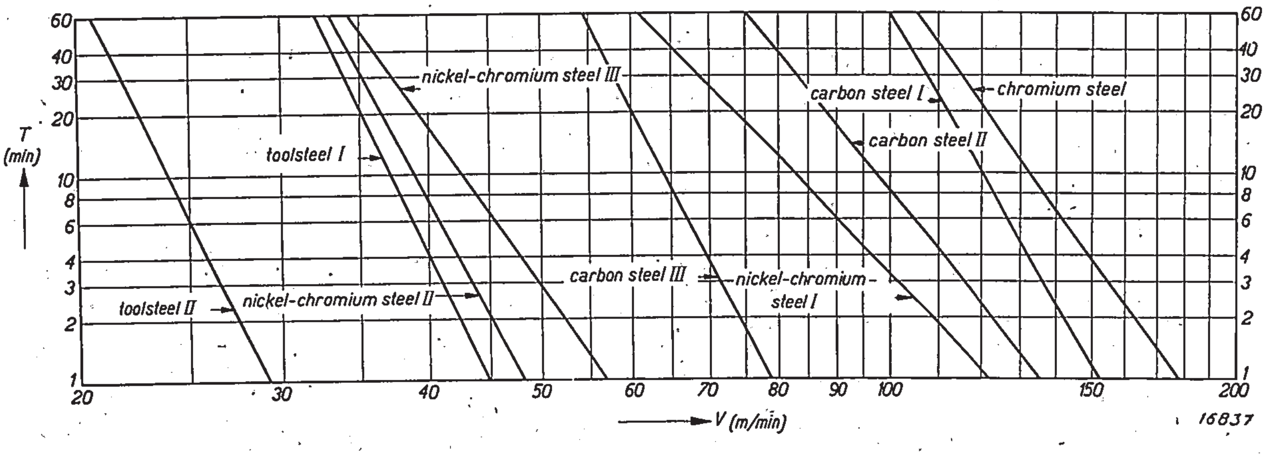

Fig. 8: Results of Taylor tests with various types of steel. For each steel the durability periods T for several different cutting speeds v were determined and plotted in a double-logarithmic diagram.

---

[9]) J. R. J. van Dongen and J. G. C. Stegwee, Metaalbewerking 3, 1 and 49, 1936. Special attention is called to the second part of this paper, which gives a comprehensive summary of all quantitative measurements.

[10]) In other words, after plotting one point of the v-T curve the worn cutting tool was reground before plotting the next point, and after the whole v-T curve had been plotted the same process was repeated with each of the other two tools.

may be regarded as the averages of three complete sets of tests. Three different tools were similarly used in the disk tests and with each tool the N-v_m curves for all the steels were plotted. Here again the final result given is a mean of three complete series of tests.

The results obtained in the Taylor tests are shown graphically in *fig. 8* and those in the disk tests in *fig. 9*. The principal values derived from the two graphs being a comparison between the two tests are collated in *Table V.*

Table V. Results of Taylor and disk tests (v_m in m per min) in relation to the cutting speed.

Material	Taylor tests					Disk tests
	N	C*)	v_1*)	v_{30}	v_{60}	$v_m^{(100)}$
Chromium steel	8	178	178	115	105	282
Carbon steel I	10	152	152	107	100	243
Carbon steel II	7	135	135	87	75	225
Nickel-chromium steel I	6	122	122	68	61	167
Carbon steel III	11	79	79	57	54	112
Nickel-chromium steel III	8	57	57	37	34	83
Nickel-chromium steel II	11	48	48	35	33	64
Tool steel I	12	45	45	34	32	62
Tool steel II	11.5	29	29	22	20.5	33.5

*) The values of C and v_1 are in agreement, although the dimensions of these magnitudes are different.

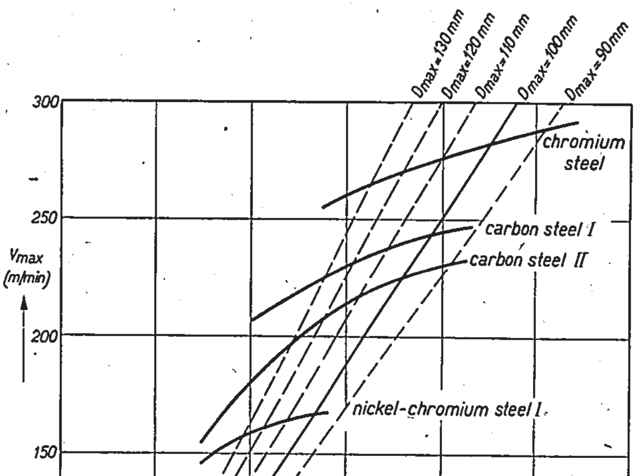

Fig. 9. Results of disk tests with various types of steel. For each steel the cutting speed v_m at the instant of collapse of the tool was determined for different lathe-speeds.

In addition, the cutting speed v_{30} corresponding to a durability of 30 min was calculated from the results of the disk tests, using equation (5). In this calculation n was obtained directly from the results of Taylor tests, since the lathe speed N in the disk tests was altered by too small an amount for each type of steel to allow n to be calculated therefrom with sufficient accuracy. The values of v_{30} calculated from equation (5) are collated in *Table VI* and fig. 5 together with those of v_{30} (see also table V) read from fig. 8. The agreement is seen to be very satisfactory. The greatest difference between the calculated and the measured values is 13 per cent, the average difference being only 7 per cent, which is not very serious when it is remembered that in Taylor tests the values of v_{30} cannot be determined with an accuracy greater than about 5 per cent.

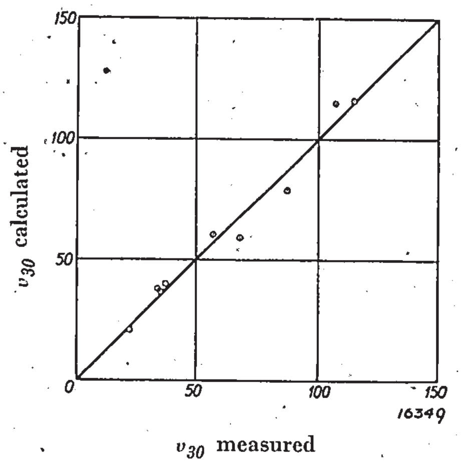

Fig. 5. Calculated values of v_{30} plotted against measured values.

Table VI. Survey of values of v_{30} as measured in Taylor tests and as calculated from disk tests (both in m per min).

Material	v_{30} measured in Taylor tests	v_{30} calculated from disk tests
Chromium-steel	115	116
Carbon steel I	107	115
Carbon steel II	87	79
Nickel-chromium steel I	68	59
Carbon steel II	57	60.5
Nickel-chromium steel III	37	40
Nickel-chromium steel II	35	37
Tool steel I	34	38
Tool steel II	22	21

As regards the possible routine testing of structural steels for their workability and machinability, it must be remembered that in the present article only the turning of small-sectional chips has been discussed and no reference has been made to rough turning, boring, planing, milling and grinding, etc. In practice it is essential to study these methods of working too. Since for round bars turning is the most common and most important operation, it should be possible to obtain satisfactory data of the machinability of various materials with the disk test by employing widely-different sections of chips.

Yet, before the disk test can be adapted to a routine test, much additional research has still to be carried out and in particular the relation between the Taylor test and the disk test should be investigated experimentally with greater accuracy and over a wider range. That an investigation over these lines is worth while is evident from a consideration of the advantages which the disk test offers over the Taylor test. It is sufficient to indicate but a few here and to emphasize the marked potential importance of the disk test for routine daily tests: practically every lathe can be readily adapted for carrying out the disk test; there is also less danger of the cutting tool crumbling owing to slag inclusions; the duration of a test is short and moreover little material is required.

Compiled by P. CLAUSING.

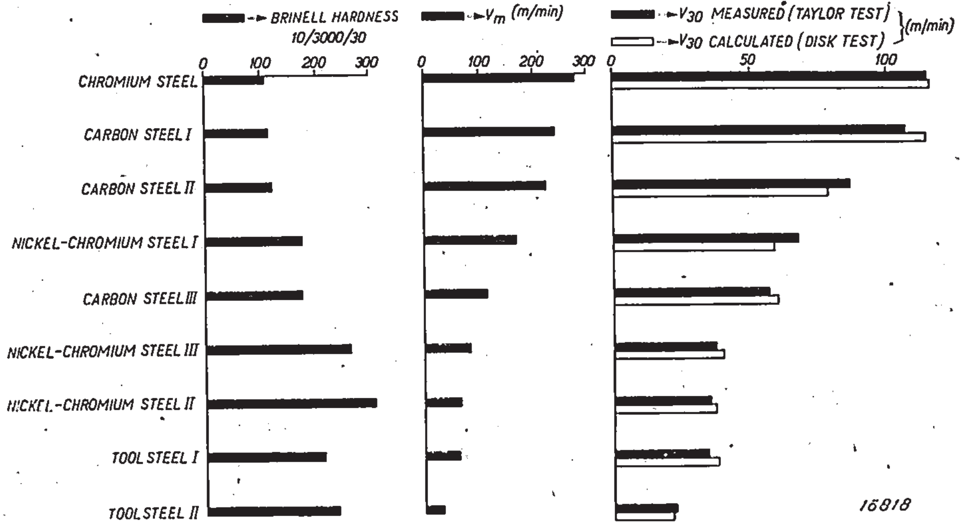

Fig. 10. Various criteria of machinability compared for a number of different steels: The Brinell hardness (10/3000/30), the maximum speed v_m measured in the disk test, the value of v_{30} calculated from the disk test, and the value of v_{30} measured in the Taylor test. It is seen that the two latter are in very good agreement. The Taylor test gives decidedly the most direct measure of the machinability. The results of the disk test, either recalculated or not, i.e. v_{30}(cal.) or v_m, lead to the same conclusion. On the other hand the Brinell hardness would lead to an entirely wrong conclusion.

---

[11] These figures give in order the diameter of the ball in mm, the pressure in kg and the time in seconds employed in measuring the hardness with the Brinnell apparatus.

AUTOMATIC STARTING RESISTANCES

("STARTO" TUBES)

By P. C. VAN DER WILLIGEN.

Summary. The starting impulse obtained with many electrical consumers can be reduced or suppressed altogether by series connection of a resistance with a negative temperature coefficient (high resistance when cold and low resistance when hot). This principle has been employed in the "Starto" starting tubes. The construction and characteristics of these tubes are described in this article, and their application to typical cases, such as for starting motors, for the gradual switching-on of lighting circuits, and for delayed circuit closing, etc., are discussed by reference to concrete examples.

Introduction

On switching on large electrical machinery heavy current impulses are frequently obtained, which are due to the fact that the working current absorbed by a motor is not limited by the resistance of the armature windings, but by the reverse voltage induced in the rotor. At the instant the motor is switched on, no counter-voltage is produced if the rotor does not immediately start to move; in this case the current may become several times greater than the normal working current. It thus usually becomes necessary to protect the armature windings against overheating when starting.

A starting rheostat is generally connected in series to the windings to prevent this overheating, this resistance being gradually reduced either by hand or automatically as the speed of the motor increases to its normal value during the starting period. At the outset the resistance must have a high value which gradually drops to a low end value. This type of resistance variation is found in semi-conductors (metalloids, metallic compounds, etc.) whose electrical resistance has a negative temperature coefficient, in other words the electrical resistance decreases as the temperature rises. When a semi-conductor of this type is connected in series with the consumer, the starting current is limited by its resistance when cold. During starting, the temperature of the resistance is raised by the passage of current and the resistance value thus gradually drops to a much lower final value.

The starting tubes which Philips are marketing under the name of "Starto" tubes have been evolved on this principle; they can be used in all cases where it is desirable to procure a gradual increase in the current.

Before passing to a detailed description of the construction and characteristics of these starting tubes it should be pointed out that these tubes are the exact opposites of the hydrogen-filled iron-filament resistors which are used as regulators. In the latter, technical use is made of the pronounced positive temperature coefficient of the resistance of the iron; with a change in the voltage applied to the resistor the current passing may remain constant in certain circumstances [1]), cf. *fig. 1*, curve A. On the other hand the operation of the starting resistances depends on the marked negative temperature coefficient of the resistance (a specific semi-conductor), and in the current-voltage characteristic there is a range in which the voltage-drop across the terminals of the tube remains practically constant, when the current is altered [2]), cf. curve B in fig. 1. The two characteristics A and B are seen to be perpendicular to each other. As we shall see below, this property is not employed in the starting tubes during starting,

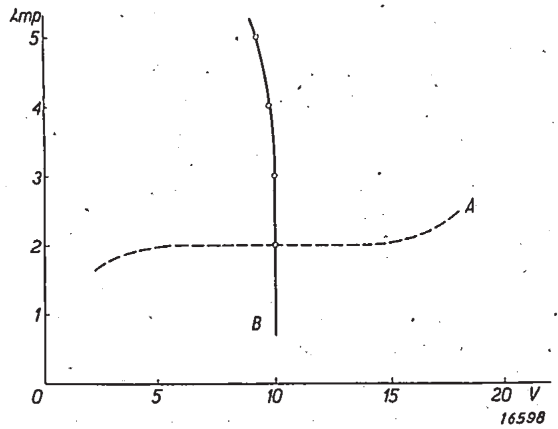

Fig. 1. Current-voltage characteristics: A - Iron filament resistor (Philips 1913). B - Starting tube ("Starto", 2-A type). The resistance of the first has a positive temperature coefficient and that of the second a negative coefficient. Each point on the curves corresponds to a condition of equilibrium.

---

[1]) For if the current E/R tends to increase as a result of an increased voltage E, the temperature rise occurring at the same time causes an increase in the resistance R, so that E/R remains practically constant, at least over a certain part of the characteristic.

[2]) For, if the voltage-drop IR tends to increase owing to a greater current I, the resistance R is reduced as a result of the temperature rise occurring at the same time, so that IR remains practically constant, at least over a certain part of the characteristic.

the operation of these tubes being in fact based on their inertia due to their marked thermal capacity.

Construction [3]) and characteristics

In "Starto" tubes, the semi-conductor used is a mixture of silicon and a ceramic binder. The resistance of silicon itself does not possess a pronounced negative temperature coefficient, but on "diluting" with a suitable binder this coefficient is considerably increased to give a very marked difference between the resistance when cold and when hot. A favorable circumstance is the fact, that these considerable differences appear with the addition of a small quantity of ceramic material (for instance 25 per cent).

The resistance material is used in the form of a rod enclosed in a glass tube filled with argon. The argon filling is required because the silicon of the rod reacts with oxygen and nitrogen.

To ensure that the characteristics of the starting resistance remain unchanged during service, the resistance material must not become too hot, i.e. it must not exceed a specific maximum in the end stage reached after starting up the current. *Figs. 2* and *3* illustrate "Starto" tubes designed for different maximum permissible currents from 1 to 100 amps. On full load the rod is raised to red heat and its temperature is then in the neighbourhood of 800 deg. C. With an overload there is the risk of altering the characteristics of the rod, which may even melt.

Characteristic Curves

The lower half of *fig. 4* gives the current-resistance characteristic for starting tubes designed for 220 volts and 1.3 amp (fig. 2) and the upper half the

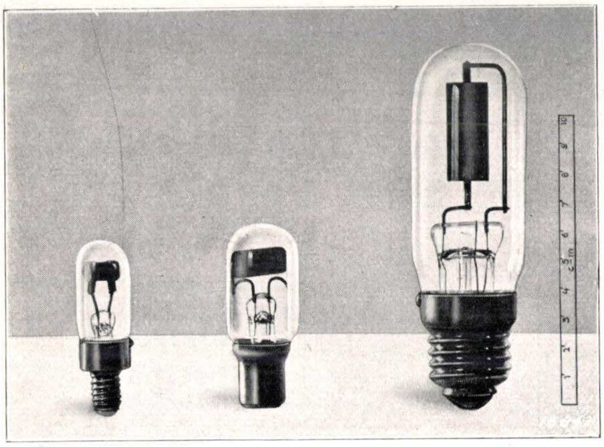

Fig. 2. "Starto" starting tubes for small currents, 1-amp, 3-amp and 6-amp types (the tubes shown here are all intended for 220 volts; tubes for 125 and 380 volts are also made).

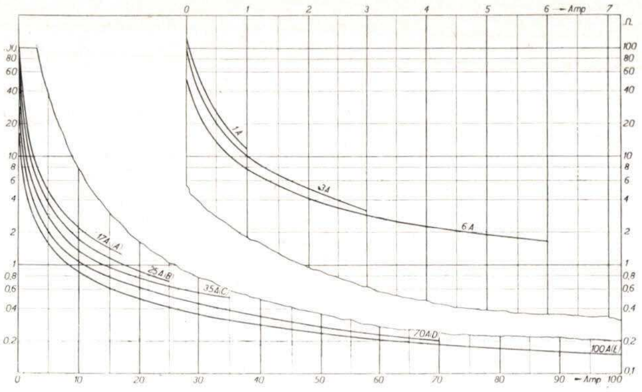

Fig. 4. Current-resistance characteristics of 220 volt starting tubes shown in fig-s 2 and 3. The ordinate (resistance in ohms) has been divided logarithmically in view of the large difference between the resistance when cold and when hot. Each curve is drawn up to the point of the maximum permissible working current for each tube.

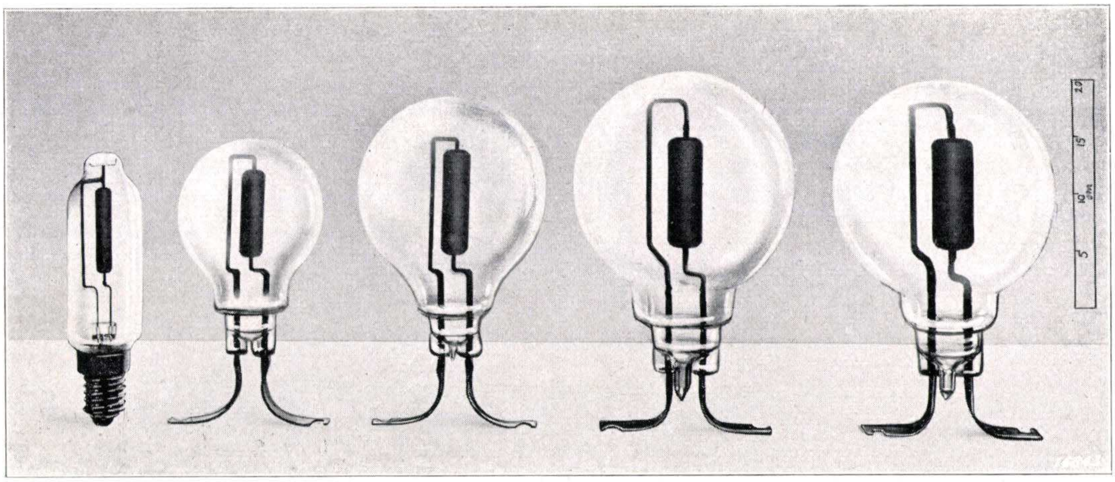

Fig. 3. "Starto" starting tubes for higher currents: *A* (17 amps), *B* (25 amps), *C* (35 amps), *D* (55 amps) and *E* (100 amps).

---

[3]) Assistance in the construction of the tubes described here was given by Messrs. Ploos van Amstel and De Schrevel.

corresponding curve for tubes designed for 220 volts and 17, 25, 35, 55 and 100 amps (fig. 3), denoted by the letters A to E. In both diagrams the ordinates have been divided logarithmically in view of the marked difference between the resistances when cold and when hot. Each curve has been drawn up to the point corresponding to the maximum permissible working current. Tubes A to E are manufactured for circuit voltages of 125, 220 and 380 volts; the only difference between an *A 125* and an *A 220* tube is in the length of the resistance material.

It follows from *fig. 4* that the final resistance will be the smaller, the greater the current for which the starting tube is designed. *Table I* gives these final resistances for tubes *A 220* to *E 220*.

Table I.

Type	Max. current in amps	Resistance in ohms	Voltage absorbed in volts
A 220	17	1.2	20
B 220	25	0.7	18
C 220	35	0.5	17
D 220	70	0.2	15
E 220	100	0.15	14

As may be seen, the voltage consumption in all types of tubes is about 12 volts, i.e. 5 per cent of the mains voltage. In the 125-volt tubes the average consumption is 8 per cent, and in the 380-volt tubes approximately 4 per cent [4]).

The resistances when cold are in the neighbourhood of 100 ohms with type *A 220* and of 15 ohms with type *E 220*; these values have been chosen such that the current on applying the full mains voltage is roughly $^1/_8$ of the maximum permissible current through the tube. By taking a suitable composition of resistance material the resistance when cold R_k can, however be altered within wide limits. Thus, a 3-amp tube can be made with a final resistance of 4 ohms and with $R_k = 200$ ohms, and also a tube for the same current rating with a final resistance of 5 ohms and with $R_k = 2000$ ohms[5]).

From the current-resistance characteristic the current-voltage characteristic can readily be deduced, being of the type given in fig. 1 for the 3-amp starting tube (curve B). The resistance varies almost in the inverse ratio of the current intensity over a very wide range of current values, so that in this range, as already indicated at the outset, the voltage consumed by the tube remains practically constant. With lower currents it is fairly difficult to trace the exact path of the curve; this is, however, of little importance since the points of this curve in fact relate only to equilibrium conditions. In practice an equilibrium is only reached when the current attains its final value, whilst during the starting period the resistance lags considerably behind the current owing to its marked inertia. As a result the voltage applied to the starting tube during starting (i.e. at low and increasing current intensities) is high and then drops to the final value of 10 volts as given in the characteristic curve.

Starting Time

The duration of the starting period, i.e. the time elapsing from the moment the switch is closed until the current reaches its maximum value, is determined by the time taken for an equilibrium to be reached between the heat supplied and the heat dissipated. The heat input is governed by the mains voltage, the resistance of the starting tube when cold R_k and the magnitude of the resistance in series with the starting tube. The heat dissipated depends on the shape and size of the tube. A consideration of the construction of the tube indicates that the starting time increases, the greater the resistance R_k when cold (small heat input) and the greater the mass and surface area of the starting resistance, (slow temperature increase owing to greater thermal capacity and rapid dissipation of heat resulting from a larger surface). With a particular starting tube a variety of starting times can be obtained, depending on the mains voltage and the value of the resistance in series. With a specific low mains voltage (or a sufficiently high series resistance) the energy input of the starting tube can be made so small that an equilibrium between the heat input and the heat dissipated is already attained with a temperature increase of 30 to 40 deg. No starting is then obtained and the current retains its small initial value. Proper starting can still be achieved in this case by heating the starting resistance from an external source, e.g. with a resistance wire wound round the starting rod and connected in parallel with it (see also below, *fig. 9*). If the tube has been once heated up, then the current intensity and hence also the heat input of the tube is so much higher that, at a certain temperature at which the tube is at red heat, a second equilibrium between heat input and the excessive dissipation of heat is reached.

---

[4]) In addition to the mains voltage R_k and the maximum permissible current, the resistance when cold is also marked on the glass bulb of the starting tube, e.g. 220 volts, 100 ohms/17 amps.

[5]) A rod of a semi-conductor served here as an incandescent body. As long as the rod absorbed little current, heating was furnished, immediately after switching on, by a resistance wire which is automatically cut out as soon as the rod becomes hot enough to conduct sufficient current to heat itself.

In nearly all applications of the starting tubes, the resistance of the series-connected consumer does not remain constant but steadily increases. When selecting a starting tube for a particular purpose, this point must also be considered in addition to those already referred to.

Cooling Period

The iron-filament resistor, which we have indicated as the opposite of the starting tube, is employed as a regulator in order to obtain a constant current in spite of a fluctuating voltage. The horizontal part of curve *A* in fig. 1 is therefore employed. A certain inertia in the resistor due to the time required for the temperature to change is, however, undesirable. The starting tube, when employed to suppress a current impulse on starting up, behaves in an exactly opposite manner. The use of this tube depends on the fact that the increase in temperature occupies a certain finite period of time; owing to the large mass of the resistance material the tube has a fairly high thermal capacity and hence exhibits a certain inertia. On the other hand, the inertia necessitates a certain period of cooling after the tube has been switched off, before it is ready to work properly on the next starting up. In most cases it is desirable for the resistance to again reach $^2/_3$ of its value when cold ⁶). *Fig.* 5 gives the cooling curves for the various types of tube illustrated in figs. 2 and 3. The cooling time is indicated in each case by a small arrow. It is seen that the cooling period is the longer the greater the starting tube.

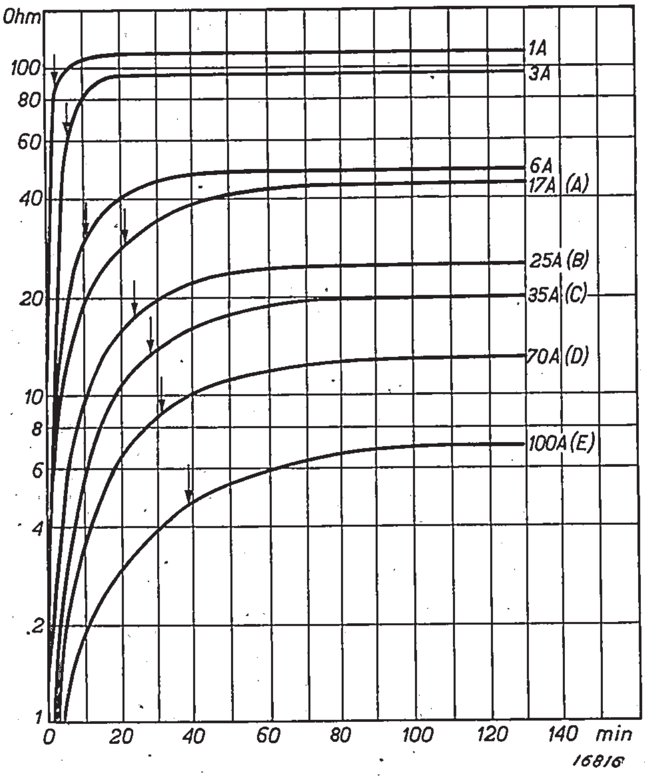

Fig. 5. Cooling curves for different types of starting tubes. The resistance in ohms is plotted as a function of the time in minutes when the tube is switched off at time 0. An arrow on each curve indicates when the corresponding tube has again reached $^2/_3$ of its resistance when cold. It is observed that the cooling time increases with the size of the starting tube.

That the "Starto" starting tubes operate at a high temperature is an advantage as regards rapid cooling. For at red heat radiation contributes appreciably more to rapid cooling, whilst in a lower temperature range cooling is due largely to convection and thus takes place much more slowly.

Applications of Starting Tubes

The use of starting resistances for reducing or preventing current impulses when switching on motors, lighting circuits, transformers, condensers, etc., offers several important advantages as compared with ordinary sliding resistances or switches. These starting resistances are fully-automatic in operation and contain no moving parts or sliding contacts which can seize. A feature of starting tubes is therefore their long life; type 3-A retains its initial characteristics when continuously loaded for more than 10 000 hours and when used 100 000 times to start a 1.3-h.p. motor. The saving in weight and space with starting tubes is also considerable; the 3-A tubes weighs only 15 gr, and the maximum overall dimensions are 2.5 × 6 cm; the corresponding data for the 100-A type are 700 gr and 9 × 25 cm.

In many cases where a consumer has hitherto been switched straight across the line because the expense of an intermediate starter was not warranted, a starting tube can now be used to advantage. Slow starting is also an advantage with impulses having a low absolute value, since for instance less maintenance is required by the motor commutators and current impulses in the mains as well the blowing of fuses are also avoided.

Starting of Motors

The resistance rod in each tube can only carry a limited amount of power without overheating, so that for each tube a maximum current rating is prescribed for continuous duty. But if the initial resistance of the current consumer is very much smaller than its final resistance, as is the case for

---

⁶) On starting motors, in most cases a smaller increase is sufficient.

instance with large motors, the heat generated in the starting tube will be too great if the latter has been selected on the basis of the maximum permissible current intensity marked on it; the heating up of the tube is then no longer uniform and local overheating may occur. To prevent this it is safest to select for a motor of specific current rating a starting tube rated for approximately double the maximum current[7]).

Example: A 3 h.p., 125 volts D.C. shunt-wound motor absorbs 12 amps on a 30 per cent load. A starting tube *B 125* (i.e. with 25 amps maximum current) is suitable for starting this motor on no load; the impulse on starting is found to be 19 amps[8]). When the motor has started and the starting tube is hot, the current may be increased in continuous duty to 25 amps above this level and for short periods even up to 50 per cent above. This temporary permissible overload of 50 per cent when hot applies in fact to all tubes.

It is evident that a fully-automatic series resistance cannot be used where speed control must also be provided for (as with certain D.C. motors). In other cases a consumer has to be switched on again immediately after being cut off. The difficulty of the higher starting impulse then occurring, can be met by shorting the starting tube after starting. The tube is then usually given sufficient time to cool, apart from the fact that the watt losses of the tube are eliminated. Shorting can be effected either by means of an ordinary switch or automatically by an electromagnetic relay. With the smaller starting tubes the watt consumption is frequently so small that it does not pay to short the tube to save the losses sustained.

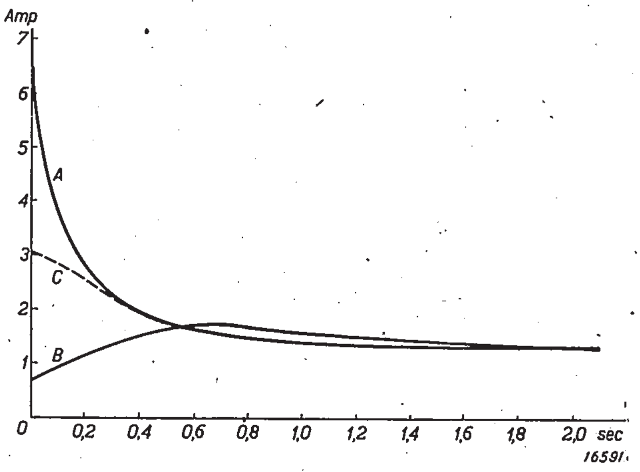

Fig. 6. Oscillogram of current on switching on a single-phase A.C. commutator motor, 220 volts, with a current consumption of 1.3 amps. *A*: straight across line, the starting impulse being 500 per cent of the working current. *B*: with "Starto" starting tube, 3-amp type, which reduced the starting impulse to 130 per cent of the normal working current. *C* with the same starting tube, switching on immediately after the motor has stopped (i.e. 7 sec. after switching off, thus representing the most unfavourable case), the impulse being 340 per cent of the normal current.

The example shown in *fig. 6* indicates the magnitude of the starting impulses, which must be reckoned with on immediately reclosing a circuit.

Slow Switching-On of Lighting Circuits

The starting impulses on closing glowlamp circuits can be suppressed with the starting tube in the same way as these tubes can be used with motors. In many cases it is desirable for the lamps to light up gradually, e.g. in cinemas, theatres, etc. The starting tube can also perform this duty, and where a comparatively long lighting-up period is necessary a tube can be selected with a maximum permissible current rating equal to double the working current of the lighting circuit (or even higher), in the same way as with large motors.

Example: Six glowlamps with a total consumption of 900 watts are connected to the 220-volts mains. The normal current is therefore 4 amps. If the lamps are to burn very weakly immediately after switching on, the initial current must be approximately half the normal, i.e. 2 amps. The resistance on switching on must therefore be 110 ohms. The six lamps in parallel have an initial resistance of approx. 12 ohms, so that the resistance when cold of the starting tube required must be approx. 100 ohms. These requirements are met by the *A 220* tube, which also has a suitable maximum permissible current rating. The current-time diagram in *fig. 7* indicates that the current increases from 50 to 90 per cent of its final value in 15 sec, a period giving every comfort to the eye.

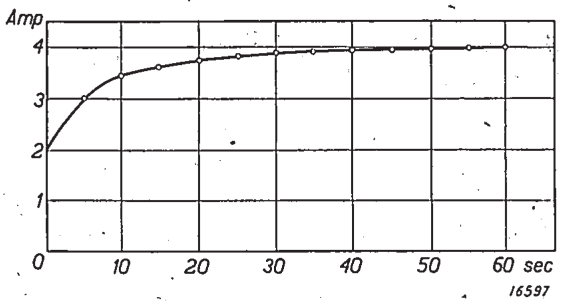

Fig. 7. Increase of current in a lighting circuit with a series-connected *A 220* starting tube. The tube has been so selected (resistance when cold), that the initial current, 2 amps, is 50 per cent of the working current. After 15 sec. the current has attained 90 per cent of its final value. This gradual lighting-up of the lamps is soothing to the eyes.

Delayed and Graduated Starting

As demonstrated particularly by the last example above, these starting tubes can also take the place of bimetallic switches for the delayed closing of electric circuits, e.g. anode circuits in rectifiers, amplifiers, relays, etc. The required time delay can be provided by suitable choice of the resistance when cold of the starting tube, and a current-time curve of the type shown in *fig. 8* can be readily obtained.

---

[7]) Thus the starting tube *A* (maximum permissible current in continuous duty 17 amps) can be used for starting a small motor which on full load takes 9 amps, and for a larger motor which on no-load takes 9 amps.

[8]) The resistance when hot of the tube *B 125* is about 0.9 ohm. If in place of the starting tube an ordinary resistance wire of 0.9 ohm is connected in series with the rotor the starting impulse will be 60 amps, i.e. three times greater.

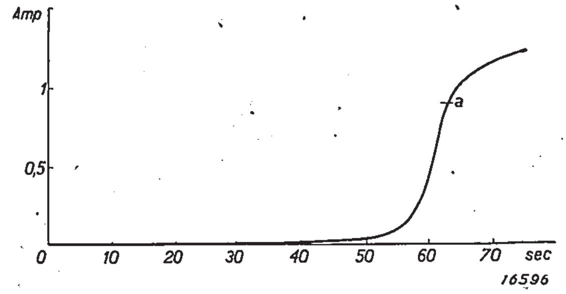

Fig. 8. Current increase with a starting tube serving as a "delay switch". This application of these tubes is chiefly suitable for switching on main feeder circuits by means of an electromagnetic relay: The auxiliary current through the relay is allowed to increase slowly by means of the starting tube connected in front of it, and only at point *a*, i.e. after a full minute, does it reach the necessary intensity to attract the electro-magnet. This offers the advantage that small types of starting tubes can still be used for heavy mains current (short cooling period).

If a specific starting current is needed, which after a definite number of minutes shall be increased, say fourfold, a starting tube of special design can be selected in which a resistance wire is connected in parallel to the starting resistance (*fig. 9*). The time delay in this case is determined by the resistance when cold of the starting rod and the heat furnished by the current flowing through the parallel resistance. In this way a great variety of currents and time delays can be obtained.

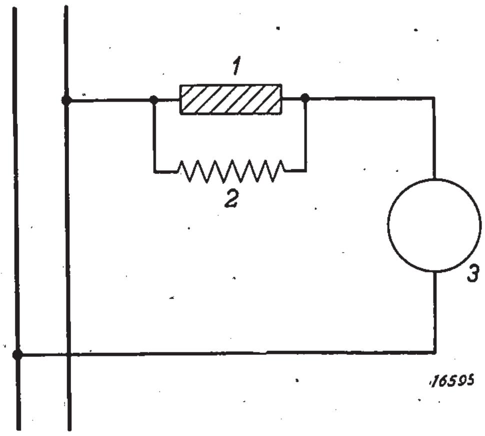

Fig. 9. Special type of starting tube for graduated starting. The glass bulb of the tube contains, in addition to the starting rod 1, also a resistance wire 2 which is connected in parallel to the rod. By this means a specific initial current is obtained at the consumer 3. The resistance when cold of rod 1 is so high that the rod cannot heat up of its own accord. The rod is gradually heated by the heat generated in coil 2; after a specific period, however, it heats up rapidly, so that the current in 3 increases to its final value.

The above considerations and examples will be sufficient to indicate that the new starting tubes possess characteristics which make them eminently suitable for many applications in electrical technology.

THE SOUND-RECORDING CUTTER IN THE PHILIPS-MILLER SYSTEM

By A. CRAMWINCKEL.

Summary. From a consideration of the requirements which the cutter used for sound recording in the Philips-Miller system has to fulfil, some dimensions are deduced for the cutter and a suitable material for it is mentioned. A brief description is also given of investigations on the durability of the cutter for sound-track recording on the "Philimil" strip.

The principles underlying the Philips-Miller method of sound recording and in particular the construction and characteristics of the sound-recording system have been discussed in detail in two previous articles in this Review[1, 2]). Sound is recorded by mechanical means by a vibrating wedge-shaped cutter S (*fig. 1*), cutting a transparent sound-modulated groove in a "Philimil" film strip. This strip is built up of a celluloid base C (similar to a photographic film), on which are laid a transparent layer of gelatin G (about 60 μ thick) and a very thin opaque coating D (about 3 μ thick). A transparent track on an opaque background is produced by the removal of the opaque coating along the groove made by the cutter.

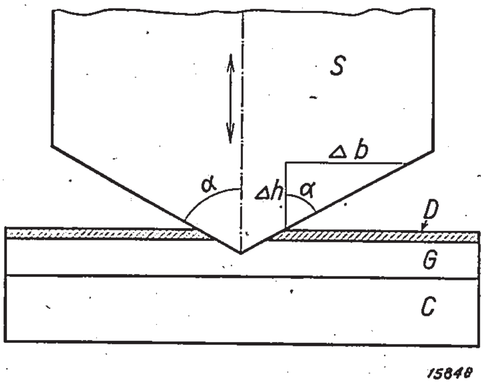

Fig. 1. The wedge-shaped cutter and the "Philimil" strip used for sound recording in the Philips-Miller system. The "Magnification" obtained in the recording of the sound track is $2\,\Delta b/\Delta h = 2 \tan \alpha$;

The cutter being shaped like a blunt wedge, small cutter amplitudes Δh are converted to magnified variations in the width $2\,\Delta b$ of the engraved track. It is just this magnification which has enabled the advantages of mechanical registration of the vibrations of a linear-amplitude system [1]) to be utilised.

In this article an outline will be given of the investigations which have been carried out regarding the shape of the cutting unit and of the results which have been obtained in this direction. The cutter has to meet the following requirements:

1) It must magnify the vibrations of the reed of the sound recorder 40 times [3]) and register them on the film without distortion, even up to the highest audio-frequencies with the maximum amplitudes which may occur in the vibrations to be registered.
2) It must be so stable that during recording no wear takes place that is likely to have an adverse effect on the quality of the sound reproduced.

The first requirement determines the dimensions of the cutter. Fig. 1 shows that the amplitude $2\,\Delta b$ of the modulated sound track is:

$$2\,\Delta b = \Delta h \cdot 2 \tan \alpha$$

The required magnification $2\,\Delta b\,/\,\Delta h = 40$ gives the apical angle of the cutter $\alpha = 174$ deg; the sides of the wedge therefore make an angle of only 3 deg. with the surface of the strip. The small value of this angle naturally considerably enhances the requirements which determine undistorted reproduction, as regards the smoothness of the cutting edges, the flatness of the strip and the accuracy of the attachment of the cutter.[4])

The angle β of the cutter (see *fig. 2*) may vary within certain limits. It must not, however, be too large, as the maximum gradient φ which the cutter can inscribe on penetration is limited by the rear slope R of the cutter, being determined by the relation $\varphi + \beta = 90$ deg. The maximum amplitude which can be registered is proportional to the length of the inscribed wave, and hence for a given velocity of the strip it is inversely proportional to the frequency. *Fig. 3* shows this relation for various cutter angles. Each sloping line gives the maximum width of sound track for a specific cutter angle. Thus, with the cutter angle of 55 deg. employed in actual practice a sound with a 4000-cycle frequency can be inscribed with a maximum track width of only 1 mm (instead of 2 mm wide as would be obtained with the full amplitude of the cutter of 25 μ. The curve also included in this figure represents the maximum amplitudes of the various frequencies occurring in music and speech.

---

[1]) R. Vermeulen, Philips techn. Rev. **1**, 107, 1936.

[2]) A. Th. v. Urk, Philips techn. Rev. **1**, 135, 1936.

[3]) As already stated in this Review [2]), the vibrations of the reed in a sound recorder of the type constructed here, amount to only a few hundredths of a mm. To obtain a modulated sound track with a width of 1.8 mm, high magnification is therefore indispensable.

[4]) To avoid distortion of the track, the plane of intersection of the cutter with the film must be exactly perpendicular to the direction of motion of the strip. A slight lateral displacement of the cutter axis, such that the two cutting edges make different angles with the plane of the film, is, however, not deleterious. The sound track becomes unsymmetrical as a result thereof, but no distortion occurs on reproduction.

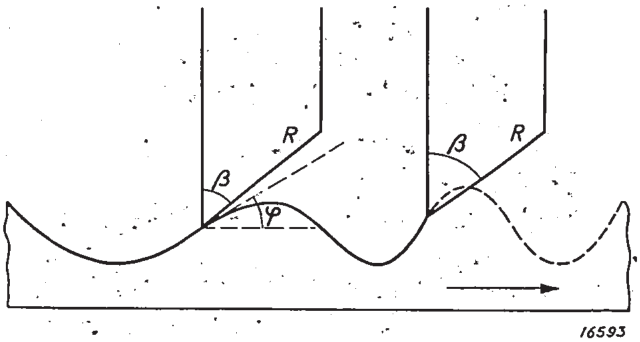

Fig. 2. Limitation of the cutter amplitude;
Left $\varphi + \beta < 90$ deg, possible.
Right $\varphi + \beta > 90$ deg, impossible.
The maximum slope φ which the cutter can inscribe on penetrating the strip; is determined by the condition that $\varphi + \beta = 90$ deg.

This curve was derived by Fletcher from measurements by Sivian, Dunn and White[5]). The maximum occurring at 300 cycles would here give the maximum amplitude of 2 mm. It is seen that at $\beta = 55$ deg. the amplitude only becomes limited by the rear of the cutter above 8000 cycles. But even at 15000 cycles the limitation in registration is only 3 decibels[6]), so that it does not appear useful to make the cutter angle smaller still (especially as the stability and durability of the cutter increase with its apical angle).

The second requirement for maximum durability and stability of the cutter called for the selection of a suitable material; since, as we have seen, the cutter angles are already fixed. In this direction it was first necessary to elucidate the exact causes responsible for the wear of the cutter.

It was found that by increasing the purity of the gelatin the life of the cutter could be considerably lengthened. It thus appeared that the cutting work done on the gelatin was not itself responsible for the wear, but that the impurities, such as dust particles, etc., which were sporadically embedded in the gelatin were the primary cause.

Owing to the great hardness of these particles the cutter must be made of a very hard material, whilst the extreme local concentration of stresses due to these particles also called for maximum homogeneity. The toughness of the cutter material

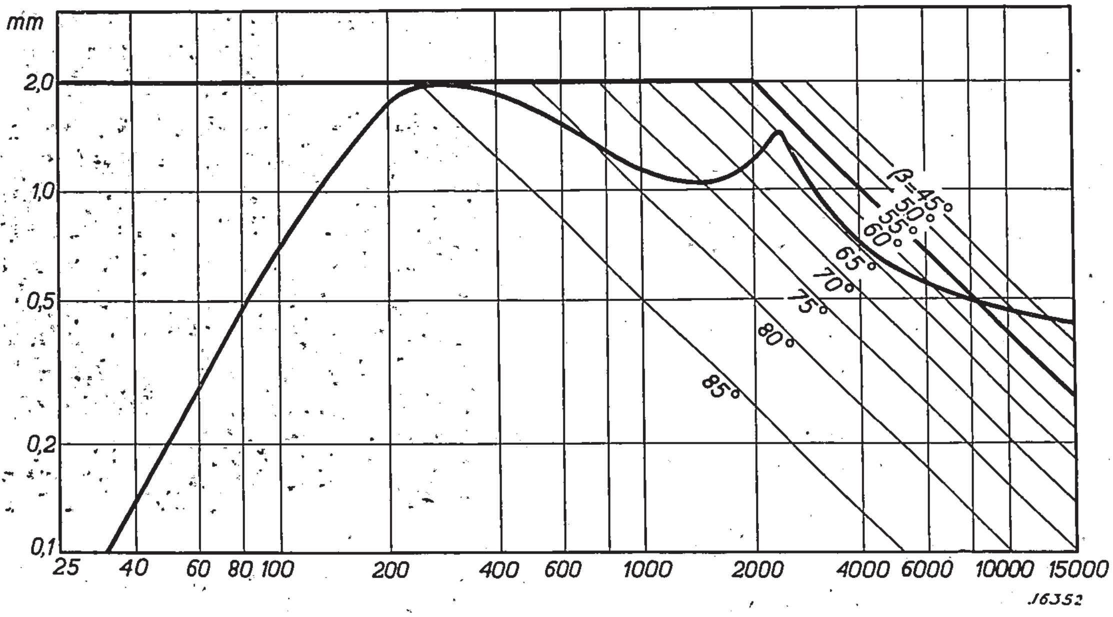

Fig. 3. Graphical representation of the limitation of the cutter amplitude a, plotted against the frequency ν. For each of a number of cutter angles β a sloping line is drawn, which indicates directly the maximum width of the sound track in mm that can be obtained at each frequency. The drawn curve indicates the actual amplitudes (widths of sound track) of all frequencies occurring in normal music and speech. Where a sloping line cuts the curve, the actual limitation of the amplitude begins at the corresponding cutter angle.

---

[5]) L. I. Sivian, H. K. Dunn, and S. D. White, J. acoust. Soc. Amer., **2**, 330, 1931.
H. Fletcher, Bell, Syst. techn. J. **10**, 349, 1931.

[6]) Corresponding to a factor 1.4 in the amplitude, which at these high sounds cannot be detected by the ear.

appears to be only of secondary importance. Various types of steel with Vickers-hardness values [7]) between 800 and 900 were not found hard enough at the outset; this may in fact be gathered from the micrograph of the sound track obtained with a worn steel cutter shown in *fig. 4*. On the other hand various sintered substances, such as the carbides of the heavy metals, which had a much greater hardness (Vickers values between 1300 to 1800) were found to be too inhomogeneous (cf. the etched section in *fig. 5*). The material finally selected, viz. sapphire in single-crystal form, incorporated the two requisite properties: Being of single-crystalline structure, it is naturally completely homogeneous (cf. the Laue diagram in *fig. 6* obtained with X-rays; an etched section similar to that in fig. 5 would have been useless here, as it would not have revealed any structural details); moreover, its Vickers hardness value is approx. 1850. On Mohs's scale of hardness sapphire has a hardness 9 as compared with diamond, the hardest substance known, which has a hardness of 10 on this scale. Between these two there is for instance silicon carbide with a Vickers hardness value of about 2100 [8]). This material was also tried as a cutter and, although it was found quite suitable, it is difficult to obtain it in the form of large crystals. The same also applies to zirconium oxide, boron carbide (Vickers hardness about 2600; this material has very nearly the same hardness as diamond [8]), and other carbides, such as the metallic carbides already referred to, which would probably also be quite

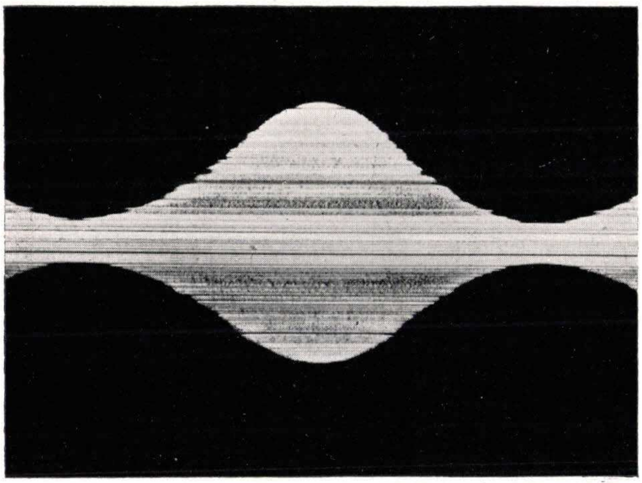

Fig. 4. Micro-photograph of a sound track obtained with an experimental cutter made of an alloy steel, after having recorded a path equivalent to a sound track on 400 or 500 m of "Philimil" strip. The cutting edge has become very jagged and has acquired a large number of notches (indicated by the thin continuous lines and the rough edge of the sound track due to the retention of the coating at certain points). The frequency of the sound registered was 150 cycles. Magnification × 18.

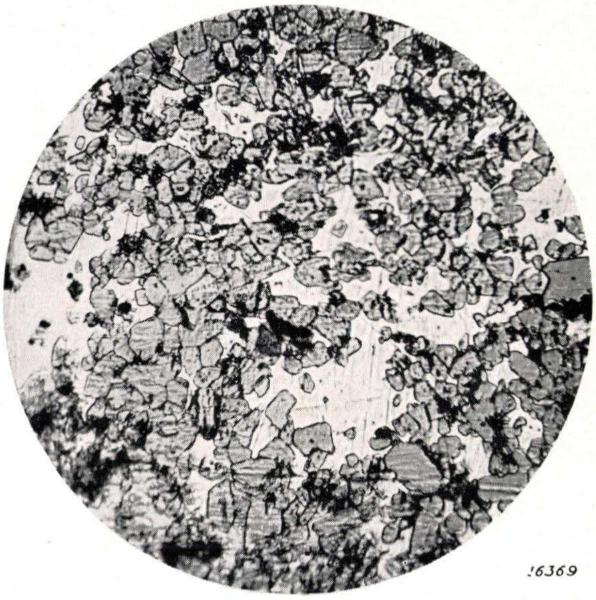

Fig. 5. Etched section through a sintered material, magnification × 100. The individual particles can be clearly picked out; these are composed of a very hard metallic carbide and held together by a soft tough binding medium. The material is evidently very inhomogeneous.

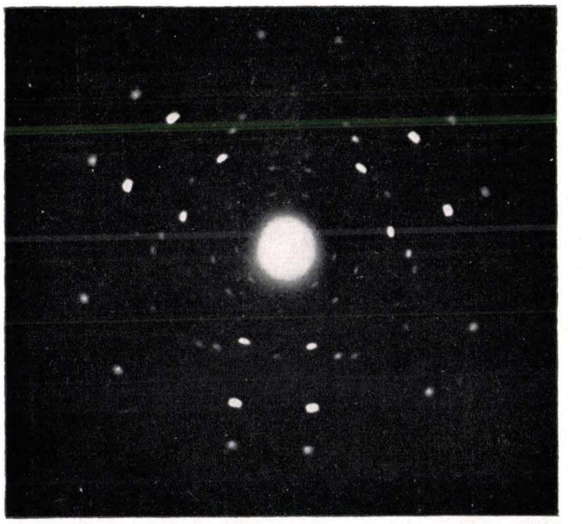

Fig. 6. X-ray diagram of a sapphire single crystal (Laue diagram). The complete homogeneity of the single crystal is indicated by the sharpness and, on suitable orientation to the crystal axes, by the symmetrical distribution of the X-ray diffraction spots (cf. also this Review, **1** 60, 1936).

---

[7]) In measuring the hardness with the Vickers apparatus, a diamond point in the shape of a square pyramid with an apical angle of 118 deg. is forced into the material with a given force. Compared with other methods for measuring hardness, the Vickers method offers the advantage that it can be used equally well for the softest and hardest materials and gives fairly accurate results. For research purposes the Vickers hardness scale is therefore always used in this Laboratory.

[8]) A Vickers hardness value cannot be very well given for diamond, which in fact follows from the definition given in footnote [7]). It would in any case be greater than 2600.

suitable materials if they could be obtained in sufficiently large single crystals. Natural and synthetic sapphire reveal no appreciable difference in quality. Also the orientation of the cutting edges of the cutter with respect to the crystal axes does not call for special consideration with sapphire, in contradistinction to the other crystals tested, such as spinel, corundum and silicon carbide. Micro-photographs of a sound track obtained with a sapphire cutter, on first use and after recording a length of track corresponding to 500 m of "Philimil" strip, are shown in *fig. 7*. It is seen that comparatively few notches have been produced in the cutter edge, these not being detectable acoustically; there is, moreover, no question of any pronounced jaggedness of the edges (such as may be seen on the steel cutter in fig. 4) [9]). As the standard length of a roll of "Philimil" strip is 300 m, the durability of the cutter is equal to recording the maximum sound track which can be obtained on a single film, and the general rule applies that the cutter requires changing after each roll of film.

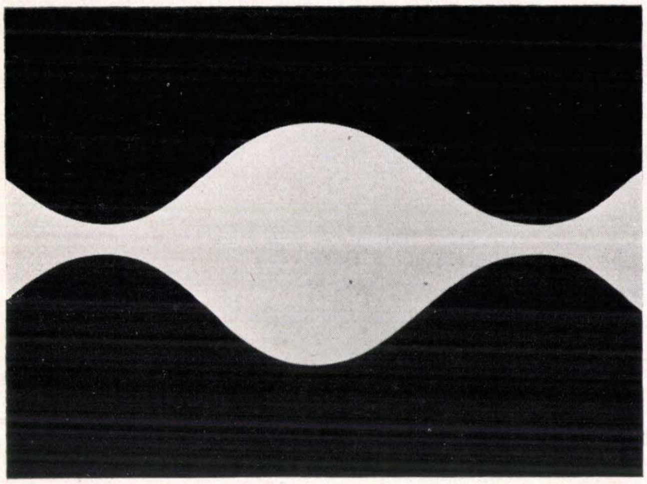

Fig. 7a. A perfect sound track recorded by a sapphire cutter on first use.

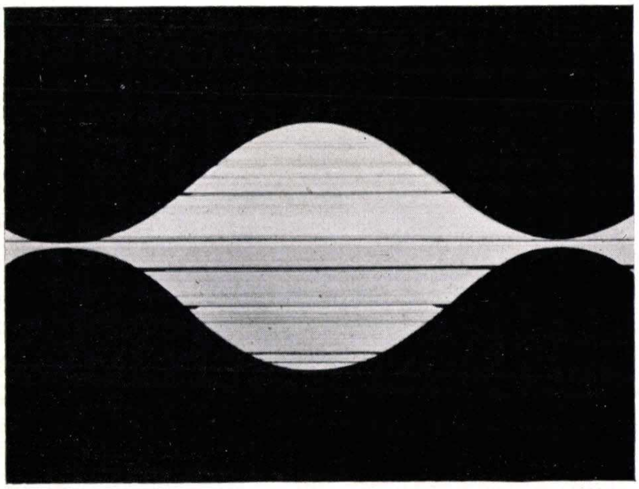

Fig. 7b. Sound track obtained with the same sapphire cutter after performing the same amount of recording as the cutter shown in fig. 4. The present cutter shows much less wear than the steel cutter in fig. 2; the edge has not become jagged and only a few notches are visible (indicated by the continuous lines and jagged edges of the sound track). Frequency and magnification are the same as in fig. 4.

The ease with which the cutter can be fixed in the sound recorder and changed for a new one may be gathered from *fig. 8*.

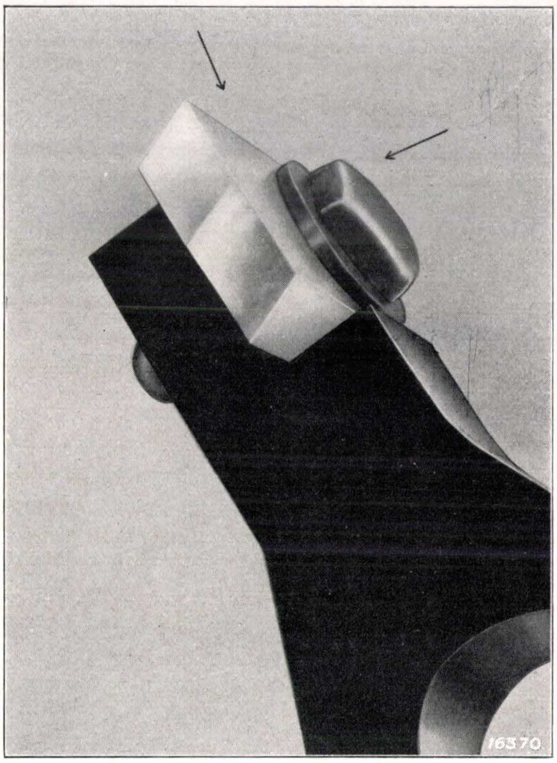

Fig. 8. Attachment of cutter to the armature extension of the sound recorder. When inserting, the cutter is pressed against the machined contact surfaces in the direction of the two arrows and is screwed tight by means of a small spanner (strongly magnificated).

In designing the clamping arrangement, the principle followed was that the cutter and the end of the recorder reed must be as light as possible in order that the recorder shall not be unnecessarily burdened with a high inertia when registering high frequencies.

---

[9]) Although the micro-photograph applies to the low frequency of 150 cycles it is nevertheless applicable to average working conditions, for during recording the sound generator traversed all frequency values. A point corresponding to a lower frequency was photographed solely for the sake of clarity. It was found, moreover, that the wear of the cutter depended to no appreciable extent on either the frequency or the amplitude.

VISUAL ACUITY AND SPEED OF VISION IN ROAD LIGHTING

By P. J. BOUMA.

Summary. The relationship is investigated between the visual acuity on the one hand and the brightness levels of the object and the background, the type of illumination (monochromatic and other types of light), the distance of the observer from the object and monocular or binocular vision on the other hand. With technical sources of light the visual acuity is considerably greater with sodium and mercury light than with ordinary glow lamp and neon light. The speed of vision is investigated for various types of light: a) For stationary objects mercury and sodium lamps are better than glow lamps and neon light, b) for moving objects the descending sequence is sodium light, glowlamps, mercury light.

In observing objects on artificially-illuminated high-ways the first requirement is to perceive the presence of the object. This perception is rendered possible by the existence of a contrast between the object and the road surface; contrast sensibility and contrast richness are determining factors here.

When an object has been once perceived it is then necessary to recognise it, i.e. to observe its exact form and to estimate its distance. This recognition is governed directly by another property of the eye, viz, its visual acuity, which is defined as the ability to differentiate between the form of certain objects which are viewed with a small angle of vision, or the ability to distinguish as separate entities objects situated close together (e.g. two dots or a number of parallel lines).

In addition to visual acuity, the speed of vision is also an important factor in visual recognition; rapid recognition of an object on a highway is of the greatest importance.

As a numerical measure of visual acuity we could, for instance, take the angle of vision at which two parallel lines are still just perceptible as separate entities. But since it is preferable to allot to the greatest visual acuity the highest numerical value, the visual acuity is usually expressed as the reciprocal of this angle (in minutes). Another method of measurement would be to give the distance at which a circle and a square with a diameter of 1 cm could still just be differentiated. These measures are inter-related as follows:

$$1 \text{ minute}^{-1} \text{ corresponds to } 690 \text{ cm.}$$

The visual acuity is determined, *inter alia*, by the following factors:

A) Physical Factors
  1) The brightness of the object perceived.
  2) The brightness of the background.
  3) The physical composition of the light.
  4) The distance at which the object is perceived.

B) Characteristics of the Eye
  5) Myopia (shortsightedness) or hypermetropia (longsightedness).
  6) Astigmatism.
  7) Chromatic and spherical aberration.
  8) Size of the photo-sensitive elements of the retina.

C) Methods of Measurement
  9) Choice of object.
  10) Monocular or binocular vision.
  11) Disturbing secondary influences. Glare.

Certain of these factors require only very brief reference. We shall consider only a "normal" or emmetropic eye; for monochromatic light from the centre of the visible spectrum this eye will exhibit neither myopia, hypermetropia nor astigmatism. We shall not discuss the question of glare either but shall assume that any similar disturbing influences are entirely absent. All other factors will be dealt with in some detail.

The relation between visual acuity and the two contrasting brightnesses can be represented in different ways. To read off directly the visual acuity for two given brightness levels, the best method is to employ a diagram with the brightness levels H_1 (background) and H_2 (object) plotted as abscissa and ordinate and to insert the lines of constant visual acuity G. This has been done in *fig. 1* for sodium light; the objects viewed here consisted of a series of circles and squares, and the distance at which the square with a length of side of 1 cm would still just be distinguished was taken as a measure of G. The results apply to ordinary conditions of road lighting, where the brightness of the object is smaller than that of the background ($H_2 < H_1$). The following points may be deduced, *inter alia*, from the diagram:

1) An increase in H_2 results in a diminution of the contrast and hence a decrease of G.
2) An increase in H_1 results in an increase in the contrast and hence an increase in G.

The increase does not, however, exceed a certain limit, which in the present case is about 860 cm (1.25 minute^{-1}). This limit is reached when the image on the retina of the feature to be differentiated becomes the same size as the photo-sensitive elements. Under ordinary road lighting conditions, e.g. $H_1 = 0.3$, $H_2 = 0.06$ candles per sq. m, where $G = 530$, we are usually far below this limit.

3) Increasing H_1 and H_2 in the same ratio, in fig. 1, proceeding in a direction parallel to the line $G = 0$ (for instance by increasing the intensity of illumination), results in an increase in G; thus, if we double H_1 and H_2 in the example cited above, G will already increase to 600; here again the limit $G = 860$.

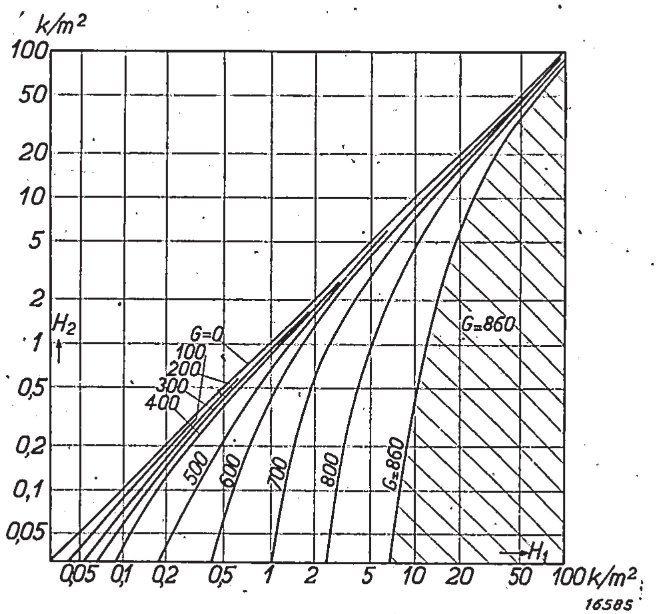

Fig. 1. Visual acuity G as a function of the brightness (in candles per sq. m) of the background (H_1) and of the object (H_2) with sodium light (Bouma).

To compare the visual acuity with different types of light, a diagram such as that shown in *fig. 2* will be found more useful and suitable. In this diagram the visual acuity G is plotted as a function of the brightness H for the following types of light: *1* mercury light; *2* sodium light; *3* neon light; *4* neon light (only the red lines); *5* white light (glow lamps), and *6* the blue mercury line, taking in every case a fixed ratio of H_1 to H_2 (here 1 : 12, i.e. for a bright object on a dark background). The curves for the green and the yellow mercury lines almost coincide with those for the total mercury light. It is seen from the diagram that the visual acuity with mercury light and with sodium light is considerably greater than that with white light. A correct idea of the magnitude of the difference between sodium light and white light is afforded by the ratio of the brightness levels required with white light and with sodium light in order to obtain an equivalent visual acuity G in both cases. This factor f is on the average 2.5 for the range under measurement, in other words the same visual acuity G is obtained when the brightness with white light is 2.5 times greater than that with sodium light. The main reason for this difference is the chromatic aberration of the eye, which adversely affects the definition of the image on the retina in the case of white light, an effect which is absent with the almost-monochromatic sodium light. Closer investigation shows that all monochromatic colours (with the exception of the shortest wave lengths, viz, blue and violet) give a greater visual acuity than white light. This difference also can be expressed by a corresponding factor f. In *fig. 3*, f is plotted as a function of the wave length λ for monochromatic light: Curve *1* is based on the average of measurements made

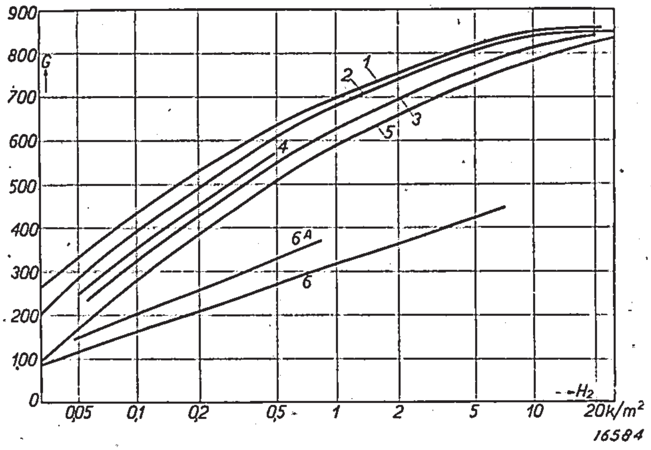

Fig. 2. Visual acuity G as a function of the brightness H_2 (in candles per sq. m) of the object (brightness of background $H_1 = 1/12\ H_2$) for: *1* mercury light; 2 sodium light; *3* neon light; *4* red neon light; 5 glowlamp light; *6* blue mercury line; *6a* as *6* after correction for myopia (Bouma).

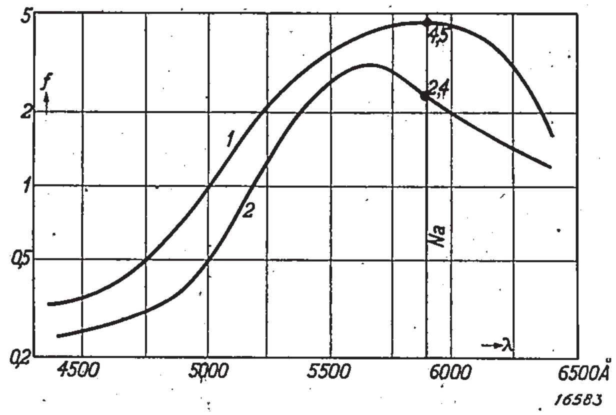

Fig. 3. Ratio f of the brightness levels of white and monochromatic light required to obtain the same visual acuity (various investigators): *1* for line grating as object; 2 for other objects.

by Ives and Luckiesh, and curve *2* on the average of measurements made by Arndt, Bouma, Korff-Petersen and Ogata (in all cases at approx. 1 candle per sq. m). That these curves do not coincide, is due to the fact that different objects were employed in the two series of experiments; the first-named investigators used a grating of parallel lines, and the latter more symmetrical objects, such as letters, Landolt rings, circles and squares. The difference is particularly pronounced in the case of sodium light (5890 Å): $f = 4.5$ for the line grating and 2.4 for the other objects. For practical purposes curve *2* is the more important, and according to this curve the greatest visual acuity is obtained at 5600 Å (not far from the point where the visibility factor of the eye is also a maximum), whilst the acuity for red rays is practically the same as for white light, but that for blue light is much lower. The fact that mercury light gives such a high visual acuity, is also accounted for by fig. 3: the intense green and yellow mercury lines (5461, 5770 and 5790 Å) are both in very favourable positions, and since they are still close together they do not create any marked interference; the blue line (4358 Å) also causes little trouble owing to its very low intensity.

The low visual acuity with blue light is partly due to the fact that the eye is myopic for this short wave length. That the main cause is, however, of different origin is indicated by curve 6^A in fig. 2 where a correction for myopia has been made. The improvement is seen to be only slight.

Of the various factors referred to at the outset we have not dealt with two of these in detail, viz, monocular and binocular vision and the effect of the distance of the object.

Regarding the first factor, it has been found (Blondel, Ferree, etc.) that binocular vision gives a better visual acuity than monocular vision, provided both eyes are identical (either naturally or after suitable correction); where the eyes are not equivalent, visual acuity in binocular vision is determined by the eye with the best accomodation; closing the other eye then has no effect.

In conclusion the effect of distance should be discussed. It seems reasonable to assume that for the normal eye the visual acuity (which is ultimately determined by the *angle* of vision) is independent of the distance; in other word, if a square of 1 cm can still just be distinguished at a distance of 6 m, it might be expected that a square of 2 cm would still just be distinguishable at a distance of 12 m. This has, however, been found not to be quite the case. Measurements by Freeman, Luckiesh, Bouma and Mouton indicate that for distances less than 2 m the visual acuity G increases with the distance d, that for d between 2 and 7 m, G is practically independent of the distance, and for greater distances gradually diminishes with the distance. *Fig. 4* shows this relation graphically; the cause of this phenomenon is still unknown. The diagram applies to the normal eye; a myopic eye would for instance exhibit a much greater decrease of G at greater distances.

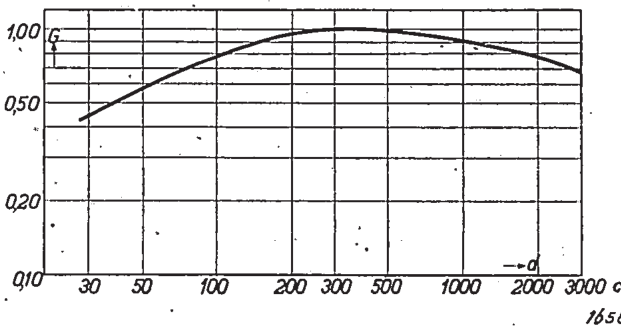

Fig. 4. Visual acuity G as a function of the distance d (various investigators).

In the above discussion an important factor has been left entirely out of consideration, viz, the time, a factor which in reality plays an important part on the road. In all the measurements referred to, the eye has been given an opportunity to observe the stationary object for an unlimited period. These experiments may be extended in two directions:

1) The eye is allowed to observe the object for only a short time.
2) The object is caused to move in the field of vision.

Restricting ourselves first to the first-named case, it is interesting to know the time τ during which an object must remain in the field of vision in order to make recognition possible. This time interval depends on the nature and size of the object, on the distance separating it from the observer, and on the brightness levels of the object and the background. If we alter only the intensity of illumination (such that the two brightness levels are altered in the same ratio) it will be found that below a certain brightness H_0 of the object the latter will no longer be distinguishable at all; this limit H_0 may be deduced from the measurements of visual acuity. At brightness levels which are only slightly above H_0, τ becomes very large and the magnitude $1/\tau$, which is frequently termed the speed of vision, approaches zero. *Fig. 5* gives an example of the variation of this factor $1/\tau$ being plotted as a function of the brightness H of the object (a number of circles and squares of 1 cm diameter were viewed from a distance of 2 m). The ratio of the brightness levels of the object and the background was here 12 : 1; the short exposure times were obtained by means of a Compur shutter. Curve *1* applies to sodium light and curve *2* to glowlamp light. The following points may be noted:

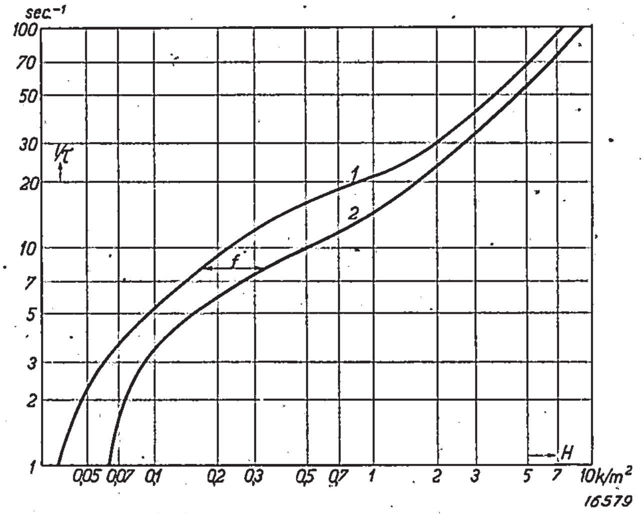

Fig. 5. Speed of vision $1/\tau$ (τ is the time for which the **stationary** object must be illuminated in order to be perceived) as a function of the brightness H (in candles per sq. m) of the object (**Bouma**): *1* sodium light; *2* glowlamp light.

1) The curves do indeed approach zero for the values $H_0 = 0.032$ and $H_0 = 0.060$ which we can also obtain from fig. 2 for $G = 200$.
2) The speed of vision is always greater for sodium light than for white light, or expressed otherwise: To obtain the same $1/\tau$ values a higher brightness level is required with white light than with sodium light. If we represent the ratio of the required brightness levels again by f (exactly as in the measurements of visual acuity), we see that at low brightness levels f is roughly equal to 2, whilst at high brightness levels (above the brightness level of road lighting) f is about 1.2.
3) At high brightness levels $1/\tau$ becomes proportional to H, i.e. whether an object is perceived depends solely on the magnitude τH and hence on the total quantity of light falling on the eye. Over these short time intervals the eye integrates the brightness within the period of exposure (exactly as does a photographic plate).

It was found for various monochromatic and technical sources of light that the values of f occurring at the speed of vision are in agreement with those from measurements of the visual acuity (**Arndt**). In particular the speed of vision is thus also greater with sodium and mercury light than with glowlamp light; this applies especially to objects which are viewed under a small angle of vision (**Luckiesh**).

The conditions are somewhat different if at the same time the object is moved (thus simultaneously extending the visual acuity experiments in the two directions indicated). Investigations on these lines were carried out, *inter alia*, by **Weigel**, who determined the time τ' during which a moving object must be visible in order to be recognised. The velocity of the object was in all cases such that during the time in which the object was visible the same distance was always traversed. *Fig. 6* shows some of the results obtained, where for various types of light (*1* sodium light, *2* glowlamp light, *3* mercury light) $1/\tau'$ is plotted as a function of the brightness of the background (the brightness of the object was always 2.2 times greater). As in the measurements made by **Arndt** and **Bouma**, sodium light is again also seen to give much better results than glowlamp light. Compared with the previous measurements there are, however, two important differences:

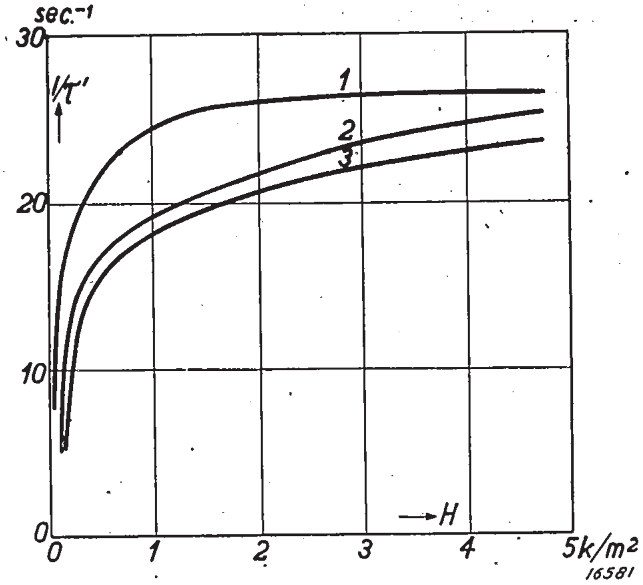

Fig. 6. Speed of vision $1/\tau'$ (τ' is the time during which a **moving** object must be illuminated in order to be perceived) as a function of the brightness H (in candles per sq. m) of the background (**Weigel**).
1 sodium light; *2* glowlamp light; *3* mercury light.

1) The magnitude τ' rapidly reaches a saturation value of about $^1/_{25}$ of a second, whilst τ measured for stationary objects may be reduced with high brightness levels to $^1/_{200}$ (**Bouma**, **Cobb**) and even to $^1/_{500}$ of a second (**Ferree**, **Rand**).
2) For moving objects, the speed of vision with mercury light is in fact smaller than with glowlamp light (**Weigel**), whilst it is much greater with stationary objects (**Arndt**).

These differences can to some extent be accounted for. At very short exposure times **Weigel** employed very high velocities for the object, so that the eye was no longer able to follow the movements of the object. Even at the highest brightness levels such short times of perception are therefore no longer able to give satisfactory vision, hence the saturation value. That the chromatic relationship of τ' may differ from that of τ is evident when it is remembered that here entirely different properties of the eye are called into operation, particularly the speed at which the image disappears from the retina. If we assume that this speed is smaller with blue light than with other kinds of light, it is clear that sodium light under these conditions is considerably superior to both mercury light and glowlamp light.

It may be advanced against the above discussion that on the highway we are not only interested in the time during which an object must be visible to us, but also particularly in the time elapsing between the first appearance of the object and the instant at which an impression has been conveyed to the brain, and the object is actually recognised for what it is. This interval obviously also embraces a psychological reaction time, viz, the time elapsing between the formation of the complete image on the retina of the eye and the instant at which it has been registered on the brain and the latter reacts to it. Although it appears plausible that this reaction time will be the same for different types of light, it is nevertheless important to investigate whether, in this respect also, sodium light offers any advantages over ordinary glowlamp light.

Information of the total time taken by the whole operation of a registration on the brain is given by the results of experiments on the speed of reading. *Fig.* 7 shows the speed of reading in letters per second for various brightness levels of the page and for both white light and sodium light. It is seen that also in this repect sodium light is superior to white light, and for f we again get, as was to be expected, approximately the same value as was determined for visual acuity and speed of vision ($f \sim 2$).

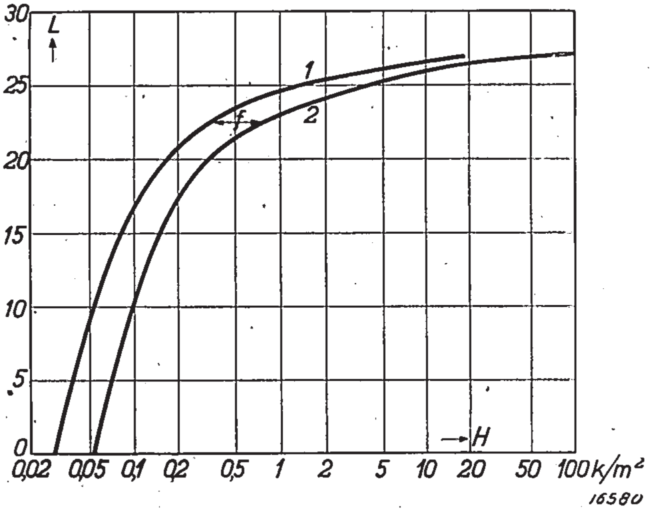

Fig. 7. Speed of reading L (in letters per second) as a function of the brightness H (in candles per sq. in) of the page (Bouma): 1 sodium light; 2 glowlamp light.

Unlike fig. 5, fig. 7 naturally reveals a saturation value determined by the speed at which our mind is able to "digest" the matter, this saturation value is the same for both types of light.

BIBLIOGRAPHY

Arndt, Das Licht, **3**, 213, 231, 1933. (Visual acuity and speed of vision for various types of light.)

Blondel, Rev, Opt., **13**, 247, 1934. (Monocular and binocular vision.)

Bouma, Ingenieur, **49**, A 31 and 243, 1934. (Visual acuity and speed of vision for various types of light; dependence on the two brightness levels and on the distance; comparison between different test objects; speed of reading.)

Cobb, Trans. Ill. Eng. Soc., **19**, 150, 1924. (Speed of vision with white light.)

Cobb and Moss, Trans. Ill. Eng. Soc., **23**, 496, 1928. (Visual acuity with white light.)

Ferreé and Rand, Trans. Ill. Eng. Soc., **22**, 79, 1927. (Speed of vision with white light.)

Freeman, J. Opt. Soc. Am., **22**, 285, 402 and 729, 1932; **26**, 271, 1936 (Visual acuity as a function of the distance.)

Ives, Phil. Mag., **24**, 845, 1912. (Visual acuity with monochromatic light.)

Korff-Petersen and Ogata, Licht und Lampe, **15**, 41, 1926. (Visual acuity and speed of vision with different types of light.)

Kruyswijk and Zwikker, Physica, **1**, 225, 1934. (Visual acuity with sodium light and white light; monocular and binocular vision.)

Luckiesh, Taylor and Sinden. J. Franklin Inst., **192**, 757, 1921. (Speed of reading.)

Luckiesh and Moss, J. Opt. Soc. Am., **10**, 275, 1925; J. Franklin Inst., **215**, 401, 1933. (Visual acuity with different types of light.)

Luckiesh and Moss, J. Optic. Soc. Am., **23**, 25, 1933. (Visual acuity as a function of the distance.)

Luckiesh, J. Opt. Soc. Am., **24**, 6, 1934. (Speed of vision with sodium and white light.)

Mouton, Recherches sur les propriétés physiques et les effets physiologiques d'une lumière colorée, Paris, 1935. (Visual acuity and speed of reading with yellow light; effect of distance.)

Weigel, Das Licht, **5**, 211, 1935. (Visual acuity and speed of vision with different types of light.)

PRACTICAL APPLICATIONS OF X-RAYS FOR THE EXAMINATION OF MATERIALS

By W. G. BURGERS.

Up to the present we have discussed in this section only X-ray photographs of pure compounds having a specific chemical composition and in which the various elements are present in fixed quantitative proportions. Where mixtures of such compounds were considered, as in the two previous articles, the compounds were present as independent physical entities. But substances are known which are composed of several elements or compounds in varying proportions, although one phase is present. In these cases we speak of solid solutions or mixed crystals, and in the case of metals frequently of alloys.

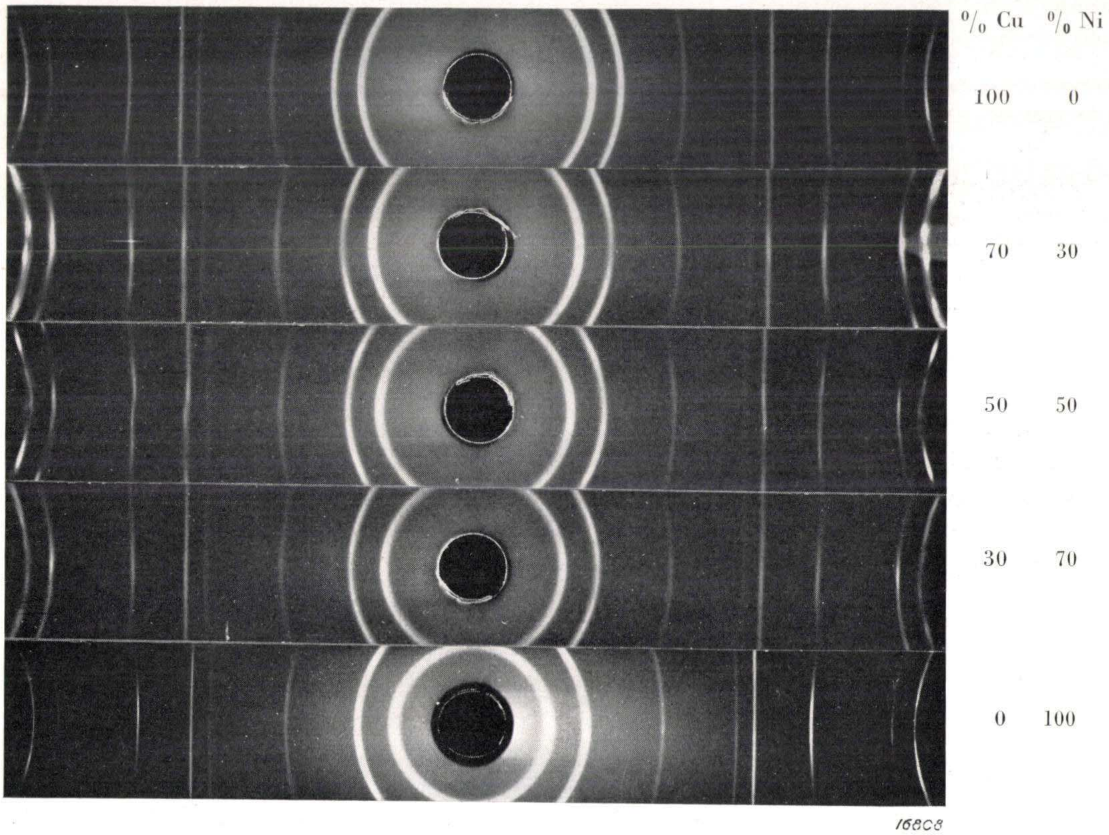

Fig. 1. X-ray photographs of copper-nickel alloys of different compositions.

Mixed crystals are frequently formed by elements or compounds having identical crystal lattices in which only the interatomic distances may have different values. Examples of these "isomorphous" crystal structures are found in many metals as well as in compounds of corresponding composition, e.g. barium and strontium carbonate, $BaCO_3$ and $SrCO_3$. Hence these elements or compounds are often "miscible" with each other in all proportions. The conception is that, for instance, in the case of $BaCO_3$ and $SrCO_3$ the barium and strontium atoms, which occupy very definite positions in the crystal lattices of the homogeneous compounds, are arbitrarily distributed over these positions in the mixed crystal.

Owing to the difference between the interatomic distances in isomorphous crystals referred to above, it must be expected — and this is actually found to be the case — that the interatomic distances in a mixed crystal (in which only a "mean" interatomic distance can be assumed owing to the different atoms alternating with each other) have values between those for the two components. Closer investigation has shown that the interatomic distances in a series of mixed crystals vary in general in proportion to the composition.

The occurrence of isomorphism and the formation of mixed crystals are readily brought into evidence by X-ray photographs, for since in isomorphous crystals the same arrangement of atoms is found, with only a difference in their distances, they give

X-ray photographs in which the interference rings occupy the same relative positions but have different diameters. These diameters are in fact determined by the angles of dispersion of the incident X-ray beam produced at the atomic lattice, the angles varying with the interatomic distances.

Thus, if we compare the X-ray photographs obtained with a series of isomorphous crystalline bodies, the corresponding rings are found to be displaced with respect to each other.

Fig. 1 a-e shows a series of photographs for mixed crystals, which were obtained with copper-nickel alloys containing 0, 30, 50, 70 and 100 per cent nickel respectively. The progressive increase in the diameter of the corresponding interference rings is brought out very clearly here.

The presence of an alloy or a solid solution can therefore be assumed when the X-ray photograph of the substance under examination is comparable to those obtained with the isomorphous substances concerned, but differs from the latter in the size of the interference rings. From the magnitude of this difference, bearing in mind the above-mentioned consideration, it is possible to deduce the approximate composition of the solid solution.

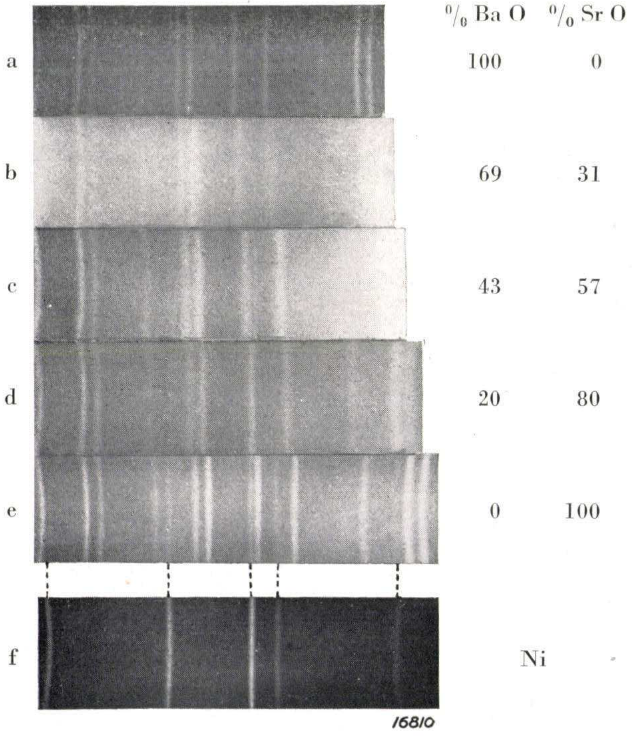

Fig. 2. Formation of mixed crystals between Ba0 and Sr0. Fig. e contains some lines which, on comparison with the nickel diagram *f*, are seen to be due to the nickel tube which carries the oxide layer.

A number of examples are given below in which the occurrence of mixed crystals or solid solutions was of interest.

12. Mixed crystal formation in oxide cathodes

The "oxide layer" of oxide cathodes consists principally of barium oxide and strontium oxide, these oxides being formed by decomposition of the corresponding carbonates. The latter are sprayed on the cathode (e.g. a short nickel tube) in the form of a paste and during preparation are decomposed by strongly heating *in vacuo*. At the high temperature of formation applied the oxides form mixed crystals as a result of diffusion [1]. This can be proved by X-ray methods as demonstrated by *fig. 2 a-e*. This figure reproduces a series of X-ray photographs of oxide preparations obtained by strongly heating carbonate mixtures containing different proportions of $BaCO_3$ and $SrCO_3$. It was found that the formation of mixed crystals influenced the emissivity of the cathode [2]).

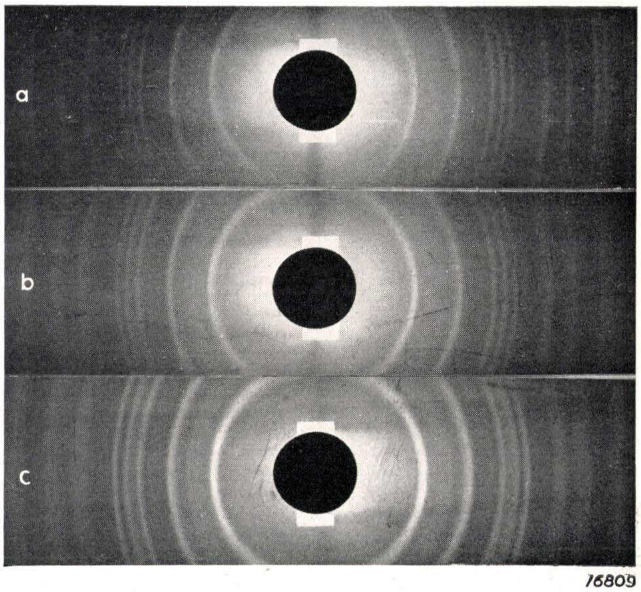

Fig. 3. Formation of mixed crystals between $BaCO_3$ and $SrCO_3$ on simultaneous precipitation from a solution of the nitrates.
a) $BaCO_3$; b) $BaSr(CO_3)_2$; c) $SrCO_3$.

Radiographic examination of a number of cathodes from standard valves showed, however, that mixed-crystal formation was not always complete. In some cases the photographs indicated that the separate oxides were still present [3]), probably owing to the fact that in the preparation of the cathodes the duration of heating and the temperature were not the same in all cases, the time being too short in some for complete formation of mixed crystals.

---

[1]) W. G. Burgers, Z. Phys. **80**, 352, 1933.

[2]) M. Benjamin and H. P. Rooksby, Phil. Mag. **15**, 810, 1933.

[3]) W. G. Burgers, loc. cit. The diagrams showed no lines due to metallic barium, the proportion of barium in the mixed crystals being far too small.

If, however, on spraying the cathode a mixed crystal of the carbonate is present at the outset, it may be expected that the solid solution of oxides will be formed directly by decomposition of this mixed crystal and as a result the interdiffusion of the oxides is eliminated. A carbonate mixture precipitated from a solution containing both Ba and Sr ions, e.g. a mixture of their nitrates, appears suitable for this purpose; as shown by the X-ray photograph in *fig. 3*, such a solution does indeed give a mixed crystal of $BaCO_3$ and $SrCO_3$.

13. Nickel-iron alloy

The next example is of the same class as the one just discussed. X-ray photographs confirmed the conclusion drawn from microscopic examination, that mixed crystals are formed on precipitating a mixture of nickel oxalate and iron oxalate from a solution of nickel chloride and iron chloride. The oxide obtained on heating the precipitate gives on reduction a nickel-iron powder composed of a solid solution of iron and nickel. In this way, therefore, a nickel-iron alloy is directly obtained.

14. Fluorescent Preparations for Luminescent Tubes and Fluorescent Screens.

Zinc sulphide containing a varying proportion of cadmium sulphide is in common use as a fluorescent preparation, the colour of the latter being determined by the relative proportions of the two substances. These substances are isomorphous and form mixed crystals in all proportions. By comparing X-ray photographs of these preparations with standard diagrams of the separate sulphides, the approximate composition of the preparations can be readily determined (to within several per cent).

ABSTRACTS OF RECENT SCIENTIFIC PUBLICATIONS OF THE N.V. PHILIPS' GLOEILAMPENFABRIEKEN

No. 1072: R. Houwink: The strength and modulus of elasticity of some amorphous materials, related to their internal structure (Trans. Faraday Soc. **32**, 133-141, Jan. 1936).

A general discussion is given of the tensile strength and the modulus of elasticity of matter on the basis of the cohesive forces of matter. The principal theories regarding the internal structure of asphalts, resins and glass are briefly outlined. The elastic properties particularly of hardening resins are studied. For a phenol-formaldehyde resin, a modulus of elasticity of 1050 kg per sq. mm and a tensile strength of 7.8 kg per sq. mm were found at 195 deg. C. This tensile strength is only 1/550th of the theoretical value (cf. **No. 1071** by J. H. de Boer). An explanation is offered by assuming the occurrence of irregularities ("Lockerstellen") in the structure of the macro-molecules of the resin. Causes responsible for the presence of these "Lockerstellen" are enumerated and discussed, both for resins and for other amorphous substances, e.g. glass. For the modulus of elasticity the measured value is 1/10th of the theoretical value. That this difference is so many times smaller than in the case of the tensile strength is probably due to the part which the secondary bonds (resulting from Van der Waals' forces) play in addition to the primary bonds in the macro-molecules of the resin.

No. 1073: R. Houwink: High elasticity of three-dimensionally polymerised amorphous materials in relation to their internal structure (Trans. Faraday Soc. **32**, 131-143, Jan. 1936).

In this paper the relationship is given between the maximum elastic energy which can be stored in a substance and the energy content of the bonds. In particular the elastic properties of hardening resins are discussed. A high possible elastic deformation (up to 240 per cent) is found at a definite degree of polymerisation of the resin (B state) at a temperature of 120 deg. C. The relationship between these elastic properties and the formation of insoluble, elastic three-dimensional networks is given. A similar behaviour may be observed with asphalt and glass, but it is not so pronounced as with the resins. With these former substances the highest possible elastic deformation is only of the order of 20 per cent. It is shown that a highest possible elastic deformation of this order may generally occur with amorphous substances if the viscosity is of the order of 10^{11} to 10^{13} poises (1 poise $=$ 1 dyne cm^{-2} sec). Calculations are given to explain the changes which occur in Young's modulus, in the tensile strength and in the yield point when matter is transformed from a compact to an open reticulated structure. From the bonding energy which is stored in the intramolecular bonds in asphalt, glass and resins, the author attempts to give a rough explanation for the high possible elastic deformation of these materials.

No. 1074: W. Elenbaas: Über die mit den wassergekühlten Quecksilber-Super-Hochdruckröhren erreichbare Leuchtdichte (Z. techn. Phys., **17**, 61-62, Febr., 1936).

It is shown in this article that in ultra-high pressure mercury vapour discharge tubes equipped with water cooling the brightness hitherto attained can be further increased by reducing the internal and external diameters of the tubes. In the first place the power input and the pressure are kept constant; the brightness increases slightly less than would be proportional to $1/R$ ($R =$ radius). By reducing the internal diameter to 1 mm and with an input of 1400 watts per cm length of the tube (805 volts and 2.1 amp) brightness values of 180 000 candles per sq. cm have been obtained.

No. 1075: M. J. O. Strutt: Diode frequency changers (Wirel. Eng., **13**, 73-80, Febr. 1936).

In this article the most important properties of diode frequency changers are set forth theoretically and experimentally. The conversion gain is $g = R/(R + R_i)$, where R is the tuned impedance on the primary side of the intermediate frequency transformer and R_i the effective internal resistance of the diode for the incoming signal. If oscillator voltages of over 4 volts are used and a proper bias applied to the diode, the value of R_i may be about 0.1 megohm. Owing to the low input impedance, it is preferable to use the diode in sets with a high-frequency valve before it. In this case the noise due to shot effect is negligible; whistling noises are sufficiently low if the input signal amplitude on the diode is only a few millivolts, while at the same time distortion effects are negligible. Compared to the octode, the diode circuit for frequency changing generally offers the advantage that it is more suitable for short waves. Contrary to other mixers, higher harmonics of the oscillator frequency for frequency changing can also be used with this diode circuit without loss of gain, as may be sometimes advisable for short waves.

No. 1076*: W. F. Brandsma: Het onderzoek van de beitelpunt (Metaalbewerking, **2**, 541-545, Febr. 1936).

This article describes the application of the so-called facing-lathe test by means of which the quality of a cutting tool edge can be determined. In these tests the distance from the shaft is measured at which the tool loses its edge when a disk rotating at a uniform angular velocity is turned by the tool from the centre towards the periphery. A fuller abstract of this paper will be omitted here as this subject is dealt with in detail in a separate series of articles appearing in this journal (Philips techn. Rev., **1**, 183 and 200, 1936).

No. 1077: Balth. van der Pol: On oscillations (Norsk Rikskringkastings Forelesninger, Oslo, 1936, pp. 243-275).

This paper presents a general mathematical review of the principal properties of oscillations which are of interest in different branches of science and technology. In addition to standard functions represented by a sinusoidal time diagram, special attention is also directed to functions with a rectangular time diagram, for which, analogous to ordinary sine functions, an orthogonal system of functions can also be derived, thus permitting an ordinary sine function to be expanded on the basis of these functions. After discussing those oscillations which can be represented by linear differential equations, the author passes to a consideration of non-linear phenomena. The relationship between harmonic and so-called relaxation oscillations is analysed. The paper concludes with a discussion of various types of relaxation oscillations of frequent occurrence in nature and technology, such as the beat of the heart, the multivibrator of Abraham and Bloch and the so-called "sleeping actions" of plants.

(A translation of these papers appeared in Ned. T. v. Natuurk., **3**, pp. 65-85 and 97-108, 1936).

No. 1078: J. L. Snoek: On the "Permalloy Problem" (Nature, **137**, 493, 1936).

According to Lichtenberger the exceptionally high permeability of Permalloy may be ascribed to the fact that three particular points in the iron-nickel system are situated close together; at 71 per cent the crystal anisotropy vanishes; at 82 per cent the absolute value of magnetostriction passes through a minimum, and at 85.5 per cent the anistropy of magnetostriction also vanishes. Various recent researches carried out by the author and other investigators lead the former to conclude that Lichtenberger's hypothesis is valid. On slow cooling in the absence of a magnetic field magnetostriction is able to disturb the magnetic orientation, resulting in a lower permeability. If on the other hand slow cooling takes place in the presence of a magnetic field, the disturbance due to magnetostriction is eliminated in the direction of this field and the action of crystal anisotropy becomes much more pronounced.

No. 1079: K. F. Niessen: Erdabsorption bei vertikalen Dipolantennen in grosser Höhe über ebener Erde (Ann. Physik, **25**, 673-687, Apr., 1936).

For the case where the quotient of the heitgh h of a vertical dipole-aerial above the ground and the radiated wave length satisfies a certain inequality, the author deduces a formula for that fraction T of the total energy radiated from the aerial which is absorbed by the earth. This absorbed portion is determined by the absolute value n and the argument of the complex refractive index and hence by the dielectric constant and by the conductivity of the soil. Simple formulae are given for the practical case where $1/n^3$ can be neglected compared with unity. The absorbed portion T at a finite height h of the dipole aerial is greater than $T(\infty)$ for an infinite height. This additional absorption due to placing the aerial at height h may be expressed as a function of h/λ. From this expression it follows that it is of advantage to locate the dipole aerial at a height which is equal to an odd multiple of the quarter wave length, whilst practically no further gain accrues when the aerial is located at a height of more than four wave-lengths above the ground.

---

*) A sufficient number of reprints for purposes of distribution is not available of those publications, marked with an asterisk *). Reprints of other publications may on application be obtained from Philips laboratory, Kastanjelaan, Eindhoven, Holland.

VOL. 1 No. 8 AUGUST 1936

Philips Technical Review

DEALING WITH TECHNICAL PROBLEMS
RELATING TO THE PRODUCTS, PROCESSES AND INVESTIGATIONS OF
N.V. PHILIPS' GLOEILAMPENFABRIEKEN

EDITED BY THE RESEARCH LABORATORY OF N.V. PHILIPS' GLOEILAMPENFABRIEKEN, EINDHOVEN, HOLLAND

THE PROBLEM OF GLARE IN HIGHWAY LIGHTING

By P. J. BOUMA.

Summary. After a short discussion of the concept of glare or dazzle and a survey of the various types of glare (direct, indirect, simultaneous and successive glare) as well as of the effects of glare (reduction in the visual faculties of the eye, fatigue, diversion of attention), the influence of glare on contrast sensitivity is analysed in some detail. An approximate formula given by Holladay is dealt with. Consideration is then given in turn to the effect of successive glare (after-effects), the feeling of discomfort and differences between observations by different observers (on the basis of investigations with 100 observers). A number of practical conclusions are then drawn.

One of the most important and at the same time one of the most difficult problems encountered in the study of highway lighting is that relating to glare or dazzle. The difficulties to be overcome are very varied in character. In the first place there appears to be no agreement as to what actually constitutes glare, whilst it is also difficult to determine what type of glare plays the principal part. No criterion for measuring the intensity of glare exists and there is perhaps no other branch of physiological optics, in which the personal equation enters more deeply than in this problem of glare or dazzle.

What do we understand by glare ?

The various phenomena which are included under the generic term of "glare" may be classified under two heads:

1) The reduction in all visual functions of the eye which results when a portion of the retina is stimulated by a brightness which is far above the average brightness level at which normal vision and perception operate.
2) The feeling of discomfort (with the simultaneous diversion of attention and various fatigue effects) which an object of such exceptional brightness creates.

Frequently both phenomena occur simultaneously and in many cases it is thus essential to distinguish clearly between these two groups: The visual faculty of the eye can in fact already be appreciably reduced before the second group of phenomena exercise any influence.

A characteristic difference between these two groups is to be found in the fact that the ocular faculties of the human eye can be measured and expressed numerically in many different ways, whilst a similar evalution as regards discomfort phenomena is much more difficult and is often quite impossible.

That portion of the retina on which the dazzling light impinges, may be the same as that which we employ for visual perception. We then speak of direct glare. (This occurs, for instance, when we make an attempt to determine the form of a light source and also when we look directly at a light source and then try to distinguish an object with the same mean retinal area). A still more common case is when the exposed area of the retina does not coincide, with the area utilised for perception, (e.g. when our perception of objects on a highway is disturbed by insufficiently-screened stationary sources of glare or by the headlights of an approaching motor car). In this case we speak of indirect glare: the visual acuity of a portion of the retina is reduced because another part of the retina is over-stimulated [1]).

---

[1]) This diminution may be partly attributed also to the dispersion of the glare light in the various parts of the eye.

As is already apparent from the examples given above, the functioning of the eye can be affected during the presence of a dazzling source as well as subsequently after its removal from the field of vision. In the first case we have simultaneous glare and in the second successive glare ("after-effects"). In the investigation of the latter phenomenon the time is naturally an important factor.

Criteria for Measuring Simultaneous Glare

To investigate the dazzling effects of different sources of light under different conditions, we must evaluate the effect produced numerically. For this purpose a measurement is usually made of how far a specific property of the eye is adversely affected by the presence of a source of glare. Thus we can measure the reduction in contrast sensitivity, in visual acuity, and in the speed of perception, etc., for all of which the following general considerations apply:

1) The dazzling effect will be the greater, the higher the intensity of illumination E which the source of glare produces at the eye.
2) The dazzling effect will be the greater, the smaller the angle of vision a between the object perceived and the glare source.
3) A given source of glare will have the greater effect, the lower the brightness values at which objects are to be perceived.
4) The differences between different types of light are very small.

Exhaustive measurements have been carried out regarding the effect of glare on contrast sensitivity; these measurements will now be discussed in some detail.

Contrast sensitivity in the absence of a source of glare is defined as:

$$K = \frac{H}{\Delta H}$$

where ΔH is the difference in brightness which can still be just distinguished against a background brightness of H 2)). Glare causes a reduction in the contrast sensitivity by a fraction P times its original value, thus:

$$K' = P\,K = H : \left(\frac{\Delta H}{P}\right).$$

In other words, in the presence of a source of glare the difference in brightness just perceptible to the eye is $\Delta H/P$.

The diminution in contrast sensitivity due to glare can also be expressed as the so-called "equivalent veiling brightness" H' instead of by the magnitude P. The equivalent veiling brightness is defined by Holladay as follows:

The difference in brightness still just perceptible would be similarly raised from ΔH to $\Delta H/P$ if in place of the source of glare an additional brightness H' were introduced into the whole field of view. For H' Holladay gave the following approximate formula:

$$H' = C\,\frac{E^{n}}{a^{m}} \quad \ldots\ldots \quad (1)$$

where H', E and a represent the same as above and C, n and m are constants, which Holladay found had the following values: $C = 9.2$ (when H' is expressed in candles per sq. m, E in lux and a in degrees), $n = 1$ and $m = 2$.

Hence the veiling brightness is proportional to the amount of light emitted from the glare source and is inversely proportional to the square of the angle of vision between the object and the source of glare. We shall discuss the application of this formula for a specific case. We must take as a basis the relationship existing between the magnitudes ΔH and H — in the absence of dazzling light sources — and which is shown in *fig. 1* for white light. It is seen from this figure that, for instance, with a brightness $H = 0.3$ candle per sq. m, a brightness difference of 0.013 candle per sq.m is still just perceptible (contrast sensitivity $K = 23$). Now assume that a source of glare is introduced which has an intensity of 810 candles in the direction of vision and is 2 m to the side of the object to be perceived. The distance

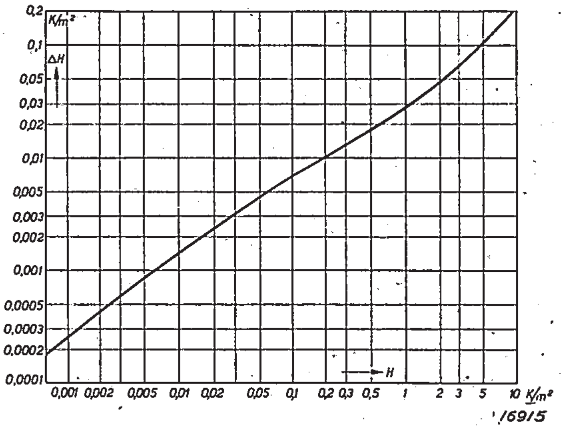

Fig. 1. Difference in brightness ΔH which is still just detectible, plotted as a function of the brightness H of the background, both expressed in candles per sq.m. The figure is applicable for white light. The ratio of abscissal to ordinal values gives the contrast sentitivity.

---

2) See also Philips techn. Rev., 1, 166, 1936 (fig. 4).

between the eye and the source of glare is assumed to be 30 m, so that the intensity of illumination at the eye (due to the source of glare) is $E = 0.9$ lux and $\alpha = 3.82°$ This case is described in the report of the Illumination Committee of the Royal Dutch Automobile Club and of the National Dutch Cycling Association (1925) as "just embarrassing glare". From (1) we get:

$$H' = 0.568 \text{ candles per sq. m}$$

Fig. 1 gives, for a brightness $H + H' = 0.868$ candles per sq.m, a value of ΔH of 0.03 candle per sq.m, so that the contrast sensitivity K' is $0.3/0.03 = 10$ and has hence dropped to half.

It should be emphasised that Holladay's formula only gives the order of magnitude of the glare. Various investigators have found that it is subject to a number of deviations:

a) The value of m varies from 1.5 (Stiles) to 4 (Rep. Roy. Dutch Auto. Club), whilst we have found that m is closely dependent on the angle of view α; for α between 2 and 15° an average value of $m = 2$ was found.

b) A source of glare situated above the object being viewed, has less effect than a glare source placed beside or below the object (Weigel, Bouma); this phenomenon is not taken into consideration in equation (1).

c) The values given by Holladay indicate that n is also dependent on α; as the angle of view increases n diminishes; between 2.5 and 5° n has a mean value of 90. We found a value of 0.89 for n when $\alpha = 3.5°$, so that the proportionality to E is not strict.

d) In equation (1) the brightness H_B of the glare source and the angle δ at which it is viewed are included only in the general term E which is proportional to $H_B \delta^2$. The law which assumes that the effect of the glare source, with equivalent E, is independent of the particular values of H_B and δ only holds good for sufficiently small sources of glare, i.e. where $\delta < \delta_0$. The limits for δ_0 given by different investigators are: 3° (Bordoni), 1° (Stiles), 0.5° (Nat. Dutch Cycl. Assoc. A.N.W.B.). We have found that the law still gives satisfactory values at $\delta = 0.6°$

e) According to our measurements H' was independent of H, as well as of E and α.

These deviations indicate, that the "equivalent brightness" cannot be regarded as a brightness value, which actually falls on the retina owing to light dispersion in the eye, but merely as a fictitious magnitude which facilitates the correlation of practical results. Measurements based on the reduction in visual acuity, speed of perception, etc., as a criterion lead to analogous results, but these cannot be so easily collated by introducing a veiling brightness.

The effect of the colour of the glare source is very slight in all cases. On comparing glowlamp and sodium light many investigators have, for instance, arrived at the same values apart from unavoidable experimental tolerances, whilst others have observed a slight advantage in favour of sodium light. In investigations carried out in these laboratories, in which 100 observers participated, a slight advantage in favour of sodium light was also found. The permissible intensity of the sodium glare source was on the average 1.086 times greater than that of a white glare source. The probable error in this value was 3%. In the case of 61% of the observers the sodium glare source gave a lesser reduction in K than a white glare source of equivalent intensity, whilst 39% found the opposite.

Successive Glare

The following must be considered as criteria for the degree of successive glare:

a) The time during which an after-image of the glare source persists.

b) The time, following the removal of the glare source until the eye again adapts itself to its normal visual capacity.

Few comprehensive measurements have as yet been carried out on this aspect of the problem, although certain tentative conclusions may already be drawn from the measurements which have been made. Thus it has been found that in general the rays of shortest wave length (blue, violet) are the most trying in successive glare. In this respect, for instance, sodium light offers considerable advantages over glowlamp and mercury-vapour light. It was also observed that light sources with a high luminous intensity and of small dimensions produce more intense successive dazzle than light sources of the same degree of brightness but of greater surface area.

Discomfort due to Glare

The feeling of discomfort and disturbance, etc., caused by a source of glare is difficult to express numerically. Attempts have been made to adjust two sources of light to have the "same discomfort values" (Harrison), but without conspicuous success.

Measurements of fatigue based on the gradual reduction in the visual capacity of the eye in the presence of a source of glare persisting for a long time (e.g. a reduction in the speed of reading) have not led to any noteworthy results. Measurements carried out by Mouton indicate that in this particular case there is practically no difference between white glowlamp light and the light obtained when all wave lengths below 5000 Å (blue-green, blue, violet) are cut out ("Selectiva" light).

Since no reliable measurements have been made in this direction, an estimate of this factor must be based on general practical experience. The following conclusions appear to be justified:

1) Exactly as in the case of successive glare, a light source of high brightness and small dimensions here again produces more discomfort than an equally bright source of light with a larger surface of radiation.
2) In general the blue rays are mainly responsible for the discomfort produced. Hence yellow light (both monochromatic light given by the sodium lamp and "Selectiva" light) results in less discomfort than white light.

The Personal Equation

In all the measurements described relating to glare, differences due to the personal equation of the observers are extremely marked. The extent of these differences will be shown by an outline of the results of measurements obtained in this laboratory with 100 collaborators.

For a given set of conditions (background brightness $H = 0.3$ candle per sq.m, illumination falling on the eye from the glare source $E = 2.1$ lux, angular distance between the object and the glare source 3.1 °) each observer had to determine the contrast sensitivity without the glare source, with a sodium glare source and with a white glare source, the latter of equivalent brightness. The average deviation of the result of an observer from the mean values was about 40 per cent; some deviations were as much as 300 per cent. In spite of this lack of agreement the following general conclusions could be drawn:

1) The 32 persons wearing spectacles exhibited a lower average contrast sensitivity than the other observers (1.2 times) even in the absence of a glare source. They also experienced greater discomfort from the glare source, so that their contrast sensitivity with this source was much lower (1.4 to 1.5 times) than that found by the other observers.
2) The ratio of the above factors P for sodium and white light glare was on an average: $P_{Na} : P_{white} = 1.059$ (probable error approx. 0.022). The slight advantage in favour of sodium light is due mainly to the results obtained by the observers wearing spectacles (with an average of 1.128), whilst the observers wearing no spectacles found practically no difference (on an average 1.024).
3) The contrast sensitivity, both in the absence and presence of the dazzle source, was lower with older persons than with the younger observers. The reduction between 18 and 50 years of age was 1.48 without a glare source, 1.57 with a sodium source, and 1.69 with a white-light glare source. An example of this reduction with a sodium source of dazzle is shown in *fig. 2*. Each point represents the mean value of a definite group of observers. The horizontal arrows through these points indicate the particular age group, over which the mean value was obtained; the vertical arrows indicate the magnitude of the probable error.

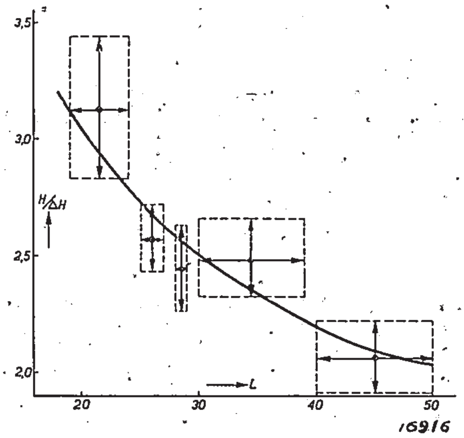

Fig. 2. The contrast sensitivity $H/\Delta H$ with glare due to sodium light as a function of the age of the observer (in years). The horizontal arrows represent the age group over which an average was taken, and the vertical arrows give the probable error. This curve was drawn on the basis of results obtained with 100 observers.

4) The observers were also asked whether they found the sodium light or the white light more discomforting. 25 $^0/_0$ expressed no opinion, whilst of the remainder 66 $^0/_0$ suggested the sodium light was the more trying and 34 $^0/_0$ the white light. The ratio $P_{Na} : P_{white}$ referred to above had a mean value of 1.092 for the first group, and a mean value of 0.947 for the second group. It was also found that there is some connection between the greater comfort afforded by one type of light on the one hand and better perception on the other hand, although it frequently happened that one light source gave

greater comfort whilst the other gave a greater ease of perception.

The experiments just described indicate, that measurements based on a small number of observers can only be employed with the greatest reserve for arriving at any conclusions.

Practical Conclusions from the Above Considerations

In every respect it is desirable for the eye to be exposed for as short a time as possible to a permanent source of glare which passes through its field of view. Precautions must therefore be taken that the light source does not radiate light over a small angle only (e.g. less than 15° against the horizon).

In view of successive glare and the discomfort produced it is desirable to give light sources low brightness values (i.e. large surfaces of radiation). In this respect an unscreened sodium light offers marked advantages over mercury light.

For the same two reasons it is advantageous to use light sources emitting few or no blue rays ("Selectiva" light for motor-car and cycle lamps, sodium light for stationary lamps).

By raising the brightness level of the highway surface, either by increasing the intensity of illumination or by improving the coefficient of reflection of the highway surface, the dazzle caused by various light sources can usually be reduced.

Glare due to other light sources on the highway is many times more powerful than that due to insufficiently screened stationary light sources, but the latter cause more discomfort than might appear on first consideration, mainly owing to their repetitive occurrence. The ideal solution is therefore to illuminate the highway principally by stationary light sources and to screen these sources in a proper way, so that they do not have a small angle of radiation against the horizon.

References

Weigel, Licht und Lampe, **18**, 955 and 1051, 1929. (Discussion of various types of glare).

Harrison, Trans. Ill. Eng. Soc., **15**, 34 1920. (Direct comparison of the discomfort produced by two sources of glare).

Holladay, J. Opt. Soc. Am., **12**, 271, 1926; **14**, 1, 1927. (Dealing, *inter alia*, with the approximate formula discussed above).

Stiles, Ill. Eng., **22**, 195 and 304, 1929. (Holladay's approximate formula with $m = 1.5$).

Rapport permanente verlichtings-commissie van de K. N. A. C. en de A. N. W. B., 1925. (Visibility measurements under conditions of glare; proposals for official regulations).

Luckiesh, Holladay, Taylor, J. Opt. Soc. Am., **11**, 311, 1925. (The effect on contrast sensitivity is practically independent of the colour).

Bouma, Polytechn. Wkbl, **29**, 625, 1935. (Deviations from Holladay's formula; duration of after-images; time of recovery after exposure to glare; monocular or binocular vision).

Bordoni, Int. Comm. Ill. Proc., 349, 1924. (In the case of glare sources subtending an angle less than 3° the total luminous intensity is alone the determining factor).

Mouton, Recherches sur les propriétés physiques et les effets physiologiques d'une lumière colorée (Paris, 1935), pp. 83-89. (Readaptation times; fatigue with yellow and white light).

THE NEW SODIUM LIGHTING SCHEME OF THE PURLEY WAY, CROYDON

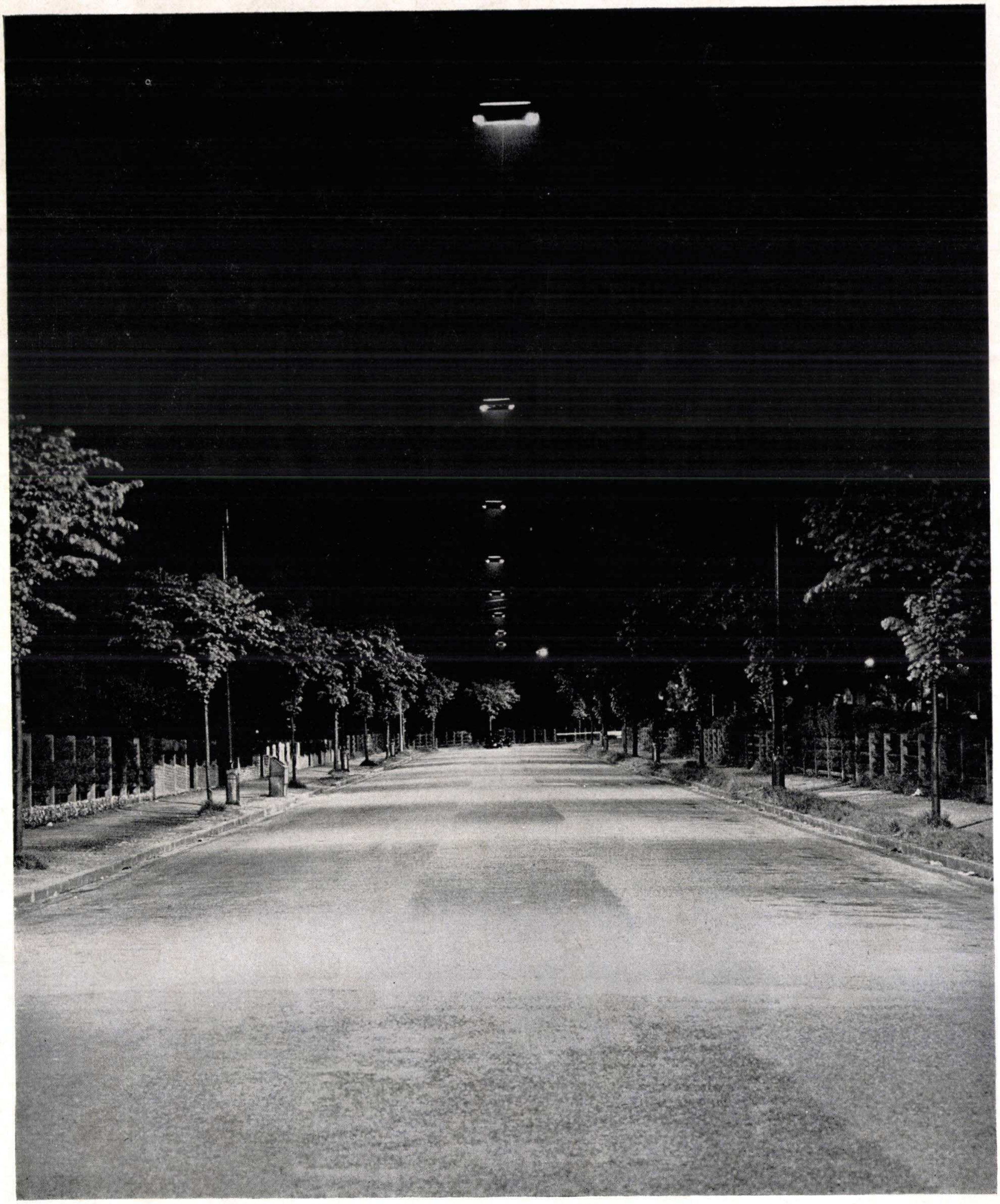

Some time ago the extended sodium lighting scheme on Purley Way Croydon was put into operation. 235 "Philora"-SO-150 W.-lamps in Wardle Units provide an illumination of 1 footcandle under the lamps and 0.7 footcandles in the mid-span points on a stretch of road four miles long.

THE RECORDING STRIP IN THE PHILIPS-MILLER SYSTEM

By C. J. DIPPEL.

Summary. A special registration strip has had to be evolved for the Philips-Miller system of sound recording, whose characteristics are discussed in the present article. The strip is composed of a gelatine layer at least 50 μ thick, the actual recording layer, which is deposited on a celluloid base. The recording layer carries a black covering layer of colloidal mercury sulphide, which is only 3 μ thick and entirely free from grain. By chemical treatment of the gelatin and the addition of special substances, it has been possible to obtain a transparent modulated sound track with sharp boundaries. Both coatings are made with a high degree of uniformity and within narrow thickness tolerances.

Introduction

As already indicated in previous articles ¹), the "Philimil" strip, on which the sound track is traced by a mechanical sound recorder in the Philips-Miller system has to meet certain specific requirements.

A recording strip of this type consists of two coatings laid down on a celluloid base, viz, the recording layer, which must be at least 50 μ thick in view of the modulation width required and the form of cutter used, and the very thin covering layer. The latter must be completely or nearly opaque to those light rays for which the photo-electric cell has its maximum sensitivity. With the standard types of photo-electric cells this range of maximum sensitivity is situated in the infra-red of the spectrum. In addition the covering layer must absorb the light rays used for photographic printing of the inscribed positive, and also be as thin as possible.

The search for a suitable strip has thus a twofold purpose:

1) The production of a recording layer in which a sound track sharply defined at the edges can be cut without meeting an excessive resistance; and
2) The coating of this recording layer with a covering surface meeting the requirements set forth above.

Requirements regarding Blackening and Transparency of a Transversal Sound Track

A number of requirements which the sound strip has to meet can be specified immediately.

It is naturally desired to obtain an adequate volume of sound from the sound track with a given amplification. The volume range is governed on the one hand by the ground noise, as the softest sounds must still be above the interference level, and on the other hand by the difference in transmission of light between the transparent and black portions of the sound track. For a given width of the stationary track this difference in fact determines the maximum variation in the fluctuations of light intensity falling on the photo-electric cell. If T_H is the transmissibility for the bright portion of the strip and T_Z that of the black portion ²), then with a 100 % modulation the maximum amount of light falling on the photo-electric cell, and hence also the photo-electric current generated, is proporti-

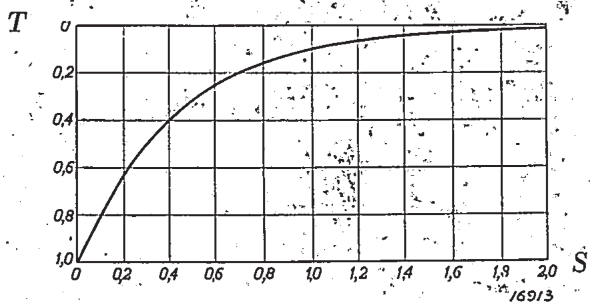

Fig. 1. The logarithmic relation between transparency (T) and blackening ($S = \log_{10} 1/T$) of the covering layer. The photo-electric current is proportional to the transmitted light, whilst for a given substance the blackening is proportional to the thickness of the covering layer. It is seen from the diagram that above $S = 1.4$ the transparency (and hence the photo-electric current through the cell), diminishes only slightly, so that as regards maximum volume on reproduction, it is not necessary to make the covering layer thicker than is requisite for this intensity of blackening. With lesser blackening intensities the transparency diminishes much more rapidly. To bring the difference between the transparencies of the clear and black sound tracks (T_H—T_Z) as close as possible to the maximum value of unity it is therefore primarily necessary to make T_H as great as possible.

---

¹) See Philips techn. Rev. 1, 107, 135 and 211, 1936.

²) The transparency is $T = I_1/I_0$ where I_0 is the intensity of the incident light and I_1 the intensity of the transmitted light.

onal to T_H, and the smallest amount of incident light proportional to T_Z, so that the amplitude of luminous intensity is proportional to $(T_H - T_Z)$. The maximum value of $(T_H - T_Z)$ is unity, i.e. when the covering layer is completely opaque $(T_Z = 0)$ and the transparent layer has nil absorption $(T_H = 1)$.

How thick must the covering layer be so that $T_H - T_Z$ is sufficiently close to unity? In *fig. 1* the transparency is plotted logarithmically against the "blackening" S, the latter being defined in photography as $S = \log_{10} 1/T$ where T is the transparency.

Hence at $T = 1, \quad S = 0$
$T = 0, \quad S = \infty$
$T = 0.1, \quad S = 1$, and so on.

The blackening is proportional to the thickness of the black covering layer. If two layers with a blackening of $S = 1$ are laid one over the other, we get $S = 2$ (transparency = 0.01). Fig. 1 thus gives directly the required thickness of the covering layer. Little is to be gained by making the blackening of the covering layer greater than $S = 1.4$ $(T = 0.04)$ as measured with infra-red rays which are used for the reproduction, since above $S = 1.4$ the transparency is no longer much reduced, in other words by making the covering layer thicker the volume is not appreciably increased. For if a covering layer with $S = 4$ $(T = 0.0001)$ were used, which would no longer be transparent, the maximum volume would only be increased by 0.36 decibel, but to this end the covering layer should be three times thicker than with $S = 1.4$ [3]).

Summarising, we thus see that in order to reproduce a high volume sweep with a constant amplification it is essential for:

1) the blackening of the covering layer to be at least 1.4; a higher value offers little practical advantage.
2) the transparency of the bright portion to be as great as possible; (a slight fog of say S = 0.06, would already reduce the light transmission from 1 to 0.87, i.e. by 13 per cent);
3) all causes liable to augment background noises to be avoided; the definition of the edges of the inscribed sound track must therefore be very sharp and the track itself must be as uniform as possible.

The Recording Layer

A wide variety of materials may be used for making the recording layer. A choice was made of gelatin, since investigations had indicated that this material offered better prospects of successful

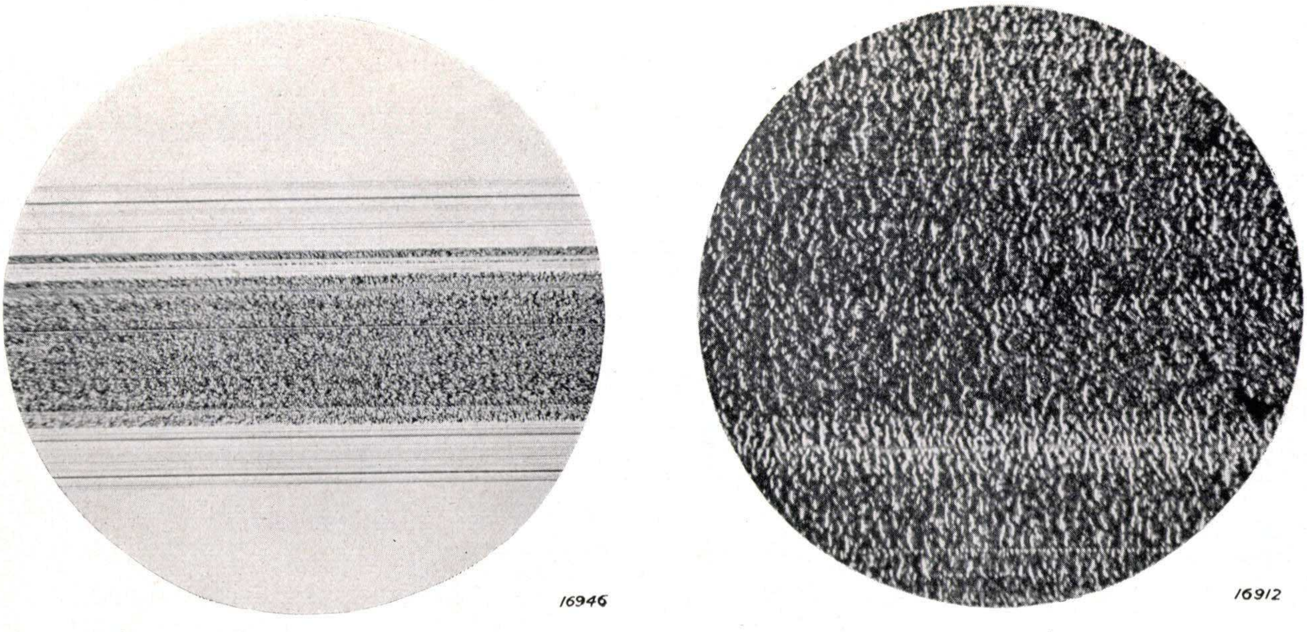

Fig. 2. The micro-photograph on the left (magnification × 60) shows a partially matt sound track in a clear gelatin layer. It is clearly seen how the matt portion strongly disperses the light and that the boundary between the matt and the bright areas is not sharp. The photograph on the right shows a matt sound track of 200 × magnification.

---

[3]) For if T_H is put equal to unity the increase in the difference $T_H - T_Z$ is $1 : (1 - 0.04) = 1.042$, and the increase in volume is equal to the square of this value, viz, 1.086. The number of decibels is obtained by multiplying the common logarithm of this value (0.035) by 10. If the practical value of $T_H = 0.93$ is taken, we get 0.38 decibel.

results than, for instance, nitro- and acetyl-cellulose coatings. In addition gelatin is comparatively cheap and the technology of producing multi-coated products has been thoroughly mastered in photographicfilm factories.

The sound track traced has to meet the following requirements:

1) The track traced must be well-defined and transparent.
2) The edges of the sound track must be smooth and straight.
3) The removed shaving must peel off easily; it must not adhere to the cutter and must not crumble.
4) The wear on the cutter must be reduced to a minimum.

Special attention has been given to the first requirement, viz., the transparency of the sound track. In many materials only a matt track can be inscribed, which has an appearance under the microscope as shown in *fig. 2.* The surface of this type of trace is wholly or partially rough, which naturally results in dispersion of the light rays and hence in reduced transmissibility, and if the matt effect extends to the edges this also leads to a want of definition at the track boundaries, which in turn is responsible for ground noise.

To ensure that the sound track is adequately transparent the gelatin must be subjected to specific chemical treatment, viz, partial decomposition.

Gelatin is a product of an albuminous nature and is made from animal albumens found in the connective tissues (muscles, tendons and corium) and in bones. The albumen occurs in these in the form of complex molecular chains with a more or less regular configuration in space. By treatment with bases the albuminous bodies are caused to swell, i.e. water is absorbed. If they are then heated (thermolysis) the weak bonds are broken and smaller molecular complexes of colloidal dimensions are produced. The resultant product is a colloidal gelatin solution made up principally of albumen molecules, except that the complex molecules have become so reduced in size that they form a colloidal solution in water. The configuration of the albumen chains is also much reduced as a result of this treatment.

The product so obtained, with which everyone is acquainted as household gelatin and as the principal constituent of glue, was found to be a suitable raw material for making the recording layer. The gelatin manufacturer, however, does not always supply a uniform product, since neither the final decomposition product he aims at producing, nor the raw material he uses, has to meet very specific requirements. This perhaps accounts for the fact, that one product exhibits better sound-registration characteristics than another. To obtain the desired characteristics and to ensure a supply of gelatin of uniform quality the decomposition process is continued a stage further under controlled conditions, during which the albumen molecules are themselves also attacked. The chains become shorter and the viscosity of the aqueous solutions drops considerably. If this process were continued indefinitely a molecular solution of amino acids (the well-known end products obtained on the total decomposition of albumens) would result, from which a coating could no longer be prepared. The process has therefore to be continued under well-defined conditions as regards hydrogen-ion concentration, temperature, density, etc., but only to a specific limit as measured by the viscosity.

What is achieved by this?

In the first place the differences between various gelatin deliveries are more or less eliminated and at the same time the resistance of the recording layer to the motion of the cutter is reduced. The most important point for the sound track traced in thus treated gelatin is to be perfectly transparent. Supplementary decomposition has, moreover, the great advantage that any foreign bodies present adhere less tenaciously to the recording layer and that filtration of the gelatin mass before coating is easier owing to the lower viscosity.

To prevent gelatin treated in this way from giving a brittle recording layer a water-soluble oil is added to the gelatin solution. The addition of this oil makes the dried recording layer very much more pliable and soft, so that the presence of the oil permits decomposition to be carried much further, than would otherwise be possible. On a correct choice of the hydrogen-ion concentration in the final coating product a little free oleic acid is retained in the dried recording layer and acts as a lubricant for the cutter, this being an advantage owing to the friction of the removed chip along the front of the cutter.

In this way decomposition and the addition of an oil furnish a recording strip giving a transparent sound track, a satisfactory continuous shaving and very good definition at the edges; moreover, any particles in the gelatin can be readily removed by filtering, and all impurities introduced later have a much less serious effect than with undecomposed gelatin.

The Covering Layer

As is well known, [4]) a trace registered photographically is not sharply defined owing to the grain of the coating. In photographic films granulation has been a hitherto unavoidable consequence of the processing required to arrive at a high light sensitivity. As the "Philimil" strip does not need to be light-sensitive, the covering layer can be made entirely free from grain. Recent investigations have shown this to be desirable, since a granular edge on the sound track causes a by no means negligible increase in background noise.

It is obvious that the application of the covering layer must not in any way affect the characteristics of the recording layer. If, for instance, an exposed and grain-free silver-halide gelatin emulsion were deposited on the recording layer and subsequently developed as free from grain as possible, the finished product would have to be passed through developing and fixing baths which have a specific alkalinity and at the same time produce a more or less hardening effect. Even if developing, fixing and washing could be carried out under closely reproducible conditions, there is still the difficulty that the treatment required by the covering layer would adversely affect the cutting properties. It was therefore found necessary to apply the covering layer to the recording layer in such a way that no finishing operations were required; moreover, this also makes it technically easier to meet the very severe requirements as regards freedom from impurities and foreign substances.

As a rule the material for the black, covering layer is prepared separately and spread on the recording surface in the form of a black solution mixed with gelatin. It is obvious from the above considerations that the covering power of the black substance must be very high, in other words the requisite blackening of at least 1.4 must be attainable with very thin layers. Many dyes which, when mixed with gelatin or adsorbed in it, give a satisfactory blackening in thick layers, cannot be used owing to their lack of covering power. It must be remembered in this connection that at the edges of the sound track the thickness of the covering layer decreases to zero owing to the wedge-shaped form of the cutter. The greater the covering power, the smaller will be the area at the wedge having a blackening of less than 1.4.

The covering layer of the "Philimil" strip consists of a black mercury sulphide sol which is easily prepared by chemical means and which, similar to other metallic sulphide sols and metal sols, possesses a high covering power. (A sol is defined as a colloidal solution containing no grains visible under the microscope).

With a colloidal mercury-sulphide solution 1 mg per sq. cm already gives a blackening in the infrared of 2.5 to 5, according to the method of preparation. It is seen from *fig. 3* that the blackening in the visible part of the spectrum and particularly in the ultra-violet is much greater still. This feature is of great advantage in the photographic printing of the "Philimil" positive.

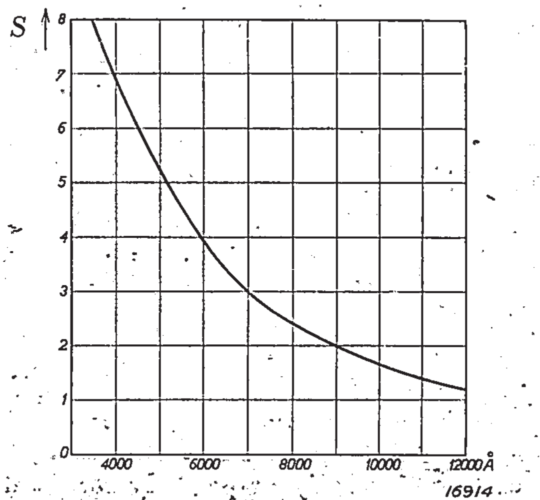

Fig. 3. Light absorption by the covering layer of a "Philimil" strip. The covering layer of this strip was 2.4 μ thick. It is seen, that the blackening with the light used for printing (approx. 4000 Å) is three to four times greater than with the light used for reproduction (approx. 8000 Å), in other words the "covering power" of this coating is three to four times greater with the printing light.

The thickness of the covering layer is 3 μ, although it is technically possible to obtain the requisite blackening with much thinner layers. To guard against mechanical damage a lesser thickness is, however not used.

No granulation can be observed even under the microscope in the mercury-sulphide covering layer, if it is carefully prepared. On comparing under the microscope a high frequency registered by the Philips-Miller process with the same frequency registered photographically, the greater definition of the former will be apparent at once (see *fig. 4*). This is due to the fact that the absence of grain in the "Philimil" strip firstly ensures high definition at the edges of the track and secondly makes it impossible for the apices to be masked by light dispersion at the grains. The latter point constitutes a reduction in amplitude and, in photographic registration, always results in losses in the high-frequency range. Fortunately, in the Philips-Miller

---

[4]) See Philips techn. Rev. 1, 107, 1936.

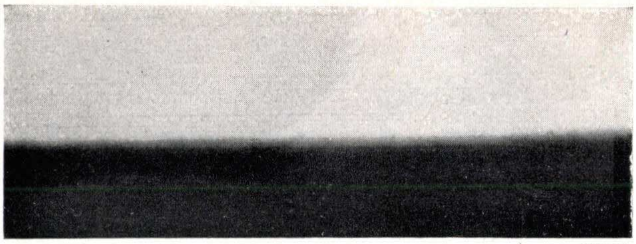

Fig. 4. a) Edge of an unmodulated Philips-Miller sound track, magnification × 100. The absence of granulation is clearly visible also in the transparent part removed by the cutter wedge.

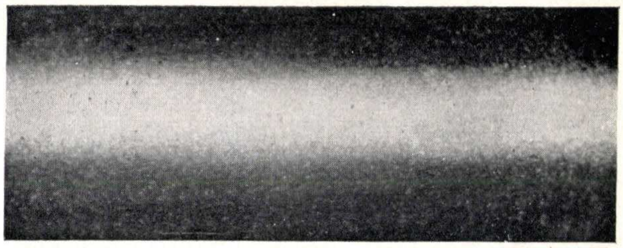

b) For comparison with fig. 4a: a micro-record of a stationary track on an experimental film of good quality (photographic process).

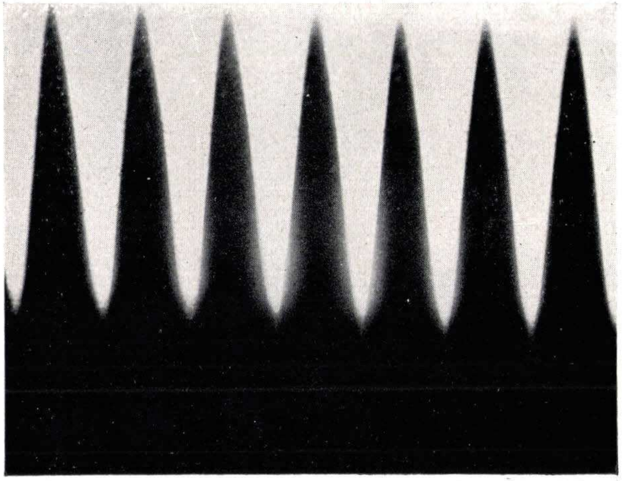

c) Micro-photograph with same magnification (× 100) of a sound track obtained by the Philips-Miller process (positive) for a frequency of 5000 cycles.

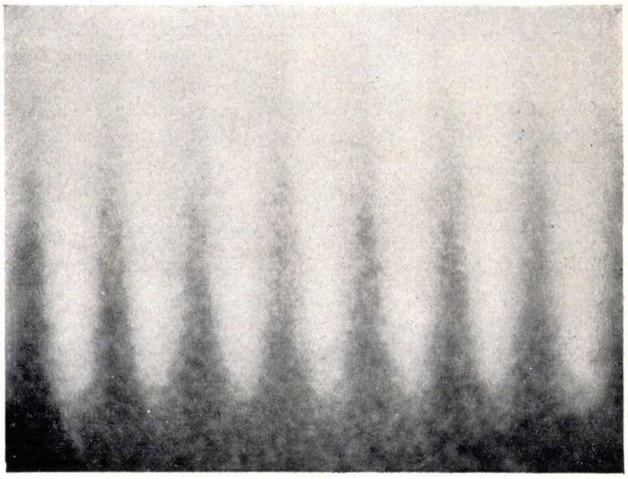

d) The same as obtained on the experimental film (photographic positive).

mechanical-registration system there is no limitation in this direction.

Finishing

The manufacture of the "Philimil" strip on the basis of the experimental results indicated above was, however, at the outset still fraught with various difficulties, which have in the meantime been overcome.

Attention must first be called to the very important requirement that the finished product must cause the minimum amount of wear of the cutter. Wear of the cutter is principally due to the impact of the instrument during registration against inhomogeneities in the gelatin layer. By the special method of pre-treatment of the recording layer cutter wear has been reduced as far as possible; nevertheless any impurities or foreign bodies present may still cause damage to the cutter edge. Every care must therefore be taken to avoid all impurities and to keep the materials as clean and free from dust as is practicable in each finishing stage.

Foreign bodies must naturally be avoided both during the preparation of the coating material and during the coating process itself. Thorough straining through various filter units is repeated many times, after which the now thoroughly clean material has to be spread on a large surface of celluloid. This is done by passing the celluloid base over a roller to bring it in contact with the solutions, a certain portion being taken up by the strip. A greater or smaller part of the gelatin layer or of the covering layer sol adheres to the base and is caused to flow over it, the amount depending on the temperature and rate of travel of the base and the viscosity of the solution. After drying, the celluloid is coated with a black layer $50\ \mu$ thick. It is evident that both the coating and the drying processes must take place in a perfectly dust-free atmosphere. Also in all subsequent operations, such as cutting to the requisite width of say 7 or 17.5 mm, and perforation, no precaution must be omitted to prevent dust from being deposited on the film. After manufacture the product is scrupulously tested for potential cutter wear.

Uniformity in Thickness

A further source of error in sound registration and reproduction is introduced by variations in thickness of the "Philimil" strip, for the sound recording system with cutter are stationary and the registration strip is stretched taut on a recording drum. A gradual reduction in thickness of say a total of 25 μ would reduce the width of a stationary track from 1 mm down to zero. Variations in thickness over the whole length of a strip, 300 m long, must therefore be kept within narrow limits of a few μ. The finishing processes are so devised, that the total variation in thickness cannot exceed about 6 μ and over short lengths not more than 4.5 μ, whilst the thickness of the recording layer is not below a certain minimum.

Uniformity in the thickness of the covering layer, i.e. in the blackening, is largely dependent on the case with which the covering layer sol can be spread on the recording layer. By adding various substances, which, *inter alia*, reduce the surface tension of the sol, the spreading power can be favourably influenced. The covering layer is made extremely uniform by suitable adaptation of the two layers to one another.

The above considerations indicate that the product in question here is one which has to meet very severe requirements. By systematic research it has been found possible to satisfy these desiderata in every respect.

AN IMPULSE-VOLTAGE GENERATOR FOR TWO MILLION VOLTS

By A. KUNTKE.

Summary. The method of operation and the construction of an impulse voltage generator rated for 2 000 000 volts with symmetrical voltage distribution against earth is described. By suitable construction the dimensions of the equipment have been made extremely small.

A few months ago an impulse-voltage generator with an output of 2 × 1000 kilovolts against earth and 2000 kilovolts across the poles was constructed at the Philips X-Ray Laboratory. The method of operation and construction of this generator are described in the present article.

As is well known, impulse-voltage generators are in common use in electrical engineering, e.g. for testing insulators and leading-through units, since impulse voltages afford a ready means of simulating artificially the effects of over-voltages created in high-tension networks as a result of atmospheric disturbances and switching operations.

Short-period voltage impulses are usually produced by imparting a heavy charge to a condenser and then passing the charge to a resistance through a suitable switch — a flash-over spark gap being used in practice for this purpose. The voltage applied to the resistance thus abruptly increases from zero to the potential of the condenser at the instant the flash-over occurs; it then falls again as the condenser discharges through the resistance.

This simple case is illustrated in *fig. 1*. If the condenser C is slowly charged from an undefined D.C. source through the resistance R_L a spark-over will occur at the sphere gap V when the breakdown voltage is reached.

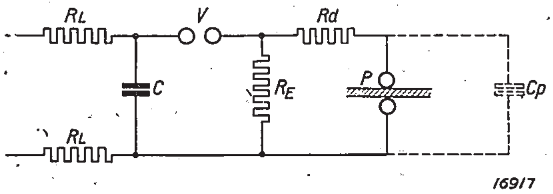

Fig. 1. Diagrammatic sketch of an impulse voltage circuit. The object P under test (with capacity C_p) is connected to the condenser C through a series resistance R_d and the spark gap V. The condenser is charged through R_L and at the flash-over at V is discharged through R_E. A voltage impulse is thus applied to the object P under test.

Thus, by choosing a suitable rating for the resistance

R_E the rate of voltage-drop at the resistance can be varied for a specific size of condenser.

If only the discharge resistance R_E is present in the circuit, its voltage will increase in an infinitely short period of time to the voltage U_c applied to the condenser at the instant the flash-over occurs, and then decreases again according to the equation:

$$U_R = U_C \cdot e^{-t/C\,R_E}$$

The object P to be submitted to the impulse voltage is connected in parallel to the discharge resistance R_E; in general P has a capacity C_p. To avoid an oscillation being superimposed on the impulse, such as might be produced by the series capacity of C and C_p and the self-induction of the circuit, a damping resistance R_d is provided which suppresses these oscillations.

The damping resistance R_d in its turn affects the character of the voltage impulse applied to the test object P, since its self-capacity C_p must be charged through the resistance R_d at the beginning of the voltage impulse.

The voltage impulse applied to the test object P is thus made up of two components:

1) The voltage increase (the wave "front") which is determined principally by the damping resistance R_d and the capacity C_p of the test object, and
2) the voltage drop (the wave "tail") which is governed mainly by the capacity C and the discharge resistance R_E. It is assumed here that C_p is small compared to C.

The variation of a voltage impulse with time is shown graphically in *fig. 2*.

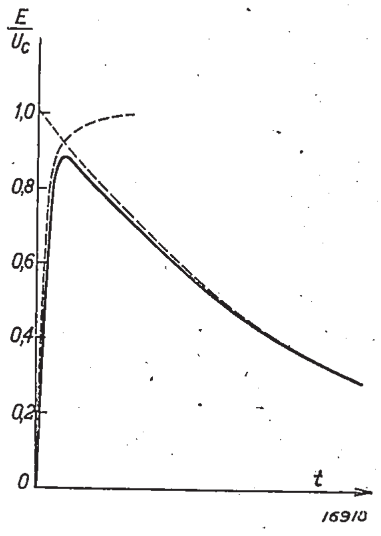

Fig. 2. Time function of a voltage impulse. The front is determined by the charging of the self-capacity C_p through resistance R_d, whilst the descending portion of the curve is determined by the discharge of the capacity C through the resistance R · U_c is the charging potential of the condenser C; the voltage applied to the test object is smaller than U

For testing insulators the time gradients of the front and of the tail have been standardised in a number of countries in order to furnish comparable results of tests. The gradient of the front is defined by the time taken for the voltage applied to the test object to rise from zero to half the maximum potential, whilst the gradient of the tail is expressed by the time taken for the voltage to drop from its peak value to half that value. An impulse wave of 0.5/50, i.e. in which the half-value time of the front is $0.5 \cdot 10^{-6}$ sec and the half-value time of the tail is $50 \cdot 10^{-6}$ sec, is in common use.

To generate very high impulse voltages (over approx. 200 kilovolts) the method of voltage multiplication described by Marx is universally adopted. The impulse generator built by Philips is also constructed on this principle, whose method of application may be suitably described with reference to the circuit diagram of Philips impulse generator given in *fig. 3*. In Marx's multiplication circuit a group of condensers are charged in parallel and then connected in series by the flashover at the spark gap. In fig. 3, C are the condensers which are shunted by the resistances r and charged through the charging resistance R from a 180-kilovolt D.C. generator. To ensure that all condensers have the same charging characteristic and are all raised to the same potential after a specific charging period, the resistances r have been made small as compared with the common charging resistances R_L. Spark gap V — the ignition spark gap — of the group of spark gaps shown in the figure is somewhat smaller than the other gaps, and thus gives the first flash-over. The potential at the succeeding spark gap is in consequence increased and thus also gives a flash-over, in this way initiating in succession the flash-overs of the succeeding spark gaps. This sequence of spark-overs takes place in an extremely short interval of time so that all condensers C are connected in series through the spark gaps and are discharged through the two discharge resistances R_E. The discharge circuit is indicated in fig. 3 by the heavy lines.

As indicated in the diagram, the impulse generator is built in two halves, each made up of 7 condensers together with the associated resistances and spark gaps; each condenser is charged to 150 kilovolts, thus giving a total potential of 2000 kilovolts in series. The maximum voltage against earth occurring at each discharge resistance and in each half of the generator is 1000 kilovolts.

The two halves of the impulse generator are shown in *fig. 4*; in the background is the 180-kilovolt D.C. source enclosed in a suitable housing, the direct

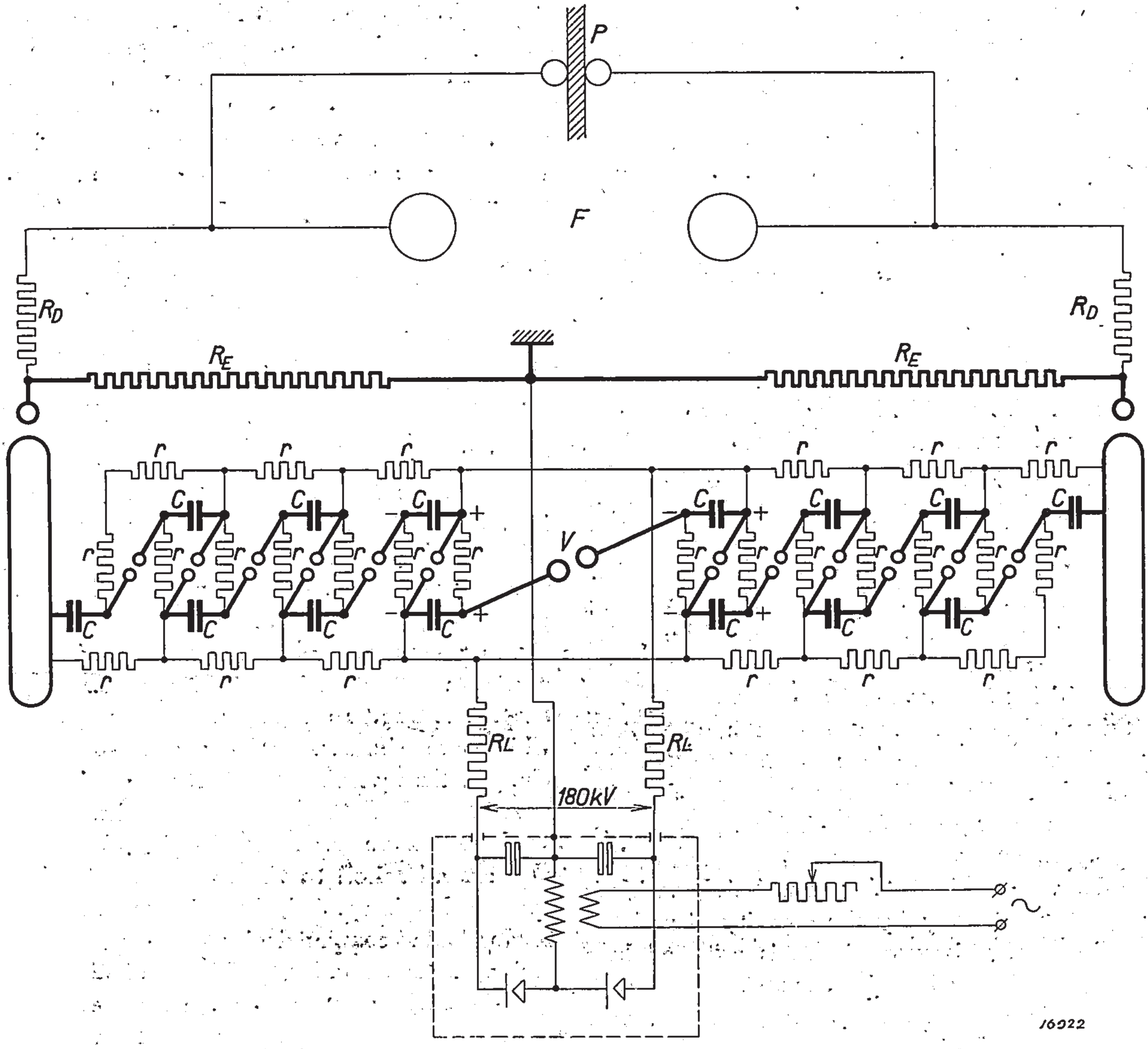

Fig. 3. Circuit diagram of the 2000 kilovolt impulse-voltage generator. All condensers C are charged from the 180-kilovolt D.C. source through the resistances R_L and r. At the instant of flash-over at the spark gap V the potential at the other spark gaps is raised, so that a flash-over is obtained at these also. The circuit, then set up, is shown by the heavy line in the diagram; it is seen that all condensers C are discharged in series through the two discharge resistances R_E. By adopting a construction in two halves and earthing the centre of the resistances R_E, the potential is symmetrical with respect to earth. The voltage applied to the test object P is measured by means of the spark gap F.

voltage being furnished by high-tension rectifying valves. At floor level between the two pillars are the spark gaps and on the front of each pillar is the discharge resistance in the form of a wire resistance oil-immersed in a glass tube. The spark gaps with 10 cm spheres and the liquid resistances acting as charging resistances are also shown.

The small overall height of the equipment is due to the compact design of the condensers. By making the outer walls of exceptionally strong insulating material it has been possible to employ the condensers as supporting members for the rest of the equipment. The constructional details are the same as adopted in certain of our X-ray apparatus ¹). A new feature as regards impulse voltage generators is the large metal electrode at the top, which has been found to serve a useful purpose in preventing flash-overs between the top constructional members at the instant the voltage impulse is applied. If this electrode is absent, premature discharges to earth occur at the high-tension metal units during the application of the voltage impulse, which in certain circumstances may induce the flash-over at a partial potential level, e.g. at the top condenser. The

---

¹) See Philips techn. Rev., 1, 6 and 178, 1936.

field intensities are reduced by the screen electrode to such an extent that these flash-overs are avoided.

The technical data of the equipment are given below:

The 2 × 7 condensers are rated for 0.01 μF per unit. At 150 kilovolts per condenser an impulse voltage of 2000 kilovolts is obtained. The impulse energy is then approx. 1.5 kilowatts per sec. The discharge resistance (oil-immersed metal resistance) is rated for 2 × 70 000 ohms, this giving a half-period value of the wave tail of $70 \cdot 10^{-6}$ sec.

To retain the general simplicity in design of the equipment, means for the common regulation of the intermediate spark gaps have been dispensed with; the spark gaps must be adjusted individually, although if required a common control for the gaps can be provided without appreciable modification in design.

The overall height of the pillars is 3 m, each pillar having a base area of 0.8 · 1.3 m. Compared with the performance of the equipment these dimensions are extremely small.

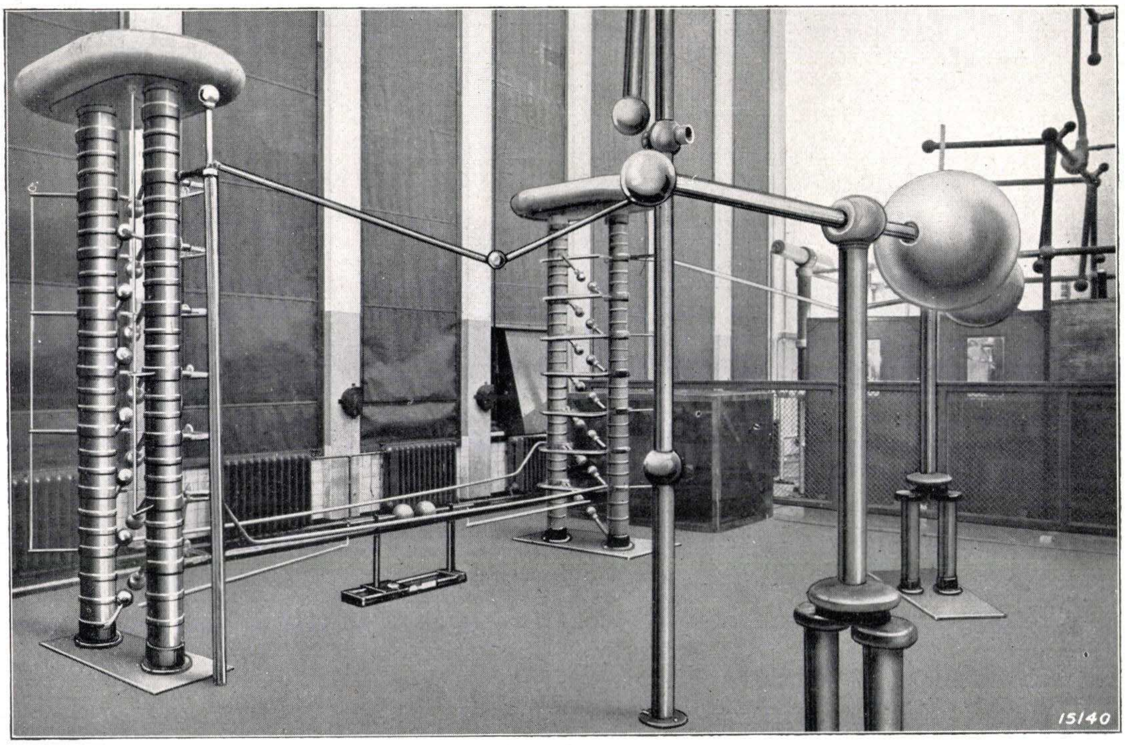

Fig. 4. Construction of the 2000-kilovolt impulse-voltage generator. At the rear is the enclosed 180-kilovolt D.C. source; between the two pillars is the ignition spark gap V. The discharge resistances R_E are located on the fronts of the pillars, the condensers being constructional members of the two pillars. The upper screen electrodes, which prevent partial flash-overs, are also shown. The sphere gap for measuring the total voltage and the connected test object are not shown in the picture.

ELECTRICAL FILTERS I

Vacation Course, held at Delft, April 1936.

By BALTH. VAN DER POL and TH. J. WEIJERS.

Summary. In this series of articles (originally forming a vacation course) the theoretical and practical constructional principles relating to electrical filters are discussed. The general characteristics of networks compounded of an arbitrary choice of impedances provide a starting point; various equivalent networks for any arbitrary filter are also dealt with. The properties of the simplest types of filter units in common use are deduced and then applied to high-pass, low-pass and band-pass filters. It is shown how, from these filter units, a compound filter can be built up to meet specific requirements. Finally, circuit-closing phenomena with low-pass and high-pass filters are discussed. In this first article an introduction is given to the general characteristics of linear networks and filters.

Introduction

Electrical filters are networks with a number of external terminals whose branches are composed of impedances of which all or some are dependent on the frequency. The most common form of filter has two primary and two secondary terminals. A network with four external terminals is called a four-pole or quadripole; if there are two primary and two secondary terminals the network is termed a di-dipole. As the impedances are dependent on the frequency, the ratio of the secondary current to the primary current is also dependent on the frequency. The general purpose of filters is to permit, the free passage with minimum attenuation of frequencies within one or more specific frequency ranges, the frequencies in all other ranges being attenuated. The transmitted frequency range is termed the transmission band and the latter the attenuation band.

The filters in most common use are the following:

a) Low-pass filters, which permit those frequencies to pass with minimum attenuation which are below a specific limiting value and attenuate all frequencies above this limit.

b) High-pass filters, which permit frequencies to pass with minimum attenuation which are above a specific limiting frequency and attenuate all frequencies below this limit.

c) Band-pass filters, which permit only frequencies to pass with minimum attenuation which are situated within specific frequency limits and suppress all frequencies beyond these limits.

Between the transmission and attenuation bands there is always a transition range; in fact it is fundamentally impossible to obtain a discontinuous (sharply-defined) limit between these two bands if all frequencies pass through the filter with the same velocity, such that the phase lag is proportional to the frequency. For it can be shown mathematically that such a filter would cause a signal to arrive before it has been transmitted, which is naturally impossible.

Electrical filters find their principal use in telegraphy and telephony as well as in cable and wireless circuits and in television.

The fundamental principles on which the theory and construction of filters are based, were developed by Lagrange (1736—1813), Heaviside (1893), Campbell and K. W. Wagner (both in 1915) and in subsequent years by Zobel, Carson, Le Corbeiller, Brillouin, David, Cauer, Bode, Küpfmüller and others.

The theory of filters may be divided into two sections:

Filters with a sinusoidal e.m.f.; and

Filters operating under the action of an impulse or an abruptly-applied and subsequently-constant voltage (transient phenomena).

1) Filters with sinusoidal e.m.f.

The theory of these filters can be developed in a variety of ways. In their most recent analysis the theory of matrices and groups, as well as complex functions, occupies a prominent position. If consideration is restricted to the practical design of filters, the application of elementary mathematical analysis already permits substantial progress to be made. The hyperbolic sine and hyperbolic cosine functions are extensively employed, being defined as follows:

$$\sinh T = \frac{1}{j} \sin j T = {}^1/_2\,(e^T - e^{-T});$$

$$\cosh T = \cos j T = {}^1/_2\,(e^T + e^{-T}).$$

and analogous to: $\cos^2 T + \sin^2 T = 1$ we also have:

$$\cosh^2 T - \sinh^2 T = 1.$$

2) Behaviour of filters under impulses (transient phenomena).

The study of this subject requires the application of the higher branches of mathematics, although with the aid of the operational calculus of Heaviside we can in many cases reduce the requisite calculations to an elementary form.

Division of Lectures

The subjects to be dealt with have been spread over four lectures as follows:

Lecture I (van der Pol): Introduction into the general characteristics of linear networks and filters;

Lectures II & III (Weijers): Application of fundamental principles to the practical treatment of special filters with sinusoidal e.m.f.;

Lecture IV (van der Pol): Switching operations with low-pass and high-pass filters.

INTRODUCTION INTO THE GENERAL CHARACTERISTICS OF LINEAR NETWORKS AND FILTERS.

Consideration will be restricted to networks which are:

1) Linear, i.e. the components (resistances, self-inductances, capacitances and mutual inductances) are independent of the current or voltage;
2) Passive, i.e. having no internal source of energy;
3) Containing only positive components, except mutual inductances, which can also be negative;
4) Invariable, i.e. the characteristics of the components do not vary with time;
5) Free from gyroscopic terms, thus conforming to the reciprocal theorem described below. This condition is always fulfilled under the conditions 1—4, if the elements of the filtor are not coupled with a mechanical system or if this coupling is purely electrically.

These networks conform to three fundamental principles:

1) Principle of Superposition

If in a circuit an e.m.f. $E_1(t)$ applied to the branch A produces a current $I_1(t)$ in another branch B, and a subsequent e.m.f. $E_2(t)$ in A produces a current $I_2(t)$ in B, then according to the principle of superposition, if the sum of the electromotive forces $E_1(t) + E_2(t)$ is applied in A, the current obtained in B will be the sum of the current $I_1(t) + I_2(t)$, or in other words; if two forces act at the same time, the result is the sum of the results obtained if either of the two forces act alone.

2) Reciprocity Theorem

The reciprocity theorem states that if an e.m.f. $E_k(t)$ applied to the k-th branch produces a current of $I_{kl}(t)$ in the l-th branch, then if subsequently the same e.m.f. $E_k(t)$ is applied to the l-th branch, the same current $I_{kl}(t)$ as previously obtained in the l-th branch will be obtained in the k-th branch.

3) Conservation of Frequency

The principle of the conservation of frequency states that if a sinusoidal e.m.f. with a frequency ν_o is applied to any branch circuit of the system, then all other voltages and currents in the system will have the same frequency ν_o.

Simplification of Networks

In networks with the above characteristics a node with n converging branches can always be converted into a complete n-sided polygon for a specific frequency, without the voltages and currents in any of the other branches being altered. By a "complete" n-gon is implied that in addition to the n sides all diagonals are also present. A complete n-gon thus has a total of $^1/_2\, n\, (n-1)$ branches.

By a single application of this transformation the number of nodes in the network is reduced by one; so that by repeated transformation it is possible to eliminate all the nodes from a network with the exception of the external terminals. We shall discuss here only networks with four external terminals, so that the network can be reduced to a complete quadrilateral (see *fig. 1*) made up of $^1/_2 \cdot 4 \cdot (4-1) = 6$ elements. The most

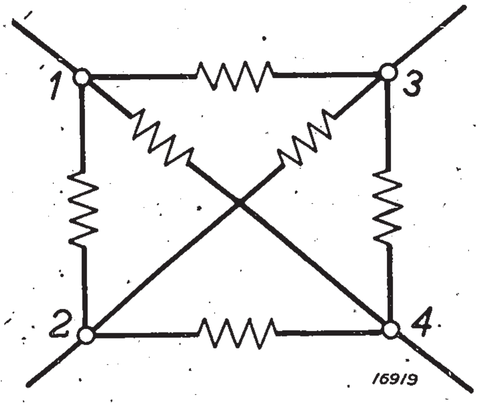

Fig. 1. Six impedances forming a complete quadrilateral and to which any arbitrary quadripole can be reduced.

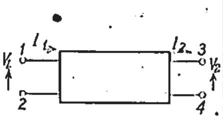	$V_1 = \alpha V_2 + \beta I_2$ $I_1 = \gamma V_2 + \delta I_2$ $\alpha\delta - \beta\gamma = 1$	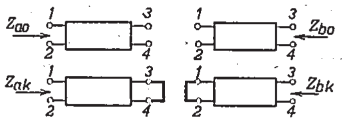 Z_{ao} Z_{bo} Z_{ak} Z_{bk} 1 2 3 4 $\frac{Z_{ak}}{Z_{ao}} = \frac{Z_{bk}}{Z_{bo}} \left(=\frac{Z_k}{Z_0}\right)$	„IMAGE IMPEDANCE" 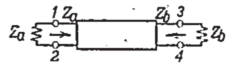 $\frac{I_2}{I_1} = \sqrt{\frac{Z_a}{Z_b}}\, e^{-T}$
$V_1 = \alpha V_2 + \beta I_2$ $I_1 = \gamma V_2 + \delta I_2$ $\alpha\delta - \beta\gamma = 1$		$\alpha = \sqrt{\frac{Z_{ao}}{Z_{bo}}}\ \frac{1}{\sqrt{1-\frac{Z_k}{Z_0}}}$ $\beta = \frac{\sqrt{Z_{ak}\ Z_{bk}}}{\sqrt{1-\frac{Z_k}{Z_0}}}$ $\gamma = \frac{1}{\sqrt{Z_{ao} Z_{bo}}}\ \frac{1}{\sqrt{1-\frac{Z_k}{Z_0}}}$ $\delta = \sqrt{\frac{Z_{bo}}{Z_{ao}}}\ \frac{1}{\sqrt{1-\frac{Z_k}{Z_0}}}$	$\alpha = \sqrt{\frac{Z_a}{Z_b}} \cosh T$ $\beta = \sqrt{Z_a Z_b} \sinh T$ $\gamma = \frac{1}{\sqrt{Z_a Z_b}} \sinh T$ $\delta = \sqrt{\frac{Z_b}{Z_a}} \cosh T$
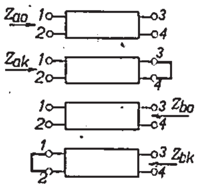 Z_{ao} Z_{ak} Z_{bo} Z_{bk} 1 2 3 4 $\frac{Z_{ak}}{Z_{ao}} = \frac{Z_{bk}}{Z_{bo}} \left(=\frac{Z_k}{Z_0}\right)$	$Z_{ao} = \frac{\alpha}{\gamma}$ $Z_{ak} = \frac{\beta}{\delta}$ $Z_{bo} = \frac{\delta}{\gamma}$ $Z_{bk} = \frac{\beta}{\alpha}$		$Z_{ao} = Z_a \coth T$ $Z_{ak} = Z_a \tanh T$ $Z_{bo} = Z_b \coth T$ $Z_{bk} = Z_b \tanh T$
„IMAGE IMPEDANCE" 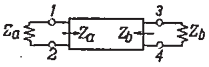 $\frac{I_2}{I_1} = \sqrt{\frac{Z_a}{Z_b}}\, e^{-T}$	$Z_a = \sqrt{\frac{\alpha\beta}{\gamma\delta}}$ $Z_b = \sqrt{\frac{\beta\delta}{\alpha\gamma}}$ $\cosh T = \sqrt{\alpha\delta}$	$Z_a = \sqrt{Z_{ao}\ Z_{ak}}$ $Z_b = \sqrt{Z_{bo}\ Z_{bk}}$ $\tanh T = \sqrt{\frac{Z_k}{Z_0}}$	
„ITERATIVE IMPEDANCE" 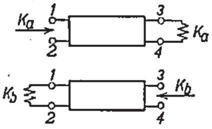 $\frac{I_2}{I_1} = e^{-\Gamma}$	$K_a = \frac{\sqrt{(\alpha+\delta)^2-4}+\alpha-\delta}{2\gamma}$ $K_b = \frac{\sqrt{(\alpha+\delta)^2-4}+\delta-\alpha}{2\gamma}$ $\cosh\Gamma = \frac{\alpha+\delta}{2}$	$K_a = \tfrac{1}{2}(Z_{ao}-Z_{bo}) + \tfrac{1}{2}\sqrt{(Z_{ao}-Z_{bo})^2 + 4\, Z_{ao}\, Z_{bk}}$ $K_b = \tfrac{1}{2}(Z_{bo}-Z_{ao}) + \tfrac{1}{2}\sqrt{(Z_{ao}-Z_{bo})^2 + 4\, Z_{ao}\, Z_{bk}}$ $\cosh\Gamma = \frac{Z_{ao}+Z_{bo}}{2\sqrt{Z_{ao}(Z_{bo}-Z_{bk})}}$	$K_a = \tfrac{1}{2}(Z_a-Z_b)\coth T + \tfrac{1}{2}\sqrt{(Z_a-Z_b)^2\coth^2 T + 4 Z_a Z_b}$ $K_b = \tfrac{1}{2}(Z_b-Z_a)\coth T + \tfrac{1}{2}\sqrt{(Z_a-Z_b)^2\coth^2 T + 4 Z_a Z_b}$ $\cosh\Gamma = \tfrac{1}{2}\left(\sqrt{\frac{Z_a}{Z_b}} + \sqrt{\frac{Z_b}{Z_a}}\right)\cosh T$
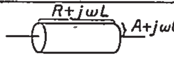 $Z = \sqrt{\frac{R+j\omega L}{A+j\omega C}}$ $\Gamma' = \sqrt{(R+j\omega L)(A+j\omega C)}$	$R+j\omega L = \sqrt{\frac{\beta}{\gamma}}\ \text{arc}\cosh\alpha$ $A+j\omega C = \sqrt{\frac{\gamma}{\beta}}\ \text{arc}\cosh\alpha$	$R+j\omega L = \sqrt{Z_0 Z_k}\ \text{arc}\tanh\sqrt{\frac{Z_k}{Z_0}}$ $A+j\omega C = \frac{1}{\sqrt{Z_0 Z_k}}\ \text{arc}\tanh\sqrt{\frac{Z_k}{Z_0}}$	$R+j\omega L = Z\, T$ $A+j\omega C = \frac{T}{Z}$
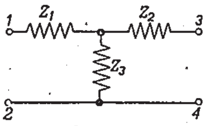	$Z_1 = \frac{\alpha-1}{\gamma}$ $Z_2 = \frac{\delta-1}{\gamma}$ $Z_3 = \frac{1}{\gamma}$	$Z_1 = Z_{ao} - \sqrt{Z_{ao} Z_{bo}}\sqrt{1-\frac{Z_k}{Z_0}}$ $Z_2 = Z_{bo} - \sqrt{Z_{ao} Z_{bo}}\sqrt{1-\frac{Z_k}{Z_0}}$ $Z_3 = \sqrt{Z_{ao} Z_{bo}}\ \sqrt{1-\frac{Z_k}{Z_0}}$	$Z_1 = \frac{Z_a\cosh T - \sqrt{Z_a Z_b}}{\sinh T}$ $Z_2 = \frac{Z_b\cosh T - \sqrt{Z_a Z_b}}{\sinh T}$ $Z_3 = \frac{\sqrt{Z_a\ Z_b}}{\sinh T}$
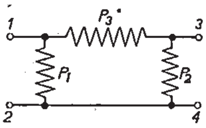	$P_1 = \frac{\beta}{\delta-1}$ $P_2 = \frac{\beta}{\alpha-1}$ $P_3 = \beta$	$P_1 = \frac{Z_{ak}}{1-\sqrt{\frac{Z_{ao}}{Z_{bo}}}\sqrt{1-\frac{Z_k}{Z_0}}}$ $P_2 = \frac{Z_{bk}}{1-\sqrt{\frac{Z_{bo}}{Z_{ao}}}\sqrt{1-\frac{Z_k}{Z_0}}}$ $P_3 = \frac{\sqrt{Z_{ak}\ Z_{bk}}}{\sqrt{1-\frac{Z_k}{Z_0}}}$	$P_1 = \frac{Z_a\sinh T}{\cosh T - \sqrt{\frac{Z_a}{Z_b}}}$ $P_2 = \frac{Z_b\sinh T}{\cosh T - \sqrt{\frac{Z_b}{Z_a}}}$ $P_3 = \sqrt{Z_a Z_b}\sinh T$
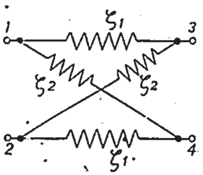 ζ_1 ζ_2 ζ_2 ζ_1 1 2 3 4	$\zeta_1 = \frac{\beta}{\alpha+1}$ $\zeta_2 = \frac{\beta}{\alpha-1}$	$\zeta_1 = Z_0\left(1-\sqrt{1-\frac{Z_k}{Z_0}}\right)$ $\zeta_2 = \frac{Z_k}{1-\sqrt{1-\frac{Z_k}{Z_0}}}$	$\zeta_1 = Z\tanh\frac{T}{2}$ $\zeta_2 = Z\coth\frac{T}{2}$

1694

„ITERATIVE IMPEDANCE“ 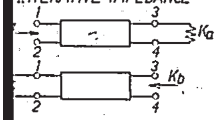 $\frac{I_2}{I_1} = e^{-\Gamma}$	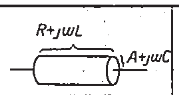 $Z=\sqrt{\frac{R+j\omega L}{A+j\omega C}}$ $\Gamma'=\sqrt{(R+j\omega L)(A+j\omega C)}$	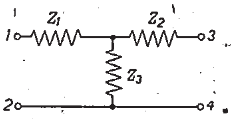 	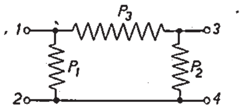 	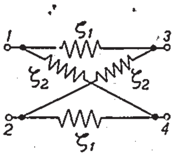 ζ_1 1 3 ζ_2 ζ_2 2 4 ζ_1
$= \frac{K_a e^{\Gamma} + K_b e^{-\Gamma}}{K_a+K_b}$ $= \frac{2K_a K_b}{K_a+K_b} \sinh\Gamma$ $= \frac{2}{K_a+K_b}\sinh\Gamma$ $= \frac{K_b e^{\Gamma}+K_a e^{-\Gamma}}{K_a+K_b}$	$\alpha=\delta=\cosh\Gamma^1$ $\beta=Z\sinh\Gamma^1$ $\gamma=\frac{1}{Z}\sinh\Gamma^1$	$\alpha=1+\frac{Z_1}{Z_3}$ $\beta=\frac{Z_1Z_2+Z_2Z_3+Z_3Z_1}{Z_3}$ $\gamma=\frac{1}{Z_3}$ $\delta=1+\frac{Z_2}{Z_3}$	$\alpha=1+\frac{P_3}{P_2}$ $\beta=P_3$ $\gamma=\frac{P_1+P_2+P_3}{P_1P_2}$ $\delta=1+\frac{P_3}{P_1}$	$\alpha=\delta=\frac{\zeta_2+\zeta_1}{\zeta_2-\zeta_1}$ $\beta=\frac{2\zeta_1\zeta_2}{\zeta_2-\zeta_1}$ $\gamma=\frac{2}{\zeta_2-\zeta_1}$
$o=\frac{K_a e^{\Gamma}+K_b e^{-\Gamma}}{2\sinh\Gamma}$ $k=\frac{2K_aK_b\sinh\Gamma}{K_b c^{\Gamma}+K_a e^{-\Gamma}}$ $=\frac{K_b e^{\Gamma}+K_a e^{-\Gamma}}{2\sinh\Gamma}$ $k=\frac{2K_aK_b\sinh\Gamma}{K_a e^{\Gamma}+K_b e^{-\Gamma}}$	$Z_{ao}=Z_{bo}=Z\coth\Gamma^1$ $Z_{ak}=Z_{bk}=Z\tanh\Gamma^1$	$Z_{ao}=Z_1+Z_3$ $Z_{ak}=\frac{Z_1Z_2+Z_2Z_3+Z_3Z_1}{Z_2+Z_3}$ $Z_{bo}=Z_2+Z_3$ $Z_{bk}=\frac{Z_1Z_2+Z_2Z_3+Z_3Z_1}{Z_1+Z_3}$	$Z_{ao}=\frac{P_1(P_2+P_3)}{P_1+P_2+P_3}$ $Z_{ak}=\frac{P_1P_3}{P_1+P_3}$ $Z_{bo}=\frac{P_2(P_1+P_3)}{P_1+P_2+P_3}$ $Z_{bk}=\frac{P_2P_3}{P_2+P_3}$	$Z_{ao}=Z_{bo}=\frac{1}{2}(\zeta_1+\zeta_2)$ $Z_{ak}=Z_{bk}=\frac{2\zeta_1\zeta_2}{\zeta_1+\zeta_2}$
$=\sqrt{K_aK_b}\sqrt{\frac{K_a e^{\Gamma}+K_b e^{-\Gamma}}{K_b e^{\Gamma}+K_a e^{-\Gamma}}}$ $=\sqrt{K_aK_b}\sqrt{\frac{K_b e^{\Gamma}+K_a e^{-\Gamma}}{K_a e^{\Gamma}+K_b e^{-\Gamma}}}$ $h\,T=\sqrt{\frac{4K_aK_b}{(K_a+K_b)^2}\cosh^2\Gamma+\left(\frac{K_a-K_b}{K_a+K_b}\right)^2}$	$Z_a=Z_b=Z$ $T=\Gamma^1$	$Z_a=\sqrt{\frac{(Z_1+Z_3)(Z_1Z_2+Z_2Z_3+Z_3Z_1)}{Z_2+Z_3}}$ $Z_b=\sqrt{\frac{(Z_2+Z_3)(Z_1Z_2+Z_2Z_3+Z_3Z_1)}{Z_1+Z_3}}$ $\cosh T=\frac{1}{Z_3}\sqrt{(Z_1+Z_3)(Z_2+Z_3)}$	$Z_a=P_1\sqrt{\frac{P_3(P_2+P_3)}{(P_1+P_3)(P_1+P_2+P_3)}}$ $Z_b=P_2\sqrt{\frac{P_3(P_1+P_3)}{(P_2+P_3)(P_1+P_2+P_3)}}$ $\cosh T=\sqrt{\frac{(P_1+P_3)(P_2+P_3)}{P_1P_2}}$	$Z_a=Z_b=\sqrt{\zeta_1\zeta_2}$ $\tanh\frac{T}{2}=\sqrt{\frac{\zeta_1}{\zeta_2}}$
	$K_a=K_b=Z$ $\Gamma=\Gamma^1$	$K_a=\frac{1}{2}(Z_1-Z_2)+\frac{1}{2}\sqrt{(Z_1+Z_2)^2+4Z_3(Z_1+Z_2)}$ $K_b=\frac{1}{2}(Z_2-Z_1)+\frac{1}{2}\sqrt{(Z_1+Z_2)^2+4Z_3(Z_1+Z_2)}$ $\cosh\Gamma=1+\frac{Z_1+Z_2}{2Z_3}$	$K_a=\frac{P_3(P_1-P_2)+\sqrt{P_3^2(P_1+P_2)^2+4P_1P_2P_3(P_1+P_2)}}{2(P_1+P_2+P_3)}$ $K_b=\frac{P_3(P_2-P_1)+\sqrt{P_3^2(P_1+P_2)^2+4P_1P_2P_3(P_1+P_2)}}{2(P_1+P_2+P_3)}$ $\cosh\Gamma=1+\frac{1}{2}P_3\left(\frac{1}{P_1}+\frac{1}{P_2}\right)$	$K_a=K_b=\sqrt{\zeta_1\zeta_2}$ $\tanh\frac{\Gamma}{2}=\sqrt{\frac{\zeta_1}{\zeta_2}}$
$+j\omega L=K\,\Gamma$ $+j\omega C=\frac{\Gamma}{K}$		$R+j\omega L=\sqrt{Z_1^2+2Z_1Z_3}\,\operatorname{arc\,cosh}\left(1+\frac{Z_1}{Z_3}\right)$ $A+j\omega C=\frac{1}{\sqrt{Z_1^2+2Z_1Z_3}}\,\operatorname{arc\,cosh}\left(1+\frac{Z_1}{Z_3}\right)$	$R+j\omega L=P_1\sqrt{\frac{P_3}{2P_1+P_3}}\,\operatorname{arc\,cosh}\left(1+\frac{P_3}{P_1}\right)$ $A+j\omega C=\frac{1}{P_1}\sqrt{\frac{2P_1+P_3}{P_3}}\,\operatorname{arc\,cosh}\left(1+\frac{P_3}{P_1}\right)$	$R+j\omega L=2\sqrt{\zeta_1\zeta_2}\,\operatorname{arc\,tanh}\sqrt{\frac{\zeta_1}{\zeta_2}}$ $A+j\omega C=\frac{2}{\sqrt{\zeta_1\zeta_2}}\,\operatorname{arc\,tanh}\sqrt{\frac{\zeta_1}{\zeta_2}}$
$=\frac{K_a-K_b\,e^{-\Gamma}}{1+e^{-\Gamma}}$ $=\frac{K_b-K_a\,e^{-\Gamma}}{1+e^{-\Gamma}}$ $=\frac{K_a+K_b}{2\sinh\Gamma}$	$Z_1=Z_2=Z\tanh\frac{\Gamma^1}{2}$ $Z_3=\frac{Z}{\sinh\Gamma^1}$		$Z_1=\frac{P_1P_3}{P_1+P_2+P_3}$ $Z_2=\frac{P_2P_3}{P_1+P_2+P_3}$ $Z_3=\frac{P_1P_2}{P_1+P_2+P_3}$	$Z_1=Z_2=\zeta_1$ $Z_3=\frac{1}{2}(\zeta_2-\zeta_1)$
$=\frac{K_aK_b(1+e^{-\Gamma})}{K_b-K_a\,e^{-\Gamma}}$ $=\frac{K_aK_b(1+e^{-\Gamma})}{K_a-K_b\,e^{-\Gamma}}$ $=\frac{2K_aK_b\sinh\Gamma}{K_a+K_b}$	$P_1=P_2=Z\coth\frac{\Gamma^1}{2}$ $P_3=Z\sinh\Gamma^1$	$P_1=\frac{Z_1Z_2+Z_2Z_3+Z_3Z_1}{Z_2}$ $P_2=\frac{Z_1Z_2+Z_2Z_3+Z_3Z_1}{Z_1}$ $P_3=\frac{Z_1Z_2+Z_2Z_3+Z_3Z_1}{Z_3}$		$P_1=P_2=\zeta_2$ $P_3=\frac{2\zeta_1\zeta_2}{\zeta_2-\zeta_1}$
$=K\tanh\frac{\Gamma}{2}$ $=K\coth\frac{\Gamma}{2}$	$\zeta_1=Z\tanh\frac{\Gamma^1}{2}$ $\zeta_2=Z\coth\frac{\Gamma^1}{2}$	$\zeta_1=Z_1$ $\zeta_2=Z_1+2Z_3$	$\zeta_1=\frac{P_1P_3}{2P_1+P_3}$ $\zeta_2=P_1$	

16948

general quadripole is thus determined by six elements.

The quadripoles such as are represented by filters are, however, of a special type. We are here only interested in the voltages between the primary poles 1 and 2 on the one hand and between the secondary poles 3 and 4 on the other. Outside of the filter there is no electrical connection between the pair of terminals 1 and 2 and the pair 3 and 4 (*fig. 2*).

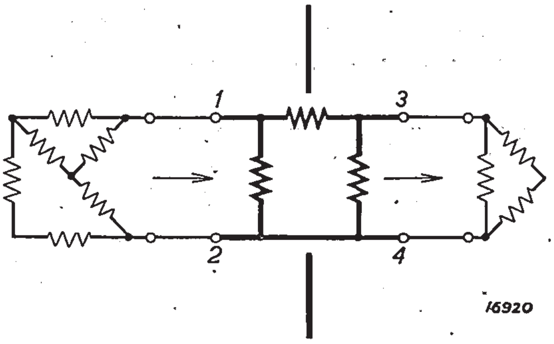

Fig. 2. Di-dipole, a special form of quadripole, which is defined by only three impedances, where the four external terminals *1*, 2, 3 and *4* are divided into two primaries *1* and 2 and two secondaries 3 and *4*. Externally to the di-dipole there is no electrical connection between the primary terminals on the one hand and the secondary terminals on the other.

It may be shown that, owing to these restrictions, applied to the general quadripole and which reduce the latter to a di-dipole, only three impedances are required for defining the characteristics of the network.

Various Ways of Defining a Filter by Three Parameters

The three impedances which are sufficient for defining a filter can be regarded as distributed in a quadripole in various ways, the different configurations being mutually transformable without the external characteristics of the filter being altered in any way. If the filter is symmetrical, i.e. if the external currents and voltages remain unaltered, when the primary terminals are made the secondary terminals and the secondary the primary, two impedances will be sufficient for defining the filter. In the large table on pp. 242 and 243 the three determinant impedances (for symmetrical filters, two impedances) are represented in various ways, together with the conversion formulae for transformation from one system of variables to another. In place of three determinant impedances three other mutually independent parameters can also be used, or also four parameters with one interrelation.

In the table each filter is defined in succession by:

a) the four coefficients of its analytical expression:

$$\begin{cases} V_1 = \alpha V_2 + \beta I_2 \\ I_1 = \gamma V_2 + \delta I_2 \end{cases}$$

in which the four coefficients α, β, γ and δ are connected by the expression:

$$\alpha\,\delta - \beta\,\gamma = 1$$

b) the primary input impedance Z_{ao} with the secondary terminals open-circuited, the primary input impedance Z_{ak} with the secondary terminals short circuited, the secondary input impedance Z_{bo} with the primary terminals open circuited and the secondary input impedance Z_{bk} with the primary impedances, where these four terminals short circuited are interrelated as follows:

$$Z_{ak}/Z_{ao} = Z_{bk}/Z_{bo}\,;$$

c) the primary image impedance Z_a, the secondary image impedance Z_b and the propagation constant T, being defined as follows: If the secondary side is terminated in an external impedance Z_b', then the impedance between the primary terminals is Z_a; if the primary side is terminated in an external impedance Z_a', leaving the secondary terminals open-circuited, then the impedance between the secondary terminals is Z_b. If the values of Z_a' and Z_b' are so chosen that $Z_a = Z_a'$ and $Z_b = Z_b'$ then Z_a and Z_b are termed the primary and secondary image impedances. The propagation constant is then defined as:

$$\frac{I_2}{I_1} = \sqrt{\frac{Z_a}{Z_b}}\, e^{-T}\,;$$

d) the primary iterative impedance K_a, the secondary iterative impedance K_b and the propagation constant Γ, being defined as follows: On shorting the secondary side with an impedance K_a the filter when seen from the primary side, similarly has the impedance K_a; on shorting the primary side through an impedance K_b, the filter similarly has an impedance K_b as seen from the secondary side. These impedances K_a and K_b are termed the primary and secondary iterative impedances; the propagation constant Γ is then defined as:

$$\frac{I_2}{I_1} = e^{-\Gamma},$$

(this propagation constant Γ is only equal, to the propagation constant referred to under c in the case of a symmetrical filter);

e) cable defined by its impedance $R + j\omega L$ and its parallel admittance $A + j\omega C$;

f) a network in the form of a T with the three impedances Z_1, Z_2 and Z_3;

g) a network in the form of a Π with the three impedances P_1, P_2 and P_3;

h) a symmetrical lattice network with the two impedances ζ_1 and ζ_2, each occurring twice (this circuit corresponds to an ordinary bridge circuit, *fig.* 3).

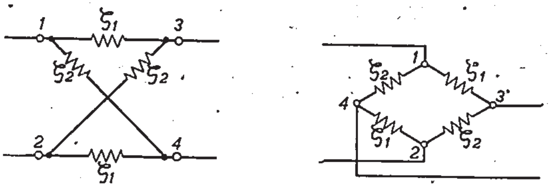

Fig. 3. Two methods of representing the same di-dipole; a symmetrical lattice network and a bridge circuit.

It should be noted that definitions *e*) and *h*) apply only to a symmetrical filter; the other definitions are based on an unsymmetrical filter, but become simplified when applied to a symmetrical filter. Thus for a symmetrical filter $a = \delta$; $Z_{ak} = Z_{bk}$; $Z_{ao} = Z_{bo}$; $Z_a = Z_b$; $K_a = K_b$; $Z_1 = Z_2$; $P_1 = P_2$.

As already indicated, any arbitrary filter can be regarded as compounded in any one of the ways *a*), *b*), *c*), *d*), *e*), *f*), *g*) and *h*), where *e*) and *h*) apply to symmetrical filters only, and in place of a filter, it is thus possible to substitute that network which will be the simplest for the particular case under consideration. In principle all networks given are equivalent and the table enables each method of representation to be transformed to any other. On transformation to another frequency independent calculation should in general be carried out, as impedances are usually obtained whose frequency dependence cannot be realised in practice.

The general characteristics found are employed in the solution of practical problems relating to the construction of high-pass, low-pass or band-pass filters to meet specific requirements, a subject to be discussed in subsequent lectures.

THE COMMUNAL AERIAL

By J. VAN SLOOTEN.

Summary. This article describes the electrical construction and method of operation of the aerial-signal amplifier "Antennaphil". With this apparatus it is possible, to supply aerial signals to a large number of receiving sets in a block of flats by using a single aerial only. Aerial-signal amplification also eliminates interference in reception.

Introduction

In large towns and cities the provision of a good aerial is usually fraught with serious difficulties, particularly in houses divided up into self-contained flats. As a rule it is not an easy matter to erect on one and the same roof a large number of separate aerials which would satisfy the requirements of all listeners. There is also the additional difficulty that in some places radio reception is practically impossible owing to interference from electric motors and other apparatus.

To surmount these difficulties a communal aerial system was evolved some years ago in these Laboratories and marketed under the name of the "Antennaphil". Briefly, this system operates in the following manner: An aerial of suitable dimensions and quality is erected at a point where interference is limited, e.g. 20 ft. above the roof. Through a specially-screened lead-in, which is made as short as possible, the aerial is connected to a so-called aerial-signal amplifier from which the incoming signals are transmitted to a number of receiving sets through a screened distributing circuit (lead-covered cable). As a rule up to 50 sets can be connected to an aerial fitted with this form of amplifier. The arrangement can also be employed quite satisfactorily with a smaller number of sets where reception sufficiently free from interference can only be obtained at a distance of several hundred to a thousand yards. These Laboratories have had an aerial of this type in use for several years in order to ensure reception free from all interference. The aerial and the aerial-signal amplifier are located about 200 yards from the laboratory on a building estate, and the supply cable for the amplifier and the high-frequency distribution cable from the amplifier are laid underground.

The amplifier consists essentially of:

a) an electrical filter unit,
b) a number of amplifying valves (high-frequency pentodes) and
c) two output transformers for matching the valves to the distribution cable.

In addition to the characteristics of the amplifier, those of the high-frequency distributing cable are also important, and as these closely determine the operation and design of the amplifier a brief discussion of the cable characteristics will not be out of place here.

The High-Frequency Distributing Cable

For the present purpose the best type of cable to use is a coaxial or concentric high-frequency cable, a diagrammatic section of which is shown in *fig. 1*. The diameter of the core is $2a$ and the internal diameter of the sheath $2b$, the external $2c$.

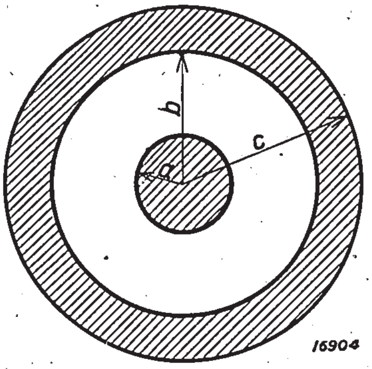

Fig. 1. Section through a high-frequency cable. a — Radius of core, b and c — internal and external radius of sheath. For a specific value of b/a the attenuation of the cable is a minimum. With a copper core and a lead sheath b/a must for instance be 5.2.

The intervening space is usually filled with a dielectric (paper or rubber), but may also have a partial air space. This insulating medium can be characterised by two constants, the dielectric constant ε and the phase difference δ. The tangent of the phase difference is given by the ratio of the effective current to the capacity current (per unit of length) and with air as dielectric is nearly unity. In cables with a good quality paper or rubber insulation δ is 0.01 to 0.025. Over the range of radio wave lengths δ is practically independent of the frequency. In addition to the sectional linear dimensions of the cable, this phase difference also determines the attenuation sustained by the oscillations during their passage through the cable.

The principal factor governing the practical efficiency of the cable is the so-called characteristic impedance. A remarkable property of a homogeneous cable is that its impedance measured at the input terminals tends towards a specific limiting resistance (the characteristic impedance) when the cable is made infinitely long. If the frequency is made sufficiently high, this resistance is practically independent of the frequency.

It follows from this property of an infinitely long cable that the input impedance of a finite cable will also become equal to the characteristic impedance if the resistance of the load at the output terminals is equal to the characteristic impedance; for in this way the same effect is produced as is obtained by prolonging the cable with an infinite length of equivalent cable. Under these circumstances no reflection therefore occurs at the ends and a true progressive wave is produced. This is the result desired, since the reflected wave travelling in the opposite direction may interfere with the advancing wave and thus generate nodes and antinodes in the voltage, which would prove very disturbing. With this type of disturbance an inadequate signal voltage would be obtained in any receiver connected to a nodal point of the cable. It is apparent from the above considerations that the cable must be a straight-through conductor without any taps or branches.

When designing the distributing system the first point to be considered is the choice of the optimum characteristics of the cable. The characteristic impedance should be fairly low, e.g. 60 ohms, for the cable is also loaded with the input impedances of the connected receivers. Hence, by using a cable with a high characteristic impedance the voltage distribution through the cable would be subject to serious interference. Another consideration also indicates the need for a low characteristic impedance. The question must be raised as to what must be the core thickness in a cable with a given thickness of lead sheathing (as determined, for instance, by cost considerations) in order to obtain the lowest possible drop in amplitude per unit length of the cable.

With a lead sheath and a copper core we get for the ratio of b to a (see fig. 1):

$$\frac{b}{a} = 5.2 \quad . \; . \; . \; . \; . \; . \; . \; . \quad (1)$$

and for this ratio the characteristic impedance is similarly of the order of 60 ohms [1]), independently of the absolute value of the diameter.

Having determined the value of this ratio, we can also calculate the lowest absolute values for these diameters. The attenuation losses in the cable can be resolved into the copper losses in the insulation, which are determined by the ohmic resistances of the core and the sheath, taking into consideration the skin effect and the dielectric losses in the insulation, which are proportional to the phase difference already referred to. The latter damping effect is determined solely by the insulating material and is independent of a and b.

Analysis of the copper losses gives equation (1); these losses can also be reduced as required by increasing the cross-section of the cable, but this is naturally of use only as long as the dielectric losses do not predominate [2]).

A practical example is, for instance, the following cable in which the attenuation due to the copper losses is equal to that due to the dielectric losses at a wave length of 200 m.

$$2a = 2.5 \text{ mm}, \; 2b = 13 \text{ mm}, \; \varepsilon = 2.5;$$
$$\delta = 0.02, \; Z = 63 \text{ ohms}.$$

With a wave length of 200 m this cable produced an overall attenuation of 1 neper, i.e. a transmission loss factor of 2.72 per km. With higher

---

[1]) The exact formula is:

$$\ln \frac{b}{a} = 1 + \frac{a}{b} \sqrt{\frac{\varrho_2}{\varrho_1}} \; ; \quad . \; . \; . \; . \; . \quad (1a)$$

where ϱ_2 and ϱ_1 are the specific resistances of the materials of the sheath and the core. The relationship between the characteristic impedance Z, the values a, b and the dielectric constant ε of the insulating material is:

$$Z = \frac{60}{\sqrt{\varepsilon}} \ln \frac{b}{a} \text{ Ohm} \quad . \; . \; . \; . \; . \; . \; . \quad (2)$$

If e.g. we put $\varepsilon = 2.5$ and take $\frac{b}{a}$ from equation (1), we get $Z = 63$ ohms.

[2]) For further details and the derivation of equation (1a) see Radio-Nieuws, **17**, 77, 1934.

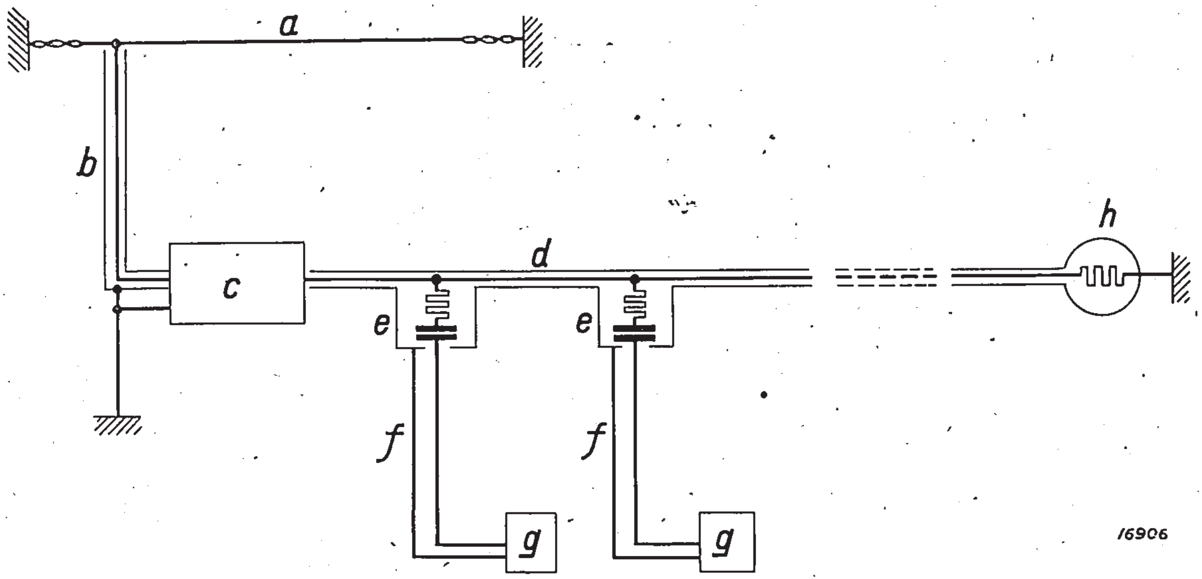

Fig. 2. General view of the aerial distributing system. a — aerial, b — lead in, c — aerial-signal amplifier, d — high-frequency distributing cable, e — branch boxes, f — lead, g — receiving set, h — terminating resistance.

wave lengths the attenuation diminishes, whilst with shorter wave lengths it increases; in the latter case dielectric losses also predominate.

Actually this cable is more than adequate for the purpose intended. For a receiving system where the cable is not more than 200 to 300 yards long a much thinner cable could also be employed with still satisfactory results, and it is then also possible to use one of the many low-capacity cables, which in general have a characteristic impedance of 100 to 150 ohms, for the screened aerial lead-in.

Fig. 2 gives a general view of the receiving system, where a is the aerial, b the aerial lead-in for which a screened low-capacity should be used for preference, c is the aerial-signal amplifier, and d the high-frequency distributing cable. The phantom aerials for eliminating the effect of the cable on the tuning of the receiver and which consist of a 200 $\mu\mu$F condenser and a 30-ohm resistance connected in series are accommodated in the branch boxes e inserted in the cable. To connect a branch box to a receiver g a flexible screened cable f with a low capacity not exceeding 40 $\mu\mu$F per metre and not more than 3 to 4 yards long should be used. The earthing terminal of the receiver is connected directly to the cable sheath and is not separately earthed. A box with a terminal resistance h is located at the end of the cable, through which the sheath is earthed.

The Aerial-Signal Amplifier

A simplified circuit diagram of an aerial-signal amplifier is given in *fig. 3*. The aerial voltages are passed to the grid of an amplifying valve (preferably a tetrode or pentode), the anode of this valve being connected to the cable impedance Z through an output transformer T. As the valve has a high internal resistance and the impedance of the cable is low, it is necessary to step down n times through T.

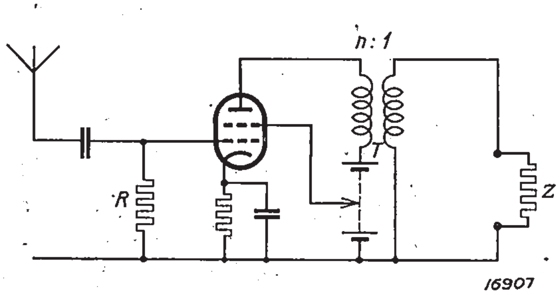

Fig. 3. Simplified circuit of an aerial-signal amplifier. The alternating voltages generated at the resistance R are amplified and passed to the distributing cable Z through a transformer T, which serves for matching the characteristic impedance of the cable to the valve.

Closer investigation indicates, however, that a simple amplifier of this type is unsuitable for transmitting a wide frequency sweep. The principal reason for this is the limitation sustained in the frequency as a result of the adverse capacity connected through the primary winding. This undesirable capacity is principally made up of the capacities of the valve and leads and the self-capacity of the winding.

The explanatory circuit in *fig. 4* shows how the voltage E_1 is produced through the primary winding of the transformer. The valve has been replaced by the current source V_gS (S = slope, V_g = grid alternating voltage); C_1 represents the total undesirable capacity, L_1 is the self-induction of the primary winding and n^2Z the secondary load resistance transformed on to the primary side. The secondary output voltage is n times smaller than E_1.

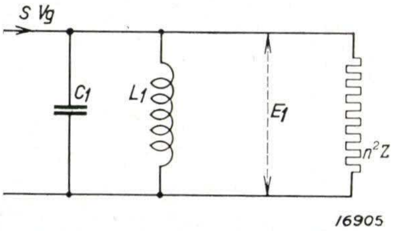

Fig. 4. Explanatory circuit for the circuit shown in fig. 3. L_1 — primary self-induction of the output transformer T, C_1 — adverse capacity. The current source $s\,V_g$ takes the place of the amplified aerial voltage and the impedance n^2Z is in place of the transformed load resistance. At very low frequencies the alternating current is removed through L_1 and at very high frequencies through C_1. A maximum amplification is obtained at $\omega^2 L_1 C_1 = 1$.

It may be seen from *fig. 4* that in the absence of C_1 and with a sufficiently high self-induction L_1 the primary impedance is determined by n^2Z, and would require a high ratio of transformation n. This also applies when C_1 is present and is of sufficiently low rating, or when the circuit $L - C_1$ is in resonance with the incoming wave. But if C_1 becomes so great that its impedance determines the voltage E_1, the highest cable voltage is obtained with a low ratio of transformation n. Thus, C_1 determines the ratio which must be employed and with a higher wave length will be greater than with a short one, as the impedance of C_1 increases with the wave length.

The following conclusions may therefore be drawn:

1) The adverse influence of the undesirable capacity increases as the wave length is reduced.
2) The smaller the wave range to be amplified, the better can use be made of a resonance between the primary capacity C_1 and the self-induction L_1 for eliminating the adverse effect of C_1.
3) It is therefore advantageous not to amplify the whole wave range through a single amplifier and output transformer but to divide it up and amplify the components separately in parallel amplifying stages, whose output voltages can again be combined. In practice the wave range is divided into two components: the broadcasting range with wave lengths from 200 to 2000 m and the short-wave range from 20 to 55 m.

Fig. 5 gives a view and *fig. 6* circuit details of the aerial-signal amplifier. On the right are two valves *III* and *IV* in parallel for amplifying the broadcast wave range, and further to the left two valves *I* and *II* for amplifying the short-wave

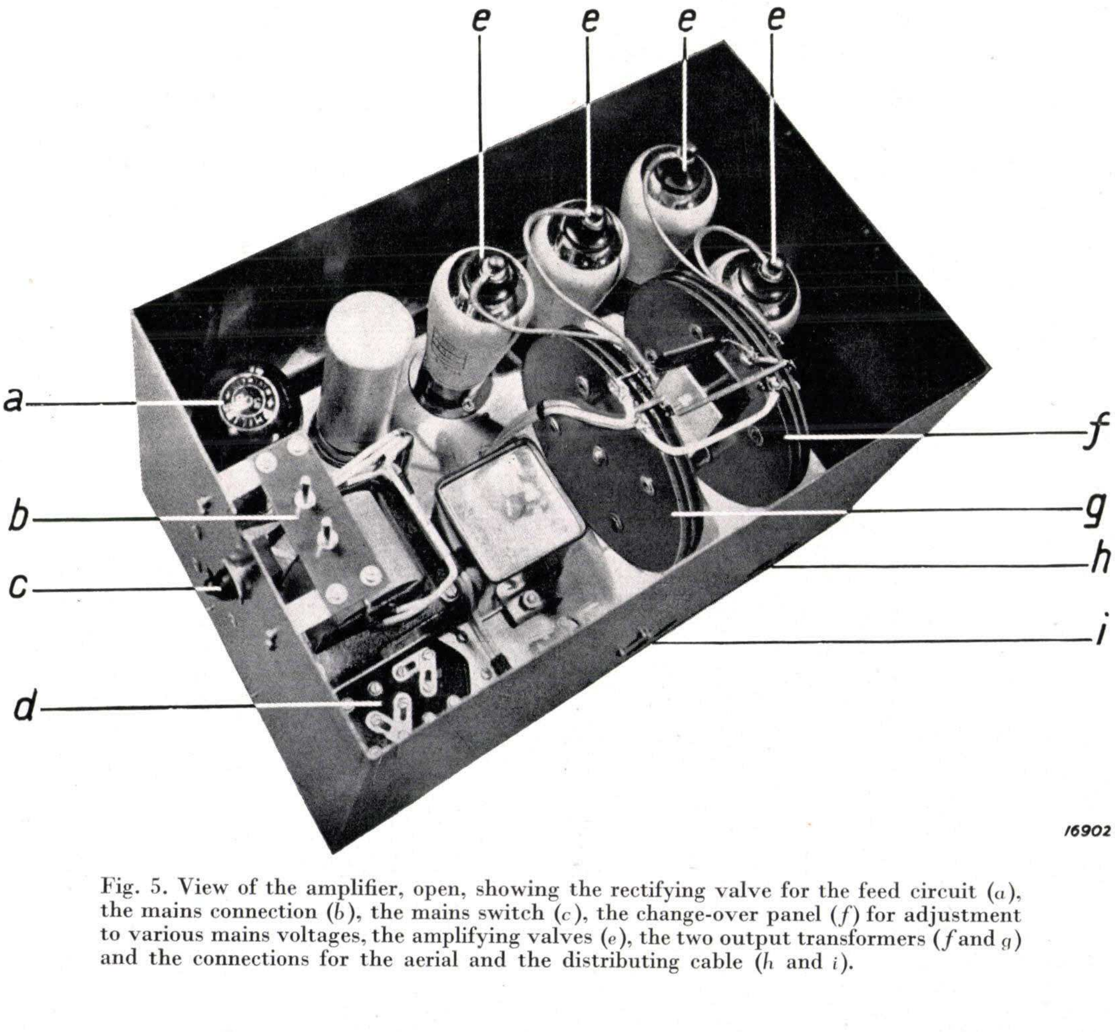

Fig. 5. View of the amplifier, open, showing the rectifying valve for the feed circuit (a), the mains connection (b), the mains switch (c), the change-over panel (f) for adjustment to various mains voltages, the amplifying valves (e), the two output transformers (f and g) and the connections for the aerial and the distributing cable (h and i).

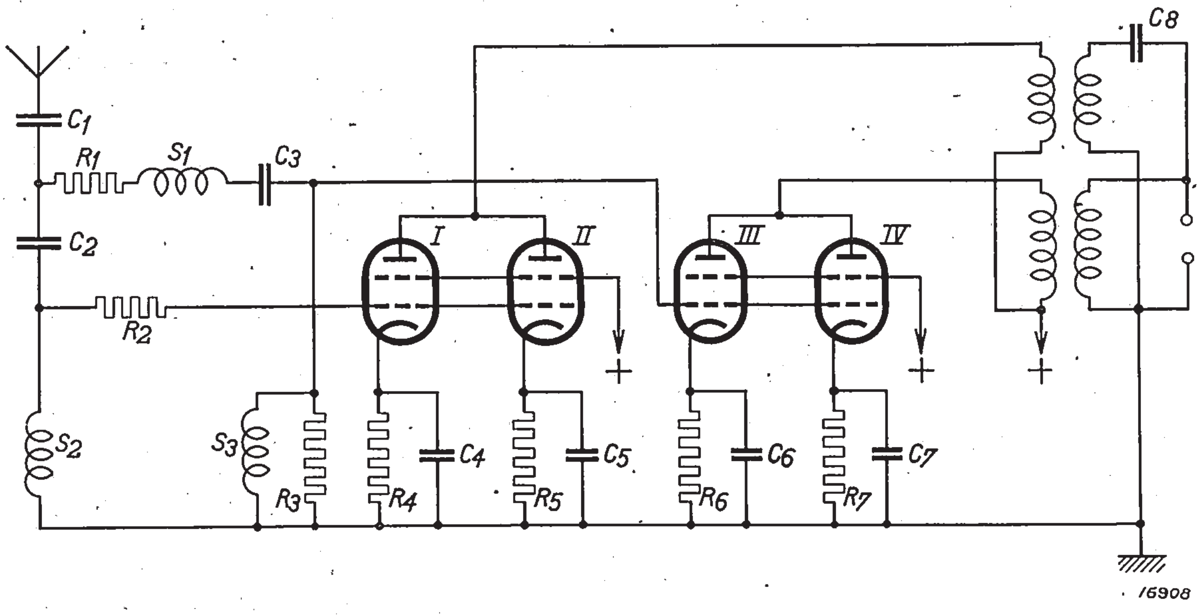

Fig. 6. Circuit cable of the aerial-signal amplifier. The valves *I* and *II* amplify the short waves and valves *III* and *IV* the broadcast waves. The circuit components C_1, C_2, C_3, S_1, S_2, S_3, R_1, R_2, R_3, constitute the filters for the two wave-length ranges. C_8 prevents the winding of the short-wave transformer from shorting the broadcast-wave transformer[3]).

range. The secondary windings of the two output transformers are connected to the input terminals of the cable. The condenser C_8 is necessary here to prevent the secondary winding of the transformer for the short-wave range from shorting the winding of the broadcast-range transformer with which it is in parallel.

On the left of fig. 6 there are a number of condensers, coils and resistances, which are inserted between the aerial and the grid of the amplifying valves. The main purpose of these units is to allow only those frequencies to pass to the valve grids which are to be amplified, for owing to the curved characteristic of the valve (anode current plotted against grid volts) it is possible for disturbing oscillations to be generated in the valve with frequencies which are the sum or difference of the frequencies passed to the grid. The risk of this interference materialising is considerably reduced if unnecessary frequencies are prevented from reaching the valve grids.

The units inserted between the aerial and the grids constitute a filter system which may be regarded as a combination of the simple filters shown in *figs.* 7 and 8. The filter in fig. 7 allows low frequencies to pass, and that in fig. 8 high frequencies. The limiting frequency is given in both cases by $\omega_0^2 L C = 1$ ($\omega = 2\pi f$, where f is the frequency). The resistances R serve for suppressing the peaks in the neighbourhood of a frequency of ω_0. In both figures *I* is the transmission curve with a low resistance R, and *II* the transmission curve for a high resistance.

The various circuit components in fig. 6 serve the following purposes: C_2 and S_2 prevent wave lengths exceeding 55 m from reaching the grids of valves *I* and *II*. The input capacity of these valves is in parallel to S_2, so that resistance R_2 is required to suppress any disturbing resonance.

S_1 and the input capacity of valves *III* and *IV* prevent wave lengths of less than 200 m being impressed on the grids of these valves. Finally, C_3 and S_3 prevent wave lengths of over 2000 m reaching the grids of valves *III* and *IV*.

R_1 and R_3 are damping resistances which are so rated that the resonance peak is not entirely suppressed with wave lengths between 200 and 2000 m.

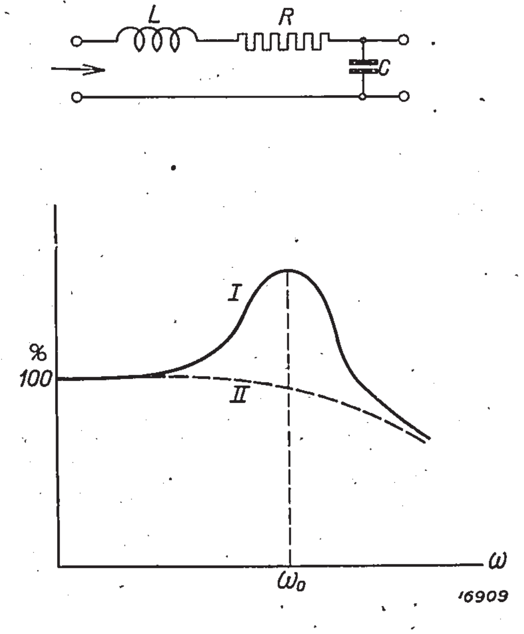

Fig. 7. A filter which suppresses frequencies above a limiting frequency of $\omega_0/2\pi$ (low-pass filter).

---

[3]) The latest design also contains two filter circuits, which suppress interference from any powerful local transmitting stations. To simplify the circuit diagram these have not been included here.

In *fig. 9* the aerial voltage furnished by the amplifier to a load of a resistance of 50 ohms is plotted against the wave length. The graph shows the subdivision into a short wave range and a broadcast wave range, which are obtained with resonance peaks partially smoothed by resistances. The resonance peaks *2* and *5* are due to filters of the type shown in fig. 8; peak *3* is due to a filter of the type shown in fig. 7, whilst peaks *1* and *4* correspond to resonance frequencies of the output transformers for the short-wave and broadcast-wave ranges.

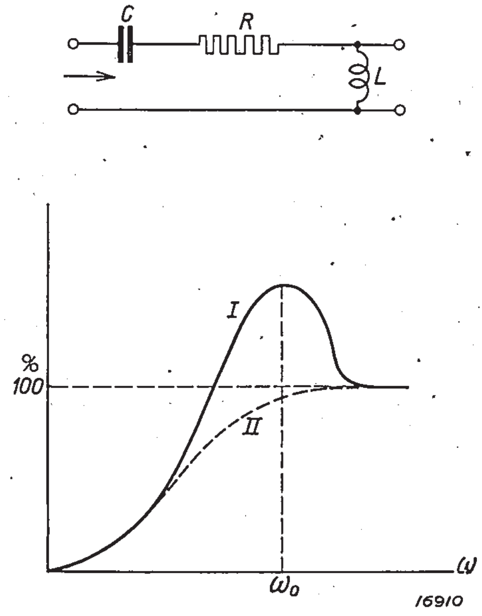

Fig. 8. A filter which suppresses frequencies below a certain limiting frequency $\omega_0/2\pi$ (high-pass filter). The limiting frequency is determined by $\omega_0^2LC = 1$. Figs. 7 and 8 also show the transmission curves for the two filters: *I* for a low resistance *R* and *II* for a high resistance *R*.

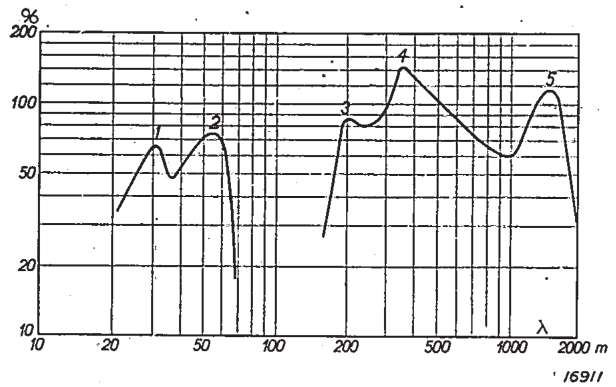

Fig. 9. Aerial voltage at a resistance of 50 ohms plotted against the wavelength. The peaks *2* and *5* are due to the high-pass filter and *3* to a low-pass filter; *1* and *4* are the resonance frequencies of the output transformers.

SHORT NOTICES

Sodium lighting of tennis courts

The problem of lighting tennis courts is of special interest as two requirements in particular have to be satisfied which, although also of importance in all illumination problems, yet have a special significance in this case; these are complete freedom from glare and high speed of discrimination. Both these requirements are exceptionally well fulfilled by a lighting system employing sodium lamps. As regards the danger of glare, experience has shown that the presence of a source of light in the field of vision is less disturbing with sodium lamps than with other light-sources of an equivalent total candle power. This fact is obviously due to the comparatively low luminous density of sodium lamps, although no satisfactory agreement has yet been obtained in the various attempts to arrive at quantitative determination of the disturbing effect of the glare produced with different types of light. With reference to the second factor, viz, high speed of discrimination, Arndt, Bouma, and Luckiesh and Moss established almost simultaneously that — as was recently confirmed by Weigel — the speed of discriminating objects is greater with sodium light than with other types of light. The speed of discrimination is defined as the time during which an observer must view an object in order to be able to recognise a specific detail of it with more than fifty per cent certainty. A similar task has to be performed by tennis players, who must be able to detect the exact location of the ball during its rapid flight.

Modern sodium lamps thus give a very satisfactory solution to the problem of illuminating tennis courts. As the glare factor is small, the lamps can be given a wide angle of radiation, and as a result uniform illumination is obtained even when the lamps are suspended at a low level, a low mounting height being desirable in order to obtain intensive illumination at a minimum of cost.

The illumination of tennis courts is particularly important in regions with a tropical climate where the heat renders play during the day impossible, and where during the evening, when the atmosphere is cooler, darkness sets in very quickly. Three open-air tennis courts in the Netherlands East Indies were recently equipped with sodium lamps, viz, one at Banjermasin and two at Sourabaya. Good results have been obtained in this case with an arrangement of eight sodium lamps ("Philora" SO, 150 watts) in two rows on both sides of the courts. These lamps are situated 20 ft. above the ground. Since little experience is as yet available of this special lighting problem it is possible that a still better arrangement of the lamps may yet be evolved (e.g. more lamps placed closer together). *Fig. 1* shows the suspension of the lamps and *fig. 2* an illuminated tennis court.

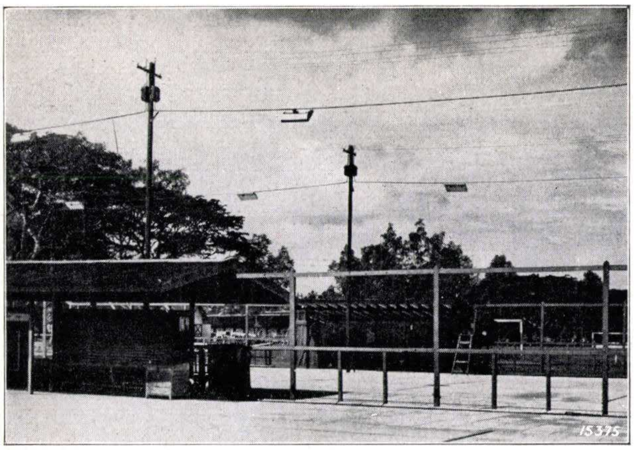

Fig. 1. Lighting fixtures of tennis courts with sodium lamps illuminated.

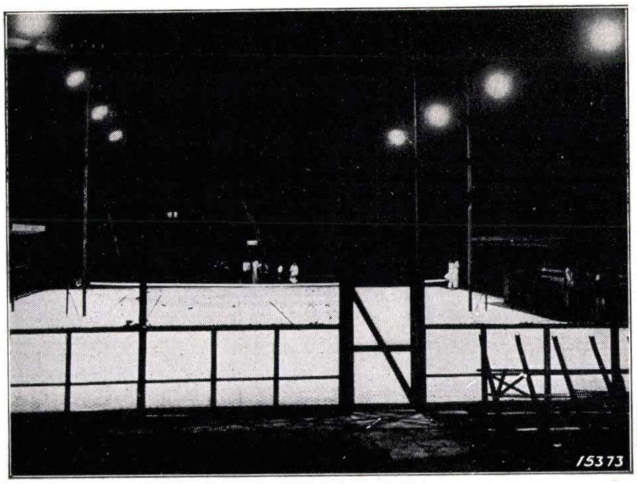

Fig. 2. Tennis court with sodium illumination.

PRACTICAL APPLICATIONS OF X-RAYS FOR THE EXAMINATION OF MATERIALS VII

By W. G. BURGERS.

The X-ray photographs, obtained with mixed crystals (solid solutions), which were described in the previous article in this series, can frequently be utilised for the "indirect" detection by radiographic means of an admixture in a specific compound. In many cases the principal constituent is able, to take up an impurity in "solid solution", in other words the admixed body is not present as a separate phase, but forms a mixed crystal or solid solution with the chief substance present. This behaviour is observed, not only with substances having a similar crystal structure, i.e. with the formation of isomorphous crystals, but also with bodies which crystallize in entirely different systems and even when one of the components is a gas. The mixed crystal then assumes the crystalline form of the predominating component.

As was indicated in the previous article (VI), this phenomenon becomes apparent in X-ray analysis by a displacement of the interference lines for the principal component, such displacement being exhibited by a greater or lesser angle of deviation of the dispersed X-rays from the direction of the incident beam, according as the crystal lattice of the principal component is either "expanded" or "contracted" by the admixture. Although the impurity is not necessarily detected by this means and cannot therefore be identified, it is yet possible to establish that the principal product is not entirely pure, which in many cases is already of great importance. The two following examples illustrate these points.

Examination of the radiographs of the series of copper-nickel mixed crystals reproduced in fig. 1 of the previous article will show that the inner lines have suffered much greater mutual displacement than the outer lines. This striking effect is due to the method used in making the photographs. The "sensitivity" of the angle of diffraction to a change in the interatomic distances is in fact greatest for those lines produced by rays, which are deflected to the greatest extent from the direction of the incident radiation. These lines are situated at the two ends of the film in a "normal" exposure, where the film is so fixed in the camera, that the undeflected X-ray, on leaving the camera, passes through a hole in the middle of the film (cf. *fig. 1a*; see also fig. 2 of article I in this series, Philips techn. Rev. **1**, 29 1936). Better results are obtained when the film is placed in the camera in the manner described by van Arkel [1]), so that the X-ray passes through a hole in the film, not on leaving but on entering the camera (see *fig. 1b*): With such a „reversed“ film the „sensitive“ lines are situated at the middle, which has the advantage, that the accuracy in measuring the interatomic distances for the sensitive lines is less affected by the shrinking of the film during drying. *Fig. 2* again shows clearly the marked difference in displacement between the inner and outer lines. The top exposure was obtained with thorium oxide $Th0_2$, and the lower one with metallic thorium these two bodies being "isomorphous", as regards the mutual arrangement of the thorium atoms, except that the distance between the Th atoms is much greater in the oxide than in the metal.

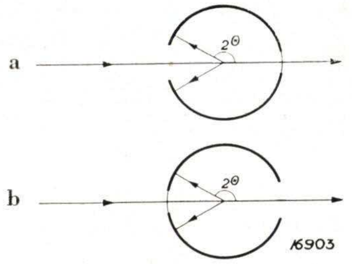

Fig. 1a. Normal position of film. The "sensitive" lines ($2\,\Theta$ slightly smaller than 180 deg.) are situated at the ends of the film.
b. "Reversed" film. The "sensitive" lines are at the middle, giving the advantage, that the measurement of the distances of the sensitive lines is less affected by shrinkage of the film during drying.

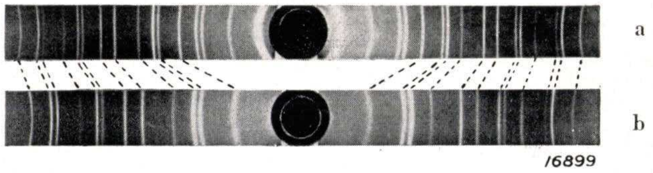

Fig. 2. "Reversed" X-ray photographs of isomorphous crystalline preparations.
a) Thorium oxide, ThO_2
b) Metallic thorium, Th.
Corresponding lines on both diagrams are connected with each other. It is clearly shown that the inner lines have undergone much greater mutual displacement than the outer lines.

15. Excessive Tantalum Content of Tantalum Carbide [2])

It was stated in example 9 (article V, Philips techn. Rev. **1**, 188, 1936) that in the preparation of carbides of highly refractory metals the isolation of the metal itself sometimes takes place.

---

[1]) A. E. van Arkel, Z. Kristallogr. **67**, 235, 1928.

[2]) W. G. Burgers and J. C. M. Basart, Z. anorg. allg. Chem., **216**, 223, 1924.

The radiographs of certain filaments of zirconium carbide thus contain, in addition to lines due to the carbide itself, also those due to metallic zirconium (loc. cit. fig. 1). In these cases the metal has at least partially become separated in the free state as an independent phase alongside the carbide.

In making filaments of tantalum carbide the same phenomenon has been sometimes observed, whilst other wires were obtained which gave a pattern of only the carbide lines. These wires, which appeared identical on examination with the naked eye (having a light to golden yellow metallic lustre), could, however, be distinguished when strongly heated *in vacuo*, a behaviour which was naturally carefully observed in view of their possible use as incandescent filaments for lamps: Even at comparatively low temperatures (about 2000 °C.) the variation in resistance was found to differ from wire to wire and the bulbs became covered with a metallic mirror which differed in thickness from case to case. It was concluded from ("reversed") radiographs of the wires that the diameter of the inner interference line was different for each wire, corresponding to alterations in the interatomic distance of about 1 per cent. Two exposures illustrating this are shown in figs. *3a* and *b* [3]). It appeared very probable that the wires had absorbed in solid solution different amounts of metallic tantalum in excess, an assumption which was subsequently confirmed for several wires by chemical (combustion) analysis, which gave a molecular composition corresponding to Ta : C = 6 : 5. By heating in methane the metallic tantalum in excess could be converted to carbide and the latter thus obtained in the pure state. The diameter of the inner interference ring for pure TaC was determined and has permitted X-ray analysis to be adopted as a routine testing method in the preparation of this carbide.

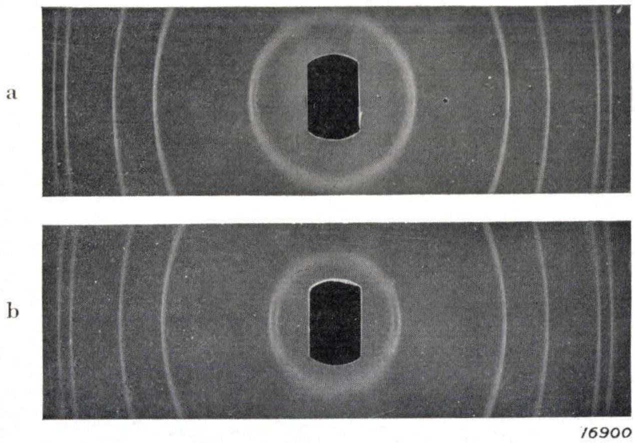

Fig. 3. X-ray photographs of:
a) Pure tantalum carbide, Ta C
b) Tantalum carbide containing excess of tantalum in solid solution.
The inner ("sensitive") interference ring has a much smaller diameter in fig. b) than in fig. a).

16. Hydrogen in Tantalum

Metallic tantalum can be deposited on a strongly-heated core wire [4]) by thermal decomposition of tantalum pentachloride, Ta Cl_5, this method closely resembling the isolation of tungsten from W Cl_6 as first achieved by van Arkel [5]). The ductility of the product was found to be by far the best when the Ta Cl_5 used had first been sublimed *in vacuo* (such treatment making it, moreover, far more active).

It appeared feasible that this improvement was due to the expulsion of absorbed gases from the Ta Cl_5 during sublimation: If theses gases were still present on the isolation of the tantalum, they could be absorbed by the metal and for instance form a solid solution, thus resulting in a reduction in ductility.

This assumption was confirmed by X-ray analysis, for small differences in interatomic distances were found for tantalum wires prepared by different means, a result which could again be deduced from the difference in diameter of the inner interference ring (registered on a "reversed" film). Two exposures so obtained are reproduced in figs. *4a* and *b*, the former relating to metal deposited from pure Ta Cl_5 and the latter to metal obtained by decomposition of the chloride in a hydrogen atmosphere. The difference between the diameters of the inner interference rings (a doublet) is 2 mm, which here corresponds to a difference in the lattice constants of approx. 0.2 per cent, the tantalum lattice having been slightly expanded by the absorption of hydrogen.

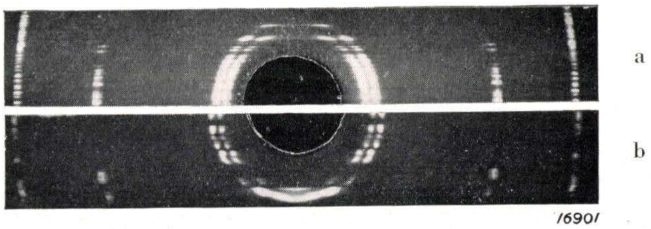

Fig. 4. X-ray photographs of tantalum prepared from tantalum chloride by thermal decomposition a) with and b) without hydrogen. The greater diameter of the inner interference ring in fig. b) is due to the presence of hydrogen in the metal, which is thus made less ductile.

---

[3]) The exposures again show clearly the greater "sensitivity" of the inner lines with respect to the lines further out.

[4]) W. G. Burgers and J. C. M. Basart, Z. anorg. allg. Chem., **216**, 223, 1924.

[5]) A. E. van Arkel, Physica, **3**, 76, 1923.

ABSTRACTS OF RECENT SCIENTIFIC PUBLICATIONS OF THE N.V. PHILIPS' GLOEILAMPENFABRIEKEN *)

No. 1080: A. Bouwers: Röntgenapparaten (Ingenieur, **51**, E 27-30, March, 1936).

In this paper the author, with the aid of examples, traces how X-ray technology has succeeded in evolving, from the X-ray tube used in experimental physics, a perfectly safe electrotechnical equipment with *a priori* calculated characteristics. The author discusses the problem of insulating high-tension equipment, with special reference to a simplified method for calculating and providing insulation on high-tension equipment capable of withstanding a uniform stress at a specific field strength, the production of high outputs for short periods, and the generation of very high tensions of the order of several million volts. A series of demonstrations were given, including a small complete X-ray equipment weighing only $3^1/_2$ kg and high-tension generators for a million volts direct voltage and impulse voltages of 2 million volts.

No. 1081: R. Vermeulen: Geluidsfilm-apparaten (Ingenieur, **51**, E 30-34, March, 1936).

In the Philips-Miller method, sound films are produced by mechanical means in the same way as gramophone records, whilst the sound track is reproduced by optical means similar to the method employed with the photographically-registered sound film.

As a series of articles on this subject is appearing in this journal (Philips tech. Rev., **1**, 107, 135, 211 and 231, 1936), a fuller abstract of this paper will not be given here.

No. 1082: J. van der Mark: Een experimenteele televisiezender en -ontvanger (Ingenieur, **51**, E 37-40, March, 1936).

This paper is almost identical with a paper of the same title contributed by the author to the first number of this journal (cf. Philips techn. Rev., **1**, 16, 1936).

No. 1083: M. J. Druyvesteyn: Electron emission of the cathode of an arc (Nature, **137**, 580, Apr. 1936).

In carbon and tungsten arcs electron emission is in general due to the high temperature of the cathode. In the case of the mercury arc it is assumed that electron emission of the cold cathode is due to the powerful electric field produced in front of the cathode by those positive ions which travel towards this electrode. In addition the author assumes also a third mechanism for electron emission from the cathode. According to this hypothesis the cathode is coated, at least partially, with a thin layer of an insulating substance. The positive ions which accumulate on this layer can generate such a powerful field that the metal emits electrons through the insulating layer. These electrons traverse at great speed the space charge of the positive ions, thus having little opportunity to recombine with them. The greater part of the cathode drop is obtained at the insulating layer.

No. 1084: J. A. M. van Liempt: Die Dampfdrücke des Caesiums (Rec. Trav. chim. Pays-Bas, **55**, 157-160, March, 1936).

On the basis of previous investigations (cf. Abstract No. 1051) the author deduces a formula expressing the vapour pressure of caesium as a function of the temperature, which is valid for temperatures between 300 and 1000 deg. K. The most probable sublimation curve is given for temperatures between 270 and 300 deg. K.

No. 1085: J. L. Snoek: Sur une nouvelle expérience de magnétostriction (Physica, **3**, 205-206, Apr., 1936).

The reversible torsion phenomena, which according to Perrier are exhibited by a nickel wire after special pre-treatment when temperature changes are produced in the neighbourhood of the Curie point, are no longer observed when the wire has been corroded by hydrogen chloride or when oxidation during pre-treatment is prevented. According to the author these phenomena must be regarded as due to the oxide layer and not to reversible changes in texture as assumed by Perrier.

No. 1086: W. Elenbaas: Der Einfluss des Zündgases auf die Quecksilber-Hochdruckentladung (Physica, **3**, 219-236, Apr., 1936).

By measuring the reduction in radiation the author has determined the additional loss in energy per cm of tube length in a high-pressure discharge

---

*) A sufficient number of reprints for purposes of distribution is not available of those articles marked with an asterik (*). Reprints of other papers may be obtained on application from Philips' Laboratory, Kastanjelaan, Eindhoven, Holland.

through mercury vapour due to the addition of rare gases. This increased loss was found to be practically independent of the energy input per cm of tube length, and could be calculated from the increase in thermal conductivity. On the assumption, that in pure mercury the heat dissipated per cm of tube length is 10 watts, the measurements could be described with the aid of a formula due to Enskog for the thermal conductivity of a gas mixture. In a previous paper (Physica, **2**, 757, 1935) the author arrived at an energy loss of 9 watts per cm from the relationship between the voltage gradient and the energy input. If the additional losses due to the rare gases introduced are also taken into consideration, the influence of the rare gases on the gradient can be calculated by a theoretical method given previously.

No. 1087: J. R. J. van Dongen and J. G. C. Stegwee: De beteekenis van de schijfproef als verkorte standtijdproef (Metaalbewerking, **3**, 1-6 and 49-56, March and Apr., 1936).

As a number of articles dealing with this subject have already appeared in this Review (Phil. techn. Rev., **1**, 183 and 200, 1936) a full abstract of this paper is superfluous.

No. 1088: K. Posthumus: Richtantennes met identiek richtingsdiagram, maar ongelijke stroomverdeeling (aequivalente antennes). (T. Ned. Rad. Genoot., **7**, 115-139, Apr., 1936).

The author points out that the directional distribution of an aerial made up of a number of similar components situated in a straight line at uniform intervals and having an arbitrary current distribution, can in general also be obtained with several other forms of aerial and a different current distribution. In the aggregate there are 2^{n-1} equivalent aerials from n components. It is shown how these equivalent aerials can be deduced from the data for an arbitrary aerial. In conclusion the author points out that the more common aerials in use have no equivalent aerial.

No. 1089: J. H. de Boer, W. G. Burgers and J. D. Fast: The transition of hexagonal α-titanium into regular β-titanium at a high temperature (Proc. kon. Akad. Wet. Amsterdam, **39**, 515-519, Apr., 1936).

In isolating zirconium by thermal decomposition of ZrJ_4 the metal is deposited in a form with regular symmetry (β-modification), whilst at ordinary temperature it is obtained with hexagonal symmetry (α-modification). Titanium is isomorphous with zirconium and at high temperatures is deposited together with zirconium in the form of mixed crystals. It thus appeared that titanium also would pass over into a regular β-modification at high temperatures; this was in fact found to be the case from both resistance curves and X-ray photographs. The transition temperature was 882 deg. C and thus differs little from that for zirconium (862 deg. C). Also, as with zirconium, (see Abstract No. **1095**) a well-defined transition temperature is only found when the metal contains no oxygen or nitrogen.

No. 1090: J. A. M. van Liempt and J. A. de Vriend: Das Flimmern von Glühlampen bei Wechselstrom (Z. Phys., **100**, 263-266, Apr., 1936).

The flickering of various types of electric lamps when run on a low-frequency alternating current supply was investigated with the aid of a cathode ray tube and a caesium photo-electric cell. At an equivalent wattage spiral filament vacuum lamps showed the least flickering, being followed by straight-filament vacuum lamps and gas-filled coiled-coil lamps; the greatest comparative flickering was obtained with gasfilled single-coil lamps.

No. 1091: Balth. van der Pol: Trillingen (Ned. T. Natuurk., **3**, 65-84 and 97-108, Apr., 1936).

A translation of the paper read in English, abstracted under No. **1077**.

No. 1092: H. Ziegler: Shot effect of secondary emission. II. (Physica, **3**, 307-316, May, 1936).

The coefficient of secondary emission and the variation in secondary current are governed by the energy of the primary electrons and by the nature of the electrode bombarded. In continuation of a previous paper (cf. Abstract No. **1066**) the author examines the multiple electronic charges composing the current impulse. The quotient of the coefficient of secondary emission and of the coefficient of secondary current fluctuations is a measure of the proportion of effective primary electrons and of the quality of the amplification due to secondary emission in respect of fluctuations in operating conditions. These phenomena are studied for a nickel plate with an activated barium and strontium surface in relationship to the velocity of the primary electrons.

VOL. 1 No. 9 SEPTEMBER 1936

Philips Technical Review

DEALING WITH TECHNICAL PROBLEMS
RELATING TO THE PRODUCTS, PROCESSES AND INVESTIGATIONS OF
N.V. PHILIPS' GLOEILAMPENFABRIEKEN

EDITED BY THE RESEARCH LABORATORY OF N.V. PHILIPS' GLOEILAMPENFABRIEKEN, EINDHOVEN, HOLLAND

PROPERTIES AND APPLICATIONS OF ARTIFICIAL RESIN PRODUCTS

By R. HOUWINK.

Summary. The chemical nature of artificial resins is briefly outlined with the principles on which their manufacture is based. As artificial resins are *per se* electrical insulating materials, this property is compared with that for other insulators; the differences between "Philite" and other insulators are also referred to. Various applications of "Philite" resins are then enumerated and discussed, followed by reference to products with special properties designed to meet the specific requirements of the consumer.

Introduction

The progressive development and expansion of the electrical industry has led to an increasing demand for cheaper and better raw materials. That the demand has not by any means been met is shown by the call for materials with low dielectric losses (low values of tan δ), which during recent years has become very heavy in view of developments in short-wave technology. The demand is not merely for an insulating material *per se*, for the material required has also to meet a host of other requirements. For example a material, such as mica, which has an exceptional suitability for making certain articles is yet frequently found useless in mass production as soon as it becomes a question of making units of complicated shape by an inexpensive process and which have to be within close dimensional tolerances. It may be noted that these requirements present insulating technology with entirely new problems, especially as the consumer is not merely concerned with the insulating properties and the mechanical strength, but frequently makes a point of specifying a pleasing appearance, which can only be obtained by very complex and highly perfected finishing processes.

In this article we will show that one of the chief reasons why "Philite", an artificial resin, which can be readily shaped by hot pressing, has found extensive applications is mainly because it can satisfy a host of practical requirements at one and the same time. *Fig. 1* shows a selection of "Philite" products, and brings out the wide variety of objects into which this material can be moulded and for which it can be utilised.

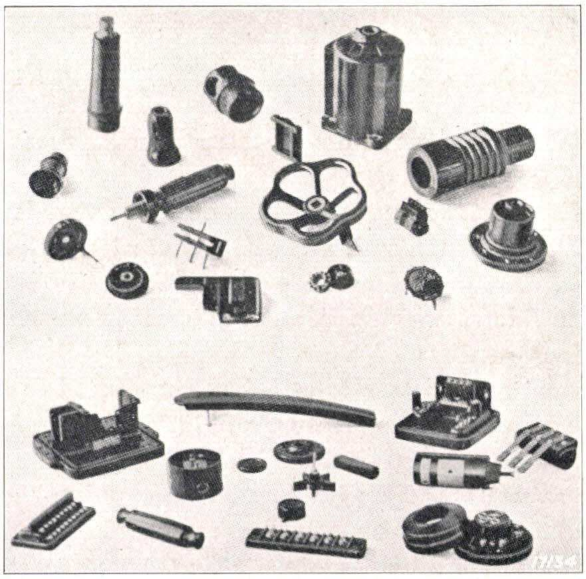

Fig. 1. Various "Philite" products for technical uses.

Basis of Manufacture of Artificial Resin

Even twenty years ago resinified products obtained by chemical reaction were disposed of as useless waste. At the present time the exact reverse is the case, and in a large number of industrial laboratories systematic search is proceeding for still further artificial resins. Of the great variety of artificial resins which have been evolved in recent years, consideration will be limited here to the phenol-formaldehyde resins, since these form important constituents of various types of Philite materials. It would lead too far to discuss in detail the chemistry of these resins, although an attempt will be made with the aid of *fig. 2* to explain the fundamental principles on which the formation of such a resin is based. If phenol and formaldehyde are caused to interact at a high temperature, then as shown in fig. 2, the molecules of these bodies combine to form a reaction product which in the figure is denoted by the word "resin". It is seen that by condensation a very large molecule is produced, and the assumption is justified that a pressed product of artificial resin (apart from fillers, which for various reasons must be added) consists of a single large molecule. This gradual growth to a so-called macro-molecule is the basis of manufacture of "Philite" materials. If we remember that the initial materials are fluid (or at least solids with low melting points) and the final product is a hard mass resembling ebonite in appearance, it is evident that in the course of the finishing process considerable changes must have taken place. In practice it may be observed that the transition to the solid finished product takes place very gradually. At first the phenol and formaldehyde form a resin-like viscous fluid, which on further heating gradually hardens to a consistency comparable to that of asphalt, finally being converted into a very hard and infusible end product. The essential factor here is the formation of an asphaltic intermediate product, for in this stage the mass can be readily liquified in heated matrices (150 °C.) under hydraulic pressure, the artificial resin filling every corner of the matrix or mould. If the body is kept at this high temperature for a few minutes longer the hardening process already referred to takes place, with the result that the mass hardens in the mould and can therefore be removed from the warm mould without the latter having to be cooled.

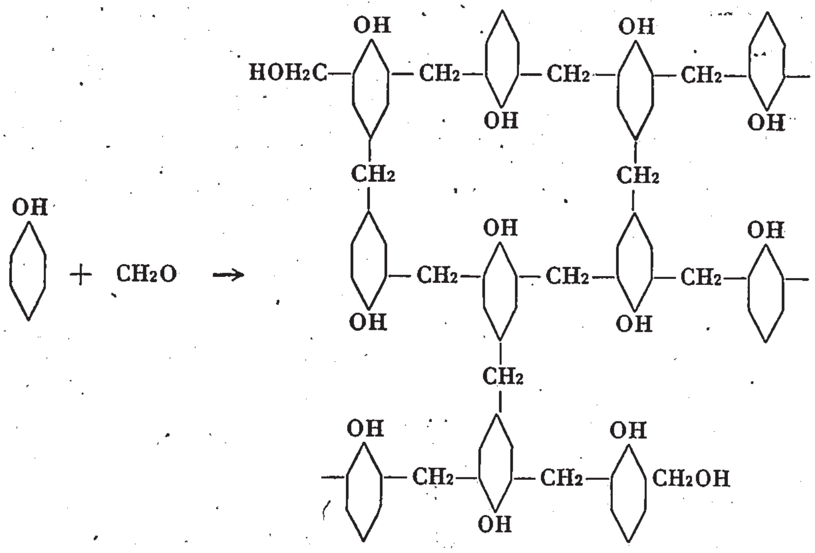

Fig. 2. Formation of phenol-formaldehyde resin. This method of representation is purely diagrammatic. The benzene nuclei must be regarded as arranged specially and linked to one another in some sort of haphazard arrangement, without giving a "pattern" as indicated in this figure.

The moulding process in the case of artificial resins is thus fundamentally different from that employed with metals, such as cast iron, which is molten and then poured into a cold mould in which it is allowed to cool. The raw material for "Philite" is introduced into a hot mould in which it hardens as a result of chemical reaction specifically promoted by the application of a high temperature.

To make this important characteristic still more clear, compare the moulding process employed with that which must be used for producing moulded articles from a substance, such as asphalt.

Asphalt can also be liquified by placing into a hot mould and applying a pressure, although there is here no chemical reaction which results in a hardening process taking place. Hence to remove the shaped asphaltic article from the mould, the latter must be cooled and again reheated before pressing of the succeeding article can commence. With artificial resin this is naturally unnecessary, thus considerably accelerating the process of manufacture. But, as in most cases this advantage is not obtained without overcoming certain difficulties, since to obtain a satisfactory shape very high pressures are required of the order of 300 kg/sq cm. The matrices thus have to sustain very high stresses and for this reason are usually fairly expensive.

Fig. 3 shows the variations in certain properties of the artificial resin with time during the pressing process. It is seen that the tensile strength, as well as the stability to heat, increases considerably. This is readily accounted for by a further glance at the reaction product shown in fig. 2 and when it is remembered that the various chemical bonds in this molecule have a high energy value (100 to 200 kilo-cals per gr. equivalent). The significance of this is that a considerable amount of energy has to be absorbed either in the form of mechanical or thermal energy to split these bonds again, thus accounting for the mechanical and thermal stability.

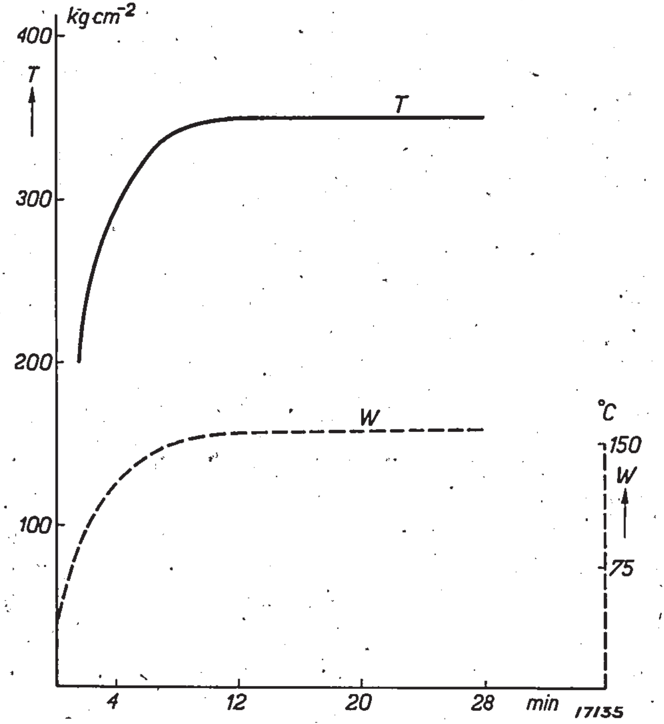

Fig. 3. Increase in the tensile strength T and the stability to heat W of an artificial resin with increasing duration of pressing.

In this brief survey we have limited ourselves merely to the artificial resin constituent and have made no mention of the fillers in "Philite", since a discussion of these latter does not enter into the scope of the present article. In this connection it may, however, be mentioned that these fillers have a marked effect on both the electrical and the mechanical properties of the finished material, such that by a rational combination of various types of artificial resins and different fillers a very varied range of products can be obtained. This is indeed one of the reasons why "Philite", as already indicated, can frequently be very easily adapted to meet specific requirements.

Comparison with other Insulating Materials

It has already been pointed out that "Philite" is able to satisfy simultaneously a number of different requirements and just for this reason it is frequently better than other insulating materials. To obtain a closer insight into this comparison the principal requirements generally determining the choice of an insulating material have been collated in Table I. This summary is, of course, not complete since in the first place a comparison is limited to merely some of the principal properties. Other properties entering into question will be indicated later, as well as the position of "Philite" in respect of these.

The most important property of interest in insulating materials, the disruptive strength, has in the case of *Philite S* the not too high value of approx. 8 kV per mm. For ordinary low-voltage applications this disruptive strength is however quite adequate, the difference as compared with the higher values given for the three other materials being of no special moment. In fact where for high-

Table I. Comparison of the Properties of Different Insulating Materials

	Tensile strength	Impact value	Stable up to temperatures of		Disruptive strength	Specific gravity	Tolerances	Ease of surface treatment
			Long periods	Short periods				
	in kg cm^{-2}	in kg cm^{-2}	°C	°C	in kV mm^{-1}	gr/cm^3	%	
"Philite" moulding material (Type S)	350	7	140	160	8*	1.35	0.2	Good
"Philite" sheet material (Philitax)	750	30	140	150	25	1.35	—	Good
Porcelain	300	2	about 1000	about 1000	30	2.5	1	Bad
Cellulose derivatives (Philite A)	300	50	50	50	50	10	1.3—1.6	Very good
Ebonite	400	10	60	60	10		1.1—1.7	Very good

*) Other types of "Philite" have a higher disruptive strength, up to 30 kV/mm.

tension purposes, a greater value is desirable this can also be met as shown in Table II.

With the aid of Table I let us compare the other principal properties of other insulating materials with those of "Philite" S. Consider first the mechanical strength as expressed by the tensile strength and the impact value; it is seen that porcelain has a very low impact value of 2 kgcm per sqcm, the wellknown fragility of porcelain making it in fact quite unsuitable for many purposes. Again as regards stability to heat it is observed that just those bodies, such as cellulose derivatives and ebonite, which have quite satisfactory mechanical values, give low values for this property, mainly because the maximum temperature they can sustain is below 100 °C., a temperature level which is of very great importance in technology. In this respect porcelain naturally offers a quite unmistakable advantage, which organic bodies, such as the artificial resins, can perhaps never hope to equal. This range of high temperatures will, it appears, therefore remain the preserve of the inorganic substances; but the applications at which such a high temperature level is not required are so numerous that a very wide field still remains for the organic insulators. And just in these applications the various kinds of "Philite" can prove of inestimable value, since e.g. specific temperature requirements in the tropics can be very readily met, even if an extra although not excessive amount of heat is evolved in the electrical apparatus itself.

As regards the dimensional tolerances which can be obtained in the products, a factor frequently of paramount importance, it is well known that in mass production the choice of a material is often determined by the tolerances within which a moulded product can be made. This is another reason why very often porcelain is rejected in favour of "Philite" S with its fivefold smaller tolerance of approx. 1 per cent., particularly as porcelain, as indicated in the last column, is very difficult to work, so that any deviations in dimensions are difficult to correct.

On the whole the principal advantages of "Philite" over porcelain are its greater impact strength and its greater accuracy in workmanship. Other advantages are its low specific gravity, its pleasing appearance and the wide range of colours in which it can be made. "Philite" is of the same colour throughout and is not merely covered with a thin varnish which can be readily damaged.

For outdoor use and under conditions in which temperatures exceeding 150 °C. may occur, porcelain is naturally to be preferred to "Philite".

Comparing "Philite" S with cellulose derivatives and ebonite, the very low stability to heat of the two latter is the chief reason for serious objection being frequently raised against their use. It is thus seen that each of the insulating materials listed possesses at least one important property which does not compare with that of "Philite" S.

In addition to its suitability for making all standard moulded products, "Philite" can also be employed for making special compound products in which metal or other parts are pressed into the material. *Fig. 4* shows a radiograph of a moulding where the metal component has been completely embedded in the "Philite". *Fig. 5* shows diagrammatically how such a metal part, here a threaded nut *M*, is pressed into the "Philite". The nut is placed on the pin *P* of the opened matrix *O*, which is then filled with the powdered raw material (*Ph*) (Fig. 5b). During pressing the mass does not fill all the cavities in the matrix but also flows round the metal parts (fig. 5c). Fig. 5d shows how the

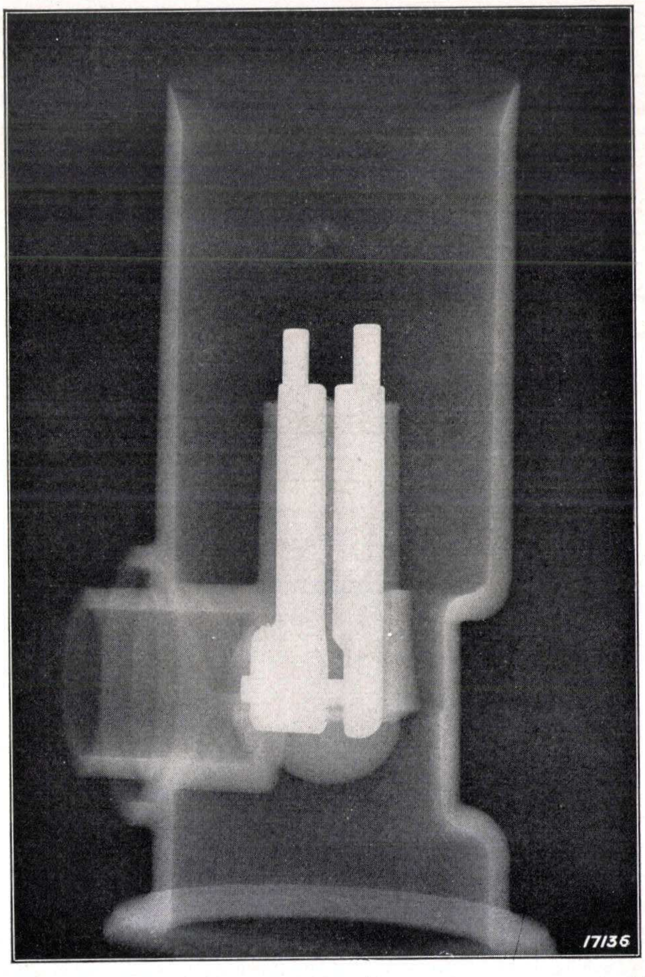

Fig. 4. Radiograph of a moulded product made of "Philite" into which metal parts have been pressed (shown white in the picture).

"Philite" (*Ph*) after hardening in the matrix has completely surrounded the brass nut *M*, holding it firmly. Here again it is possible to work to narrow tolerances, for the position of the brass nut is determined entirely by the pin *P*, which is attached to a solid part *O* of the matrix. This method of embedding metal parts is much simpler than the process employed in which holes are first drilled in the moulded article and the metal part then secured by putty or screwed in.

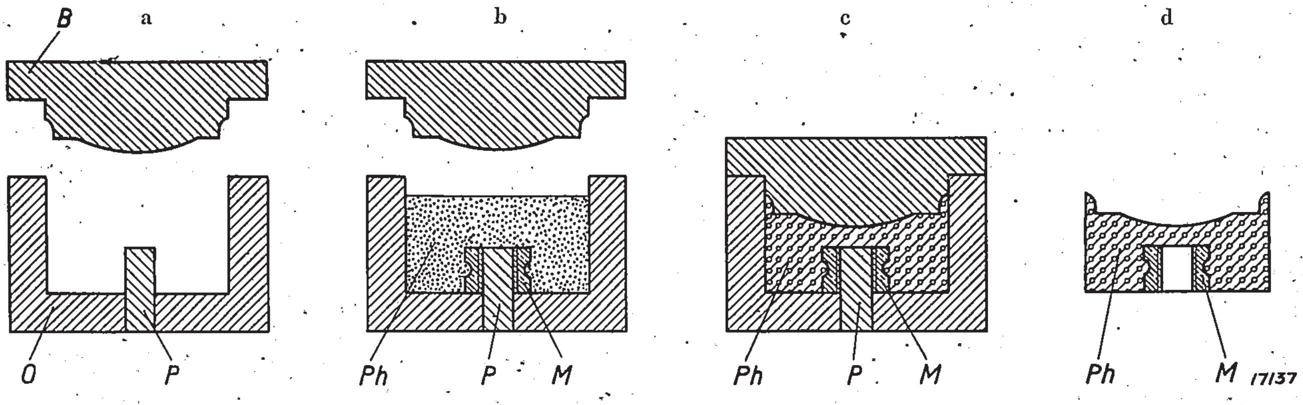

Fig. 5. Manufacturing process for pressing in a brass nut *M* into "Philite" *Ph* which is moulded by pressing in a lower matrix *O* and an upper matrix *B*.

a) Matrix open.
b) Inserting the brass nut *M* and filling with raw mixture.
c) Closing the matrix.
d) Finished product with embedded nut.

Special Kinds of "Philite"

In the following, brief reference will be made to several variaties of "Philite", each of which differs in some particular or other from "Philite" S referred above, the latter being regarded as a standard of comparison.

It is evident that in view of the wide variety of demands which technology makes as regards an insulating material it is practically impossible to find a single substance which will satisfy every single requirement. For this reason a large range of special types of "Philite" have been evolved and are employed for various products. *Table II* gives a survey of a selection of these varieties and also includes, to facilitate comparison, the corresponding properties of the standard "Philite" S. For the other kinds of "Philite", figures are only given where the relevant properties differ appreciably from those of "Philite" S.

Tabel II. Some of the Principal Properties of Special "Philite" Products *)

	Tensile strength	Impact value	Stable up to temperatures of (long period)	Disruptive capacity	Tan δ in 10^{-4} at 200 m ($1.5 \cdot 10^6$ cycles)	Other characteristics
	in kg cm^{-2}	in kg cm cm^{-2}	in °C.	in kV mm^{-1}		
"Philite" S	350	7	140	8	500	See Table I.
"Philite" I	—	—	180	1 tot 5	—	For high temperatures.
High-tension "Philite" . . .	—	—	—	30	—	High tension material for indoor situations.
High-frequency "Philite" P	—	—	60	20	2 tot 5	20 000 per matrix and per week; not stable to heat.
High-frequency "Philite" 160 (in various kinds)	Between 200 and 300, according to kind	—	180	30	55	General high-frequency use.
Flaked "Philite"	—	10—15	—	about 1	—	High impact strength.
"Transphilite"	—	—	—	—	—	Transparent.
Acidproof "Philite"	—	—	—	—	—	*Inter alia*, unattacked by strong HCl, 30 per cent sulphuric acid and HF.

*) For the sake of simplicity only those values are given for each material which differ considerably from the corresponding values for "Philite" S. On application the exact values for the properties of each specific material will be gladly supplied.

The first requirement specified by users of artificial resins is their ability to withstand high temperatures. It is obvious that in the case of an organic body, such as an artificial resin, the same high stability cannot be attained as with, for instance, porcelain. Nevertheless a satisfactory stability to prolonged heating up to 180 °C. can be attained as indicated for "Philite I" in Table II, and which is quite satisfactory for a large number of technical applications.

The very frequent demand for a material with a very high electrical disruptive value is met by *High-Tension Philite* which has a disruptive strength of 30 kV per mm, a value roughly the same as that for porcelain. Although the use of this material is limited to indoor locations, it yet offers many advantages over porcelain in view of its high mechanical stability and the low dimensional tolerances to which it can be worked, as well as the ease with which metal parts can be pressed into it, so much so that it has already found very extensive use.

Two types of high-frequency "Philite" have been evolved to meet the increased demand for materials with low dielectric losses. *High-frequency Philite P* with a value of $\tan \delta = 2$ to $5 \cdot 10^{-4}$ offers exceptional advantages in this respect, and enables values to be obtained which are nearly equal to the best other materials in this class, such as mica and quartz, but which are not susceptible to moulding. On the other hand, this material has the disadvantage that its stability to heating is low, viz., about 60 ° C. To overcome this difficulty *High-Frequency Philite 160* was evolved which can be produced with different tensile values, and similarly to "Philite I" can withstand heating to a temperature of 180 °C. Although this advantage has been gained to a certain extent at the expense of the phase difference, yet $\tan \delta = 55 \cdot 10^{-4}$ as compared with "Philite S" ($\tan \delta = 500 \cdot 10^{-4}$) is so low that Philite 160 still has many practical applications.

The mechanical strength will naturally always remain an important consideration, especially as "Philite" has in recent years become extensively employed in directions other than those for which it was originally intended, viz., as an insulating material, and in these supplementary applications properties entirely foreign to good insulation have been required. The impact value of 10 to 15 kg-cm per sq cm of "*Flaked Philite*" closely approaches that of various kinds of wood, and components made of this material thus possess very high mechanical values. Whilst the insulation properties have become slightly reduced, the final product is still an insulating material with exceptional impact strength.

"*Transphilite*" is a material which is made with a variety of transparent colours and is used for certain lighting fittings.

A special "Philite" product which must be mentioned is the *acid-proof variety of "Philite"* which has been evolved for use in chemical works, being practically unattacked by various concentrated acids. It is interesting to note that contrary to glass this product is not attacked by hydrofluoric acid, and in view of this property it is frequently employed in place of glass.

Flat sheets of "Philite"

Up to the present reference has been limited to artificial resins which could be moulded to any desirable shape. In addition there is a series of artificial resins which are only suitable for manufacturing flat sheets which can be easily cut with the saw. Sheet "Philite" is supplied in various kinds, distinguished for exceptional mechanical properties, in this respect being comparable to wood.

"Philitax", whose principal properties are enumerated in Table I, is one of the best materials for making insulating sheets. In small thicknesses (e.g. 1.5 mm) it can be easily cold stamped, as well as hot stamped up to a thickness of 7 mm. In this way simple mass-production articles can be produced from it as shown in *fig.* 6, and similar to stamped metal plates and sheets. It is not only extensively used in the construction of switchboards, but also for interior components in a large range of electrical apparatus since owing to the ease with which it can be worked it combines cheapness with desirable mechanical and electrical properties, without requiring expensive matrices.

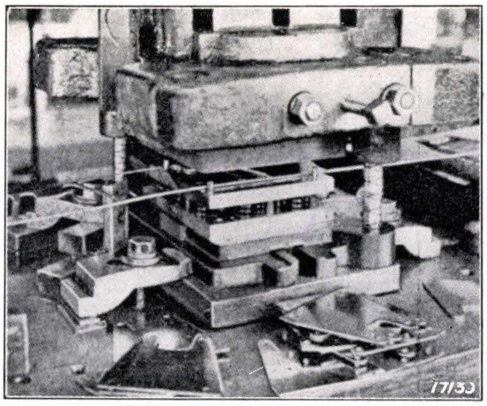

Fig. 6. Stamping of articles from "Philitax" sheet material.

"Philitext" meets the need for a very high impact value, which in the case of this material is 50 kg cm cm^{-2}. Electrically, this material is not quite comparable to "Philitax" whose electrical characteristics are high; it has become widely adopted since it is suitable for manufacturing bearings which can be water lubricated, as well as for making silent gear wheels, a selection of which is illustrated in *fig. 7*. In these directions in particular "Philitext" offers a number of still further potentialities. It should be mentioned in this connection that the friction of bearing materials made with artificial resin as a base is roughly comparable to that of good bearing metals (coefficient of friction 0.1). In addition artificial resins have the advantage of being unattacked by acids and alkalies, permitting lubrication with water and offering a long life.

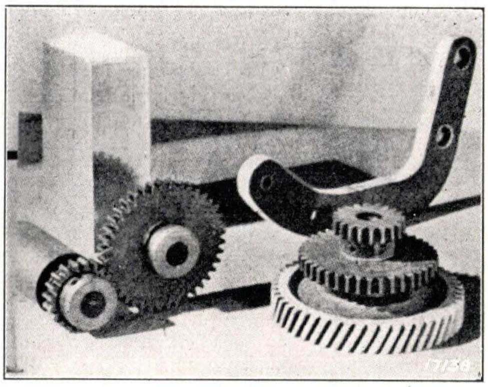

Fig. 7. Silent gears made of "Philitext".

This brief outline of the characteristics and properties of the "Philite" range of artificial resins will suffice to indicate to what extent the varied requirements of consumers can be met. Technological advances, however, continue to be made and it may be confidently expected that in the course of the next few years further additions will be made to the comprehensive list of existing "Philite" products and which will in their turn meet other specific requirements.

IMPROVEMENTS IN RADIO RECEIVERS

By C. J. VAN LOON.

Summary. Two important improvements in radio receivers, viz., touch tuning and low-frequency counter-coupling, are discussed in detail.

In touch tuning sharp tuning is indicated by the turning of the tuning knob suddenly becoming stiffer; in the circuit employed a braking magnet which brakes the tuning-knob shaft is magnetised on sharp tuning. This device has been supplemented by an arrangement which by mechanical means keeps the set perfectly silent as long as no station has been sharply tuned in.

With low-frequency counter-coupling the distortion occurring in low-frequency amplification is reduced to a small fraction of its value in the absence of counter-coupling, the frequency relationship of amplification being favourably influenced at the same time.

Introduction

The most important characteristics of radio receivers are unquestionably their purity of reproduction, their selectivity and their sensitivity. In the course of the technical development of receiving sets the quality of reproduction has been improved in various directions, thus the acoustic reproduction of the loudspeaker, which during the first few years of broadcasting was limited to a comparatively narrow range of audio-frequencies, has steadily been improved upon such that a range of for instance 40 to 10 000 cycles/sec. can now be reproduced with satisfactory uniformity. Furthermore, the technical design and construction of the various amplifying stages in a receiver and the outputs of the amplifying and output valves have been raised to a high stage of development, these advances being naturally also to the marked advantage of purity of reproduction.

Controllable Band Width

Similar far-reaching improvements have also been achieved in regard to the selectivity of sets, such refinement having become indispensable under present-day conditions of broadcasting with powerful transmitters utilising frequencies which are extremely to those employed by weak stations. On the other hand, however, a very high selectivity cannot be coupled with the requisite purity of reproduction. A small resonance curve as shown in *fig. 1a* results in the side bands of the incoming signal being damped, so that high modulation frequencies are far too weak and reproduction sounds heavy or "flat". An improvement is obtained by making the resonance curve less sharp (see *fig. 1b*), when as large as possible a portion of the side bands is transmitted undamped. Further investigations in this direction have led to the so-called "controllable band width" which is used to an increasing extent in superheterodyne receivers. By adjustment of the coupling between the circuits in the intermediate frequency section, the resonance curve can be made narrower (as shown in fig. 1*b*) or wider (as in *fig. 1c*) just as required. A wide transmission band is employed where a high selectivity is not required, since the transmitter tuned in is powerful or there is no interference from adjoining stations; the high audio-frequencies are then not weakened so that reproduction is of an exceptionally high quality. Where a high selectivity is required under the conditions ruling, a narrower transmission band is chosen, which

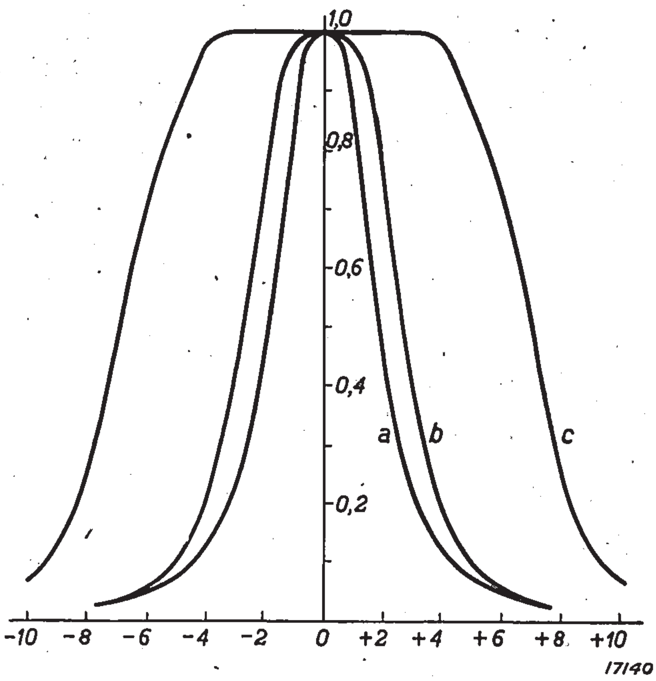

Fig. 1. Resonance curves, with intensity plotted as a function of the detuning in kilocycles.

a) Small resonance curve; the higher modulation frequencies are reproduced much too weakly.
b) Smoother resonance curve: a greater part of the side bands is transmitted undamped and the selectivity is lower.
c) Example of a resonance curve as obtained with controllable band width on adjustmant to "wide".

however unavoidably leads to a loss of the high notes.

Automatic Volume Control

An improvement which has been incorporated in a large number of radio-receiving sets for several years is the automatic control of volume, consisting in producing an automatic decrease in the amplification of a set as the signal at the detector becomes more powerful. The marked differences between the input signal voltages (a medium-strength signal, for instance, gives 0.1 millivolt in the aerial, and the signal from a powerful local station, 500 millivolts) are reduced considerably in the set itself by the automatic volume control.

The pronounced advantages of automatic volume control both as regards fluctuations in the strength of the station tuned in (fading effects) and when listening in to a number of stations of different outputs in succession, are too well known to require detailed discussion. Such control, however, introduces a number of difficulties; for instance it is more difficult with an A.V.C. to determine sharp tuning of a station. In receiving sets without automatic volume control sharp tuning presents no difficulty, for tuning by ear is merely continued until a maximum volume of reception is obtained. On the other hand, accurate, audio-tuning is much more difficult in those sets equipped with automatic volume control and also having a resonance curve with a flat peak; on slight detuning of the set there is no detectible difference in volume since automatic control compensates for any reduction.

It thus becomes necessary to employ as a criterion of correct tuning a maximum volume of the low notes or a minimum of distortion. This method of tuning requires, however, considerable skill with the result a set of this type is frequently flat tuned, thus affecting the purity of reproduction owing to the absence of the low notes and the occurrence of distortion.

"Touch" Tuning

It is not surprising, therefore, that means have sought to eliminate these difficulties and which would indicate in a simple manner when sharp tuning was realised. One method evolved for this purpose was that of "visual" tuning in which a maximum or minimum deflection of a pointer was obtained when tuning was sharp. Circuits were also evolved with which, as in early receiving sets, a fairly definite maximum volume was obtained when sharp tuning was attained so that tuning was again an audible process. In this laboratory an entirely new method of tuning has however been developed, viz., a method of "touch" tuning, which considerably facilitates accurate adjustment. Sharp tuning is here indicated by a sudden braking of the tuning knob, being achieved by means of a circuit in which as sharp tuning is approached there is a sudden increase in current which is utilised to hold the tuning shaft by means of a magnet. An arrangement can also be quite easily incorporated with this circuit which by mechanical means keeps the receiver completely silent until it has been sharply tuned to the station (socalled "silent" tuning); as soon as the braking magnet is energised a contact is closed at the same time which connects up the loudspeaker system. In this way "touch" tuning is combined with "silent" tuning.

We shall discuss the operation of the "touch" tuning circuit with the aid of a number of diagrams. Assume that the receiving set which has to be equipped with the "touch" tuning system is a heterodyne receiver of the type shown diagrammatically in *fig. 2*.

When the set is sharply tuned the high-frequency portion is adjusted to the frequency of the incoming signal and at the same time the oscillator tuned to a frequency such that the differential frequency generated in the mixer valve is exactly equal to the intermediate frequency f_0 to which the intermediate-frequency portion is tuned. On a slight departure from the sharp-tuning position by giving the tuning knob a little turn, the oscillator becomes detuned. The differential frequency has thus been altered and no longer coincides with the intermediate frequency. The circuits in the high-frequency portion are also detuned, so that in consequence there is a slight change in the amplitude of the signal passed to the mixer valve. If detuning is not excessive, then owing to the operation of the automatic volume control it may be expected that to a first approximation a signal whose frequency varies while the amplitude remains substantially the same will be obtained at the output of the intermediate-frequency amplifier, i.e. at P; on sharp tuning the frequency is exactly equal to the intermediate frequency f_0.

The circuit shown in *fig. 3* is now connected to P through a small condenser C_1. This arrangement consists of a circuit ($L\,C\,r$) which is tuned to the intermediate frequency f_0. The oscillating alternating voltage in this circuit is rectified by the diode D, so that a direct voltage is obtained at

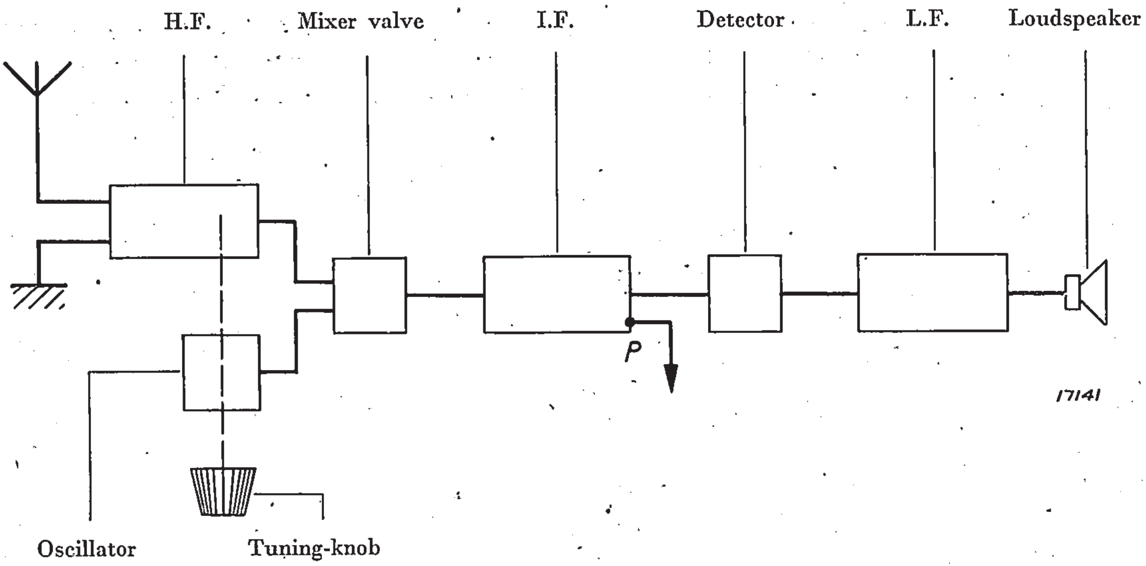

Fig. 2. Circuit of a super-heterodyne receiver. The intermediate-frequency signal for touch tuning is tapped from the point P.

the resistance R, which is by-passed by the condenser C_2. R is also connected in series with a direct-current source V_B whose negative pole is connected to the anode, so that in the absence of alternating voltage in the circuit the anode of the diode is negative with respect to the cathode. It should be noted that a rectified current only commences to flow when the amplitude of the alternating voltage is greater than the threshold voltage V_B.

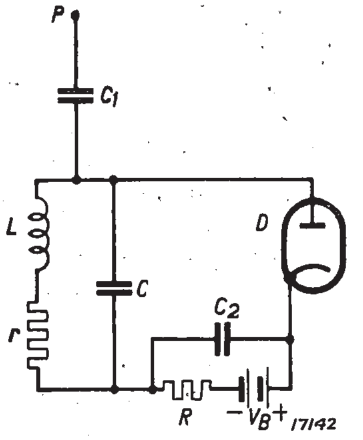

Fig. 3. Equivalent circuit for "touch" tuning. On sharp tuning of the set a voltage is obtained at P (see also fig. 2) which is passed through C_1 to the oscillating circuit LCr tuned to the intermediate frequency; on sharp tuning the voltage in this circuit is greater than V_B so that the diode D with which the threshold voltage V_B is connected in series acts as a rectifier and furnishes a direct voltage at the resistance R which serves for operating a braking arrangement. As detuning becomes greater the voltage in circuit LCr become smaller, so that from a certain degree of detuning V_B prevents rectification and the brake no longer operates.

When the receiver is sharply tuned pole P, as we have seen, will have a voltage with the frequency f_0. The voltage resulting therefrom in the oscillating circuit will have an amplitude V_0. On slight detuning the amplitude of the voltage in P will remain practically unchanged. If the frequency is altered to $f_0 + \Delta f$ (or $f_0 - \Delta f$) the circuit voltage will then drop to:

$$V_o \frac{1}{\sqrt{1+\left(\frac{4\pi\Delta f}{r/L}\right)^2}} .$$

If $V_0 > V_B$ the diode will pass current at tuning and a direct voltage will be produced at R. On detuning this current ceases to flow as soon as Δf reaches a limiting value Δf_{lim} as expressed by the equation:

$$V_o \frac{1}{\sqrt{1+\left(\frac{4\pi\Delta f_{lim}}{r/L}\right)^2}} = V_B \quad . . . (1).$$

Thus by a suitable choice of the threshold voltage V_B it is possible to determine in what frequency range on both sides of the resonance frequency f_0 rectification will occur and a direct voltage be obtained at resistance R. This direct voltage can, for instance, be utilised for modulating an amplifying valve such that a magnet inserted in the anode circuit of this valve will brake the tuning-knob shaft.

By this method "touch" tuning of stations of a specific strength becomes possible. But if a station is chosen with e.g. a much greater strength, the voltage in P, in spite of automatic volume control, can be as much as several times greater than in the case just considered. As a result the frequency sweep over which "touch" tuning is effective will also increase. Consider the example of a circuit in which $r/L = 6280\ \mathrm{sec}^{-1}$ and $V_B/V_0 = 0.86$. From equation (1) we get $\Delta f_{lim} = 300$ cycles/sec. If for a more powerful station V_0 is, say, twice as powerful, V_B/V_0 will be 0.43 and hence Δf_{lim} will be 1050 cycles/sec. The range over which touch tuning operates thus varies fairly considerably for transmitters of different strengths, so much that the tuning knob in the case of the powerful stations becomes already braked at an excessive distance from the sharp-tuning position.

This difficulty may be overcome in the following way. It follows from equation (1) that for a given value of r/L the term Δf_{lim} will also have a definite value, provided the ratio of V_B to V_0 is unchanged. This would be the case if in the circuit shown in fig. 3 the threshold voltage V_B were not constant but increased in proportion to V_0. *Fig. 4* shows how this is achieved and represents two circuits, *I* and *II*, which are both tuned to the intermediate frequency, as well as two rectifying diodes. C_3 is a small condenser.

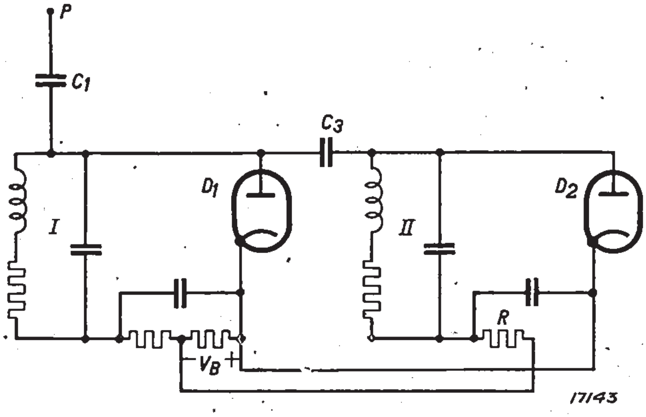

Fig. 4. Improvement of the circuit shown in fig. 3. The voltage of circuit *I* is rectified by the diode D_1. A part of the direct voltage obtained serves as the threshold voltage V_B for the second rectifying circuit (circuit *II*, diode D_2, resistance *R*). By means of this circuit the diode D_2 always rectifies in the same frequency range on both sides of the sharp tuning position, almost independently of the signal strength in *P*.

The diode D_1 rectifies the voltage in circuit *I*, part of the rectified voltage constituting the threshold voltage V_B for the rectifying circuit of D_2. This circuit ensures that the rectifying action of the diode D_2 always commences at the same degree of detuning Δf_{lim} irrespective of the signal strength in *P*, whereby a direct voltage is obtained at the resistance *R* which through an amplifying valve energises the braking magnet.

In the practical design of this arrangement as shown in *fig. 5* circuit *I* is not connected directly to *P* in the intermediate-frequency section, but is linked up through an amplifying valve *L*. Valve *L* is modulated by the rectified voltage at *R*; in the sharp tunning range the voltage at *R* makes the grid of *L* more negative so that the relay inserted in the anode circuit of *L* trips and thus closes a contact in a circuit which energises the braking magnet. If the relay simultaneously closes a second contact, for instance for switching on the loudspeaker, a "silent" tuning system is arrived at in a very simple way.

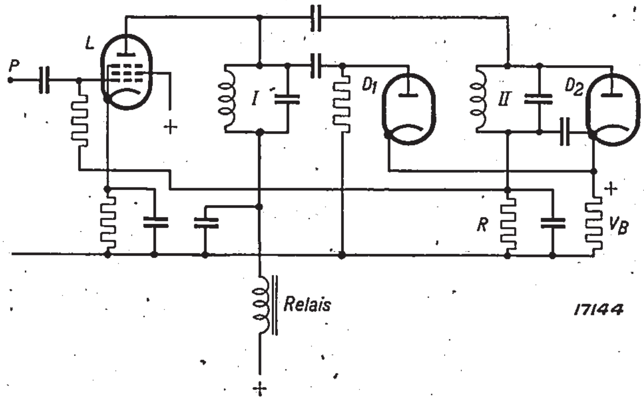

Fig. 5. Practical design of a circuit for touch tuning. Circuit *I* (cf. also fig. 4) is not connected directly to the intermediate frequency portion at *P* but through an amplifying valve *L*. The direct voltage obtained at *R* on sharp tuning is passed to the grid of *L* and reduces the anode current in this valve; as a result the relay trips and the brake comes into operation.

Fig. 6 gives a view of the braking system where an iron disc is attached to the tuning-knob shaft opposite to the braking magnet. This disc is secured on the shaft by a spring and cannot be turned about the shaft but only displaced along it, so that it is attracted towards the braking magnet when the latter is energised

Counter-coupling

Brief reference has already been made above to the fact that developments in radio valves, and in particular in output valves, have also included an improved purity in reproduction. The immediate means for reducing the distortions in reproduction has appeared to be the introduction of high-output last-stage valves. At the same time a circuit was evolved in this laboratory, which has been employed in a variety of receiving sets and which may be termed that of low-frequency counter-coupling. With this circuit the distortion occurring in the low-frequency part of a receiver is reduced to a very small fraction of its initial value, while at the same time the frequency characteristics of reproduction are also favourably influenced.

If an alternating voltage V_g is applied to the grid of an output valve, an amplified alternating voltage V_a will occur at the load resistance in the anode circuit. A part $n\ V_a$ of this output voltage can be fed back to the input circuit. If this fedback voltage is in phase opposition to the input voltage V_i we can speak of counter-coupling (or opposed coupling). The amplification is reduced by this counter-coupling, as well as the distortion in almost the same ratio.

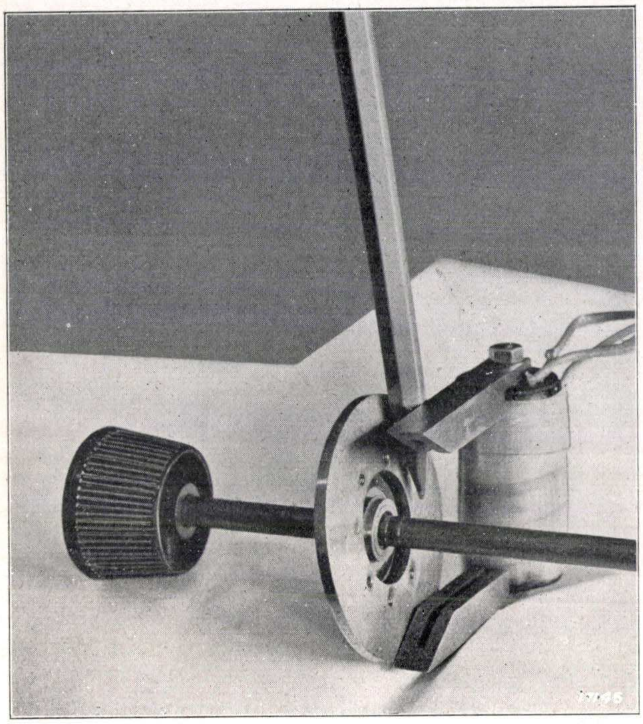

Fig. 6. Brake. An iron disc is fixed on the tuning-knob shaft opposite to the braking magnet. The disc is attached to the shaft by means of a specially-shaped spring and is thererefore constrained to move along the shaft only, so that it is drawn towards the brake magnet when the latter is energised.

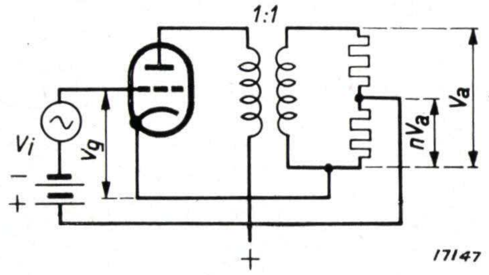

Fig. 7. Circuit of a counter-coupled output valve. A part $n\ V_a$ of the anode alternating current V_a, which is generated by the grid alternating current V_g, is fed back to the grid in phase opposition to the input voltage V_i.

The circuit of a counter-coupled output valve is shown in *fig.* 7; the load is not inserted directly in the anode circuit but is connected up through an ideal transformer with a 1 : 1 ratio in order to be independent of the direct voltage of the anode battery. If the amplification of the valve is m, we have $V_a = m\ V_g$. As furthermore $V_g = V_i - n\ V_a$ we thus get $V_a = m\ V_i - m\ n\ V_a$, or:

$$V_a = \frac{m}{1 + m\,n}\, V_i\,,$$

so that the amplication has been reduced by a factor $(1 + m\,n)$ by counter-coupling. If n is made so great that $m\,n \gg 1$ then V_a will approach the value V_i/n. Thus as the counter-coupling increases the amplification becomes pregressively more independant of m, i.e. of the characteristics of the valve, so that the distortion also becomes steadily smaller owing to the non-linearity of the valve characteristics.

For a closer investigation, express the non-linearity between V_a and V_g as follows:

$$V_a = \alpha\, V_g + \beta\, V_g^{\,2} + \gamma\, V_g^{\,3} + \;.\;.\;.\;.\;.\;.\;.\;.\quad (2).$$

The alternating voltage V_g is equal to $V_{gm} \cos \omega t$, which substituted in equation (2) gives:

$$V_a = \alpha\, V_{gm} \cos \omega t + \beta\, V_{gm}^{\,2} \cos^2 \omega t + \gamma V_{gm}^{\,3} \cos^3 \omega t\ ,$$

To a first approximation¹) this expression may be written as follows:

$$V_a = {}^1/_2\, \beta\, V_{gm}^{\,2} + \alpha\, V_{gm} \cos \omega t + {}^1/_2\, \beta\, V_{gm}^{\,2} \cos 2\, \omega t$$
$$+ {}^1/_4\, \gamma\, V_{gm}^{\,3} \cos 3\, \omega t.$$

We thus have terms containing 2ω and 3ω, i.e. distortions due to the second and third harmonics respectively.

If we denote the amplitudes of the first, second and third-over-tones of V_a by V_{a_1}, V_{a_2} and V_{a_3}, we then get:

$$V_{a_1} = \alpha\, V_{gm},\quad V_{a_2} = {}^1/_2\, \beta\, V_{gm}^{\,2} \text{ and } V_{a_3} = {}^1/_4\, \gamma\, V_{gm}^{\,3}$$

With counter-coupling we get for the relationship between V_i and V_g:

$$V_g = V_i - n\, V_a \quad .\;.\;.\;.\;.\;.\quad (3).$$

Equations (2) and (3) together express the relationship between V_a and V_i. Let us write V_a also as a power series of V_i; to do this we must first "invert" equation (2), thus getting:

$$V_g = \frac{1}{\alpha} V_a - \frac{\beta}{\alpha^3} V_a^{\,2} + \frac{2\,\beta^2 - \alpha\,\gamma}{\alpha^5} V_a^{\,3} + \;.\;.\;.\;.$$

Substituting from equation (3) we find:

$$V_i = \left(\frac{1}{\alpha} + n\right) V_a - \frac{\beta}{\alpha^3} V_a^{\,2} + \frac{2\,\beta^2 - \alpha\,\gamma}{\alpha^5} V_a^{\,3} + \;.\;.\;.\;.$$

After "inversion" this equation becomes:

$$V_a = \frac{\alpha}{1 + \alpha\, n} V_i + \frac{\beta}{(1 + \alpha n)^{\,3}} V_i^{\,2} + \frac{\gamma\,(1 + \alpha\, n) - 2\,\beta^2 n}{(1 + \alpha\, n)^5} V_i^{\,3}\ .$$

which neglecting the small terms as usual may be written as follows:

$$V_a = \alpha \frac{V_i}{1 + \alpha\, n} + \frac{\beta}{1 + \alpha\, n}\left(\frac{V_i}{1 + \alpha\, n}\right)^2 + \frac{\gamma}{1 + \alpha\, n}\left(\frac{V_i}{1 + \alpha\, n}\right)^3.$$

We have thus obtained the non-linear relationship between V_a and V_i with counter-coupling.

In the same way as adopted above we get for the amplitudes of the first, second and third harmonics the following expressions:

---

¹) We neglect $^3/_4\, \gamma\, V_{gm}^{\,2}$ against α

$$V_{a_1} = a\frac{V_{im}}{1 + an},$$

$$V_{a_2} = {}^1/_2\,\frac{\beta}{1 + an}\left(\frac{V_{im}}{1 + an}\right)^2,$$

$$V_{a_3} = {}^1/_4\,\frac{\gamma}{1 + an}\left(\frac{V_{im}}{1 + an}\right)^3.$$

We thus see that to obtain the same output voltage V_{a_1} when introducing counter-coupling an input voltage $V_{im} = (1 + an)\,V_{gm}$ is required, so that the amplification is reduced $(1 + an)$ times; at the same time V_{a_2} and V_{a_3} are reduced in the same ratio.

This is shown graphically in *fig. 8* where for the AL 4 output valve with an anode load of 7000 ohms the distortion with and without counter-coupling is plotted as a function of the energy passed to the anode load; the factor $(1 + a\,n)$, which denotes the degree of counter-coupling was here taken as approximately = 4.

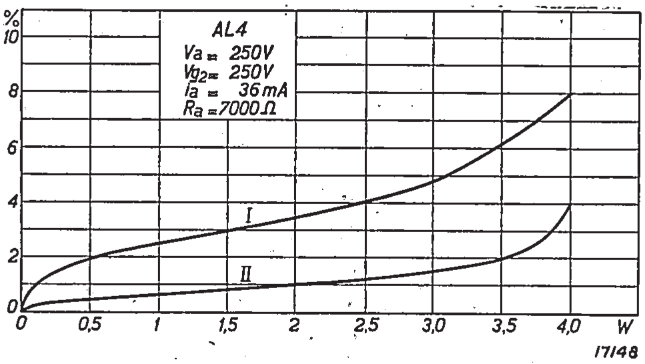

Fig. 8. Distortion in the AL 4 output valve with an anode resistance of 7000 ohms plotted as a function of the power developed in the anode resistance, without counter-coupling (curve *I*) and with fourfold counter-coupling (curve *II*).

In the above discussion we have in every case assumed an anode resistance independent of the frequency. Actually the load is provided by a loudspeaker whose impedance varies fairly considerably with the frequency. At the resonance point, which is usually situated between 50 and 100 cycles/sec. the impedance is a maximum. Above this point it is practically constant over a specific range, increasing again at still higher frequencies. It is evident that this variation in impedance will affect the fluctuations in loudspeaker current or the loudspeaker voltage as the frequency varies and hence also the purity of reproduction. Counter-coupling thus offers a means whereby an arbitrary choice of the frequency characteristic can be made. If for instance for all frequencies the same fraction of the voltage V_a at the load is taken as the counter-coupled voltage, which will correspond to a fixed fraction n, the voltage V_a will vary progressively less with the frequency as the counter-coupling increases; eventually $V_a = V_i/n$, i.e. quite independent of the frequency. If, on the other hand, more powerful reproduction is desirable over a specific frequency range, for instance in the higher notes, the counter-coupling can be so adjusted that it is smaller for the range in question than for other frequencies.

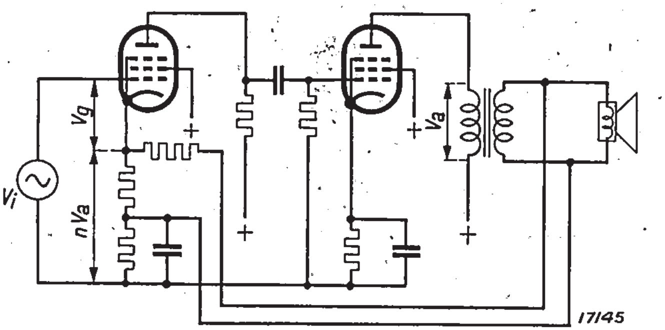

Fig. 9. Circuit for a counter-coupled amplifier in which the voltage is not fed back to the grid circuit of the output valve but to the grid circuit of the preceding amplifying valve.

Fig. 9 shows a further circuit in which the counter-coupling is not applied to the grid circuit of the output valve but to the grid circuit of the preceding amplifying valve. This offers, *inter alia*, the advantage that not only is the distortion in the output valve reduced but also the distortion in the whole of the two-stage low-frequency amplifier.

ELECTRICAL FILTERS II

Vacation course, held at Delft, April 1936.

By BALTH. v. d. POL and TH. J. WEIJERS.

PRACTICAL CALCULATION OF FILTERS WITH SINUSOIDAL E.M.F.

Summary. In this article the characteristics of filter sections are systematically discussed by the method of Campbell and Zobel[1]), in which the filters are defined by their image impedances Z_a and Z_b and the propagation constant T. Some simple fundamental types (T-sections, Π-sections and half-sections) are analysed in detail. From the characteristics of the filter sections the characteristics of compound filters can be directly derived, the filter sections of the latter being closed by their image impedances. Particularly useful for obtaining a systematic survey of the subject is a study of filters composed of non-dissipative impedances (inductances and capacities). In these cases there are sharply-defined transmission and attenuation bands in the frequency range. In the sections dealing with the m_T-transformation and the m_π-transformation, a method is outlined for deriving from T-or Π-sections a series of new filters having the same image impedances and transmission and attenuation bands, but a different propagation constant, the latter being defined by equations (25) and (31). If this transformation is applied to the asymmetrical half-sections only one of the image impedances remains unchanged, the other being altered as determined by equations (24) and (30).

Magnitudes, defining the filters

As indicated in the first article [2]) the characteristics of a filter can be expressed in terms of three parameters. In the following [1]) we shall select for these three parameters the primary image impedance Z_a, the secondary image impedance Z_b and the propagation constant T. The calculation of these magnitudes for a given filter is based on another system of variables whose values can be readily determined, viz., the primary and secondary open-circuit and short-circuit impedances Z_{ao}, Z_{ak}, Z_{bo} and Z_{bk}, which being impedances of simple networks can be easily calculated. After determining these magnitudes we can calculate from them Z_a, Z_b and T using the formulae in the table on pp. 242 and 243 of the previous issue of this Review:

$$Z_a = \sqrt{Z_{ao}\,Z_{ak}}\,; \quad \ldots\ldots \quad (1)$$

$$Z_b = \sqrt{Z_{bo}\,Z_{bk}}\,; \quad \ldots\ldots \quad (2)$$

$$\tanh T = \sqrt{\frac{Z_k}{Z_o}} \quad \ldots\ldots \quad (3)$$

As $Z_{ak}/Z_{ao} = Z_{bk}/Z_{bo}$, in equation (3) this quantity has been abbreviated for the sake of simplicity to Z_k/Z_o. Equation (3) can also be written in the following form:

$$e^{-2T} = \frac{1-\sqrt{\frac{Z_k}{Z_o}}}{1+\sqrt{\frac{Z_k}{Z_o}}} \quad \ldots\ldots \quad (4)$$

In general Z_k and Z_o, and hence also T, are complex. If we put:

$$T = \alpha + j\,\beta$$

we get:

$$\frac{I_2}{I_1} = \sqrt{\frac{Z_a}{Z_b}}\cdot e^{-T} = \sqrt{\frac{Z_a}{Z_b}}\cdot e^{-\alpha - j\beta} \quad \ldots\ldots \quad (5)$$

It is thus seen that α determines the attenuation and β the phase difference between I_1 and I_2.

Filter sections

The design of a filter to meet specific requirements usually consists of a stepwise process of compounding a certain number of filter sections. We shall limit discussion below to the symmetrical T-section, the symmetrical Π-section and the half-section. As already indicated two impedances are all that are required for a symmetrical filter to define the characteristics of the filter. To construct a filter section we therefore start from two impedances Z_1 and Z_2 (*fig. 1a*) which are termed "full branches" and from these build up the sections enumerated in the manner shown in *fig. 1b, c, d* and *e*. If two half-sections are suitably connected in series, we get a symmetrical T-section or a symmetrical Π-section (*fig. 2*). A half-section can therefore be regarded as half a T-section or as half a Π-section.

---

[1]) Campbell, Bell Syst. techn. J., vol. 1, No. 2, 1922. Zobel, Bell Syst. techn. J., vol. 2, No. 1, 1923.

[2]) Cf. Philips techn. Rev., 1, 240, 1936. For the following see the large table line 3, column 3.

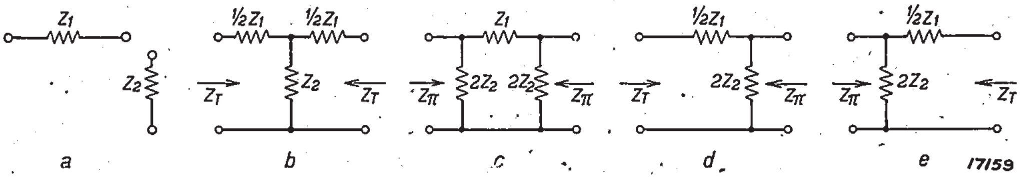

Fig. 1. Filter sections made up of the "full branches" Z_1 and Z_2,
a) Full branches,
b) Symmetrical *T*-section,
c) Symmetrical *Π*-section,
d) Half-section,
e) Half-section.

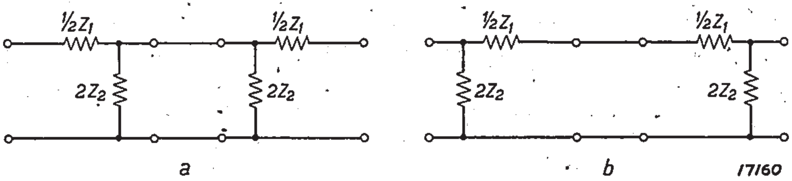

Fig. 2. a) *T*-section composed of two half-sections,
b) *Π*-section composed of two half-sections.

Compound Filters

A compound filter is obtained by connecting individual filter sections in series. The image impedance and the propagation constant of this compound filter may be determined from the corresponding value of the separate sections.

As already pointed out the primary image impedance Z_a is the impedance across the primary terminals *1* and *2* when the secondary terminals *3* and *4* are closed with the secondary image impedance Z_b (*fig. 3*).

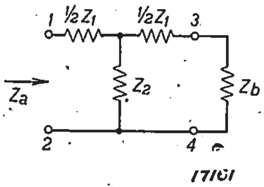

Fig. 3. Filter section, secondary closed with the corresponding image impedance.

It is immaterial how the impedance Z_b is produced; it can, for instance, even consist of a filter with a primary image impedance Z_b, whose secondary is closed by its own secondary image impedance Z_c. In the diagram (*fig. 4*) this second filter is equal to the given filter, so that $Z_a = Z_b = Z_c$; this is naturally not imperative, for the only condition which must be met is that the interconnected image impedances must be equal and the output of the second filter must be terminated with the corresponding image impedance.

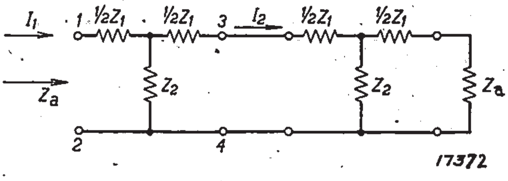

Fig. 4. Filter section, secondary closed with a closed filter section.

In this way filter chains can be compounded of any number of sections, the primary image impedance Z_a of the whole filter remaining equal to the primary image impedance of the first section. Hence the secondary image impedance of the whole filter is equal to the secondary image impedance of the last section. If the image impedance of the sections are different, the image impedance of the compound filter will not be equal to that of the terminal sections and will in general be an irregular, fluctuating function of the frequency. This gives the undesirable result that I_2/I_1 also will vary irregularly with the frequency. Thus in the practical design of filters it is usually to make the two image impedances at the junctions of two sections equal to each other. This is assumed to be so in every case in the following analysis.

The propagation constant T of the compound filter is calculated from the propagation constants $T_1, T_2, T_3 \ldots T_n$ of the individual sections. We have seen above (5) that $I_2/I_1 = \sqrt{Z_a/Z_b} \cdot e^{-T}$. It follows from fig. 4 that the secondary current I_2 of the first section is the primary current of the second section. Similarly the secondary current I_3 of the second section is equal to the primary current of the third section, and so on. For a compound filter made of n sections we have therefore:

$$\frac{I_2}{I_1} = \sqrt{\frac{Z_a}{Z_b}}\, e^{-T_1}\,;$$

$$\frac{I_3}{I_2} = \sqrt{\frac{Z_b}{Z_c}}\, e^{-T_2}\,;$$

$$\vdots$$

$$\frac{I_{n+1}}{I_n} = \sqrt{\frac{Z_n}{Z_{n+1}}}\, e^{-T_n}\,.$$

The continued product of these equations is:

$$\frac{I_{n+1}}{I_1} = \sqrt{\frac{Z_a}{Z_{n+1}}}\, e^{-(T_1 + T_2 + \dots + T_n)} \quad . \; . \; . \; . \quad (6)$$

The propagation constant of the compound filter is hence equal to the sum of the propagation constants of the individual sections.

The relationship between the primary and the secondary currents of the filter is deduced from the assumption that on the secondary side the filter is closed with its image impedance. In practice this is however never the case at all frequencies, so that I_2/I_1 is found to be a non-uniform function of the frequency in the transmitting bands; the deviations from uniform variation will be the greater the greater the secondary terminating resistance deviates from the secondary image impedance. An endeavour must therefore be made to match these two impedances as closely as possible in the transmission bands. As we have already seen, the image impedances of compound filter sections are equal to those of the terminal sections. In the following chapter it will be shown that the image impedance in the transmission band is a pure real resistance, which however varies with the frequency. We shall later discuss several special forms of terminal sections, in which the image impedance throughout the greater part of the transmission band is practically independent of the frequency. If a terminal section of this character is closed by a suitable constant resistance, a very close approximation to the above ideal case is obtained. The very tedious, accurate calculation of I_2/I_1 will not be dealt with in this series of lectures.

We shall study a large number of different classes of filter sections of which a few will have the same image impedances but different propagation constants which vary with the frequency. Filter sections will also be included with propagation constants of the same function of the frequency but with different image impedances. To construct a filter with a propagation constant meeting specific requirements, a number of known types of filter sections are linked up, their choice being such that the sum of the propagation constants of the individual sections gives the requisite frequency function. Furthermore from the sections with the same propagation constant those types are selected that give the same image impedances at all junctions of the sections.

Filters composed of non-dissipative reactances.

Optimum energy conditions are required in the transmission band. If the filter contains resistances energy will be lost so that as a rule a filter will be built up from reactances, self-inductances, capacities and mutual inductances having the minimum possible dissipation. True non-dissipative reactances cannot be realised, but the loss can be reduced to a minimum. We shall therefore first consider some characteristics of ideal filters composed of non dissipative reactances.

For these filters the open-circuit and short-circuit impedances Z_{ao}, Z_{ak}, Z_{bo} and Z_{bk} are imaginary (for certain specific frequencies zero or infinite), as they are impedances of networks composed exclusively of imaginary impedances. Z_k/Z_o as a quotient of two imaginary quantities is however real.

If in a certain frequency band Z_k/Z_o is negative then it follows from equations (1) to (5) that Z_a and Z_b are real and T is imaginary, i.e. $\alpha = 0$. A real impedance in a passive network is never negative, so that Z_a and Z_b are here positive and real. It thus follows from (5) that:

$$\frac{|I_2|}{|I_1|} = \sqrt{\frac{Z_a}{Z_b}}$$

Hence $|I_2|^2\, Z_b = |I_1|^2\, Z_a$, i.e. the apparent power input on the primary side of the filter is also available at the secondary. The filter thus causes no attenuation; this frequency band is thus a transmission band. The propagation constant is here $T = j\,\beta$ signifying that the phase angle between I_1 and I_2 is β. If in a particular case $Z_a = Z_b$ then $I_1^2 = I_2^2$; the amplitudes of the primary and secondary currents are then equal.

If in a particular frequency band Z_k/Z_o is positive, then we have *pari passu* that Z_a and Z_b are imaginary and $T = \alpha + j\,\beta =$ complex, where $\alpha > 0$ and β is a multiple of $\pi/2$. We then have $I_2^2\, Z_b < I_1^2\, Z_a$; the apparent power output on the secondary side of the filter is thus smaller than the input of the primary side. The filter thus has an attenuating effect, so that this frequency band is therefore an attenuating band.

It is found from the above that for a filter composed of non-dissipative reactances the image impedances in the transmitting bands are real and in the attenuating bands imaginary; they are therefore never complex.

The frequency at which a transmission band passes over into an attenuating band is termed the limiting frequency; Z_k/Z_o here changes from a negative to a positive value and is therefore zero or infinite.

Special importance attaches to the frequencies at which $Z_k/Z_o = +1$. For from equation (4) it follows that for these frequencies $e^{-2T} = 0$, so that from equation (5) $I_2 = 0$, i.e. the filter allows no current to pass with these frequencies, which are termed frequencies with infinite attenuation. It is also evident that the attenuation is infinite at $Z_k/Z_o = +1$, i.e. when $Z_k = Z_o$. $Z_{ak} = Z_{ao}$ signifies that shorting or opening the secondary terminals does not affect the impedance between the primary terminals and hence does not alter the current distribution in the filter. With the secondary terminals open just as little voltage is present as when these terminals are shorted. If an external impedance is connected across these terminals, no current will pass through it. But zero secondary current signifies an infinite attenuation.

These considerations naturally apply only approximately to non-ideal filters in which the coils and condensers always have a finite resistance. The transmitting and attenuating bands, the limiting frequencies and the frequencies with infinite attenuation are then defined as above, at the same time neglecting the resistances. In the transmitting bands there is a certain attenuation present; for "frequencies with infinite attenuation" the attenuation is then not infinite but has a maximum. In determining the image impedances the resistances in the filter coils and condensers can as a rule be neglected without introducing any error.

Image Impedances and Propagation Constants of Filter Sections after fig. 1.

The following three parameters are taken as defining a filter: the image impedances Z_a and Z_b and the propagation constant T. The filter sections in fig. 1 are however determined by the impedances Z_1 and Z_2. We shall express the open-circuit and short-circuit impedances in terms of Z_1 and Z_2 and then with the aid of equations (1) to (4) obtain the image impedances Z_a and Z_b and the propagation constant T.

If we form a T-section from two half-sections (fig. 2*a*) then at the junction of the half-sections the condition is satisfied that equal image impedances close each other: each of the two half-sections is the image of the other. If a Π-section is constituted from two half-sections (fig. 2*b*) this condition is similarly met. It thus follows that the image impedances of the T-section are the same as the image impedances of the half-section on the left of fig. 1*d* and that the image impedances of the Π-section are the same as the image impedances of the half-section on the right hand side of fig. 1*d*. Thus in fig. 1*b* to *e* there are only two different image impedances, which for the sake of clarity we shall no longer refer to as Z_a and Z_b but as Z_T and Z_π, as indicated in fig. 1. The image impedances and the propagation constant are most easily calculated for the half-section from the open-circuit and short-circuit impedances Z_o and Z_k. For the left-hand side of the half-section after fig. 1*d* we have:

$$Z_o = {}^1/_2\, Z_1 + 2\, Z_2; \quad \dots \dots \quad (7)$$

$$Z_k = {}^1/_2\, Z_1 \quad ; \quad \dots \dots \quad (8)$$

$$Z_T = \sqrt{Z_o\, Z_k} = \sqrt{Z_1\, Z_2}\sqrt{1 + \frac{Z_1}{4\, Z_2}} \quad ; \quad . \; . \quad (9)$$

For the right hand side of the half-section according to fig. 1*d* (left hand side of fig. 1*e*) we have:

$$Z_o = 2\, Z_2; \quad \dots \dots \quad (10)$$

$$Z_k = \frac{2\, Z_1\, Z_2}{Z_1 + 4\, Z_2}; \quad \dots \dots \quad (11)$$

$$Z_\pi = \sqrt{Z_o\, Z_k} = \frac{\sqrt{Z_1\, Z_2}}{\sqrt{1 + \dfrac{Z_1}{4\, Z_2}}} \quad \dots \quad (12)$$

For both sides of the half-section we therefore get:

$$\frac{Z_k}{Z_o} = \frac{1}{1 + \dfrac{4\, Z_2}{Z_1}} \quad \dots \dots \quad (13)$$

The propagation constant T of the half-section then satisfies the equation:

$$e^{-2T} = \frac{\sqrt{1 + \dfrac{Z_1}{4\, Z_2}} - \sqrt{\dfrac{Z_1}{4\, Z_2}}}{\sqrt{1 + \dfrac{Z_1}{4\, Z_2}} + \sqrt{\dfrac{Z_1}{4\, Z_2}}} \quad ; \quad . \; . \quad (14)$$

which is obtained by substituting equation (13) in equation (4).

For a whole section, which whether of the T-or the Π-type may be regarded as a series combination of two half-sections, the propagation constant from equation (6) is double as great as for the half-section: thus for both the T-section and the Π-section we have:

$$e^{-T} = \frac{\sqrt{1 + \frac{Z_1}{4 Z_2}} - \sqrt{\frac{Z_1}{4 Z_2}}}{\sqrt{1 + \frac{Z_1}{4 Z_2}} + \sqrt{\frac{Z_1}{4 Z_2}}}\,; \quad \ldots \quad (15)$$

We thus see that the magnitudes which define our filter sections[3] viz., Z_T, Z_π and T can be expressed in terms of $Z_1 Z_2$ and $Z_1/4 Z_2$. Since T depends merely on $Z_1/4 Z_2$, we will not calculate T but only $Z_1/4 Z_2$ and read T from a graph giving its value as a function of $Z_1/4 Z_2$. The method of graphical representation will be discussed in the next article.

As shown at the outset, in the case of filters composed of non-dissipative reactances Z_k/Z_o is negative and real in the transmission band. Expressed in terms of Z_1 and Z_2 this condition may be written according to equation (13) as follows:

$$-1 < \frac{Z_1}{4 Z_2} < 0 \quad \ldots \ldots \quad (16)$$

It follows herefrom that for the limiting frequencies one of the two relationships:

$$\frac{Z_1}{4 Z_2} = \begin{cases} 0 \\ -1 \end{cases} \quad \ldots \ldots \quad (17)$$

is satisfied. $Z_1/4 Z_2 = 0$, when $Z_1 = 0$ and $Z_2 \neq 0$, or when $Z_1 \neq \infty$ and $Z_2 = \infty$; $Z_1/4\ Z_2 = -1$, when $Z_1 = -4 Z_2$.

For frequencies with infinite attenuation the condition applies: $Z_k/Z_o = +1$, from which through equation (13) we get:

$$\frac{Z_1}{4 Z_2} = \infty. \quad \ldots \ldots \quad (18)$$

i.e. $Z_1 = \infty$ and $Z_2 \neq \infty$, or $Z_1 \neq 0$, $Z_2 = 0$. This may in fact be directly inferred, for if $Z_1 = \infty$, the branch will allow no current to pass and the secondary current is therefore zero; if $Z_2 = 0$, the voltage between the two ends of the branch will be zero and behind this branch, i.e. also between the secondary terminals, no current will flow. The cases where Z_1 and Z_2 are both zero or infinite require closer analysis.

m-Transformations

In the T- and Π-sections as shown in *fig. 1b* and *c* we have studied sections which have the same propagation constant but different image impedances. We shall now analyse a method by which from a given filter section which may be regarded as the fundamental type and whose characteristics are denoted by an accent, other sections can be derived which have the same image impedance, but different propagation constants. It has been shown above (p. 272) that the image impedances in the transmitting band are real and in the attenuating band imaginary. It follows from the fact that the derived filters have the same image impedances as the fundamental filter that both types also have the same transmitting and attenuating bands.

a) m_T-Transformation. We shall first analyse how from the half-section in fig. 1*d* another half-section can be derived, which on the left has the same image impedance $Z_T = Z_T'$. If in the expression $Z_T = \sqrt{Z_o Z_k}$ we multiply the short-circuit impedance Z_k with a positive real number m and divide the open-circuit impedance Z_o by the same value m, Z_T will remain unchanged. For the original half section $Z_k' = {}^1/_2\, Z_1'$, and for the transformed section we therefore have:

$$Z_k = {}^1/_2\, m\, Z_1'\,; \quad \ldots \ldots \quad (19)$$

thus for the original section $Z_o' = {}^1/_2\, Z_1' + 2\, Z_2'$ and for the transformed section:

$$Z_o = \frac{Z_1'}{2\,m} + \frac{2\,Z_2'}{m} \quad \ldots \ldots \quad (20)$$

The question now arises as to the composition of the filter section conforming with this conditions. If Z_1 and Z_2 are the impedances of the full branches of the transformed section, then it follows from equations (7), (8), (19) and (20), that:

$$Z_1 = m\, Z_1'\,; \quad \ldots \ldots \quad (21)$$

$$Z_2 = \frac{1 - m^2}{4\,m} Z_1' + \frac{1}{m} Z_2' \quad \ldots \quad (22)$$

With these values for Z_1 and Z_2 for a full section, a T-section, a Π-section and a half-section can be formed (*fig. 5*).

As the image impedance Z_T of the T-section (fig. 5*b*) is the same as the primary image impedance Z_T of the half-section (fig. 5*d*), the image impedances Z_T of the T-section (fig. 5*b*) and Z_T' of the fundamental type (fig. 1*b*) are equal, so that we have:

$$Z_T = Z_T', \quad \ldots \ldots \quad (23)$$

independent of the choice of the parameter m. From equations (12) and (14) we get however that in the transformed half-section Z_π and T differ from Z_π' and T'. For these sections we then get from equations (12), (19), (20), (21) and (22) on putting $1 - m^2 = 1/a^2$:

---

[3] There is a duality between T-sections and Π-sections. If in Π-sections the admittance $1/Z$ is introduced as a variable in place of the impedances Z, formulae are obtained for equations (10) to (12) which are almost identical with equations (7) to (9) for T-sections. In this way it is possible to apply the results of calculation for T-sections to Π-sections and vice versa. Equations (21) to (25) for the "m_T-transformation" and equations (27) to (31) for the "m_π-transformation" are examples of this.

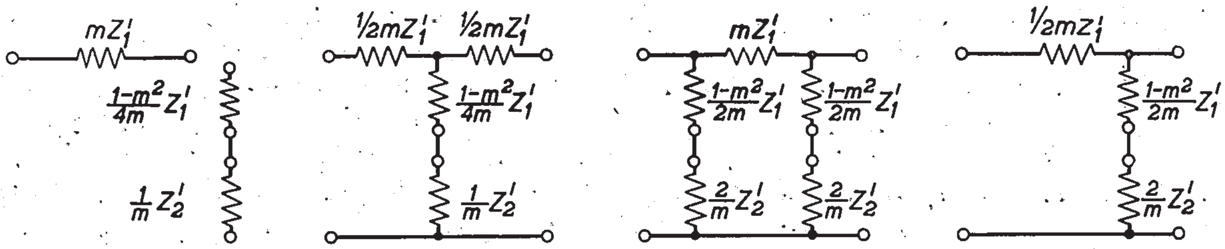

a) Full branches b) T-section c) Π-section d) Half-section 17163

Fig. 5. m_T-Transformation. The image impedances Z_T of the T-section (b) are equal to the primary image impedance Z_T of the half-section (d, left) and are also equal to the image impedance Z_T' of the fundamental type (fig. 1b). The image impedances Z_π of the Π-section (c) are equal to the secondary image impedance Z_π of the half-section (d, right), which is however not equal to the image impedance Z_π' of the fundamental type (fig. 1c). The propagation constant T of the T-section (b) and the Π-section (c) are equal but not equal to the propagation constant T' of the fundamental types (figs. 1b and c).

$$Z_\pi = Z_\pi' \left(1 + \frac{1}{a^2}\frac{Z_1'}{4\,Z_2'}\right); \quad \ldots \quad (24)$$

$$\frac{Z_1}{4\,Z_2} = \frac{Z_1'}{4Z_2'}\,\frac{m^2}{1 + \frac{1}{a^2}\,\frac{Z_1'}{4\,Z_2'}} \quad \ldots \quad (25)$$

If therefore T-sections of the fundamental type and the transformed type are connected in series, equal image impedances will always be obtained at the junctions. This does not however apply to Π-sections.

It follows from equation (22) that an m_T-transformation is only rational when:

$$0 \leqslant m \leqslant 1 \quad \ldots \quad (26)$$

If $m = 0$ the filter disappears; for $m = 1$ we arrive back at the fundamental type.

Since by this transformation of the fundamental type Z_T does not change, this method is termed that of m_T-transformation.

b) *m_π-transformation.* m_π-transformations are defined as those in which Z_π remains constant. A method analogous to that employed in the m_T-transformation can also be used in the m_π-transformation:

$Z_1 =$ the parallel combination of $m\,Z_1'$ and $\frac{4\,m}{1-m^2}Z_2'$; (27)

$$Z_2 = \frac{1}{m}\,Z_2'\,; \quad \ldots \quad (28)$$

$$Z_\pi = Z_\pi'\,; \quad \ldots \quad (29)$$

$$Z_T = Z_T'\,\frac{1}{1 + \frac{1}{a^2}\,\frac{Z_1'}{4\,Z_2'}}\,; \quad \ldots \quad (30)$$

$$\frac{Z_1}{4\,Z_2} = \frac{Z_1'}{4\,Z_2'}\,\frac{m^2}{1 + \frac{1}{a^2}\,\frac{Z_1'}{4\,Z_2'}} \quad \ldots \quad (31)$$

Here again condition (26) must be satisfied. It is seen from equations (25) and (31) that at the same

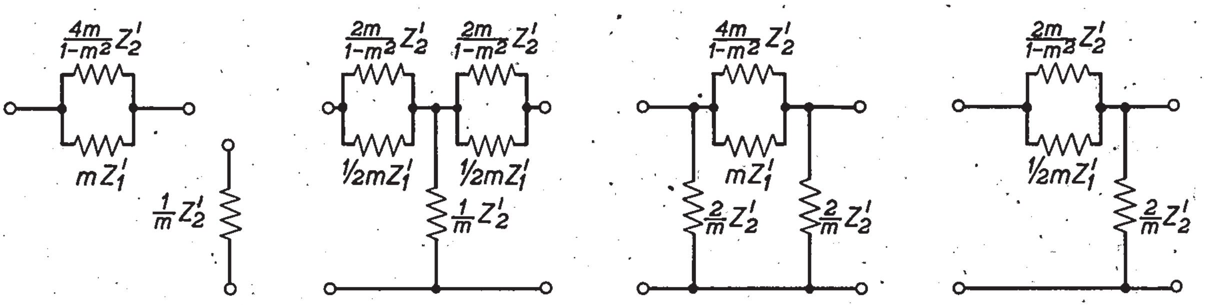

a) Full branches b) T-section c) Π-section d) Half-section 17164

Fig. 6. m_π-Transformation. The image impedances Z_π of the Π-section (c) are equal to the secondary image impedance Z_π of the half-section (d, right) and also equal to the image impedance Z_π' of the fundamental type (fig. 1c). The image impedances Z_T of the T-section (b) are equal to the primary image impedance Z^T of the half-section (d, left), but are not equal to the image impedance Z_T' of the fundamental type (fig. 1b). The propagation constants T of the T-section (b) and of the Π-section (c) are equal to each other, and are also equal to the propagation constant for T- and Π-sections in m_T-transformation (fig. 5, b and c), but are to the propagation constant T' of the fundamental types (figs 1b and c).

value of m, $Z_1/4\,Z_2$ and hence the propagation constant T is the same for both transformations. *Fig. 6* shows how from these transformed branches of a T-section, a Π-section and a half-section can be produced. If Π-sections of the fundamental and transformed types are connected in series, the same image impedances will always be obtained at the junctions. This does not however apply to T-sections.

It is evident that, for instance, after applying the m_T-transformation the transformed section can again be regarded as a new fundamental type and an m_π-transformation applied to it and vice versa.

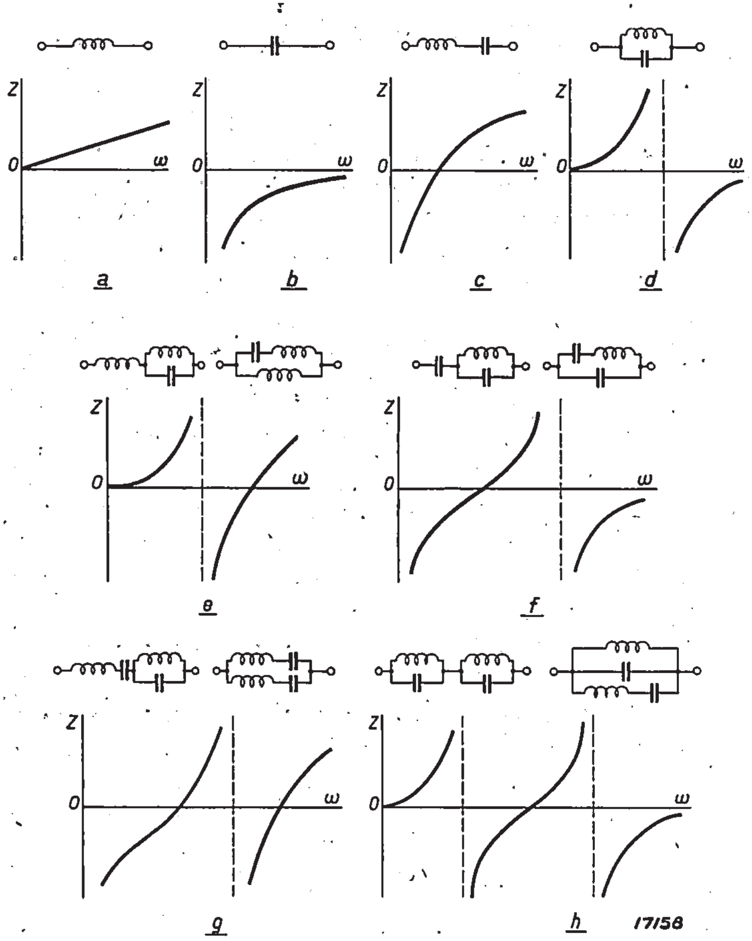

Fig. 7. Reactances composed of 1, 2, 3 or 4 elements.

Reactance Diagrams.

A general characteristic of networks composed of non-resistive reactances is a monotonic increase in the impedance with rising frequency, apart from discontinuous transitions from $+j\infty$ to $-j\infty$. As an example *fig. 7* gives the reactances, which will be used later as filter branches, the reactance being plotted as a function of the frequency. In the case of reactances having more than two elements, several equivalent circuits can be obtained (figs. 7*e* to *h*).

These reactance diagrams offer a simple means for deriving at least qualitatively, the most important characteristics of the propagation constant of a specific filter section.

In the next article it will be shown how these reactance diagrams are utilised in the analysis of the various simple types of sections for low-pass, high-pass and band-pass filters.

A NEW APPARATUS FOR TESTING THE FASTNESS-TO-LIGHT OF MATERIALS

By J. F. H. CUSTERS.

Summary. A testing device is described, which allows to investigate the fastness-to-light of materials by means of a short time exposure.

Introduction

The colour of no substance is absolutely fast to light, and experience teaches that sunlight affects every material to a more or less extent, causing a permanent photochemical change in the colour and frequently also some change in the fibrous structure. The changes produced differ from material to material, both as regards intensity and nature. Some materials become lighter in colour, others darker, while again others acquire a colour totally different to their original colour. An instructive example of decoloration was observed by the author in a tobacconist's window display, where a dark chocolate-brown packing had been converted to a greenish colour. On prolonged illumination the chocolate-brown paper became gradually changed to a very stable bright grass green.

How can the stability of a substance against the action of light be tested and how can the fastness-to-light be standardised? Where information of the fastness of a colour or material under the action of sunlight and daylight is required, a suitable method of determining this appears to be the exposure of a sample of the material to sunlight to observe if after a time an appreciable change in colour is obtained. To arrive at standards of fastness-to-light it is further necessary to know the variation in intensity of the radiation falling on the sample of material during its period of exposure, since the intensity of illumination is not constant. In addition to changes in the altitude of the sun (diurnal and annual motion of the sun), there are also changes in intensity due to the very pronounced fluctuations in the meteorological conditions of the earth's atmosphere. In the course of an investigation the cloud conditions are liable to vary very considerably; but even without this change the intensity also varies owing to the state of humidity of the atmosphere. The spectral composition of solar radiation is itself subject to fluctuation, thus during the winter sunlight contains much less short-wave ultra-violet rays than summer sunlight, and finally the composition of direct sunlight differs appreciably from that of indirect daylight, where again the cloud conditions play an important part. These fluctuations can be taken into account by recording with a suitable instrument (photo-electric cell or thermopile) the solar intensity during the exposure of the sample and expressing the quantity of light found in this way in terms of a standard unit, for instance the amount of light which falls on unit surface of the sample in unit time on a bright cloudless summer day. It is, however, then tacitly assumed that the relative spectral energy distribution of the light falling on the material remains constant. On the basis of a method of test worked out on these lines, fastness-to-light standards could be evolved by defining various fastness-to-light classes, each corresponding to a specific number of the arbitrary standard units of light quantity.

This method of investigation is, however, very cumbersome and tedious, especially when carrying out fastness-to-light tests during the winter months. It is evident that simpler means must be evolved, and to some extent this need has been met. The methods arrived at are of two types. On the one hand, endeavours have been made to avoid the inconvenience already referred to, by starting with a series of type colours each of which represents a specific fastness-to-light class; the sample under investigation is then compared with this standard series. On the other hand, an artificial source of light has been evolved as a substitute for natural sunlight, which has usually a constant intensity and with which the given sample is illuminated either with or without simultaneous exposure of standard type colours. The principal requirement which this artificial light source has to meet is that the light emitted must have exactly the same relative spectral energy distribution as sunlight. It is sufficient merely to point out that a low-pressure mercury lamp, which is frequently employed for this purpose, is actually quite unsuitable, for it emits a line spectrum containing only a few lines, while the ultra-violet spectral lines radiated have too great an intensity.

With the artificial sources of light employed hitherto, it was a common difficulty that to obtain an appreciable change in colour in the sample irradiation had to be continued for a very long period. In the case of the new apparatus described below this difficulty was overcome by concentrating the light from a special type of glowlamp in such a way that the sample, whose fastness-to-light was under test, could be irradiated with 50 times the intensity of sunlight. At the same time the spectral composition of the light is modified by a suitable filter so that it is closely comparable to that of sunlight.

Principle of Operation of Apparatus

The concentration of the irradiation on the sample under test is based on the property of an ellipsoid of rotation that every beam of light radiating from one focus is reflected at the surface of the ellipsoid along a line passing through the other focus. This property is utilised in the apparatus described here by placing a nearly punctiform source of light at one focus of the ellipsoid and the sample under test at the other focus.

Fig. 1 shows the energy distribution $E(\lambda)$ of the light from the glowlamp as a function of the wave length in λ (curve a). The light source is a 750-watt gas-filled tungsten filament lamp, burning at a temperature of 3100 deg. K. at which it emits a total luminous flux of 20 000 lumens and has a life of approximately 100 hours. For purposes of comparison the energy distribution in sunlight is also given (curve b).

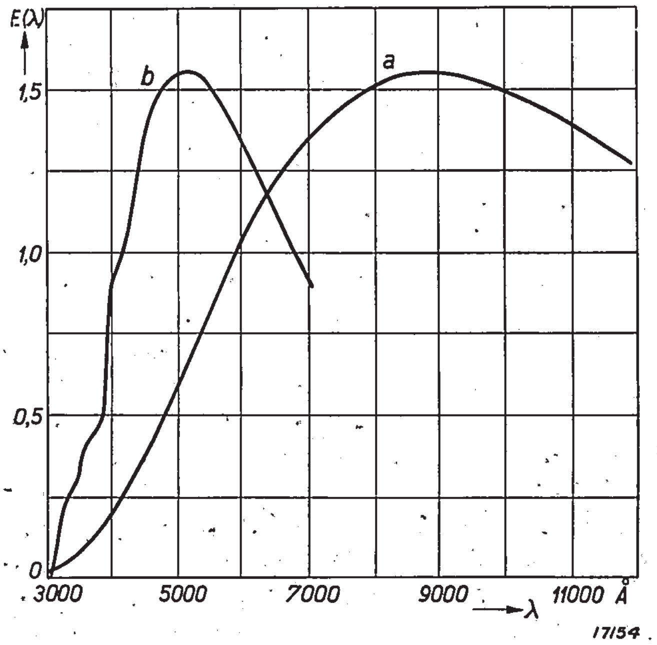

Fig. 1. Spectral energy distribution curves:
a) Glowlamp light.
b) Solar light.

It is seen that the two curves of energy distribution differ considerably. By means of suitable filters they can however be made comparable. The transmission factor of an ideal filter for this purpose would at every wave length be proportional to the ratio of $E(\lambda)$ for the sun and the glowlamp. In the present case, there is the additional important requirement to be met that the filter itself must be perfectly stable to the action of light, so that very few materials can be used as filters. An aqueous solution of copper sulphate of a certain concentration satisfies these two essential requirements very well, as may be seen from the following. *Fig. 2* shows the spectral transmission curve of a quartz vessel filled with a filter liquid of this type.

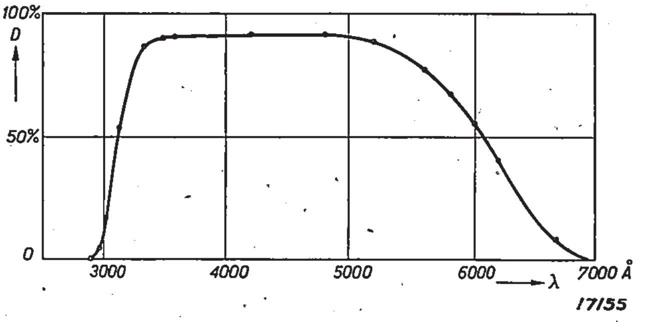

Fig. 2. Spectral transmission curves for a copper sulphate filter. Together with curve a in fig. 1 this curve shows that the filter absorbs a considerable portion of glowlamp light.

This filter is placed near the focus so that the radiation incident on the sample passes through the filter and is thus partially absorbed. The absorbed portion is quite considerable, as may be gathered from a comparison of fig. 1 (curve a) and fig. 2, since all radiation emitted from the glowlamp with a wave length above approx. 7000 Å — and this is more than 85 per cent of the total energy radiated — is absorbed by the filter and converted to heat. As a result there is a marked temperature rise in the filter vessel, which must be avoided in some way or other, e.g. by filtering out the long-wave energy before the light reaches the filter vessel. A column of water of suitable thickness is very useful for this purpose, as shown by *fig. 3* which gives the spectral transmission curves for water columns 1 cm and 27 cm thick.

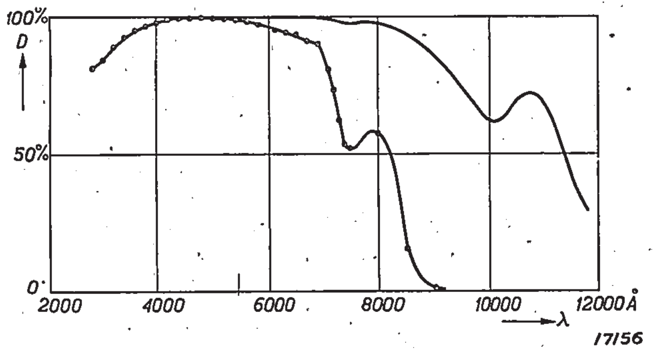

Fig. 3. Spectral transmission curves for water columns 1 and 27 cm thick.

The second curve applies to the method employed here, for in the practical design adopted for the apparatus the whole ellipsoid is filled with pure water. The dimensions of the ellipsoid are so chosen that the path traversed by the light rays from focus to focus via the surface of the ellipsoid is 27 cm. It may be seen from the figure that pure water is transparent for all rays from 3000 to 7000 Å, while above 9000 Å all the incident rays are absorbed. The light energy absorbed by the water is indeed so great that special provision has to be made for dissipating the heat evolved; details of the method adopted are given below. *Fig. 4* shows the energy distribution in the plain glowlamp light (*1*), in the light after passing through the column of water (*2*), and after being passed through the second (copper sulphate solution) filter (*3*), as well as that in the sunlight which reaches the earth (*4*). It is seen that there is very good agreement between the relative spectral energy distributions in sunlight and the light issuing from the apparatus under discussion. The deviation is greatest at wave-lengths above approximately 6000 Å. In this wave-length range the photochemical effect of the light is however so small that this difference may be neglected. It has been shown by investigations made by **Rein**[1]) that the photochemical changes observed in materials are due principally to the visible radiation with very high energy. By comparative illumination experiments of objects through quartz glass (complete exposure to solar radiation) and through window glass (elimination of wave range below approx. 3250 Å) **Rein** showed that contrary to common opinion the short ultra-violet of sunlight contributes only very little to the action of sunlight on all kinds of coloured materials. It depends entirely on the absorption spectrum of the material under investigation which range of wave-lengths causes the most marked decoloration. White and yellow pigments (e.g. white or undyed textiles or dyes, white paper, films, etc.) which absorb ultra-violet light exclusively and whose absorption usually increases with diminishing wave length, exhibit very marked differences on illumination through quartz glass and window glass. It is therefore desirable for the artificial light source to contain wave-lengths down to 3000 Å. Coloured materials not only absorb in the ultra-violet, but also a considerable proportion of waves in the visible part of the spectrum, and since the sun is richest in just these rays the photochemical action of sunlight is particularly due to this range of wave lengths.

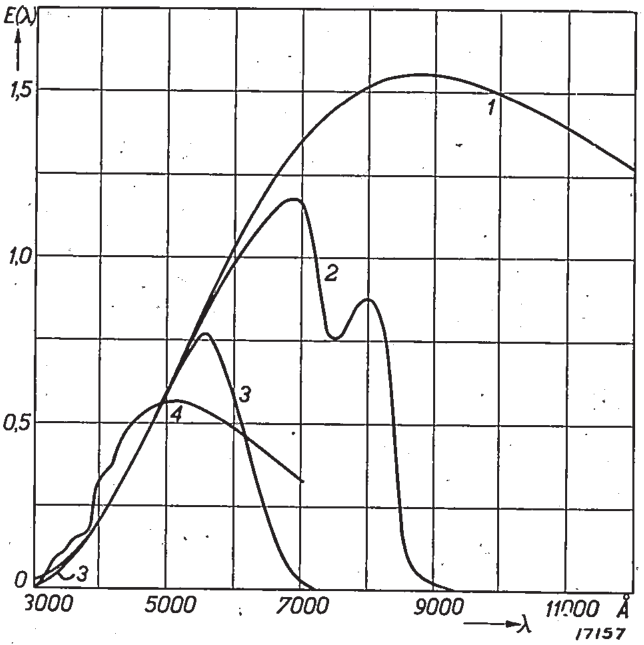

Fig. 4. Distribution of spectral energy in glowlamp light:
1) In plain lamp,
2) After the light has been passed through 27 cm of water, and
3) After it has also been passed through the second filter,
4) Energy distribution in sunlight (for comparison with curve *3*).

Construction of Apparatus

The general construction of the apparatus evolved is shown in *fig. 5*. Owing to the difficulties encountered in the construction of a complete ellipsoid, only the upper half of the ellipsoid has been employed and fitted at the top with a neck. The lower side consists of a conical jacket which at the bottom is closed by a quartz plate *K*. On the interior the ellipsoid is bright chromium-plated. The coefficient of reflection of chromium for vertically incident light varies in the wave-length range in question here (from 3000 to 7500 Å) from 62 to 71 per cent. Since the greater part of the light from the glowlamp strikes the surface at a fairly flat angle, the average coefficient of reflection is in fact much greater. The ellipsoid and the cone are filled with water up to the edge of the neck. The incandescent filament of the lamp is situated at the focus *B'*, this lamp being made from a specific kind of glass to prevent the immersed part of the bulb from cracking. The liquid filter vessel is located at *C* and is also immersed in the water filling the ellipsoid, for in spite of preliminary filtering through water so much heat is still generated in *C* that if the vessel were placed in air it would crack. In the arrangement adopted here, the heat developed in *C* is absorbed by the water. To provide additional means for the dissipation of the heat, the ellipsoid has been fitted with a cooling jacket *N* connected to a water tap at *c*; *d* is the outlet for the cooling water. The sample of material irradiated is located at the focus *B''* which is slightly below *K*. The sample is clamped to a metal holder under a circular diaphragm 15 mm in diameter (for which springs *V'* and *V''* have been provided), so that one part is exposed to radiation and the other part is screened. In spite of the extensive measures taken to absorb the long-wave energy in the two light filters supplementary cooling of the sampling has been found necessary in some cases. This is indeed not surprising when it is remembered that the effective intensity of illumination of the sample is about 50 times the intensity of sunlight. A considerable proportion of the light falling on the sample is converted to heat and to dissipate this heat energy cooling water is circulated through the centre of the sample holder and flows out through *b*, entering the cooling jacket *N* at *c*. In this way an excessive temperature rise at the sample is effectively avoided, provided that the material itself is a good conductor of heat (or is sufficiently thin) and a heat conducting path is established with the metal holder. If this cannot be achieved, as with woollen or rough materials which are able to accumulate warm air between the fibres, cooling from above is essential, and is provided by a rapid current of air directed by the electric blower *B* against the surface of the material.

---

[1]) H. **Rein**, Z. angew. Chem. **47**, 157, 1934.

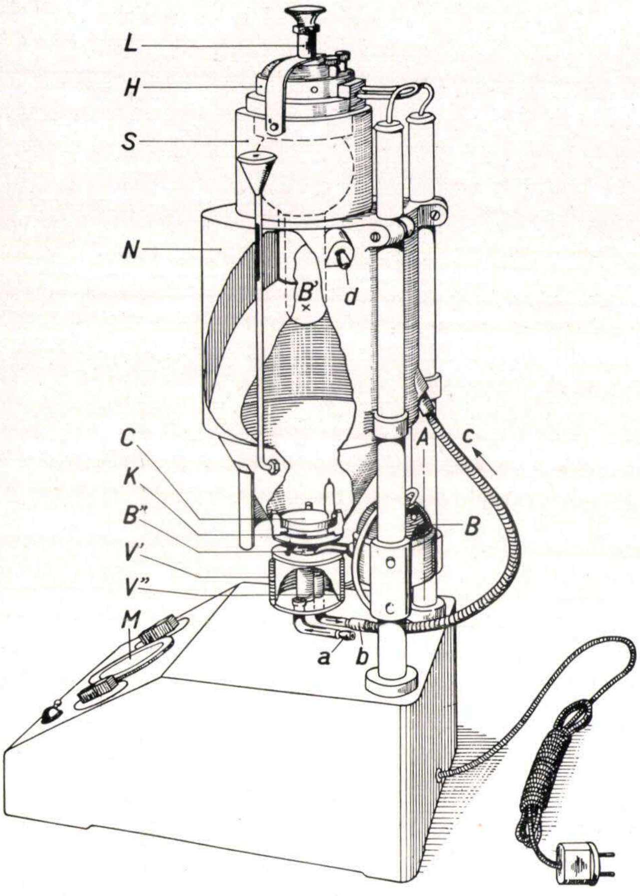

Fig. 5. Construction of the fastness-to-light meter. *B'* is the incandescent filament of the lamp situated at one focus of the ellipsoid. The glowlamp is always accurately positioned at the focus *B'* as it is secured to the holder *H* by a positioning flange. *C* is the copper sulphate filter. The sample under test is placed at the other focus *B''* and is fixed to a turntable holder; it can be cooled by the electric blower *B*.

In regard to the fixing of the light source it should be mentioned that the glowlamp is fitted with a so-called positioning flange with which the lamp is secured in the holder *H* in an invariable position; the holder *H* rests against the head *S* and is secured with the clip *L*. The incandescent filament of the lamp is thus always brought exactly into the focus of the ellipsoid. A mains-fed transformer is employed for feeding the lamp and motor and is accomodated in the foot of the apparatus. The current consumption of the lamp is indicated on the ammeter *M* and can be regulated by means of two switches. A general view of the whole apparatus is shown in *fig. 6*, while *fig. 7* shows the rotary plate holder for the sample of material under test.

Although tungsten, which volatilises during the running of the lamp, rapidly blackens the lamp

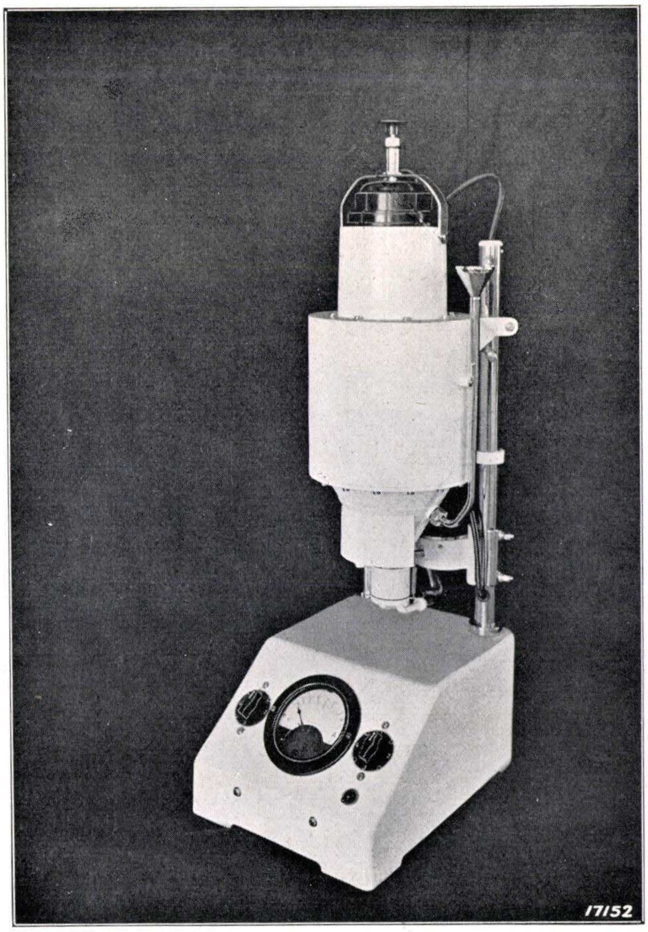

Fig. 6. General view of fastness-to-light meter. The total height of the apparatus is approx. 85 cm.

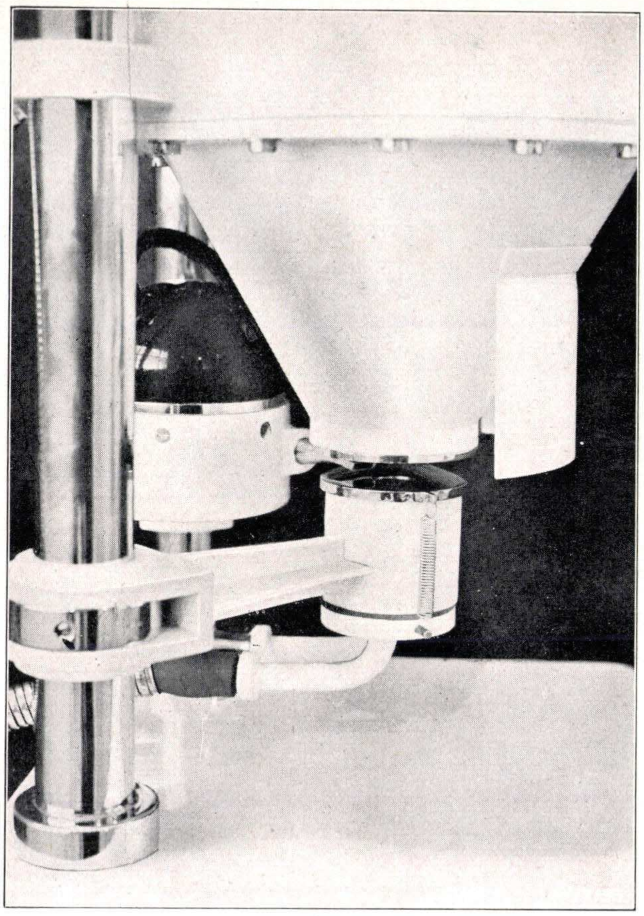

Fig. 7. View of the lower side of the meter showing the turntable holder for the sample under test and the fan with blower hood for cooling the sample when necessary.

bulb the surface round the incandescent filament remains perfectly clear in view of the special design of the lamp adopted. The luminous flux of the apparatus is thus maintained constant throughout the life of the lamp.

Results of Investigations with the New Apparatus

Apart from extensive experiments carried out to determine the comparative illumination intensities of the apparatus and the sun, a series of comparative tests were also made with a variety of samples of material. Thus 30 kinds of offset printed colours of different shades and degrees of fastness-to-light were irradiated, every colour showing the same degree and type of fading after 30 minutes exposure in the apparatus as obtained with exposure to sunlight for a period of eight sunny days in September. The yellowing of various kinds of white paper was found to be exactly the same in this apparatus as on irradiation by sunlight; the normal colour of newsprint was altered after two hours illumination to a yellowish brown. Coloured samples of paper with a low fastness-to-light exhibited a marked fading already after three minutes irradiation, while after 30 minutes they had been completely bleached.

Samples of textile materials were also tested. An apt example is the series of standard blues already referred to, which under the fastness-to-light meter became decoloured in the same way and in the same order as when exposed to solar radiation. This series contained eight examples, numbered from I to VIII, the fastness-to-light coefficient increasing from I to VIII. No. I exhibited a distinct decoloration already after three minutes exposure in the meter, and No. V a just detectible change after an hour's exposure. If a textile material shows no distinct decoloration, after one hour's exposure it appears to be adequately fast to light.

Owing to the variety of practical requirements which have to be met, the time of exposure to light which a sample must be able to sustain without decoloration varies according to the nature of the sample. In the case of textiles it is reasonable to prescribe a minimum period of exposure of at least an hour, for printed colours (black and other colours) on paper at least half an hour, and for varnished colours at least two hours before a change in colour takes place.

With certain textiles a striking behaviour was observed. On exposure to irradiation they became darker and during a subsequent period of non-irradiation they regained their original colours almost completely, only a slight residual change being detectible. Owing to the weak intensity of sunlight this behaviour is barely or not at all visible under normal conditions (many lithopones), since the material has an opportunity to recover. Actually after suitable solar irradiation the residual effect alone is observed. In general, only materials with a pronounced fastness-to-light exhibited this reversible behaviour in tests with the apparatus. In practice the same standards can be retained here as adopted for materials showing a normal behaviour; after irradiation a short period must be allowed to elapse to see whether the darkening in colour disappears or not.

In conclusion, reference must be made to the possibility of using the apparatus described for formulating fastness-to-light standards. To standardise this property in terms of solar exposure hours has very little practical value. Since the apparatus described here permits a constant intensity of irradiation to be maintained, and according to experience produces the same fading as the sun, it offers a standard illumination for use in fastness-to-light tests.

FESTIVE ILLUMINATION OF THE NETHERLANDS CRUISER "DE RUYTER"

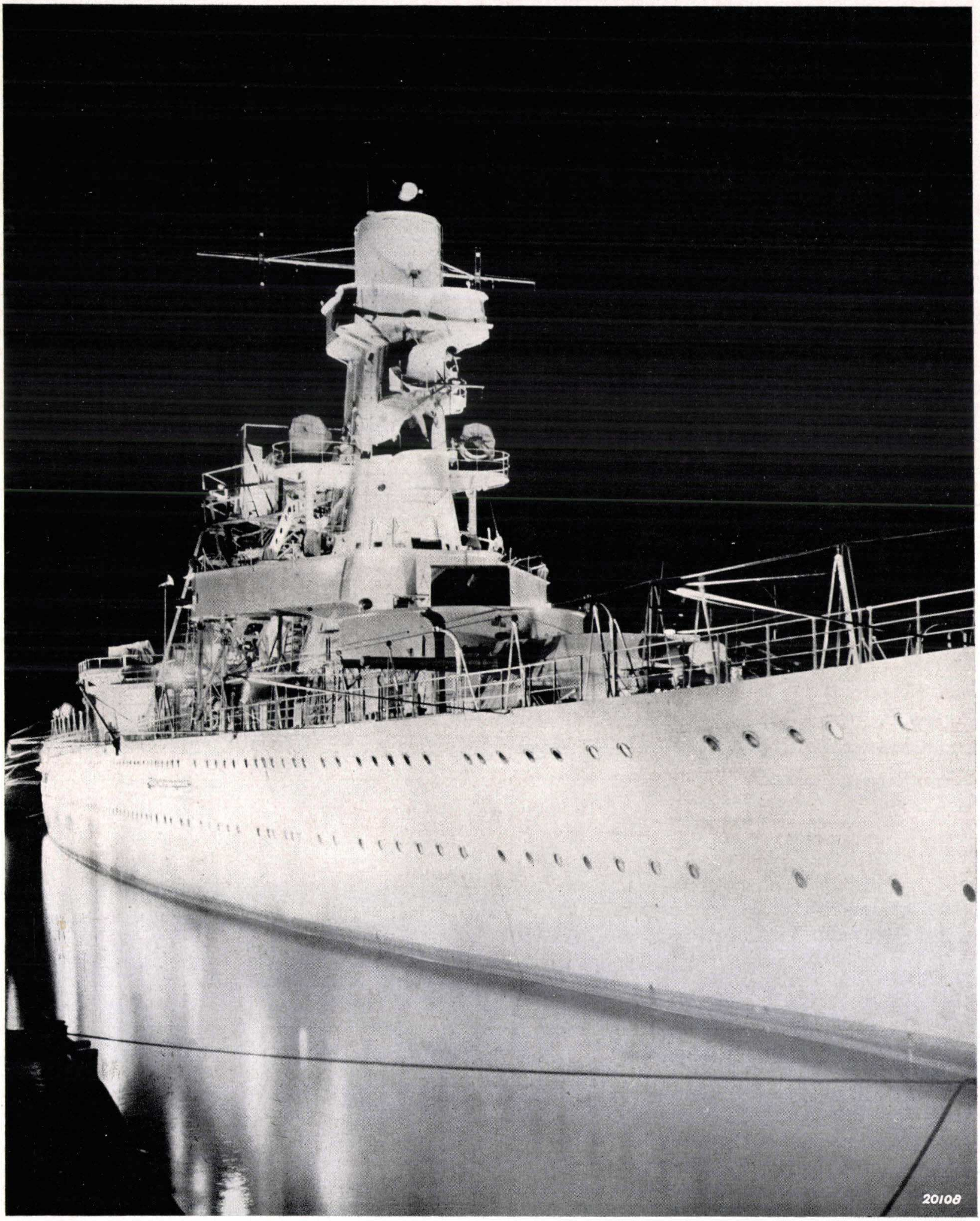

For visits in foreign harbours this new cruiser has been equipped with an installation by means of which the entire vessel can be brightly illuminated, without having to depend upon search-lights on the shore. The grey hull is lighted by 24 incandescent lamps of 500 watts in enamelled reflectors, which are hung outboard from suspension poles 20 ft. long. The fire-control tower, which is about 65 ft. high, is illuminated by six 750-watt lamps in mirrored reflectors. The gun-turrets, the boats and other accessories are lighted separately. Altogether, 30 kilowatts have been installed for this festive illumination.

THE PERCEPTION OF COLOUR

By P. J. BOUMA.

Summary. The principles of colour vision are discussed in this article, consideration of the problem being limited to its qualitative aspects. An investigation is made of the conditions determining the production of a colour sensation. Following consideration of the effect of the nature of the incident light and the characteristics of the object illuminated, the properties of the eye are discussed. It is shown that all colour sensations or impressions can be represented graphically in a plane. The effects of very low brightness levels and of simultaneous and successive contrast are then considered, and finally brief reference is made to the theory of colour vision.

"When I look out of the window, I see that the grass is green".

We all agree with this statement, but as a rule we do not realise the vast complexity of phenomena which lead us to draw this apparently simple conclusion.

The sun illuminates the grass with light containing practically all wave-lengths of the visible spectrum in definite proportions. Of the incident light the grass reflects a certain portion, but not the same proportion of each of the various wave-lengths is reflected. A portion of the reflected light — whose spectral composition is thus different from that of the incident sunlight — impinges on the eye, penetrates into it and after refraction in the lens and liquids of the eye throws an image on the retina. The formation of this image produces certain stimuli in the optic nerves; these stimuli are transmitted to the brain and there become registered by our conciousness; the impression which we finally receive we describe briefly by the statement: "I see the grass is green".

This step by step analysis of the process of vision also teaches us the conditions determining the production of a specific colour sensation.

Effect of the Nature of the Incident Light

The nature of the light falling on the grass can differ in two particulars, viz.,

1) In character (spectral composition).
2) In quantity (intensity of illumination).

To visualise the effect which the spectral composition of the incident light has on the colours of illuminated objects, let us consider a few important practical examples:

a) If sunlight is replaced by nearly monochromatic sodium light, then all objects are almost exclusively illuminated with wave lengths of 5890 and 5896 Å. Whatever may be the properties of reflection of the objects, they can never reflect any light other than rays of these particular wave-lengths [1]). The net result is that the same type of light impinges on the eye from every object: We see all objects as yellow, and only the "dark" objects, which reflect only a small amount of light, appear a brownish yellow. It cannot be expected that in these circumstances the grass will still appear green.

b) In light from a mercury vapour lamp our surroundings already have a much closer resemblance to their appearance in the "world of daylight"; nevertheless it is observed that various objects exhibit an unnatural, i.e. abnormal, colour. This is mainly due to the fact that the red rays are absent in mercury light and all blue rays have been concentrated to a single wave length (4358 Å). Since the incident light has a different spectral composition to daylight, this will also be the case with the reflected light, with the net result that the colours appear different to us.

c) Also when we use the light from ordinary electric glowlamps our surroundings will again appear different to what we see in daylight. That the difference in this case is less striking is partly due to the fact that we have become more accustomed to this type of light, and partly because the light from a glowlamp with its continuous spectrum differs much less from sunlight than, for instance, sodium and mercury light. Very striking are, however, the differences when we view the same surroundings in quick succession in daylight and glowlamp light, or when a sheet of paper is illuminated half with daylight and half with glowlamp light (for instance when the paper is held in front of a gap in the curtains in a room from which daylight is excluded, and the two halves are separated by another sheet of paper fixed perpendicular to them). In this case the half sheet illuminated with daylight will appear slightly bluish and the other half a pale orange yellow [2]).

---

[1]) We must here make an exception of the so-called fluorescent substances, i.e. chemical substances which transform incident light into light of different (longer) wave length. Thus rhodamine converts yellow sodium light into red light and is therefore employed in practice for making traffic signals (boards) appear red on sodium illumination.

These examples show clearly that colour is not a property of the objects themselves but a result of the combination of the source of light, the object viewed and the eye.

If the spectral composition of the light is left unchanged, we can vary the amount of the incident light (intensity of illumination) and hence also the quantity of the reflected light (brightness of the object) within wide limits, without observing a marked alteration in the nature of the colour sensations produced by the objects viewed: Grass will appear green both on a bright sunny day and in dull weather. Only when the objects have very low brightness values (e.g. in a moonlight landscape) will the brightness have an appreciable effect on the nature of the colour. We shall return later to a discussion of this point in greater detail.

Effect of the Characteristics of the Object

The yellow flower which grows among the grass receives exactly the same sunlight, but reflects different proportions of the various wavelengths than those reflected by the grass. As a result the light from the flower which impinges on the eye has a different spectral composition to the light coming from the grass. Owing to the specific characteristics of the eye we perceive this difference in composition as a difference in colour: the flower appears yellow, and the grass appears green.

The part played by the object in producing a colour sensation consists therefore exclusively in the fact that it reflects a specific portion $R(\lambda)$ from light of a particular wavelength λ. If $E(\lambda)$ is the spectral composition of the incident light, then the spectral composition of the reflected light is $R(\lambda) \cdot E(\lambda)$.

If R is the same for all wave lengths, the reflected light will have the same spectral composition as the incident light and will also produce the same colour sensation (provided R is not too small). Viewed in daylight such an object will appear white (or grey if R is small), and it is usual therefore to speak in this case of a "white object", although the same object viewed in sodium light will naturally appear to be yellow.

If R is not the same value for all wave lengths, the reflected light will have a different composition to the incident light. In daylight such an object will then usually not appear to be white, and in this case we generally ascribe a specific colour to the object, although with another kind of incident light it will as a rule produce a different colour sensation (in certain circumstances even appearing to be white).

The "Normal" Mixing Characteristics of the Eye

The "Visual organ" [3]) acts simultaneously as a receiver, transformer and reproducer for colours and thus constitutes the most complex link in the chain of generating a colour sensation.

We shall first summarise briefly the various problems entailed here.

1) How does the eye operate as a mixer for rays of different wavelength, i.e. what colour sensations do the various spectral mixtures produce which can impinge on the eye?
2) How do these characteristics change with very small brightness values?
3) How is the eye's ability to discriminate colours affected by the simultaneous presence of objects of different colour in the field of vision?
4) Are the characteristics of the eye affected by light sensations to which it is exposed just previously to viewing a particular object?
5) What individual variations occur in the "colour characteristics" of the eye?

To obtain an insight into the first problem, consider the four other influences as absent, i.e. an object with a brightness above a certain limit (about 3 candles per sq. m) is viewed with a non tired normal eye, no objects of another colour being present in the field of vision. For these conditions let us determine the various colour sensations corresponding to different spectral compositions of the light incident on the eye [4]).

Each specific spectral distribution produces a definite colour sensation in the eye. Is the converse also true? Can we deduce the spectral composition of the light from the nature of the colour sensation obtained? This question must be answered in the negative. A specific colour sensation can be produced by entirely different spectral compositions.

---

[2]) The difference is emphasised here by simultaneous contrast, which is referred to in greater detail below.

[3]) "Visual organ" is defined as the combination of the eye proper, the optic nerve and that part of the brain which assists in creating a colour impression. The term "eye" is usually also defined in this broad sense, for of many phenomena in vision we are unable to determine in which part of the organ they actually take place.

[4]) Consideration is omitted here of whether the light which impinges on the eye is derived directly from the light source or is first reflected by an object.

The well-known phenomenon of complementary colours should be recalled: A combination of two spectral colours (e.g. blue 4800 Å and yellow 5800 Å) can produce exactly the same colour impression as the continuous solar spectrum.

In the same way as we have here simulated the colour of sunlight by mixing two colours of the spectrum, it has been found possible by suitably mixing three spectral colours (e.g. red 7000 Å, green 5200 Å and blue 4800 Å) to obtain practically all compound colours[5]).

An interesting survey of these mixtures is afforded by a graph in which every colour sensation is indicated by a specific point on the plane of the paper. In *fig. 1* the three primary colours of the spectrum mentioned above are indicated by the points *1*, *2* and *3*. To represent other colour sensations in the diagram the mixture of two colours be represented by the points in the line joining the two points for these colours. We thus get the line *1—2* for all colour sensations which can be simulated by a suitable mixture of *1* and *2*. The position of the mixture on the line is determined by the ratio in which we must mix the two components; the greater the percentage of colour *1* required the closer will be the point to *1*, which represents this colour[6]). To determine the position of a particular colour, e.g. white, we must first assume a mixture of the requisite amounts of *1* and *2*. This mixture is represented by the point *B*. White is now produced by a suitable mixing of *B* and *3* (*B* is thus a complementary colour to *3*). The point *W* is therefore on the line *B—3*, its position on this line being determined by the ratio of *B* and *3* in the mixture. In this way every colour sensation which can be produced by a mixing of the three primary colours can be represented by a point within the triangle *1-2-3*. What are now the relative positions of the various colours in this triangle?

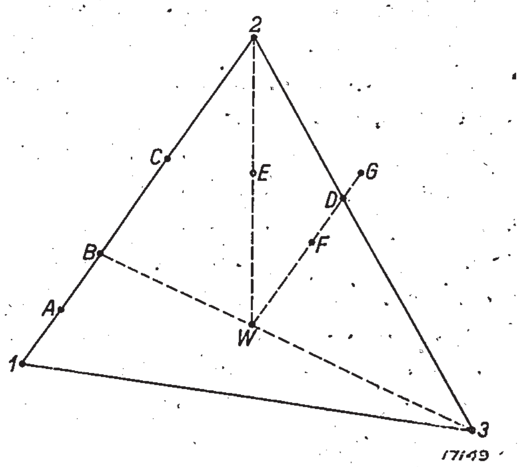

Fig. 1 — Mixing of colours from three primary colours: *1*) Red 7000 Å; *2*) green 5200 Å; *3*) blue 4800 Å. *W* represents white; *A*, *B*, *C*, *D* are orange, yellow, yellowish-green and bluish-green respectively; the line *1—3* embraces the shades of purple. *G* represents the spectral blue-green, which must be mixed with white (*W*) in order to give the blue-green *D*. *E* is produced by mixing *W* and *2*.

The mixtures of *1* and *2* are: orange (*A*), yellow (*B*) and yellowish green (*C*). Along the line *2-3* the various shades of bluish-green (e.g. *D*) are situated, while along the line *1-3* are the different shades of purple. From the method of representing the colour mixtures adopted here it follows that two colours are complementary when the point *W* lies on the line joining them. The pair of colours *B-3* is an example of this. Furthermore we see that the colour sensation *E* can be simulated by mixing spectral green (*2*) with white (*W*); this mixture produces a sensation of an "unsaturated" (pale, bleached, dull) green. The closer this point *E* is moved towards *2* the deeper will be the colour, finally reaching its maximum saturation at *2*.

If the point *F* is moved along the line *W D* a progressive intensification in the bluish-green colour is similarly observed, but contrary to the previous example the maximum saturation is not yet reached at *D*. For among the spectral colours there is still a deeper bluish-green, which must be mixed with a certain amount of white (bleached) in order to give the point *D*. Thus in our method of representing mixed colours we must represent this spectral bluish-green by a point *G* on the line *W-D* produced: The point *D* must be situated between *W* and *G*.

Similar considerations apply to all spectral colours, and these are all (with the exception of *1*, *2* and *3*) represented by points outside the triangle *1-2-3*.

In *fig. 2* the same triangle *1-2-3* has again been drawn but with the spectral colours included. The numbers relate to the wave lengths. If we also draw the line *1-V*, connecting the two ends of the spectrum with each other, we again find by our method of representing colour mixtures that all colour sensations can be represented by points situated within the figure enclosed by the curve of spectral colours and the line *1 V*. (For all colour sensations are produced by mixing spectral colours and these mixtures are all situated within the figure referred to).

---

[5]) The type mixture referred to here must not in any way be confused with the mixing of dyes which follows entirely different laws. The two methods of mixing are fundamentally different: In the first case one type of light is mixed with another, both being allowed to fall on the eye simultaneously or with the aid of a sector disk being thrown into the field of vision in rapid sucession, whilst in the second case each of the two dyes absorbs a specific proportion of the incident light. The results achieved by these two forms of mixing are also quite different: If yellow and blue are mixed by the sector method they will give, as complementary colours, white or grey on a correct choice of the ratio. But if a blue dye is mixed with a yellow dye, the former will absorb red and yellow rays and the latter the blue rays of solar light, so that a green colour is left.

[6]) Quantitative scales can be always so chosen that the method of representation never results in contradictions. The quantitative side of the problem will be discussed in a later article.

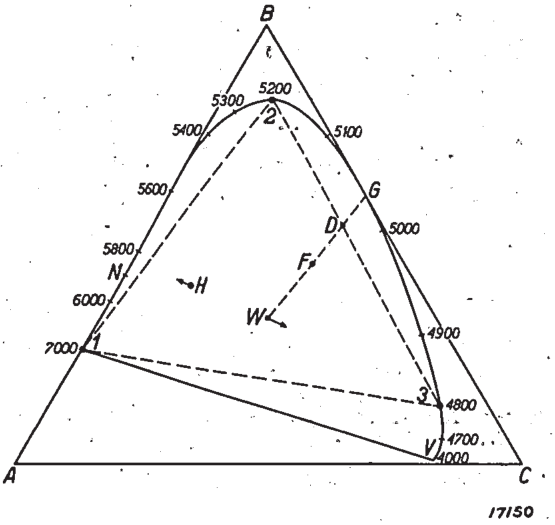

Fig. 2. The same graphical representation as in fig. 1; the curve represents the spectral colours and is enclosed in a triangle *ABC* in order to enable the colours to be expressed numerically. *H* represents glowlamp light and *N* sodium light.

The wave-length of the spectral colour *G* is termed the predominant wave-length of the colour sensation *F*. If *F* can be simulated by mixing a luminous flux L_1 of white light with a beam L_2 of the spectral light *G*, the ratio $L_2/(L_1+L_2)$ is termed the colorometrie purity of the colour *F*. For white this ratio is thus equal to zero; it increases progressively along the line *W-G* and reaches its maximum value at the spectral curve (i.e. *1*). The strongest saturated purples are situated along the line *1-V*.

To express the various colour sensations numerically, an isosceles triangle *ABC* (fig. 2) is drawn which completely encloses the spectral curve, and the position of the point which produces a specific colour sensation, is than expressed by the ratio of the distances of the point from the three sides of *ABC*. In this way every colour sensation is expressed by the ratio of three numbers.

Effect of Brightness on the Mixing Properties of the Eye

As already indicated the "standard" mixing characteristics of the eye discussed above are valid only above a certain brightness level (approx. 0.3 candles per sqft.). Below this limit the rods come into action in addition to the cones [7]. The resulting effect on colour vision can be described in broad outline as follows: When vision is restricted to the rods exclusively (extremely low brightnesses), no colour differences are apparent and everything appears to be grey. If the brightness is in that range in which both cones and rods operate, we may expect to see a composite colour formed from the colour apparent on using the cones (e.g. *F* in fig. 2) and the grey colour seen with the rods. Applying this rule of mixtures and starting with a colour *F* and gradually reducing the brightness (retaining the same spectral distribution) we shall eventually arrive at a colour sensation corresponding to a point between *W* and *F*. In other words: In the transmission range from "cone" vision to "rod" vision colours become steadily paler, finally all passing over into the grey of "rod" vision at very low brightness levels. This phenomenon is in fact observed when dusk falls. The rate at which the colours become paler depends on the choice of colour. The brightness ratio between individual colours also changes when dusk falls [8].

Simultaneous Contrast

Up to the present we have made the assumption that the colour under investigation is the only one in the field of vision. If a second colour appears alongside the first colour, the remarkable phenomenon is observed that the first colour appears to have undergone a change as compared with when it was present alone. The difference between the two colours becomes intensified by their appearance simultaneously (simultaneous contrast). With the aid of fig. 2 we can in fact state in advance in which direction the chromatic displacement will approximately occur: The two points in the colour triangle sum to move further apart and will repel each other equally. This behaviour explains the result obtained in the experiment described above in which white daylight (*W*) was compared with yellow glowlamp light (*H*); as a result of simultaneous contrast the points move further away from each other; the daylight appears bluish and the artificial light has a definite orange-yellow. The well-known phenomenon that when sodium light (*N*a) and glowlamp light (*H*) are present simultaneously the latter appears bluish can also be explained on these lines [9].

---

[7] Regarding the functions of the rods and cones, see Philips techn. Rev. 1, 105, 1936.

[8] On this point, see Philips techn. Rev. 1, 142, 1936.

[9] The effect is here very marked owing to the high saturation of the sodium light.

The colour sensation is also affected in quite another way by the surrounding conditions. The reader will have noticed that in discussing the colour triangle no mention was made of grey and brown. As already pointed out the impression of "grey" is obtained when the object being viewed emits the same type of light as a "white" object, although having at the same time a low coefficient of reflection. Grey is thus really the same as white, in the sense that a white object in general has a brightness higher than that of its surroundings and a grey object a lower brightness: As a result of simultaneous contrast the surroundings make white appear grey. If a white paper and a grey paper are separately illuminated in dark surroundings, the grey e.g. receiving about five times more light, it is quite readily possible to make the two sheets appear to have exactly the same colour.

In the same way as grey may be produced from white by simultaneous contrast, brown may be obtained from yellow, orange or red. This can also be demonstrated by a similar experiment. To a lesser extent the same phenomenon occurs with green, and at low coefficients of reflection the so-called olive green is produced.

Finally, it should be pointed out that simultaneous contrast in the same way as it intensifies colour differences also emphasises differences in brightness: A small white spot in a large black field appears much brighter than the same white in a large white field.

Successive Contrast

By successive contrast we understand the effect of a prior illumination of the eye on the subsequent differentiation of colour. These phenomena are of a similar type to simultaneous contrast: When the eye has become accustomed for some time to a sodium light a white light will again appear to be bluish.

If the intensity of prior illumination were very powerful (we have for instance looked directly at a lamp for a time), this phenomenon will result in the appearance of an after-image; For a brief period an image of the object previously viewed will persist, sometimes dark and sometimes bright against the background and frequently with quite different colours than possessed by the original object. Such after-images are very disturbing to vision and play an important part in glare problems.

Theory of Colour Vision

Only brief reference will be made to this subject; as it is beyond the prescribed scope of this Review. Moreover, as yet very little definite information has been gathered of the mechanism of colour vision.

The study of the phenomena of colour vision has led to the enunciation of two different sets of theories, which subsequently have become expanded in a variety of directions.

The first, due originally to Young and Helmholtz, assumes that three sensations can take place in the eye; the first sensation is excited to the greatest extent by red light, the second by green light and the third by blue light. On the basis of this assumption the mixing laws established experimentally are readily explained: each colour provides a stimulus for the three fundamental sensations in a specific ratio, and it can thus be actually expressed by the ratio of these magnitudes. With this theory we can moreover readily account for the occurrence of different types of colour blindness on the simple assumption that in these one or other of the three fundamental sensations is absent.

The other theories, due initially to Hering, assume three sensations each of which can take place in two directions: A blue-yellow sensation, a red-green sensation and a black-white sensation; blue light displaces the first sensation in the one direction and yellow light displaces it in the opposite direction, etc. A theory on these lines gives us a better insight into the sensations experienced with simultaneous and successive contrast, after-images and fatigue phenomena, etc., but does not give such a natural and simple explanation of the representation of colours in a colour triangle as is offered by the Helmholtz theory.

It has hitherto not been possible to demonstrate anatomically that three kinds of nervous elements exist in the retina or that three kinds of chemical phenomena take place there.

In conclusion a few words may be added regarding binocular colour mixing. If the two eyes are exposed to light of different colours, a mixed colour is obtained with most persons, the same mixing rules applying in general to this sensation as to ordinary mixing. With other persons such a mixture cannot be obtained and as a rule these will see only one of the two original colours. From the existence of binocular mixing it may be concluded that the mixing processes — at least the combination of the primary colours to give a simple colour sensation — do not take place on the retina or the optic nerve, but at some deeper point, possibly not before the brain is reached.

ABSTRACTS OF RECENT SCIENTIFIC PUBLICATIONS OF THE N.V. PHILIPS' GLOEILAMPENFABRIEKEN

No. 1093: A. E. **van Arkel**, E. J. W. **Verwey** and M. G. **van Bruggen**: Ferrites I (Rec. Trav. chim. Pays-Bas, **55**, 331-339, May, 1936).

Radiographs were made of mixtures of oxides of bivalent metals (MO) with ferric oxide (Fe_2O_3) in different proportions, which had been strongly heated from 1200 °C up to 1300 °C. for several hours. The radiographs indicated that mixtures containing a high percentage of Fe_2O_3 have comparable structures. At high temperatures (up to 1300°C.) the ferrite phase (with spinel structure) stretches far towards the Fe_2O_3 side. At lower temperatures (800° to 1000 °C) this area is considerably contracted. From a crystallographic standpoint, solid solutions in which the iron content is greater than corresponding to the ratio $MO : Fe_2O_3 = 1 : 1$ may be regarded as "differential phases" as defined by **Hägg**. Compounds with a composition 2 MO. 3 Fe_2O_3 as assumed by **Hilpert** do not exist.

No. 1094: E. J. W. **Verwey**, A. E. **van Arkel** and M. G. **van Bruggen**: Ferrites II (Rec. Trav. chim. Pays-Bas, **55**, 340-347, May, 1936).

At high temperatures (up to 1400 °C) the proportions in which ferrites are miscible with metallic oxides are investigated. Hausmannite (Mn_3O_4) dissolves considerable quantities of Fe_2O_3 (at 1300° up to $Mn_3O_4 : Fe_2O_3 = 1 : 6$), whereby its tetragonal lattice gradually passes over into the cubic lattice of ferrite. Solid solutions of MgO with $MgFe_2O_4$ and of NiO with $NiFe_2O_4$, which are formed at high temperatures, segregate slowly at about 1000 °C. The elementary cell for ferrite is almost exactly double as great as that for the oxides. Segregation can therefore be investigated by X-ray methods only on the basis of calculated and observed intensities of the diffraction lines. Magnetic measurements reveal the segregation far more accurately than X-ray measurements, and the latter much better than observations with the microscope.

With a ratio of $CuO : Fe_2O_3 = 3 : 1$ a new compound is formed in copper ferrite.

No. 1095: J. H. **de Boer** and J. D. **Fast**: The α-β transition in zirconium in the presence of hydrogen (Rec. Trac. chim. Pays-Bas, **55**, 350-356, May, 1936).

Both α and β zirconium absorb hydrogen. The solubility decreases in both modifications with rising temperature. Hydrogen is absorbed when α zirconium is converted into β zirconium at rising temperature and in a hydrogen atmosphere. On cooling β zirconium passes over into the α modification and at the same time liberates hydrogen. The transition of α zirconium into the β modification appears to be responsible for the very rapid absorption of hydrogen observed by **Clausing** and **Ludwig** when a zirconium wire is allowed to cool.

No. 1096: A. G. **Boer**, E. H. **Reerink**, A. v. **Wijk** and J. v. **Niekerk**: A naturally occurring chicken provitamin-D (Proc. Roy. Soc. Amst., **39**, 622-632 May, 1936).

This paper describes the preparation and properties of provitamin-D which is a constituent of cholesterol. The probable structural formula deduced from various data is confirmed by different reactions and proved by comparison with pure synthetic 7-dehydrocholesterol with which the new provitamin D is identical. By irradiation a vitamin D is obtained whose anti-rachitic action on chickens is comparable with vitamin D from cod-liver oil.

No. 1097: W. **Uyterhoeven** and C. **Verburg**: Température des électrons (T_e) dans une décharge en colonne positive dans un melange Ne-Na (C.R. Acad. Sci., Paris, **202**, 1498-1500, May, 1936).

In a previous paper (see Abstract No. **1047**) the authors have indicated that the addition of a little sodium vapour to neon causes the voltage drop in the positive column to increase considerably. In the present paper probe measurements in a column of Ne-Na are described. The temperature of the electrons (T_e) and the concentration of the ions (n_p) are determined as a function of the temperature of the wall of the tube, i.e. as a function of the Na concentration. The electron temperature attains a maximum of approx. 23 000 °K. with one atom of sodium to 10 000 atoms of neon; in the case of pure neon and other conditions being equal the temperature is 19 500 °K.

VOL. 1 No. 10 OCTOBER 1936

Philips Technical Review

DEALING WITH TECHNICAL PROBLEMS
RELATING TO THE PRODUCTS, PROCESSES AND INVESTIGATIONS OF
N.V. PHILIPS' GLOEILAMPENFABRIEKEN

EDITED BY THE RESEARCH LABORATORY OF N.V. PHILIPS' GLOEILAMPENFABRIEKEN, EINDHOVEN, HOLLAND

5/

THE "PHOTOFLUX"

A LIGHT-SOURCE FOR FLASHLIGHT PHOTOGRAPHY

by J. A. M. VAN LIEMPT and J. A. DE VRIEND.

Summary. The "Photoflux" is a light-source suitable for flashlight photography. It consists of a bulb containing oxygen in which a long wire of a combustible alloy is ignited electrically. This article deals with the method employed for measuring the quantity of light emitted and the luminous intensity as a function of the time.

Introduction

The art of photography is now one hundred years old and is almost as old as are attempts to devise means of artificial illumination enabling photographs to be taken when natural sunlight is either lacking or too weak. At the present time two types of artificial light sources are employed in photography:

1) Light-sources for studio lighting by means of which a large number of photographs can be taken in rapid succession.
2) Light-sources which can be used once only and which furnish a very powerful light for a brief period of time, this characteristic being implied in their ordinary name of "flashlights".

A light-source of the latter type is exceptionally suitable for taking snapshots and must satisfy, *inter alia*, the following requirements:

a) It must generate an intense light which must however not be embarrassing to the subject being photographed.
b) It must operate without even the least complex or heavy current source.
c) It must not introduce any fire hazard or other undesirable condition, such as smoke or odour.
d) It must always be ready for use, also during rainy and stormy weather.
e) It must be compact in design and light in weight.

It is comprehensible therefore why flashlight powder, which only satisfies requirements b) and e) and not by any means requirements c) and d), has been rapidly replaced during recent years by flash bulbs in which the whole process of the rapid light-generation by combustion takes place in a totally-enclosed glass bulb. This class of light generator includes the "Photoflux" in which the duration of the flashlight is only about 1/40 of a second, thus being considerably below the reflex time of the eye of approx. 1/10 sec. The use of this source thus eliminates that screwing-up of the eyes in flashlight photographs, which has been a common fault of these photographs in the past.

Description

The "Photoflux" (*fig. 1*) consists of a glass bulb 55 or 70 mm in diameter filled with oxygen and enclosing a wire of an aluminium alloy containing approx. 8 per cent magnesium. This wire is only 0.035 mm thick and is in the form of a crumpled mass, so that it is distributed as uniformily as possible over the whole interior of the bulb. The volume occupied by the whole wire is not greater than that of a hailstone. After careful evacuation the bulb is filled with pure dry oxygen at a low pressure. In the middle of the bulb and thus completely surrounded by the crumpled wire is a small incandescent filament carrying a weak charge of priming paste. If the filament is brought to incandescence, e.g. by connecting the lamp to a flashlamp battery, the priming is ignited. Ignition is transmitted to the wire which burns very rapidly in the oxygen atmosphere. Since the length and thickness of the wire are the same in all lamps and the quantity of light evolved is proportional to the weight of the wire, there is every guarantee that all lamps of the same type will give the same intensity of light.

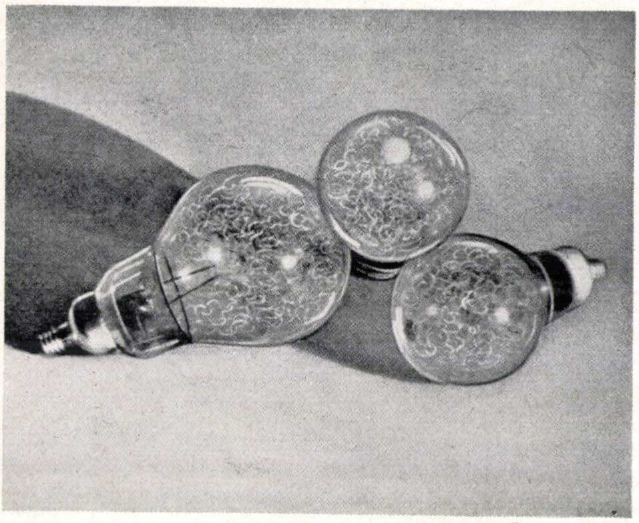

Fig. 1. The "Photoflux" flashbulb.

Should inleakage develop in the lamp after leaving the works, for instance through a crack in the bulb, the latter will fill with air through the crack owing to the low pressure of the contained oxygen. A lamp of this type with a thin-walled bulb and a much higher gas pressure than the initial oxygen filling would prove dangerous on ignition, since the bulb cannot withstand the sudden increase in pressure generated on combustion. To avoid this hazard a deep-blue spot of a cobalt salt is provided in the bulb which turns a light rose colour by absorption of moisture when air leaks into the lamp. The salt used is so sensitive that the humidity of the air even on the driest and coldest days is sufficient to produce a change in colour. Lamps with a bright rose instead of a blue indicator spot are therefore defective and must not be used owing to the liability of shattering the bulb.

Since the combustion responsible for the generation of light takes place in a sealed bulb, the "Photoflux" operates with complete reliability in all weathers. The fire hazard has been completely eliminated and the combustion-products formed remain in the bulb.

The "Photoflux" is preferably used with a reflector so that the greater part of the spherically-radiated light is utilised to good purpose and the light is intensified four to five times in the required direction. The simple Photoflux millboard reflector makes a very good reflector, where a more efficient and hence more expensive unit is not essential. The "Photoflux" is fitted with either a miniature cap, similar to that on flashlamp bulbs, or with standard screw and bayonet caps as on ordinary incandescent lamps. The „Photoflux" with incandescent lamp cap can be used with either a 4-volt battery or a lighting mains supply. For the latter case a rapid-acting fusible element is incorporated in the lamp to protect the house fuses. The actinic energy of the light from the „Photoflux" is given in the following table, which applies to the smallest Type I now on sale.

Illumination Table for „Photoflux" Type I when using a lamp with reflector

Distance (in metres) from the light source to the object being photographed for different apertures.

Negative Material	Aperture							
	3.5	4.5	6.3	11	12.5	18	21	32
Normal orthochromatic	8	6.5	4.5	2.6	2.3	1.6	—	—
Rapid orthochromatic	12	9	7	3.7	3.2	2.2	1.9	—
Normal panchromatic	14	11	8	4.5	4	2.8	2.4	1.6
Rapid panchromatic	20	16	11	6.5	6	4	3.4	2.2

Quantity of Light and Light Yield

The photographic value of a flashlight is expressed essentially by the quantity of light (luminous flux multiplied by the time). It may be measured with a photo-electric cell in conjunction with a spherical integrating photometer and an electrostatic voltmeter. In our measurements we used a type 3510 photo-electric cell (a vacuum cell with potassium cathode) whose characteristic is given in *fig. 2*. This figure shows that the photo-

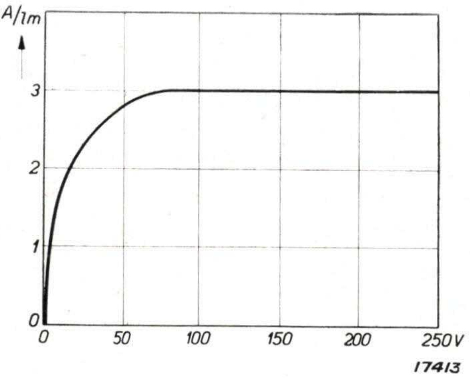

Fig. 2. Characteristic of the Philips type 3510 photo-electric cell.

electric current in the cell is practically independent of the anode voltage as long as the latter does not drop below 50 volts, a feature which is very convenient for the present measurements. The colour sensitivity of the cell is roughly the same as that of an orthochromatic plate, the red limit being approximately at 7500 Å.

To measure the light output the following arrangement was used (*fig. 3*). The "Photoflux" *2* was suspended in an Ulbricht sphere, and the photoelectric cell *6* connected to the electrostatic voltmeter *7*. The condenser which is incorporated in the design of this voltmeter is initially charged to 300 volts by a Wimshurst machine. As soon as light falls on the cell, the condenser is discharged by the photo-electric current and since the current is independent of the anode voltage (above 50 volts), the quantity of light generated is proportional to the voltage difference measured on the electrostatic voltmeter before and after discharge, provided the lowest voltage is not under 50 volts. The capacity of the condenser referred to is matched to the quantity of light expected by connecting one or more other condensers in parallel.

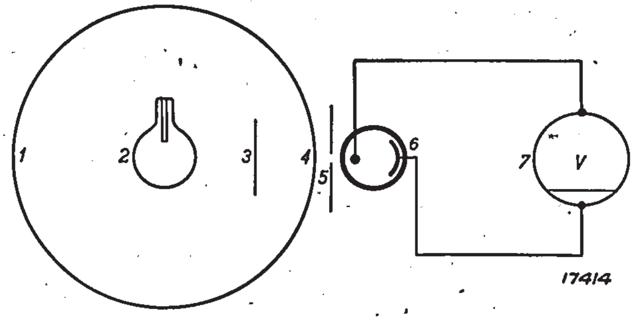

Fig. 3. Arrangement for photometric examination of the flashbulbs. *1* Ulbricht sphere; 2 "Photoflux"; 3 screen; *4* opal glass plate protected by the screen 3 against direct radiation from the "Photoflux"; 5 diaphragm; *6* photo-electric cell; *7* electrostatic voltmeter.

After the photometer has been calibrated with an incandescent lamp whose luminous flux has itself been calibrated and which is switched on for a definite period, the light output of the flash-bulb can be calculated in lumens per sec. Thus for the "Photoflux type" I a value of 25 000 lumen secs was obtained and for type II 50 000 lumen secs. Since the duration of the flash is about 1/40 of a second, the light output of 25 000 lumen secs or 1 000 000 lumens in 1/40 of a sec corresponds to the light emitted in the same time by 1000 lamps of 100 Dekalumen.

The heat of combustion of the alloy wire was measured in a calorimetric bomb and was found to be 28.9 watts-secs per mg. Since the "Photoflux" type I contains 27 mg of alloy wire, the light output is:

$$\frac{25000}{27 \cdot 28.9} \doteq 32 \text{ lumens per watt}$$

This corresponds to the light output of a black body at a temperature of 3100 °K.

Luminous Intensity as a Function of the Time

In addition to the total light-output of the flashbulb the variation of the light output as a function of the time is also of interest. The measuring apparatus used consists essentially of a photoelectric cell and a cathode ray tube. The photoelectric current generated by the light from the "Photoflux" produces a voltage drop at a noninductive resistance of 50 000 ohms. The terminals of this resistance are connected to the deflecting plates which deflect the cathode ray perpendicularly to its direction; the second pair of deflecting plates is not employed and is earthed.

In *fig. 4* the arrangement of the apparatus used is shown diagrammatically. At the top is the high-vacuum cathode ray tube (*1*), and on the right the mains connection for furnishing the heating current for indirectly heating the cathode and, through a series of potentiometer tappings, the D.C. voltages for the grid and the two anodes. At the bottom left is the photo-electric cell (*2*) whose anode voltage is furnished by a 360-volt battery. The cell with battery is bridged by a 50 000-ohm resistance and connected in parallel with two series-connected resistance leaks of 10 megohms, whose junction is connected to the deflection plates and the earthed anode of the cathode ray tube. In the arrangement shown a vacuum cell with caesium cathode, type 3512, was used, since no amplifier

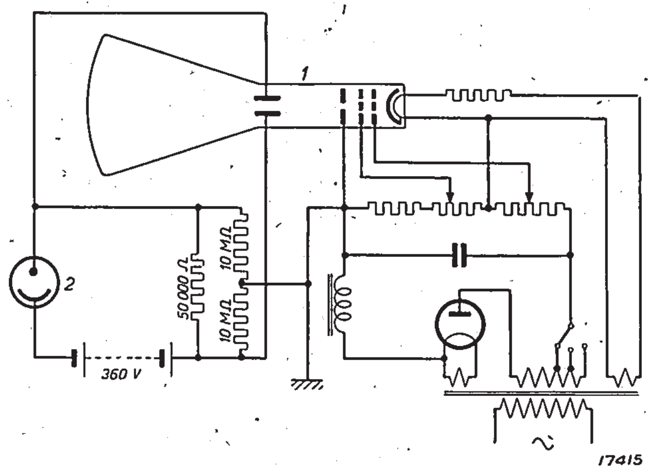

Fig. 4. Apparatus for measuring the light intensity as a function of the time. *1* cathode ray tube; 2 Type 3512 photo-electric cell.

is employed here and a high sensitivity is therefore essential. The photo-electric cell is enclosed in a metal housing mounted on the Ulbricht sphere. Between the sphere and cell an adjustable diaphragm is fixed. When the flashlight is burnt in the spherical photometer, a beam of light falls on the photo-electric cell which is reduced to a suitable intensity by the diaphragm. The voltage drop at the 50 000-ohm coupling resistance is then used to control the cathode ray.

The vertical deflection of the cathode ray produced in this way is registered by means of an oscillograph camera with extra high-power optical system. The photographic plate is displaced horizontally in the camera by means of a released spring. On unlatching the locking pawl, which releases the stretched spring in the camera, a switch is released at the same time which switches on the "Photoflux", so that the cathode ray is deflected the moment the camera plate starts moving. A small neon lamp fed from a 50-cycle A.C. mains supply is also photographed to provide a time base, a black mark being produced on the plate at intervals of 0.01 sec. The oscillogram obtained can, if necessary, be enlarged four to five times with an enlarger and can be converted to absolute units since the total quantity of light in lumens per second is known. The variation in light intensity of the type I bulb as a function of time is shown in *fig. 5*.

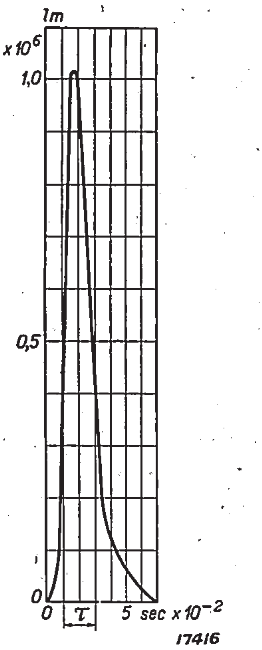

Fig. 5. Light-intensity-time curve of the "Photoflux". τ is the speed of the flash.

Lag on Ignition

In addition to the light intensity-time curve the socalled lag on ignition is also an important characteristic, i.e. the time elapsing between the moment the lamp is switched on and the instant the "Photoflux" commences to radiate light. To measure this lag the arrangement just described has been slightly amplified. A Philips E 499 radio valve is connected in parallel with the photo-electric cell (*fig. 6*), the valve being fed from e.g. a 240-volt battery. On operating the camera switch *O* a relay *K* is energised which connects the "Photoflux" to a 4-volt accumulator through two contacts (which are here connected in parallel in order to ensure good circuit-closing contact). A 2-ohm resistance is connected in series with the accumulator to adapt the arrangement to the working conditions obtaining when using a pocket-lamp battery.

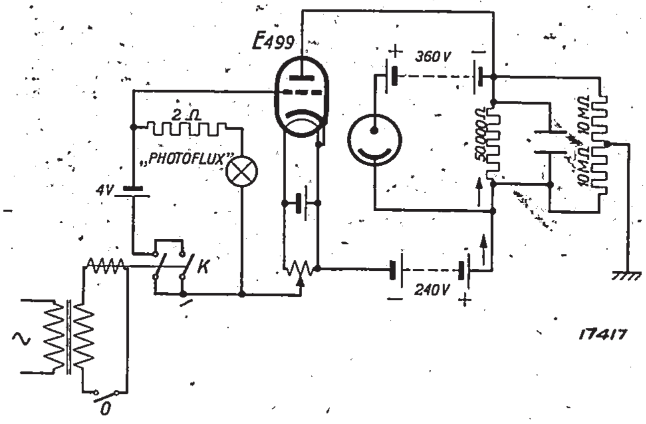

Fig. 6. Diagram of arrangement for measuring the lag in ignition of the "Photoflux".

On switching on the "Photoflux" the accumulator is inserted, at the same time and through the same contact, between the cathode and the grid of the E 499 valve, so that the grid bias of the valve is increased by 4 volts as compared with that previously adjusted at the potentiometer through the filament voltage of the E 499 valve, whereby the anode current of the valve is suppressed. This anode current previously flowed through the 50 000-ohm coupling resistance and caused a deflection in the cathode ray tube which disappeared on switching on the "Photoflux". When light commences to be radiated from the "Photoflux" the cathode ray is again deflected. The time elapsing between these two deflections is the required lag on ignition. In addition to the lag the oscillogram also includes the whole of the light intensity-time curve.

An oscillogram of this type is reproduced in *fig. 7*, which includes not only the light-time diagram, as shown in fig. 5, but also the actual lag on ignition. The lag in the "Photoflux" is about 0.035 sec;

it varies very little from bulb to bulb and is also not appreciably affected by the resistance in the circuit, i.e. ignition is obtained just as rapidly with a new as with a partially-exhausted pocket-lamp battery.

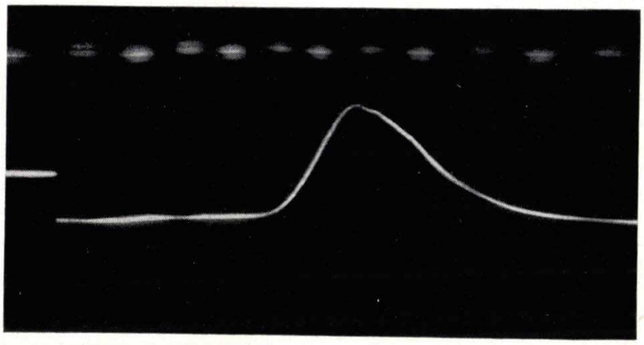

Fig. 7. Oscillogram of the lag in ignition of the "Photoflux" and the variation of light intensity with time.

The absolute value of the lag is of less moment than the fact that it is practically constant, an important characteristic when using the "Photoflux" in conjunction with synchronised shutter releases. The latter are small units mounted on the camera for synchronising the shutter with the flash-bulb. The simplest arrangement of this type consists of an electric switch which is operated at the same time as the shutter cable release. With a single manual operation the shutter is first opened and a very short time later the flash-bulb is switched on (for the sake of convenience the bulb is mounted in a holder on the camera), 0.035 sec later light is emitted and lasts for only about 0.05 sec, when the shutter is automatically reclosed. To ensure satisfactory exposure the shutter in this arrangement must remain open for about 1/10 of a second.

In a more refined arrangement the flash-bulb can, for instance, be switched on first and immediately after the shutter released, so that its opening coincides with the emission of light. To obtain well-defined exposures and to avoid any interference from artificial light sources and windows in the field of view, the shutter speed can be reduced to 1/100 to 1/500 of a second without disadvantage. The only precaution necessary here is that the shutter is open during the short time the maximum quantity of light is emitted from the flash-bulb. It is evident that in both cases, and particularly in the latter, the lag on ignition of the flash-bulb must be very constant if light emission is to be obtained exactly at the moment required.

Practical Speed of the Flash

It will be apparent that the time during which the light is strong enough to act on the photographic plate is smaller than the base of the light-time curve diagrams in figs. 5 and 7. The spurs at the two ends of the light-time curve are of negligible importance since the sensitivity of the plate drops considerably below a certain intensity threshold.

To determine the actual speed of the flash we can compare exposures of a moving object obtained with the flash-bulb with similar exposures made with a uniform illumination and using an ideal, previously calibrated, instantaneous shutter, and estimating at which exposure time photographs of equal definition are obtained.

This has been done by photographing with the "Photoflux" a rotating black disc on which several hexagonal white and grey stars with black letters are arranged at different distances from the centre. The requisite distance of the "Photoflux" from the disk was determined from an illumination formula [1]), so that the correct blackening of the negative was realised. The exposures obtained were compared with those of the disk rotating at the same velocity when illuminated by a light-source giving a uniform luminous flux and with previously calibrated shutter speeds of 1/10, 1/25, 1/35, 1/50 and 1/100 of a second [2]). In this way the practical speed of the flash was found to be 1/35 to 1/50 of a sec, which is in agreement with fig. 5, if it is assumed that the spurs on both sides of the light-time curve produce no latent blackening of the plate up to light intensities of 20 to 30 per cent of the maximum value. For these comparative exposures a shutter should be used in which the inertia of the blades is very small. With shorter exposure times (below 1/25 sec) a diaphragm can be used with advantage, in order that the illuminated diagram of the shutter is a rectangle.

Colour of the Light

The spectrum of the light emitted by the "Photoflux" was recorded with a Hilger spectrograph Type E 3 with quartz prism on Ilford Special Rapid panchromatic plates. The negative was printed through a grey wedge using the method of Visser [3]) so that the length of the spectral lines on the print increases with their intensity. The result obtained is indicated in *fig. 8*. The spectrum is seen to be continuous and reaches from about 3500 Å into the infra-red. A more intense band and a stronger line occur at 5200 Å (Mg) and 5900 Å (Na).

---

[1]) J. A. M. van Liempt, Rec. Trav. chim. Pays-Bas, **53**, 471, 1934.

[2]) For information on the calibration of instaneous shutters using the cathode ray tube see:. J. A. M. van Liempt and J. A. de Vriend, Z. Phys., **95**, 198, 1935.

[3]) S. H. R. Visser, Physica, **1**, 497, 1934.

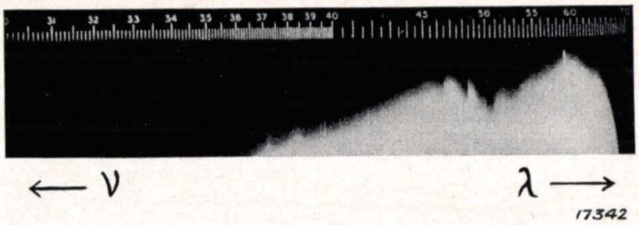

Fig. 8. Spectrum of the "Photoflux".

Furthermore, the chromatic reproduction on different plates was measured with the Agfa graded colour table [4]). We found the following values:

Plate [5])	Red	Yellow	Green	Blue
Blue-sensitive plate	30	15	30	160
Isochromatic plate	30	30	30	160
Orthochromatic plate	30	20	30	180
Panchromatic plate I	180	80	30	100
Panchromatic plate II	70	60	50	120
Panchromatic plate III	90	50	40	120

For comparison, the results are given below of measurements on the same plates using daylight with a clear sky and facing the north. As may be seen the reproduction of colours with "Photoflux" illumination is better than with daylight.

Plate [5])	Red	Yellow	Green	Blue
Blue-sensitive plate	30	10	25	180
Isochromatic plate	30	20	30	180
Orthochromatic plate	30	15	30	180
Panchromatic plate I	90	40	30	180
Panchromatic plate II	60	40	40	140
Panchromatic plate III	60	30	30	160

The colour-scale temperature of the light from the "Photoflux" was determined by comparing the photographic reproduction of colour with other light sources of known colour-scale temperature. The colour diagram of von Lagorio[6]) was obtained for these light sources and for the "Photoflux" on different panchromatic plates. It was found that the colour-scale temperature of the "Photoflux" is slightly higher than that of the carbon filament lamp, viz., about 4000 deg. abs. [7]).

---

[4]) H. Arens and J. Eggert, Z. wiss. Phot., **29**, 239, 1930.

[5]) The panchromatic plates I, II and III were obtained from three of the principal makers.

[6]) A. von Lagorio, Phot. Ind., **23**, 629, 1930.

[7]) J. A. M. van Liempt and J. A. de Vriend, Z. wiss. Phot., **34**, 237, 1935.

RECTIFIERS FOR TELEPHONE EXCHANGES

Summary. For telephone installations a D.C. supply is required with very constant voltage and low internal resistance. A rectifier is described which satisfactorily meets these requirements, being designed for feeding small telephone installations without the aid of a battery.

Charging of Telephone Batteries

Batteries are employed in telephone exchanges all over the world for furnishing the current requirements of microphones and relays. Initially it was usual to equip these exchanges with a double set of batteries, each set being employed alternately so that the idle batteries could be recharged while the other set was in service. During recent years charging arrangements have been constructed by means of which the batteries can be charged during service, thus making spare battery sets superfluous. For this socalled "buffer operation" in telephone exchanges the rectifier is a very suitable supply unit since it has no moving parts, requires no attendance, operates quite noiselessly and also has a satisfactory efficiency. Moreover, the rectifier can be set up close to the battery, thus considerably shortening the connecting cables.

The batteries can be charged by either of two methods:

a) By means of a rectifier which is set in operation automatically as soon as the charge has dropped below a specific minimum, and which again disconnects itself when the battery has been fully charged;

b) By means of a socalled "buffer rectifier" which is in continuous operation.

With the buffer rectifier the charging current is so adjusted that the rectifier just makes up the average discharge current. The battery can then be made much cheaper as its capacity has to be merely sufficient to maintain the service on a temporary failure of the mains supply or when during peak traffic periods a greater amount of current is consumed than can be supplied from the rectifier.

A Rectifier as a Battery Substitute

By using the buffer rectifier, the battery can in fact be dispensed with altogether and the rectified alternating current smoothed by a filter. The problem whether this method offers advantages in certain cases has long been the subject of investigation.

A feature in favour of batteries is that a disturbance in the mains supply does not interfere with the telephone service itself. But a battery is not always necessary. In most private telephone installations a breakdown in the supply is not to be anticipated, since a failure in the power supply occurs only rarely and is then only of short duration. Moreover, a large telephone installation, such as is commonly used in large buildings and warehouses, can be connected to two different sections of the mains supply where a failure cannot take place in both together.

When using a rectifier for a direct supply of a telephone network the direct voltage must as far as possible be independent of the load; a filter must also be provided as otherwise the ripple of the current furnished by the rectifier will produce an audible hum in the telephone circuits.

A valve rectifier is described below which operates without a battery and which is suitable for feeding small telephone exchanges, e.g. house telephone installations in warehouses and factories.

Fig. 1 gives the general circuit diagram. The principal components of the rectifier are the rectifying valves B_1, B_2 and the filter which is made up of the choke coils L_1, L_2 and the condensers C_1, C_2. Of the various types of rectifying valve available the gasfilled valve offers the advantage of having a voltage loss independent of the load, so that a compensating arrangement can be dispensed with. Gasfilled rectifying valves with oxide cathodes are particularly suitable for the present purpose.

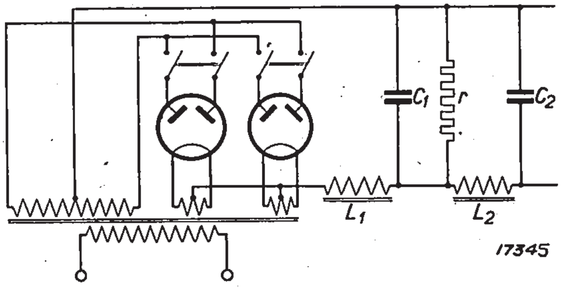

Fig. 1. Diagrammatic circuit of the telephone rectifier. The principal components are the rectifying valves and the filter composed of C_1, C_2, L_1 and L_2. When one valve is running, the other valve cannot start as its starting voltage is higher than the running voltage of the other valve. The idle valve however starts to operate automatically as soon as the other valve ceases to function.

This valve has moreover a very long life. *Fig. 2* shows the efficiency of the two-phase 10-amp rectifying valve type 1788 plotted as a function of the current for direct voltage outputs of 100 volts (maximum) and 50 volts. At 50 volts the efficiencies at 5 and 10 amps current are 76 and 79 per cent respectively. At 100 volts the efficiencies are 86 and 89 per cent respectively.

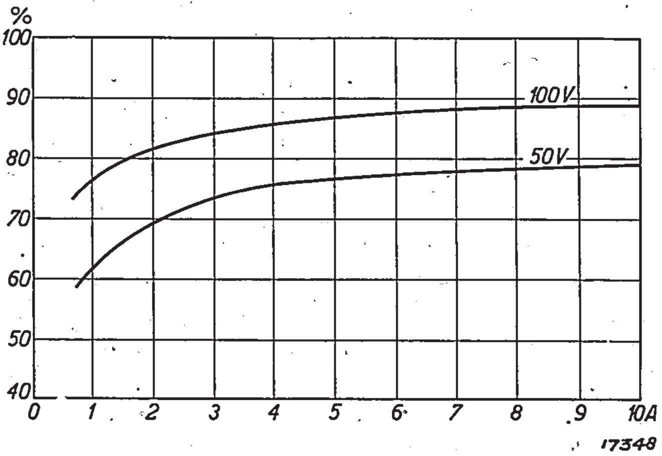

Fig. 2. Efficiency of the gas filled rectifying valves Type 1788 for voltages of 50 and 100 volts plotted as a function of the current intensity.

The filter

A two-phase rectified alternating voltage of 50 volts, 50 cycles, has *inter alia* an A.C. component of 100 cycles and approx. 25 volts eff., which must be suppressed sufficiently so that no humming is audible in the telephones [1].

The filter consists in its simplest form of a choke coil through which the charging current passes and a condenser in parallel with the output terminals of the rectifier. As necessary a series of these stages are connected in series (see e.g. fig. 1). The filter circuit employed for a rectifier used for directly feeding a telephone network must have an extremely small D.C. resistance in order to keep the output voltage constant and independent of the load.

The degree of smoothing is determined to a first approximation by the product of self-induction L of the choke coil and the capacity C of the condenser. Within certain limits L can be made small and C very large or vice versa [2]. To avoid cross-talking the A.C. resistance of the source of supply must be low. The self-induction values are therefore made as low as possible and the capacity C_2 very large. Electrolytic condensers are particularly suitable for this purpose as they enable high capacities to be coupled with compact dimensions and with a low weight.

The voltage furnished by the rectifier is practically constant over a wide current range, but increases with a very low load up to the peak value of the rectified alternating voltage, while the normal running voltage E_0 is much smaller. To avoid the voltage fluctuations which may result therefrom a resistance r is connected in parallel with the condenser C_1, this resistance shown in fig. 2 permits a minimum load to be applied. The value of r is so chosen that the voltage of the rectifier on no load has dropped to E_0.

In many telephone installations the feed circuits for the microphones and relays can be kept separate. Since the direct current for the relays does not have to be smoothed to the same degree as the microphone current, while the direct voltage in the microphone circuit need not be kept as rigidly constant as in the relay circuits, the filter at the rectifier can with advantage be split up. *Fig. 3* gives the general circuit details for an arrangement of this type. The relays are connected to the terminals R and the microphones to the terminals M.

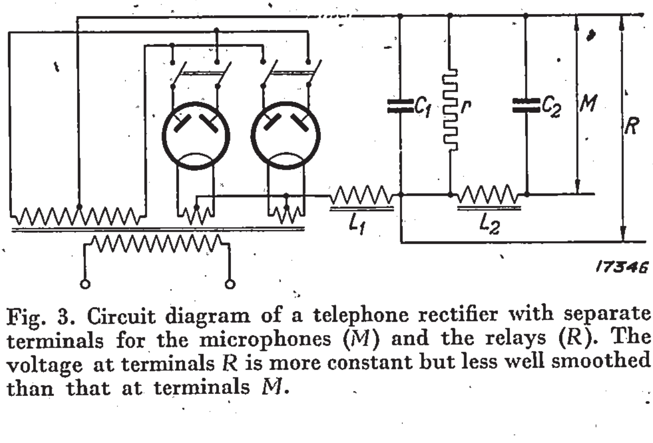

Fig. 3. Circuit diagram of a telephone rectifier with separate terminals for the microphones (M) and the relays (R). The voltage at terminals R is more constant but less well smoothed than that at terminals M.

The last portion of the filter composed of L_2 and C_2 here also acts as an interference-suppression filter eliminating the crackling noises emanating from the relays, in addition to smoothing the direct current. In a rectifier designed on the lines of the circuit in fig. 1 these disturbances are suppressed by the condenser C_2 which for this purpose must therefore have a much greater capacity.

Reliability in Operation

As may be seen from the circuits in figs. 1 and 3 two rectifying valves connected in parallel are employed. The starting voltage of gas-filled valves differs slightly from valve to valve, but is always greater than the arc voltage so that of two valves in parallel the one with the lower starting voltage will come into operation first and at the same time prevent the starting of the other valve. In this way one valve acts as a reserve and takes over automatically immediately the other valve fails. The temperature of the filament in these valves is only about 950 °C., and is thus so low that vaporisation is of no account so that the spare valve remains in excellent condition. The current consumption of the hot cathode in the 10-amp valve in only 20 watts, so that also in this direction there is no objection against a second filament being continuously in circuit. A double pole anode switch is incorporated in the rectifier for each valve, such that immediately the working valve is switched of the other valve is switched on. In this way it is possible to test each valve without breaking the continuity of supply. A defective valve can be replaced without any interruption in service.

---

[1] At 100 cycles this limit is located at approx. 0.2 volt. Cf. for further information J. G. W. Mulder and D. M. Duinker, Over het afvlaksysteem bij het laden van telefoonbatterijen gedurende het bedrijf. De Ingenieur **46**, E 27, 1931.

[2] Cf. D. M. Duinker, Discussion on "Some considerations in the design of hot cathode mercury-vapour rectifier circuits", J. Inst. el. Eng., **76**, 421, 1935.

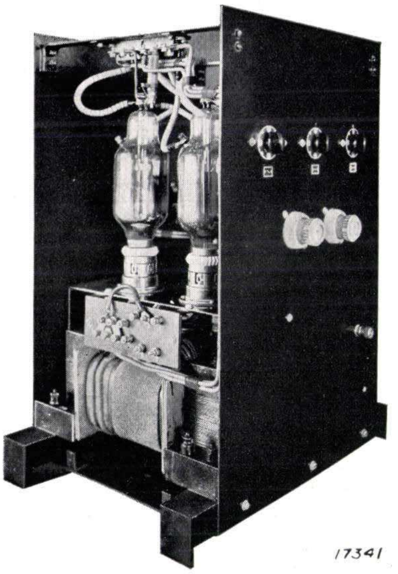

Fig. 4. View of a telephone rectifier for 50 volts and 7 amps D.C. The unit is wired as shown in the diagram in fig. 3. It is suitable for connection to a single-phase A.C. mains supply and can be adjusted for various supply voltages between 190 and 260 volts (50 cycles).

Electrical Construction

The apparatus shown in *fig. 4* is suitable for connection to a single-phase A.C. mains supply and can be adjusted for various supply voltages. It is constructed for a voltage of 50 volts with a maximum current of 7 amps. The efficiency is shown graphically in *fig. 5*. The voltage ripple occurring at the output terminals is less than 0.1 volt at 100 cycles, and with this rippling no hum is audible.

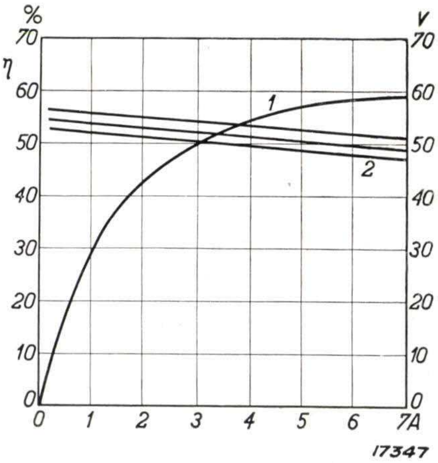

Fig. 5. *1* Efficiency of the rectifier shown in fig. 4, plotted as a function of the current intensity. *2* Direct voltage output plotted as a function of the current intensity. As the current increases up to full load the voltage gradually drops with about 8 per cent. To correct for small voltage fluctuations the transformer primary is provided with three tappings, which correspond to the three curves in the figure.

Rectifiers of this type for furnishing a direct supply to telephone installations and for buffer operation are now supplied for outputs up to several kilowatts.

Compiled by H. J. J. BOUMAN.

ELECTRICAL FILTERS III

Vacation course, held at Delft, April, 1936.

By BALTH. VAN DER POL and TH. J. WEIJERS.

LOW-PASS FILTER SECTIONS.

Summary. In this article the characteristics of non-dissipative low-pass filter sections are analysed by the method described in the previous issue of Philips Technical Review. A short discussion follows of the effect of the losses and the design of compound filters, whose input and output impedances are practically equivalent to pure resistances independent of the frequency. In conclusion a diagrammatic summary is given of the data and formulae for the design of low-pass filter sections. The appendix contains a summary of the formulae which were deduced in the article: Electrical Filters II.

Introduction

The general characteristics of *T*-sections, *Π*-sections and half-sections which were deduced in the previous article will now be applied for deriving the simplest forms of low-pass, high-pass and band-pass filter elements and their characteristics. In each case we shall take a simple form of filter element as the fundamental type and from this derive the other type with the aid of *m*-transformations. We shall see later how from the sections available a compound filter can be built up to satisfy specific requirements.

Low-Pass Filter Sections

The function of a low-pass filter consists in transmitting all frequencies below a certain limiting frequency with the minimum degree of attenuation and to damp all frequencies above ν_1 in a given ratio. We shall in the first instance consider ideal filter sections composed of pure reactances. We shall see later what effect the real resistances of filter elements can exercise.

a) *Fundamental Form.* As a basic form we shall take the simplest form of low-pass filter section. We shall again denote all magnitudes relating to the fundamental form with an accent. The complete sections Z_1' and Z_2' are made up of a self-inductance L_1' and a capacity C_2' respectively, thus:

$$\left.\begin{aligned} Z_1' &= j\omega L_1'\,; \\ Z_2' &= \frac{1}{j\omega C_2'}\,. \end{aligned}\right\} \quad \ldots\ldots \quad (32)$$

A *T*-section, a *Π*-section and a half-section can be formed from these elements in the usual way. As shown in the previous article (p. 274) the transmission bands of these sections coincide and are determined by $-1 < Z_1/4\,Z_2 < 0$; Z_1 and $4\,Z_2$ are in this region of opposite sign, while Z_1 and $-4\,Z_2$ are of the same sign. Moreover $|Z_1| < |4\,Z_2|$. If now in one graph Z_1 and $-4\,Z_2$ are plotted as a function of the frequency, the transmission band is characterised by the fact that Z_1 lies between the abscissa and $-4\,Z_2$. For the filter section considered *fig. 8* represents this diagram of reactances. From this we see that Z_1' lies between the abscissa and $-4\,Z_2'$ for all frequencies between $\nu = 0$ and $\nu = \nu_1$. The transmission band thus reaches from $\nu = 0$ to $\nu = \nu_1$. The attenuation band reaches from $\nu = \nu_1$ to ∞. The limiting frequencies are therefore $\nu = 0$ and $\nu = \nu_1$. For the sake of simplicity we shall express the frequency with the limiting value ν_1 as unity and thus put:

$$\frac{\nu}{\nu_1} = x \quad \ldots\ldots\ldots \quad (33)$$

The limiting frequencies are therefore given by $x = 0$ and $x = 1$. According to equation (17) we have for a limiting frequency:

a) $Z_1 = 0$, $Z_2 \neq 0$ or
b) $Z_2 = \infty$, $Z_1 \neq \infty$ or
c) $Z_1 = -4\,Z_2$.

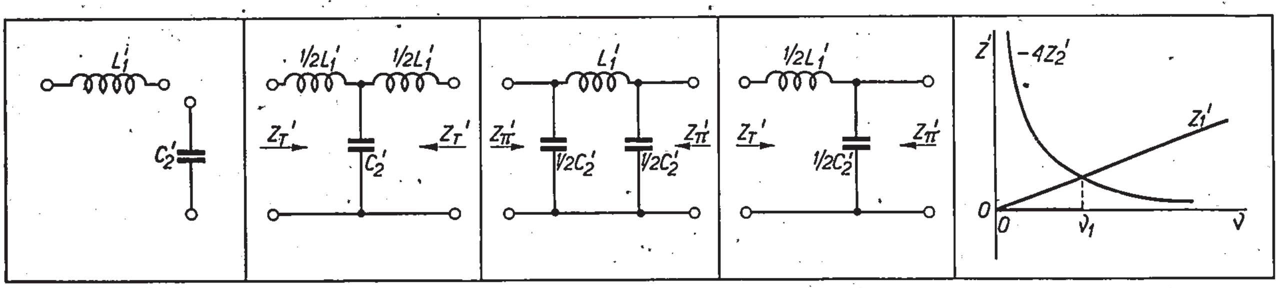

complete branches   *T*-section   *Π*-section   half section   reactance-diagram

Fig. 8. Low-pass filter section. Basic form: $L_1' = R'/\pi\,\nu_1$; $C_2' = 1/R\pi\,\nu_1$.

---

[1] Philips techn. R. 1, 272, 1936.

For $x = 0$ ($\nu = 0$) *a*) and *b*) are satisfied, for $x = 1$ ($\nu = \nu_1$) condition *c*) is satisfied. According to equation (18) we have for frequencies with infinite attenuation:

a) $Z_1 = \infty$, $Z_2 \neq \infty$ or
b) $Z_2 = 0$, $Z_1 \neq 0$.

These conditions are satisfied when $x = \infty$ ($\nu = \infty$).

In the previous article we have seen that the characteristics of filter sections are determined by Z_1Z_2 and $Z_1/4\,Z_2$. For the sections in fig. 8 these magnitudes are expressed in the filter elements L_1' and C_2':

$$Z_1'\,Z_2' = \frac{L_1'}{C_2'} \quad ; \quad \dots\dots\dots \quad (34)$$

$$\frac{Z_1'}{4\,Z_2'} = -{}^1/_4\,\omega^2\,L_1'\,C_2' \quad \dots\dots \quad (35)$$

$Z_1'\,Z_2' = L_1'/C_2'$ is real, positive and independent of the frequency. We can therefore write:

$$Z_1'\,Z_2' = \frac{L_1'}{C_2'} = R^2 \quad \dots\dots \quad (36)$$

We shall soon see the physical meaning of this resistance R.

For the limiting frequency $x = 1$ we have $Z_1'/4\,Z_2' = -1$, so that:

$$^1/_4\,\omega_1^2\,L_1'\,C_2' = 1 \quad \dots\dots \quad (37)$$

From equations (36) and (37) we get L_1' and C_2' expressed in terms of R and ν:

$$\left.\begin{aligned} L_1' &= \frac{R}{\pi\,\nu_1}\,; \\ C_2' &= \frac{1}{R\,\pi\,\nu_1}. \end{aligned}\right\} \quad \dots\dots \quad (38)$$

Substitution of (33) and (38) in (32) gives:

$$\left.\begin{aligned} Z_1' &= j\,2\,R\,x \quad ; \\ Z_2' &= \frac{R}{j\,2\,x} \quad ; \end{aligned}\right\} \quad \dots\dots \quad (39)$$

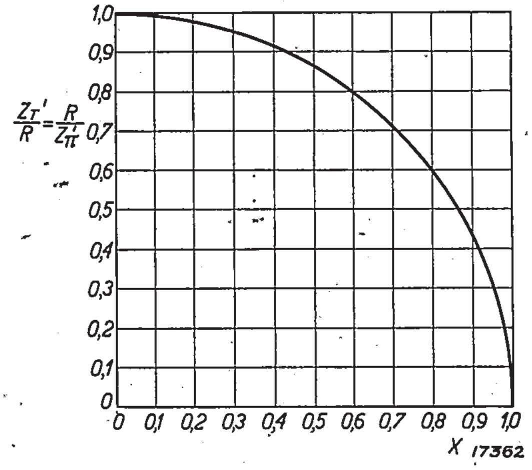

Fig. 9. $Z_T'/R = R/Z_\pi'$ plotted as a function of the frequency $x = \nu/\nu_1$ in the transmission range for the basic type of a low-pass filter.

$$\frac{Z_1'}{4\,Z_2'} = -x^2 \quad \dots\dots\dots \quad (40)$$

The image impedances now follow from (9) and (12)

$$Z_T' = R\,\sqrt{1 - x^2} \quad ; \quad \dots\dots \quad (41)$$

$$Z_\pi' = \frac{R}{\sqrt{1 - x^2}} \quad \dots\dots \quad (42)$$

The physical meaning of the resistance R is thus the image impedance (both Z_T' and Z_π') of this filter section for $x = 0$ ($\nu = 0$). *Fig. 9* gives:

$$\frac{Z_T'}{R} = \frac{R}{Z_\pi'}$$

for these filter sections as a function of the frequency x ($= \nu/\nu_1$) in the transmission band. In the attenuation band $x > 1$ and Z_T' and Z_π' are therefore imaginary according to (41) and (42), thus conforming with the general conclusions previously reached. The value of the image impedances in the attenuation range is in most cases of no practical use.

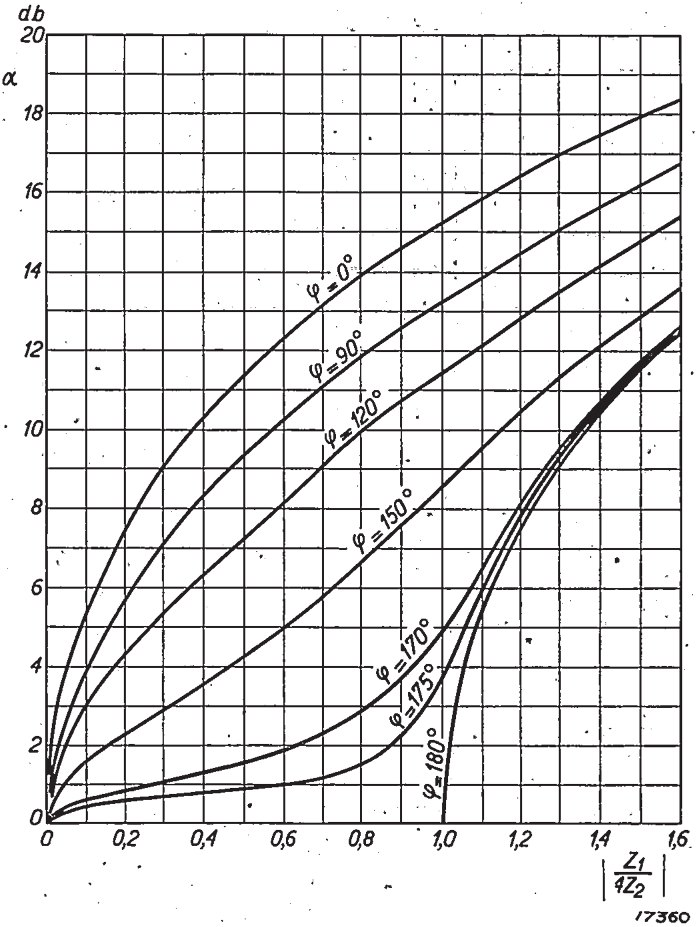

Fig. 10. Attenuation equivalent α (real part of the propagation constant Γ) in decibels as a function of $Z_1/4\,Z_2$ for T- and Π-sections.

$Z_1/4\,Z_2 = U + j\,V$; $\tan\varphi = V/U$

The attenuation equivalent α is determined by means of *fig. 10* in which α for the whole section (whether of the T-form or the Π-form) is represented as a function of $|Z_1/4\,Z_2|$, for which x^2 may be substituted according to equation (40). For the half section α is half as great. α is expressed in decibels, i.e. 20 times the value found for the real part of the exponent when e^{-T} is written as a power of 10, as is almost universally the practice at the present day. We must here take the curve with the parameter $\varphi = 180$ deg. (Further reference will be made later to the significance of this parameter and the other curves in these illustrations). We see from the figure that the loss in the transmission band ($x < 1$, or $|Z_1/4\,Z_2| > 1$) is zero and in the attenuation band ($x > 1$, $|Z_1/4\,Z_2| > 1$) it increases from zero to ∞ as the frequency rises.

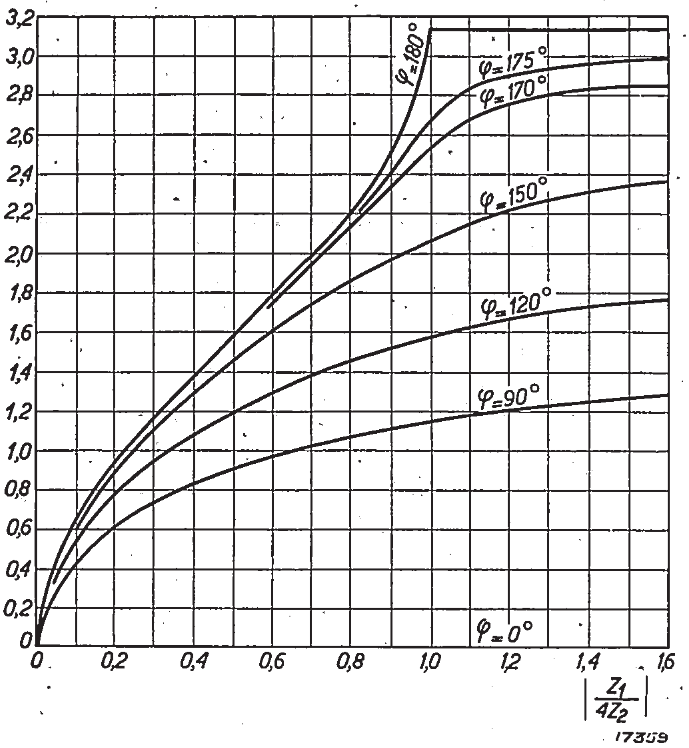

Fig. 11. Phase constant β (imaginary part of the propagation constant T) as a function of $|Z_1/4\,Z_2|$ for T- and Π-sections.

The phase constant β is obtained from *fig. 11*, where again the curve with the parameter $\varphi = 180$ deg. is the operative one. It is seen that β in the transmission band increases from 0 to π as the frequency rises and is constant in the attenuation band.

b) *m_T-Transformation.* Applying equations (21) and (22) to the section in fig. 8 as the basic type, we get the complete sections, the T-section, the Π-section, the half-section and the reactance diagram given in *fig. 12*. We thus have:

$$Z_1 = m\,Z_1' \;;$$

$$Z_2 = \frac{1-m^2}{4\,m}\,Z_1' + \frac{1}{m}\,Z_2' \;;$$

i.e.

$$\left.\begin{aligned} L_1 &= m\,L_1' \;; \\ L_2 &= \frac{1-m^2}{4\,m}\,L_1' \;; \\ C_2 &= m\,C_2' \;; \end{aligned}\right\} \quad \ldots\ldots \quad (43)$$

$$\left.\begin{aligned} Z_1 &= j\,2\,R\,m\,x = m\,Z_1' \;; \\ Z_2 &= j\,2\,R\,\frac{1-m^2}{4\,m}\,x + \frac{R}{j\,2\,m\,x} = \\ &= Z_2'\,\frac{1-x^2\,(1-m^2)}{m}. \end{aligned}\right\} \quad (44)$$

(L_1' and C_2' are the elements of a fundamental type whose values are obtained from equation (38).

For the three magnitudes Z_T, Z_π and $Z_1/4\,Z_2$ which determine the characteristics of the filter section, we get from equations (23), (24) and (25) if we again put $1 - m^2 = 1/a^2$:

$$Z_T = Z_T' = R\sqrt{1-x^2} \;; \quad \ldots\ldots \quad (45)$$

$$Z_\pi = Z_\pi'\left(1 - \frac{x^2}{a^2}\right) = R\,\frac{1-\dfrac{x^2}{a^2}}{\sqrt{1-x^2}} \;; \quad \ldots\ldots \quad (46)$$

$$\frac{Z_1}{4\,Z_2} = \frac{a^2-1}{1-\dfrac{a^2}{x^2}} \quad \ldots\ldots \quad (47)$$

We have already found that the transmission band, the attenuation band and the limiting frequencies are the same for the transformed type as for the fundamental type. The frequency with

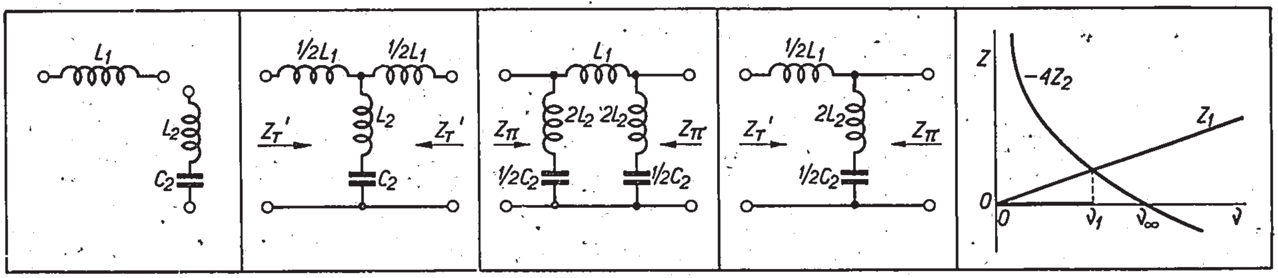

complete branches T-section Π-section half-section reactancediagram

Fig. 12. Low-pass filter section. m_T-transformation: $L_1 = mL_1'$; $L_2 = \frac{1-m^2}{4\,m}\,L_1'$; $C_2 = mC_2'$.

infinite attenuation, x_∞, is the resonance frequency of Z_2, since for this frequency $Z_2 = 0$ and $Z_1 \neq 0$. For $x = \infty$, both Z_1 and Z_2 are ∞. To obtain the attenuation for this frequency, we put $x = \infty$ in equation (47) and obtain:

$$\frac{Z_1}{4\,Z_2} = a^2 - 1 = \frac{1}{1 - m^2} - 1,$$

which only becomes ∞ for $m = 1$, i.e. for the basic type. In the transformed types the attenuation for $x = \infty$ ($\nu = \infty$) is thus finite. The frequency with infinite attenuation ν_∞ is obtained by putting $Z_2 = 0$ in equation (44), i.e.

$$x_\infty = a = \frac{1}{\sqrt{1 - m^2}} \quad \quad (48)$$

We have seen before that m lies between 0 and 1. It follows herefrom that x_∞ lies between 1 and ∞. By a suitable choice of m infinite attenuation can thus be obtained for any arbitrary frequency in the attenuation band.

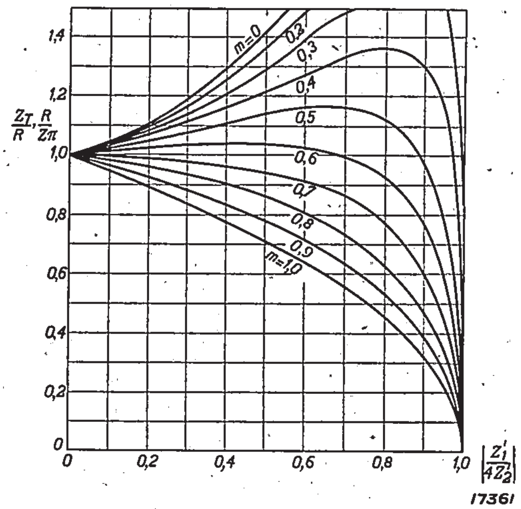

Fig. 13. $Z_T/R = R/Z_\pi$ plotted as a function of $Z_1/4\,Z_2$ for non-dissipative filters. The image impedances Z_T for the m_π-transformation and Z_π for the m_T-transformation in the transmission range are derived from this figure for all types of filter sections.

The attenuation equivalent a and the *phase constant* β are again determined for each given frequency from figs. 10 and 11 by means of equation (47). For $x < a$ (i.e. $x < x_\infty$) we find from equation (47) that $Z_1/4\,Z_2$ is negative and in the figures we take the curves with the parameter $\varphi = 180$ deg; for $x > a$ (i.e. $x > x_\infty$) $Z_1/4\,Z_2$ is positive and here we take the curve with the parameter $\varphi = 0$ deg.

The image impedances $Z_T = Z_T'$ and Z_π in the passing band can be found in *fig. 13*, where Z_T/R and R/Z_π are plotted as a function of:

$$\left|\frac{Z_1'}{4\,Z_2'}\right| = x^2$$

In the m_T-transformation $Z_T/R = Z_T'/R$ is indicated by the curve with the parameter $m = 1{:}0$, for all different values of m to be used in this transformation, while R/Z_π is to be found from the curve with the value of m used as parameter.

c) *m_π-Transformation.* Applying the equations (27) to (31) to the basic filter in fig. 8, we get the complete sections, the T-section, the Π-section, the half-section and the reactance diagram shown in *fig. 14*. We thus get:

$$\left.\begin{aligned} L_1 &= m\,L_1'\,; \\ C_1 &= \frac{1 - m^2}{4\,m}\,C_2'\,; \\ C_2 &= m\,C_2'\,. \end{aligned}\right\} \quad \quad (49)$$

$$\left.\begin{aligned} Z_1 &= j\,\frac{2\,R\,m\,x}{1 - x^2\,(1 - m^2)} = Z_1'\,\frac{m}{1 - x^2\,(1 - m^2)}\,; \\ Z_2 &= \frac{R}{2\,j\,m\,x} = \frac{Z_2'}{m}\,; \end{aligned}\right\} \quad \quad (50)$$

$$Z_T = Z_T'\,\frac{1}{1 - \frac{x^2}{a^2}} = R\,\frac{\sqrt{1 - x^2}}{1 - \frac{x^2}{a^2}}\,; \quad \quad (51)$$

$$Z_\pi = Z_\pi' = \frac{R}{\sqrt{1 - x^2}}\,; \quad \quad (52)$$

$$\frac{Z_1}{4\,Z_2} = \frac{a^2 - 1}{1 - \frac{a^2}{x^2}}\,; \quad \quad (53)$$

$$x_\infty = a = \frac{1}{\sqrt{1 - m^2}} \quad \quad (54)$$

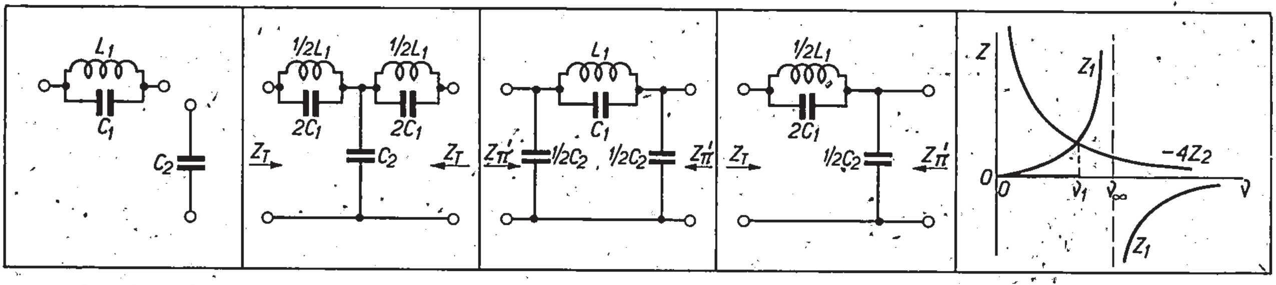

Fig. 14. Low-pass filter section. m_π-transformation: $L_1 = mL_1'$; $C_1 = \frac{1 - m^2}{4\,m}\,C_2'$; $C_2 = mC_2'$.

Obviously $Z_1/4\,Z_2$ and hence x_∞, a and β for the same value of m are the same for the m_π-transformation as for the m_T-transformation.

It follows from equations (46) and (51) that Z_T/R for the m_π-transformation is equal to R/Z_π for the m_T-transformation. Z_T and Z_π are now also found from fig. 13. $R/Z_\pi = R/Z_\pi'$ is now represented independent of m by the curve with the parameter $m = 1.0$, while Z_T/R is given by the curve with the value of m used as parameter.

d) *Effect of Losses in the Filter Components.* Up to the present it has been assumed that the components of the filters are non-dissipative. But the coils and condensers always have a certain resistance. To determine the effect of this resistance we regard the losses in the coils as a series resistance r_L and that in the condensers as a parallel resistance R_C, writing:

$$\frac{r_L}{\omega L} = d_L, \qquad \frac{1}{R_C\,\omega\,C} = d_C.$$

We also assume that d_L is the same for all coils in the filter and d_C is the same for all condensers in the filter. Hence in the equations for the non-dissipative filter we must substitute for $j\,\omega\,L$ and $j\,\omega\,C$ the expressions:

$$r_L + j\omega L = j\omega L\left(1 - j\frac{r_L}{\omega L}\right) = j\omega L\,(1 - j\,d_L)\,;$$

$$\frac{1}{R_C} + j\omega C = j\omega C\left(1 - j\,\frac{1}{R_C\,\omega\,C}\right) = j\,\omega\,C\,(1 - j\,d_C) \qquad (55)$$

We then get for the fundamental form:

$$\left.\begin{aligned} Z_1' &= j\cdot 2\,R\,x\,(1 - j\,d_L)\ ; \\ Z_2' &= \frac{R}{j\,2\,x\,(1 - j\,d_C)}\ ; \end{aligned}\right\} \quad .\ .\ .\ .\ (56)$$

$$\frac{Z_1'}{4\,Z_2'} = -\,x^2\,(1 - j\,d_L)\,(1 - j\,d_C) \quad .\ .\ (57)$$

As already indicated above, the effect of the losses in the filter components on the image impedances can as a rule be neglected. The image impedances are therefore always calculated without consideration of the losses.

It follows from equation (57) that $Z_1/4\,Z_2$ is now complex, we must therefore put:

$$\frac{Z_1'}{4\,Z_2'} = U' + j\,V' \ ; \quad .\ .\ .\ (58)$$

$$\frac{V'}{U'} = tg\,\varphi' \quad .\ .\ .\ .\ .\ .\ .\ .\ (59)$$

As a rule d_L and d_C are small (0.005 to 0.05). In many cases when using high-grade condensers d_C can in fact be neglected altogether. To a very close degree of approximation we can therefore write:

$$\frac{Z_1'}{4\,Z_2'} = -\,x^2\,[1 - j\,(d_L + d_C)]\ ; \quad (60)$$

$$\left.\begin{aligned} U' &= -\,x^2 \\ V' &= x^2\,(d_L + d_C); \end{aligned}\right\} \quad .\ .\ .\ .\ (61)$$

$$tg\,\varphi' = -\,(d_L + d_C) \quad .\ .\ .\ .\ (62)$$

For the transformed types we can similarly deduce $Z_1/4\,Z_2$ from the results for the non-dissipative case, by substituting $x^2\,(1 - j\,d_L)\,(1 - j\,d_C)$ for x^2. We then get:

$$\frac{Z_1}{4\,Z_2} = \frac{a^2 - 1}{1 - \dfrac{a^2}{x^2\,(1 - jd_L)\,(1 - jd_C)}} \qquad (63)$$

We now also put $Z_1/4\,Z_2 = U + j\,V$, $\tan\varphi = V/U$. In figs. 10 and 11 a and β are plotted as a function of $|Z_1/4\,Z_2|$ with φ as parameter.

In the transmission band the effect of the losses is most marked in the neighbourhood of the upper limiting frequency, where the attenuation may be fairly high owing to the losses, as may be seen from fig. 10. In the attenuation band the effect of the losses is greatest at the "frequency with infinite attenuation", resulting in the attenuation actually remaining finite. For x_∞, $x = a$ we get from equation (63) to a sufficiently close degree of approximation:

$$\frac{Z_1}{4\,Z_2} = j\,\frac{a^2 - 1}{d_L + d_C} \quad ;\ .\ .\ .\ (64)$$

$$\left|\frac{Z_1}{4\,Z_2}\right| = \frac{a^2 - 1}{d_L + d_C} \quad ;\ .\ .\ .\ (65)$$

$$\varphi = 90^\circ \quad .\ .\ .\ .\ .\ .\ .\ (66)$$

e) *Compound Filters.* It was shown in the previous article how a filter can be compounded from a number of individual sections. By connecting in series various sections of the types discussed having different values of m (also with $m = 1$, i.e. the fundamental type), the attenuation in the attenuation band can be made to satisfy specific requirements. At the points of interconnection of the sections equivalent image impedances must be contiguous; if the only sections employed are wholly T sections after m_T-transformation or Π cells after m_π-transformation, this requirement will be met. Also by inserting a half-section of the basic form T-sections can be transformed into Π-sections. It is also essential for the image impedances of the whole filter, i.e. the image impedances of the terminal sections, to be as closely equivalent as possible in the transmission band to the resistances R_1 and R_2 connected across the external terminals of the filter. It is assumed that these external resistances R_1 and R_2 are real and equal to each other. If they are not real, complications occur, to which further reference must be dispensed with here. If they are different they can be made equivalent to each other by inserting a transformer (*fig. 15*). It follows from fig. 13 that for $m = 0.6$ the impedances Z_T for the m_π-transformation and Z_π for the m_T-transformation are practically independent of the frequency over nearly the whole of the transmission band. This interesting property can be employed to advantage for providing a filter with suitable terminals sections. A filter built up of T sections whether of the fundamental form or after m_T-transformation is terminated on both sides with a half-section after m_T-transformation with an image-impedance Z_π' at the terminating side and $m = 0.6$; a filter made up of Π-sections is terminated with half-sections after m_π-transformation with an image-impedance Z_π at the terminating side and $m = 0.6$. *Fig. 16* gives an example of each of these two cases. At the interconnection of the sections equivalent image impedances are everywhere contiguous in the filter, and the image impedances of the whole filter are practically constant over nearly the whole of the transmission band. The values of the filter components are calculated from the equations discussed, where for R the value of the (equal) external resistances is taken.

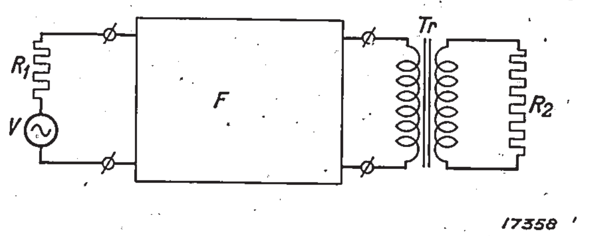

Fig. 15. Filter whose primary and secondary are terminated by the resistances R_1 and R_2 and a generator of voltage V. The ratio of the transformer Tr is $\sqrt{R_2/R_1}$. If $R_1 = R_2$ the transformer can be dispensed with.

By employing the multiple m-transformation referred to on p. 276 terminals sections can be obtained whose image impedances are still more closely constant in the transmission band. But very complex circuits are then obtained which in most cases can be dispensed with.

f) Diagrammatic Survey of the Filter Sections discussed. (*Fig. 17*). The composition and most important characteristics of the filter sections discussed are given diagrammatically in *fig. 17.* Column 1 refers to the basic form, column 2 to the m_T-transformation, column 3 to the m_π-transformation. In the first row the complete sections are given; the second row contains the values of the components of these complete sections expressed in R, ν and m. How a T-section, a Π-section and a half-section can be made up from these complete sections is shown in figs. 8, 12 and 14. The subsequent rows gives the qualitative values of Z_T, Z_π, α and β as a function of the frequency. In each picture the frequency x is represented as the abcissa such that $x = \infty$ falls in each case at the end of the axis. By adopting a similar diagrammatic method the value ∞ on the ordinate also has a finite location, except for β which is plotted linearly. In these four series the filter sections are regarded as non-dissipative. How the sketches are affected by the losses in the filter

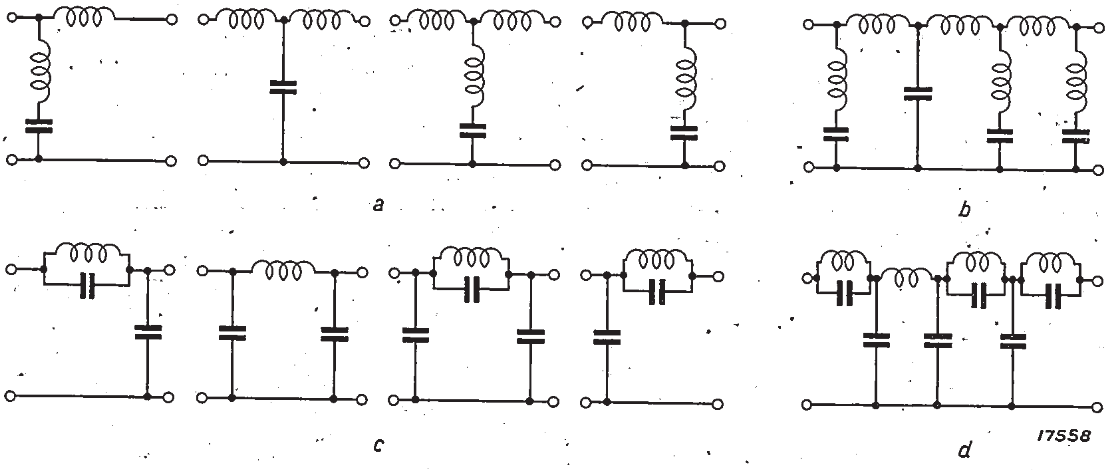

Fig. 16. Low-pass filter composed of a section of the fundamental type, a section after m-transformation with an arbitrary value of m, and two terminal half-sections after m-transformation with $m = 0.6$, giving an image impedance for the whole filter which is practically constant in the transmission band. *a* the individual section of T form; *b* these sections combined to form a filter, *c* the individual sections of Π form; *d* these sections combined to form a filter. The filters *b* and *d* are equivalent.

components may be deduced by means of the analysis given above for each particular case. In the next row $Z_1/4\,Z_2$ is given both for the ideal case ($d = 0$) as for the practical case ($d \neq 0$). By means of these equations $Z_1/4\,Z_2$ can be calculated for each frequency and the values of α and β then obtained from figs. 10 and 11. The last row of the table then gives the definitions of the magnitudes employed.

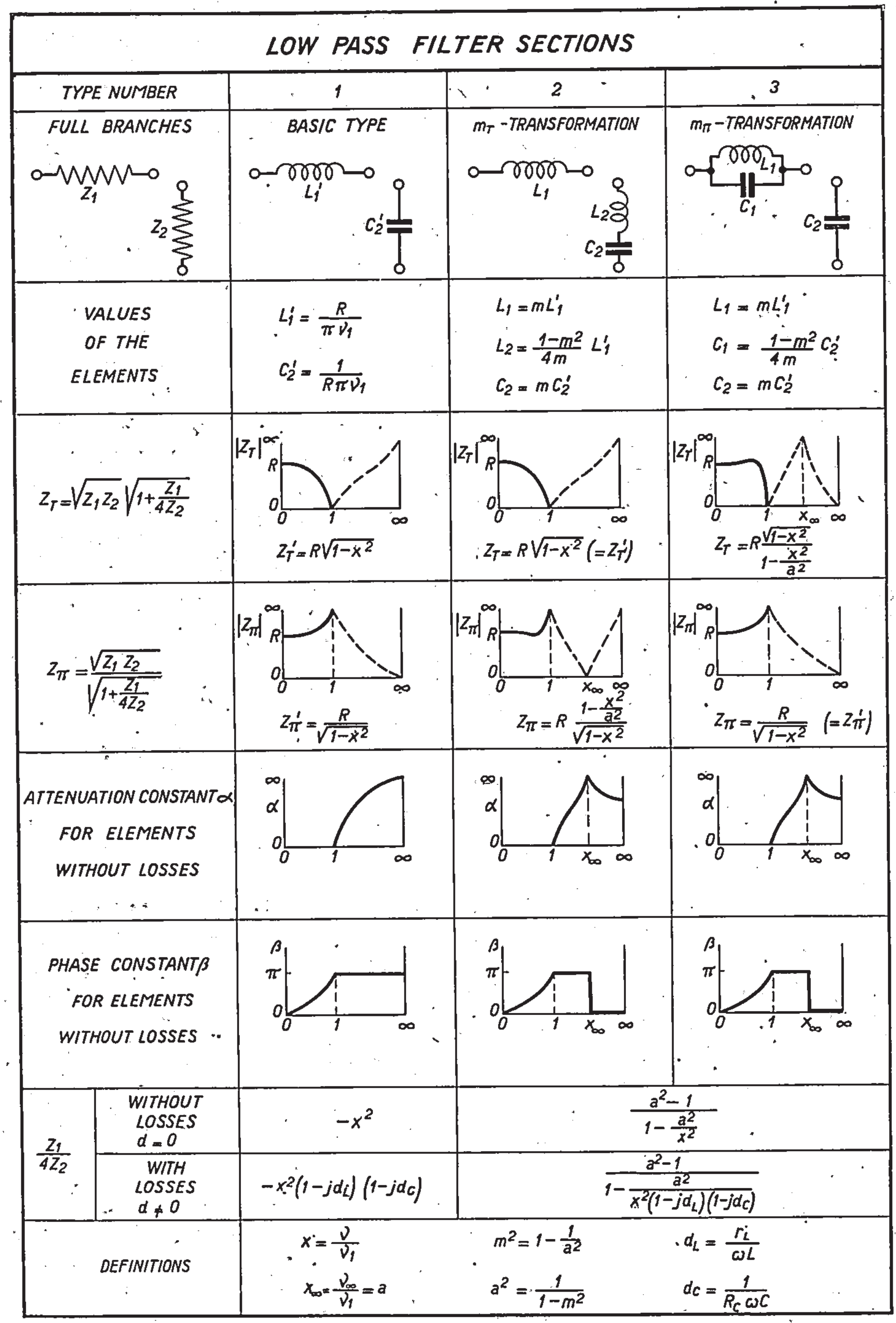

LOW PASS FILTER SECTIONS			
TYPE NUMBER	1	2	3
FULL BRANCHES Z_1, Z_2	BASIC TYPE L_1', C_2'	m_T-TRANSFORMATION L_1, L_2, C_2	m_π-TRANSFORMATION L_1, C_1, C_2
VALUES OF THE ELEMENTS	$L_1' = \frac{R}{\pi \nu_1}$ $C_2' = \frac{1}{R\pi\nu_1}$	$L_1 = mL_1'$ $L_2 = \frac{1-m^2}{4m} L_1'$ $C_2 = mC_2'$	$L_1 = mL_1'$ $C_1 = \frac{1-m^2}{4m} C_2'$ $C_2 = mC_2'$
$Z_T = \sqrt{Z_1 Z_2}\sqrt{1+\frac{Z_1}{4Z_2}}$	$Z_T' = R\sqrt{1-x^2}$	$Z_T = R\sqrt{1-x^2}\ (=Z_T')$	$Z_T = R\frac{\sqrt{1-x^2}}{1-\frac{x^2}{a^2}}$
$Z_\pi = \frac{\sqrt{Z_1 Z_2}}{\sqrt{1+\frac{Z_1}{4Z_2}}}$	$Z_\pi' = \frac{R}{\sqrt{1-x^2}}$	$Z_\pi = R\frac{1-\frac{x^2}{a^2}}{\sqrt{1-x^2}}$	$Z_\pi = \frac{R}{\sqrt{1-x^2}}\ (=Z_\pi')$
ATTENUATION CONSTANT α FOR ELEMENTS WITHOUT LOSSES			
PHASE CONSTANT β FOR ELEMENTS WITHOUT LOSSES			
$\frac{Z_1}{4Z_2}$ WITHOUT LOSSES $d = 0$	$-x^2$	$\frac{a^2-1}{1-\frac{a^2}{x^2}}$	
$\frac{Z_1}{4Z_2}$ WITH LOSSES $d \neq 0$	$-x^2(1-jd_L)(1-jd_C)$	$\frac{a^2-1}{1-\frac{a^2}{x^2(1-jd_L)(1-jd_C)}}$	
DEFINITIONS	$x = \frac{\nu}{\nu_1}$ $x_\infty = \frac{\nu_\infty}{\nu_1} = a$	$m^2 = 1-\frac{1}{a^2}$ $a^2 = \frac{1}{1-m^2}$	$d_L = \frac{r_L}{\omega L}$ $d_C = \frac{1}{R_C\,\omega C}$

20347

Fig. 17. Data and formulae for the construction of low-pass filter sections.

Appendix. Formulae in the article: "Electrical Filters II".

Meaning of symbols:

$$\left.\begin{array}{l} Z_{ao} \text{ Open-circuit impedance} \\ Z_{ak} \text{ Short-circuit impedance} \end{array}\right\} \text{Input side.}$$

$$\left.\begin{array}{l} Z_{bo} \text{ Open-circuit impedance} \\ Z_{bk} \text{ Short-circuit impedance} \end{array}\right\} \text{Output side.}$$

Z_a, Z_b Image impedances.

T Propagation constant.

α Attenuation equivalent.

β Phase constant.

I_n Primary current of the n^{th} section = secondary current in $(n - 1)^{\text{th}}$ section.

Z_T, Z_π Image impedances of the T- and Π-sections respectively.

Z_1, Z_2 Complete sections.

Z_1'. Z_2' Complete sections of basic form.

m Parameter of "m-transformation".

Formulae:

$$Z_a = \sqrt{Z_{oa} Z_{ak}} \tag{1}$$

$$Z_b = \sqrt{Z_{bo} Z_{bk}} \tag{2}$$

$$\tanh T = \sqrt{\frac{Z_k}{Z_o}} \tag{3}$$

$$e^{-2T} = \frac{1 - \sqrt{\frac{Z_k}{Z_o}}}{1 + \sqrt{\frac{Z_k}{Z_o}}} \tag{4}$$

$$\frac{I_2}{I_1} = \sqrt{\frac{Z_a}{Z_b}} \cdot e^{-T} = \sqrt{\frac{Z_a}{Z_b}} \cdot e^{-\alpha - j\beta} \tag{5}$$

$$\frac{I_{n+1}}{I_1} = \sqrt{\frac{Z_a}{Z_{n+1}}}\, e^{-(T_1 + T_2 + \dots T_n)} \tag{6}$$

$$Z_o = {}^1/_2\, Z_1 + 2\, Z_2 \tag{7}$$

$$Z_k = {}^1/_2\, Z_1 \tag{8}$$

$$Z_T = \sqrt{Z_o Z_k} = \sqrt{Z_1 Z_2}\sqrt{1 + \frac{Z_1}{4\, Z_2}} \tag{9}$$

$$Z_o = 2\, Z_2 \tag{10}$$

$$Z_k = \frac{2\, Z_1 Z_2}{Z_1 + 4\, Z_2} \tag{11}$$

$$Z_\pi = \sqrt{Z_o Z_k} = \frac{\sqrt{Z_1 Z_2}}{\sqrt{1 + \frac{Z_1}{4\, Z_2}}} \tag{12}$$

$$\frac{Z_k}{Z_o} = \frac{1}{1 + \frac{4\, Z_2}{Z_1}} \tag{13}$$

For half-section:

$$e^{-2T} = \frac{\sqrt{1 + \frac{Z_1}{4\, Z_2}} - \sqrt{\frac{Z_1}{4\, Z_2}}}{\sqrt{1 + \frac{Z_1}{4\, Z_2}} + \sqrt{\frac{Z_1}{4\, Z_2}}} \tag{14}$$

For T-section and Π-section:

$$e^{-T} = \frac{\sqrt{1 + \frac{Z_1}{4\, Z_2}} - \sqrt{\frac{Z_1}{4\, Z_2}}}{\sqrt{1 + \frac{Z_1}{4\, Z_2}} + \sqrt{\frac{Z_1}{4\, Z_2}}} \tag{15}$$

Valid for transmitting band:

$$-1 < \frac{Z_1}{4\, Z_2} < 0 \tag{16}$$

Boundaries at passing bands:

$$\frac{Z_1}{4\, Z_2} = \begin{cases} 0 \\ -1 \end{cases} \tag{17}$$

Condition for infinite attenuation:

$$\frac{Z_1}{4\, Z_2} = \infty \tag{18}$$

m_T-transformation:

$$Z_k = {}^1/_2\, m\, Z_1' \tag{19}$$

$$Z_o = \frac{Z_1'}{2\, m} + \frac{2\, Z_2'}{m} \tag{20}$$

$$Z_1 = m\, Z_1' \tag{21}$$

$$Z_2 = \frac{1 - m^2}{4\, m} Z_1' + \frac{1}{m} Z_2' \tag{22}$$

$$Z_T = Z_T' \tag{23}$$

$$Z_\pi = Z_\pi' \left(1 + \frac{1}{a^2} \frac{Z_1'}{4\, Z_2'}\right) \tag{24}$$

$$\frac{Z_1}{4Z_2} = \frac{Z_1'}{4Z_2'} \frac{m^2}{1 + \frac{1}{a^2}\frac{Z_1'}{4Z_2'}} \quad \ldots \ldots \ldots (25)$$

$$0 \leqslant m \leqslant 1 \quad \ldots \ldots \ldots (26)$$

m_π-transformation:

$$Z_1 = \text{parallelconnection of } mZ_1' \text{ and } \frac{4m}{1-m^2} Z_2' \quad (27)$$

$$Z_2 = \frac{1}{m} Z_2' \; ; \quad \ldots \ldots \ldots (28)$$

$$Z_\pi = Z_\pi' \; ; \quad \ldots \ldots \ldots (29)$$

$$Z_T = Z_T' \frac{1}{1 + \frac{1}{a^2}\frac{Z_1'}{4Z_2'}} \; ; \quad \ldots \ldots \ldots (30)$$

$$\frac{Z_1}{4Z_2} = \frac{Z_1'}{4Z_2'} \frac{m^2}{1 + \frac{1}{a^2}\frac{Z_1'}{4Z_2'}} \quad \ldots \ldots \ldots (31)$$

A SURVEILLANCE SYSTEM USING INFRA-RED RAYS

By A. L. TIMMER and A. H. VAN ASSUM.

Summary. Description of a surveillance system with infra red alternating light intensity, which works over a distance of 425 metres. In addition to the light source a foto-electric cell and a two valves amplifier is used.

Introduction

At the present time it is becoming increasingly the practice to entrust the protection and surveillance of rooms containing valuable objects no longer to human attendants, but to automatic alarm systems which become actuated immediately an unauthorised person enters the protection area. The advantage of an arrangement of this type is that surveillance is continuous and that if required the competent public authorities, such as the police, can be directly warned of any intrusion, etc. The close surveillance offered by these systems is particularly useful and desirable, for instance, on strong rooms of banks, valuable collections in museums, shop premises, etc.

A reliable and efficiently alarm system must satisfy the following requirements:

1) . It must not be capable of being easily rendered inoperative.
2) It must give an alarm on any interference with its normal state of preparedness (e.g. a failure of the current supply).
3) It must not be recognised as an alarm system.
4) It must not be subject to interference or put out of action by normal activities and operations in the vicinity.

Various mechanical protective arrangements, such as door contacts or step contacts, are naturally quite practicable, but important advantages are offered by a method using invisible rays which on being intercepted in any way release an alarm system. Fundamentally the method depends on the operation of a photo-electric cell, which furnishes a current as long as infra-red radiation falls on it. After amplification this very weak current can be used for controlling an alarm system.

In the simplest form of such a system the photo-electric current is used directly for energising a relay. The current generated is however only of the order of a few micro-amperes, as may be gathered from the following example. If a glowlamp of say 25 candles is used as a light source, the total luminous flux radiated will be about 250 lumens. When a photo-electric cell with a window opening of e.g. 20 sq. cm is placed about 1 m from the lamp, the light falling on the cell will be:

$$\frac{20}{4\pi 100^2}\, 250 \approx 0.04 \text{ lumen.}$$

A vacuum cell is employed which for white light has a sensitivity of approx. 25 micro-amps per lumen so that a current of about 1 micro-amp is generated. This extremely weak current can be intensified by inserting a lens between the light source and the photo-electric cell (*fig. 1*). If for this purpose a lens of 25 cm focal length and 10 cm diameter is used and the distance between the cell and the light source is made only so great that the image of the incandescent coil still falls completely within the cell window, then the whole of the light collected by the lens will fall on the cell.

The coil covers roughly a square of 2 mm side, while the cell window is a circle of 5 cm diameter. The filament must then be placed 26 cm in front of the lens, and the image is produced 460 cm behind the lens, so that a space of 4 m wide can be readily kept under surveillance.

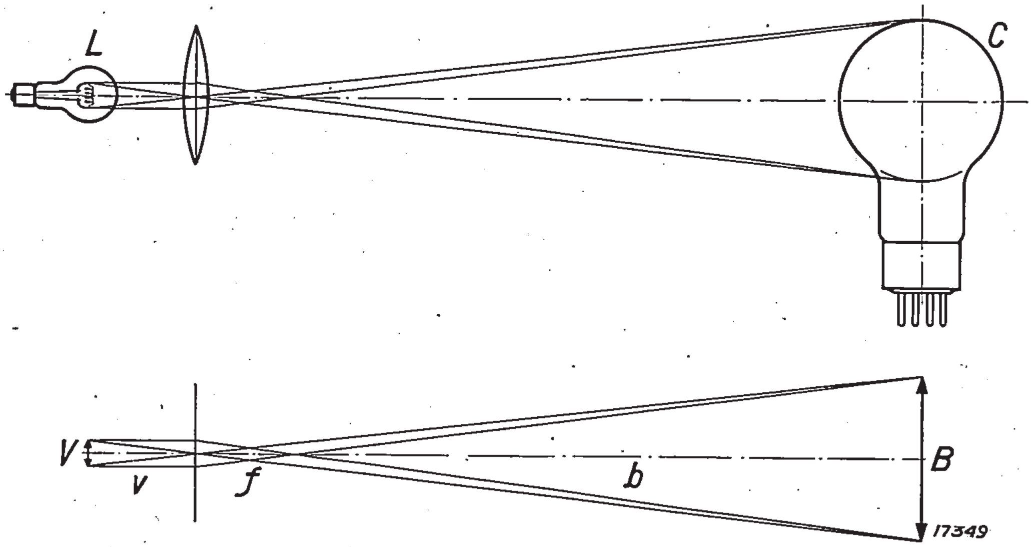

Fig. 1. The image of the incandescent filament of a glowlamp L is produced in such a way that it exactly fills the aperture of a photo-electric cell C. In the lower half of the figure V is the size of the incandescent coil, v its distance from the lens, f the focal length of the lens, b the distance of the cell from the lens, and B the size of the image V on the cell.

Although the lens throws a much greater portion of the spherically-radiated light on the photo-electric cell than would be incident thereon without a lens, even with this arrangement only 2.32 lumens of the 250 lumens radiated will reach the cell, the absorption losses in the lens being still left out of account. The photo-current is then 58 microamperes. It is not a simple matter to construct a relay responding to this small current, while moreover the space of $4^1/_2$ m wide controlled is not particularly large. If in place of a vacuum cell a gasfilled cell is used which is six times as sensitive, but also critical in adjustment, the electric current generated is 350 microamps, which is still too small. We are employing visible light in this example, which therefore does not satisfy condition 3) above.

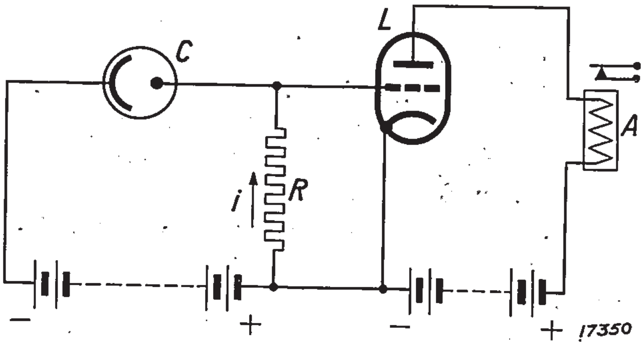

Fig. 2. If no light falls on the cell C a current flows through the relay A which attracts the armature. If C is illuminated, the current i generated as a result of this illumination produces a voltage drop at R. The control grid of the valve L becomes negative, and the anode current through A is reduced so that the armature is released.

Since the photo-electric cell under consideration is however fairly sensitive to infra-red rays, the light beam can be rendered invisible by passing it through a glass plate which allows only the infra-red rays to pass through (infra-red filter). This adaptation reduces the photo-current to about a third. In order to be able to operate a relay it has thus been found necessary to amplify the photo-current.

The Amplifier

A simple circuit for amplifying the photo-electric current is shown in *fig. 2.*

The current generated in the photo-electric cell C by illumination is passed through a resistance R, which is connected to the grid and cathode of the amplifying valve L, so that the voltage of the grid is negative with respect to the cathode. The method of operation is then as follows: No current passes through the resistance R when no illumination falls on the cell. The grid of the valve L is then at the same potential as the cathode, and a definite anode current is circulating which maintains the attraction of the armature of the relay A. When the cell is illuminated the grid becomes negative, and as a result the anode current diminishes, thus releasing the relay armature. In this position the whole system is therefore in the "safe" setting. If the beam of light is interrupted, the current through the relay rises, the armature is attracted and an "alarm" arrangement can be operated.

This method of operation obviously does not satisfy the second condition enumerated above. Any failure or interference in the amplifier remains undetected, since the relay current is then zero and the armature is hence not attracted. This shortcoming can however be readily overcome by using the circuit shown in *fig. 3*, where the grid of the amplifying valve L has a negative grid bias, so that a small feed current flows through the relay A which does not actuate the latter. Since the photo-electric cell is connected in the opposite way to that shown in fig. 2, the photo-current through the resistance R generated on illumination will reduce the negative grid bias, so that the anode current rises and the relay operates. If the system is in the "safe" setting, then contrary to the circuit in fig. 2 current flows through the relay such that the armature remains attracted. Any interference of whatever nature will then release the alarm system. The width of the area protected can be increased by using a more powerful source of light, but this introduces the need for greater amplification; one valve is not sufficient for this purpose and several have to be used.

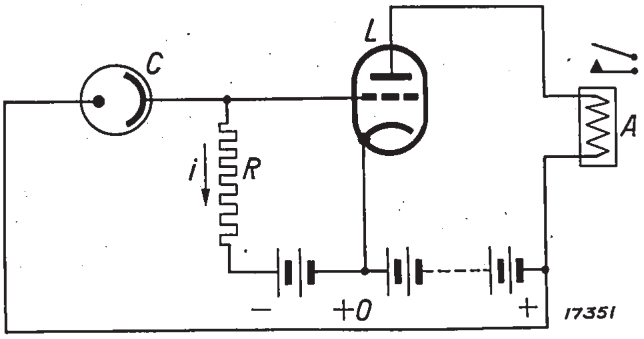

Fig. 3. If no light falls on C a very weak current flows through A which causes no other component to operate. If C is illuminated then, contrary to fig. 2, the grid of L becomes more *positive*, since here the current from C flows through R in the *opposite* direction; the current through A increases and may cause the attraction of the armature.

The fundamental circuit of the apparatus evolved in this Laboratory is reproduced in *fig. 4*. It will be seen that a condenser has been inserted between the photo-electric cell and the grid of the first amplifying valve. This has been done for the following reason: The circuits in figs. 2 and 3 are fundamentally those for D.C. amplifiers. It is, however, difficult without complicated precautions to obtain a D.C. amplifier with more than one stage, while on the other hand the construction of a multi-stage amplifier for A.C. is very simple. Fig. 4 is thus a circuit for an A.C. amplifier, so that it is necessary to furnish the cell with A.C. also.

Two methods can be used for generating alternating current:

1) Alternating voltage can be passed to the anode of the cell.

2) The cell can be illuminated with an intermittent or fluctuating light.

The second method is naturally the more advantageous. The apparatus no longer responds to a continuous beam of light, so that one cannot walk through the beam and direct a beam from a pocket lamp on to the cell as a substitute for the screened light. For this reason the second method was selected.

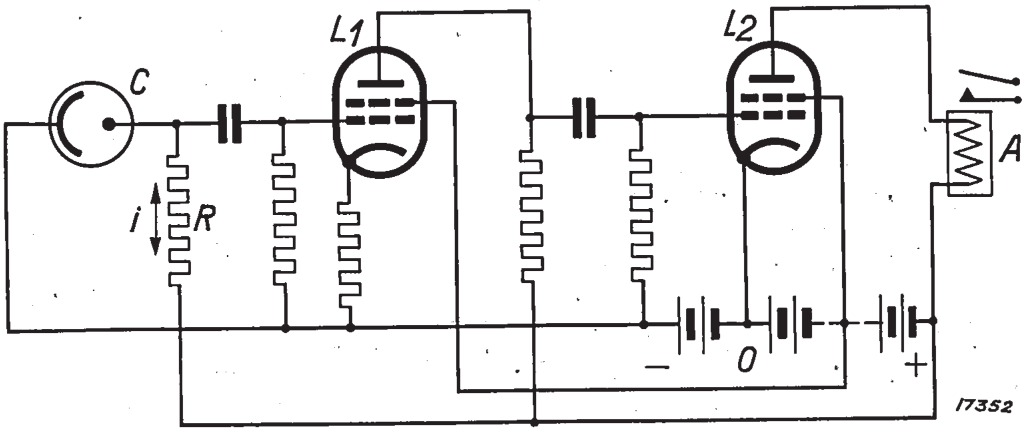

Fig. 4. The intermittent illumination system. Light of fluctuating intensity falls on the photo-electric cell C; *inter alia*, an alternating voltage is thus generated across R. This voltage is amplified by L_1 and is then applied to L_2, whereupon the current through the relay A increases, as shown in fig. 6.

The fluctuating light is generated in the following way: A steel spring is substituted for the armature in a magnetised coil (such as that from a loudspeaker) which is energised by alternating current. A small disk is attached to the spring at its free end. On connecting the coil to the A.C. mains supply the disk will vibrate with a frequency of 50 times per second (*fig. 5*). This arrangement is set up in the beam between the glowlamp and the lens in such a way that the disk, when at rest, just bisects the beam of light falling on the lens. In this way the beam can be entirely cut off or given a free passage by a minimum deflection of the spring. One might be inclined to employ resonance phenomena, i.e. make the natural frequency of the spring equal to the A.C. frequency, in order to obtain a large deflection with a small power. This method cannot however be used satisfactorily since then a small variation in frequency will immediately result in a marked diminition of the deflection. The natural frequency must exceed the frequency superposed on it, as otherwise the spring would vibrate about a node.

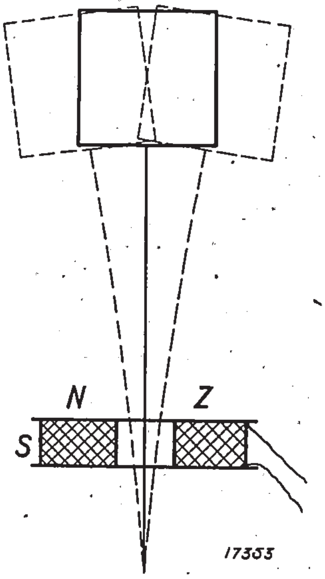

Fig. 5. Oscillating spring for generating the intermittent beam. 50-cycle alternating current is passed through the coil S, so that the spring is set in vibration with the aid of the horseshoe magnet with poles N and Z.

In this way the photo-electric cell receives an intermittent beam of light so that on a voltage drop in R an alternating voltage is obtained at the grid of the first amplifying valve. After amplification this voltage is impressed on the grid of the second valve, which acts as an anode rectifier and whose anode current therefore increases with increasing (alternating) voltage at the grid. The grid of L_2 has a negative bias of such a value that a very weak anode current flows (*fig. 6*). If alternating voltage is now applied to the grid the anode current as shown in the figure will become pulsating; the pulsations are not however registered if measured by a moving coil instrument which at a sufficiently high frequency of pulsation indicates the mean current. This anode current is employed for actuating the alarm relay.

The currents at which the relay attracts or releases the armature are determined by the dimensions. From the characteristic of the rectifier, i.e. from the variation of the anode current as a function of the grid alternating voltage, the voltage required at the grid can be found so that the relay attracts its armature. The rest current which flows when no alternating voltage is present, i.e. when the light beam is cut off, must therefore be a little smaller than the current at which the armature is released (see *fig. 7*).

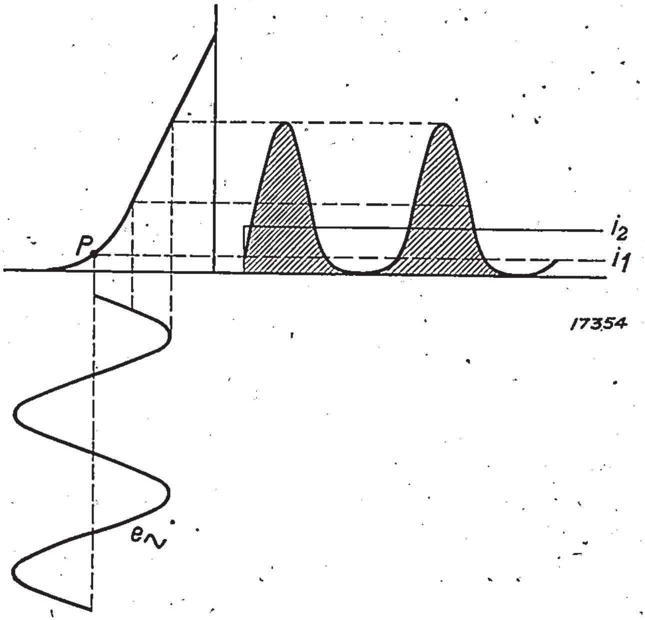

Fig. 6. In the absence of alternating voltage at the grid the amplifying valve operates at the point P of the characteristic (current intensity i_1). If an alternating voltage is applied to the grid a pulsating anode current with an average value of i_2 is obtained.

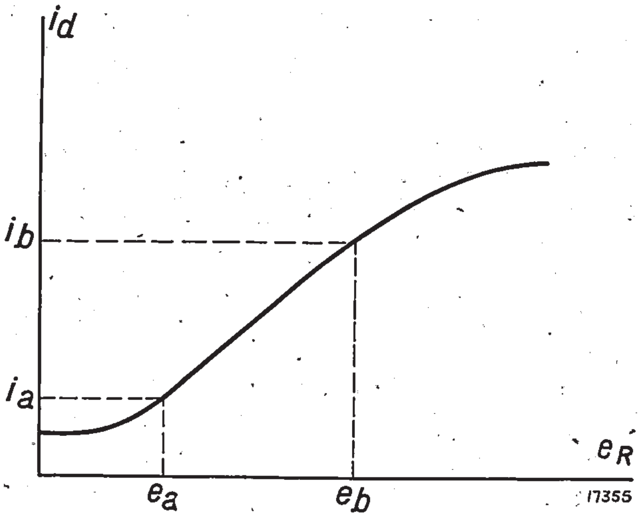

Fig. 7. Characteristic of the rectifier, i.e. anode current of the rectifier (which therefore flows through the relay A) as a function of the alternating voltage at the resistance R of fig. 4. At the current i_b the relay armature is attracted; at i_a it is released.

Sensitivity of the system

The sensitivity of the system is mainly determined by the current sensitivity of the relay, which in its turn is governed *inter alia* by the windings on the relay core. The power of a relay is determined solely by the product of the current intensity and the number of turns, so that up to a point the sensitivity of the relay can be raised by increasing the number of turns and reducing the diameter of the wire. Since the photo-electric cell must generate such a current that the amplifier can furnish the difference between the currents at which the relay armature is attracted and released, it is evident that these currents will preferably be made small since the ratio between them is constant.

It has been found possible to wind a relay having a "response current" of 0.6 mA and a "release current" of 0.2 mA. To obtain this current difference a grid alternating voltage of 0.015 volt is required at the first amplifying valve. The photo-electric cell must therefore furnish 0.015 μA (through an impedance of 1 megohm). This is the effective value, the peak value is $\sqrt{2}$ times greater. The light however fluctuates from zero to a maximum, and the curve of the intermittent light must be compared with the "zero line" A, as shown in *fig. 8*. This indicates that the peak value of the current which the cell must furnish is:

$$2 \cdot 0.015 \cdot \sqrt{2} = 0.042 \ \mu\text{A}.$$

When using a gasfilled photo-electric cell whose sensitivity for white light is approx. 150 μA per lumen, the 0.042 μA required would need an intensity of 0.00028 lumen of white light. With infra-red rays the sensitivity is however three times smaller, so that then 0.00084 lumen (expressed as white light) must impinge on the photo-electric cell.

Distance of Surveillance

To calculate the length of beam corresponding to an intensity of 0.00084 lumen at the cell window, it must be remembered that over this great distance the whole of the light emerging from the lens no longer falls on the photo-electric cell; the size of the image of the lamp coil is on the other hand a multiple of the cell window (*fig. 9*). In this case the amount of incident light is inversely proportional to the square full distance of the light source. Since the focal length f, the size V of the lamp coil and the quantity of light L falling on the lens are fixed, and also the amount of light l required for illuminating the cell cannot be improved in the particular construction adopted, the length of the beam b between the lens and the cell can only be increased by enlarging the surface A^2 of the cell. The photo-electric cell must receive a minimum of

$$l = \frac{A^2}{B^2} \cdot L = \frac{A^2 f}{b^2 V^2} L$$

which gives for the permissible distance of the photo-electric cell:

$$b = \frac{f}{V} \cdot \sqrt{\frac{A^2 L}{l}} .$$

The magnitude A^2, the operative area of the cell, can in fact be further increased. For if the cell is placed at the focus of a parabolic mirror, the effective surface of the cell will be equal to that of the mirror.

The above-mentioned magnitudes have the following values in our apparatus:

f = 25 cm,
V = 0.2 cm,
A^2 = 200 sq cm,
L = 2.32 lm (see above),
l = 0.00084 lm

so that for infra-red light the distance of surveillance can be:

$$b = \frac{0.2}{25} \sqrt{\frac{200 \cdot 2.32}{0.00168}} = 93000 \text{ cm}$$

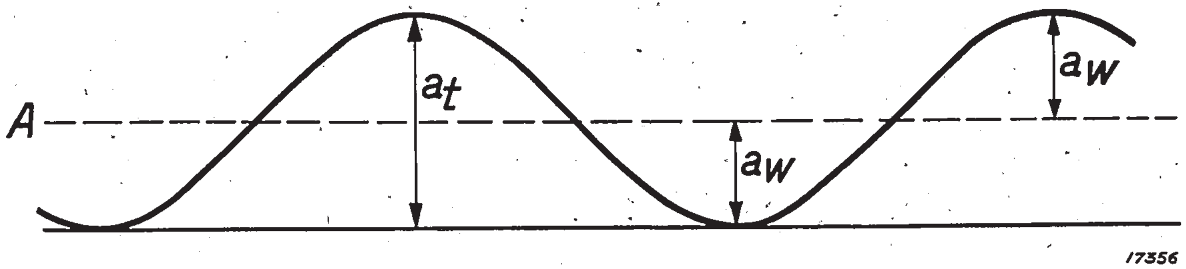

Fig. 8. Fluctuation of the intermittent beam as a function of the time. The average value is represented by the line A and is a_w. The curve may be regarded as made up of two components, viz., a D.C. component with the value a_w and an A.C. component with the amplitude a_w.

In practice the attainable length of beam is smaller since absorption losses must also be taken in consideration. A more comprehensive system of surveillance with rays will in fact require a larger number of mirrors, e.g. for reflecting the beam of light to and fro. The lens and the parabolic mirror referred to above also absorb light. If five plane mirrors are used and each optical unit absorbs 20 per cent of the light incident on it, then the quantity of light L must be multiplied by a factor $(0.8)^7 = 0.21$.

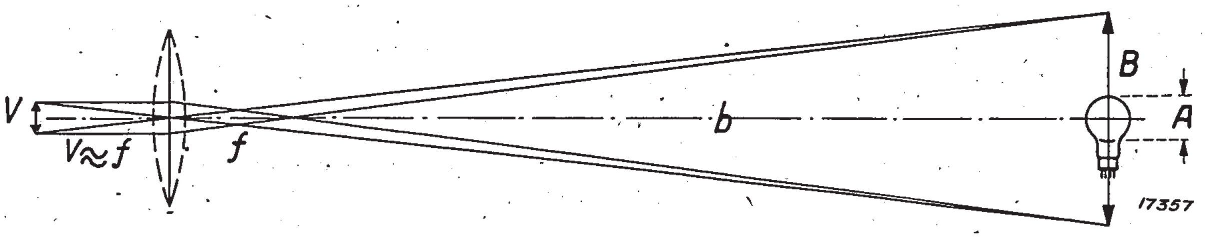

Fig. 9. Layout of a surveillance system in which the window A of the photo-electric cell is considerably smaller than the image B of the lamp coil.

The maximum path of surveillance is then:

$$b' = 93000 \sqrt{0.21} \approx 42500 \text{ cm}.$$

The apparatus could therefore be used for surveillance over a distance of 425 m.

Advantages and Disadvantages

One disadvantage of all systems run from alternating current mains is that any failure in the supply immediately causes a false alarm to be given. The apparatus will also give an alarm when a failure or defect develops in one of the components; yet, according to the point of view, this can also be regarded as an advantage.

The principal advantage of the system is the fact that the beam of light is itself a fluctuating magnitude. A second and less important advantage is that, owing to the provision of the parabolic mirror which concentrates all incident rays at its focus, a screen with a small hole can be placed at this level at the focus itself. Extraneous light rays impinging at an angle, emanating from the general illumination or from passing light sources and concentrated next to the actual focus, do not then reach the photo-electric cell which is therefore screened against these rays. This renders interference with the apparatus by means of a light source with the same characteristics extremely difficult, since the direction of incidence of the rays has also to be very accurately adjusted.

THE ELECTRON MICROSCOPE AS AN AID IN METALLOGRAPHIC RESEARCH

By W. G. BURGERS and J. J. A. PLOOS VAN AMSTEL.

10

Summary. The crystalline structure of a metallic surface heated to a high temperature can be registered by employing thermo-electronic emission of the metal utilising an electron beam. For this purpose in a cathode ray tube of suitable construction the electrons emitted from the metal surface must be focussed on a fluorescent screen in the tube by means of electrical or magnetic fields.

This article describes a suitable tube for this purpose and also discusses the activation process which must be applied to the metal under investigation, in order to raise its electron emissivity to such a level that a "visible" fluorescence is obtained. In conclusion it is shown that the emission and etched diagrams are in substantial agreement.

Investigation of Crystalline Structure by Etching

To bring out the crystalline structure of a metallic surface, the usual method adopted in metallography is to polish the surface of the test specimen under examination and then to etch the surface with a suitable chemical reagent. Owing to their anisotropic structure the crystallites are not uniformily attacked by the etching medium, and certain atomic surfaces are thus subjected to a more intense action than others, such that the crystallites acquire a tiered or stepped surface. This result is shown in *fig. 1*, which illustrates diagrammatically a section drawn perpendicularly through the etched surface (the depth of the step is of the order of several microns). Since the orientation of the crystal lattice is quite abrupt on passing from one crystallite to another, the same will also apply to the direction of the steps. If therefore a beam of light is directed against the surface at a specific angle of incidence, the rays will be reflected in different directions by the different crystallites such that when viewed from a certain direction the crystallites will appear with unequal brightnesses. This phenomenon is shown clearly in *fig. 2* for an aluminium plate which is composed of comparatively large crystals and which has been etched with hydrofluoric acid and aqua regia.

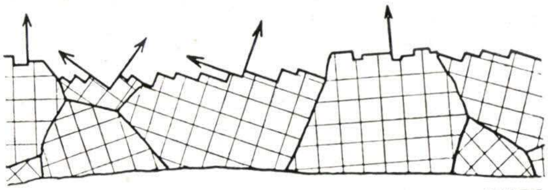

Fig. 1. *) Reflection of incident light from an etched metal surface (diagrammatic). This illustration shows a section perpendicular to the surface of the etched specimen. The thick lines indicate the boundaries of the various crystallites, and the thin lines the position of the atomic lattice in each crystallite.

*) This illustration is taken from: G. Sachs, Z. Metallk., **17**, 299, 1925.

It is obvious that etching at room temperature can only reveal the crystalline structure existing at that temperature, and that to investigate the structure obtaining at higher temperatures the specimen must be etched in the hot state. Although this can indeed be done [1]) the requisite procedure is cumbersome and difficult.

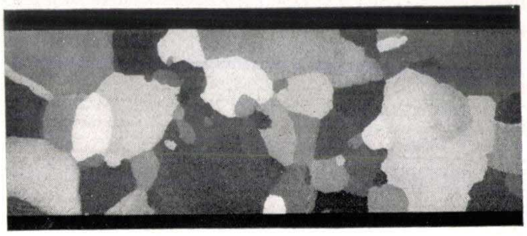

Fig. 2. Etched aluminium sheet composed of large crystals (half natural size).

Investigation of the Crystalline Structure with an Electron Beam

As already indicated in a previous issue of this Review [2]) the crystalline structure of a metallic surface at high temperatures can also be investigated by means of a beam of electrons.

The practicability of such socalled electron-optical representation depends on the following two fundamental principals:

a) The emission of electrons of metals at a hot temperature is determined by the composition of the metallic phase and for a specific composition by the surface of the crystal lattice through which the electrons emerge. This latter factor applies particularly following activation (see section below).

b) If in a vacuum tube an electron-emitting cathode of suitable form is used, then by employing suitable electrical and magnetic fields it is possible to concentrate all electrons emitted from a specific point of the cathode on to a given point of a screen situated at a given distance away. The luminous pattern obtained on the fluorescent coating of this screen will then correspond point for point to the distribution of intensity over the emitting cathode surface. As may be gathered from the previous article in this Review, a magnification or reduction of the image of the structure can be realised according to requirements. Magnification is employed in the "electron microscope" in order to obtain a maximum size of image on the cathode surface. If this surface forms part of the specimen under examination, then in view of the differences in emissivity referred to above the different crystallites will be distinguishable from each other by differences in brightness on the fluorescent screen. The emission diagram obtained in this way closely resembles that obtained by etching the surface.

---

[1]) Thus e.g. in an investigation by A. E. van Arkel and P. Koets (Z. Phys., **41**, 701, 1927) Iron was etched with chlorine gas at a temperature above 900 ° C.

[2]) G. P. Ittmann, Philips techn. Rev. **1**, 33, 1936.

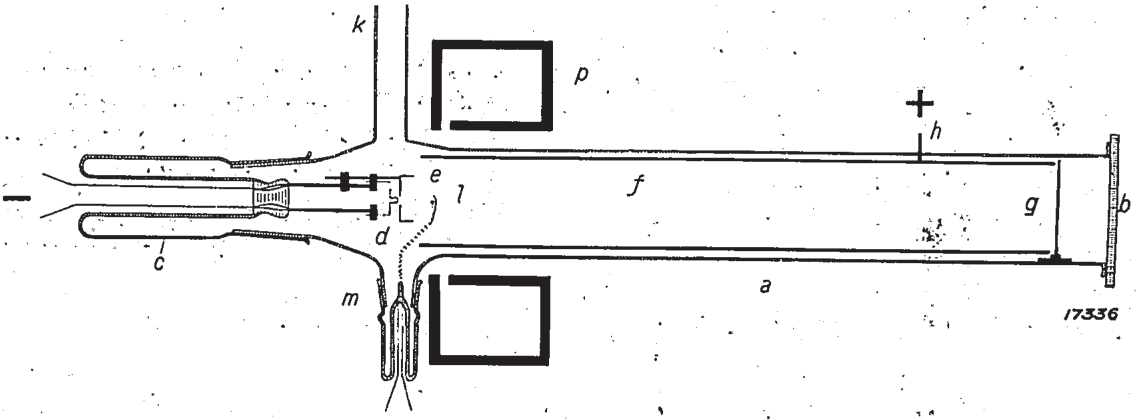

Fig. 3. Cathode ray tube with magnetic focusing for the investigation of metallic surfaces. *a* Cylindrical glass tube (length approx. 45 cm, diameter approx. 6 cm). *b* Plane glass plate. *c* Ground connection securing the cathode. *d* Cathode, made of a rolled strip of the metal under investigation. *e* Brass cap in front of cathode. *f* Anode, a wide brass cylinder. *g* Fluorescent screen. *h* Anode pole. *k* Connection for vacuum pump. *l* Tungsten coil for depositing the activating coating on the cathode. *m* Ground connection. *p* Magnet coil enclosed in mild steel sheath (internal diameter approx. 8 cm, external diameter approx. 20 cm, height approx. 6 cm).

The first study of metallographic problems by the electron-optical method outlined above was carried out by Brüche and his collaborators during investigations in the Research Institute of the A. E. G. [3]) Investigations in similar lines [4]) have also been carried out in this Laboratory. Some results of this work will be described in two articles to show what has been achieved in this direction. In this, the first article, discussion will be devoted to the experimental method adopted, while the second article will deal in detail with the application of the method to a specific example.

Experimental Procedure

The experimental problems entailed fall into two groups:

1) Construction of the cathode-ray tube, and
2) Preparation of the metallic surface to be used as cathode.

Construction of the Cathode Ray Tube

The design and construction of the cathode-ray tube depend on the magnification required. With the comparatively low linear magnification of 15 to 25 employed in this Laboratory, the most practicable method was to focus the electrons by means of a magnetic field. A number of investigators [5]) have published constructional data for tubes of this type, and the tube employed by us, shown diagrammatically in *fig. 3*, was designed on the basis of these data. It consists of a glass cylinder *a* about 45 cm long and 6 cm wide, which is closed at one end by a flat glass plate *b*. At the other end there is a ground connection for the union with a tube holder *c* in which the metal testpiece *d* to be used as cathode is fixed; the specimen is adjustably mounted on two nickel poles. One of the nickel poles carries a brass cap *e* with an aperture at the centre. A brass cylinder *f* located in the glass cylinder *a* serves as anode.

---

[3]) See in particular the work by E. Brüche and O. Scherzer, Geometrische Elektronenoptik (Julius Springer, Berlin, 1934). Some new work at this laboratory will be referred to in the course of this and subsequent articles.

[4]) W. G. Burgers and J. J. A. Ploos van Amstel, Nature, **136**, 721, 1935.

[5]) M. Knoll, F. G. Houtermans and W. Schulze, Z. Phys., **78**, 340, 1932.
J. Pohl, Z. techn. Phys., **15**, 579, 1934.

At the end of the brass cylinder is the fluorescent screen *g*, usually coated with blue-fluorescing calcium tungstate (for making photographic exposures). The connection to the anode is passed out at *h*. The tube *k* connects up with a vacuum pump. By means of a tungsten coil *l* in a small tube holder any suitable substance, such as barium carbonate (if necessary produced by decomposition), can be deposited on the cathode to activate the latter. By means of the ground joint *m* the coil can be turned through a right angle after the material has been deposited, so that it no longer lies between the cathode and the fluorescent screen (as shown in the figure). Finally, *p* is a coil acting as a "magnetic lens" and which except for a slot several millimetres wide, is completely covered with mild steel to a depth of about 5 mm, as described by Ruska and Knoll. *Fig. 4* gives a general view of the whole apparatus, the cathode ray tube and the "magnetic lens" being easily picked out. With a tube of this type diagrams subject to very little distortion can be readily obtained. Naturally to ensure good diagrams at a given anode voltage (with respect to the cathode which is earthed in this arrangement) the current through the magnet coil must be of such a value that the rays can be sharply focussed on the fluorescent screen. The optimum current intensity through the magnet coil and the optimum anode voltage depend on the emissivity of the cathode and also on the relative positions (cf. fig. 3) of the surface of the cathode *d*, the brass cap *e*, the magnet coil *p*, the brass anode *f*, and the fluorescent screen *g*. The voltages employed in our apparatus were of the order of 3000 to 6000 volts when about 1 A current was passed through the magnet coil (2000 ampere-turns).

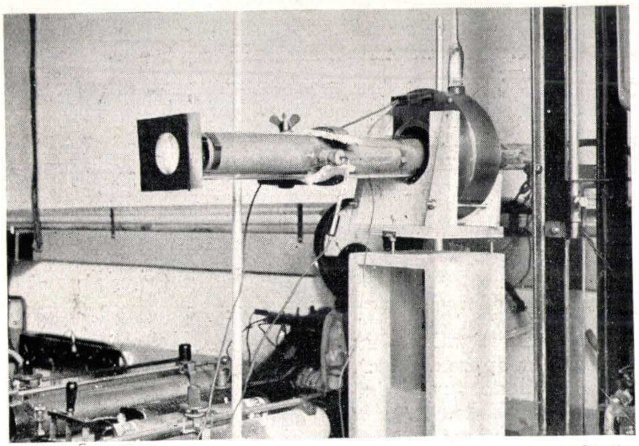

Fig. 4. View of experimental apparatus; the cathode ray tube, viewing window and enclosed magnet coil can be easily picked out.

To obtain a sharply-defined image the voltage and the current intensity must be maintained sufficiently constant. The constant voltage was supplied from a suitably-rated anode voltage unit [7]) and the constant current derived from an accumulator. Naturally the cathode ray tube as a whole had also to be adequately protected against vibration, etc.

Preparation of the Metallic Surface to be used as Cathode

Shape of the cathode

It was found that a plane cathode located perpendicular to the axis of the tube gave an image of satisfactory definition on the fluorescent screen. We employed the metal under examination in the form of a rolled strip about 2.5 mm wide and 0.1 mm thick, the shape of which is shown in fig. 3*d*. Only the front position (a small square of about 2.5 mm side) served as the actual cathode surface for which a diagram was obtained. This surface was polished [8]) and set up perpendicular to the axis of the tube immediately behind the aperture approx. 5 mm wide, in the brass cap *e*.

Activation of the Cathode

Frequently the emission of electrons from metals at temperatures at which e.g. a transformation is to be observed, is far too small to give fluorescent images of sufficient intensity for visual observation or photographic registration. It then becomes necessary to "activate" the surface of the metal, i.e. to raise its emissivity. Such activation can be realised by coating the surface with a layer of electro-positive atoms, as of barium, strontium or caesium.

As a result of such activation the aggregate emissivity of the metal is very considerably increased. But apart from this effect, an intensified contrast in the emission pattern can frequently

---

[6]) E. Ruska and M. Knoll, Z. techn. Phys., **12**, 448, 1931. In this way the magnetic field is concentrated mainly in a plane perpendicular to the axis of the cathode ray tube, permitting the ampere-turns required to obtain a given "refractive action" to be reduced. Cf. also M. Knoll and E. Ruska, Z. Phys., **78**, 318, 1932.

[7]) The anode voltage unit employed by us gives a maximum output of 20 watts. The energy taken from it is however much smaller, since the anode current is normally less than 0.1 mA.

[8]) Inequalities of the surface (as a result of deep etching), which affect the potential distribution in the immediate neighbourhood of the cathode, render the focusing action of the electrical and magnetic fields difficult and should be avoided.

[9]) Compare J. H. de Boer, Electron emission and adsorption phenomena (Cambridge 1935).

also be obtained, since the different planes in the crystal lattice adsorb varying amounts of electropositive atoms so that the differences in their emissivities are intensified.

Activation may be performed in several ways, e.g. by coating the metal surface with an aqueous solution of barium azide or, with the aid of the tungsten coil *1* in fig. 3 which is suitably coated with barium or strontium carbonate, by depositing on the metal surface metallic barium or strontium or the oxides of these metals and then submitting the specimen to a specific, frequently complex, heat treatment, usually consisting of strongly heating the metal surface to different temperatures, with or without the simultaneous applications of the anode voltages.

The choice of activator depends *inter alia* on the temperature at which observations of the crystal structure are to be made. If this temperature is comparatively high, an activating atomic layer should be sought which does not volatilise too readily from the surface of the cathode. For observations at low temperatures activation with the most powerful electropositive atoms is necessary, thus Schenk [10]) has obtained good results with caesium already at 400 ° C. The emission of electrons from a metal can also be induced by photo-electric means by irradiating the surface with ultra-violet light. Using this method, diagrams of the crystalline structure can already be produced at room temperature [11]).

The series of photographs shown in *fig. 5* indicate the changes visible during the activation process. These photographs relate to an iron strip activated with strontium carbonate and represent various stages of the activation process [12]).

Immediately after vaporisation a more or less uniform emission is observed (*a*) at a comparatively low temperature (approx. 800 to 900 ° C.), such emission revealing no crystalline structure. The temperature is then raised, e.g. to 1010 ° C., whereupon the emission slowly decays (*b-c*), until eventually[13]) it disappears altogether (*d*). The temperature of the cathode is then again reduced, as a result of which emission recommences (*e-i*) and spreads visibly over the surface.

The emission now obtained reveals the crystalline structure of the cathode surface. *Fig. 6* enables a comparison of an electron-optical image (*a*) with the photograph of the etched cathode (*b*) taken immediately after. It is seen that the emission and etched diagrams are practically identical. The small differences observed are due to the fact that the emission diagram corresponds to the uppermost surface of the iron strip, while the etched diagram relates to a surface situated at a greater depth.

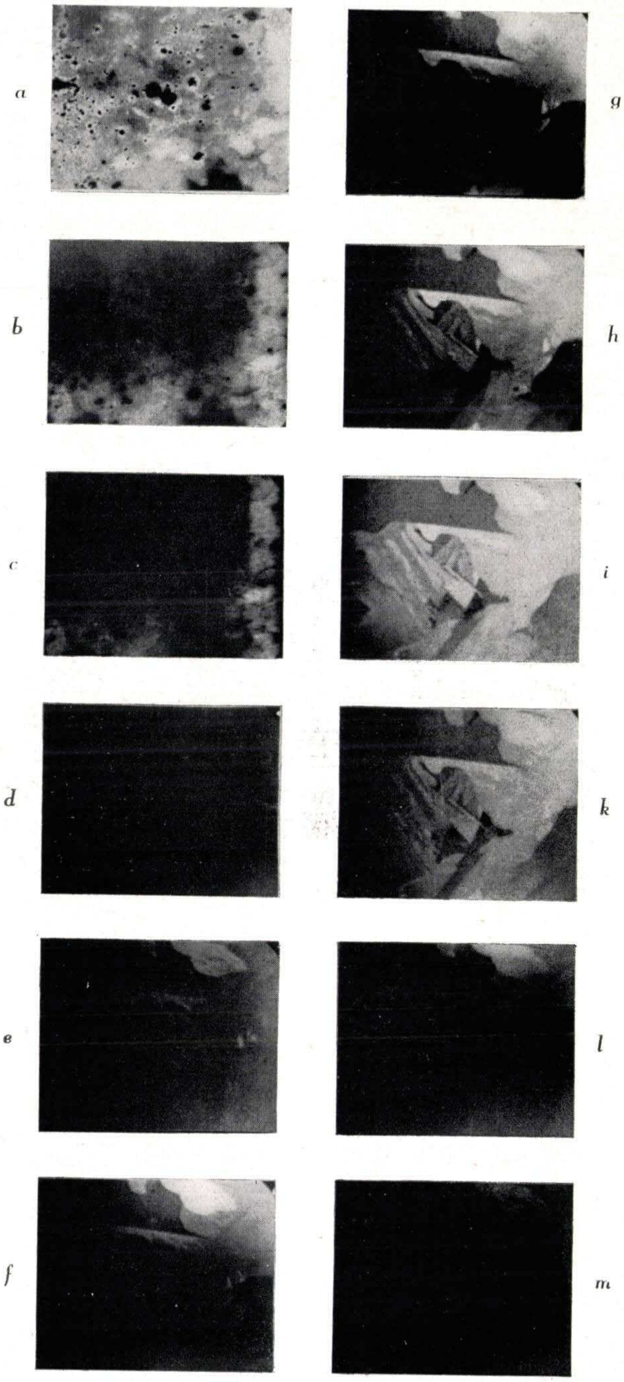

17338

Fig. 5. Appearance and disappearance of the crystal-structure diagram on activating an iron strip with strontium carbonate.

a After depositing the activator on the cathode, in the first instance forming a comparatively thick coating of strontium or strontium carbonate.

b to *d* On heating to a high temperature the activating coating disappears and the emission becomes reduced.

d to *l* The temperature is lowered and an image of the crystalline structure is obtained.

k to *m* On again raising the temperature this image also disappears.

---

[10]) E. Schenk, Z. Phys., **98**, 753, 1935.

[11]) J. Pohl, Z. techn. Phys., **15**, 579, 1934.
H. Mahl and J. Pohl, ibid, **16**, 219, 1935.

[12]) For this purpose a standard film camera was set up in front of the glass plate *b* with which exposures were made with exposure times of 1 to 2 seconds.

[13]) A temporary increase in emission may occur here. For details of these characteristics in the activation process reference should be made to a paper to be published in Physica.

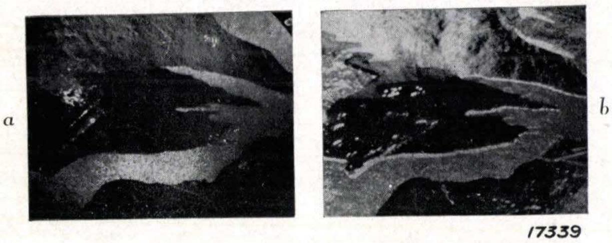

Fig. 6. Crystalline structure diagram of iron on magnification 20 times: Agreement between *a* the emission diagram (at 880 ° C) and *b* the etching diagram (at 20 ° C).

The process of activation described above may perhaps be explained on the following lines. After depositing the activating coating, the iron strip is in the first place covered with a comparatively thick coating of strontium or strontium oxide, and the emission obtained originates from this coating. As the temperature is subsequently raised, this coating disappears from the surface of the metal, part being removed by volatilisation and part by diffusion inwards. The emission therefore becomes reduced to that of the iron itself, i.e. it disappears almost wholly since the emission of iron at 1100 ° C is very small. If the temperature is now reduced the volatilisation of the strontium from the surface of the iron diminishes to a greater extent than the back-diffusion of the strontium out of the iron. When the temperature has been sufficiently reduced, diffusion will predominate over volatilisation so that the metal coating required for activation is able to form on the surface. On again raising the temperature this coating also volatilises and the emission again falls, as may be seen from the photographs *k-m* in fig. 5 [14]).

Revealing the Crystalline Boundaries

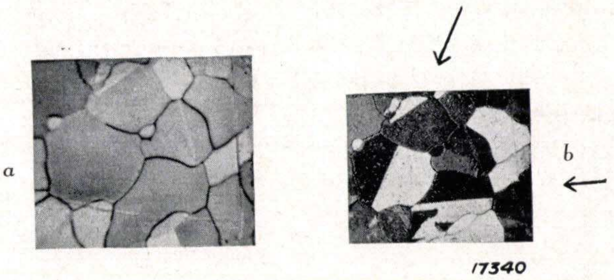

Fig. 7. Emission diagram *a* (at 1100 ° C) and etched diagram *b* at room temperature of nickel iron: In the emission diagram the boundaries of the crystallites can be clearly picked out, while the socalled "twinning boundaries" marked in the etched diagrams by arrows are barely visible.

In the emission diagrams reproduced in figs. 5 and 6 the emission is seen to differ for different crystallites. With different methods of activation diagrams are obtained in which as in *fig. 7a* only the boundaries of the crystallites are well defined. A diagram of this type is obtained particularly on heating cathodes which are still covered with such a thick coating of activating material that the coating itself emits electrons and not the metal beneath it. Since at the boundaries of the crystallites any admixtures in the metal are frequently accumulated, it is possible that the activating coating above these boundaries is present in a different state, i.e. reacts chemically or volatilises more rapidly, than over the crystallites themselves, and that as a result a different emission is obtained [15]). Fig. 7*a* was obtained with nickel iron at a temperature of approx. 700 ° C., and fig. 7*b* with a cathode etched with hydrochloric acid and picric acid. In addition to a number of irregular boundary lines, the etched diagram also includes several which are quite straight (marked with arrows). These are the socalled boundaries, i.e. they separate two crystal lattice areas mutually orientated in twin positions. These boundaries are thus entirely different from ordinary crystal boundaries, where, as already indicated, e.g. admixtures or impurities may be accumulated. It should be noted that the difference in character of these two types of boundary lines is clearly brought out in the electron-optical diagram. While the ordinary crystal boundaries appear very dark, the twinning boundaries can be barely distinguished.

Correction. In the article on the „Development of the Coiled-Coil Lamp" Philips techn. Rev. I, 97, 1936 the following corrections to printer's errors should be noted:

1. (Table p. 98): The figures in the last column relate to a wire 0.1 mm in diameter (and not to one of 0.01 mm).
2. (Footnote p. 100) : 1 m^3 of air contains approximately 1 cm^3 of krypton and 0.1 cm^3 of xenon (instead of 10 and 1 cm^3 respectively).
3. (Fig. 8, p. 101): In the caption *A* and *B* have been interchanged; the caption should read: *A* for a coiled-coil lamp, *B* for a single-coil lamp. Hence the diminution in efficiency is lower in the case of the coiled-coil lamp.

---

[14]) According to the above experiment the activation process described here bears a close analogy to observations made in the activation of tungsten containing thorium oxide, cf. E. Brüche and H. Mahl, Z. techn. Phys., **16**, 623, 1935.

[15]) A generally valid explanation of this phenomenon has not yet been advanced as far as we are aware. Cf. e.g. E. Brüche, Z. Phys., **98**, 77, 1935.

VOL. 1 No. 11 NOVEMBER 1936

Philips Technical Review

DEALING WITH TECHNICAL PROBLEMS
RELATING TO THE PRODUCTS, PROCESSES AND INVESTIGATIONS OF
N.V. PHILIPS' GLOEILAMPENFABRIEKEN

EDITED BY THE RESEARCH LABORATORY OF N.V. PHILIPS' GLOEILAMPENFABRIEKEN, EINDHOVEN, HOLLAND

ELECTRON-OPTICAL OBSERVATIONS ON THE TRANSITION OF ALPHA TO GAMMA IRON

By W. G. BURGERS and J. J. A. PLOOS VAN AMSTEL

Summary. To investigate the process of transformation or recrystallisation in a metal by the standard etching method used in metallography, etching must in general be performed during the transformation itself. In most instances this introduces considerable difficulty, particularly at high transformation temperatures. In such cases the electron-optical method of exhibiting the crystal structure of a metal at a high temperature can prove of great service. The present article describes how this procedure may be applied to the investigation of the transformation of iron from the γ to the a phase which occurs at about 900° C.

In the previous issue [1]) of this Review it was shown how the crystalline structure of a heated metal surface could be rendered visible by electron-optical means in the cathode ray tube. This method consists in focusing the electrons emitted from the metal acting as a cathode, on to a fluorescent screen in the tube by applying suitable electrical and magnetic fields to the electron beam. A fluorescent image is produced on the screen whose brightness corresponds point for point to the emitting cathode surface and which can moreover be enlarged to give a much magnified image of this surface. Since the individual crystals of which the cathode is composed in general emit electrons to a varying degree owing to differences in composition and axial orientation, fluorescent areas of varying intensity are produced on the screen. The screen thus reveals a pattern very similar to an etched figure, a feature very aptly shown in fig. 6 of the previous paper.

This method of rendering visible the crystalline structure of a metal specimen at a high temperature can prove particularly instructive where the metal undergoes a transformation on heating and it is desirable to investigate the stable phase above the transition point. By the etching process commonly used in metallography and briefly outlined in the previous article, this can only be done by etching at room temperature when the phase in question can be supercooled by reducing the temperature of the heated testpiece at a sufficient velocity ("quenching"). But frequently retention of this phase is impossible even on the most rapid cooling. In order to investigate in such case the phase existing at a high temperature the testpiece must be etched at this temperature.

That the etched figure then obtained remains stable in spite of the transformation occurring during cooling is demonstrated by the following. As already explained in the previous article the surface of the crystallites becomes "stepped" as a result of etching. These steps are of "microscopic size", i.e. they are composed of a large number of atoms, and their direction conforms with specific surfaces of the crystal lattice. An etched surface of this type is again reproduced in *fig. 1* with the crystals shown by continuous lines. Assume that the crystals owing to a transformation during cooling have been altered to the state as shown by the broken lines. In general these changes are not directly observable, for as the alterations in structure in many cases take place atom for atom, the new crystals completely occupy the same space as previously taken up by the original crystals, except for deviations of atomic dimensions (approx. 10^{-8} cm) at the surface. These changes are however much too small to alter the visible shape of the steps, so that no difference is detected in the etched figure[2]). Only on further etching does the old surface disappear and in place of it there appears a surface formed by the newly-constituted crystals.

---

[1]) Philips techn. Rev., 1, 312, 1936.

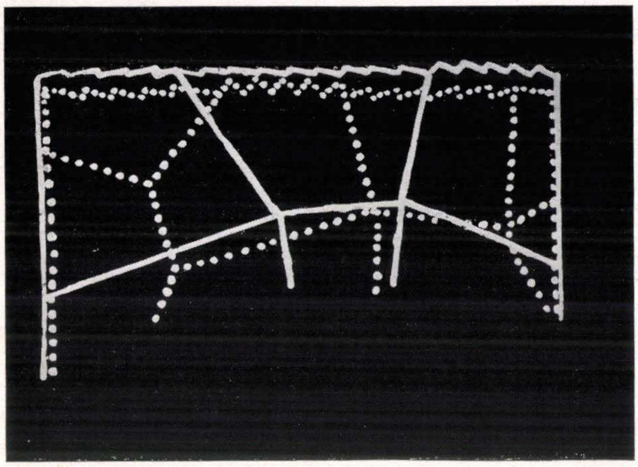

Fig. 1. Structural changes in a metal during recrystallisation (diagrammatic representation after van Arkel and Koets). The figure shows a section drawn perpendicular to the surface of the test specimen. The continuous lines indicate the boundaries of the crystals originally present, at which a step-shaped surface is exposed by etching. The crystals produced by transformation and indicated by broken lines completely fill the space occupied by the previous phase, except for differences of atomic dimensions (of a magnitude of 10^{-8} cm). Only after renewed etching is the old step-shaped surface displaced by one corresponding to the new crystals formed, so that the latter becomes apparent.

In many cases the etching of surfaces at a high temperature is a difficult matter, particularly where not only the phase formed by a specific transformation, but also the development of such transformation itself is to be studied.

The intrinsic suitability of the electron-optical method for investigating a transformation taking place at a high temperature is shown by the study described below of the transformation of the alpha modification of iron stable at temperatures below about 900 °C into the gamma modification [3]) stable above this temperature.

Brüche and Knecht [4]) were the first to study this transformation by electron-optical means. In their experiments the iron was activated to such a degree by a thin coating of barium volatilised on an oxide cathode that at a temperature of about 1000 ° C a well-defined fluorescent image of the crystalline structure, embracing all crystals of the gamma modification stable above 900 ° C, was produced which moreover could be readily photographed. At the transition point itself and particularly at still lower temperatures, the emission was however too weak, in spite of activation, to give the fluorescent pattern, if adequate adaptation in a darkened room were not provided. Photographic registration of the variation in structure at the transformation point was thus not possible [5]).

In our experiments the iron, which was used in the form of a rolled strip several mm wide and 0.1 mm thick, was electrically heated, and activated by a volatilised coating of Sr (or Sr0) deposited from a tungsten coil coated with SrCO$_3$. By suitable heat treatment it was found possible to obtain such powerful and sustained emission that both above and below the transformation point well-defined patterns of the structure were obtained; these did not exhibit any appreciable reduction in intensity during a period of 10 minutes and could be successfully photographed with a standard film camera (through the glass plate *b* in fig. 3, loc. cit.) employing an exposure time of about 2 secs.

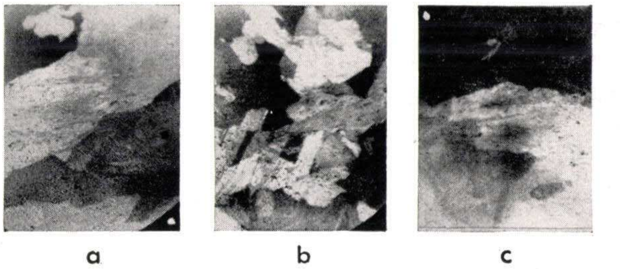

a b c

Fig. 2. Electron-optical images of crystal structure (magnification approx. 15) of a heated iron strip whose temperature is *a*) a little above, *b*) a little below, and *c*) again above the transformation temperature of the two modifications. The figures thus show: *a*) γ crystals, *b*) α crystals, and *c*) again γ crystals. Figures *a* and *c* are seen to be quite different.

The mechanism of activation on these lines has already been described in detail in the previous article on the basis of a series of photographic records. The photographs reproduced in fig. 5 of that article relate to iron. In *fig. 2* of the present article three crystal-structure patterns obtained by the same method are reproduced. These were obtained with the same strip and at temperatures just above, just below and also directly at the transformation point. The patterns thus show in 15-fold magnification: *a*) γ crystals, *b*) α crystals, and *c*) again γ crystals. From a metallographic standpoint the fact is interesting that the two γ structures are different: The first transformation from the γ into the α phase was probably very complete and left no γ nuclei, which on subsequent transformation could have caused the re-generation of the original crystals.

---

[2]) There are however exceptions. So the growth of martensite needles can immediately be observed without etching. This transformation was cinematographically recorded by H. J. Wiester. Z. Metallk., 24, 276, 1932.

[3]) As is well known the iron atoms in both modifications form a cubic lattice, with the sole difference that in the case of α iron the centres of the cubic cells are occupied in addition to the corners (space-centred structure), while in γ iron the cubic surfaces are occupied in addition to the corners (face-centred structure). That the modification stable above 900 ° C is denoted by γ and not by β is associated with the fact that magnetic α iron stable at room temperature becomes non-magnetic at about 760 ° C (Curie point) and this non-magnetic phase, which has the same crystal structure as the magnetic phase, is already designated as β iron. It would in fact be more logical to term the transformation at 900 ° C the β-transformation.

[4]) E. Brüche and W. Knecht, Z. techn. Phys., **15**, 461, 1934; **16**, 95, 1935.

[5]) These investigations could however quite definitely conclude from the alteration in the crystal pattern, if any, whether the transformation point was passed or not on reducing the temperature, by making all observations at 1000 ° C. and reducing the cathode temperature for a short time between successive observations to a temperature in the neighbourhood of the transformation point.

The progress of transformation itself can also be very well followed by varying the electric current passing through the iron when the latter is heated in the neighbourhood of the transformation point. The occurrence of a temperature gradient in the strip (as a result of the marked cooling at the clamped ends) causes a displacement along the surface of the strip of the line of separation between the crystalline states above and below the transformation temperature. In consequence transformation is seen to proceed from one side of the fluorescent screen to the other. By very slowly altering the current the duration of transformation could be extended to a period of 5 minutes, thus permitting the whole process to be filmed using an exposure time of 2 secs per picture as indicated above.

The observation of the transition of the γ phase stable above the transformation temperature into the α phase stable below this temperature was particularly successful. Since the ends of the strip are always at room temperature, α crystals are always present in the colder part of the strip; these serve as nuclei and ensure a uniform development of the transformation process. Conditions are however different on inverse transformation: At the beginning of the experiment γ crystals are then absent and it may occur that transformation is only initiated when some point or other is superheated to a few degrees. When this has once occurred the nuclei generated then frequently commence to grow suddenly and very rapidly (owing to the high temperature) and it is no longer possible to register the development of growth photographically using the comparatively long exposure time of 2 secs per picture.

In *figs. 3* and *4* two series of photographs taken from a film are reproduced which bring out well the transition of γ crystals into α crystals. A point to be noted is how the nuclei of the α phase formed on the left develop into more or less elongated crystals filling the whole strip. The rate of growth of these crystals has thus kept pace with the velocity of transformation, so that practically no other nuclei are formed. The photographs, which are in fact enlargements of standard film pictures, show the crystal structure with a magnification of approx. 20 (fig. 3) and approx. 35 (fig. 4). The photographs in fig. 3 were made at the beginning of the investigation, i.e. before sufficient attention has been given to setting up the cathode ray tube on a vibrationless base, which thus accounts for their somewhat blurred appearance. This defect has in the meantime been eliminated. Fig. 4 with a still higher magnification demonstrates extremely well the suitability of the electron-optical method for investigating the transformation processes. Further investigation of this method of analysis will show how far the procedure can prove of general application.

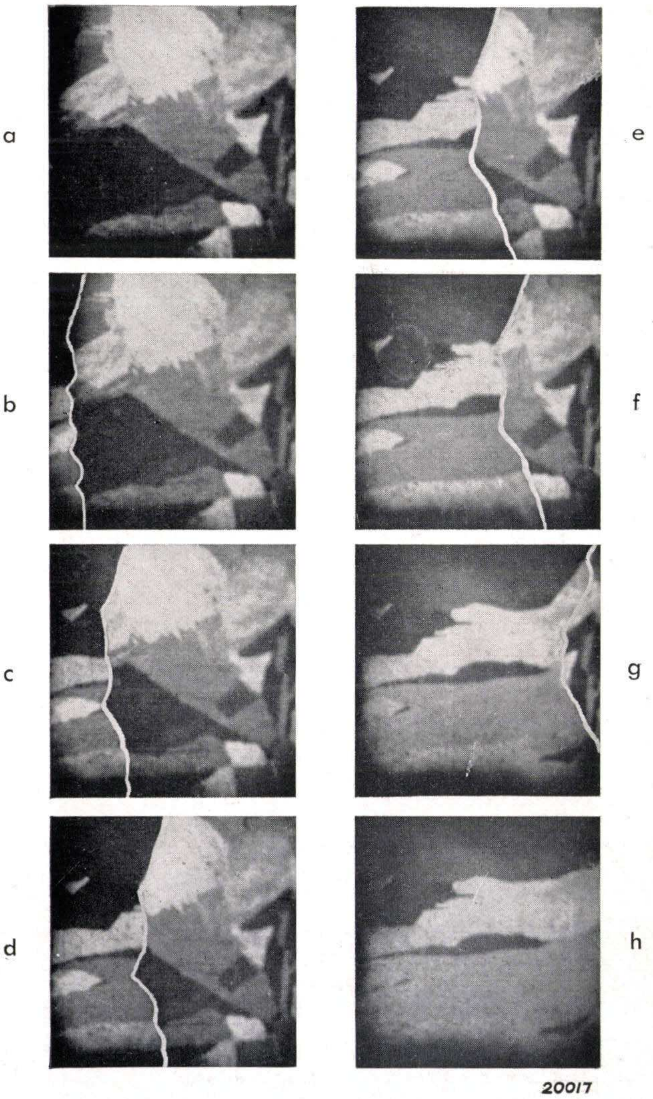

Fig. 3. Electron-optical representation of the transformation of γ crystals *a*) stable above 900 ° C into α crystals *b*) stable below 900 ° C on slowly lowering the temperature of the strip. The new crystals grow from left to right, as indicated by the white line of separation.

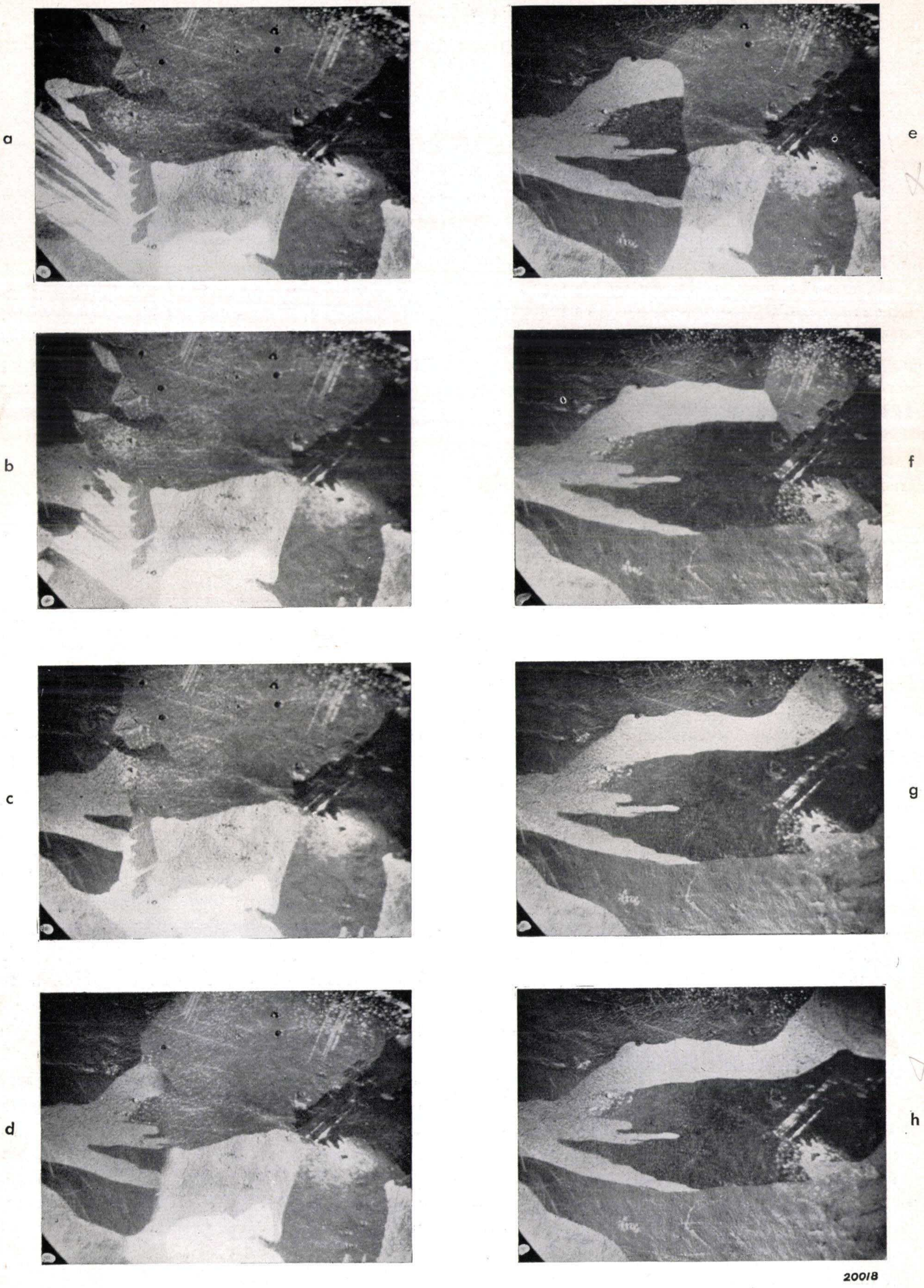

Fig. 4. As fig. 3. The line of separation between the growing α and the disappearing γ crystals is not shown here, since it can be quite clearly picked out.

TELEVISION

by J. VAN DER MARK.

Summary. The television transmitter in the Philips Laboratory which has already been described in the first number of this review [1]) has now been adapted for transmitting with a wide variety of line frequencies using sequential and interlaced scanning systems. These extensions are discussed, as well as a number of circuit details which were not referred to in the first article.

In a previous article [1]) in this Review the television transmitter in this Laboratory has already been described in broad outline. In the present article details are given of a number of points on which further information has been gathered during experience with the experimental transmitter.

It should be pointed out at the outset that the transmitter in its present form, as indeed already indicated in the previous article, is suitable for transmitting purposes employing a wide choice of scanning lines per picture. Before passing to a closer consideration of this point we shall again briefly describe the scanning process employed.

The earlier description related to a unit for transmitting 25 pictures per second and 180 lines per picture. These pictures were on the whole quite satisfactory, but suffered from a very undesirable defect, viz., the bright parts in the field of vision were subject to flicker. This flickering produced an unsteady visual impression which made it very fatiguing to view the pictures for any length of time. The reason for this was that when an adequate brightness of the field of view was obtained the picture frequency of 25 per second was insufficient to produce a perfectly steady impression. This flickering could be avoided by transmitting at a higher picture frequency, e.g. 50 pictures per second, at which no fluctuations in the brightness impression occur [2]), but this would mean doubling the maximum modulation frequency to retain the same picture definition: a very undesirable alteration.

Flickering can, however, be suppressed without altering the maximum modulation frequency, viz., by adopting a suitable artifice. For if with an odd number of scanning lines per picture, e.g. 405, at a picture frequency of 25 per second, the picture frequency is doubled, i.e. to 50, then 202.5 scanning lines per picture will be obtained, i.e. not an integral number of lines. The scanning of the picture then commences alternately in the left-hand top corner and in the middle of the top edge of the picture. *Fig. 1* shows that this results in bringing the lines of the "even" pictures exactly midway between the lines of the "odd" pictures. Although the whole picture surface is written in 1/25 of a second, i.e. in the same time as formerly, directly contiguous lines in the picture are now reproduced alternately at intervals of 1/50 of a second. Since a televised picture must be viewed from such a distance that the individual lines cannot be seen separately (in the same way as the impression of a screen block must be viewed from such a distance that the screen dots are not seen individually), no flickering will be observable. This effect is shown in fig. 1 for a picture with only 7 lines.

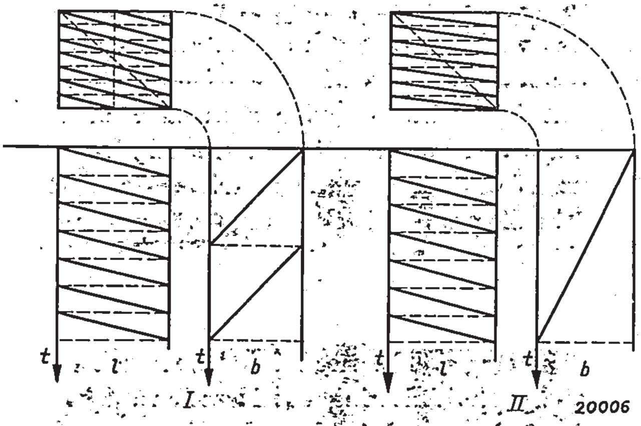

Fig. 1. Interlaced and sequential scanning of a picture of 7 lines. Both systems employ the same saw-tooth movement in scanning the lines (*I l* and *II l*); in interlaced scanning the saw-tooth movement of the lines across the frame has double the frequency as in sequential scanning (*I b* and *II b*). The net result is that by both systems the whole surface of the frame is scanned in the same time; with sequential scanning (right) the lines are scanned in direct succession, while in interlaced scanning (left) first all odd lines and then all even lines are scanned.

The maximum modulation frequency in this system of scanning, called interleaved scanning, interlacing or line jump scanning, remains unchanged, for the number of picture elements transmitted per second is not increased.

---

[1]) Philips techn. Rev., 1, 16, 1936.

[2]) For reasons given later on in this article, there is in practice only a choice between 25 and 50 pictures per second when using a mains frequency of 50 cycles.

The transmitting equipment at the present moment is suitable for the use of the following scanning systems:

	Picture frequency per second	Scanning lines per picture	Scanning system	Picture
1)	50	90	Sequential	Non-flicker
2)	50	120	,,	,,
3)	50	180	,,	,,
4)	25	180	,,	Flickering
5)	25	240	,,	,,
6)	25	360	,,	,,
7)	25	375	,,	,,
8)	25	405	,,	,,
9)	2 × 25	$187^{1}/_{2}$	Interlaced	Non-flicker
10)	2 × 25	$202^{1}/_{2}$	,,	,,

A number of examples is reproduced in *fig. 2*. The oscillator, the frequency demultiplicator and the various saw-tooth generators are adjusted by switches to the various requisite frequencies, so that by switching over a number of knobs a change can be made instantaneously from one system of scanning to the other.

In the diagrammatic sketch in *fig. 3*, a number of additional components not included in the previous layout (page 19 of this Review) are shown on the left next to the oscillator and the frequency demultiplication stages. The need for these auxiliaries is shown by the following considerations. The television receiver, and in fact also the transmitter, must be fed from the mains. The direct voltages employed, which are generated by rectification, will always indicate their origin by the presence of ripples, if no costly additional apparatus is included to avoid this effect, these ripples are apparent in the images by one or more slightly dark bands and a slight displacement of the lines. As long as the bands are stationary with respect to the frame, this effect can be tolerated, but the bands constitute a serious disturbance as soon as they commence to wander across the picture. Stationary bands are only obtained by synchronising the picture frequency with the A.C. mains supply. If interlaced scanning is used for transmission, synchronising becomes still more imperative, since adjoining lines are not scanned in direct succession, so that without synchronising the lines of the odd and the even pictures will move with respect to each other, the definition of the picture naturally suffering in conseqeunce. If scanning is synchronised with the A.C., the two frames used with interlaced scanning follow each other at intervals of 1/50 of a sec., as indicated in the table, i.e. with the same periodicity as the mains supply, with the result that the adjoining lines are distorted to the same extent by the voltage ripple. It is also essential to synchronise the picture frequency with the mains also when transmitting films in which the projector is driven by a synchronous motor.

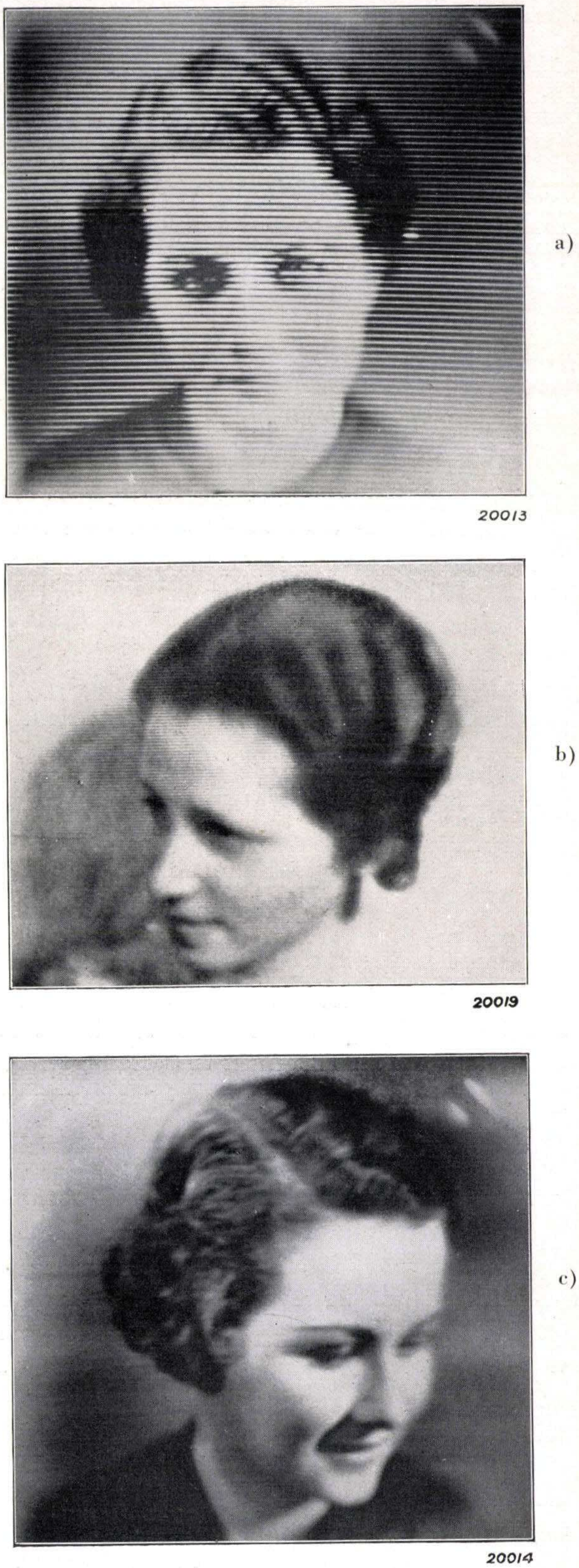

Fig. 2 Pictures obtained with: *a*) 90 linies, *b*) 180 lines, *c*) 405 lines

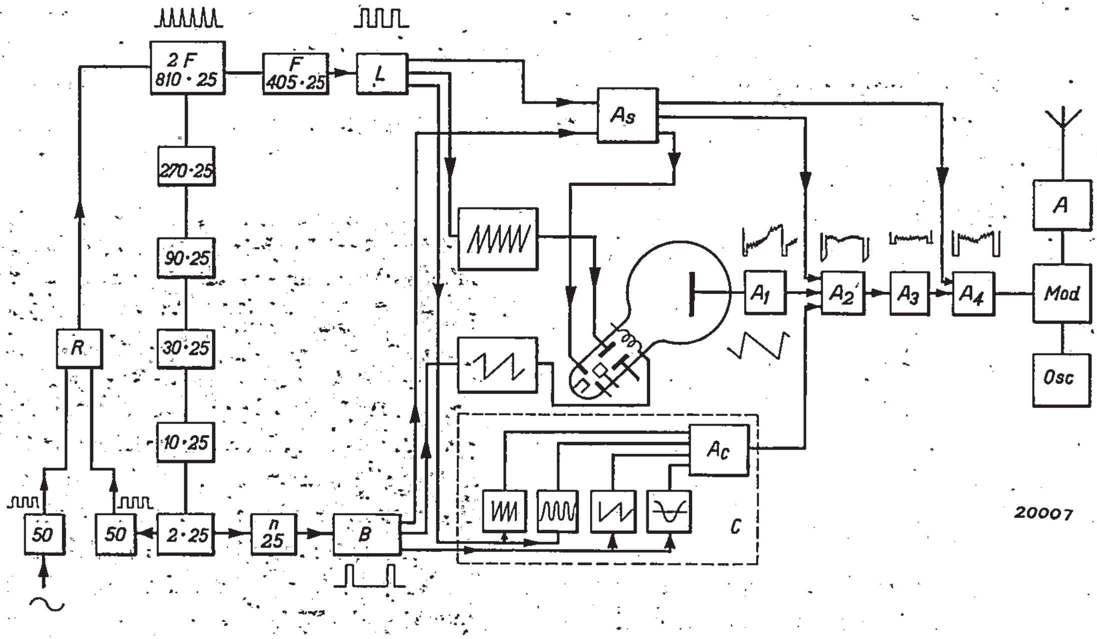

Fig. 3. Diagrammatic layout of the transmitter. In the oscillator 2 F in the top left, impulses are generated with a frequency $2f$ (f is the line frequency, being equal to the product of the picture frequency n per second and the number of lines N per picture). In the stages depicted below this frequency is demultiplied until a 50-cycle frequency is obtained. In this way the picture frequency n (25 or 50 cycles) is arrived at on the one hand, and on the other hand (going to the left in the diagram) the oscillator, which furnishes a voltage with a rectangular time diagram, is controlled. This voltage, together with an equal mains-controlled voltage is passed to a component marked R; the latter furnishes a direct voltage which is a measure of the phase difference between the two alternating voltages. This direct voltage serves as the control voltage for the oscillator 2 F which in this way is stabilised as described in the text. The impulses furnished by F and n are converted in L and B to synchronising signals with rectangular voltage characteristics. These signals are mixed and amplified in the amplifier A_S; they also serve for operating the two saw-tooth generators for controlling the electron beam in the iconoscope, and are finally passed to the complex C which furnishes the compensating signals. From the amplifier A_S the synchronising signals are *inter alia*, passed to the control electrode of the iconoscope in order to suppress the electron beam during each flyback.
Four different compensating signals are given in the diagram (although actually more are used), viz., the saw-tooth voltages with line and picture frequencies, and sinusoidal voltages with the same frequencies. These voltages, each of which can be regulated, are mixed in the amplifier A_C. The picture signals of the iconoscope are first amplified in the amplifier A_1. As shown diagrammatically these signals increase, for instance, from left to right, while they should have a horizontal mean value throughout. By mixing a suitable compensating signal from A_C in the amplifier A_2, this horizontal level may be obtained. The end of the synchronising signal is however then distorted. To eliminate this distortion the distorted end is cut out in A_3, by limiting the amplitude, whereupon a synchronising signal is added in A_4 in order to obtain the correct amplitude for the synchronising signal. The signal is then passed to the transmitter.

The frequency of the oscillator, which controls scanning, must therefore be of such a value that the picture frequency which is derived from it by a series of demultiplications is maintained in synchronism with the mains. This is done in the following way: The oscillator is designed on such lines that its frequency can be regulated within specific limits by altering a direct voltage. The latter is furnished by a circuit in which a 50-cycle alternating voltage derived from the mains is balanced against another 50-cycle alternating voltage generated by frequency demultiplication. This circuit is so designed that the direct voltage obtained is a measure of the phase difference between these two voltages. As soon as the picture frequency deviates slightly from the mains frequency, this phase difference will be altered and hence also the direct voltage. This change in the direct voltage now reacts on the oscillator frequency in such a way that the initial change is compensated. In this way the line and picture impulses are maintained in a strict proportionality by demultiplication in frequency and phase, and the latter are always synchronised with the mains supply and in a definite adjustable phase relationship with it.

The circuit diagram in fig. 3 also includes a number of other alterations whose purpose will also be described in some detail. It has already been indicated in the previous article that the iconoscope furnishes a voltage whose magnitude at every instant is a measure of the illumination incident on that part of the light-sensitive plate being scanned at that moment. In addition to this signal, the iconoscope can also generate a further, and undesirable, signal owing to a small part of the electrons emitted from the signal plate returning to it and impinging at points different from their initial points of emission. There thus results a charge transport from one part of the signal plate to other parts, such transport becoming apparent in the final picture as blurred bright and dark patches. The definition of the picture does not suffer in consequence, but the average brightness over certain areas deviates from the correct value. Since this phenomenon makes itself apparent as large blurred spots, it is possible to eliminate it by means of an auxiliary signal.

If, for instance, a picture is obtained at the receiver which is too bright on the left and too dark on the right, this condition can be improved by superposing in the transmitter a compensating signal in the form of a saw-tooth voltage with the line frequency on the voltage furnished by the iconoscope (the line frequency is entailed here since the lines are scanned from left to right). In this way the average brightness is reduced on the left and increased on the right, so that with a suitable choice of voltage the correct value is obtained over the whole frame. The result is checked with a monitor receiver.

To permit this method of compensation to be used in all cases, various compensating voltages are available, such as e.g. saw-tooth voltages of picture and line frequency and alternating voltages of various frequencies, which are derived from the synchronising impulses. As Fourier components the synchronising impulses contain a large number of harmonics of the picture and line frequencies. All these voltages can be continuously and controllably mixed or modulated with respect to each other, both in magnitude and direction, and impressed on the picture. Naturally the compensating signals must be subsequently regulated by hand, the result being checked on a monitor reproduction tube. It should also be noted that by the addition of the compensating signals the synchronising signals become distorted, as shown in fig. 3 in the diagrams drawn above A_2 and A_4. As this is not permissible if efficient operation of the receiver is to be ensured, the distorted part of the synchronising signals is eliminated in a special amplifier A_3 by limiting the amplitude, and after a new synchronising signal has been superposed in A_4 the total signal is then passed to the actual transmitter.

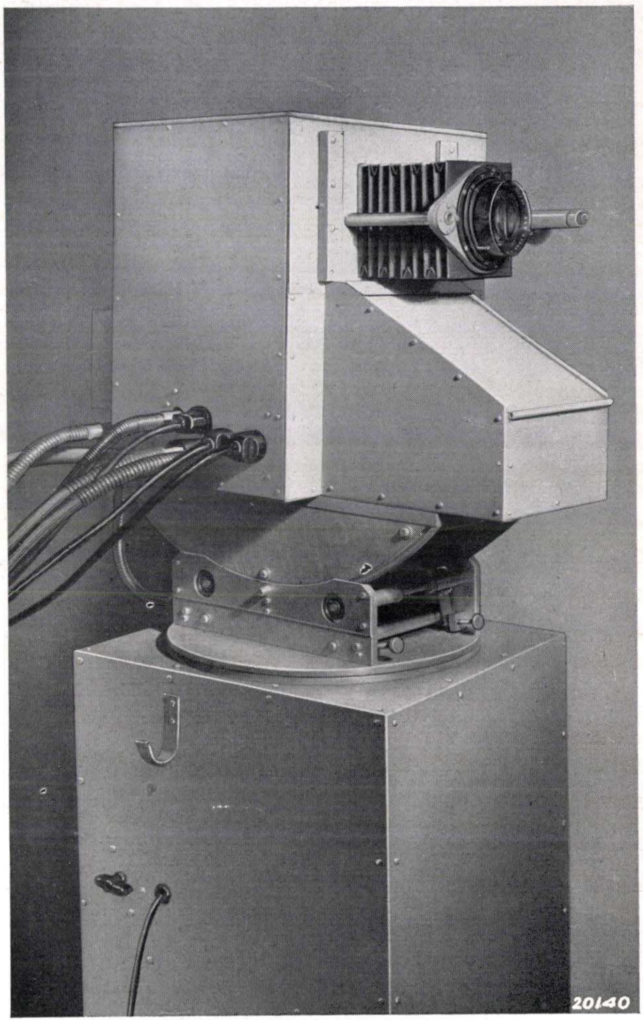

Fig. 4. Iconoscope camera.

A small temporary transmitting room has been equipped in which the television camera was set up; the camera is as mobile as an ordinary film camera and is connected by cables with the feed-voltage supplies and the control board. The iconoscope was electrically controlled from this control board. By means of a mirror the cameraman is able to check directly the definition of the optical image on the iconoscope screen. Since the focal length of the lens is fairly large (21 cm) owing to the size of the iconoscope, the depth of contrast is very small with the diaphragm fully open (f/2.9),

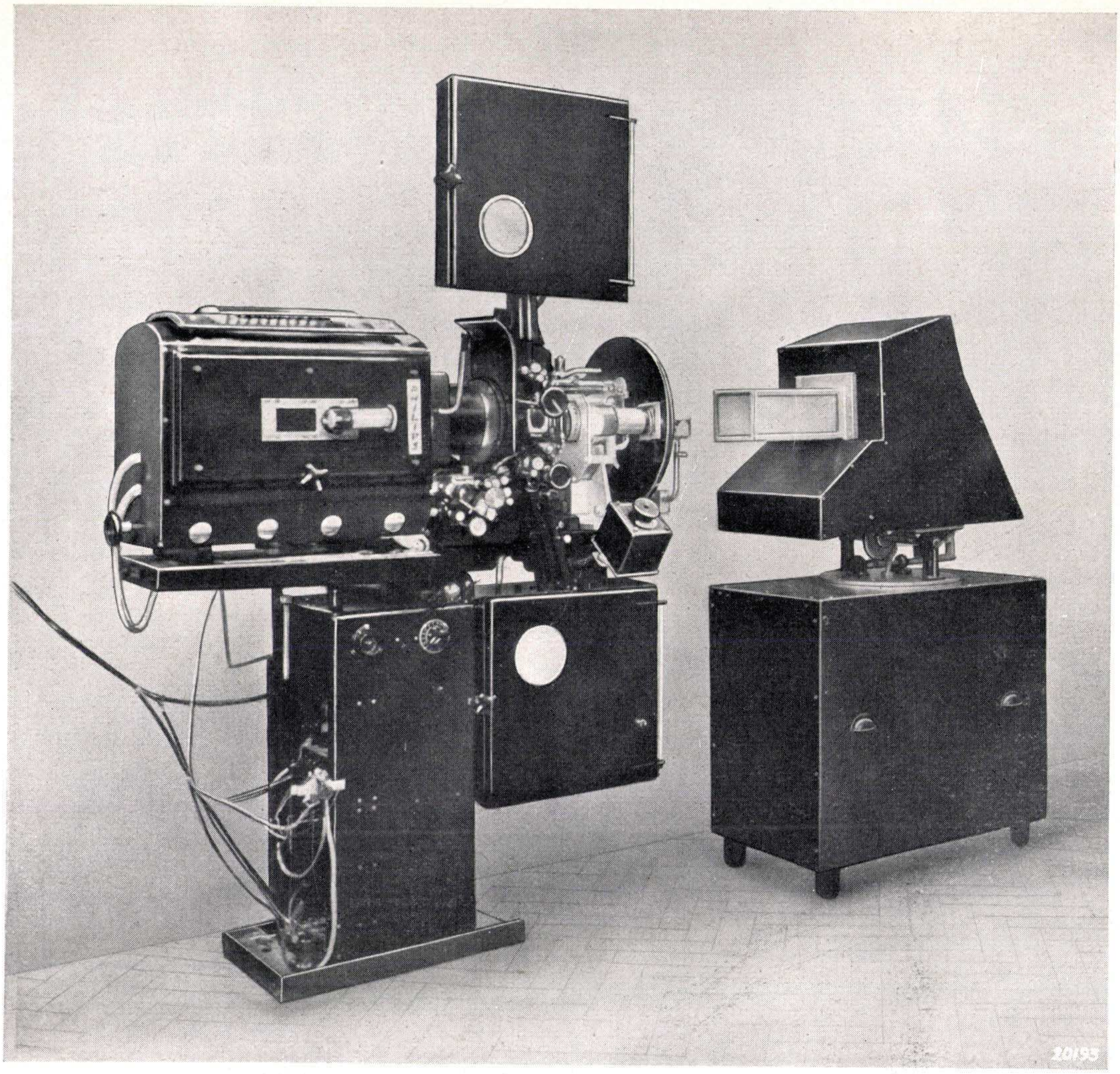

Fig. 5. Filmprojector and iconoscope

so that focusing requires very great care. In this respect, the conditions are less satisfactory than when filming.

Regarding the sensitivity, it has been found that as a rule outdoor scenes which can be suitably filmed can also be satisfactory picked up with the iconoscope.

For direct-transmission from the transmitting room Philips water-cooled high-pressure mercury lamp was used as a light source. The general lighting was provided by a combination of three of these lamps, which owing to their compact dimensions could be placed close together; when fed from three-phase alternating-current mains this group gave a practically constant light output. (In television the light source must not be subject to fluctuation, as the various parts of the object are reproduced in succession and light fluctuations are liable to appear as dark and bright strips.) The aggregate output of the group of three lamps referred to is 7.5 kilowatts.

Small mercury lamps were used as auxiliary lighting to illuminate areas in shadow.

This method of illumination represents an important advance, mainly because of the small amount of heat radiated. With incandescent lamps and arc lamps the radiation of heat is frequently intolerable to the speakers or artists being televised, while the mercury lamps radiate only very little heat. This is a very important point in television, since here the persons must usually face the camera for longer periods than when being filmed, where the individual scenes usually do not exceed more than a few minutes in duration.

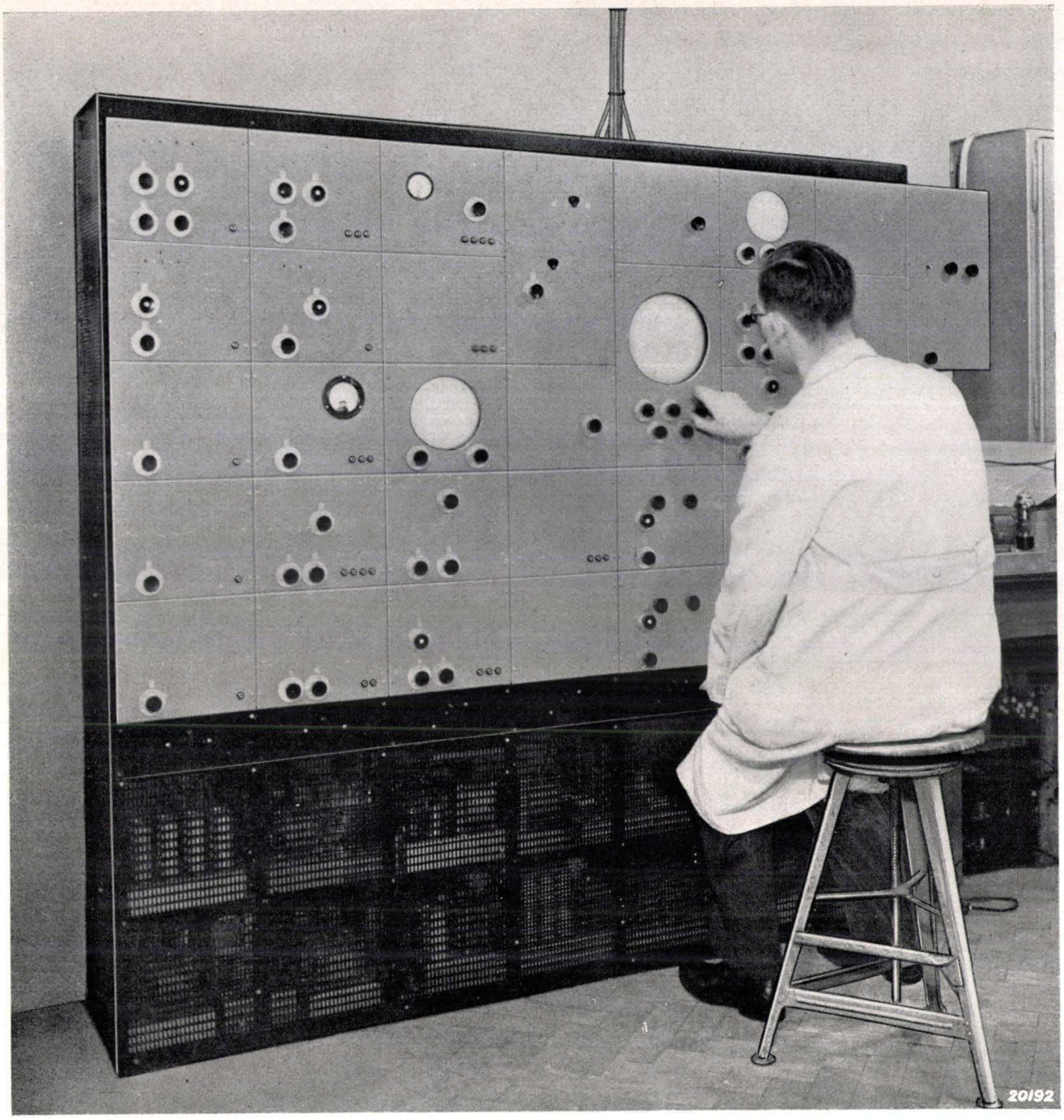

Fig. 6. Control board.

ELECTRICAL FILTERS IV.

Vacation Course, held at Delft, April 1936

By BALTH. VAN DER POL and TH. J. WEIJERS.

HIGH-PASS AND BAND-PASS FILTER SECTIONS

Summary. The method described in the previous article for investigating low-pass filter sections (basic types and m-transformations) are applied in this article to high-pass and band-pass filters. Furthermore, in the section on "double m-transformation" an extension of the m-transformation is given, which can be applied to band-pass filters and, *inter alia,* can also give rise to sections of a particularly simple construction. All data obtained in this way for the design of low-pass, high-pass and band-pass filter sections are collated in Tables II and III. In conclusion, the design of a low-pass filter which has to meet specific requirements is discussed by way of example.

Basic Types and m-Transformations

In the previous articles it was shown how the image impedances, the propagation constant and the transmission and attenuation bands for T-sections, Π-sections and half-sections could be represented as functions of the impedances Z_1 and Z_2 of the "complete branches".

Thus the transmission band is expressed by the condition that $Z_1/4\,Z_2$ must lie between -1 and 0.

For the low-pass filter sections discussed in the previous article this condition was found to be satisfied for frequencies below a certain limiting frequency ν_1. This condition may also be derived from the reactance diagrams of the fundamental types shown in *fig. 18.* The transmission band commences at the frequency 0 with $Z_1' = j\,0$ and $-4\,Z_2' = j\,\infty$. $Z_1' = j\,\omega\,L_1'$ increases with the frequency, $-4\,Z_2' = j\,4/\omega\,C_2'$ diminishes with increasing frequency; the point of intersection of the two curves determines the limiting frequency ν_1.

These considerations also show the values which the impedances Z_1' and Z_2' must have in order to obtain a high-pass or a band-pass filter. For high-pass filter sections (fig. 18*b*) the transmission band reaches from the frequency ν_1 to ∞, and for band-pass filter sections from ν_1 to ν_2. In the case of all three basic types there is a frequency ν_0 for which $Z_1' = 0$ and $Z_2' = \infty$. For low-pass filter sections this frequency is 0 and, for high-pass filter sections ∞, while for the band-pass filter sections it is finite and lies between ν_1 and ν_2.

The figure shows diagrammatically the variation of the reactances Z_1' and $-4\,Z_2'$, as a function of the frequency for the three basic types. The circuits of the complete branches giving these functions are shown at the side. In the case of the high-pass filter section Z_1' is a capacity C_1', and Z_2' a self-inductance L_2'. With the band-pass filter section Z_1' is a self-inductance L_1' with a condenser C_1' in series, and Z_2' is a self-inductance L_2' with a

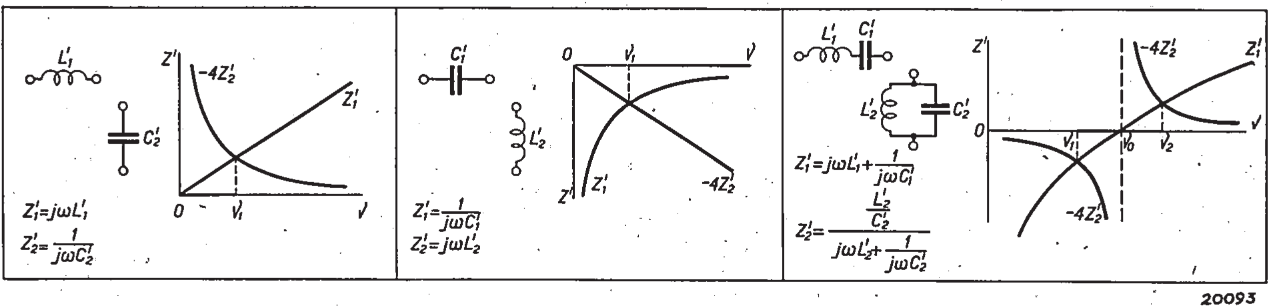

a) b) c)

Fig. 18. Reactance diagrams. Reactances Z_1' and $-4\,Z_2'$ for filters of the basic type as a function of the frequency ν. a) Low-pass filter, b) High-pass filter, c) Band-pass filter. A filter has a passband when $-4\,Z_2'$ lies between Z_1' and the axis. The transmission bands are indicated on the axis by a thicker stroke. On the left of each diagram, it is indicated how the reactances can be made up from self-inductances and condensers and how they can be represented analytically as a function of the angular frequency.

condenser C_2' in parallel, where $L_1' C_1' = L_2' C_2'$ so that the impedance Z_2' becomes infinite at the same frequency ν_0 at which the impedance Z_1' disappears [1]).

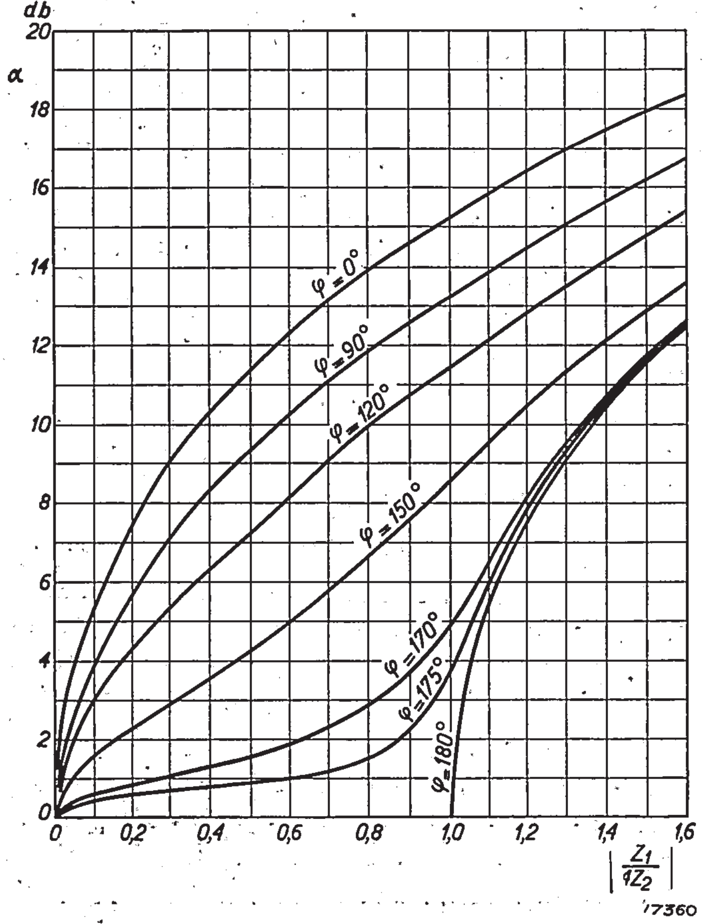

Fig. 19. Attenuation constant α (real component of the propagation constant T) in decibels expressed as a function of $|Z_1/4\ Z_2|$ for T-sections and Π sections.

In the previous article (see e.g. p. 305, equation 9, 12, 15, 23, 24, 25, 29, 30 and 31) it was shown that the image impedances and the propagation constant could be expressed for all sections (basic types and m-transformations) in terms of $Z_1' Z_2'$ and $Z_1'/4\ Z_2'$. Now for the low-pass, high-pass and band-pass filter sections of the basic type $Z_1' Z_2'$ has a real, positive value independent of the frequency, which in conformity with equation (36) in the previous article is denoted by R^2. If now $Z_1'/4\ Z_2'$ expressed as a function of the frequency is known for an arbitrary filter section of the basic type, then from the equations enumerated above the image impedances and the propagation constant can similarly be obtained as functions of the frequency (hence also the transmission bands and the frequencies with infinite attenuation) for both the basic type and those types obtained after m-transformation.

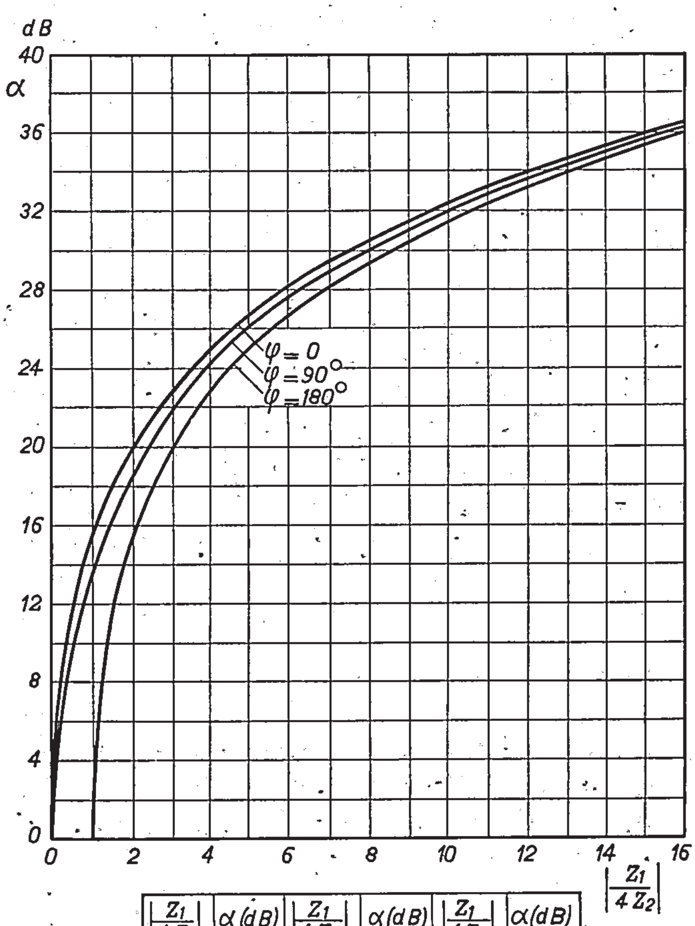

$\left\lvert\frac{Z_1}{4Z_2}\right\rvert$	α (dB)	$\left\lvert\frac{Z_1}{4Z_2}\right\rvert$	α (dB)	$\left\lvert\frac{Z_1}{4Z_2}\right\rvert$	α (dB)
20	37,9	50	45,8	200	58,1
25	39,8	60	47,3	300	61,6
30	41,3	70	48,8	400	63,8
35	42,7	80	50,0	500	66,0
40	43,8	90	51,0	1000	72,1
45	44,8	100	51,9	2000	78,2

20059

Fig. 20. Attenuation constant α in decibels for high values of $|Z_1/4\ Z_2|$. For $|Z_1/4\ Z_2| < 1.6$ fig. 19 is used. The table under the figure is a continuation of the graph for $|Z_1/4\ Z_2| > 16$. In the latter case the effect of φ on α can be neglected in practice.

The results obtained by this method have been collated in *Table I*. In addition the requisite data for laying out filters are also given in *Tables II* and *III*, on similar lines as already deduced for low-pass filter sections in the previous article (p. 304) [2]).

---

[1]) If these frequencies are different, then $Z_1'/4\ Z_2'$ will change its sign between ν_1 and ν_2, and will therefore not lie wholly between 0 and — 1. Between the frequencies at which Z_1' and Z_2' become zero and infinity respectively, there is an attenuation band, which interrupts the transmission band.

[2]) These two tables are inserted in this issue of Philips techn. Rev. as separate sheets. The broken lines in the diagrams of the image impedances are intended to show that the image impedance is imaginary in the corresponding frequency band, being positive or negative according as the absolute value increases or decreases respectively with rising frequency.

All expressions in Table I, with the exception of the third line, apply for non-dissipative filter sections ($d = 0$). In the previous article (p. 302) a brief discussion was given on the effect of the losses in low-pass filter sections. The same remarks also apply to high-pass and band-pass filter sections.

The physical interpretation of the resistance $R = \sqrt{Z_1' \, Z_2'}$ was in the case of low-pass filter sections the image impedance (both Z_T and Z_π) at the frequency $\nu = 0$, and this was in fact true for both the basic type and the results of m-transformation. With high-pass filter sections R is the image impedance at the frequency $\nu = \infty$, and for band-pass filter sections that at the frequency $\nu = \nu_0$, the resonance frequency of the two branches Z_1 and Z_2. This frequency ν_0 is the mean proportion between the two limiting frequencies ν_1 and ν_2 and also at the same time the mean proportion of the two frequencies with infinite attenuation $\nu_{1\infty}$ and $\nu_{2\infty}$.

One of these frequencies with infinite attenuation can be chosen arbitrarily, and then determines the other frequency with infinite attenuation which lies in the other attenuation band, as well as the parameter m. In the following section (double m-transformation) we will however encounter band-pass filter sections, in which the two frequencies with infinite attenuation can be arbitrarily chosen independent of each other.

As in the case of the low-pass filter sections, so also with the high-pass and band-pass filter sections, Z_T in the m_π-transformation and Z_π in the m_T-transformation are comparatively constant throughout the transmission band, if m is made about 0.6 (see fig. 13 in the previous article). Thus as a rule, here also, half-sections with m equal to approx. 0.6 can be chosen as terminal half-sections in a compound filter.

When $Z_1/4\,Z_2$ has been determined for one filter section, then *figs. 19, 20* and *21* can be employed to derive the attenuation constant α and the phase constant β by the method discussed in the previous article for low-pass filter sections.

How a T-section, a Π-section and a half-section are derived from the full branches given in the tables and how a compound filter can be built up from these sections require no further elucidation here, in view of the full analysis already given for low-pass filters.

Double m-Transformations of Band-Pass Filter Sections

In addition to the m-transformations already discussed, other transformations can also be performed with band-pass filters, which similarly permit other types of filter sections to be derived from the basic type, in which the limiting frequencies and one of the image impedances remain the same, while the other image impedance and the propagation constant T are different. In certain cases these transformations give sections of simpler construction, which are frequently employed for building up compound filters.

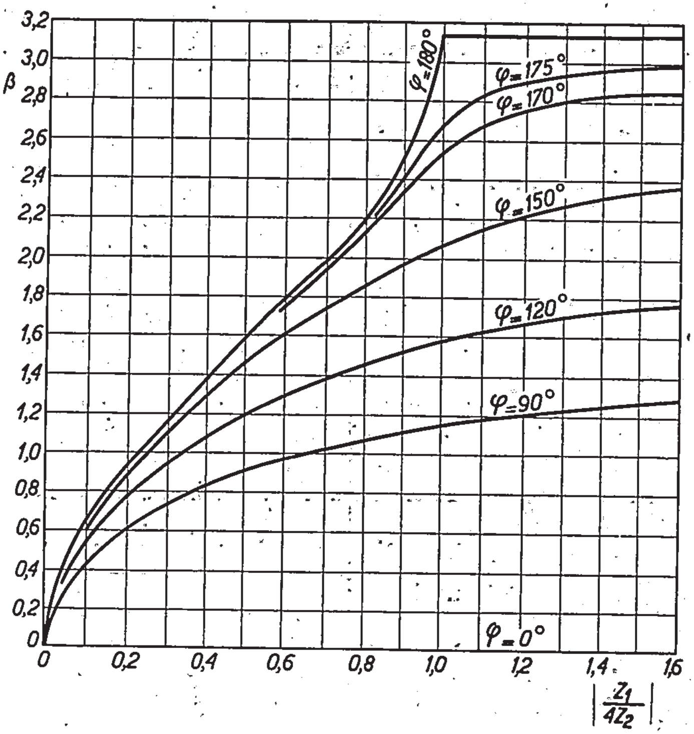

Fig. 21. Phase constant β (imaginary component of the propagation constant T) as a function of $|Z_1/4\,Z_2|$ for T- and Π-sections.

For the basic type we have found:

$$Z_1' = j\,\omega\,L_1' + \frac{1}{j\,\omega\,C_1'}\,.$$

On m_T-transformation we get:

$$Z_1 = m\,Z_1' = j\,m\,\omega\,L_1' + \frac{m}{j\,\omega\,C_1'}\,,$$

and Z_2 is defined such that $Z_T = \sqrt{Z_1\,Z_2}\,\sqrt{1 + Z_1/4\,Z_2}$ remains the same as for the basic type. But if we multiply L_1' by a positive, real number m_1 and divide C_1' by another positive, real number m_2, we then get

$$Z_1 = j\,m_1\,\omega\,L_1' + \frac{m_2}{j\,\omega\,C_1'}\,.$$

If we now seek for a corresponding impedance Z_2, such that $Z_T = Z_T'$, then these values of Z_1 and Z_2 represent the full branches of another filter section, whose Z_T is the same for all frequencies as that of the basic type. This signifies that the limiting

Tabel I

		Lowpass filter sections	Highpass filter sections	Bandpass filter sections
Basic type				
$Z_1' Z_2' = R^2$		$\frac{L_1'}{C_2'}$	$\frac{L_2'}{C_1'}$	$\sqrt{\frac{L_1' L_2'}{C_1' C_2'}}$
$\frac{Z_1'}{4 Z_2'}$	Without losses $d = 0$	$-x^2$	$-1/x^2$	$-y^2 = -\frac{(x-1/x)^2}{(x_2-x_1)^2}$
	With losses $d \neq 0$	$-x^2 (1-j d_L)(1-j d_C)$	$\frac{-1}{x^2 (1-j d_L)(1-j d_C)}$	$-\frac{1}{(x_2-x_1)^2} \cdot \frac{1-j d_C}{1-j d_L} \cdot \left[x (1-j d_L) - \frac{1}{x (1-j d_C)} \right]^2$
Transmission band $-1 < Z_1'/4 Z_2' < 0$		$0 < x < 1$	$1 < x < \infty$	$x_1 < x < x_2$
Infinite attenuation $\lvert Z_1'/4 Z_2' \rvert = \infty$		$x_\infty = \infty$	$x_\infty = 0$	$x_{1\infty} = 0;\ x_{2\infty} = \infty$
$Z_T' = \sqrt{Z_1' Z_2'} \sqrt{1 + \frac{Z_1'}{4 Z_2'}}$		$R \sqrt{1-x^2}$	$R \sqrt{1 - \frac{1}{x_2}}$	$R \sqrt{1-y^2}$
$Z_\pi' = \frac{\sqrt{Z_1' Z_2'}}{\sqrt{1 + Z_1'/4 Z_2'}}$		$\frac{R}{\sqrt{1-x^2}}$	$\frac{R}{\sqrt{1-1/x^2}}$	$\frac{R}{\sqrt{1-y^2}}$
m-transformations $(\alpha = 1/\sqrt{1-m^2})$				
$\frac{Z_1}{4 Z_2} = \frac{Z_1'}{4 Z_2'} \frac{m^2}{1 + \frac{1}{a^2} \frac{Z_1'}{4 Z_2'}}$		$\frac{a^2-1}{1 - \frac{a^2}{x^2}}$	$\frac{a^2-1}{1 - a^2 x^2}$	$\frac{a^2-1}{1 - \frac{a^2}{y^2}}$
Transmission band		As basic type	As basic type	As basic type
Infinite attenuation $Z_1'/4 Z_2' = -a^2$		$x_\infty = a$	$x_\infty = \frac{1}{a}$	$y_\infty = \pm a$ $x_{2\infty} - x_{1\infty} = a (x_2 - x_1)$ $x_{1\infty} x_{2\infty} = 1$
m_T-transformation				
$Z_T = Z_T'$		$R\sqrt{1-x^2}$	$R\sqrt{1-1/x^2}$	$R\sqrt{1-y^2}$
$Z_\pi = Z_\pi' \left(1 + \frac{1}{a^2} \frac{Z_1'}{4 Z_2'}\right)$		$R \frac{1 - \frac{x^2}{a^2}}{\sqrt{1-x^2}}$	$R \frac{1 - \frac{1}{a^2 x^2}}{\sqrt{1-1/x^2}}$	$R \frac{1 - \frac{y^2}{a^2}}{\sqrt{1-y^2}}$
m_π-transformation				
$Z_T = Z_T' \frac{1}{1 + \frac{1}{a^2} \frac{Z_1'}{4 Z_2'}}$		$R \frac{\sqrt{1-x^2}}{1 - \frac{x^2}{a^2}}$	$R \frac{\sqrt{1-1/x^2}}{1 - \frac{1}{a^2 x^2}}$	$R \frac{\sqrt{1-y^2}}{1 - \frac{y^2}{a^2}}$
$Z_\pi = Z_\pi'$		$\frac{R}{\sqrt{1-x^2}}$	$\frac{R}{\sqrt{1-1/x^2}}$	$\frac{R}{\sqrt{1-y^2}}$
Definitions		$x = \frac{\nu}{\nu_1}$; $2 \pi \nu_1 = \frac{2}{\sqrt{L_1' C_2'}}$	$x = \frac{\nu}{\nu_1}$; $2 \pi \nu_1 = \frac{1}{2 \sqrt{L_2' C_1'}}$	$x_1 x_2 = 1;\ x_2 - x_1 = 2 \sqrt[4]{\frac{L_2' C_1'}{L_1' C_2'}}$; $x = \frac{\nu}{\nu_0};\ 2 \pi \nu_0 = \frac{1}{\sqrt[4]{L_1' L_2' C_1' C_2'}}$

frequencies are also unchanged; for on exceeding the limiting frequencies, the image impedances change from a real to an imaginary value and *vice versa*. Calculation shows that this impedance Z_2 is of the form shown in *fig. 22*; in this figure the values of the components are also given. It can also be substituted by the equivalent circuit shown in Table II; Band-pass filter sections II_1. Usually the latter circuit will be given preference, since the values of the self-inductances and the condensers are then as a rule neither too large nor too small, as might frequently happen with the circuit shown in fig. 22. Yet to derive still further filter sections we will for the sake of simplicity employ the circuit shown in fig. 22.

The impedance Z_2 can only be realised when m_1 and m_2 satisfy the following conditions:

$$\left.\begin{array}{l} 0 < m_1 < 1\,; \\ 0 < m_2 < 1\,; \\ \dfrac{x_2}{x_1} \geqslant \dfrac{m_1}{m_2} \geqslant \dfrac{x_1}{x_2}. \end{array}\right\}$$

The sections obtained by "double m-transformation" are composed of the same L's and C's as the band-pass filter sections I_2 obtained by simple m-transformation, although $x = 1$ is now no longer valid for the resonance frequencies of the two branches and the two frequencies with infinite attenuation $x_{1\infty}$ and $x_{2\infty}$ are no longer inter-related by the equation $x_{1\infty} \cdot x_{2\infty} = 1$. By a suitable value of m_1 and m_2, $x_{1\infty}$ and $x_{2\infty}$ can be arbitrazily chosen independent of each other, provided a frequency with infinite attenuation is located in each attenuation band.

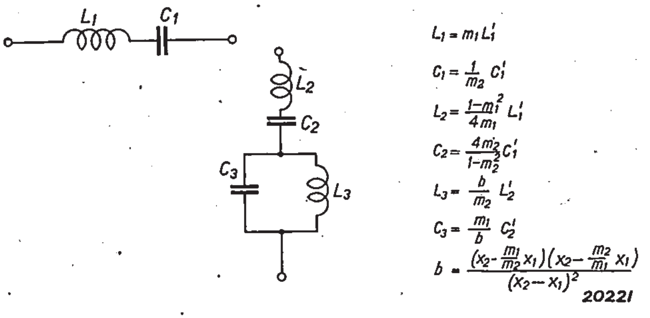
L_1
C_1
L_2
C_2
C_3
L_3
$L_1 = m_1 L_1'$
$C_1 = \frac{1}{m_2} C_1'$
$L_2 = \frac{1-m_1^2}{4m_1} L_1'$
$C_2 = \frac{4m_2}{1-m_2^2} C_1'$
$L_3 = \frac{b}{m_2} L_2'$
$C_3 = \frac{m_1}{b} C_2'$
$b = \frac{(x_2 - \frac{m_1}{m_2} x_1)(x_2 - \frac{m_2}{m_1} x_1)}{(x_2 - x_1)^2}$
20221

Fig. 22. Full branches of a band pass filter obtained by double m-transformation from the basic type. L_1', L_2', C_1', C_2' are the values of the components for the basic type, and x_1 and x_2 are the limiting frequencies (see Table II, column I_1).

A double m-transformation may be performed on exactly the same lines on the basic type in such a manner that Z_π remains equal to Z_π' of the basic type.

In Table II: Band-pass filter sections, II, the circuits for the full branches after double m_T and double m_π transformations are given, as well as the values of the components. L_1', C_1', L_2' and C_2' are the values of the elements of the basic type (see column I_1). If the limiting frequencies x_1 and x_2, the frequencies with infinite attenuation $x_{1\infty}$ and $x_{2\infty}$ and the image impedance R for the frequency $x = 1$ are given, as is usually the case in practice, the values of the components can be calculated. The propagation constant $T = \alpha + i\,\beta$ for these sections is most easily calculated by adding the propagation constants of two simpler types of section, which have still to be analysed, as indicated in Table II. The qualitative variation of α and β as a function of the frequency is similar to that found with the single m-transformation.

Special Cases of Double m-Transformation. Simpler Sections.

For certain values of m_1 and m_2 the sections assume a simpler form; these special cases are summarised in Table III.

The following special cases are differentiated in the double m_T-transformation.

$m_1 = m_2 \neq 1$	The twofold m-transformation passes over into single m-transformation. The filter section corresponds to type	II_1
$m_1 = m_2 = 1$	The fundamental type is obtained	I_1
$m_1 \neq 1,\ m_2 = 1$	In fig. 22, C_2 becomes infinity, and a filter section is obtained aequivalent with type	V_1
$m_1 = 1,\ m_2 \neq 1$	In fig. 22, C_2 becomes zero, and a filter section is obtained aequivalent with type	V_2
$\dfrac{m_1}{m_2} = \dfrac{x_2}{x_1}$	In fig. 22, b becomes zero, from which follows: $L_3 = 0$, $C_3 = \infty$, and a filter section is obtained of type	IV_1
$\dfrac{m_1}{m_2} = \dfrac{x_1}{x_2}$	Similarly $b = 0$, $L_3 = 0$ and $C_3 = \infty$; and a filter section is obtained of type	IV_2
$m_1 = 1,\ m_2 = \dfrac{x_1}{x_2}$	In fig. 22, $L_3 = 0$, $C_3 = \infty$, $L_2 = 0$, and a filter section is obtained of type	III_1
$m_2 = 1,\ m_1 = \dfrac{x_1}{x_2}$	In fig. 22 $L_3 = 0$, $C_3 = \infty$, $C_2 = \infty$, and a filter section is obtained of type	III_2

The same eight special cases occur under the same conditions in the double m_π-transformation, for which the relevant formulae and the data are also given in Table III. Sections after m_T-transformation are only used in the T form and those after m_π-transformation only in the Π form, as otherwise it is not possible to connect up separate sections of a compound filter with equal image impedances side by side. No formulae are given in the figures for those image impedances having no direct bearing on such compounding, but only qualitative curves, whose irregular shape in the transmission band is already sufficient indication of their unsuitability and of the need for avoiding them.

For the sections of types II and V the propagation constant $T = \alpha + i\beta$ is best determined not by calculating $Z_1/4 Z_2$, but by addition of the values of α and β for two simpler sections, which are given in the Table II and III for each section of type II or V. The propagation constants of the simpler sections are calculated by substituting in the indicated formulae those values of $x_{1\infty}$ and $x_{2\infty}$ which are employed for the sections of type II or V under consideration. Thus for type II the sections IV_1 and IV_2 are indicated, and in order to determine α for these filter sections $Z_1/4 Z_2$ is first calculated for the IV_1 section with that value of $x_{2\infty}$ as employed in Π, then deriving the corresponding attenuation coefficient α from fig. 19 or 20. This is followed by the calculation of $Z_1/4 Z_2$ for section IV_2 with the same value of $x_{1\infty}$ as given for the type II section, again reading the corresponding value of α from fig. 19 or 20, and finally adding the two attenuation values of α so obtained. The imaginary term β of the propagation constant is derived in exactly the same way with the aid of fig. 21.

If a thorough grasp has been obtained of the theory of electrical filters outlined in this series of articles, the data given in Tables II and III and in figs. 19, 20 and 21 will be found sufficient for evolving any filter to meet specific requirements included among the usual types employed in practice. This may be suitably demonstrated by a specific example.

Example

It is required to design a low-pass filter to meet the following requirements: The filter is to be used in the anode circuit of a triode with an internal resistance of 10 000 ohms. With a constant alternating voltage applied to the grid of the triode, the secondary voltage of the filter must not vary more than 1 decibel from a specific mean value for frequencies below 900 cycles/sec (the voltage must therefore be maintained between 0.89 and 1.12 per cent of this mean value), and for frequencies above 1100 cycles/sec it must be less than 1/500 of this mean value. The attenuation must therefore be at least 54 decibels. The losses in the coils, which it is proposed to use, at frequencies above 1000 cycles/sec, and those of the condensers throughout the whole frequency sweep have such values that $r/\omega L = R\omega C = 0.02$. It is further assumed that the losses in the coils below 1000 cycles/sec are exclusively due to a D.C. resistance, and are thus independent of the frequency. Then for $\nu > 1000$ cycles/sec, $d_L = d_C = 0.02$; for $\nu < 1000$ cycles/sec, $d_L = 0.02 \cdot 1000/\nu$.

No conditions are laid down for the frequency band between 900 and 1100 cycles/sec; this is therefore the transition range between the transmission and the attenuation bands. The limiting frequency ν_1 is taken in the middle of this band, so that $\nu_1 = 1000$ cycles/sec.

Firstly, the type and number of the filter sections required are determined; this is followed by the determination of the ratings of the filter components. In the transmission band required ($\nu = 0$ to 900 cycles, i.e. $x < 0.9$), the attenuation must be adequately constant. To satisfy this condition

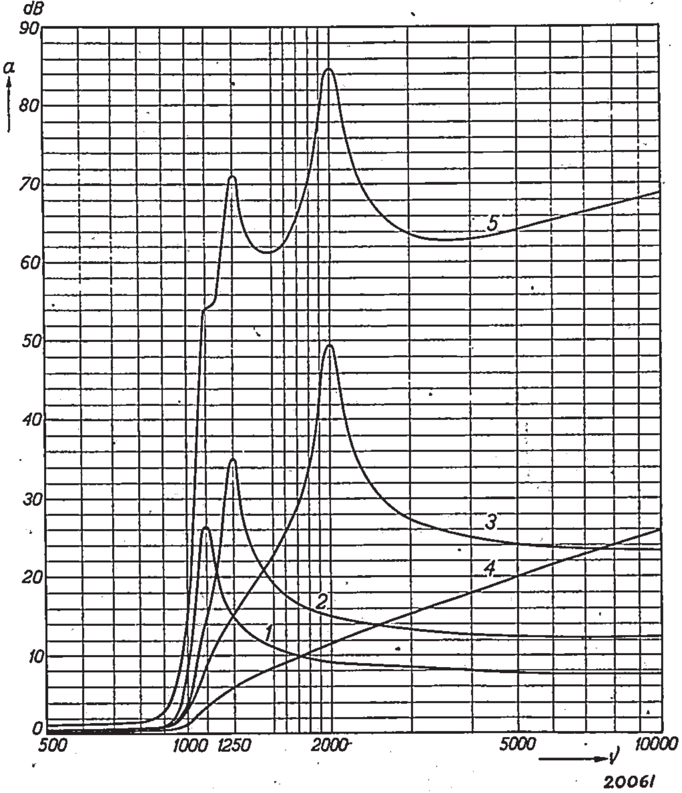

Fig. 23. Attenuation constant α of a low-pass filter composed of four sections, plotted as a function of the frequency.

1. Attenuation of a section with $x_\infty = 1.1$.
2. Attenuation of both terminal half-sections with $m = 0.6$ ($x_\infty = 1.25$), which together may be regarded as a single section.
3. Attenuation of a section with $x_\infty = 2.0$.
4. Attenuation of a half-section of the basic type.
5. Total attenuation.

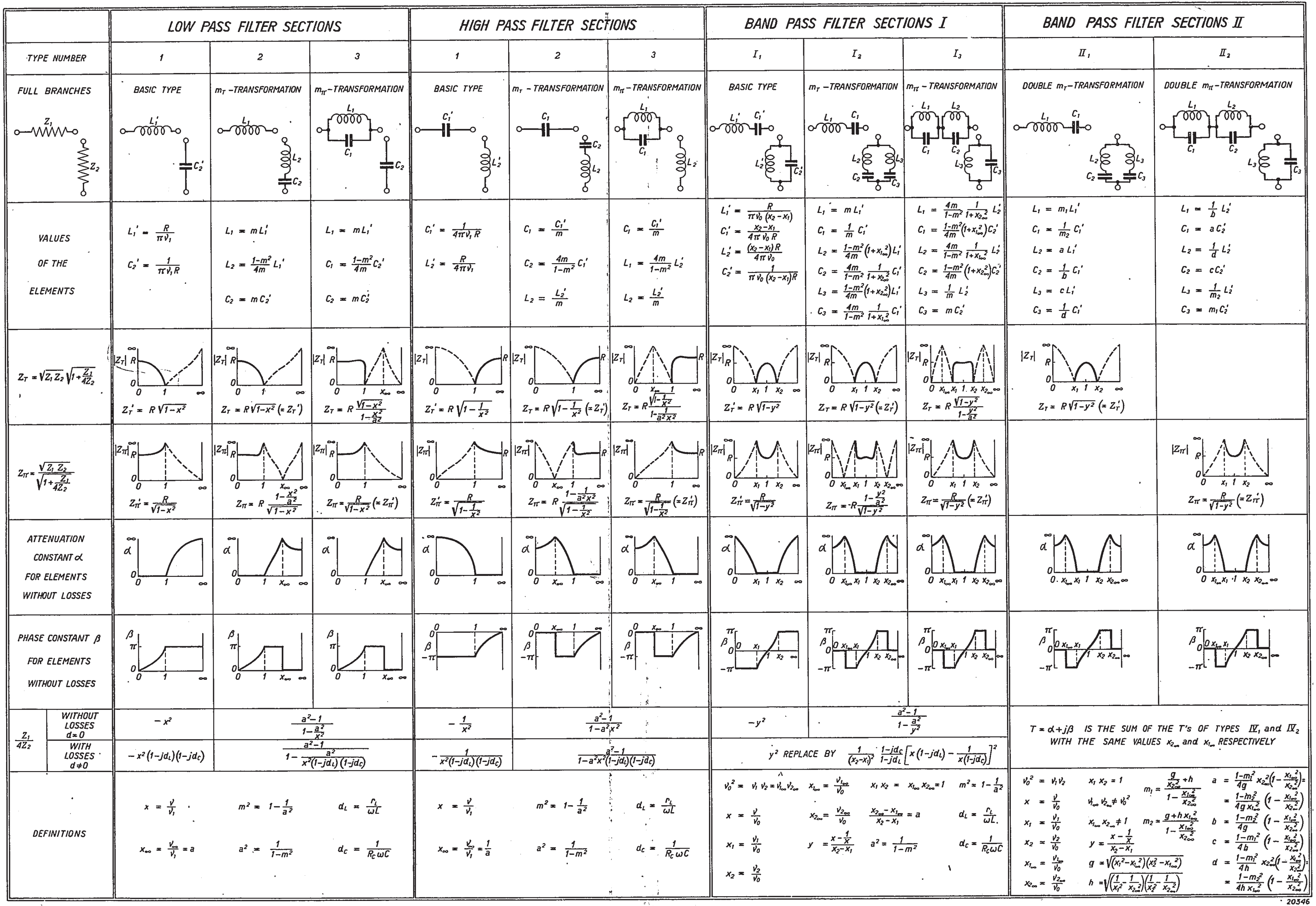

	LOW PASS FILTER SECTIONS			HIGH PASS FILTER SECTIONS			BAND PASS FILTER SECTIONS I			BAND PASS FILTER SECTIONS II	
TYPE NUMBER	1	2	3	1	2	3	I_1	I_2	I_3	II_1	II_2
FULL BRANCHES	BASIC TYPE	m_T-TRANSFORMATION	m_π-TRANSFORMATION	BASIC TYPE	m_T-TRANSFORMATION	m_π-TRANSFORMATION	BASIC TYPE	m_T-TRANSFORMATION	m_π-TRANSFORMATION	DOUBLE m_T-TRANSFORMATION	DOUBLE m_π-TRANSFORMATION
VALUES OF THE ELEMENTS	$L_1' = \frac{R}{\pi\nu_1}$ $C_2' = \frac{1}{\pi\nu_1 R}$	$L_1 = mL_1'$ $L_2 = \frac{1-m^2}{4m}L_1'$ $C_2 = mC_2'$	$L_1 = mL_1'$ $C_1 = \frac{1-m^2}{4m}C_2'$ $C_2 = mC_2'$	$C_1' = \frac{1}{4\pi\nu_1 R}$ $L_2' = \frac{R}{4\pi\nu_1}$	$C_1 = \frac{C_1'}{m}$ $C_2 = \frac{4m}{1-m^2}C_1'$ $L_2 = \frac{L_2'}{m}$	$C_1 = \frac{C_1'}{m}$ $L_1 = \frac{4m}{1-m^2}L_2'$ $L_2 = \frac{L_2'}{m}$	$L_1' = \frac{R}{\pi\nu_0(x_2-x_1)}$ $C_1' = \frac{x_2-x_1}{4\pi\nu_0 R}$ $L_2' = \frac{(x_2-x_1)R}{4\pi\nu_0}$ $C_2' = \frac{1}{\pi\nu_0(x_2-x_1)R}$	$L_1 = mL_1'$ $C_1 = \frac{1}{m}C_1'$ $L_2 = \frac{1-m^2}{4m}(1+x_{1\infty}^2)L_1'$ $C_2 = \frac{4m}{1-m^2}\frac{1}{1+x_{2\infty}^2}C_1'$ $L_3 = \frac{1-m^2}{4m}(1+x_{2\infty}^2)L_1'$ $C_3 = \frac{4m}{1-m^2}\frac{1}{1+x_{1\infty}^2}C_1'$	$L_1 = \frac{4m}{1-m^2}\frac{1}{1+x_{2\infty}^2}L_2'$ $C_1 = \frac{1-m^2}{4m}(1+x_{1\infty}^2)C_2'$ $L_2 = \frac{4m}{1-m^2}\frac{1}{1+x_{1\infty}^2}L_2'$ $C_2 = \frac{1-m^2}{4m}(1+x_{2\infty}^2)C_2'$ $L_3 = \frac{1}{m}L_2'$ $C_3 = mC_2'$	$L_1 = m_1L_1'$ $C_1 = \frac{1}{m_2}C_1'$ $L_2 = aL_1'$ $C_2 = \frac{1}{b}C_1'$ $L_3 = cL_1'$ $C_3 = \frac{1}{d}C_1'$	$L_1 = \frac{1}{b}L_2'$ $C_1 = aC_2'$ $L_2 = \frac{1}{d}L_2'$ $C_2 = cC_2'$ $L_3 = \frac{1}{m_2}L_2'$ $C_3 = m_1C_2'$
$Z_T = \sqrt{Z_1Z_2}\sqrt{1+\frac{Z_1}{4Z_2}}$	$Z_T' = R\sqrt{1-x^2}$	$Z_T = R\sqrt{1-x^2}\ (=Z_T')$	$Z_T = R\frac{\sqrt{1-x^2}}{1-\frac{x^2}{a^2}}$	$Z_T' = R\sqrt{1-\frac{1}{x^2}}$	$Z_T = R\sqrt{1-\frac{1}{x^2}}\ (=Z_T')$	$Z_T = R\frac{\sqrt{1-\frac{1}{x^2}}}{1-\frac{1}{a^2x^2}}$	$Z_T' = R\sqrt{1-y^2}$	$Z_T = R\sqrt{1-y^2}\ (=Z_T')$	$Z_T = R\frac{\sqrt{1-y^2}}{1-\frac{y^2}{a^2}}$	$Z_T = R\sqrt{1-y^2}\ (=Z_T')$	
$Z_\pi = \frac{\sqrt{Z_1Z_2}}{\sqrt{1+\frac{Z_1}{4Z_2}}}$	$Z_\pi' = \frac{R}{\sqrt{1-x^2}}$	$Z_\pi = R\frac{1-\frac{x^2}{a^2}}{\sqrt{1-x^2}}$	$Z_\pi = \frac{R}{\sqrt{1-x^2}}\ (=Z_\pi')$	$Z_\pi' = \frac{R}{\sqrt{1-\frac{1}{x^2}}}$	$Z_\pi = R\frac{1-\frac{1}{a^2x^2}}{\sqrt{1-\frac{1}{x^2}}}$	$Z_\pi = \frac{R}{\sqrt{1-\frac{1}{x^2}}}\ (=Z_\pi')$	$Z_\pi' = \frac{R}{\sqrt{1-y^2}}$	$Z_\pi = -R\frac{1-\frac{y^2}{a^2}}{\sqrt{1-y^2}}$	$Z_\pi = \frac{R}{\sqrt{1-y^2}}\ (=Z_\pi')$		$Z_\pi = \frac{R}{\sqrt{1-y^2}}\ (=Z_\pi')$
ATTENUATION CONSTANT α FOR ELEMENTS WITHOUT LOSSES											
PHASE CONSTANT β FOR ELEMENTS WITHOUT LOSSES											
$\frac{Z_1}{4Z_2}$ WITHOUT LOSSES $d=0$	$-x^2$	$\frac{a^2-1}{1-\frac{a^2}{x^2}}$		$-\frac{1}{x^2}$	$\frac{a^2-1}{1-a^2x^2}$		$-y^2$	$\frac{a^2-1}{1-\frac{a^2}{y^2}}$		$T = \alpha + j\beta$ IS THE SUM OF THE T's OF TYPES IV_1 and IV_2 WITH THE SAME VALUES $x_{2\infty}$ and $x_{1\infty}$ RESPECTIVELY	
$\frac{Z_1}{4Z_2}$ WITH LOSSES $d \neq 0$	$-x^2(1-jd_L)(1-jd_C)$	$\frac{a^2-1}{1-\frac{a^2}{x^2(1-jd_L)(1-jd_C)}}$		$-\frac{1}{x^2(1-jd_L)(1-jd_C)}$	$\frac{a^2-1}{1-a^2x^2(1-jd_L)(1-jd_C)}$		y^2 REPLACE BY $\frac{1}{(x_2-x_1)^2}\frac{1-jd_C}{1-jd_L}\left[x(1-jd_L)-\frac{1}{x(1-jd_C)}\right]^2$				
DEFINITIONS	$x = \frac{\nu}{\nu_1}$ $x_\infty = \frac{\nu_\infty}{\nu_1} = a$	$m^2 = 1-\frac{1}{a^2}$ $a^2 = \frac{1}{1-m^2}$	$d_L = \frac{r_L}{\omega L}$ $d_C = \frac{1}{R_C\omega C}$	$x = \frac{\nu}{\nu_1}$ $x_\infty = \frac{\nu_\infty}{\nu_1} = \frac{1}{a}$	$m^2 = 1-\frac{1}{a^2}$ $a^2 = \frac{1}{1-m^2}$	$d_L = \frac{r_L}{\omega L}$ $d_C = \frac{1}{R_C\omega C}$	$\nu_0^2 = \nu_1\nu_2 = \nu_{1\infty}\nu_{2\infty}$ $x = \frac{\nu}{\nu_0}$ $x_1 = \frac{\nu_1}{\nu_0}$ $x_2 = \frac{\nu_2}{\nu_0}$ $x_{1\infty} = \frac{\nu_{1\infty}}{\nu_0}$ $x_{2\infty} = \frac{\nu_{2\infty}}{\nu_0}$ $y = \frac{x-\frac{1}{x}}{x_2-x_1}$	$x_1x_2 = x_{1\infty}x_{2\infty} = 1$ $\frac{x_{2\infty}-x_{1\infty}}{x_2-x_1} = a$ $a^2 = \frac{1}{1-m^2}$	$m^2 = 1-\frac{1}{a^2}$ $d_L = \frac{r_L}{\omega L}$ $d_C = \frac{1}{R_C\omega C}$	$\nu_0^2 = \nu_1\nu_2$ $x = \frac{\nu}{\nu_0}$ $x_1 = \frac{\nu_1}{\nu_0}$ $x_2 = \frac{\nu_2}{\nu_0}$ $x_{1\infty} = \frac{\nu_{1\infty}}{\nu_0}$ $x_{2\infty} = \frac{\nu_{2\infty}}{\nu_0}$ $x_1x_2 = 1$ $\nu_{1\infty}\nu_{2\infty} \neq \nu_0^2$ $x_{1\infty}x_{2\infty} \neq 1$ $y = \frac{x-\frac{1}{x}}{x_2-x_1}$ $g = \sqrt{(x_1^2-x_{1\infty}^2)(x_2^2-x_{1\infty}^2)}$ $h = \sqrt{\left(\frac{1}{x_1^2}-\frac{1}{x_{2\infty}^2}\right)\left(\frac{1}{x_2^2}-\frac{1}{x_{2\infty}^2}\right)}$	$m_1 = \frac{\frac{g}{x_{2\infty}^2}+h}{1-\frac{x_{1\infty}^2}{x_{2\infty}^2}}$ $m_2 = \frac{g+hx_{1\infty}^2}{1-\frac{x_{1\infty}^2}{x_{2\infty}^2}}$ $a = \frac{1-m_1^2}{4g}x_{2\infty}^2\left(1-\frac{x_{1\infty}^2}{x_{2\infty}^2}\right) = \frac{1-m_2^2}{4gx_{1\infty}^2}\left(1-\frac{x_{1\infty}^2}{x_{2\infty}^2}\right)$ $b = \frac{1-m_2^2}{4g}\left(1-\frac{x_{1\infty}^2}{x_{2\infty}^2}\right)$ $c = \frac{1-m_1^2}{4b}\left(1-\frac{x_{1\infty}^2}{x_{2\infty}^2}\right)$ $d = \frac{1-m_1^2}{4h}x_{2\infty}^2\left(1-\frac{x_{1\infty}^2}{x_{2\infty}^2}\right) = \frac{1-m_2^2}{4hx_{1\infty}^2}\left(1-\frac{x_{1\infty}^2}{x_{2\infty}^2}\right)$

Table II. Data for the designs of low-pass, high-pass and band-pass filters.

	BAND PASS FILTER SECTIONS III				BAND PASS FILTER SECTIONS IV				BAND PASS FILTER SECTIONS V			
TYPE NUMBER	III₁	III₂	III₃	III₄	IV₁	IV₂	IV₃	IV₄	V₁	V₂	V₃	V₄
FULL BRANCHES 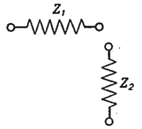	m_T − TRANSFORMATION 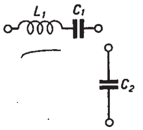	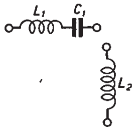	m_π − TRANSFORMATION 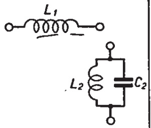	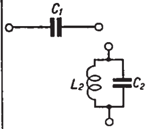	m_T − TRANSFORMATION 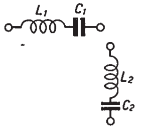	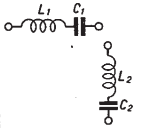	m_π − TRANSFORMATION 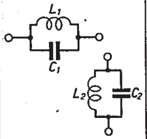	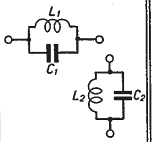	m_T − TRANSFORMATION 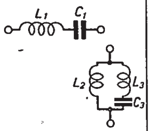	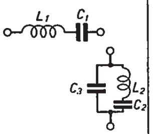	m_π − TRANSFORMATION 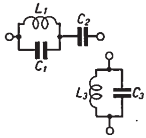	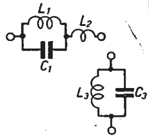
VALUES OF THE ELEMENTS	$L_1 = \frac{R}{\pi\nu_0(x_2-x_1)} = L_1'$ $C_1 = \frac{x_2-x_1}{4\pi\nu_0 x_1^2 R}$ $C_2 = \frac{1}{\pi\nu_0(x_1+x_2)R}$	$L_1 = \frac{x_1^2 R}{\pi\nu_0(x_2-x_1)}$ $C_1 = \frac{x_2-x_1}{4\pi\nu_0 R} = C_1'$ $L_2 = \frac{(x_1+x_2)R}{4\pi\nu_0}$	$L_1 = \frac{R}{\pi\nu_0(x_1+x_2)}$ $L_2 = \frac{(x_2-x_1)R}{4\pi\nu_0 x_1^2}$ $C_2 = \frac{1}{\pi\nu_0(x_2-x_1)R} = C_2'$	$C_1 = \frac{x_1+x_2}{4\pi\nu_0 R}$ $L_2 = \frac{(x_2-x_1)R}{4\pi\nu_0} = L_2'$ $C_2 = \frac{x_1^2}{\pi\nu_0(x_2-x_1)R}$	$L_1 = m_1 L_1'$ $C_1 = \frac{1}{m_2}C_1'$ $L_2 = \frac{1-m_1^2}{4m_1}L_1'$ $C_2 = \frac{4m_2}{1-m_2^2}C_1'$ $m_1 = \sqrt{\frac{x_{2\infty}^2-x_2^2}{x_{2\infty}^2-x_1^2}}$ $m_2 = x_1^2 m_1$	$L_1 = m_1 L_1'$ $C_1 = \frac{1}{m_2}C_1'$ $L_2 = \frac{1-m_1^2}{4m_1}L_1'$ $C_2 = \frac{4m_2}{1-m_2^2}C_1'$ $m_1 = \sqrt{\frac{x_1^2-x_{1\infty}^2}{x_2^2-x_{1\infty}^2}}$ $m_2 = x_2^2 m_1$	$L_1 = \frac{4m_2}{1-m_2^2}L_2'$ $C_1 = \frac{1-m_1^2}{4m_1}C_2'$ $L_2 = \frac{1}{m_2}L_2'$ $C_2 = m_1 C_2'$ $m_1 = \sqrt{\frac{x_{2\infty}^2-x_2^2}{x_{2\infty}^2-x_1^2}}$ $m_2 = x_1^2 m_1$	$L_1 = \frac{4m_2}{1-m_2^2}L_2'$ $C_1 = \frac{1-m_1^2}{4m_1}C_2'$ $L_2 = \frac{1}{m_2}L_2'$ $C_2 = m_1 C_2'$ $m_1 = \sqrt{\frac{x_1^2-x_{1\infty}^2}{x_2^2-x_{1\infty}^2}}$ $m_2 = x_2^2 m_1$	$L_1 = m_1 L_1'$ $C_1 = C_1'$ $L_2 = p L_1'$ $L_3 = \frac{1-m_1^2}{4h}L_1'$ $C_3 = \frac{h}{p}C_1'$	$L_1 = L_1'$ $C_1 = \frac{1}{m_2}C_1'$ $L_2 = \frac{q}{g}L_1'$ $C_2 = \frac{4g}{1-m_2^2}C_1'$ $C_3 = \frac{1}{q}C_1'$	$L_1 = \frac{h}{p}L_2'$ $C_1 = \frac{1-m_1^2}{4h}C_2'$ $C_2 = p C_2'$ $L_3 = L_2'$ $C_3 = m_1 C_2'$	$L_1 = \frac{4g}{1-m_2^2}L_2'$ $C_1 = \frac{q}{g}C_2'$ $L_2 = \frac{1}{q}L_2'$ $L_3 = \frac{1}{m_2}L_2'$ $C_3 = C_2'$
$Z_T = \sqrt{Z_1 Z_2}\sqrt{1+\frac{Z_1}{4Z_2}}$	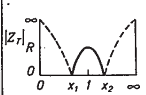 $Z_T = R\sqrt{1-y^2} (= Z_T')$	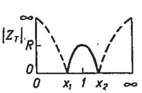 $Z_T = R\sqrt{1-y^2} (= Z_T')$	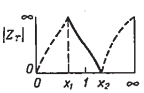	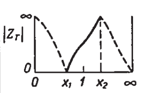	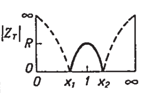 $Z_T = R\sqrt{1-y^2} (= Z_T')$	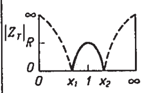 $Z_T = R\sqrt{1-y^2} (= Z_T')$	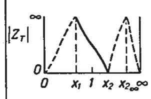	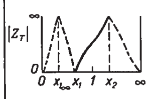	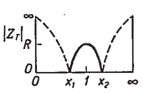 $Z_T = R\sqrt{1-y^2} (= Z_T')$	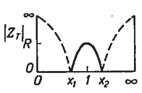 $Z_T = R\sqrt{1-y^2} (= Z_T')$	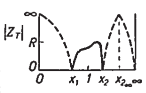	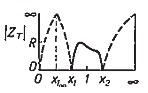
$Z_\pi = \frac{\sqrt{Z_1 Z_2}}{\sqrt{1+\frac{Z_1}{4Z_2}}}$	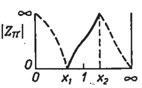	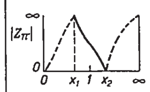	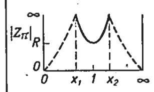 $Z_\pi = \frac{R}{\sqrt{1-y^2}} (= Z_\pi')$	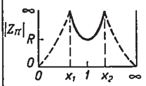 $Z_\pi = \frac{R}{\sqrt{1-y^2}} (= Z_\pi')$	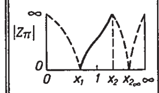	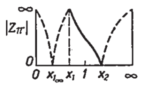	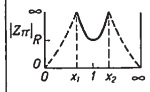 $Z_\pi = \frac{R}{\sqrt{1-y^2}} (= Z_\pi')$	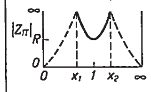 $Z_\pi = \frac{R}{\sqrt{1-y^2}} (= Z_\pi')$	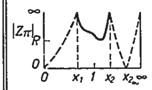	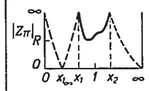	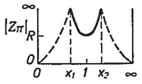 $Z_\pi = \frac{R}{\sqrt{1-y^2}} (= Z_\pi')$	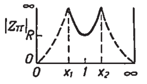 $Z_\pi = \frac{R}{\sqrt{1-y^2}} (= Z_\pi')$
ATTENUATION CONSTANT α FOR ELEMENTS WITHOUT LOSSES	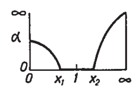	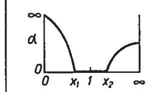	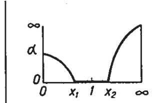	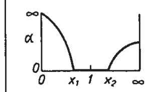	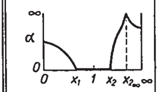	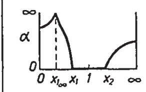	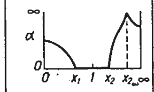	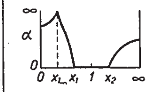	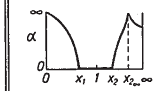	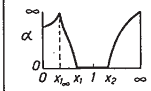	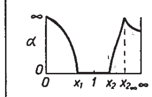	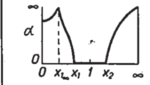
PHASE CONSTANT β FOR ELEMENTS WITHOUT LOSSES	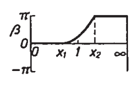	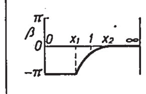	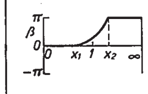	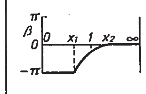	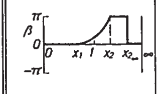	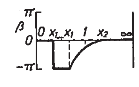	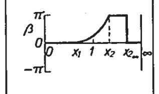	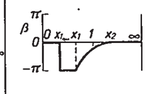	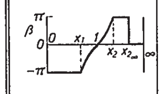	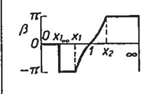	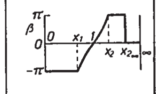	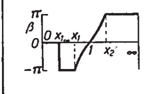
$\frac{Z_1}{4Z_2}$ WITHOUT LOSSES d = 0	$\frac{x_1^2-x^2}{x_2^2-x_1^2}$	$\frac{x_1^2-\frac{1}{x^2}}{x_2^2-x_1^2}$	$\frac{x_1^2-x^2}{x_2^2-x_1^2}$	$\frac{x_1^2-\frac{1}{x^2}}{x_2^2-x_1^2}$	$\frac{(x_2^2-x_{2\infty}^2)(x^2-x_1^2)}{(x_2^2-x_1^2)(x_{2\infty}^2-x^2)}$	$\frac{(x_1^2-x_{1\infty}^2)(x^2-x_2^2)}{(x_1^2-x_2^2)(x_{1\infty}^2-x^2)}$	$\frac{(x_2^2-x_{2\infty}^2)(x^2-x_1^2)}{(x_2^2-x_1^2)(x_{2\infty}^2-x^2)}$	$\frac{(x_1^2-x_{1\infty}^2)(x^2-x_2^2)}{(x_1^2-x_2^2)(x_{1\infty}^2-x^2)}$	$T = \alpha + j\beta$ IS THE SUM OF THE T's OF TYPES LISTED BELOW WITH THE SAME VALUES $x_{1\infty}$ and $x_{2\infty}$			
WITH LOSSES d ≠ 0	x^2 REPLACE BY $x^2(1-jd_L)(1-jd_C)$				x^2 REPLACE BY $x^2(1-jd_L)(1-jd_C)$				III₂ en IV₁	III₁ en IV₂	III₂ en IV₁	III₁ en IV₂
DEFINITIONS	$\nu_0^2 = \nu_1 \nu_2$ $x = \frac{\nu}{\nu_0}$	$x_1 = \frac{\nu_1}{\nu_0}$ $x_2 = \frac{\nu_2}{\nu_0}$	$y = \frac{x-\frac{1}{x}}{x_2-x_1}$ $x_1 x_2 = 1$	$d_L = \frac{r_L}{\omega L}$ $d_C = \frac{1}{R_C \omega C}$	$\nu_0^2 = \nu_1 \nu_2$ $x = \frac{\nu}{\nu_0}$	$x_1 = \frac{\nu_1}{\nu_0}$ $x_2 = \frac{\nu_2}{\nu_0}$	$x_{1\infty} = \frac{\nu_{1\infty}}{\nu_0}$ $x_{2\infty} = \frac{\nu_{2\infty}}{\nu_0}$	$y = \frac{x-\frac{1}{x}}{x_2-x_1}$ $x_1 x_2 = 1$ $d_L = \frac{r_L}{\omega L}$ $d_C = \frac{1}{R_C \omega C}$	$\nu_0^2 = \nu_1 \nu_2$ $x = \frac{\nu}{\nu_0}$ $x_1 = \frac{\nu_1}{\nu_0}$ $x_2 = \frac{\nu_2}{\nu_0}$ $x_1 x_2 = 1$	$x_{1\infty} = \frac{\nu_{1\infty}}{\nu_0}$ $x_{2\infty} = \frac{\nu_{2\infty}}{\nu_0}$ $y = \frac{x-\frac{1}{x}}{x_2-x_1}$	$g = \sqrt{(x_1^2-x_{1\infty}^2)(x_2^2-x_{1\infty}^2)}$ $h = \sqrt{\left(\frac{1}{x_1^2}-\frac{1}{x_{2\infty}^2}\right)\left(\frac{1}{x_2^2}-\frac{1}{x_{2\infty}^2}\right)}$ $m_1 = \frac{1}{x_{2\infty}^2} + h$ $m_2 = x_{1\infty}^2 + g$	$p = \frac{1-m_1^2}{4} x_{2\infty}^2$ $q = \frac{1-m_2^2}{4} \frac{1}{x_{1\infty}^2}$

20345

Table III. Data for the design of special band-pass filters.

the supplementary attenuation produced at the two terminals of the filter by the deviation of the image impedances from the terminating resistances must be small. As already indicated on p. 302, this may be achieved by terminating the filter at both ends with half-sections obtained by m-transformation, where $m = 0.6$. The image impedances of the whole filter, which are equal to the image impedances of the terminating sections, are then nearly constant for $x < 0.9$, and to a first approximation the supplementary attenuation just referred to can be neglected. Since this conforms with the most common practical case, the calculation of the supplementary attenuation will be omitted here in order to simplify the analysis. The two half-sections together give the same attenuation as a whole section. If the attenuation of this section is calculated for a number of frequencies, the attenuation curve *2* in *fig. 23* is obtained. The "frequency with infinite attenuation" (for which, as already shown in a previous article, the attenuation with a dissipative filter is not really infinite but has a maximum value) is $x_\infty = a = 1/\sqrt{1-m^2} = 1.25$. For frequencies in the neighbourhood of the frequency with infinite attenuation ($x = 1.25$) and close to the limiting frequency (but $x > 1$), the value of $Z_1/4\,Z_2$ including into consideration the losses may be obtained from the expression:

$$\frac{Z_1}{4\,Z_2} = \frac{a^2-1}{1-\dfrac{a^2}{x^2\,(1-jd_L)\,(1-jd_C)}} =$$

$$= \frac{0.5625}{1-\dfrac{1.5625}{x^2\,(1-j\,0.04)}}$$

(At $x < 1$ we must insert a higher value for d_L, viz., $0.02/x$.) For the remaining frequencies (in the present case for $x \geqslant 1.5$) the effect of the losses in the filter components can be neglected and the following simplified equation found applicable to a sufficient degree of approximation:

$$\frac{Z_1}{4\,Z_2} = \frac{a^2-1}{1-\dfrac{a^2}{x^2}} = \frac{0.5625}{1-\dfrac{1.5625}{x^2}}.$$

As an example, we calculate the attenuation constant of the section under consideration for $x = 1.2$:

$$\frac{Z_1}{4\,Z_2} = \frac{0.5625}{1-\dfrac{1.5625}{1.44\,(1-j\cdot 0.04)}} = -5.31 + j\cdot 2.76.$$

From this it follows:

$$\left|\frac{Z_1}{4\,Z_2}\right| = \sqrt{5.31^2+2.76^2} = 5.98;$$

$$tg\,\varphi = -\frac{2.76}{5.31} = 0.520;$$

$$\varphi = 152^\circ\,30'.$$

From fig. 20 we then get for this frequency: $a = 28$ decibels.

We must now investigate which forms of sections can be inserted between these two half-sections in order to satisfy the requirements as regards attenuation. The lowest frequency for which a given attenuation is stipulated is $x = 1{\cdot}1$, which is fairly close to the limiting frequency. To obtain adequate attenuation at this frequency a section with $x_\infty = a = 1.1$ must be used, since sections with higher values of a give too low an attenuation so close to the limiting frequency. Exactly as for the terminal sections with $a = 1.25$ ($m = 0.6$), the attenuation curve is deduced for this section (fig. 23, curve *1*). It is found that both sections together give an attenuation of only 41 decibels at $x = 1.1$, which is thus not enough. Apart from the consideration of other points, further sections must therefore be added, which for $x = 1.1$ all add something to the attenuation. We must then examine whether the attenuation of the complete filter is adequate at $x = 1.1$.

It follows from curves *1* and *2* that the attenuation is still too low at $x > 1.5$. We therefore add a section with $x = a = 2$. The choice of this value of x_∞ is to some arbitrary, but with some experience in the construction of filters a reasonable close approximation to the correct value of x_∞ can be readily made. For this section we again calculate the attenuation curve (fig. 23, curve *3*). On plotting the attenuation curve for the three sections connected in series, which is equivalent to the sum of the attenuations of the separate sections, it is observed that the attenuation above $x > 2$ progressively diminishes with increasing frequency. To obtain adequate attenuation for $x > 3$, still another section must hence be added which will give a high attenuation particularly at high frequencies, e.g. a section of the basic type. The attenuation of a half-section of the basic type, i.e. half the attenuation of a whole section, is found to be already sufficient. The attenuation of this half-section is shown in curve *4* in fig. 23, while curve *5* gives the attenuation of the whole filter.

It now remains to be seen whether all conditions laid down at the outset have been fully met. In the prescribed transmission band ($0 < x < 0.9$) the attenuation is between 1 and 3 decibels. The average is 2 decibels, and the attenuation does not vary from this by more than 1 decibel. The requirements as regards the transmission band have thus been met. In the required attenuation band ($x > 1.1$) the attenuation has to be $2 + 54 = 56$ decibels. We see that for $x = 1.1$ the attenuation is only 54 decibels; nevertheless this condition is adequately met for higher frequencies. In the majority of practical cases this difference of only 2 decibels is quite permissible (being moreover in a very narrow frequency range). In our case, however, there are several ways available for increasing the attenuation for $x = 1.1$. For instance, another filter section can be added, although this way out of the difficulty is rather expensive; also at the same time attenuation in the whole attenuation range becomes much greater than is necessary, and the filter becomes unnecessarily bulky and costly. A usually simpler solution consists in using a self-inductance of somewhat better quality, i.e. with a slightly lower value for $d_L = r/\omega L$ in the section with $a = 1.1$. As a result the attenuation for $x_\infty = a = 1.1$ is made much greater. But in the present case a still simpler solution can be adopted. For the section with $x_\infty = a = 2$ the value 2 was selected rather arbitrarily. If a is made 1.9 or 1.8, the attenuation of this section at $x = 1.1$ becomes slightly greater and is then adequate. Above $x > 2$ the attenuation is indeed reduced, but this is of no moment since the attenuation in this frequency band is even then more than enough. The values eventually arrived at in this analysis correspond to a filter with $x_\infty = a = 1.8$ for this section.

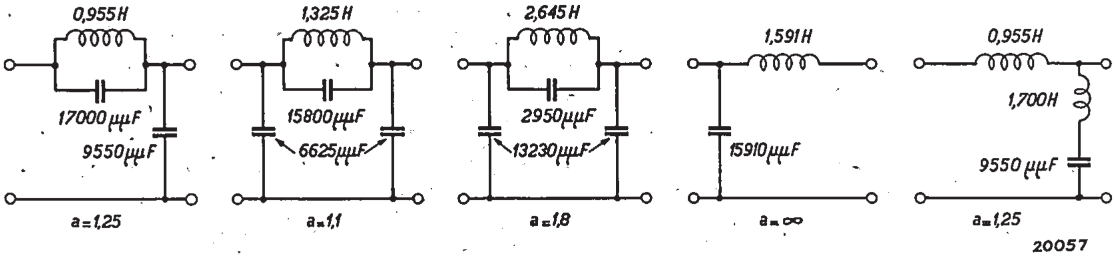

Fig. 24. Filter sections for a low-pass filter with a limiting frequency of 1000 cycles/sec. This filter satisfies the requirements set out on p. 336, if the coils and condensers have the ratings as stated there.

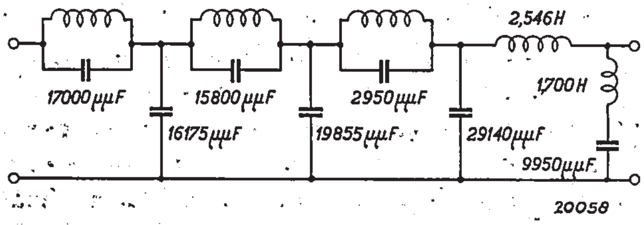

Fig. 25. Low-pass filter composed of the filter sections given in fig. 24.

Finally, it must be decided whether the various sections are to be used in the T or the Π form. As regards attenuation these two forms are identical, only in the one case more coils are required and in the other more condensers. In general the circuit with the smaller number of coils is the less costly, so that if at all possible the Π type will be preferred here. Since, *inter alia*, a half-section of the fundamental type occurs, in which there is a spontaneous transition from Π sections to T sections, the one terminal half section will correspond to the m_T-transformation and the other to the m_π-transformation. We thus arrive at the sequence of sections shown in *fig. 24*. The numerical values indicated there for the components are calculated by the formulae in Table II by inserting $R = 10\,000$ ohms, and $\nu_l = 1000$ cycles/sec. If the individual sections are interconnected and the condensers in parallel are replaced by a single condenser equivalent to the sum of the two, and the self-inductances in series are also replaced by a single unit equivalent to the pair, then the filter shown in *fig. 25* is obtained, which on the secondary side must be terminated by a resistance of 10 000 ohms.

The accuracy with which the self-inductances and condensers are calculated and calibrated must as a rule by so high that the ratings of the finished filter components do not differ more than 1 per cent from the theoretical values. Only for filters which have to satisfy particularly severe requirements is a higher degree of accuracy necessary.

SYSTEMATIC X-RAY EXAMINATION FOR THE DETECTION OF PULMONARY TUBERCULOSIS

By J. G. A. VAN WEEL.

Summary. A description is given of the application of X-ray screening as adopted by the medical welfare section of N.V. Philips for the detection of pulmonary tuberculosis. Examinations are made on all new entrants to the Works, the whole of the permanent staff, school-children and the families of patients suffering from pulmonary tuberculosis.

Introduction

The applications of X-rays in medical practice have steadily gained in importance during the last few decades, their progressive utilisation being due to the simultaneous development of theory and practice in two outstanding directions. Firstly, there has been the marked technological advance made in the construction of apparatus having a much greater range of application and affording both the patient and the radiologist better protection against the injurious action of the rays [1]) than hitherto. The other development is the recognition of the fact that in certain circumstances diagnosis cannot be based solely on the findings of ordinary clinical examination, and radiological examination is necessary to supplement clinical diagnosis. The omission to avail oneself of the advantages of a radiological examination is in many instances due to a lack of appreciation of its potentialities and value.

The aim of the radiological methods as an aid in diagnosis is to render visible the internal organs of the human body, either by radiography or by screening. Such examination can be based on either a natural contrast, (e.g. in pulmonary diagnosis) or on an artificial contrast as produced for the stomach, intestines and kidneys when using barium or other substance which has a marked absorption for X-rays.

A very important field of X-ray diagnosis lies in the examination of the thoracic cavity. Owing to the contained air the lungs produce a natural contrast with respect to surrounding organs, such as the heart and vascular system, and it is just this characteristic which can be used to advantage in the investigation of one of the most common diseases of the thoracic cavity, viz., pulmonary tuberculosis.

It may be recalled that X-ray examination was originally employed to obtain a closer insight into the processes developing in the tubercular lung. At the present time it is also used for the active detection of tuberculosis. Pulmonary tuberculosis frequently develops without the patient at the outset complaining of any symptoms, and these cases of "unsuspected" tuberculosis can only be detected by systematic X-ray examination.

It would lead us too far to discuss fully all the advantages and disadvantages of the two methods employed for this purpose, viz., screening and radiography, and only the more important characteristics will be referred to.

The high cost of making radiographs is still the principal obstacle in the way of the general application of radiography for these investigations. Screening owing to its simple procedure and low cost is however eminently suitable for this purpose. One drawback of this method is that certain tubercular foci may escape detection. It would of course be far better if both methods could be applied simultaneously in all cases, but the high cost of radiography precludes this. The marked technical advances made have opened up a large field of application for screening, and large groups of persons can now be examined by screening almost at any place (offices, factories, schools, barracks, etc.), mainly owing to the construction of simple and portable screening equipment.

In a large industrial undertaking with a large staff, the active detection of tuberculosis among the employees enables early treatment to be given to those infected. Healthy persons, moreover, benefit by the reduced danger of infection when established cases of active tuberculosis are located in their early stages and given timely treatment.

A brief description is given here of the systematic X-ray examinations for the diagnosis of tuberculosis which are carried out in connection with the staff of the Philips Works at Eindhoven.

---

[1]) It should be noted in this connection that modern X-ray tubes, such as the Metalix, have been so thoroughly screened that no radiation is obtained outside the actual X-ray beam. It must not, however, be concluded from this that the radiologist is exposed to no danger at all provided he remains outside the beam, for although the primary beam has been adequately cut off the patient disperses rays which as a rule are of such intensity that in most cases additional precautions must be taken.

Procedure and Results

To combat resolutely the spread of pulmonary tuberculosis it is essential that every single individual is submitted to a proper examination; since tuberculosis is an infectious disease its origin must be sought among all persons (family, dependents, colleagues, apprentices, etc.) which have come in contact with an infected case. A more or less isolated group of individuals in fact offers an excellent opportunity for the intensive fighting of tuberculosis.

At the beginning of 1932 the medical and welfare services of N. V. Philips' Gloeilampenfabrieken commenced the systematic screening of all applicants for employment, and proposed the gradual extension during subsequent years of this examination to the whole staff of employees. The school children in the Philips schools had also to be included in this systematic investigation, followed by the families of patients.

The various groups submitted to periodical X-ray examination were:

A) New employees.

B) Existing staff.

C) The schoolchildren.

D) Employees' families.

A) New Employees. In addition to the ordinary medical examination, all new employees (above the age of 14 years) were submitted to screening. On the detection of any pathological abnormality this examination was supplemented by an examination of the blood, radiography, etc. Unsuitable and rejected applicants were reported to their own doctors or to the competent medical institution.

The results of this examination are given in *Table I* [2].

Table I. Incidence of Tuberculosis among New Employees.

	Active		Doubtful active
	Open	Latent	
Females	0.1 %	10 %	7 %
Males	3.8 %	4 %	12 %
Total	2.7 %	6 %	10 %

B) Existing Staff. In general all employees on engagement are submitted to a medical examination; subsequently to April, 1932, this examination was also supplemented by screening. It was, however, found that persons who originally exhibited no foci on X-ray examination later developed a diseased condition of the lungs, thus indicating the extreme importance of periodical X-ray examination: It thus becomes necessary to examine all members of the existing staff by screening at regular intervals of, say, one to two years.

Persons showing pathological abnormalities in these routine examinations are submitted to closer examination; viz., general medical examination, blood tests and if necessary sputum tests, tuberculin reaction, and radiography. The examination shows whether the patient requires treatment (surgical, rest, hospital or sanatorium treatment) or merely observation (repeated blood tests and radiological examination) under favourable conditions of employment.

The family doctor is sent reports of these examination; a summary of the results achieved is given in *Table II*.

Table II. Incidence of Tuberculosis among Existing Staff

	Active		Doubtful active
	Open	Latent	
Females	0.9 %	4.2 %	9 %
Males	1.4 %	3 %	14 %
Total	1.27 %	3 %	13 %

Non-tubercular changes in the thoracic cavity, i.e. of the heart , vascular system, etc., were found to total 4 per cent in all cases examined in groups A) and B).

Table III shows the results obtained by systematic screening of all new applicants for employment; employees (approx. 10 000) engaged before April 1, 1932, were not screened during their initial examination, but all applicants subsequently engaged (approx. 5 000) were submitted to radiological examination.

Table III. Reduction in the number of tuberculosis cases among permanent staff since the introduction of radiological examination on April 1, 1932.

		Total	Examined	
			Before April 1, 1932	After April 1, 1932
Active	Open	14	13	1
	Latent	32	29	3
Doubtful Active		142	127	15
Total		188	169	19

C) Schoolchildren. Originally all children in Philips schools were screened once a year, but for practical reasons this periodical examination has now been limited to those children which give a positive reaction in the tuberculin test (Moro ointment). This reduces the number of children coming up for examination to about $^{1}/_{6}$ to $^{1}/_{7}$ of the total.

---

[2] Compiled by J. G. A. van Weel, Thesis, Utrecht, 1935.

Results of these examinations were as follows: Of 1246 children of the Philips schools who were screened 1.2 per cent had active and 2.7 per cent doubtfully active symptoms. The former class thus required treatment and the latter careful observation.

D) *Examination of Families.* For the effective suppression of tuberculosis it is absolutely imperative to examine in addition to the patients all those persons coming in daily contact with them, either in their own homes or at works (apprentices, etc.), viz., the socalled "contacts".

For the periodical examination of these contacts the medical department of N.V. Philips has organised a consultative section for tuberculosis sufferers which works in collaboration with the local medical institution at Eindhoven.

The functions of the Philips consultative section include the examination of the following groups:

1.) Persons who report of their own accord complaining of symptoms, or who require examination as a precautionary measure (marriage) or those suspecting infection (open tuberculosis in the neighbourhood).
2.) Persons sent by their own physician owing to the detection of a lung disease.
3.) Persons sent by other employers to ensure that they are not suffering from an infectious lung disease (e.g. domestic employees).
4.) Contacts with all cases of active (open and latent tuberculosis) and with doubtfully active cases enumerated under *A*, *B*, *C* and *D* 1), 2) and 3).

The importance and necessity for treating or keeping under observation all contacts with tubercular patients is indicated by the fact that among contacts with patients suffering from active tuberculosis (open and latent) six times as many infections of all kinds were found than among the rest of the community, while among contacts with doubtfully active cases there were twice as many infected cases.

The ratio of the number of cases established by the active diagnosis of tuberculosis (systematic radiological examination of all members of the staff and their contacts) to the number of passive cases (sent by the patient's family physician or patient reporting of his own accord) is shown by the proportion of cases passing through the consultative section which have been detected by each of the two methods. The relevant data are given in *Table IV*, which indicates that nearly three-quarters of all cases were detected as a result of direct examination.

Table IV. Distribution of cases according to method of detection

		Direct	Indirect
Active tuberculosis	Open	50 %	50 %
	Latent	70 %	30 %
Doubtfully active		77 %	23 %
Total		73 %	27 %

The great value of submitting large groups of persons to systematic radiological examination is shown by *Table V*, where the cases detected by radioscopy are compared with the number of cases diagnosed by family physicians and by the examination of contacts.

Table V. Value of Group Radioscopy for the detection of tuberculosis.

		Screening	Family physicians and examination contacts
Active tuberculosis	Open	36 %	64 %
	Latent	27 %	76 %
Doubtfully active tuberculosis		62 %	38 %

It may be concluded from this table that without routine screening of large groups of persons more than a third of the infections cases (open cases) would have remained undetected. Moreover, routine screening on these comprehensive lines reveals the greater part of the doubtfully active cases; this is particularly important since it is just these cases which provide the later active and open cases of

Table VI. Decrease in number of days of sick leave as a result of anti-tuberculosis measures.

Year	Average number of days of sick leave 3)
1932	1.38
1933	1.24
1934	1.21
1935	0.80

---

3) Calculated per head and per annum with a maximum of 375 days of sick leave per head (including Sundays).

infection. By the periodical supervision of these cases the formation of unknown foci of infection can thus be, to a large extent, prevented.

It is interesting to note that during the periodical repetition of radiological examinations over a large mass of people the number of new cases detected gradually diminishes since all old cases are already known and the families where the greatest danger of infection and spread of the disease obtains are kept under constant supervision by the consultative officials.

In conclusion *Table VI* gives data covering the period 1932 to 1935 which show the reduction in the average number of days of sick leave.

THE PHILIPS TWIN CURRENT WELDING UNIT

By H. A. W. KLINKHAMER.

Summary. A description of a unit for arc welding with direct current and alternating current is given. The transformer which feeds the rectifier during D.C. welding is used as a welding transformer during A.C. welding.

Introduction

Since some 5 years ago Philips first employed their hot-cathode valves in direct-current welding units the welding rectifier has continued to justify its place in welding practice. In these five years the wealth of practical experience gathered both in our own works and in other works has enhanced the reputation of this new unit, and a wide field of application has been developed in which the welding rectifier has shown itself as particularly apt and efficient.

These applications include:

A) The welding of thin sheets from 0.02 to 0.1 inch thick, for which alternating current is not very suitable; thicker sheets also can be welded with direct current more quickly, easier and better than with alternating current especially if the direct current is furnished by a welding rectifier.

B) Difficult welding work, such as vertical and overhead seams; direct current is the much more preferable for this purpose than alternating current.

C) The welding of special metals, such as rustless steels, aluminium, and bronze. Aluminium cannot in fact be welded at all with alternating current.

For the welding jobs included under A) direct current of approx. 10 to 80 A is required; for B) and C) current intensities of up to 140 A are frequently needed and welding rods up to 0.15 inch in thickness used.

The applications of the welding rectifier are however not by any means limited to the above jobs for it can be used to advantage in all cases where a welding transformer is suitable. According to a large number of practical users work with the welding rectifier is more convenient and agreeable, and hence over long periods much more rapid. This is however to some extent purely a matter of individual taste, while the nature of the welding job also is a determining factor.

The welding rectifier competes with the welding transformer and the rotary converter. In the above enumeration under A), B) and C) of the specific fields of application of the welding rectifier, we had a comparison with the welding transformer particularly in mind. The jobs referred to can as a rule also be performed with direct current furnished by a rotary converter, but compared with the latter, the welding rectifier offers the important advantages of lower first cost and lower weight.

The speed with which a welding unit adapts its voltage to the rapidly fluctuating voltage of the arc is a point of paramount importance. Without entering into this question in great detail it may be recalled that during welding there is a continuous sequence of striking and re-striking of the arc. To strike the arc the point of the welding rod is brought into brief contact with the workpiece, which causes a powerful current to be built up, and is then removed from the surface again when the arc is struck. The length of the arc and hence also the minimum voltage for maintaining the arc increase rapidly during this operation. There is now a race between the minimum arc voltage and the voltage output of the unit. If the voltage of the latter lags behind the arc breaks down and must be struck afresh. But with every collapse of the arc there is the danger of a weak spot being produced in the welded seam, so that it is absolutely essential to keep the voltage output of the supply unit continuously matched to the arc voltage.

It is just in this respect that the welding rectifier shows to better advantage than the welding converter. The unidirectional voltage furnished by the welding converter is in fact proportional to the field about the poles of the welding dynamo. This field cannot alter its magnitude abruptly, since any alteration in the field produces currents in the exciter winding and in certain circumstances also in the solid poles and yoke, which counteract a change in field. In the welding rectifier no similar lag is naturally found since no exciter winding is used.

There are various types of welding dynamo in which this lag is to a large extent eliminated by adopting a suitable circuit and appropriate lamination of the yoke and poles. But by these modifications in construction the cost of the converter is increased, although it can nevertheless never be made entirely comparable in efficiency with the welding rectifier.

The rapidity with which the voltage of the welding rectifier recovers after a short-circuit may be gathered from the oscillogram in *fig. 1*, which shows the variation in voltage when in a type 1306 Philips welding rectifier, the short-circuit current in the highest setting of the regulator is interrupted by a high-speed switch. It is seen that the time required for completely re-establishing the open-circuit voltage is less than 0.002 sec. An accurate time scale is here provided by the waves of the voltage oscillogram, and since four-phase rectification is employed each wave corresponds to 0.005 sec.

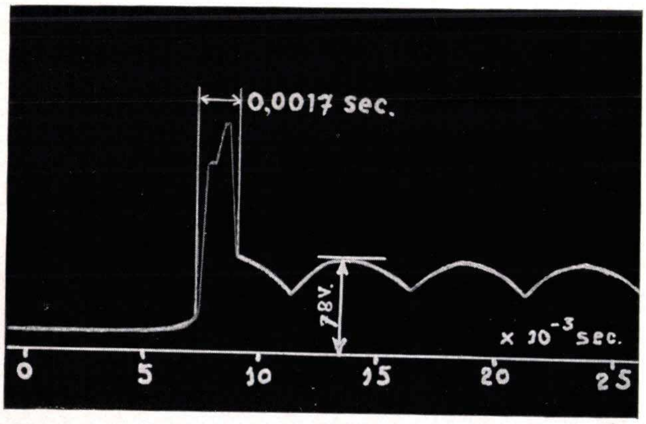

Fig. 1. Voltage oscillogram for Philips welding rectifier, type 1306, when suddenly interrupting the short-circuit current with a high-speed switch.

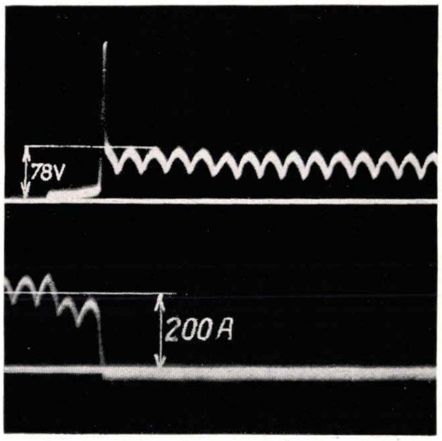

Fig. 2. Voltage and current oscillograms for the same operation as in fig. 1 but registered at a slower film speed.

Fig. 2 reproduces a second oscillogram of the same operation, except that here the speed of the film, i.e. the time scale, is about five times smaller. The top curve represents the welding voltage, and the lower curve the welding current.

Philips Twin-Current Welding Unit

The special applications of the welding rectifier enumerated under A), B) and C) include only work which can be performed with comparatively low currents. At higher currents the welding rectifier frequently does not show to such good advantage as the welding transformer, and usually one of the latter type can be used quite satisfactorily.

Now a welding rectifier includes, in addition to the valves, also a transformer which is less efficiently loaded than as in normal circumstances. It thus seemed reasonable to adapt this transformer also for welding with high-intensity alternating current, especially as this would permit a considerable increase in the application of the equipment without entailing much extra cost.

These considerations led to the development of the twin-current welding unit, which can be used as a welding rectifier for lower currents and as a welding transformer for higher currents.

Circuit Layout of the Twin-Current Welding Unit

The unit is run off a three-phase mains supply. It is equipped with a switch, in one extreme position of which the unit operates as a welding rectifier and in the other extreme position as a welding transformer, while in the middle position the output terminals are dead and all circuits are disconnected from the supply.

The unit contains two single-phase leakage transformers, whose leakage resistances can be simultaneously altered by adjusting a magnetic leakage regulator. This permits continuous variation of the welding current between wide limits.

If the switch is moved into the D.C. welding position, the primaries of the transformers are interconnected to a T-circuit, and they transform the three-phase mains current into low-voltage four-phase current which is then rectified by the thermionic valves.

In the A.C. position of the switch one pole of the three-phase mains supply is off circuit. The two single-phase transformers are then interconnected in parallel across the two other poles; the four secondary coils, which in the rectifier circuit constitute the arms of the four-phase star connection, are then interconnected in parallel and each carries one fourth of the welding current.

Fig. 3 shows a simplified circuit for the D.C. position of the switch. The points U, V and W are connected to the phases of the three-phase network and H is connected to K. The windings are dimensioned to give the vector diagram shown in *fig. 5a*, and the K—R section of the winding remains dead. The secondary windings form a symmetrical four-phase star connection, whose neutral point is connected to the negative output terminal. The positive output terminal is connected to the centre of the heating windings, which surround the primary coils and whose voltage is therefore independent of the load.

On changing over to A.C. welding, the simplified circuit shown in *fig. 4* is obtained. The points H and K of the primary winding are now no longer interconnected; but U and R are linked to each other, as well as W and V, and these terminals are connected to the delta voltage of the three-phase mains supply, so that the fields of the two transformers are in phase with each other and no longer have a displacement of 90 deg. as in the previous case (see fig. 5*b*). The left hand terminations of the four secondary windings are connected with one output terminal, and the right hand terminations with the other terminal. In this position of the change-over switch the D.C. windings are open-circuited, so that no D.C. power is unnecessarily wasted during welding with A.C. As indicated in the circuit diagram, the secondary windings

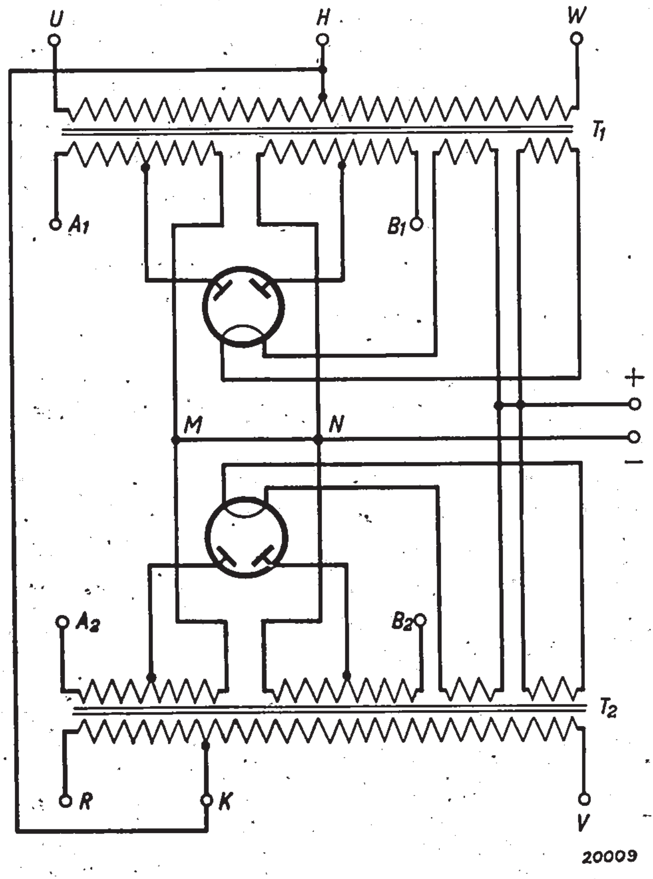

Fig. 3. General circuit layout for D.C. welding with the Philips twin-current welding unit.

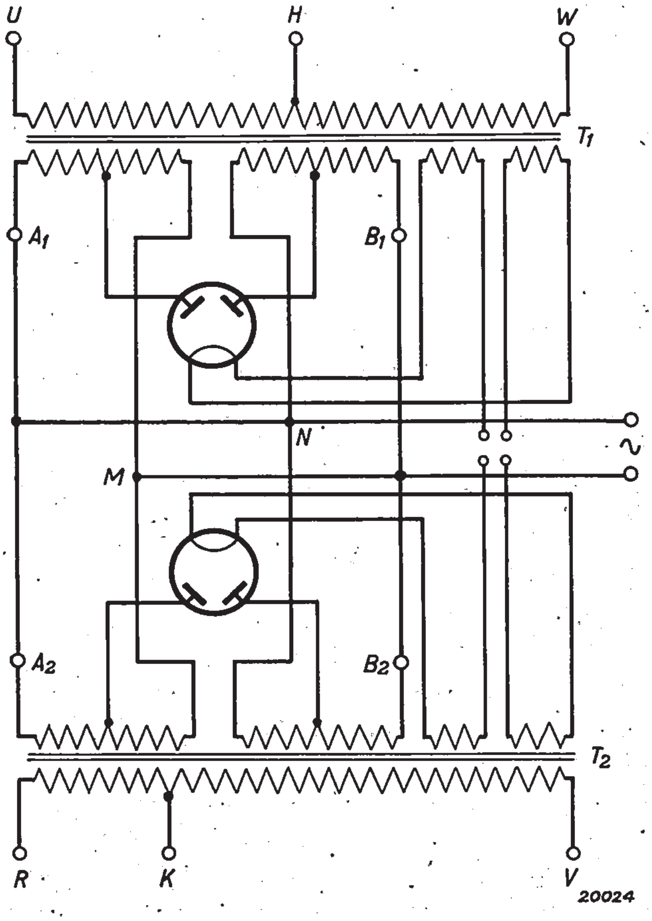

Fig. 4. General circuit layout for A.C. welding with the Philips twin-current welding unit.

in this circuit have been lengthened by several supplementary windings, such that the open-circuit voltage is raised to the value required for A.C. welding. These supplementary windings are wound above the primary coil, thus making the leakage resistance just equal to the value at which the unit furnishes alternating current at 300 A in the extreme outer position of the leakage regulator. This maximum value of 300 A was selected out of consideration of the practical need of obtaining efficient welding with sheathed welding rods 0.3 inch thick.

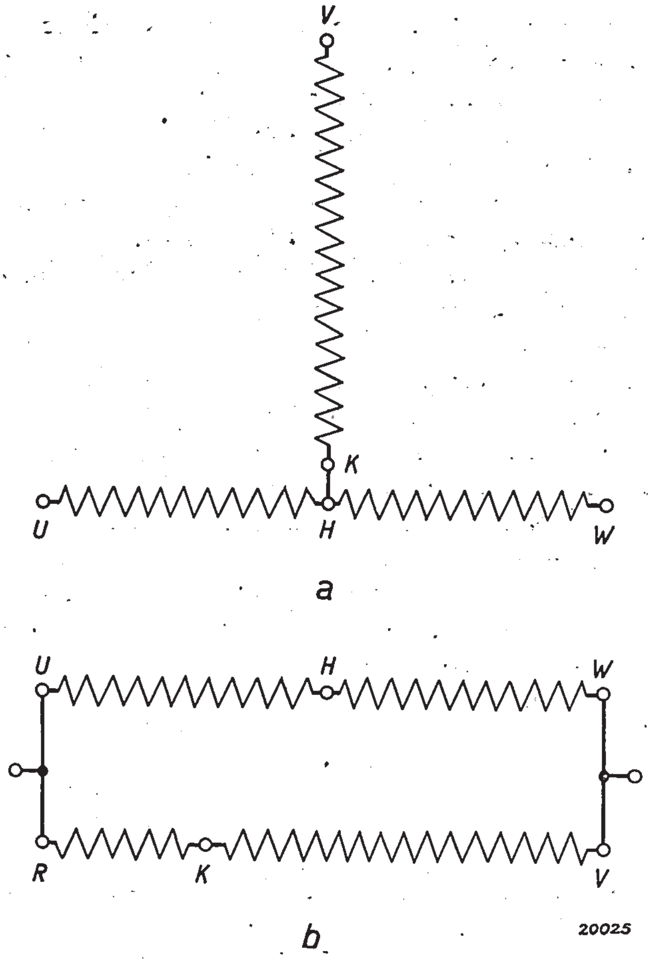

Fig. 5. a) Diagram of connections of primary windings when using the welding unit as a welding rectifier.
b) Diagram of circuits when using the welding unit as a single-phase transformer.

The primary winding is also provided with a number of taps not shown in the diagram, these permitting the unit to be connected to three-phases supplies of other voltages, e.g. 220 and 380 volts or 190 and 220 volts. Changing over from one voltage to the other is done by readjusting four small clips on a terminal board located under the cover.

Construction of the Transformers and the Regulator.

The use of leakage transformers in heavy-current technology introduces a number of difficulties which are the greater the larger the transformer used. If, for instance, an ordinary leakage transformer rated for several 10 kVA is enclosed in an iron housing, the powerful leakage field surrounding the transformer will induce eddy currents in the magnetic material of the housing, framework and constructional elements, these eddy currents being the direct cause of losses, overheating und humming of the iron structure. It therefore becomes necessary to make the framework and housing from expensive non-magnetic material, a method which has been adopted by various constructors of welding transformers using brass for the framework and wood for the housing.

A different method was adopted in the twin-current welding unit. Instead of making the transformers of the core-type as commonly adopted for units of this rating, the shell-type construction was favoured, although a little more material is perhaps entailed in this design of transformer. With this design the leakage field does not indeed constitute a source of disturbance, as may be seen from *figs.* 6 and 7.

Fig. 6 is a diagrammatic sketch of a leakage transformer of the core type, while fig. 7 shows the same transformer of the shell type. Between the primary coil *I* and the secondary coil *II* is the magnetic shunt *C*, which in the core-type unit is of one piece and in the shell-type is in two pieces. To alter the leakage resistance it is sufficient to insert the shunt to a greater or less depth in the aperture, so that regulation is obtained by displacement perpendicular to the plane of the paper.

When the transformer is on load, then neglecting the magnetising current the ampere-turns on the primary coil are equal to those on the secondary. The two coils thus give the same magnetic field intensity; the direction of this intensity at a particular moment is shown by arrows in the figure. In fig. 6 this produces a positive magnetic potential in the whole of the upper yoke *B* and a negative magnetic potential in the lower yoke *A*. The magnetic field strength at any surrounding point, e.g. at the point *P*, which is compounded of a component from each *A* and *B*, is readily seen to be of the same order of magnitude as the components themselves.

In fig. 7, however, the part *B* of the middle limb between the coils is separated from the surroundings by the shell *A* which may be regarded as a

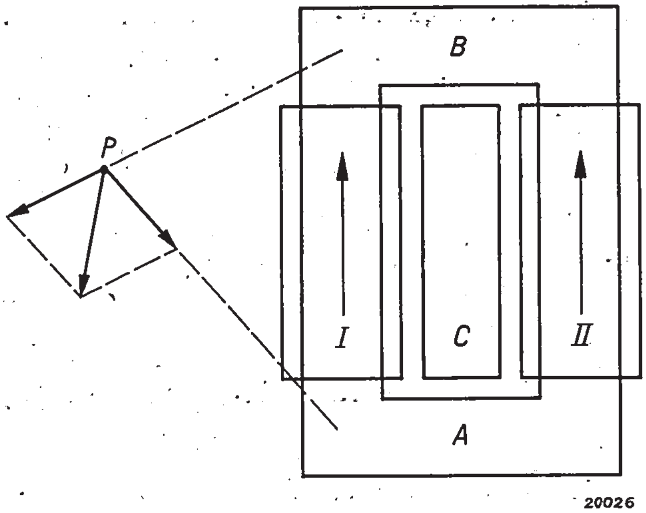

Fig. 6. Leakage transformer, core type.

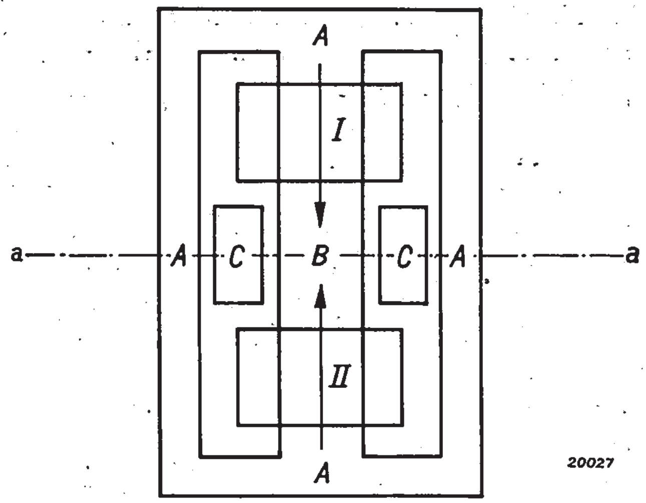

Fig. 7. Leakage transformer, shell type.

magnetic short-circuiting ring. In this way the whole of the surroundings are completely screened from magnetic effects which may emanate from the transformer.

This does not, however, entirely apply to points outside the plane of the paper; nevertheless it is definite that the leakage field in the design shown in fig. 7 is concentrated to a greater extent towards the interior of the transformer than in the design shown in fig. 6. The difficulties with the core-type transformer mentioned above are not experienced with the shell-type, so that the frame and housing of the latter can without any apprehension be made of iron.

Nevertheless the core-type transformer with its powerful external leakage field could not be used here for an entirely different reason: In an experiment using two core transformers in the circuit shown in fig. 3 it was found that on load one rectifying valve carried almost double the current passing through the other valve, although the open-circuit voltages and the short-circuit currents were the same. The valves had exchanged their functions when the phase sequence of the mains supply was reversed. Although the currents could be balanced by increasing the distance between the transformers, this way out of the difficulty was naturally out of the question in a welding unit.

The cause of this behaviour is to be sought in the mutual influence of the transformers produced by their leakage fields, as a result of which transformer T_1 generates a supplementary voltage $-jkI_1$ in the secondary winding of T_2 and T_2 a supplementary voltage $-jkI_2$ in the secondary winding of T. Here k is a coefficient of mutual induction. If each transformer has a leakage resistance jx and carries of load of resistance R, and V_1 and V_2 are the open-circuit voltages, then the equations for the two circuits are found to be:

$$V_1 = jxI_1 + RI_1 + jkI_2$$
$$V_2 = jxI_2 + RI_2 + jkI_1$$

If the first equation is multiplied by j and is then subtracted from the second equation, then since $V_2 = jV_1$ we get:

$$\frac{I_2}{I_1} = j\,\frac{R + jx - k}{R + jx + k}$$

i.e. $I_2 \neq jI_1$ for $k \neq 0$, in other words we get an asymmetrical three-phase load when the transformers influence each other through their leakage fields. On short circuit ($R = 0$), although the currents are equal, the phase difference is yet not equal to 90 deg. With the shell-type transformer k was found to be so small that the valve currents were practically equal, also when the unit was on load.

If the secondary circuits are not kept separate as in the above example, but are coupled together on the D.C. side of the valves, this factor can be taken into consideration by assuming that one transformer carries a load R_1 and the other a load R_2, where $R_1I_1 = R_2/I_2$. Calculation is then not so simple but gives the same qualitative result.

The shell type of transformer also offers advantages as regards the construction of the regulating device. To make a movable magnetic shunt is never a simple matter, since powerful magnetic forces have to be taken into consideration. Thus with an air gap with an induction B, the force acting on the contiguous iron surfaces is $B^2/25000$ gr per sq. cm, i.e. approx. 600 kg per sq. dm with an induction of 12000 gauss. With a mains frequency of 50 cycles this force fluctuates 100 times per second between zero and its maximum value.

Owing to the elastic response of the structure a loud hum is then very quickly produced, particularly where the whole structure does not constitute a rigid unit, and the magnetic shunt has to be made to slide along the guide bars.

Although in the design shown in figs. 6 and 7 the magnetic forces which act on the shunt regulator have indeed been compensated theoretically, yet high unbalanced magnetic forces immediately make their appearance in service owing to small discrepancies in erection, such as a slight twist of the regulator about its axis perpendicular to the plane of the paper.

The whole construction has therefore to be made extremely rigid. Heavy guide bars must be used whose supports in their turn must be very rigidly connected to the transformer.

In order not to make the unit excessively costly, another method was adopted which although suitable for the shell type was not applicable to the core type of transformer: it consisted of clamping the shunt cores after adjustment firmly against the middle core. During service they then form a rigid aggregate with the middle core, so that the magnetic forces acting between the shunt cores and the middle core produce no displacement and hence also no hum is heard.

To illustrate this the section *a—a* in fig. 7 is shown in *fig. 8*. The middle cores are denoted by *B*, the outer cores by *A*, and the hatching indicates the direction of the laminations. The two shunt cores L_1 are made up of sheets packed on a brass rod with the same thickness, and so combined to form a rigid bar. The two shunts L_2 are constructed on similar lines. To adjust the welding current these bars are displaced longitudinally and then clamped against the middle core by a bolt whose axis is indicated by *bb* in the figure.

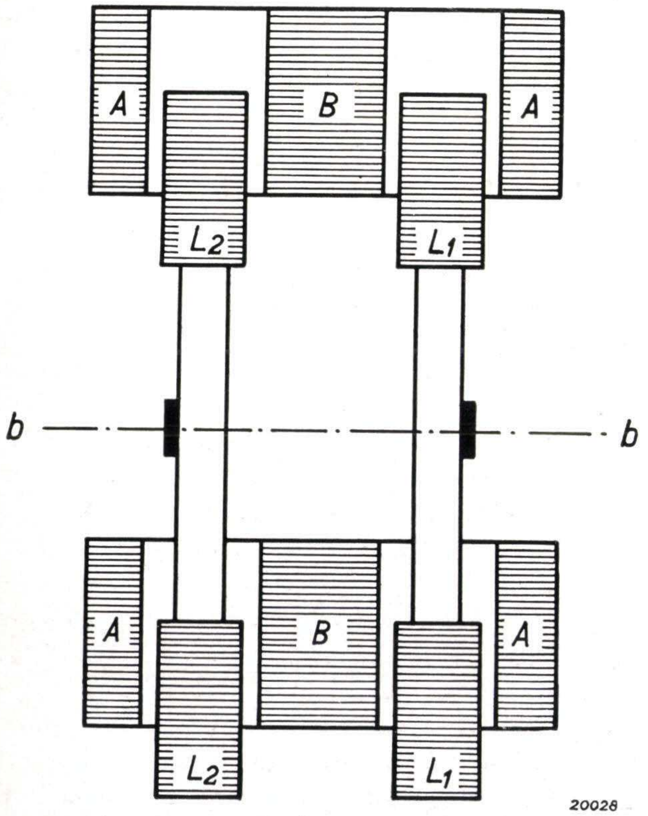

Fig. 8. Leakage transformer with locking-type regulator (section through *a—a* in fig. 7).

The Twin-Current Welding Units, Types 1306 and 1307

Two types of welding units have been built to date on the principles outlined above, viz., 1306 (*fig. 9*) for high outputs and 1307 (*fig. 10*) for low outputs. The welding current can be regulated between the following limits:

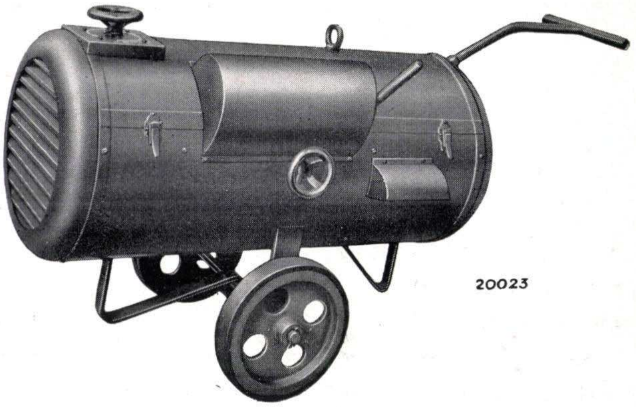

Fig. 9. Twin-current welding unit, type 1306. The lever change-over switch serves for changing over from alternating to direct current. The current intensity is regulated by means of the upper handwheel; the magnetic shunt cores are clamped against the middle core by menas of the side handwheel.

Type 1306:	Direct current	25—140 A.
	Alternating current	60—300 A.
Type 1307:	Direct current	10— 80 A.
	Alternating current	30—175 A.

The D.C. range of type 1306 is suitable for the duties enumerated under A) above, viz., on sheets of 0.04 inch thick upwards, also for the work given under *B* and *C* using welding rods up to 0.15 inch thick. With alternating current welding rods up to 0.25 inch thick can be employed with this unit.

In type 1307 the D.C. range will permit welding on sheets from 0.02 inch thick upwards, as well as the use of welding rods up to 0.1 inch thick. With alternating current welding rods up to 0.15 to 0.2 inch thick can be used with this unit.

Type 1306

The type 1306 welding unit is shown in fig. 9. It is of rainproof design and mounted on two wheels with solid rubber tyres; fan cooling is provided. The housing is in the form of a cylindrical wind tunnel in which the two transformers are mounted one behind the other and behind the two type 1069 valves; the latter are fixed side by side in a light frame held in a spring suspension. Then follows the fan which forces out the hot air through louvres on the pusher bar side. On the side of the housing is a semi-cylindrical cover under which the change-over switch is situated, whose top, middle and bottom positions correspond to alternating current, "off", and direct current.

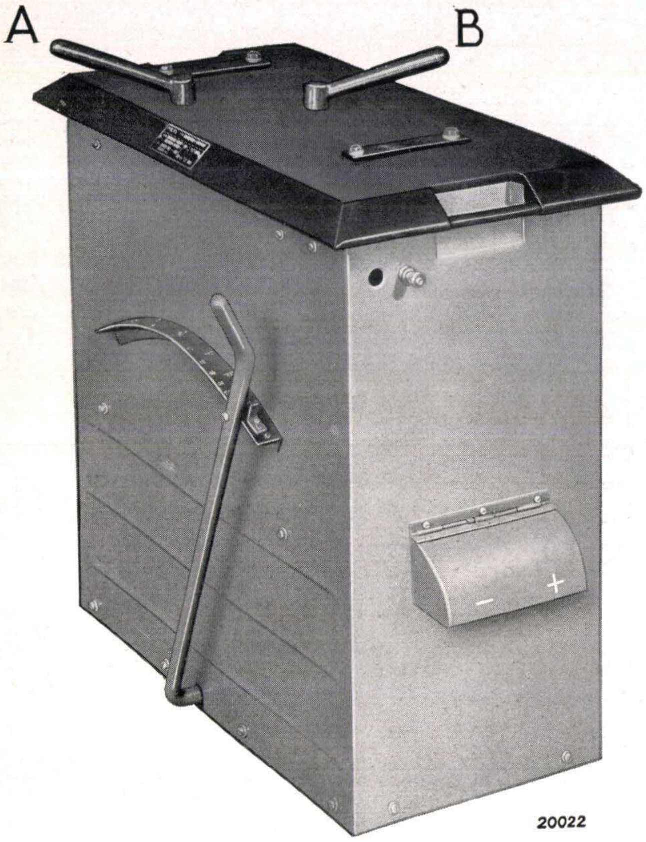

Fig. 10. Twin-current unit, Type 1307. The side lever serves for adjusting the current, while changing over from alternating to direct current is performed by means of the switch *B* on the cover. The clamping arrangement is operated by means of the crank *A*.

The handwheel on the top side serves for adjusting the welding current; through a vertical shaft and gearwheel and rod it controls the magnetic shunts which can be displaced in the axial direction of the cylindrical housing. A pointer is attached to the handwheel to indicate the welding current on a scale.

The handwheel at the side of the housing operates the clamping arrangement; on a complete revolution the shunt cores are clamped tight against the middle core.

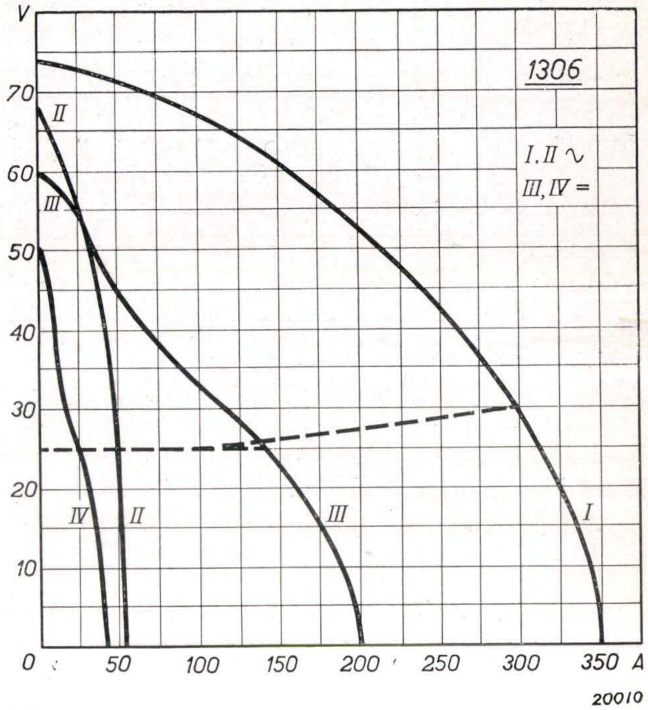

Fig. 11. Current-voltage characteristics of the twin-current welding unit, Type 1306.

I on adjustment to highest alternating current,
II ,, ,, ,, lowest ,, ,,
III ,, ,, ,, highest direct ,,
IV ,, ,, ,, lowest ,, ,,

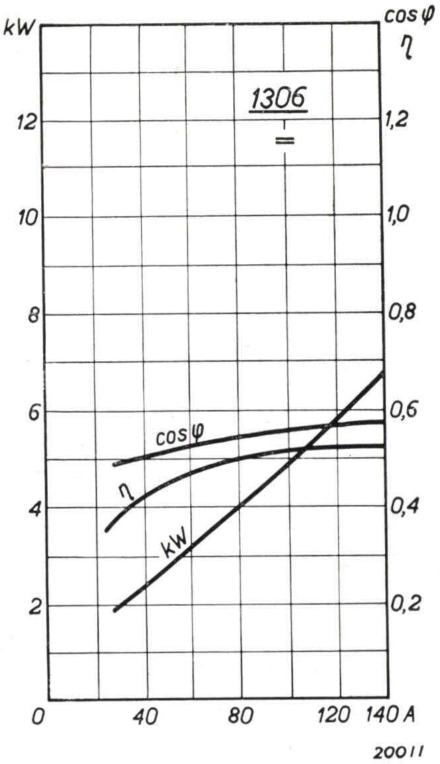

Fig. 12. Curves for the efficiency, power factor and power consumption of the twin-current welding unit, type 1306, used as welding rectifier for an arc voltage of 25 volts.

To inspect the interior the carrying ring is screwed off, the handwheel detached, the clips at the side opened and the upper part of the housing which is hinged to the lower half is tilted upwards.

Fig. 11 shows the static volt-ampere characteristics of the unit in the two extreme positions of the regulator; curves *I* and *II* are those for the A.C. circuit and curves *III* and *IV* those for the D.C. circuit. *Fig. 12* gives a few D.C. curves and *fig. 13* the corresponding curves for A.C.

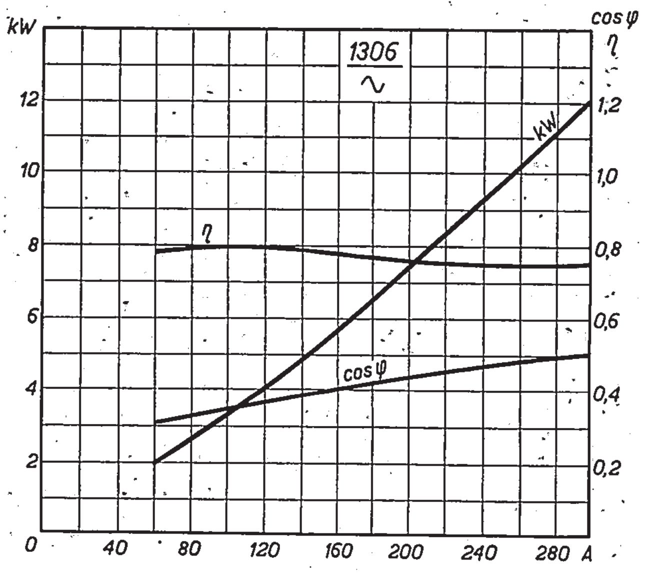

Fig. 13. Curves for the efficiency, power factor and power consumption of the twin-current welding unit, type 1306, used as welding transformer with an arc voltage varying from 25 to 30 volts along the broken line in fig. 11. Where a reduction in mains current consumption is desired, the power factor can be improved with the aid of a condenser.

Where it is desirable to reduce the power consumption from the mains, the power factor can be improved by means of a condenser.

Type 1307

A view of the type 1307 welding unit is shown in fig. 10. This type is splashproof and can be carried short distances by means of the handles. It is not provided with a fan but is designed for natural air cooling. The construction of the transformers and the regulator is exactly the same as in the 1306 type, except that the shunt regulator is not controlled by means of a gearwheel but by two forked levers. These levers are pivoted on the level of the base where they are attached to a horizontal shaft. The shaft can be turned from the outside through about 50 deg by means of a lever, which is shown in the figure at the front of the unit. The crank *A* on the cover of the unit actuates the clamping arrangement, and the crank *B* operates the changeover switch. The two valves of type 1054 are mounted above the transformers.

The characteristics and the curves for efficiency and power factor are very similar to those for type 1306.

ABSTRACTS OF RECENT SCIENTIFIC PUBLICATIONS OF THE N.V. PHILIPS GLOEILAMPENFABRIEKEN

No. 1098: H. van der Tuuk: Moderne Röntgentechniek (Ned. T. Natuurk. 3, 129 to 140, May, 1936).

This paper surveys the principal stages in the development of X-ray technology during recent decades. The requirements are set out which X-ray tubes for diagnosis and therapy have to fulfil.

No. 1099: F. M. Penning De beweging van electronen in een homogeen electrisch en homogeen magnetisch veld (Ned. T. Natuurk. 3, 141 to 154, May, 1936).

The author discusses the equations of motion of an electron under the action of a homogeneous electrical and a homogeneous magnetic field. If two long plates parallel to each other are employed as cathode and anode, then at a minimum angle φ between the magnetic field and these plates part of the electrons deflected by the magnetic field will not return to the cathode. For a number of special cases this angle φ is calculated from the magnetic field strength, the electrical field strength and the components of the velocity of emergence. The results are applied to gas discharges at a very low pressure in a magnetic field.

No. 1100: J. L. Snoek: Action of an alternating magnetic field on disks made of magnetic steel (Physica, 3, 361 to 370, June, 1936).

The author has observed that small disks of magnetic steel rotated in an alternating magnetic field situated parallel to the plane of the plates are subject to an accelerating moment even if the initial velocities are extremely small, until finally their revolution synchronises with the 50-cycle alternating field. This lability phenomenon is due to ferro-magnetic hysteresis and only occurs when amplitude of the magnetic field strength is of the same order of magnitude as the coercivity. The equations deduced are confirmed quantitatively. The lability also continues to occur at 500 cycles.

No. 1101: Balth. van der Pol: On potential and wave functions in n dimensions (Physica 3, 385 to 392, June, 1936).

Analogous to the derivation of the wave equation in n dimensions from one in $n+1$ dimensions, by making the latter independent of one of the dimensions concerned ("méthode de descente" of Hadamard), the same solutions can also be arrived at by means of problems in $n-1$ dimensions ("méthode de montée"). This gives a simple method for deriving the classical Whittaker potential and wave functions in three dimensions in a generalised form and at the same time constitutes an extension of these functions to n dimensions. The integral expressions so derived also cover the Hankel functions and spherical functions of the second degree.

No. 1102: Balth. van der Pol: A generalization of Maxwell's definition of solid harmonics to waves in n dimensions (Physica 3, 393-397, June, 1936).

A solution of the potential equation in three dimensions derived by Maxwell with the aid of spherical functions is generalised for n dimensions and also for the wave equation, by the derivation of analogous solutions containing Bessel and Gegenbauer functions.

No. 1103: J. F. H. Custers and J. H. de Boer: Die Lichtabsorption des absorbierten Paranitrophenols (Physica 3, 407 to 417, June, 1936).

As already demonstrated for the adsorption of paranitrophenol by CaF_2, adsorption at a BaF_2 surface also takes place in two different layers. The molecules of the lower layer are linked electrostatically with their OH dipoles to the fluorine ions of the surface. They have an absorption spectrum which compared to that of pure paranitrophenol is displaced considerably towards the red, the displacement being greater with BaF_2 than with CaF_2. The molecules of the upper layer are linked to the molecules of the lower layer by Van der Waals's adsorption forces. The absorption spectrum has also undergone slight modification and shows a displacement towards the red, which diminishes as the concentration at the surface rises.

No. 1104: J. L. Snoek: Magnetic and electrical properties of the binary systems $MO.Fe_2O_3$ (Physica 3, 463 to 483, June, 1936).

The magnetic and electrical properties of the binary systems $MO.Fe_2O_3$ composed of ferric oxide with ferrous, manganese, cupric, nickel or magnesium oxide are investigated. In addition to the two existant methods for distinguishing a homogeneous phase from a two-phase system a third method is also employed in which the demagnetising factor is derived from the socalled ideal curve. In this way it is possible to detect quite easily the presence of extremely small admixtures of a second nonmagnetic component. If as a result of the energy differences being too small segregation takes place very slowly, this method is of marked value (nickel and magnesium ferrite). Close to the Curiepoint (manganese ferrite) the deductions to be drawn from the measurements made are not conclusive, so that the method cannot be used in these cases. The results obtained coincide with those deduced from radiographs.

No. 1105: W. Elenbaas: Übergang der laminaren in turbulente Konvektions-Strömung im Hochdruckentladungsrohr (Physica **3**, 484 to 490, June, 1936).

If the pressure of the diameter of a high-pressure mercury discharge exceeds a certain value, the discharge becomes unstable. It is observed that convection flow which is initially streamline then becomes turbulent. With diameters exceeding 10 mm, the amount of mercury per cm of tube length at which instability occurs, expressed as a function of the cross-section, conforms with the laws of similitude for turbulence. The Reynolds 's number calculated herefrom is of the order of 1000, which indicates that the phenomenon is in fact caused by turbulent convection flow.

No. 1106: A. A. Kruithof and F. M. Penning: Determination of the Townsend ionisation coefficient α for pure Argon (Physica **3**, 515 to 533, June, 1936).

For determining the Townsend ionisation coefficient a new apparatus has been evolved which can be evacuated at a high temperature and on which exterior to the tube an arrangement has been fitted for displacing the cathode. The ionisation coefficient α of pure argon was determined for values of the quotient of the electrical field strength in volts per cm and the gas pressure in mm of mercury (reduced to 0 C°) between 5 and 400 volts per cm per mm. For small values of this quotient the values obtained were about 500 times smaller than stated by Ayres.

No. 1107: F. M. Penning: Verzögerungen bei der Zündung von gasgefüllten Photozellen im Dunkeln (Physica **3**, 563 to 568, June, 1936).

In certain gasfilled photo-electric cells, spontaneous discharge in the dark only takes place with a specific lag depending on the voltage employed. Very weak illumination reduces this delay considerably. Owing to the thermal emission of the cathode a current flows through the cell already at voltages which are under the starting voltage. This current has a specific discontinuous characteristic which may be ascribed to the window of the cell acting as a third electrode with a powerful secondary emission. If the previous discharge is given due consideration, it is found that the duration of the lag diminishes with increasing temperature of the photo-electric cell.

No. 1108: E. J. W. Verwey and J. H. de Boer: Molecular energy of alkali halides. (Rec. Trav. chim. Pays-Bas **55**, 431 to 442, June, 1936).

The lattice energies of the alkali halides and the dissociation energies of the halide molecules into ions are recalculated, the values of Mayer and Helmholtz being corrected by the subsequent more accurate estimation of the Van der Waals and London forces given by Mayer. The electron affinities are then found to be: F^- 92.2; Cl^- 83.0; Br^- 77.2, and I^- 69.9 kg. cals. The dissociation energies of the molecules which are deduced from lattice and sublimation energies are compared with various values deduced from molecular models (Preis, Born and Heisenberg). In place of the law of powers the exponential law is employed for the repulsion in calculating the dissociation energy, consideration also being given to the polarisation energy. If the six immediately surrounding ions are alone taken into consideration calculation is much simplified and very little difference is found in the results. In the case of molecules with nuclear distances smaller than 2 Å considerable deviations are found from the exponential law of repulsion. The calculated proportions of the polarisation energy in the linkage are as expected several kgcals too high, assuming homogeneous fields and constant polarisability.

No. 1109: J. H. de Boer and E. J. W. Verwey: Energy and structure of the molecules of the alkaline earth oxides. (Rec. Trav. chim. Pays-Bas **55**, 443 to 450, June, 1936).

With the aid of Born and Mayer's exponential law of repulsion, the lattice energies of the oxides BeO, MgO, CaO and BaO have been recalculated. The electron affinity of oxygen ($O—O^{--}$) was thus found to be −173 kgcals per gramatom. As for the alkali halides the molecular energies were also calculated for these oxides. The values obtained for ionic molecules are considerably less than those calculated from the lattice and sublimation energies, which indicates that the homopolar linkage has a marked effect on the combination energy. It follows from other considerations that the oxides of the alkaline earths although they undoubtedly form ionic lattices have a predominating homopolar valency in the vapour state and then form atomic molecules.

No. 1110: J. H. de Boer, P. Clausing and J. D. Fast: The α - β transition with mechanically-treated and with untreated zirconium (Rec. Trav. chim. Pays-Bas, **55**, 450 to 458, June, 1936).

In 1926 Zwikker observed a transition stage with zirconium wires between temperatures of 1100 and 1400 ° C; later investigations showed that there was a sharp transition temperature. In the present paper it is shown that the ill-defined character of the α - β transition in the earlier investigations was due to the heating of the material in different stages of working. The transition temperature was 865 ± 10 ° C. The total radiation of β zirconium is proportional to $T^{4.7}$.

No. 1111: J. H. de Boer and J. D. Fast: The influence of oxygen and nitrogen on the α - β transition of zirconium (Rec. Trav. chim. Pays-Bas, **55**, 459 to 467, 1936).

In zirconium two or more atoms per cent of oxygen and nitrogen can be homogeneously absorbed. The transition from hexagonal α zirconium to the regular β modification does not then, however, take place at a well-defined transition temperature of 865 ± 10 ° C., but throughout a wide transition range. The transition commences at 10 atoms per cent of oxygen at a temperature of 910 ° C. and is not yet completed at 1550 ° C. A low-oxygen β-phase is in this range always in equilibrium with a high-oxygen α-phase. The resistance of a specific test-bar was found to be free from hysteresis phenomena and to depend only on the temperature. If the zirconium absorbs oxygen and nitrogen at the same time, the resistance as a function of the temperature exhibits definite hysteresis phenomena. The resistance curves are practically unaffected by the addition of aluminium.

No. 1112: J. A. M. van Liempt: Die Dampfdrücke des Bariums (Rec. Trav. chim. Pays-Bas, **55**, 468 to 470, June 1936).

From the careful vapour-pressure measurements carried out by Rudberg and Lampert on barium between 500 and 750 ° C., the author has calculated the sublimation pressure and the sublimation velocity as a function of the temperature, using the formulae previously derived by him in another paper (**No. 1051**). Employing a formula also from a previous paper (**No. 1068**), the velocity of vaporisation in an inactive gas can now also be calculated.

No. 1113: E. J. W. Verwey and J. H. de Boer: Cation arrangement in a few oxides with crystal structures of the spinel type (Rec. Trav. chim. Pays-Bas, **55**, 531 to 540, June, 1936).

On the basis of the differences in character of the cations and in their arrangement over the crystal lattice, it is possible to account for the good conductivity for electrons possessed by Fe_3O_4 and the absence of such conductivity in Co_3O_4 and Mn_3O_4. From radiographic measurements it is concluded that Fe_3O_4 consists of divalent and trivalent ions and Co_3O_4 and Mn_3O_4 of divalent and tetravalent ions. The lattice of Fe_3O_4 is an abnormal spinel type in which probably all Fe^{++} together with half the Fe^{+++} are distributed statistically over mutually-equivalent crystallographic lattice points. Co_3O_4 and Mn_3O_4 have a normal spinel lattice: $Co^{IV}Co_2^{II}O$ and $Mn^{IV}Mn_2^{II}O_4$. The Mn_2O_3 prepared as described by Dubois is γ-Mn_2O_3. Its face-centred tetragonal cell may be regarded as a deformed elemetary cell of γ-Fe_2O_3 type. Contrary to Mn_3O_4 it contains only trivalent cations, similar to γ-Fe_2O_3.

No. 1114: E. J. W. Verwey: De electrolytische dubbellaag van kolloiden, in het bijzonder van AgI, metalen en kool γ (Chem. Wbl., **33**, 414 to 420, June, 1936).

In this report of a paper read, several fundamental problems in the theory of the electrical double layer are discussed, viz., those relating to the structure of the inner and outer surfaces of the double layer, their production, and the part played therein by differences in the contact potentials in the boundary layer. The examples discussed include the negatively charged dialysed AgI sol, the electro-kinetic behaviour of rare metals in water, and the behaviour of positive and negative carbon suspensions.

VOL. 1 No. 12 DECEMBER 1936

Philips Technical Review

DEALING WITH TECHNICAL PROBLEMS
RELATING TO THE PRODUCTS, PROCESSES AND INVESTIGATIONS OF
N.V. PHILIPS' GLOEILAMPENFABRIEKEN

EDITED BY THE RESEARCH LABORATORY OF N.V. PHILIPS' GLOEILAMPENFABRIEKEN, EINDHOVEN, HOLLAND

HOW CAN ONE JUDGE THE EFFICIENCY OF ROAD LIGHTING?

By G. HOLST and P. J. BOUMA.

Summary. To determine the efficiency of road lighting equipment neither a knowledge of the illumination intensity nor information of the brightness distribution on the highway is sufficient in itself. It is necessary to carry out in addition visibility measurements directly on the highway in question. Following a discussion of the fundamental principles which a visibility meter has to satisfy, a simple type of instrument is described. The results of measurements for different existing lighting equipments are given and discussed.

Introduction

In a number of previous articles [1]) we have discussed various characteristics of the eye which throw light on the mechanism of perception of objects on a highway and indicate the factors which affect the ability of perception either favourably or adversely. In addition, these data bring out the general principles governing the design of lighting equipment.

Our knowledge of the mechanism of vision has by no means advanced to such a stage that from the characteristics of the eye we can without further ado evolve the ideal method of illumination for a particular case. In the first place, we frequently do not know to what extent the various factors entailed, such as the visual acuity, contrast sensitivity, etc., contribute to visual perception, and moreover in every system of road lighting there are various associated factors (such as the brightness conditions of the surroundings, alterations in the reflecting powers of the road, as a result of wear and moisture), whose effect on the ability of perception it is difficult to estimate.

Both to extend our practical knowledge as well as to permit expression of the intrinsic value of a specific lighting system in practice, it is therefore extremely desirable to be able to make a reliable evaluation of the efficiency of a lighting equipment already in service and if at all possible to express its characteristics numerically.

It must be clearly emphasised that to do this measurements made on the highway itself are absolutely indispensable, for only by performing such a survey can all factors which determine perception on the highway be included in the results of measurement. Measurements made on reduced scale models of an equipment or a study of photographs and films of the illuminated highway are usually quite inadequate for this purpose.

Measurement of the Intensity of Illumination

What measurements must be conducted on the highway in order to arrive at useful and reliable values expressing the quality or efficiency of the lighting equipment?

In the past, illumination surveys were frequently limited to a measurement of the horizontal and vertical illumination, i.e. to a measurement of the amount of light, incident on different areas of the road surface and on different vertical surfaces. It is evident that such illumination measurements really give no information as to how well the eye can perceive objects. What interests us is by no means the quantity of light falling on various road areas or on the objects on the highway which we have to perceive, but rather the quantity of light which the different parts of the road and the objects radiate in the direction of our eyes and which is utilised for visual perception. In other words: It is less a question of the intensity of illumination of the highway as of the brightness. If two different roads are equipped with the same type of lamps, the results obtained can yet differ considerably, if one road surface has entirely different properties of reflection than the other (e.g. is darker or has a greater specular reflection); although the intensities of illumination are the same, the distribution of brightness is different.

---

[1]) Philips techn. Rev. 1, 102, 142, 166, 215, 225, 1936.

Measurement of Brightness

We can thus judge the quality of the illumination much better by measuring the brightness values instead of the intensity of illumination on the highway.

A practical difficulty is encountered in that the requisite measurements are very tedious. For while the intensity of illumination at a specific point on the road can be obtained by a single measurement, the brightness of the same area of surface is different in different directions, i.e. it depends on the location of the observer. To make a complete survey of the brightness conditions it therefore becomes necessary not only to move our measuring instrument in succession to all parts of the road surface, but the observer himself has also to take up various positions.

A serious disadvantage of a more fundamental character is that a determination of the brightness distribution over the roadway does not yet give the necessary answer to the question as to how well we can see on the highway. There are several reasons for this.

In the first place, perception is not determined exclusively by the brightness values of the roadway and of the objects located on it, but may also depend e.g. on the presence of sources of glare: Brightness measurements alone therefore do not afford an adequate basis for judging the lighting. At the same time they provide certain data in a not-readily usable form, for it is difficult, if not impossible, to deduce from the distribution of brightness the efficiency of vision on the highway. It is indeed possible to determine from brightness measurements, for instance, whether the highway has any bright and dark spots or not, but it is not easy to estimate the effect of this irregularity on the facility of perception.

Measurement of Visual Performances

It is seen that nothing else remains but to conduct experiments on the highway of the visibility of the objects on it.

If a number of different objects are placed at different points on a highway and it is estimated at what distance they are still perceptible or recognisable a true idea is obtained of the visibility of such objects on the highway, although the measurements themselves are very cumbersome, tedious and frequently dangerous. It is therefore important to investigate whether these experiments can be facilitated by means of an optical instrument.

In designing such an instrument, the fundamental requirement must not be lost sight of that in observations with it the eye must function under exactly the same conditions as when perception is performed with the naked eye. If there is any divergence from this equivalence, we still measure the performances of the eye, yet it will be functioning under conditions which do not occur in practice.

Practically every measurement of visual performance is based on determining a "threshold value", i.e. a determination of the conditions under which the eye can still just perceive a particular object. The first question which arises is therefore: How can we create the conditions required for determining the requisite threshold value?

The most direct way appears to be to reduce the brightness of the whole field of vision — e.g. by placing light-absorbing glasses in front of the eyes — to such a value that a test object on the highway becomes invisible, and to take the magnitude of this brightness reduction as a measure of the visibility of the object in question. An instrument ²) extensively used in America functions on this principle, but it is apparent that this method does not satisfy the fundamental requirement stated above, for in using the instrument the eye is functioning under conditions — in this case at brightness values — which never occur in practice on the highway concerned. This divergence can in many cases readily result in an entirely false evaluation of the quality of the lighting system. The greatest danger of this is incurred when the method is employed to compare the illumination values produced by different types of light sources. As has already been discussed in detail ³), the brightness level is a factor of paramount importance in making such comparisons: A system of lighting which proves efficient at the brightness levels occurring on the highway may prove less favourable than another method of lighting at low brightness values. The effect of glare on perception in general also does not remain the same if the brightness of the highway surface and of the source of glare are reduced by the same factor.

A better method for determining the threshold values is offered by making the test object variable or by selecting the still just visible test object out of a group of these objects. Since setting up a group of test objects on a roadway is a very cumbersome and time-wasting procedure, an apparatus has been devised in which a lens throws an image of

---

²) The "visibility meter" of Luckiesh (J. Frank. Inst., 220, 431, 1935).

³) Philips techn. Rev. 1, 166, 1936.

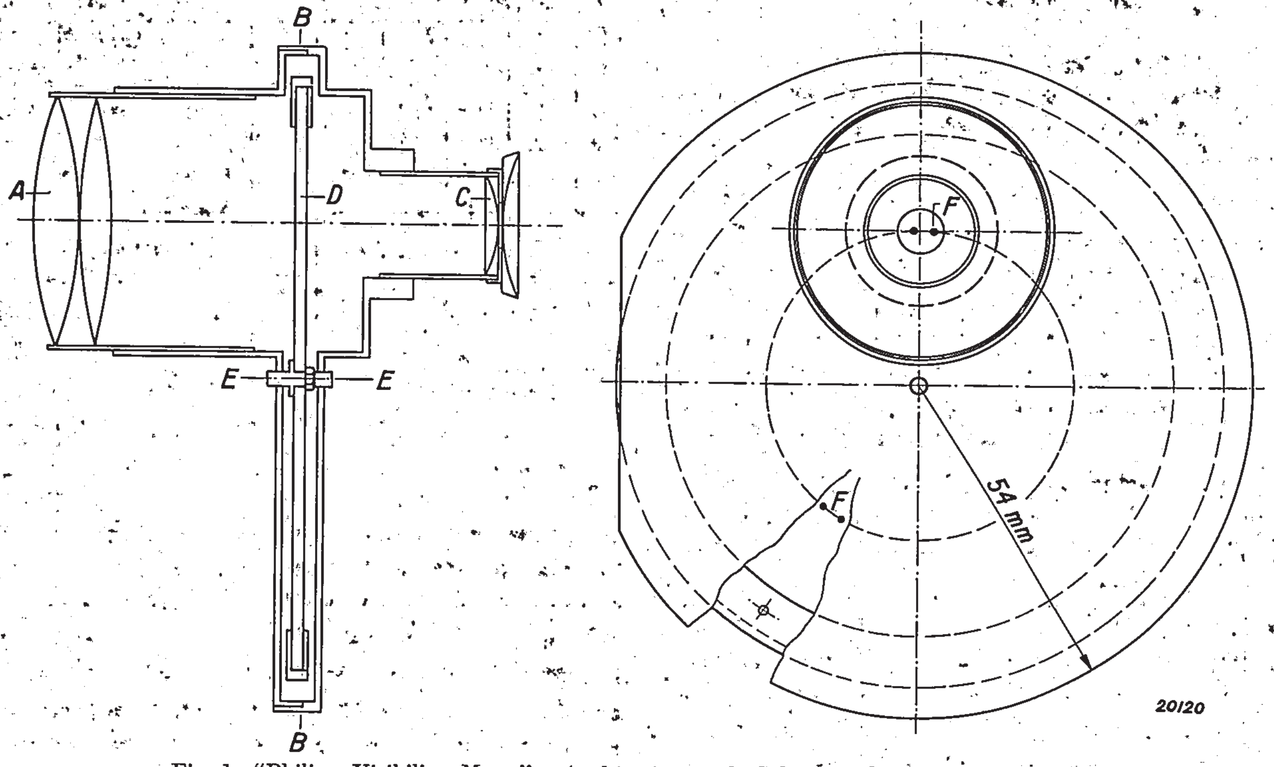

Fig. 1. "Philips Visibility Meter". *A* objective and *C* lens, with which the spots *F* with progressively increasing transmission coefficients are observed against the road surface as background.

the road on to a plane in front of the eyepiece, and in which the test-objects are also located.

Construction of the "Philips Visibility Meter"

Fig. 1 shows the construction of an apparatus designed by us on this principle. The objective *A* projects an image of the highway surface on the plane *B-B*, in which a glass disc *D* pivoted about the axis *E-E* is mounted. On the disc there are 50 small numbered circular spots *F* with different transmission coefficients which have been prepared by photographic means. These spots are viewed together with the image of the roadway through the lens *C*. Directing the instrument towards the area of road under investigation and turning the disc *D*, the spot which is still just perceptible against the highway as background can be determined.

In the practical design of this apparatus the fundamental requirement stated was to a large intent satisfied, viz., that the eye when using the instrument should function under exactly the same conditions as in normal vision. The following points are important in this respect:

1) On a highway objects nearly always appear dark against the background of the surface; the same contrast is found with the test objects.
2) To avoid sources of glare, which affect perception to a marked extent, from being screened off during observation, the field of vision has been made very large. That this reduces the definition at the edges of the image is of secondary importance.
3) The angles of vision between different objects in the field of view, for instance between an object being perceived and a source of glare, must not be altered by the instrument. This has been achieved by adopting the same focal length for *A* and *C*, as a result of which the whole optical system has a magnification of 1 : 1.
4) The angular dimensions of the test objects must be of the same order of magnitude as the obstructions present on the roadway. In the apparatus described the spots subtend an angle of about 35′, which is equivalent to the angle subtended by a pedestrian seen at a distance of about 150 yards.
5) The contrasts between the test object and the background must be comparable to those actually occurring on a highway.

Fig. 2 illustrates the calibration of one of the glass plates used. Along the abscissa the numbers of the spots *N* are plotted, and along this ordinate the contrast *K* [4]) which the spot exhibits against

---

[4]) The contrast between two brightness values is defined as:

$$K = \frac{\text{Maximum brightness — minimum brightness}}{\text{maximum brightness}}.$$

A spot with the transmission coefficient p thus produces a contrast of $K = 1 - p$.

the road surface as background. The contrasts lie between 80 per cent (an object with a reflecting power one fifth of that of the road) and 2 per cent (a contrast just still perceptible under the most favourable conditions).

Results of Measurements

The values measured naturally differ for different areas of the road surface (irregularity in brightness distribution, variable effect of glare, etc.). If we determine the highest and the lowest values for a particular highway, we shall in fact already obtain a fairly reliable picture of the efficiency of the lighting, at any rate a better idea than would be got by a complete survey of the illumination intensities or the brightness distribution.

Table I gives the results of some measurements carried out on existing lighting systems.

Table I

	Place	Type of Lighting	Installed power kW/km	Just perceptible contrast		
				Most favourable	Most unfavourable	Average
1	Eindhoven	Sodium	3	0.07	0.20	0.14
2	Cheltenham	,,	2.5			0.15
3	Vught	,,	3			0.10
4	Croydon 5)	,,	4.3			0.15
5	Vught	Blended light 6)	6.3			0.18
6	London	Mercury	10.5			0.34
7	Cheltenham	,,	9.5			0.39
8	Eindhoven	Glow lamps	5	0.19	0.31	0.25
9	,,	,,		0.34	0.47	0.40
10	Eindhoven	Gas lamps		0.39	0.70	0.54
11	London	,,				0.28
4a	Croydon	Sodium	4.3	With glare source		0.34

The following points are of interest in connection with these measurements:

The results 1 - 4 obtained on different highways illuminated by sodium are in surprisingly good agreement, while those obtained for the three roadways lighted with mercury (5 - 7) differ considerably from each other, the reason for which is immediately apparent; In the lighting system at Vught provision is made by using socalled concentrated reflectors so that the lamps radiate no light at an angle close to the horizontal, while such concentration is not employed in the other systems (distributing or dispersive reflectors). The marked difference between 5, 6 and 7 is therefore mainly due to glare resulting from the pronounced radiation of light in an almost horizontal direction.

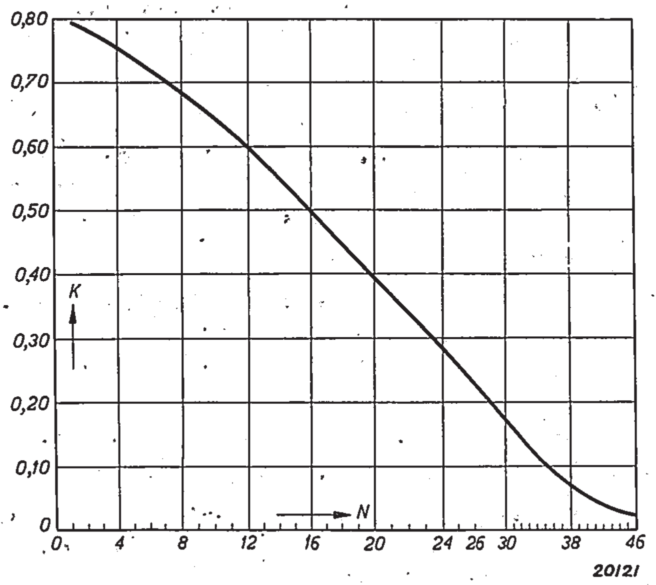

Fig. 2. The contrast K of the spots numbered from 1 to 46 against their background.

Examples 8 and 9 relate to the best and the worst of a number of lighted roadways equipped with ordinary electric lamps in the vicinity of Eindhoven, while examples 10 and 11 refer to an inefficient and a satisfactory gas lighting equipment respectively.

Example 4a applies to the same equipment as 4, but measurements were made at a moment when a motor vehicle with headlights on appeared in the field of vision at a distance of approx. 200 yards. It is seen that glare has had a pronounced adverse effect on visibility.

The best visibility values are obviously obtained with sodium and mercury lighting systems (1 - 5) if the sources are screened from direct exposure to the eye; it should be noted how this result has been achieved with a low current consumption in kilowatts per kilometer.

The general observation should be noted that the illumination is inadequate for fast traffic when contrasts of approx. 25 per cent. can no longer be perceived over greater parts of the road surface. The requirements as regards fast traffic are therefore only fully met by lighting equipments 1 - 5. (where example 4a demonstrates how necessary it becomes to traverse such well-lighted roadways with screened headlights), while the best glow lamp and gas lighting systems (8 and 11) lie just at the boundary.

---

5) See photograph on p. 312 in the October issue of Philips techn. Rev.

6) We call blended light a mixture of mercury light and glow lamps.

THE USE OF LOADING COILS IN TELEPHONY

By W. SIX.

Summary. The attention effects and distortions obtained in a telephone cable can be appreciably reduced by the insertion of induction coils (termed Pupin or loading coils) in the line at regular intervals. In this article it is shown on the basis of the theory of coil-loaded conductors that the iron cores of the loading coils have to possess the following characteristics: High permeability, low hysteresis, and high stability. By a combined rolling and heat-treatment process it has been possible to produce nickel-iron strip which adequately satisfies these requirements.

In telephone circuits the sound waves are converted by the microphone into electric waves which are transmitted by conductors and then re-converted into sound waves by the telephone receiver.

The sound waves generated by the human voice are composed of vibrations of various frequencies with extremely divergent amplitudes. Satisfactory transmission is only realised when the sound waves generated by the telephone receiver contain the different frequencies in the same mutual ratios of intensity as the sound waves picked up by the microphone. On the other hand, the ear is fairly insensitive to alterations in the phase of the individual vibrations. In a telephone circuit consisting of microphone, conductor and receiver, each of these three components affects transmission in some way or other. In the present article attention will be limited to the conductors alone. Fortunately the human ear is capable of detecting the originating sound, even in a highly-distorted sound complex. On a marked change in the ratios of the amplitudes, the tone is however altered; thus the voice sounds drummy when high-frequency vibrations have a lower amplitude than low-frequency vibrations. Yet if the higher frequencies become too attenuated, there will eventually remain only a heavy hum and speech will become quite unintelligible.

As will be shown in greater detail later, the attenuation of the line or conductor causes a reduction in the amplitude of a sinusoidal electric vibration traversing the line. The attenuation increases with the frequency. Moreover, the velocity of propagation is smaller for higher frequencies than for lower frequencies, with the net result that in the transmission of compound vibrations along the line the composition of these vibrations will vary with the attenuation and the alteration in phase. This phenomenon proved a serious obstacle in the early days of telephony to the setting up of efficient telephone channels.

In addition to its electrical resistance, a telephone line, whether in the form of a buried cable or an overhead line, also possesses capacity, self-induction and leakance. A conductor of this type can be simulated by a network with series impedances composed of resistance and self-induction and with parallel reactances composed of capacity and leakance.

In *fig. 1* the substitution scheme of a unit length of cable is shown diagrammatically. From a study of this diagram the following differential equations, which state how the current i and the voltage v vary with the longitudinal co-ordinate l of the cable, can be derived:

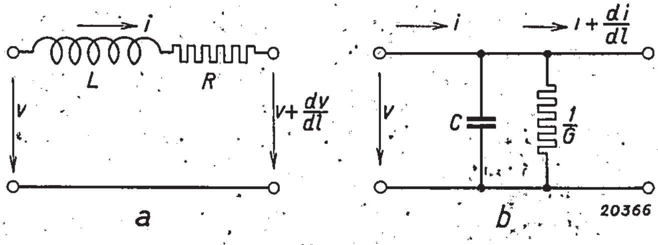

Fig. 1. Substitution diagram for a unit length of a cable.
a) Effect of resistance and self-induction on the voltages in the cable.
b) Effect of leakance and capacity on the currents.

$$\left.\begin{aligned} -\frac{\partial v}{\partial l} &= R\,i + L\frac{\partial i}{\partial t} \\ -\frac{\partial i}{\partial l} &= G\,v + C\frac{\partial v}{\partial t}, \end{aligned}\right\} \quad \ldots \ldots \quad (1)$$

where R is the resistance, L the self-induction, C the capacity and G the leakance per km of cable.

To solve these equations the voltages and currents assumed to be sinusoidal are expressed as complex functions of the time:

$$i = I\,e^{j\omega t}$$

$$v = V e^{j\omega t}.$$

We can then write the above differential equations as follows:

$$\left.\begin{aligned} -\frac{\partial V}{\partial l} &= (R + j\,\omega\,L)\;I \\ -\frac{\partial I}{\partial l} &= (G + j\,\omega\,C)\;V \end{aligned}\right\} \quad . \; . \; . \quad (2)$$

These equations are satisfied by:

$$V = V_0\, e^{-Tl},$$
$$I = I_0\, e^{-Tl},$$

where I_0 and V_0 are the current and voltage at the input of the line and:

$$T = \sqrt{(R + j\,\omega\,L)\;(G + j\,\omega\,C)} = \alpha + j\,\beta \quad . \quad (3)$$

T is termed the propagation constant and is compounded of a real component α, the attenuation constant, and an imaginary component $j\beta$, the phase constant. Voltage and current along the line are expressed by the following:

$$v = V e^{j\omega t} = V_0\, e^{-(\alpha+j\beta)l}\, e^{j\omega t},$$

$$\left.\begin{aligned} v &= V_0\, e^{-\alpha l}\, e^{j\,\omega\,(t-\beta\,l/\omega)} \\ i &= I_0\, e^{-\alpha l}\, e^{j\,\omega\,(t-\beta\,l/\omega)} \end{aligned}\right\} \quad . \; . \; . \quad (4)$$

It follows from this form of expression that the voltage and the current are propagated along the line in the form of attenuated or damped travelling waves. The attenuation is determined by α. The velocity of propagation is:

$$S = \frac{\omega}{\beta}$$

If the real parts on both sides of equation (3) are equated to each other, as well as the imaginary parts, we get:

$$\alpha = \sqrt{{}^1\!/_2 \sqrt{(R^2+\omega^2L^2)\;(G^2+\omega^2C^2)} + {}^1\!/_2\,(RG - \omega^2\,LC)}$$

$$\beta = \sqrt{{}^1\!/_2 \sqrt{(R^2+\omega^2L^2)\;(G^2+\omega^2C^2)} - {}^1\!/_2\,(RG - \omega^2 LC)}.$$

Lack of knowledge of the theory of propagation of electric vibrations along conductors, which has been briefly outlined above, was responsible for the initial failure to arrive at reliable and efficient telephone channels. It was indeed rapidly realised that the attenuation increased with the resistance and the capacity, although at the same time it was generally assumed that the principal requirement was to keep the self-induction of the line as low as possible.

In 1887 Heaviside developed the theory of propagation of electrical vibrations along conductors, and at the same time showed that the comparatively complex formulae for the propagation constant became much simplified in the special case of $LG = RC$. Then $\alpha = \sqrt{RG}$ and $\beta = \omega\sqrt{LC}$. The velocity of propagation S in this case becomes:

$$S = \frac{\omega}{\beta} = \frac{1}{\sqrt{L\,C}}$$

In a conductor satisfying this condition both the attenuation and the velocity of propagation are thus independent of the frequency, in other words a vibration compounded of a variety of frequencies can also be transmitted along the line without any distortion whatsoever being created. Although the train of waves is damped here also, yet the form of the train remains unchanged. The line is then said to be distortionless or non-distorting.

Since in normal types of cable RC is always considerably greater than LG, the question arises how the condition $LG = RC$ can be satisfied. It is possible, firstly, to make R or C smaller, and indeed it is known that the attenuation in low-capacity overhead lines is considerably smaller than that of cables and that also by increasing the cross-section of the conductor, i.e. by reducing the resistance, the attenuation can be diminished. But all possibilities in this direction have already been exhausted within commercial limits.

Secondly, it would appear possible to arrive at distortionless lines by increasing G or L. Increasing G does indeed result in making the attenuation the same for all frequencies, but also produces an increase, while by increasing L the attenuation can be reduced.

It was not till 1899 that Prof. M. I. Pupin gave a practical solution of the problem of providing telephone lines possessing a low distortion. He proposed the insertion of choke coils in the lines at regular intervals for the purpose of increasing the self-induction of the line. Pupin demonstrated that the expressions for the propagation constant of cables with a uniformly distributed self-induction are still valid when the self-inductions are concentrated at regular intervals, provided the distances of the coils are small compared with the wave-length. He calculated that the ratio of the attenuation of a line with concentrated self-inductions to the attenuation of an equivalent line with uniformly distributed self-inductions was as ${}^1\!/_2\;\beta_s : \sin\,{}^1\!/_2\;\beta_s$, when β_s is the phase displacement of the wave between two consecutive coils. For small values of β_s, i.e. where the distance between two coils is small compared with the wave length, α is roughly equal to α'. If ${}^1\!/_2\;\beta_s$ is much greater than $\sin\,{}^1\!/_2\;\beta_s$, then also α will be much greater than α'. It is therefore necessary to make the distance between consecutive coils such that also at the highest frequency to be transmitted a sufficient number of coils per wavelength are present.

The first cables equipped with Pupin or loading coils were laid at the beginning of this century. These coils were composed of an annular core made of thin steel wire which was surrounded by a toroidal winding of copper wire. The toroidal form was intentionally selected to keep the external fields of the coil as small as possible, in order to prevent the coils, of which large numbers were accommodated in large iron tanks, from influencing each other.

Since that time the laboratories of the various telephone manufacturers have been studying in great detail the core material for these coils. The result of this work has been not only a marked reduction in the dimensions of the coils, but also a considerable improvement in their characteristics.

Copper and Iron Losses

We shall first study the principal characteristics which must be possessed by loading coils.

The copper and iron losses in loading coils naturally increase the attenuation of the line and it is therefore desirable to keep them small as compared with the natural resistance of the line. The copper losses may be traced back to the ohmic resistance of the winding, which can be kept small by choosing a material for the core with the maximum permeability. These losses can, however, always be reduced by increasing the dimensions of the coil.

The iron losses can be differentiated under three heads: the eddy-current losses, the hysteresis losses and the losses due to magnetic viscosity.

The eddy-current losses are due to the production of eddy currents in the core; they are proportional to the square of the frequency and to B_0^2, if B_0 represents the amplitude of induction in the core. As is well known these losses can be reduced by subdividing the core; this subdivision is continued until the losses at the maximum frequency to be transmitted can be neglected as compared with the losses due to the ohmic resistance.

The hysteresis losses are proportional to the frequency and, for small current amplitudes, also proportional to B_0^3 1). The eddy-current and hysteresis losses can be expressed in the form of a loss resistance, multiplied by the square of the current intensity. If we put the induction B_0 proportional to the amplitude of the current, it is found that the resistance representing the eddy-current loss is independent of the current, while the hysteresis-loss resistance increases in proportion to the amplitude of the current.

As shown in another connection 2), a resistance dependent on the current results in non-linear distortion, so from this point of view it is important to make the hysteresis-loss resistance as small as possible. For this reason the induction B_0 must not be made too high.

Since B_0 is proportional to the permeability of the material, the hysteresis and eddy-current losses limit the permissible permeability. This is in contradiction with the requirements stated above as regards the copper losses, so that a compromise must be achieved.

We have also referred to the losses due to magnetic viscosity. As already indicated the eddy-current loss resistance is proportional to the square of the frequency, while the hysteresis-loss resistance is proportional to the first power of the frequencies and the current. Investigation of the iron losses at different frequencies and currents and resulting extrapolation for zero frequency and zero current demonstrates however that there is still another loss resistance. Jordan 3) has termed this phenomenon the magnetic after effect of viscosity; it is independent of the current and proportional to the frequency. It is however small compared with the other losses and can therefore be neglected in this analysis.

Stability

When the first loading coils had been in use for a few years it was discovered that the self-induction of many coils had undergone a considerable change. The cause of this was found to be due to an alteration in the permeability of the core material by magnetisation with direct current. This magnetisation was the result of abnormally high currents occasionally induced in the telephone lines by lightning or the power conductors of electric railways, etc. The change in self-induction on magnetisation

---

1) On weak magnetisation with alternating current, the following type of relationship is found between the induction B and the field strength H: $B = \mu H \pm \nu (H^2 - H_0^2)$ where H_0 is the amplitude of the field strength and the algebraical sign is negative or positive according as the field strength decreases or increases. The loss in energy per period is given by the surface F of this curve and is found to be:

$$F = \frac{8}{3} \frac{\nu}{\mu^3} B_0^3 .$$

2) Philips techn. Rev. 1, 140, 1936 (in the article dealing with the sound recorder of the Philips-Miller system).

3) H. Jordan, E.N.T. 1, 7, 1924.

by passing a direct current of 1 A through the line was taken henceforth as a measure for the stability. In the first loading coils this change might amount to as much as 30 per cent, while in modern loading coils the stability has been raised to less than 1 per cent.

As already stated the cores in the first loading coils were made of thin steel wire. A marked improvement was made in 1916 by the introduction of the compound core.

These cores were made of iron powder which had been compressed under a high pressure with an insulating material. By using powdered iron the path of the lines of force through the core is subdivided; this subdivision thus acts similarly to an air gap, except that in the compound cores this gap is spread uniformly over the whole length of the lines of force, whereby symmetry is retained and the stray field remains small.

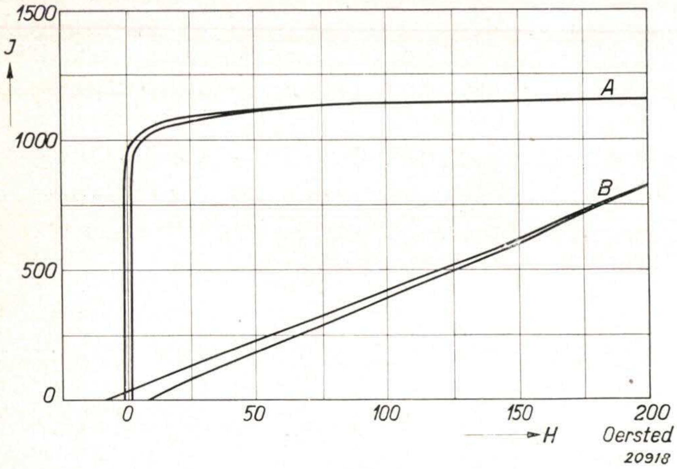

Fig. 2. Magnetisation curves of nickel-iron strip for loading coils.
A) Magnetic field perpendicular to the direction of rolling.
B) Magnetic field parallel to the direction of rolling.

Owing to the air gap the induction at constant field strength is reduced. If *A* in *fig. 2* represents the magnetisation curve of the original material, the curve for the compound core is found to be less steep, roughly as shown by *B*. This second curve has a much greater stability and smaller hysteresis losses.

Since that time progressive improvements have been made on the material used for coil cores. Better characteristics were sought in different directions, e.g. by modifying the shape of the metal particles and in the choice of insulating medium. Efforts were also made to obtain directional orientation of the metal particles by applying a magnetic field to them during the pressing process; but the principal work was directed towards the use of metallic alloys with a high initial permeability and low hysteresis losses. The best known alloys employed for this purpose are the nickel-iron alloys, such as Permalloy which was evolved in America.

Some details are given below of a material for making the cores of loading-coils, which was produced a few years ago in the laboratories of the Philips Works. The development of this material was based on the fact that the remanence must be small and *B* must be proportional to *H*. The magnetising curve had therefore to be of the form shown for the powder material Permalloy (see curve *B* in fig. *2*).

It was well known that certain nickel-iron alloys which had a very high remanence in the normal annealed state exhibited a lower remanence and a suitable hysteresis curve in the hard-rolled condition. A hard-rolled alloy of this type would therefore prove a suitable material for making cores if its necessary properties could be still further enhanced.

To investigate whether this could be done cores were made of a nickel-iron alloy which was rolled down to a strip of 60 microns, then insulated with varnish and finally wounded up to a coil core (see *fig. 3*). To enable the material to be rolled easily it was reheated several times during the rolling process.

It became immediately apparent in the first ex-

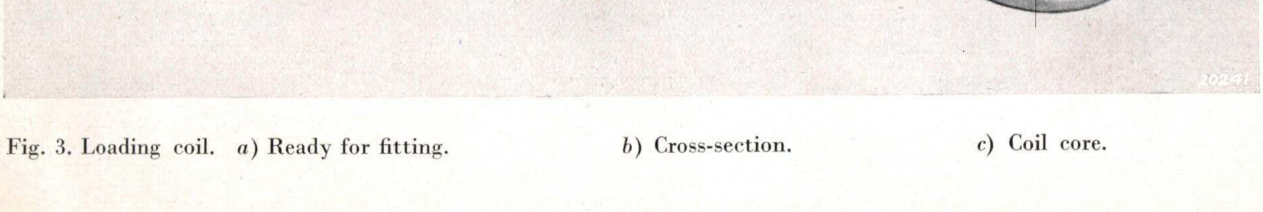

Fig. 3. Loading coil. *a*) Ready for fitting. *b*) Cross-section. *c*) Coil core.

periments made that cores manufactured by this process exhibited marked differences as regards hysteresis losses. These losses were five times greater with several coils as with others. The high hysteresis losses were always accompanied by a high remanence.

After tracking down the causes of these differences, the following manufacturing process was evolved, which furnishes a material with very low hysteresis losses and a satisfactory stability. A nickel-iron strip was rolled down to approx. 0.1 mm and recrystallisation then induced by reheating; the strip was then rolled down to 60 microns and again annealed at a temperature of approx. 400 °C during which stage no recrystallisation takes place.

Each of the four stages of this process has its own specific importance. During first rolling the nickel-iron undergoes marked deformation in the direction of rolling, as a result of which a very characteristic structure is obtained on subsequent recrystallisation: The axes of the crystals, with very low deviation, lie parallel to the length, breadth and depth of the strip.

This pronounced crystal structure causes the appearance of stresses in the material during the subsequent rolling process (reduction from 0.1 mm to 60 microns), the material also becoming magnetically anisotropic. The magnetisation curves of the rolled strip obtained on magnetisation in the direction of rolling and perpendicular to it are observed to be essentially different. The are given by the curves *B* and *A* respectively in fig. 2. We have thus obtained a material which on magnetisation in the direction of rolling has very low hysteresis losses.

The fourth stage in manufacture, annealling, is merely carried out for the purpose of reducing the internal stresses, as a result of which the permeability rises without the low hysteresis value in the longitudinal direction increasing too much.

The effect of this annealing process is shown clearly in *fig. 4*, giving the curves for the permeability μ, the hysteresis value q [4]) and the stability $\Delta L/L$ as a function of the temperature of annealing.

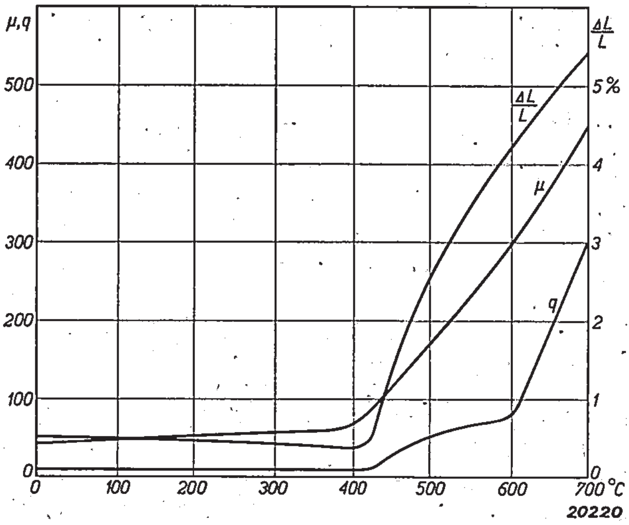

Fig. 4. Permeability μ, hysteresis value q and stability $\Delta L/L$ as a function of the temperature after last re-heating. It is seen that the hysteresis has its lowest initial value up to 400 °C. At this temperature the permeability has already considerably increased, while the stability has reached an optimum at this value.

For the type of coil shown in fig. 3 the following practical values were obtained.

Permeability $\mu = 80$

Hysteresis value $q = h/\sqrt{L} = 7$

Stability $\Delta L/L = 0.5$ per cent.

The volume of the core was 23 cm³ and that of the coil 60 cm³.

---

[4]) The hysteresis value $q = h/\sqrt{L}$ gives a figure for the hysteresis losses of the coil which is independent of the number of turns and is only determined by the dimensions and the material of the core. Here h is the hysteresis factor, i.e. the increase in the hysteresis loss resistance per henry and mA at 800 cycles/sec.

TELESCOPE MIRRORS

By H. J. MEERKAMP VAN EMBDEN.

Summary. The degree of precision to which the surface of mirrors must conform to the true shape for use in large reflecting telescopes is exceptionally high. Deviations from the true shape occur owing to sag and bending under its own weight and also owing to small temperature changes at the upper and lower surfaces of the glass disc. A process is described here in which the thick disc of glass normally employed is replaced by a chromium-iron casting, one surface of which is coated with a thin glass layer on which the reflecting surface is ground.

The history of astronomy and particularly of astrophysics is very closely related to the evolution of the instruments used for observations in these subjects. Before the invention of the refracting telescope only the paths of the planets could be observed and described; a deeper delving into the structure of the universe could not be essayed. The first refracting telescopes were made about 1580 by Giambettista della Porta in Italy and by Zacharias Jansen (1608) in Holland. The Dutch telescope, which was originally invented as an instrument for use in warfare and offered to Prince Maurits for this purpose, very soon became widely known and was also sold in Paris, Galilei in Padua thus obtaining information of its existence. He realised the importance of the invention and himself built a telescope on the same lines. From this time dates a rapid expansion of knowledge of the structure of universe: The discovery of the satellites of Jupiter, the "mountains of the moon", the starry clusters of the Milky Way, and spots of the sun, etc. By the applications of spectrum analysis and photography in the nineteenth century a more profound knowledge of these phenomena was gained.

Together with the refracting telescope, the reflecting telescope was also undergoing development. Newton (1640—1720) gave the first impetus to its evolution by his discovery that a mirror, contrary to a lens, does not possess chromatic aberration.

In the histories of the refracting and reflecting telescopes we are confronted with an example of the keenest mutual competition in which each instrument in its turn occupied the position of favour and preference. During recent years the reflecting telescope has come more and more to the fore, after a telescope with a mirror of 100″ diameter was put into commission in 1918 at the Mount Wilson Observatory. At the present time an instrument is under construction with a mirror having a diameter of 200″. It should be noted for purposes of comparison that the largest telescope, that at the Yerkes Observatory, is equipped with a lens of 40″ diameter, so that for the largest instruments the reflecting telescope holds unchallenged priority.

Yet both instruments have their own specific fields of application. The refracting telescope is employed in general for visual observations and for astronomical purposes, while the reflecting telescope, particularly those of large dimensions, is the ideal instrument for the observation of objects having a low luminosity as well as for spectrographic and photographic work. The image obtained with the refracting telescope is still sharp at some distance from the optical axis and in this respect gives better representation than the reflecting telescope; the latter is however a better condenser of the feeble light emitted from very distant objects. Moreover, reflecting telescopes are frequently favoured by amateurs since they are easier to make than refracting telescopes giving the same brightness of image.

To eliminate chromatic aberration the objective of a telescope must be composed of at least two lenses, which entails grinding and mutually centering four surfaces on each objective, as against only one surface in a reflecting telescope where chromatic aberration is absent. Furthermore, in the objective of a refracting telescope part of the incident light is reflected at the surface and absorbed by the glass; this absorption is most pronounced with short wavelengths to which photographic plates are most sensitive. The efficiency of the reflecting telescope is therefore the more satisfactory, especially as in the most modern types the surface is coated with aluminium instead of silvered, mainly because an aluminium coating gives a satisfactory reflection of that part of the spectrum required for photographic purposes. Reflection at the silvered surface of a telescope mirror is much reduced if the silver surface tarnishes by exposure to air, so that it must be renovated at regular intervals by replating.

The most important component of the reflecting telescope, the mirror, was originally made of metal.

Socalled "mirror metal", an alloy of 68.3 per cent copper and 31·7 per cent tin, has been known for many years and has proved extremely efficient. One disadvantage was, however, its brittleness and its difficulty to work, making the manufacture of large units impossible. By altering the composition it was indeed found possible to cast larger objects, but only at the expense of the surface, which after a short time lost its polish and no longer gave a good reflection. Owing to the extreme accuracy required of the surface, renovation cannot be resorted to and a metal mirror once having lost its reflecting surface cannot be reconditioned.

Nevertheless mirror metal was the only material available to the famous English builders of telescopes, Herschel, Lord Rosse and Lassell in the 19th century when constructing their large telescopes — up to a diameter of 72″ — with which they made a large number of important discoveries.

It was not until 1857 that Foucault described a new method of preparing a reflecting surface. He made a glass disc with the requisite shape of surface and by chemical means coated this surface with a very thin layer of silver. If the surface becomes dull by contact with the air, the silver was merely dissolved off and a new silver coating was deposited on it, without the shape of the surface being in the least way altered. This method was very successful and is still in general use. In recent years, however, Dr. Strong of Pasadena has evolved a process in which the silver coating is replaced by aluminium, which is deposited on the glass in a high vacuum by volatilisation. On exposure to air the aluminium becomes coated with an extremely thin film of oxide, but is subsequently not further attacked by the atmosphere.

If we examine the causes which limit the observation of extremely distant objects in the universe when using large telescope mirrors, we find that these causes fall naturally into two groups: One group is independent of the instrument used, and the other group is inherent in the instrument.

In the first group we have the lack of homogeneity of the atmosphere and the occurrence of disturbing light, and in the second group inaccuracies in the surface of the mirror and abnormalities due to stresses in the materials used and created in shaping them.

Difficulties Independent of the Instrument

The observation of objects beyond the earth's atmospheric mantle is rendered difficult because the air through which the emitted light reaches the observer is not at rest but in constant motion. If the air were homogeneous, this motion would have no effect; but owing to differences in temperature and humidity this is by no means the case, and the irregular refraction of the light rays during their passage to the instrument frequently prevents reliable observations being made.

In addition there are other disturbances due to the atmosphere surrounding the earth not being wholly transparent, but being permeated with dust and fog particles in suspension. Their presence not only causes diffuse dispersion of part of the emitted light, but has the same effect also on light from other sources, so that a star cannot be seen against a perfectly dark background but only against a background which itself appears to have a certain brightness. The greater the surface of the telescope mirror, the more light from the star under observation will be collected at the focus and the greater will be the contrast against the background.

To restrict the effect of this diffuse-dispersed light, it has been decided to erect the 200″ telescope now in course of construction in America not on Mount Wilson alongside the existing 100″ telescope, which is the largest one in use at the present time, but on Mount Palomas (3300 m) at a distance of 150 km. The reason for this is that the valleys surrounding Mount Wilson have become densely populated during recent years and it has become essential to locate the new observatory at some more distant spot.

Difficulties Inherent in the Instrument

While the difficulties described above are beyond the control of the instrument builder, he must nevertheless give the most careful consideration to the following points since they have a paramount bearing on the efficiency and utility of the instrument. We will therefore discuss these difficult points in order.

The correct theoretical shape for the surface of the mirror is a paraboloid and every deviation from this ideal shape results in a reduction in the quality of the image. The first question which therefore arises is: How far can the actual shape of the surface deviate from the ideal theoretical shape, in other words what tolerance is permissible in the preparation of the surface? The best known rule for this is that given by Lord Rayleigh, according to which the maximum deviation at any point must not exceed $^1/_8$ of the wavelength of visible light or approx. 0.07 μ. It is thus evident to what high degree of accuracy the surface must be worked, since in machining metals a precision to within several microns already calls for the most exceptional accuracy on the part of the machines used. That the difficulties in making large mirrors become rapidly greater with the size is also apparent, for it is a very different matter to work to this precision with a surface of 28″² (a mirror of 6″ diameter) than with a mirror of 30000″² surface, i.e. of 200″ diameter.

Although this requirement *per se* is already difficult enough to fulfil, it is rendered still more onerous by the fact that a telescope mirror is not a perfectly rigid body, since when the instrument is turned in different directions elastic deformation is set up within it while changes in shape are also produced by temperature gradients. As a result of these deviations a telescope may become quite useless.

Hitherto telescope mirrors have been made of glass, with the lower surface flat and the upper surface ground convex and then silvered. If a plate of this type is supported at three points in the usual way and is then turned out of its horizontal position in following the path of a star a deformation must inevitably occur. In a horizontal position the mirror bends at the centre under its own weight, while when exactly vertical the force of gravity creates a quite different type of deformation. In the case of a massive disc the deformation in the vertical position can be neglected, but this cannot be done when the plate is horizontal and has a diameter exceeding about 8″.

Consider two mirrors made of the same material, then according to investigations by Couder[1]) the sag of the mirror is proportional to R^4/h^2, where R is the radius and h the thickness of the mirror. It is thus possible to keep the deformation small by making the thickness large as compared with the diameter; but difficulties are then encountered in manufacture as well as in erection which limit the advantages to be gained by this means.

With two mirrors of the same dimensions, but of different materials, the sag at the centre was found to be proportional to d/E, where d is the density and E the modulus of elasticity. Thus if we compare glass and bronze, two materials which are commonly used for making mirrors, it is found that E is the same for both materials, viz. approx. $7 \cdot 10^5$ kg per sq cm, while the density of bronze is 8 and that of glass $2^1/_2$, so that in this case glass would be much more suitable than bronze.

In the large telescopes in use at various observatories, the mirror is usually given extra support at different points by means of a complicated system of levers with counterweights, thus eliminating the effect of the dead weight of the mirror. If these mirrors are raised towards the vertical, the opposing pressure applied by the counterweights diminishes.

We shall now turn to another factor which affects the deformation, viz., the variable temperature distribution over the mirror. Already during the manufacture of the mirror this effect becomes apparent, since the grinding media cause the evolution of heat on the worked surface, while the lower side of the mirror remains at a lower temperature. As a result the upper surface expands relative to the lower one, resulting in a deviation from the correct curvature, so that further grinding or measurement must be postponed until the temperature has again become uniform. The opposite state of affairs rules during the employment of the mirror: The surface directed towards the heavens becomes cooled during night observations, while the lower surface protected by a cushion of still air between the back of the mirror and the mount is subject to less cooling. This temperature difference again results in a change in shape, unless provision for a temperature equilibrium is made by thermal conduction of the glass and by radiation. Couder also investigated this phenomenon and found that with equivalent dimensions the deformation occurring is proportional to $a\,d\,c/k$, where:

a is the coefficient of linear expansion,
d the density,
c the specific heat, and
k the thermal conductivity.

To reduce these deformation effects Pyrex glass has been used in place of ordinary glass, the former having a lower coefficient of expansion and a greater thermal conductivity.

	Coefficient of expansion = Relative elongation per °C	Thermal conductivity cal cm^{-1} sec^{-1}
Pyrex glass	$3 \cdot 10^{-6}$	0.012
Ordinary glass	$9 \cdot 10^{-6}$	0.005

With metal mirrors a considerable improvement could be achieved in this respect, since the conductivity of metals is approx. 100 times greater than that of glass.

A third cause of deformation is that temperature differences can occur not only between the upper and lower sides of the mirror but also between the

---

[1]) A detailed investigation of this point is described by A. Couder in Bull. Astron. VII, 1931.

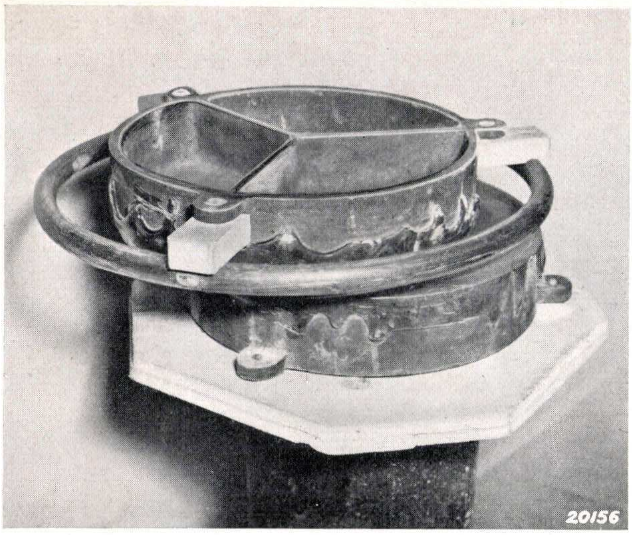

Fig. 1. Rear side of the 12″ mirror. The casting by which the mirror is later secured in the telescope can be clearly seen. During surface working which is done by hand a wood ring is attached to the casting to provide a grip.

rim and the centre. As a result of this the zone at the rim may become so highly deformed that the sole remedy possible is to place a diaphragm in front of the mirror, which naturally reduces its useful reflecting surface. In this respect again a metal mirror would be less sensitive.

Mirrors in the past have been made exclusively in the form of massive discs, except the 200″ mirror of Pyrex glass now in course of manufacture, which is made up of a plate ribbed on the lower side. A ribbed construction of this type offers various advantages, but could not be hitherto employed owing to the great difficulty of casting complicated shapes of glass.

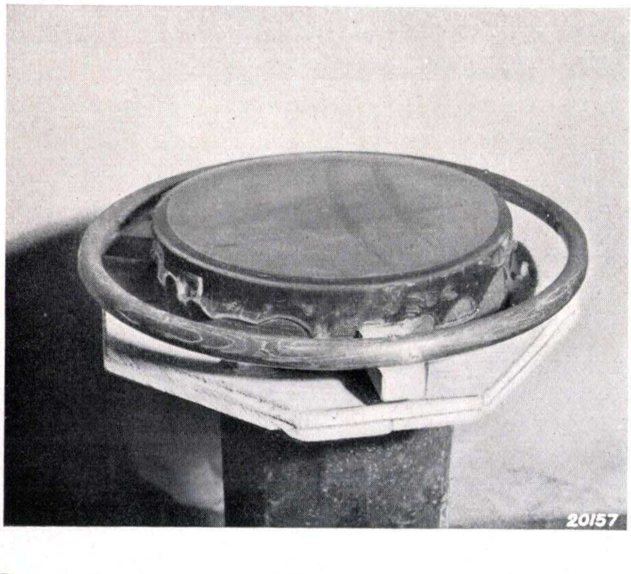

Fig. 2. Casting for a 12″ concave mirror (focal length 80″). On affixing the glass, part has run over the edge. Shaping is done by polishing two glass discs one against the other, using a suitable lubricant (carborundum, alundum or rouge).

The casting of metals is much simpler, although by using metals the important disadvantage already referred to remains, viz., that the surface of the mirror is difficult to work and rapidly deteriorates.

A way to overcome the difficulty has been investigated at this Laboratory for some time past; the new method of manufacture evolved is based on a combination of the desirable properties of glass and metal, viz., the use of a metal mirror which on the upper side is coated with a very thin skin of glass on which the mirror surface is ground.

The metal used is a special chromium-iron alloy whose coefficient of expansion is the same as that of glass and to which the glass can very tenaciously adhere. This alloy has found extensive use in vacuum-tight metal-to-glass unions, which form an important component in the larger types of rectifying valve, in transmitting valves and X-ray tubes.

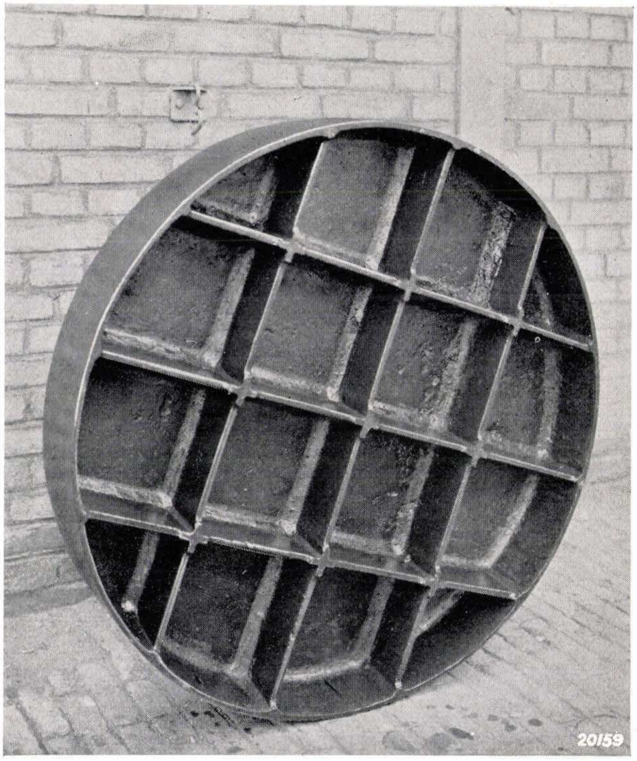

Fig. 3. Rear side of the 35″ mirror. The supporting framework provides the necessary stiffening for the thin upper surface on which the glass is fused.

The manufacture of castings from chromium-iron is not much more difficult than from steel and is much simpler than from glass.

Any shape can be cast and the strengthening ribs can be made as thin and as high as required for obtaining the requisite strength, at the same time realising a low weight. Eyes and lugs can also be readily cast on, which can be later machined and threaded to facilitate the fixing of the mirror in its support.

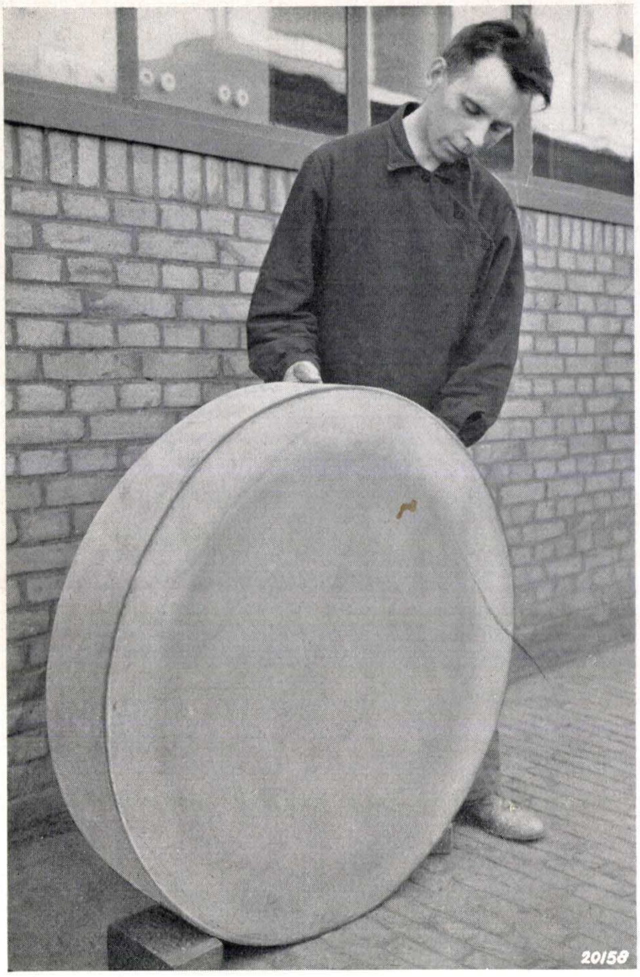

Fig. 4. Chromium-iron casting of 35″ diameter, covered on the front with glass to a thickness of 10 mm (shaded). The glass is later ground completely smooth, after which the surface is silvered.

The casting is readily relieved of internal stresses by reheating, while for the same end glass mirrors must usually be allowed to cool for several months under the most carefully controlled conditions.

The chromium-iron casting is first machined on the rear side and turned flat in a lathe so that the mirror will later lie quite flat when mounted in the polishing machine. The workpiece is then reversed and the top surface which is later covered with glass is then machined. In this operation the surface is roughly shaped to conform with the final surface contour of the mirror.

This is followed by the application of the glass coating. A glass plate is laid on the casting and the assembly then heated in a furnace to above the softening point of the glass. The glass melts and forms a bond with the metal surface below it; the fused glass must not be allowed to get too fluid so that with a concave mirror the whole of the glass collects at the centre. If this operation is correctly performed the glass coating forms a layer of uniform thickness over the whole surface and can therefore be maintained very thin. Little has then to be removed in the subsequent machining process, although the principal advantage is that the thin glass layer can be cooled very rapidly without the production of internal stresses. Cooling takes as many hours as months were required in the past. It is also possible to sort out the glass plates at the outset and reject all those with any suspicion of air bubbles, inclusions or other defects.

In this way the advantages of metal and glass can be combined, viz., the easy machinability, good conductivity and ease in fixing of metal and the excellent surface and every facility for silvering or aluminium coating offered by glass.

A concave mirror 12″ in diameter (*figs. 1* and *2)* manufactured by this process was placed at the disposal of a number of amateur astronomers at Eindhoven, who are now grinding it down to give a focal length of 80″. This mirror will be used in a telescope being built for its reception.

A plane mirror with a diameter of 36″ (*figs. 3* and *4)* was supplied to the Californian Institute of Technology. It is now being ground and is to be used as a mirror in a coelostat, i.e. an instrument which at a plane mirror rotated by clockwork reflects the light emitted from a star or other heavenly body so that the measuring instruments used can be kept stationary.

When using such coelostats for solar observations, a glass mirror introduces considerable difficulties owing to the marked differences in temperature which occur during the measuring period, while metal mirrors have the disadvantage that the surface gradually deteriorates and the power of reflection becomes considerably reduced.

The advantages of the new process thus become strikingly apparent in this application.

ELECTRICAL FILTERS V

Vacation course, held at Delft, April, 1936,

By BALTH. VAN DER POL and TH. J. WEIJERS.

Summary. In this article the transient phenomena in non-dissipative low-pass filters are analysed. With the aid of Heaviside's operational calculus the cut-in current of the n-th section of an infinitely long filter composed of a number of equivalent sections of basic type is calculated. By repeated subdivision of the filter sections the continuous cable is obtained at the limit with uniformly-distributed inductance and capacity. On passing to the limit, it is found that the impressed impulse is propagated without distortion and at a specific velocity through a non-dissipative cable. It is indicated in the last section how the transient phenomena in high-pass filters can be deduced from those derived for low-pass filters.

In the previous articles of this series the behaviour of filters when sinusoidal e.m.f. is impressed on them was investigated. From the results obtained the behaviour of the filter on the application of a non-sinusoidal but still periodically-varying voltage could also be deduced. This voltage can be expanded as a Fourier series, each term of which can be dealt with independently and the results then added by the principle of superposition (p. 242).

Conditions are, however, different where the voltage is not a periodic function, and in this case it is not possible to expand it as a Fourier series. An example of a non-periodic voltage sequence is the phenomenon obtained when closing a circuit; in this case transient phenomena are encountered.

These phenomena will be analysed in detail below. The simplest case is the sudden impression of a direct voltage which will be assumed, for the sake of simplicity, to be unity, and to remain constant after the circuit is closed, on a filter carrying neither current nor voltage. *Fig. 1* gives this voltage as a function of the time: For $t < 0$, $V = 0$ and for $t > 0$, $V = 1$.

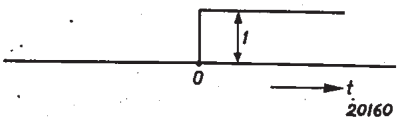

Fig. 1. The Heaviside unit function.

This function will be termed the unit function, in accordance with Heaviside, and will be represented by the symbol [1]. In this article we shall limit discussion to low and high-pass filters of fundamental form when this unit voltage-time function is impressed on them.

We shall employ the operational or symbolic calculus, which is based on the following principle: If $i(t)$ is an arbitrary function of the time, a function with another variable p can be obtained by means of the following expression (Carson's integral):

$$p \int_0^\infty e^{-pt}\, i(t)\, dt = f(p) \quad . \; . \; . \; . \quad (1)$$

The symbolic form of equation (1) is:

$$i(t) \doteqdot f(p) \quad . \; . \; . \; . \; . \; . \; . \; . \; . \quad (2)$$

For each given function $i(t)$, $f(p)$ is defined by (1) and vice versa. $f(p)$ is termed the operational representation of $i(t)$. If $i(t)$ represents a current and if at time $t = 0$ the current and all time derivatives are equal to zero, then it follows that:

$$\left.\begin{aligned} \frac{d}{dt}\, i(t) &\doteqdot p\, f(p)\;; \\ \frac{d^2}{dt^2}\, i(t) &\doteqdot p^2 f(p)\;; \\ &\vdots \\ \frac{d^n}{dt^n}\, i(t) &\doteqdot p^n f(p)\,. \end{aligned}\right\} \quad . \; . \; . \; . \quad (3)$$

Differentiation with respect to t therefore corresponds to a multiplication by p (and not by $j\,\omega$, as in the complex method). Similarly integration corresponds to a multiplication by $1/p$. We get by calculation with the aid of equation (1):

$$\int_0^t i(t)\, dt \doteqdot \frac{1}{p}\, f(p) \quad . \; . \; . \; . \; . \; . \quad (4)$$

We thus obtain a transformation from the known complex method to the operational calculus, if $j\,\omega$ is replaced by p.

The operational representation of the unit function [1], which is now under consideration, is according to equation (1):

$$[1] \doteqdot p \int_0^\infty e^{-pt}\,[1]\,dt = p \int_0^\infty e^{-pt} \cdot 1 \cdot dt = 1\,,$$

$$[1] \doteqdot 1 \quad \ldots\ldots\ldots \quad (5)$$

A potential impressed at the time $t = 0$ which subsequently remains constant is thus represented in the operational calulues by a constant which is equal to the absolute value of this potential.

Low-Pass Filter of Basic Type on the Application of the Heaviside Unit Function

Consider a low-pass filter composed of an infinite number of T-sections of basic type (*fig. 2*), or what is the same thing as regards the currents and voltages in the filter, of a finite number of sections which are terminated by the image impedance.

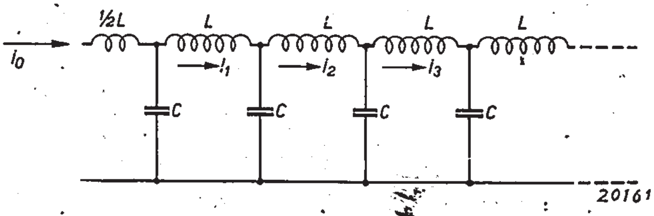

Fig. 2. Low-pass filter composed of an infinite number of T sections of basic type.

We shall discuss this filter in the first place as again having a sinusoidal e.m.f. impressed on it, using the complex method of representation $E_0 e^{j\omega t}$. We shall here make use of the formulae for low-pass filters which were derived earlier [1]) and which are collected together in a comprehensive table on p. 305 of this Review. For the image impedance Z_T', i.e. here the impedance between the primary terminals, we have:

$$Z_T' = R\sqrt{1-x^2} = \sqrt{\frac{L}{C}}\sqrt{1-\frac{\omega^2}{\omega_1^2}} \quad . \quad (6)$$

and the propagation constant T of a single section is given by the expression:

$$e^{-T} = \frac{\sqrt{1-x^2}-jx}{\sqrt{1-x^2}+jx} = \left(\sqrt{1-\frac{\omega^2}{\omega_1^2}} - j\,\frac{\omega}{\omega_1}\right)^2 \quad . \quad (7)$$

Equations (6) and (7) give Z_T' and T as functions of the angular frequency. ω_1 is the angular frequency at the boundary of the transmission band. The secondary current of the n-th section is i_n, i.e. the primary current of the n-th section (= the secondary current of the $(n-1)$th section) is i_{n-1}.

The primary current of the first section is thus i_0. If now the voltage between the primary terminals of the filter is $E_0 e^{j\omega t}$, we have:

$$i_0 = \frac{E_0 e^{j\omega t}}{Z_T'} \quad \ldots\ldots \quad (9)$$

$$i_n = \frac{E_0 e^{j\omega t}}{Z_T'}\, e^{-nT} =$$

$$= \frac{E_0\, e^{j\omega t}}{\sqrt{\frac{L}{C}}\sqrt{1-\frac{\omega^2}{\omega_1^2}}}\left(\sqrt{1-\frac{\omega^2}{\omega_1^2}} - j\,\frac{\omega}{\omega_1}\right)^{2n} \quad . \, . \quad (10)$$

What does i_n become if no sinusoidal voltage is impressed across the primary terminals of the filter, but a unit potential function [1]? We obtain the operational representation of this current $i_n(t)$ by substituting in equation (10) p for $j\,\omega$ and 1 for $E_0 e^{j\omega t}$, thus:

$$i_n\,(t) \doteqdot \sqrt{\frac{C}{L}}\,\frac{1}{\sqrt{1+\frac{p^2}{\omega_1^2}}}\left(\sqrt{1+\frac{p^2}{\omega_1^2}} - \frac{p}{\omega_1}\right)^{2n} \quad . \quad (11)$$

In order to determine to which time function this operational expression (11) corresponds, i.e. how the current in the n-th branch depends on the time, expression (11) is substituted in the integral equation (1). We have therefore to solve the integral equation:

$$p\int_0^\infty e^{-pt}\,i_n(t)dt = \sqrt{\frac{C}{L}}\,\frac{1}{\sqrt{1+\frac{p^2}{\omega_1^2}}}\left(\sqrt{1+\frac{p^2}{\omega_1^2}} - \frac{p}{\omega_1}\right)^{2n} \quad (12)$$

and to answer the question: What function $i_n(t)$ on integration gives this result?

The operational representation of a large number of functions is known; the right hand side of equation (11) belongs to the group of known expressions:

$$\int_0^{\omega_1 t} J_{2n}\,(x)\,dx \doteqdot \frac{1}{\sqrt{1+\frac{p^2}{\omega_1^2}}}\left(\sqrt{1+\frac{p^2}{\omega_1^2}} - \frac{p}{\omega_2}\right)^{2n} \quad . \quad (13)$$

It thus follows from (11) and (13):

$$i_n\,(t) = \sqrt{\frac{C}{L}}\int_0^{\omega_1 t} J_{2n}\,(x)\,dx\,, \quad . \, . \, . \quad (14)$$

where $J_{2n}(x)$ is the Bessel function of the $2n$-th order with the argument x.

Equation (14) thus gives the current obtaining behind the n-th section of a low-pass filter composed of T-sections of basic type, if at the input of the filter at time $t = 0$ a direct voltage of unit value is suddenly applied, and the filter before $t = 0$ carried neither current nor voltage.

---

[1]) Philips techn. Rev. 1, 298, 1936.

Fig. 3 shows the current in the self-induction of the fourth section, i.e.

$$i_4(t) = \sqrt{\frac{C}{L}} \int_0^{\omega_1 t} J_8(x)\, dx$$

as a function of $\omega_1 t$. It is seen that the current $i_n(t)$ remains very small up to time $t = 2n/\omega_1$; it then commences to be built up and finally fluctuates about $\sqrt{C/L}$ with gradually diminishing amplitude. This is the analogue of the finite time of transmission of a signal as found in the case of cables. In our case the current has passed through n sections in the time $t = 2n/\omega_1$, so that per second $n/t = {}^1/_2\, \omega_1$ sections are traversed. The velocity of propagation is therefore ${}^1/_2 \cdot \omega_1 = 1/\sqrt{LC}$ sections per second.

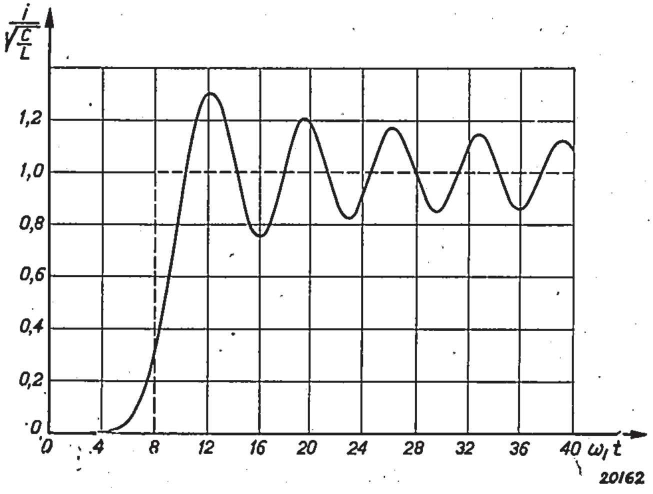

Fig. 3. The current in the self-induction of the fourth section of a low-pass filter composed of an infinite number of sections of basic type (or a finite number of sections terminated by the image impedance), when unit potential [1] is impressed at the input of the filter at $t = 0$. This current is represented by

$$i_4(t) = \sqrt{\frac{C}{L}} \int_0^{\omega_1 t} J_8(x)\, dx,$$

where ω_1 is the limiting frequency of the filter. The broken line indicates the current at the same point when the filter is transformed into a continuous cable by infinite subdivision of the filter sections.

Transition from a Low-Pass Filter to a Continuous Cable

The filter discussed in the previous section consisted of a group of equivalent T-sections connected in series. If each T-section is replaced by a series-connected group of other T-sections, with self-inductions and capacities an m-th part of the original filter, the total self-induction and total capacity will both remain unchanged. Since, furthermore, the limiting frequency of the filter $\omega_1 = 2/\sqrt{LC}$ is determined by the self-induction and the capacity per section, it will be multiplied by m on subdivision of the section. If this demultiplication is continued ad infinitum, we get the continuous cable at the limit $m \to \infty$ viz., a uniformly distributed self-induction in series and uniformly-distributed capacity in parallel throughout the cable. As m has been taken to infinity, the limiting frequency of the cable will be infinite. A cable devoid of resistance (i.e., non-dissipative) will transmit all frequencies without attenuation. The impedance of the cable is the limiting value of

$$Z_T' = \sqrt{\frac{L}{C}} \sqrt{1 - \frac{\omega^2}{\omega_1^2}}$$

i.e.

$$Z_T' = \sqrt{L/C}.$$

The behaviour of the cable on the application of the unit function [1] can be derived from the behaviour of the filter already investigated and from which we have derived the cable as the limiting case.

Consider the point A which in the original filter was located at the end of the n-th section, and assume that the current at that point is $i_A(t)$. If each section is subdivided into m sections, then for each new section the self-induction will be L/m and the capacity C/m, so that the limiting frequency of the filter is no longer $2/\sqrt{LC}$, but:

$$\omega_1 = \frac{2m}{\sqrt{LC}} \quad . \; . \; . \; . \; . \; . \quad (15)$$

The current at the point A now follows from equation (11):

$$i_A(t) = i_{mn}(t) \doteqdot \sqrt{\frac{C}{L}} \frac{\left(\sqrt{1 + \frac{p^2 LC}{4m^2}} - \frac{p\sqrt{LC}}{2m}\right)^{2mn}}{\sqrt{1 + \frac{p^2 LC}{4m^2}}}. \quad (16)$$

If subdivision of the sections is continued to infinity, i.e. $m = \infty$, the filter passes over into the continuous cable. The total self-induction between the input of the filter and the point A remains $n\,L$, and the total capacity $n\,C$. If l is the length of the cable between the input and the point A, the self-induction per unit of length is $\overline{L} = nL/l$ and the capacity per unit of length $\overline{C} = n\,C/l$. For the sake of abbreviation insert $1/\sqrt{\overline{L}\,\overline{C}} = c$ and we get:

$$LC = \frac{l^2}{n^2}\, \overline{L}\, \overline{C} = \frac{l^2}{n^2 c^2} \quad . \; . \; . \; . \quad (17)$$

Substitution in equation (16) then gives:

$$i_A(t) \doteqdot \sqrt{\frac{C}{L}}\,\frac{\left(\sqrt{1+\frac{p^2l^2}{4m^2n^2c^2}}-\frac{pl}{2mnc}\right)^{2mn}}{\sqrt{1+\frac{p^2l^2}{4m^2n^2c^2}}} \quad . \quad (18)$$

If m in this expression is taken to infinity, we get the limiting case of the continuous cable, thus:

$$i_A(t) \doteqdot \lim_{m\to\infty} \sqrt{\frac{C}{L}}\,\frac{\left(\sqrt{1+\frac{p^2l^2}{4m^2n^2c^2}}-\frac{pl}{2mnc}\right)^{2mn}}{\sqrt{1+\frac{p^2l^2}{4m^2n^2c^2}}} =$$

$$= \lim_{m\to\infty} \sqrt{\frac{C}{L}} \cdot 1 \cdot \left(1-\frac{pl}{2mnc}\right)^{2mn} =$$

$$= \sqrt{\frac{C}{L}} \cdot e^{-pl/c} \; . \; . \; . \; . \; . \; . \; . \; . \; . \; . \; . \; . \quad (19)$$

Since the impedance of the cable at every point is $\sqrt{L/C}$, the operational representation of the voltage at the point A is:

$$e_A\,(t) \doteqdot e^{-pl/c} \; . \; . \; . \; . \; . \; . \quad (20)$$

This is, the operational representation of the unit function [1], which however does not operate at $t = 0$, but at $t = l/c$, as demonstrated in *fig. 4*.

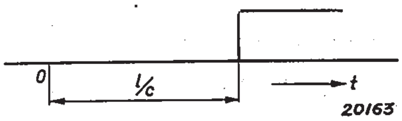

Fig. 4. Current through a continuous cable at a distance l, when the potential at the input is represented by the Heaviside unit function.

Thus the unit potential [1], which was impressed on the cable at the input end, arrives at the point A free from distortion as a unit potential after the elapse of the time $t = l/c$. Hence on the transition from a low-pass filter to a continuous cable a distortionless propagation is obtained with a time of transmission of l/c, in accordance with the elementary theory of electric cables. Propagation has in fact become free from distortion because the limiting frequency in the transmission band has been displaced to infinity. For a non-dissipative cable located in an area without dielectric losses and with a dielectric constant $\varepsilon = 1$ the self-induction and capacity assume such values that the velocity of propagation c is equal to the velocity of light. If $\varepsilon > 1$, c will be smaller than the velocity of light.

Transient Phenomena with High-Pass Filters of Fundamental Form

Hitherto we have limited discussion to transient phenomena with low-pass filters; the results obtained can be applied to high-pass filters with the aid of a mathematical transformation by which the transient phenomena in a second network can be calculated when those in the first network are known. A necessary condition before this can be done is that the second network must be a frequency-reciprocal of the first network, i.e. it must possess self-inductions at those points where the first network has capacities, and capacities at those points where self-inductions are located in the first network, while the resistances in the two networks must be the same. The values of C^*, L^* and R^* of the second network must be related to the L, C and R values of the first network according to the following expressions:

$$\frac{1}{\omega_1\,C^*} = \omega_1\,L\;,$$

$$\frac{1}{\omega_1\,L^*} = \omega_1\,C\;,$$

$$R^* = R\;,$$

where ω_1 is an arbitrary angular frequency in radians. If ω_1 is taken equal to the limiting frequency of the low-pass filter, the latter will pass on applying the above-mentioned mathematical transformation into a high-pass filter with the same limiting frequency and it becomes possible to deduce from expressions derived on highly generalised assumptions [2] the transient phenomena in high-pass filters in a closed form, directly from the known expressions for low-pass filters as demonstrated above.

Since the high-frequency components of the voltage impulse applied to the first section in this case allow current to flow instantaneously through all series-connected capacities, the retardation found with low-pass filters is absent here, and the currents in all circuits exhibit a discontinuous front, which to some extent complicates mathematical representation. We shall not consider this point in greater detail.

---

[2] Balth. van der Pol, Physica 1, 521, 1934.

GAS-FILLED TRIODES

By H. G. BOUMEESTER and M. J. DRUYVESTEYN.

Summary. In this article a description is given of a gas-filled triode, which contains in addition to a cathode, a grid and an anode a cathanode. The manner in which it works and the possibilities of its application are dealt with.

To obtain a specific amplification with the smallest number of amplifying valves, valves must be used in which a definite variation in the grid voltage produces the greatest possible change in the anode current. In receiving valves of normal ratings the ratio between these two variations, the socalled slope or gradient, is rarely greater than 10 milliamps per volt. Yet if triodes of standard ratings are filled with a small quantity of gas [1]) a slope of 30 milliamps per volt and even more can be realised. In spite of this desirable result there are, however, two important objections against the use of a valve of this type, viz., its marked noise and the fact that the steep slope is maintained only at low frequencies; at higher frequencies (roughly above 10^6 cycles) the slope drops to a much lower value. The relationship between the slope and the frequency is evident when it is remembered that the occurrence of a high slope when using a gas filling is due to ionisation by electrons in the vicinity of the anode; the resultant positive ions possess only a low velocity and thus remove from the space charge a much greater number of electrons, so that the anode current increases considerably. It is just this slow displacement of the positive ions (a result of their great mass) which is responsible for the reduced gradient at higher frequencies.

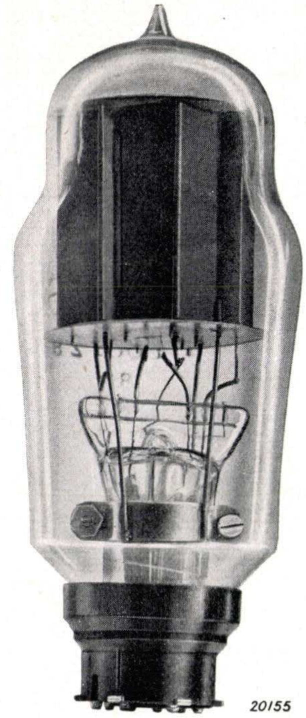

Fig. 1. The gas-filled triode.

Some time ago [2]) a valve filled with mercury vapour was described which could be used as triode and which did not possess the above-mentioned disadvantages of the gas-filled triode; in this valve a greater slope was moreover achieved in a somewhat different manner. The general appearance of the valve may be gathered from *fig. 1*, while *fig. 2* shows a section through the Philips type of this valve. *K* is an indirectly-heated cathode. At a distance of 10 mm from the cathode is a rectangular grid (*KA*) made of gauze. It is seen from the longitudinal section that the upper and lower sides of the grid are covered by mica plates *m*. Immediately behind the first gauze there is a second gauze at

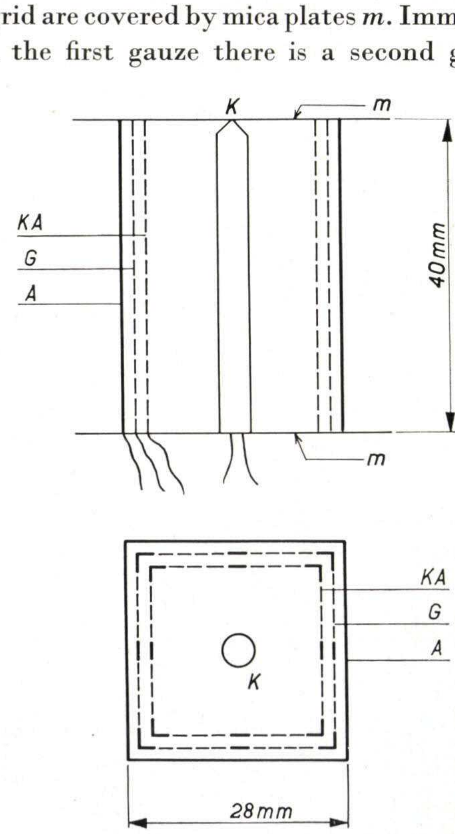

Fig. 2. Section through the gas-filled triode. *K* cathode; *KA* cathanode; *G* grid; *A* anode and *m* mica plates for limiting the discharge.

---

[1]) Gas-filled valves were used already 20 years ago.

[2]) J. R. Nelson and J. D. le Van, Q.S.T. June 1935, p. 23.

a distance of 1 to 1.5 mm, and directly behind the latter a plate bent at right angles which serves as the anode. The valve bulb contains a drop of mercury so that an atmosphere of mercury vapour is present between the electrodes. The valve functions on the following lines: Between the cathode and the first gauze an arc discharge is produced for which this gauze acts as anode. In the arc a large number of positive ions are formed which dilute the space charge of electrons, so that the running voltage of the arc (i.e. the voltage between cathode and anode) is low, for example 10 volts. Electrons pass through this gauze-like electrode and are attracted to the plate by the second gauze. The plate thus performs the same function as the anode in a vacuum valve, while the second gauze is fully comparable to the grid of a vacuum valve. The first gauze may be compared on the one hand to the cathode of a vacuum valve, and since on the other hand it constitutes the anode of the arc discharge it is termed the "cathanode".

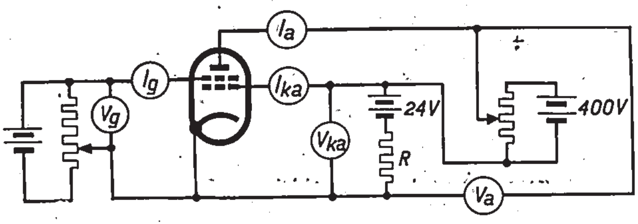

Fig. 3. Circuit for plotting the characteristics. V_a anode voltage, V_{ka} voltage at the cathanode, V_g grid potential, i_g grid current, i_{ka} cathanode current, i_a anode current and R resistance for stabilising the arc discharge.

To measure the characteristics of this valve the circuit shown in *fig. 3* is employed. The arc current, which is e.g. 500 mA, is furnished by a 24-volt battery through a resistance R. The grid and anode voltages are varied by means of potentiometers and the usual characteristics then plotted. The arc current flowing to the cathode is not altered during this measurement, but only that part of this current which flows from either the cathanode or the anode. *Figs. 4* and *5* reproduce a number of characteristics in which the anode current i_a is plotted as a function of the anode volts V_a and the grid voltage V_g respectively. In the example illustrated in the graphs the slope was 27 mA per volt, and the internal resistance 1900 ohms, so that the amplification factor was 51. It is seen that the slope increases with the arc current, while the amplification factor meanwhile changes very little.

The properties of this valve may be explained by regarding the cathanode as a cathode, the action of the valve then being identical to that of a vacuum triode [3]). Since the surface of the cathode is very large and the grid is located close to the cathode, the steep slope is readily accounted for. The number of positive ions formed between the grid and the anode is small and is not a measure of the slope. As on varying the grid voltage the anode current is also altered but not the arc current, while at the same time the number of positive ions formed between the cathode and the cathanode remains constant, it would be expected that the slope is not related to the frequency, provided the latter does not assume such high values that the time of transit of the electrons has to be taken into consideration. In fact this valve may be quite readily used as an oscillator at a wavelength of, for example, 200 m. The other disadvantage of gas-filled valves mentioned at the outset, viz., the pronounced noise, is also absent in this valve.

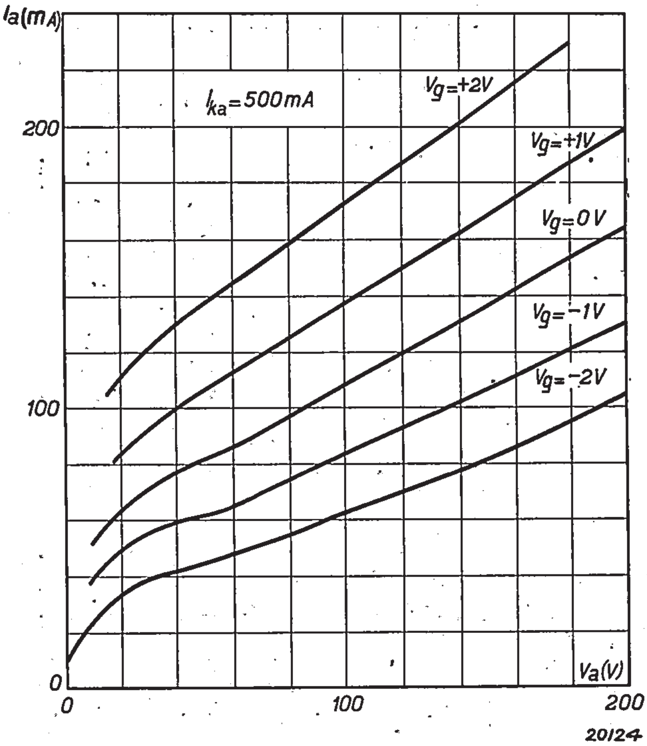

Fig. 4. Characteristics of the anode current i_a as a function of the anode volts V_a for different values of the grid potential V_g. The cathanode current i_{ka} is here 500 mA.

---

[3]) A fundamental difference between this virtual cathode and the normal oxide cathode of a vacuum valve is that the mean velocity of emission of the electrons in the second case is only about 0.1 volt as against several volts with the cathanode. It is desirable for the velocity of emission of the electrons at the cathanode to be as low as possible, since the slope increases as the velocity of emission diminishes. This velocity can be reduced by raising the gas pressure as well as by increasing the arc current; the form of the discharge space can also be made more efficient than shown in fig. 2. If, for instance, the anode is enclosed by two grids and the discharge is produced in the outer space where also the cathode must be situated, the discharge space is enlarged and the velocity of the electrons at the cathanode is reduced.

On comparing this valve with vacuum valves it is found that in spite of the absence of the disadvantages referred to above its general application is nevertheless restricted by several properties in which it differs from those of the vacuum valves. The principal divergent properties are:

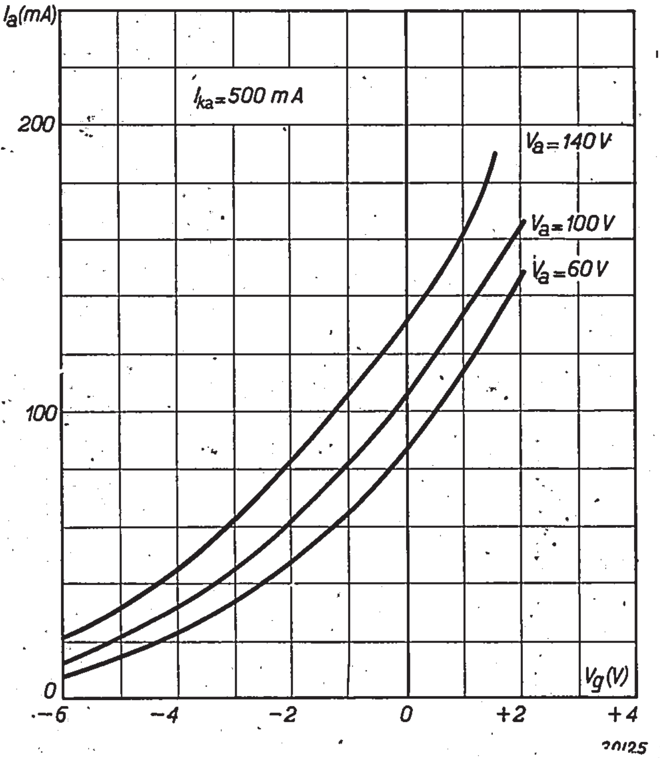

Fig. 5. Characteristics of the anode current i_a as a function of the grid volts V_g for different values of the anode voltage V_a. The cathanode current i_{ka} is here 500 mA.

1) The cathanode current introduces an additional complication, especially as it is fairly high, e.g. 500 mA, and must be kept constant to a high degree.
2) The grid currents are high, being for instance several mA [4]).
3) The grid-anode capacity is high, since the distance between the electrodes is small, this small interval being indeed necessary in order to limit the ionisation: By introducing a screen grid between these electrodes the capacity can however be considerably reduced.
4) As the pressure of the mercury is governed by the temperature, the characteristics usually vary with fluctuations in the room temperature or when the valve is cooled by a current of air [5]).
5) The i_a-V_g characteristic has a fairly pronounced curvature.

Since these properties are on the whole inherent in the valve described, they restrict considerably the possible use of the valve. It is evident that these properties will prove more undesirable in some applications than in others.

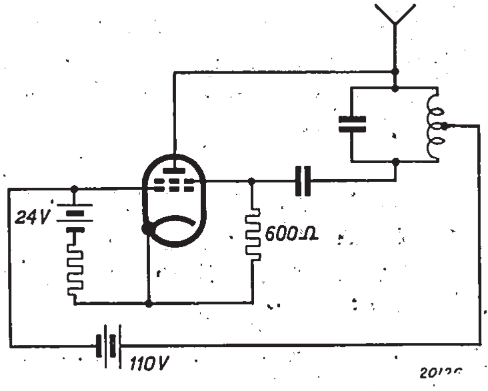

Fig. 6. Circuit for a gas-filled triode used as oscillator in a one-valve transmitter for operating on an anode voltage of 110 V. The cathanode current is furnished by a 24-volt battery.

This valve can be used with marked satisfaction as an oscillator in one-valve transmitters, the pronounced slope permitting the operation of a transmitter of the type shown in *fig. 6* from a 110-volts supply. The anode consumption is here 12 watts, the cathanode current 400 milliamps, and the high-frequency energy 6 watts at a wave-length of 670 m.

---

[4]) While with a negative grid bias (with reference to the cathode) a current of positive ions flows to the grid which hardly varies with the grid potential, a current of electrons which will vary with the grid potential will flow to the grid when the bias is positive.

[5]) This difficulty could be overcome by using an unsaturated mercury vapour instead of saturated one, or by filling the valve with a rare gas at a low pressure. In the latter case the slope is, however, smaller than when using mercury vapour.

THE DAMPING OF MECHANICAL VIBRATIONS

By A. CRAMWINCKEL, C. J. DIPPEL and G. HELLER.

Summary. Two factors: friction and the decay of the restoring stresses determine the properties of damping agents. In the present article an investigation is made as to how the damping properties depend on the frequency taking into consideration the above two factors. Two groups of damping agents can be distinguished which exhibit fundamentally different behaviours towards vibrations. In the first group, the damping depends mainly on the decay of the restoring stress, and in the second it is due mainly to internal friction. A damping agent of the second group is described, which is suitable for damping the resonances of vibrating mechanical systems.

In the construction of vibrating mechanical systems (for instance for acoustic purposes) it is frequently necessary to damp the undesirable natural vibrations without excessively reducing the sensitivity of the system. In many cases suitable damping can be obtained with air or, where a more powerful action is required, with oil or other fluid. But in many apparatus these forms of damping are not desirable or cannot be realised in practice; it becomes necessary to employ solid damping agents.

Since the damping of vibrations plays an important part in modern engineering, some of the more important aspects of damping agents will be discussed below. We shall first discuss the principal causes producing the damping of vibrations, taking as an example a rectilinear vibration of a point mass under the action of elastic and damping forces. This will be followed by the analysis of a specific technical problem.

Friction and Decay of Restoring Forces as Damping Causes

Two causes of damping will be considered below¹). The first, friction, is a general phenomenon well known in mechanics. It can be represented by a force which, contrary to elastic forces, always acts in a direction opposite to that of the motion affected and at the same time increases with the velocity. In the simplest case (liquid friction) this force is proportional to the velocity:

$$\text{Force of friction} = -a\,v = -a\frac{d\,x}{d\,t} \quad (1)$$

where x is the distance traversed and a is the coefficient of friction.

There is also a second factor causing the damping of vibrations. If a material, such as ebonite, is allowed to remain for a long time in an elastically deformed state, it will be found that on being released it does not return either at all or wholly to its initial state of equilibrium. The reason for this is that the forces of restitution do not correspond to perfect elasticity, but gradually decay with the lapse of time owing to molecular rearrangements. If with such a material the external forces impressed on it are kept constant, the material will begin to flow in such a way that a reduction of the elastic forces results. If the time of decay τ is introduced ²), we have the differential law:

$$dK = -c\,d\,x - K\frac{dt}{\tau} \quad . \; . \; . \; . \; . \quad (2)$$

This law states that the force of restitution with a sufficiently rapid vibration is proportional to the elongation ($K = -c\,x$). If the system is arrested after deflection a decay of the forces will, however, take place with a lapse of time according to the law:

$$\frac{dK}{K} = -\frac{dt}{\tau}.$$

It may be readily seen that this phenomenon also results in a damping of the vibrations. If, for instance, we represent the velocity v by an electric current i and the force K by a voltage V, then the conditions of damping resulting for a point mass are analogous to the damping of an oscillating circuit by a resistance r in series and a second resistance R in parallel to the condenser (see *fig. 1*). It is thus evident that this electrical problem satisfies exactly the same differential equations as the mechanical model, if the circuit elements are so chosen that:

---

[1] A detailed discussion of these questions is to be found in J. M. Burgers, Ned. T. Natuurk. 1, 209, 1934; First Report on Viscosity and Plasticity, Proc. Roy. Ac. Sc. A'dam, Physics I., Vol. XV, No. 3.

[2] The assumption of a time of decay τ independent of the restoring forces, as in the case of our model, signifies that the material already begins to flow at the lowest applied force. In practice, with flow phenomena one is mostly dealing with materials which only commence to flow appreciably above a specific force, the socalled yield point.

$$C = 1/c$$
$$L = m$$
$$r = a$$
$$R \cdot C = \tau$$

It is well known that both the series resistance r and the shunt resistance R produce a damping of the oscillations. Thus in our mechanical model a damping is similarly produced, both as a result of friction and of the decay of the restoring forces.

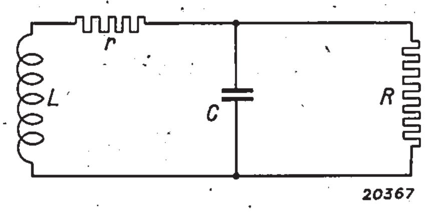

Fig. 1. Substitution circuit for a mechanical vibration with friction and decay of restoring forces. In place of the coefficient of friction a we have the resistance r, and in place of the time of decay τ of the forces of restitution the time of discharge RC of the condenser.

Behaviour of Damping Agents with respect to Forced Vibrations

The behaviour of damping agents has a much greater practical importance with respect to forced vibrations — the arresting of vibrating mechanical systems — than with regard to free vibrations. The necessary calculations can be readily carried out by introducing, in addition to the internal forces, which are the same as those for free vibrations, also an external force $k \sin \omega t$.

The following expression is obtained for the absolute value of the amplitude A of vibration:

$$A = \frac{k}{c} \frac{\sqrt{1 + (1/\omega\tau)^2}}{\sqrt{\left[1 - \left(\frac{\omega}{\omega_0}\right)^2\right]^2 + \left(\frac{\omega}{\omega_0}\right)^2 \left(\frac{\omega_0 \alpha}{c} + \frac{1}{\omega_0 \tau}\right)^2}} \quad . \; . \; (3)$$

where ω_0 is the natural frequency of the freely-vibrating system. This equation gives the "numerical amplitude" $A/k/c$ as a function of the "numerical frequency" ω/ω_0, the "numerical friction" $\alpha' = \omega_0\ \alpha/c$, and "the numerical time of decay" $\tau' = \omega_0\ \tau$.

Discussion of the relation 3

In *fig. 2* the numerical amplitude is plotted as a function of the numerical frequency for a specific case ($\tau' = 20$, $\alpha' = 0.45$). The frequency scale ω/ω_0 has been divided into four regions which will be discussed separately.

I) Decay Region

At low frequencies the amplitude becomes very great owing to the decay of the restoring forces. If the frequency is so low that ω/ω_0 is small as compared with unity, we get from equation (3) for the numerical amplitude:

$$\frac{A}{k/c} = \frac{1}{\omega\tau} \quad . \; . \; . \; . \; . \; . \quad (4)$$

It is therefore determined by the time of delay τ, and for this reason this region will be termed the decay region.

II) Static Region

In the region between approx. $^1/_{20}\ \omega_0$ and $^1/_2\ \omega_0$ the amplitude differs but little from the value:

$$A = k/c \quad . \; . \; . \; . \; . \; . \quad (5)$$

This is Hooke's law, which applies to the static loading of a material with elastic constant c with a force k This region can therefore be termed the static region.

III) Friction Region

At resonance ($\omega = \omega_0$) the amplitude in the absence of friction would increase without limit. Friction limits the amplitude in such a way that the maximum numerical amplitude is inversely proportional to the numerical friction:

$$\frac{A}{k/c} = \frac{c}{\omega_0 \alpha} = \frac{1}{\alpha'} \quad . \; . \; . \; . \; . \; . \quad (6)$$

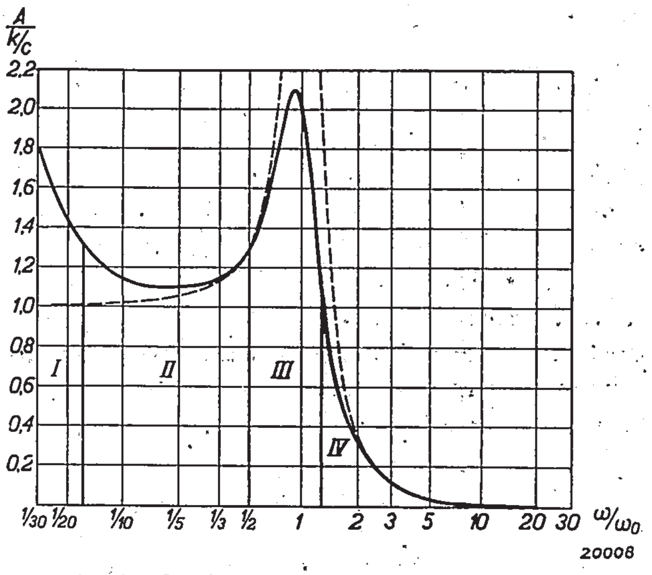

Fig. 2. Amplitude of a vibrating system as a function of the frequency when under the action of a constant energising force. At very low frequencies, the amplitude becomes very great owing to flow phenomena (decay of the restoring forces), while for the rest the usual curve for damped oscillations is obtained. The curve applies for $\omega_0\ \tau = 20$, $\omega_0\ a/c = 0.45$. *I* decay region; *II* static region; *III* friction region; *IV* mass region. The broken line shows the amplitude, in regions *I* and *III*, in the absence of friction and decay. In the latter case the amplitude at the resonance frequency becomes infinite.

IV) Mass Region

At very high frequencies $\omega \gg \omega_0$, the amplitude of the vibration becomes independent of the friction, the time of decay and the hardness of the spring. For this limiting case we get:

$$A = \frac{k}{c}\frac{\omega_0^2}{\omega^2} = \frac{k}{m\omega^2} \quad \ldots \ldots (7)$$

in other words a diminution inversely proportional to the mass and square of the frequency.

Equations (4) to (7) indicate that in each of the four frequency regions one of the four constants τ, c, a and m determines the amplitude. These results are collated in *table I*.

Table I

Region	Characteristic constant
I) Decay region	τ
II) Static region	c
III) Friction region	a
IV) Mass region	m

It is seen that the amplitude is determined in two regions (*I* and *III*) by the damping constants τ and a; the frequency range of these regions is proportional to $1/\tau$ and a. In the first region, that of decay, the decay of the restoring forces at a given amplitude of the forced vibrations leads to a reduction of the forces. In the third region (friction) the friction with given forces inducing vibration causes a reduction of the amplitudes.

A separate problem is the relationship between the damping constants on the one hand and the viscosity and decay of the damping agent on the other. This relationship cannot be immediately deduced, for it is governed by the method the vibrations are transmitted, particularly e.g. whether transversal or longitudinal vibrations are set up in the damping medium. A model for the pure transversal transmission of vibrations has been investigated theoretically and experimentally by Madelung and Flügge[3]).

Specific Applications

The above analysis indicates the existence of fundamentally different types of damping agents. The first type (flow-type damping agents) yields to slow displacements and is elastic with regard to high frequencies. These damping agents are particularly suitable for preventing the occurrence of elastic stresses on gradual deformation, e.g. in foundations. A typical example of this class of material is asphalt. Under a brisk blow from a hammer, which generates mainly high frequencies this material exhibits a true elasticity, but under a sustained pressure it commences to flow. The second group of agents (frictional damping agents) is elastic when subjected to slow displacements; the natural vibrations are, however, damped by internal friction. These agents are extremely suitable for damping instruments used for recording vibrations, particularly when the modulus of elasticity of the damping material is sufficiently small. Rubber is a typical frictional damping medium provided the impressed force is not too great, but also has a comparatively high modulus of elasticity, so that its use in vibrating systems considerably increases the rigidity in addition to the damping force.

A damping medium without this disadvantage has been employed in the sound recorder of the Philips Miller system. In this case the material has to be run into the damping chamber as a fluid and must then rapidly set, before it has a chance to flow into the air gaps of the magnetic system. These considerations, together with the need for a low modulus of elasticity, led to experiments being conducted with gelatinised systems, of which gelatin and agar-agar solutions are typical examples. Compared to fluid damping agents, a solid damping medium offers the advantage that the point of application of the damping force can be chosen arbitrarily and made of limited dimensions, and that the damping material can be applied directly where required in every case.

Mixtures of gelatin and water are unsuitable, as they rapidly dry out and also shrink considerably, so that on drying the material becomes detached from the walls. Both disadvantages can be overcome by the addition of glycerine. But a considerable amount of glycerine has to be added, which in its turn reduces the damping force too much. By adding water-soluble oils, the desired combination of a high damping and low rigidity was indeed realised, but at the same time the durability of the mixture was unsatisfactory, for in course of time shrinkage occurred and the rigidity increased.

The addition of sugar was found satisfactory from every point of view. The damping was increased, the rigidity remained small, and all shrinkage disappeared, while the adhesion of the material was excellent.

---

[3]) E. Madelung and S. Flügge, Ann. Physik, 22, 209, 1935.

The damping properties of this material may be improved by a suitable thermal treatment. It is remarkable that this implies a diminuation of the viscosity of the mass in the liquid phase. Therefore the damping properties of definite gelatinising systems cannot be deduced as a rule from the properties of the system above the gelatinising temperature in the molten state.

The total damping of the sound recorder was roughly doubled by using this damping medium, while the sensitivity was reduced by only about 5 per cent.

By varying the composition, the physical properties of the material, such as melting point, damping, rigidity, could to some extent be modified. The addition of agar-agar in place of gelatin, for instance, raises the melting point.

It should be mentioned that this damping compound can also be employed for other damping duties, such as occur in wax-disc cutters and loudspeakers. One of the authors has used the damping agent described here with complete satisfaction for filling bicycle tyres, which thus acquired marked damping properties and no longer required pumping up. Since the compound does not flow, the cycle can be left to stand for a long time without the tyres going flat.

PRACTICAL APPLICATIONS OF X-RAYS FOR THE EXAMINATION OF MATERIALS VIII

By W. G. BURGERS.

In article No. VII of this series it was shown that the expansion (or contraction) of a crystal lattice is exhibited in X-ray analysis by a displacement of the interference lines towards a smaller (or larger) angle of deflection with reference to the direction of incidence. This phenomenon can be employed as the basis for a method for revealing the elastic strains in a material by means of X-rays [1]). These strains produce elastic deformations resulting in a slight change in the interatomic distances which alteration can be brought out by radiography. According to the nature of strain distribution in the material or workpiece this can happen in different ways. In general the strains vary in direction and magnitude from area to area. If the areas of nearly constant strain are greater than the cross-section of the X-ray beam (i.e. greater than about 1 sq mm) then the distortion of the lattice is the same throughout the whole of the irradiated area: The X-ray lines are then displaced either inwards or outwards according to the local strain. Strains of this type, which may be termed "macro-strains" may for instance occur in the neighbourhood of welded seams or in workpieces under an external load or stress, such as axles, levers, etc. Elastic strains may, however, vary over much smaller areas such that in a single square millimetre every possible state of strain can be found. Such micro-strains occur for instance in cold-worked (e.g. rolled) metals, even when these are not subject to external load. In such a case the interatomic distances in the irradiated area are slightly greater at one point and slightly smaller at another point: The X-ray lines are then displaced both inwards and outwards, so that the lines become indistinct, while their distance apart is to a first approximation the same as in the absence of any strain [2]).

Frequently the mechanical state of a workpiece will include both macro and micro-strains, a condition which is revealed in the radiograph by the presence of lines which compared with the radiograph for the unstrained material are displaced *as well as* broadened out.

To obtain the X-ray strain diagram for a workpiece the arrangement shown diagrammatically in *fig. 1* may be used with satisfactory results; here only those rays reflected in a direction almost opposite to that of the incident X-ray beam are registered on the film. This arrangement is favorable in view of the low value of the possible deformation. The maximum strains are indeed to a certain extent limited by the yield point (in certain circumstances by the ultimate strength) of the material, i.e. by the strain at which permanent set (or failure) is obtained. On exceeding the yield point the interatomic distances undergo on the average no further change over small areas of for instance 1000 atoms, since the lattice then gives and the atoms slide over each other. This critical strain, particularly with metals, is less than 1 per cent of the modulus of elasticity, in general being actually a much smaller fraction. The fluctuations in interatomic distances resulting from elastic strain will therefore be at the most of this order of magnitude, so that only the most sensitive lines on a radiograph will become measurably displaced, i.e. those lines which on a specific change in interatomic distance sustain the maximum displacement. As already indicated in the previous article (Philips techn. Rev. 1, 253, 1936: fig. 1*b*) these are the inner lines of a socalled "reversed" radiograph, i.e. a radiograph in which the film is so placed that the incident X-ray beam passes through a hole in the centre of the film. This method is employed in the arrangement shown in fig. 1.

---

[1]) In certain circumstances it can also be measured, cf. A. E. van Arkel and W. G. Burgers, "Inwendige spanningen in metalen", Polytechn. Wbl. 28, 513, 1934.

[2]) This has been demonstrated by W. P. Davey and A. E. van Arkel:
W. P. Davey, Gen. Electr. Rev. 28, 586, 1925;
A. E. van Arkel, Physica 5, 208, 1925.

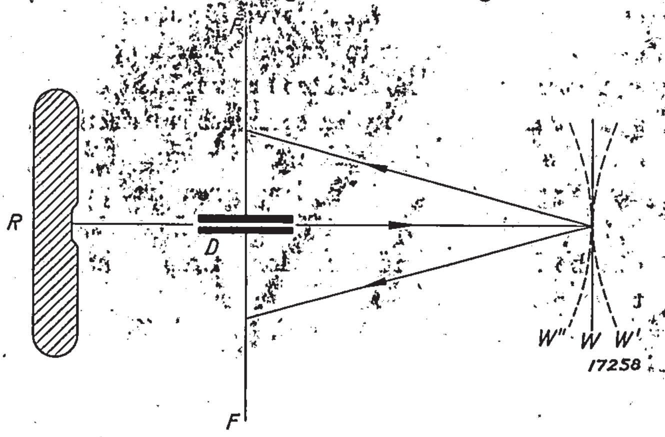

Fig. 1. Diagrammatic arrangement of X-ray tube, film and specimen for the X-ray investigation of internal strains.
R = X-ray tube. *D* = Diaphragm.
F-F = Photographic film (with a hole at the centre through which the diaphragm *D* projects).
W = Surface of workpiece or material under investigation (for the meaning of *W'* and *W''* see example 17).

As X-rays are strongly absorbed by metals, strain conditions can only be registered and investigated by the X-ray method which are located in the outer superficial layer (e.g. within a thickness of 20 μ) of the sample or workpiece under examination.

A number of simple applications of the X-ray method to the investigation of strain conditions are discussed below.

17. Detection of "Macro-strains" in an elastically-flexed Metal Strip

Fig. 2a shows the "most sensitive" interference lines in a radiograph of a rolled nickel-iron strip which was irradiated in a direction perpendicular to its surface *W* using the arrangement represented in fig. 1. *Fig. 2b* reproduces the radiograph of the same strip after it has been elastically flexed, as indicated by the hatched line *W'* in fig. 1 (the flexion between two points 4 cm apart being several millimetres). As a result of flexion the convex side of the strip has become elastically expanded parallel to the surface, and owing to transverse contraction it has become elastically constricted perpendicular to the surface.

The reduction in the interatomic distance in the latter direction causes a displacement of the sensitive X-ray lines inwards (see in particular the inner interference ring). If the band is flexed in the opposite direction (hatched line *W''* in fig. 1) so that the X-ray beam strikes the concave side, there is a displacement of the lines in the opposite direction *(fig. 2c)*. Thus from an examination of the displacement of the lines, the character of the strains in the surface (and in certain circumstances also their magnitude, cf. the article in the Polytechn. Wbl. quoted) can be approximately determined. In the example under discussion here the line displacement can be equated against the strain produced by flexion, thus providing the basis of a method for determining the macro-strains at any point of a workpiece (e.g. in a welded seam); to do this it is merely necessary to compare the radiograph obtained with the arrangement shown in fig. 1 for the stressed area with the corresponding exposure obtained for an unstressed area.

18. Effect of Heat Treatment on the "Micro-strains" in a Steel Ring

The radiographs shown in *figs. 3a* and *b* were obtained with two steel rings of which one had been reheated to 600 ° C for half an hour. The definition of the sensitive interference lines (a doublet) is very different in the two exposures: in fig. 3*a* the lines are indistinct and in fig. 3b they are quite clearly separated. It may thus be concluded that the latter radiograph applies to the reheated ring: As a result of reheating the elastic "micro-strains" in this ring have disappeared, being retained in the non-heated ring (produced probably as a result of previous working) where they are indicated by the lack of definition in the interference lines.

19. Difference in Micro-strains between the Surface Layer and Core of a drawn Tungsten Wire

Fig. 4a reproduces the "most sensitive" X-ray lines of a radiograph prepared from a cold-drawn

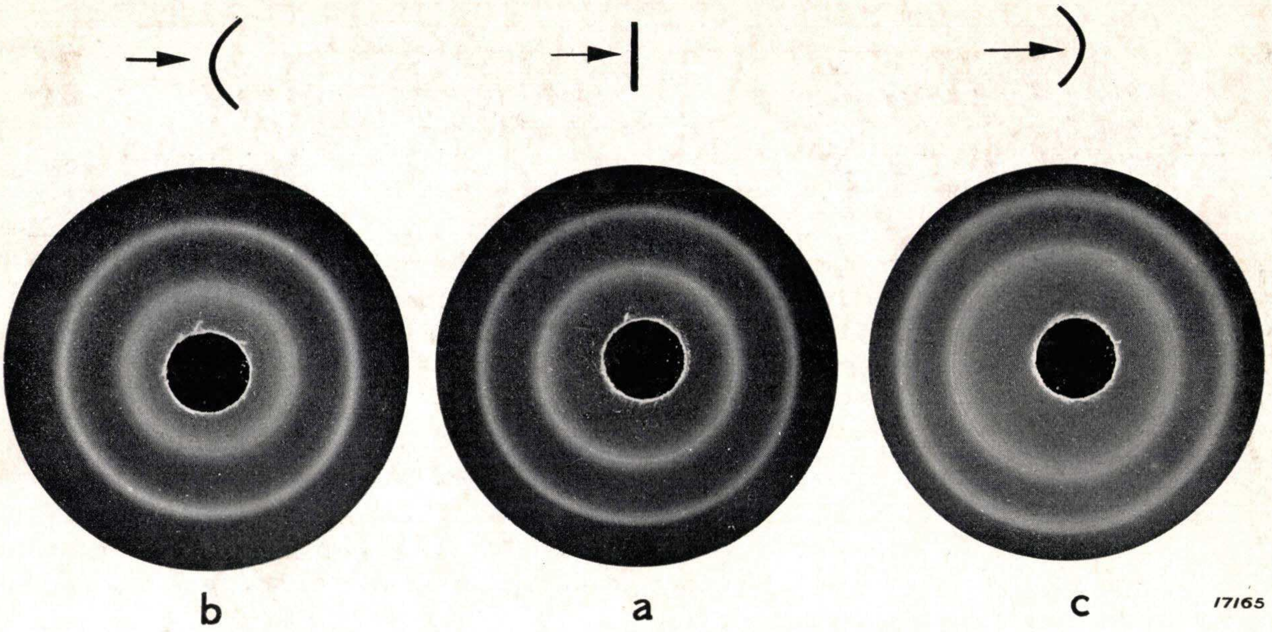

Fig. 2. Radiographs of a nickel-iron strip irradiated perpendicularly to the surface.
a Band flat . . . . (*W* in fig. 1).
b Band flexed, outer surface irradiated (*W'* in fig. 1).
c Band flexed, inner surface irradiated (*W"* in fig. 1).

fine-crystalline tungsten wire 500 μ in thickness, while *fig. 4b* gives the corresponding lines for a radiograph of the same wire after etching off the skin to a depth of about 15 μ. The lines in fig. 4*a* lack definition, while those in fig. 4*b* are sharply defined (this is particularly shown by the fact that the pictures consist of two doublets whose separation is very different in figs. *a* and *b*). It may be concluded from these radiographs that the outer layer of a drawn tungsten wire, i.e. the layer which has come in direct contact with the drawing disc, has bene subjected to variable deformation from point to point [3]).

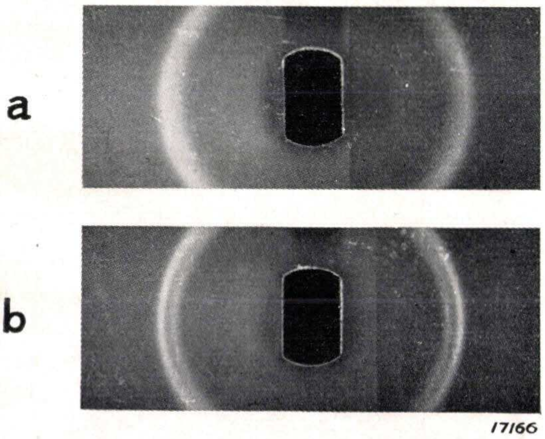

Fig. 3. Effect of heat treatment on the "micro-strains" in a steel ring.
a Non-reheated ring.
b Ring after reheating to 600 ° C for about half an hour.

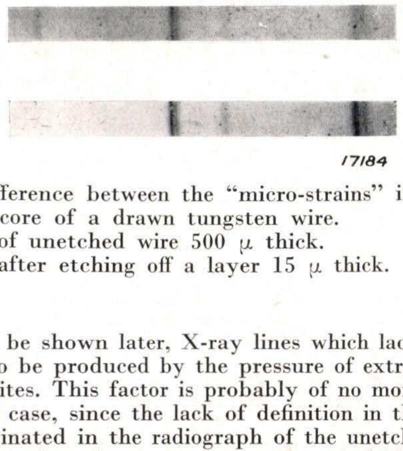

Fig. 4. Difference between the "micro-strains" in the outer layer and core of a drawn tungsten wire.
a Surface of unetched wire 500 μ thick.
b Surface after etching off a layer 15 μ thick.

---

[3] As will be shown later, X-ray lines which lack definition can also be produced by the pressure of extremely small crystallites. This factor is probably of no moment in the present case, since the lack of definition in the lines can be eliminated in the radiograph of the unetched wire by reheating the wire to a temperature at which crystalline growth (recrystallisation) is still almost completely absent, although such atomic displacement occurs that the distortions of the crystal lattice and hence also the "micro-strains" are reduced.